Shard polytopes and quotientopes for lattice congruences of the weak order

Julian Ritter

INSTITUT POLYTECHNIQUE DE PARIS

NNT : 2021IPPAX087

Thèse de doctorat

ÉCOLE POLYTECHNIQUE

IP PARIS

Shard Polytopes and Quotientopes for Lattice Congruences of the Weak Order

Thèse de doctorat de l'Institut Polytechnique de Paris
préparée à l'École polytechnique

École doctorale n°626 École doctorale de l'Institut Polytechnique de Paris (EDIPP)
Spécialité de doctorat : Informatique

Thèse présentée et soutenue à distance, le 29 octobre 2021, par

JULIAN RITTER

Composition du Jury :

Jean CARDINAL Professeur Université libre de Bruxelles (Département d'Informatique)	Président
Matthias BECK Professeur San Francisco State University (Department of Mathematics)	Rapporteur
Lionel POURNIN Professeur Université Paris 13 (LIPN)	Rapporteur
Carolina BENEDETTI Professeure assistante Universidad de los Andes (Departamento de Matemáticas)	Examinatrice
Arnau PADROL Maître de conférences Sorbonne Université (IMJ-PRG)	Examinateur
Viviane PONS Maîtresse de conférences Université Paris-Saclay (LRI)	Examinatrice
Raman SANYAL Professeur Goethe-Universität Frankfurt (Institut für Mathematik)	Examinateur
Vincent PILAUD Chargé de recherches CNRS & École polytechnique (LIX)	Directeur de thèse

Contents

Findest du also nichts hier auf den Gängen, öffne die Türen, findest du nichts hinter diesen Türen, gibt es neue Stockwerke, findest du oben nichts, es ist keine Not, schwinge dich neue Treppen hinauf. Solange du nicht zu steigen aufhörst, hören die Stufen nicht auf, unter deinen steigenden Füßen wachsen sie aufwärts.

— Franz Kafka, Fürsprecher

So if you find nothing in the corridors, open the doors, and if you find nothing behind these doors, there are more floors, and if you find nothing up there, don't worry, just leap up another flight of stairs. As long as you don't stop climbing, the stairs won't end, under your climbing feet they will go on growing upwards.

— Franz Kafka, Advocates

Si tu ne trouves rien ici dans les couloirs, alors ouvre les portes, si tu ne trouves rien derrière ces portes, il y a de nouveaux étages, si tu ne trouves rien plus haut, ce n'est pas une catastrophe, projette de nouveux escaliers devant toi. Tant que tu ne cesses pas de monter, les marches ne cessent pas, elles poussent au fur et à mesure sous tes pieds qui montent.

— Franz Kafka, Intercesseur

Acknowledgements

The person I thank first and foremost is my thesis advisor Vincent Pilaud. Enthusiastically, he introduced me to the beautiful objects of his research, while giving me plenty of opportunities to meet others and get an impression of their work as well. Tirelessly, he helped me with the questions I had, encouraged me with the answers I found, and put very much effort into my progress towards this thesis. Reliably, he met me with kindness and a lot of patience, and never ceased to impress me with his skill in organizing and his ability to master any administrative obstacle. Thank you for guiding me all the way and enabling me to make a small step into the unknown myself.

I thank Matthias Beck and Lionel Pournin for taking the time to be referees for this thesis. Thanks to all the members of the jury for accepting to be part of the thesis committee and the way each of you impacted me before. I thank Raman Sanyal (who introduced me to posets and lattices in an amazing course he taught back at FU Berlin), Viviane Pons (who encouraged me to use *SageMath* upon my arrival in Paris), Jean Cardinal (who once asked me more about quotientopes than I knew, showing me how much there was yet for me to find out), Carolina Benedetti (who co-organized *ECCO*, the most stunning mathematical gathering I have ever attended, filling the term *scientific community* with life), Lionel Pournin (who gave a thumbs-up at the mid-term defense, when he had confidence although results were sparse), Arnau Padrol (who posed a great question after a seminar talk, which was the starting point for a co-authored paper and a large part of this thesis) and Matthias Beck (who discussed that paper in a course at FU Berlin and gave me the opportunity to give a talk to his students about it).

I thank my co-authors Doriann Albertin, Arnau Padrol and Vincent Pilaud. Without their contributions, this thesis would not have been possible. Moreover, I thank Francisco Santos and Cesar Ceballos for hosting me as a visitor at FU Berlin and Uni Wien and for the opportunity to give presentations to their workgroups.

I thank the creators, developers and maintainers of *SageMath* for providing me with an immense open source software project which allowed me to experiment, to shape my intuition and to visualize what I was dealing with. In particular, I thank Viviane Pons, Florent Hivert and Nicolas Thiéry at LRI for answering my questions from installing to giving presentations with live code examples. Furthermore, thanks to Aram Dermenjian, Kevin Dilks, Samuel Lelièvre and Frédéric Chapoton for turning me from a user into a contributor. I thank Sophia Elia, Jean-Philippe Labbé and Vincent Pilaud for putting trust in my code and motivating me to write more.

I also thank my fellow PhD students at the LIX: Thibault Manneville welcomed me before I even arrived, Joël Gay brought to the office all his warmheartedness, and Mathias Lepoutre supplied me with more French words than I ever knew I needed. Thanks to all the other PhD students whose paths I crossed. In particular, I thank Doriann Albertin, Germain Poullot and Daniel Tamayo Jiménez for taking the time to go through some of my writing and help me improve it.

I thank the *équipe combi* at LIX that I had the good fortune to be part of. Thanks to Benjamin Doerr for his efforts at the interface between doctoral school and doctoral students. Finally, I am grateful for the financial support provided by the French ANR Grants SC3A, CAPPS and CHARMS as well as the French-Austrian cooperation project PHC Amadeus, which allowed me to visit workgroups and participate in conferences and summer schools from which I benefited greatly.

Introduction

This thesis gives an overview of my work on polytopes related to lattice congruences of the weak order. Two well-known examples of these polytopes are the permutahedron and the associahedron.

The permutahedron Perm_n, a subject of research since at least 1911 (see [Sch13]), is a polytope whose vertices correspond to the permutations of n elements, and whose edges are given by transpositions of adjacent entries. It can be constructed as the convex hull of the permutations of $[n]$ seen as vectors in $\mathbb{R}^n$ or as a Minkowski sum of the segments $[\mathbf{e}_i, \mathbf{e}_j]$ for $1 \leq i < j \leq n$. The associahedron Asso_n, described and studied in [Sta63], is a polytope whose vertices can be interpreted as the triangulations of a convex polygon, and whose edges are given by flips of diagonal. Another interpretation associates the vertices to all binary trees and the edges to rotations. It has been constructed in several ways, in particular as the convex hull of carefully chosen points associated to binary trees (see [Lod04]). The permutahedron and associahedron have connections to several areas of mathematics beyond the scope of combinatorics and geometry, including Hopf algebras (see [LR98, MR95, HNT05]) and mathematical physics (see [AHBHY18]).

Like all polytopes, these two can be studied from different perspectives: focusing on their shape and volume as geometric objects, or on the combinatorial information they encode in their face structure. For example, the face lattice of the permutahedron is the refinement lattice of ordered partitions of $[n]$ and the face lattice of the associahedron is the inclusion lattice of noncrossing sets of polygon diagonals. In this thesis, we are most interested in the normal fans of these polytopes. The normal fan of the permutahedron is the braid fan, given by the braid arrangement of the hyperplanes $x_i = x_j$ for $1 \leq i < j \leq n$. The normal fan of the associahedron of [Lod04] is the sylvester fan. Since it coarsens the braid fan, the associahedron is a generalized permutahedron (in the sense of [Pos09, PRW08]).

Such relationships between polytopes are not limited to the braid fan. The cones of any real central hyperplane arrangement induce a fan that is the normal fan of a zonotope. Moreover, choosing one of the regions of that fan as the base region induces a partial order on all the regions, called the poset of regions (see [Ede84, BEZ90]), which is a lattice under certain circumstances. For the braid arrangement, this poset is isomorphic to the weak order on the symmetric group $\mathfrak{S}_n$. For the Coxeter type $\mathcal{B}$ arrangement (see [BB05]), it is isomorphic to the weak order on the hyperocathedral group $\mathfrak{S}_n^{\mathcal{B}}$ (see [You30]).

Applying a lattice congruence (see [Rea04]) to a lattice of regions induces a quotient fan (see [Rea05]), where maximal cones are united if their corresponding lattice elements are equivalent under the lattice congruence. For example, the normal fan of the associahedron is a quotient fan induced by the sylvester congruence (see [LR98, HNT05]). A quotientope is a polytope whose normal fan is a quotient fan. Their existence was certified by a technical construction in [PS19] for those quotient fans based on the weak order on $\mathfrak{S}_n$.

The objective of this thesis is to study further constructions for quotientopes. Our first contribution concerns constructions as removahedra (see [Pil17]), which are polytopes obtained by removing inequalities from the facet description of the permutahedron. We show that the permutreehedra (introduced in [PP17]) are the only quotientopes that can be obtained as removahedra. Our second contribution is a simplified construction of arbitrary quotientopes as Minkowski sums of elementary polytopes we call shard polytopes due to their close relation with the shards of a hyperplane arrangement studied in [Rea16b]. In the weak order on $\mathfrak{S}_n$, our quotientope for the sylvester congruence coincides with the associahedron constructed in [Pos09], a Minkowski

sum of the faces of the standard simplex. Moreover, our construction can be adapted to construct quotientopes for all lattice congruences of the weak order on $\mathfrak{S}_n^{\mathcal{B}}$.

This thesis is made of four chapters. We start with preliminaries in Chapter 1. We then continue in Chapter 2 by analyzing the quotient fans of permutree congruences. In Chapter 3, we introduce the concept of shard polytopes. In Chapter 4, we transfer this concept to the type $\mathcal{B}$ arrangement. Next, we will give an overview of the contents of each of these four chapters.

1. Preliminaries. This chapter largely follows the concepts and notation established in [Zie07] and [Rea16b]. We start by giving an overview of some well-established concepts of discrete geometry, including hyperplanes (in Section 1.1), polyhedral cones and polytopes (in Section 1.2). In Section 1.2.4, we introduce type cones, which first appeared in [McM73]. Given a fan, a function that assigns to each of its rays a certain scalar is called a height function. The name comes from the intepretation as description of a convex set, where the function gives the maximal extent that set has in the direction of the respective ray. While the convex sets induced by arbitrary height functions can have many shapes and might be empty, we are particularly interested in those that induce a polytope whose normal fan is the fan we started with. For a complete fan, the set of these special height functions is an open polyhedral cone itself, called the type cone. They are closely related to Minkowsi sums (which we introduce in Section 1.2.5). Given two height functions from a type cone, their sum induces a polytope that is the Minkowski sum of the polytopes induced by the individual height functions.

In Section 1.3, we introduce real central hyperplane arrangements, which are sets of linear hyperplanes in $\mathbb{R}^n$. The complement of their union splits the real space into a number of connected components whose closures are called the regions of the arrangement. Each region is a polyhedral cone and they are the maximal cones of the arrangement fan, a complete fan in $\mathbb{R}^n$. This arrangement fan is also the normal fan of a family of polytopes. A zonotope is any polytope that can be written as the Minkowski sum of finitely many line segments. An arrangement zonotope is a zonotope where there is one such line segment normal to each of the arrangement hyperplanes. The normal fan of any arrangement zonotope is the arrangement fan. A well-known arrangement is the braid arrangement $\mathcal{A}_n$ containing all the hyperplanes $\{\mathbf{x} \in \mathbb{R}^n \mid x_i = x_j\}$ for $1 \leq i < j \leq n$. Its regions correspond to the permutations of $[n]$ and its fan is called the braid fan. A well-known zonotope is the permutahedron Perm_n, whose vertices are the permutation vectors for all permutations of $[n]$. The permutahedron is an arrangement zonotope of the braid arrangement.

While the fan of a hyperplane arrangement is naturally ordered by inclusion of its cones, we can introduce another partial order on the regions of an arrangement by setting one of the arrangement regions to be the base. We can then partially order all the regions by inclusion of the sets of hyperplanes that separate them from the base region. We call an arrangement together with a choice of base region an oriented arrangement, and the partial order is its poset of regions introduced in [Ede84]. For the braid arrangement, the canonical choice of base region is the one containing the point $(1, 2, \ldots, n)$ corresponding to the identity permutation $\mathsf{id} \in \mathfrak{S}_n$. The poset of regions of the oriented braid arrangement is isomorphic to the well-known weak order on $\mathfrak{S}_n$. The weak order, like any poset of regions of an oriented simplicial arrangement, is a semidistributive lattice. We introduce the basic ideas revolving around posets and lattices in Section 1.4. In particular, we introduce join-irreducible elements of a lattice, which are those that cannot be obtained as the join of other elements. In the weak order on $\mathfrak{S}_n$, these are the permutations with a single descent. As the poset of regions is semidistributive, each of its elements has a canonical decomposition as the join of some join-irreducibles. We also introduce lattice congruences which are equivalence relations that preserve meets and joins. Any lattice congruence $\equiv$ induces a quotient lattice whose elements are the equivalence classes of $\equiv$. This quotient lattice retains the induced partial order, meets and joins of the original lattice. A well-established lattice congruence on the weak order is

the sylvester congruence (see [LR98, HNT05]) and its quotient lattice is the well-known Tamari lattice (see [Tam51]).

In the poset of regions, the join-irreducibles are in bijection with certain parts of the arrangement hyperplanes, introduced in [Rea03]. These parts are obtained by following a set of rules to break the arrangement hyperplanes into pieces, which is why they are called the shards of the arrangement, commonly denoted by Σ. In Section 1.5, we introduce the construction of shards, their relation to join-irreducibles and lattice congruences through a partial order among them called forcing. Given a lattice congruence on the poset of regions, its equivalence classes can not only be understood as combinatorial objects comprising elements of the lattice, but also as geometrical objects, corresponding to unions of some of the chambers of the arrangement fan. This coarsening of the arrangement fan, where $\equiv$-equivalent chambers are united, is called the quotient fan $\mathcal{F}_{\equiv}$.

Like the arrangement fan is the normal fan of arrangement zonotopes, some quotient fans also appear as normal fans of well-known polytopes. For example, the normal fan of the classical associahedron (see [Lod04]) is the quotient fan induced by the sylvester congruence on the poset of regions of the braid arrangement. Such a polytope is called a quotientope for that congruence (see [PS19]). This leads us to the main question that served as the starting point for the research presented in this thesis: Given any lattice congruence on the poset of regions of an oriented simplicial arrangement, is there a quotientope whose normal fan is the quotient fan induced by that congruence? It is known from [PS19] that this is the case for a quotient lattice of the poset of regions of the braid arrangement. However, their construction is based on a careful but rather technical choice of height function and does not generalize easily to other arrangements. This motivated research to better understand quotient fans and find more natural ways to construct quotientopes, which we will see in Chapters 3 and 4.

In Section 1.6, we review some previous research on the type cone of the braid arrangement. Labeling the rays of the braid fan by subsets of $[n]$, its type cone can be understood as the set of strictly submodular height functions on subsets of $[n]$. We introduce the family of all polyhedra whose normal fans coarsen the braid fan. These polyhedra correspond to height functions that are submodular but not necessarily strictly submodular. They appeared in [Pos09] and [PRW08] as generalized permutahedra, but we will use the term deformed permutahedra to emphasize the special kind of generalization obtained by coarsening the normal fan.

A particularly interesting subclass of deformed permutahedra are removahedra. They can be obtained from the standard permutahedron Perm_n by removing inequalities from its $\mathcal{H}$-description. Their normal fans are called removahedral fans. Extending this notation, we call a lattice congruence on the weak order removahedral if its quotient fan is a removahedral fan. Examples of removahedra besides the permutahedron include the associahedron Asso_n, the Hohlweg-Lange associahedra (see [HL07]), and the graph associahedra (see [CD06, Dev09]) of chordful graphs (see [Pil17]).

But these are not the only special quotientopes that have already been studied in different contexts. In Section 1.7, we introduce permutrees, objects which first appeared in [PP17] and generalize a number of combinatorial objects, in particular permutations, binary sequences and binary trees. They are oriented trees drawn from bottom to top, where each internal node has one or two upper and one or two lower neighbors. The numbers of neighbors are represented by the symbols $\textcircled{1}, \textcircled{2}, \textcircled{3}$ and $\otimes$ and the sequence of these symbols is called the decoration δ of the permutree. Permutrees with decoration $\textcircled{1}^n$ correspond to permutations on $\mathfrak{S}_n$, while those with decoration $\textcircled{2}^n$ correspond to binary trees with n internal nodes and those with decoration $\otimes^n$ correspond to binary sequences of length $n-1$. Generic δ-permutrees are obtained from decorations containing various of these symbols.

Given a decoration δ, all δ-permutrees are related by sequences of rotations in the tree and can be partially ordered by fixing a natural orientation of these rotations. The resulting partial order is called the δ-permutree lattice. As a result of the correspondences discussed above, special cases of permutree lattices include the weak order on $\mathfrak{S}_n$ for $\delta = \textcircled{\scriptsize I}^n$, the Tamari lattice for $\delta = \textcircled{\scriptsize Y}^n$ and the Boolean lattice for $\delta = \otimes^n$. These correspondences go even further: Every permutree decoration induces a lattice congruence on the weak order. The special cases include the trivial congruence for $\delta = \textcircled{\scriptsize I}^n$, the sylvester congruence for $\delta = \textcircled{\scriptsize Y}^n$ and the hypoplactic congruence (see [KT97], [Nov00]) for $\delta = \otimes^n$.

In consequence, every permutree lattice is a quotient lattice of the weak order and induces a quotient fan of the braid arrangement fan, called the δ-permutree fan. Quotientopes for all permutree congruences have been constructed in [PP17]. They are called permutreehedra and can be described directly from the number of nodes in left and right upper and lower subtrees of each node of a permutree. Permutreehedra include as special cases the permutahedron for $\delta = \textcircled{\scriptsize I}^n$, Loday's associahedron (see [Lod04]) for $\delta = \textcircled{\scriptsize Y}^n$, the Hohlweg-Lange associahedra (see [HL07]) for $\delta \in \{\textcircled{\scriptsize Y}, \textcircled{\scriptsize Y}\}^n$, the parallelpiped with directions $\mathbf{e}_i - \mathbf{e}_{i+1}$ for $\delta = \otimes^n$ and some graphical zonotopes for $\delta \in \{\textcircled{\scriptsize I}, \otimes\}^n$.

2. Quotientopes and Removahedra. Chapter 2 is based on the following preprint:

- [APR20] Doriann Albertin, Vincent Pilaud, and Julian Ritter. Removahedral congruences versus permutree congruences. Preprint, arXiv:2006.00264, 2020.

A short version of the paper appears in the proceedings of the 33rd International Conference on Formal Power Series and Algebraic Combinatorics (see https://www.mat.univie.ac.at/~slc/wpapers/FPSAC2021/10.html).

In this chapter, we make some observations about congruences on the lattice of regions of the braid arrangement in general and permutree congruences in particular. We start in Section 2.1 by distinguishing essential and non-essential congruences. We call a congruence essential if the minimal lattice element and all its neighbors are in distinct congruence classes. We argue that quotientopes for non-essential congruences of the weak order on $\mathfrak{S}_n$ can be obtained as the Cartesian product of quotientopes for some essential congruences of the weak order on some $\mathfrak{S}_k$ with $k < n$. This justifies considering only essential congruences in many situations.

In Section 2.2, we discuss the rays of quotient fans of the braid fan. For a general lattice congruence, we determine whether or not a certain ray of the braid fan is a ray of the quotient fan as well. We do so by analyzing the shards that have been removed by the congruence. As the quotient fan coarsens the braid fan, this is sufficient to describe the set of rays of the quotient fan. For the special case of a permutree congruence, we translate the statement into a straightforward criterion to check for potential rays of the permutree fan using only the decoration. For example, using the conventional labeling of the rays of the braid fan by proper subsets of $[n]$, the set of rays of the δ-permutree fan is the set of all proper intervals for $\delta = \textcircled{\scriptsize Y}^n$ and it is the set of all proper initial and final intervals for $\delta = \otimes^n$.

It had been established in [PP17] that all permutree congruences are removahedral and that permutreehedra generalize the classic constructions of associahedra of [Lod04] and [HL07]. In Section 2.3.1, we show that all removahedral congruences are permutree congruences. In consequence, these two notions are equivalent for congruences of the weak order on $\mathfrak{S}_n$. Moreover, in Section 2.3.2, we introduce a special case of removahedral congruences. We call a congruence strongly removahedral if its quotient fan can be obtained not only by deleting inequalities from the standard permutahedron Perm_n but starting from any polytope P whose normal fan is the braid fan. We show that every permutree congruence is strongly removahedral. This implies that every removahedral congruence is in fact strongly removahedral, allowing to construct appropriate quotientopes not only starting with the $\mathcal{H}$-description given by the height function of Perm_n, but starting with any strictly submodular function.

In Section 2.4, we use our findings about the rays of the permutree fan to describe the type cone of a permutree fan. We give a description of the facets of the type cone, determine its number of facets and deduce a criterion to find out whether a type cone of a certain permutree fan is simplicial. Permutree fans whose associated type cone is simplicial are particularly interesting because they allow for a canonical representation of the permutreehedron as the Minkowski sum of those polytopes induced by height functions corresponding to the rays of the type cone. We complete the chapter by describing the set of all quotientopes for such a permutree fan in the kinematic space (see [AHBHY18]).

3. Shard Polytopes for the Braid Arrangement. Chapter 3 is based on part I of

- [PPR20] Arnau Padrol, Vincent Pilaud, and Julian Ritter. Shard polytopes. Preprint, arXiv:2007.01008, 2020.

A short version of the paper appears in the proceedings of the 33rd International Conference on Formal Power Series and Algebraic Combinatorics (see https://www.mat.univie.ac.at/~slc/wpapers/FPSAC2021/11.html).

In this chapter, we establish a construction of quotientopes for any lattice congruence of the weak order on $\mathfrak{S}_n$. These new quotientopes, called shardsumotopes, are built as the Minkowski sum of new elementary polytopes for each of the shards of the arrangement, called shard polytopes.

We start in Section 3.1 by generalizing shards of the oriented braid arrangement to so-called pseudoshards, a broader class of polyhedral cones with similar combinatorial representation. We introduce a number of new objects related to shards, both inspired by and compatible with the schematic representation of shards established in [Rea15]. In particular, we introduce shard matchings, which can be seen geometrically as certain sums of braid arrangement hyperplane normals $\mathbf{e}_i - \mathbf{e}_j$ that are closely related to the shard.

We then use these shard matchings to define the shard polytope $\mathsf{SP}(\Sigma)$ in Section 3.2. There is one such polytope for each shard of the braid arrangement. We give both an $\mathcal{H}$-description and a $\mathcal{V}$-description and prove that they are equivalent. We determine the dimension, the number of facets and the number of vertices of the shard polytope. In particular, we observe that shard polytopes are simplices for the up shards and that the numbers of shard polytope vertices are the Fibonacci numbers for alternating shards. We go on to describe faces of a shard polytope. We determine its edges using combinatorial properties of the associated shard matchings. Moreover, we show that any face of a shard polytope is (isomorphic to) a Cartesian product of shard polytopes. To conclude the section, we establish a number of symmetries of shard polytopes.

In Section 3.3, we analyze the normal fans of shard polytopes, called shard fans and denoted by $\mathcal{SF}(\Sigma)$. These are of particular interest as we aim to reconstruct a quotient fan as the normal fan of a Minkowski sum of shard polytopes, so the normal fan of this Minkowski sum will be the common refinement of all the associated shard fans. We describe the walls and some of the cones of the shard fans. The main result in this section guarantees that the union of walls of the shard fan $\mathcal{SF}(\Sigma)$ both contains the shard Σ as a subset and is contained in the union of all those shards Σ' that force Σ in the sense introduced in Section 1.5.3.

This property of shard fans enables us to construct shardsumotopes in Section 3.4. Given a lattice congruence $\equiv$ on the weak order, the shardsumotope $\mathsf{SP}_+(\equiv)$ is the Minkowski sum of all shard polytopes $\mathsf{SP}(\Sigma)$ for the shards Σ that appear in the quotient fan $\mathcal{F}_\equiv$. The normal fan of the shardsumotope is then equal to the quotient fan, where each shard polytope $\mathsf{SP}(\Sigma)$ summed up in the process introduces the shard Σ into the resulting fan without adding any walls not present in $\mathcal{F}_\equiv$. Prominent shardsumotopes include the parallelotope spanned by braid arrangement normals, a non-standard permutahedron and a translate of the classical associahedron (see [Lod04]) obtained as the shardsumotope of the sylvester congruence. We conclude this section with a discussion of vertices and facets of shardsumotopes and a way to construct them efficiently.

In Section 3.5, we examine the role that shard polytopes play in the type cone of the braid arrangement. We show that shard polytopes are Minkowski indecomposable, so their height functions lie in the rays of the type cone of the braid fan. We visualize the type cone of the braid fan, relating the polyhedral structure of the cone, the polytopes induced by certain height functions and the shards of the braid arrangement in one picture.

4. Shard Polytopes for the Type B Arrangement. Chapter 4 is based on part II of

- [PPR20] Arnau Padrol, Vincent Pilaud, and Julian Ritter. Shard polytopes. Preprint, arXiv:2007.01008, 2020.

A short version of the paper appears in the proceedings of the 33rd International Conference on Formal Power Series and Algebraic Combinatorics (see https://www.mat.univie.ac.at/~slc/wpapers/FPSAC2021/11.html).

In this chapter, we adapt our findings from Chapter 3 to a different class of hyperplane arrangements. While Chapter 3 covers lattice congruences on the poset of regions of the braid arrangement $\vec{\mathcal{A}}_n$ (which is isomorphic to the lattice of the weak order on $\mathfrak{S}_n$), Chapter 4 considers lattice congruences on the poset of regions of the type $\mathcal{B}$ arrangement $\vec{\mathcal{B}}_n$ (which is isomorphic to the lattice of the weak order on $\mathfrak{S}_n^{\mathcal{B}}$). The name of this arrangement is derived from its relation to the type B Coxeter group (see [Rea16a]), also known as the hyper-octahedral group (see [You30]).

In Section 4.1, we introduce the type $\mathcal{B}$ arrangement and its poset of regions isomorphic to the weak order on the group $\mathfrak{S}_n^{\mathcal{B}}$ of signed permutations. We determine the type cone of the type $\mathcal{B}$ arrangement. We describe the canonical zonotope of the type $\mathcal{B}$ arrangement, known as the $\mathcal{B}$-permutahedron. Each signed permutation on $[n]$ can equivalently be described as a centrally symmetric permutation of $[\pm n] := \{-n, \dots, -1, 1, \dots, n\}$. This translates into a geometric relationship of the associated arrangements via the centrally symmetric subspace $\mathcal{H}_n^{\mathcal{B}}$. The $\mathcal{B}$ arrangement $\vec{\mathcal{B}}_n$ can be obtained as the intersection of a braid arrangement with $\mathcal{H}_n^{\mathcal{B}}$. The $\mathcal{B}$-permutahedron can be obtained as the projection of the standard permutahedron to $\mathcal{H}_n^{\mathcal{B}}$.

In Section 4.2, we analyze the shards of the type $\mathcal{B}$ arrangement. We show that they can be obtained by intersecting the shards of the braid arrangement with $\mathcal{H}_n^{\mathcal{B}}$. We then use the geometry of the arrangement to carefully establish the forcing relation among $\vec{\mathcal{B}}_n$ shards. It would be convenient to assume that the forcing order on type $\mathcal{B}$ shards coincides with the forcing order on shards of the braid arrangement intersected with $\mathcal{H}_n^{\mathcal{B}}$. However, we prove that this is not the case. In particular, most upper sets of type $\mathcal{B}$ shards cannot be obtained from upper sets of braid arrangement shards by intersection with $\mathcal{H}_n^{\mathcal{B}}$.

It is known (see [Rea16a]) that lattice congruences on the weak order on $\mathfrak{S}_n^{\mathcal{B}}$ are in bijection with upper sets in the forcing order on type $\mathcal{B}$ shards and define quotient fans just as those on the weak order on $\mathfrak{S}_n$ do. In Section 4.3, we describe these quotient fans. With the help of the shard polytopes for the braid arrangement constructed in Chapter 3, we define shard polytopes for all type $\mathcal{B}$ shards using the projection to $\mathcal{H}_n^{\mathcal{B}}$. Again, we show that the normal fans of each of these type $\mathcal{B}$ shard polytopes contains the shard itself and is contained in the union of all shards that force it. With this result, we conclude the chapter by constructing quotientopes for all lattice congruences of the weak order on $\mathfrak{S}_n^{\mathcal{B}}$.

Software. Over the course of preparation of my thesis, I extensively used the open source software SageMath [SD19] to work with many of the objects mentioned so far. I wrote code to implement some definitions and algorithms that had not been present in the software yet. This enabled my collaborators and me to experiment with the concepts, visualize examples and shape an intuition of the objects we were dealing with. Plots obtained from this effort can be seen in a few of the figures in this thesis. This computational support was very helpful to obtain the results presented in the following chapters.

Introduction

Cette thèse donne une vue d'ensemble de mon travail sur les polytopes reliés aux congruences de treillis de l'ordre faible. Deux examples bien connus de ces polytopes sont le permutaèdre et l'associaèdre.

Le permutahèdre Perm_n, sujet de recherche depuis au moins 1911 (voir [Sch13]), est un polytope dont les sommets correspondent aux permutations de n éléments, et dont les arêtes sont données par les transpositions d'entrées adjacentes. Il peut être construit comme l'enveloppe convexe des permutations de $[n]$ vues comme vecteurs dans $\mathbb{R}^n$ ou comme la somme de Minkowski des segments $[\mathbf{e}_i, \mathbf{e}_j]$ pour $1 \leq i < j \leq n$. L'associaèdre Asso_n, décrit et étudié dans [Sta63], est un polytope dont les sommets peuvent être interprétés comme les triangulations d'un polygone convexe, et dont les arêtes sont données par les flips des diagonales. Une autre interprétation associe les sommets à tous les arbres binaires et les arêtes aux rotations. Il a été construit de plusieurs manières, notamment comme l'enveloppe convexe de points soigneusement choisis associés aux arbres binaires (voir [Lod04]). Le permutaèdre et l'associaèdre ont des liens avec plusieurs domaines des mathématiques au-delà de la combinatoire et de la géométrie, notamment avec les algèbres de Hopf (voir [LR98, MR95, HNT05]) et avec la physique mathématique (voir [AHBHY18]).

Comme tout polytope, ces deux polytopes peuvent être étudiés selon différentes perspectives : en se concentrant sur leur forme et volume comme des objets géométriques, ou sur l'information combinatoire encodée par leur structure de faces. Par exemple, le treillis des faces du permutaèdre est le treillis de raffinement des partitions ordonnées de $[n]$ et le treillis des faces de l'associaèdre est le treillis d'inclusion des ensembles sans croisement de diagonales d'un polygone. Dans cette thèse, nous nous intéressons aux éventails normaux de ces polytopes. L'éventail normal du permutaèdre est l'eventail de tresses, donné par l'arrangement de tresses des hyperplans $x_i = x_j$ pour $1 \leq i < j \leq n$. L'éventail normal de l'associaèdre de [Lod04] est l'éventail sylvestre. Comme il est raffiné par l'éventail de tresses, l'associaèdre est un permutaèdre généralisé (au sens de [Pos09, PRW08]).

De telles relations entre polytopes ne se limitent pas à l'éventail de tresses. Les cônes de tout arrangement réel d'hyperplans linéaires induisent un éventail qui est l'éventail normal d'un zonotope. De plus, le choix d'une région de l'éventail comme région de base induit un ordre partiel sur les régions, appelé l'ordre des régions (voir [Ede84, BEZ90]), qui est un treillis dans certaines circonstances. Pour l'arrangement de tresses, cet ordre est isomorphe à l'ordre faible sur le groupe symétrique $\mathfrak{S}_n$. Pour l'arrangement de Coxeter de type $\mathcal{B}$ (voir [BB05]), il est isomorphe à l'ordre faible sur le groupe hyper-octaédrique $\mathfrak{S}_n^{\mathcal{B}}$ (voir [You30]).

L'application d'une congruence de treillis (voir [Rea04]) sur un treillis de régions induit un éventail quotient (voir [Rea05]), où des cônes maximaux sont collés si leurs éléments de treillis correspondants sont équivalents sous la congruence de treillis. Par exemple, l'éventail normal de l'associaèdre est un éventail quotient induit par la congruence sylvestre (voir [LR98, HNT05]). Un quotientope est un polytope dont l'éventail normal est un éventail quotient. Leur existence a été certifiée par une construction technique dans [PS19] pour les éventails quotients basés sur l'ordre faible sur le groupe symétrique.

L'objectif de cette thèse est d'étudier plus avant des constructions de quotientopes. Notre première contribution concerne les constructions comme enlevoèdres (voir [Pil17]), qui sont des polytopes obtenus en enlevant des inégalités de la description des facettes du permutaèdre. Nous mon-

trons que les permutarbrèdres (introduits dans [PP17]) sont les seuls quotientopes qui peuvent être obtenus comme enlevoèdres. Notre deuxième contribution est une construction simplifiée de quotientopes arbitraires comme sommes de Minkowski de polytopes élémentaires que nous appelons polytopes de tessons en raison de leur étroite relation aux tessons d'un arrangement d'hyperplans étudiés dans [Rea16b]. Dans le cas de l'ordre faible sur $\mathfrak{S}_n$, notre quotientope pour la congruence sylvestre coïncide avec l'associaèdre construit dans [Pos09], une somme de Minkowski des faces du simplexe standard. De plus, notre construction peut être adaptée pour construire des quotientopes pour toute congruence de treillis de l'ordre faible sur $\mathfrak{S}_n^{\mathcal{B}}$.

Cette thèse est composée de quatre chapitres. Nous commençons par les préliminaires dans le chapitre 1. Nous poursuivons ensuite dans le chapitre 2 en analysant les éventails quotient des congruences de permutarbres. Dans le chapitre 3, nous introduisons le concept de polytopes de tessons. Dans le chapitre 4, nous transfèrons ce concept à l'arrangement de Coxeter de type $\mathcal{B}$. Dans la suite de cette introduction, nous détaillons le contenu de chacun de ces quatre chapitres.

1. Préliminaires. Ce chapitre suit en grande partie les concepts et les notations établis dans [Zie07] et [Rea16b]. Nous commençons en donnant une vue d'ensemble de quelques concepts classiques de géométrie discrète, y compris les hyperplans (dans la partie 1.1) et les cônes polyédraux et polytopes (dans la partie 1.2). Dans la partie 1.2.4, nous introduisons les cônes de type, qui sont apparus pour la première fois dans [McM73]. Étant donné un éventail, une fonction qui attribue à chacun de ses rayons un certain scalaire est appelée une fonction de hauteur. Le nom vient de la description d'un ensemble convexe, dont la fonction précise l'étendue maximale dans la direction donnée par chaque rayon. Tandis que les ensembles convexes induits par des fonctions de hauteur arbitraires peuvent avoir des formes differentes et pourraient être vides, nous sommes particulièrement intéressés par celles qui induisent un polytope dont l'éventail normal est l'éventail dont nous sommes partis. Pour un éventail complet, l'ensemble de ces fonctions de hauteur spécifiques est lui-même un cône polyédral, appelé le cône de type. Ces cônes de type sont étroitement liés aux sommes de Minkowski (que nous introduisons dans la partie 1.2.5). Étant donné deux fonctions de hauteur d'un cône de type, leur somme induit un polytope qui est la somme de Minkowski des polytopes induits par ces fonctions de hauteur.

Dans la partie 1.3, nous introduisons les arrangements réels centraux d'hyperplans, qui sont des ensembles d'hyperplanes linéaires dans $\mathbb{R}^n$. Le complément de leur union divise l'espace réel en plusieurs composantes connexes dont les clôtures sont appelées les régions de l'arrangement. Chaque région est un cône polyédral et ils sont les cônes maximaux de l'éventail de l'arrangement, un éventail complet dans $\mathbb{R}^n$. Cet éventail d'arrangement est également l'éventail normal d'une famille de polytopes. Un zonotope est un polytope qui peut être écrit comme la somme de Minkowski d'un nombre fini de segments. Un zonotope d'arrangement est un zonotope où ces segments sont des vecteurs normaux des hyperplans de l'arrangement. L'éventail normal de tout zonotope d'arrangement est l'éventail de l'arrangement. Un arrangement bien connu est l'arrangement de tresses $\mathcal{A}_n$, qui contient tous les hyperplans $\{\mathbf{x} \in \mathbb{R}^n \mid x_i = x_j\}$ pour $1 \leq i < j \leq n$. Ses régions correspondent aux permutations de $[n]$ et son éventail est appelé l'éventail de tresses. Un zonotope bien connu est le permutaèdre Perm_n, dont les sommets sont les vecteurs des permutations de $[n]$. Le permutaèdre est un zonotope d'arrangement de l'arrangement de tresses.

L'éventail d'un arrangement d'hyperplans est naturellement ordonné par l'inclusion de ses cônes. On peut aussi introduire un autre ordre partiel sur les régions d'un arrangement en fixant une des régions comme étant la région de base. On peut alors ordonner toutes les régions par inclusion de l'ensemble des hyperplans qui les séparent de la région de base. On appelle un arrangement avec un choix de région de base un arrangement ordonné et son ordre partiel est son ordre des régions introduit dans [Ede84]. Pour l'arrangement de tresses, le choix canonique de la région de base est celle qui contient le point $(1, 2, \ldots, n)$ et qui correspond à la permutation iden-

tité $\mathsf{id} \in \mathfrak{S}_n$. L'ordre des régions de l'arrangement de tresses orienté est isomorphe à l'ordre faible sur $\mathfrak{S}_n$. L'ordre faible, comme tout ordre des régions d'un arrangement simplicial orienté, est un treillis semi-distributif. Nous introduisons les bases de la théorie des ordres partiels et des treillis dans la partie 1.4. En particulier, nous introduisons les éléments sup-irréductibles d'un treillis, qui ne peuvent pas être obtenus comme un sup d'autres élements. Dans l'ordre faible sur $\mathfrak{S}_n$, ce sont les permutations avec une seule descente. Comme l'ordre des régions est semi-distributif, tout élément admet une décomposition canonique comme le sup de certains éléments sup-irréductibles. Nous introdusions aussi les congruences de treillis, qui sont des relations d'équivalence qui préservent l'inf et le sup. Chaque congruence de treillis $\equiv$ induit un treillis quotient dont les éléments sont les classes d'équivalence de $\equiv$. Ce treillis quotient retient l'ordre partiel induit, les infs et les sups du treillis d'origine. Une congruence de treillis bien connue sur l'ordre faible est la congruence sylvestre (voir [LR98, HNT05]) et son treillis quotient est le treillis de Tamari (voir [Tam51]).

Dans l'ordre des régions, les sup-irréductibles sont en bijection avec certaines parties des hyperplans de l'arrangement, introduites dans [Rea03]. Ces parties sont obtenues en suivant un ensemble de règles pour briser les hyperplans de l'arrangement en morceaux, c'est pourquoi ils sont appelés tessons de l'arrangement, généralement dénotés par Σ. Dans la partie 1.5, nous introduisons la construction des tessons, leur relation aux sup-irréductibles et aux congruences de treillis à travers un ordre partiel sur les tessons, appelé le forçage. Étant donné une congruence de treillis sur l'ordre des régions, ses classes d'équivalence peuvent non seulement être comprises comme des objets combinatoires qui fusionnent des éléments du treillis, mais aussi comme des objets géométriques qui correspondent à certaines unions de chambres de l'éventail de l'arrangement. Cet éventail, qui est raffiné par l'éventail d'arrangement, et qui unit les classes des chambres équivalentes sous $\equiv$, est appelé l'éventail quotient $\mathcal{F}_{\equiv}$.

De même que l'éventail d'un arrangement est l'éventail normal des zonotopes de l'arrangement, certains éventails quotients apparaissent comme éventails normaux de polytopes bien connus. Par exemple, l'éventail normal de l'associaèdre classique (voir [Lod04]) est l'éventail quotient induit par la congruence sylvestre sur l'ordre des régions de l'arrangement de tresses. Un tel polytope est appelé un quotientope pour cette congruence (voir [PS19]). Cela nous amène à la question principale qui servait de point de départ pour les recherches présentées ici : étant donnée une congruence de treillis sur l'ordre des régions d'un arrangement simplicial orienté, existe-t-il un quotientope dont l'éventail normal est l'éventail quotient induit par cette congruence ? Il est connu de [PS19] que c'est le cas pour toute congruence de treillis sur l'ordre des régions de l'arrangement de tresses. Cependant, leur construction est basée sur un choix minutieux mais assez technique de fonction de hauteur et elle ne se généralise pas facilement à d'autres arrangements. Cela a motivé la recherche visant à mieux comprendre les éventails quotients et à trouver des constructions plus naturelles des quotientopes, ce que nous verrons aux chapitres 3 et 4.

Dans la partie 1.6, nous passons en revue certaines recherches antérieures sur le cône de type de l'arrangement de tresses. En étiquetant les rayons de l'éventail de tresses par les sous-ensembles de $[n]$, son cône de type peut être compris comme l'ensemble des fonctions de hauteur strictement sous-modulaires sur les sous-ensembles de $[n]$. Nous introduisons la famille de tous les polyèdres pour lesquels l'éventail de tresses raffine leur éventail normal. Ces polyèdres correspondent aux fonctions de hauteur qui sont sous-modulaires mais pas forcément strictement sous-modulaires. Ils sont apparus dans [Pos09] et [PRW08] comme permutaèdres généralisés, mais nous utilisons l'expression permutaèdres déformés afin de souligner la généralisation particulière obtenue par cette relation de raffinement des éventails.

Les enlèvoèdres forment une sous-classe particulièrement intéressante des permutaèdres déformés. Ils peuvent être obtenus à partir du permutaèdre standard Perm_n en enlevant des inégalités de sa description par inégalités. Leurs éventails normaux sont appelés éventails enlèvoédraux. Par extension, nous appelons une congruence de treillis sur l'ordre faible enlèvoédrale si son éven-

tail quotient est un éventail enlèvoédral. Des exemples d'enlèvoèdres sont l'associaèdre standard Asso_n, les associaèdres de Hohlweg-Lange (voir [HL07]), et les associaèdres de graphes (voir [CD06, Dev09]) pour les graphes dont tous les cycles induisent des sous-graphes complets (voir [Pil17]).

Mais ce ne sont pas les seuls quotientopes spéciaux qui ont déjà été étudiés dans d'autres contextes. Dans la partie 1.7, nous introduisons les permutarbres, des objets qui sont apparus pour la première fois dans [PP17] et qui généralisent plusieurs objets combinatoires, y compris les permutations, les séquences binaires et les arbres binaires. Ce sont des arbres orientés dessinés de bas en haut, où chaque nœud interne a un ou deux voisins inférieurs et un ou deux voisins supérieurs. Les nombres de voisins sont représentés par les symboles $\oplus, \curlywedge, \curlyvee$ et $\otimes$ et la suite de ces symboles est appelée décoration δ du permutarbre. Les permutarbres avec la décoration $\oplus^n$ correspondent aux permutations sur $\mathfrak{S}_n$, tandis que ceux avec la décoration $\curlywedge^n$ correspondent aux arbres binaires à n nœuds internes et ceux avec la décoration $\otimes^n$ correspondent aux séquences binaires de longeur $n-1$. Des δ-permutarbres génériques sont obtenus à partir des décorations contenant différents symboles.

Étant donné une décoration δ, tous les δ-permutarbres sont reliés par des suites de rotations dans l'arbre et peuvent être ordonnés partiellement en fixant une orientation naturelle sur ces rotations. L'ordre partiel ainsi obtenu est appelé le treillis des δ-permutarbres. En conséquence des correspondances discutés ci-dessus, les cas particuliers des treillis de permutarbres comprennent l'ordre faible sur $\mathfrak{S}_n$ pour $\delta = \oplus^n$, le treillis de Tamari pour $\delta = \curlywedge^n$ et le treillis booléen pour $\delta = \otimes^n$. Ces correspondances vont même plus loin : chaque décoration de permutarbres induit une congruence de treillis sur l'ordre faible. Les cas particuliers comprennent la congruence triviale pour $\delta = \oplus^n$, la congruence sylvestre pour $\delta = \curlywedge^n$ et la congruence hypoplactique (voir [KT97], [Nov00]) pour $\delta = \otimes^n$.

En conséquence, chaque treillis de permutarbres est un treillis quotient de l'ordre faible et induit un éventail quotient de l'éventail de l'arrangement de tresses, appelé l'éventail des δ-permutarbres. Des quotientopes pour toutes les congruences de permutarbres ont été construits dans [PP17]. Ils sont appelés les permutarbrèdres et peuvent être décrits directement à partir du nombre de nœuds dans les sous-arbres gauche et droit inférieur et supérieur de chaque nœud d'un permutarbre. Les cas particuliers de permutarbres comprennent le permutaèdre pour $\delta = \oplus^n$, l'associaèdre de Loday (voir [Lod04]) pour $\delta = \curlywedge^n$, l'associaèdre de Hohlweg-Lange (voir [HL07]) pour $\delta \in \{\curlywedge, \curlyvee\}^n$, le parallélépipède avec les directions $\mathbf{e}_i - \mathbf{e}_{i+1}$ pour $\delta = \otimes^n$ et certains zonotopes graphiques pour $\delta \in \{\oplus, \otimes\}^n$.

2. Quotientopes et enlevoèdres. Le chapitre 2 est basé sur la prépublication suivante :

- [APR20] Doriann Albertin, Vincent Pilaud, and Julian Ritter. Removahedral congruences versus permutree congruences. Preprint, arXiv:2006.00264, 2020.

Une version courte de l'article apparaît dans les actes de la 33rd International Conference on Formal Power Series and Algebraic Combinatorics (voir https://www.mat.univie.ac.at/~slc/wpapers/FPSAC2021/10.html).

Dans ce chapitre, nous faisons quelques observations sur les congruences sur le treillis de régions de l'arrangement de tresses en général et les congruences de permutarbre en particulier.

Nous commençons dans la partie 2.1 par distinguer les congruences essentielles et non-essentielles. Nous appelons une congruence essentielle si l'élément minimal du treillis et tous ses voisins sont dans des classes d'équivalence distinctes. Nous observons que des quotientopes pour les congruences non-essentielles de l'ordre faible sur $\mathfrak{S}_n$ peuvent être obtenus par produit cartésien de plusieurs quotientopes pour des congruences essentielles de l'ordre faible sur un certain $\mathfrak{S}_k$ avec $k < n$. Cela justifie de ne considérer que les congruences essentielles dans beaucoup de situations.

Dans la partie 2.2, nous discutons les rayons des éventails quotients de l'éventail de tresses. Pour une congruence de treillis générale, nous déterminons si un certain rayon de l'éventail de tresses est aussi un rayon de l'éventail quotient. Pour ce faire, nous analysons les tessons qui ont été enlevés par la congruence. Comme l'éventail de tresses raffine l'éventail quotient, cela est suffisant pour décrire l'ensemble des rayons de l'éventail quotient. Pour le cas spécial d'une congruence de permutarbre, nous traduisons la proposition en un critère simple pour vérifier des rayons potentiels de l'éventail de permutarbre en n'utilisant que la décoration. Par exemple, en utilisant l'étiquetage conventionnel sur les rayons de l'éventail de tresses par les sous-ensembles propres de $[n]$, l'ensemble de rayons de l'éventail des δ-permutarbres est l'ensemble de tous les intervals propres pour $\delta = \circledcirc^n$ et il est l'ensemble de tous les intervals propres initiaux et finaux pour $\delta = \otimes^n$.

Il a été établi dans [PP17] que toute congruence de permutarbre est enlèvoédrale et que les permutarbrèdres généralisent les constructions classiques de l'associaèdre de [Lod04] et [HL07]. Dans la partie 2.3.1, nous montrons que toute congruence enlèvoédrale est une congruence de permutarbre. En conséquence, ces deux notions sont équivalentes pour les congruences de l'ordre faible sur $\mathfrak{S}_n$. De plus, dans la partie 2.3.2, nous introduisons un cas spécial des congruences enlèvoédrales. Nous appelons une congruence fortement enlèvoédrale si son éventail quotient peut être obtenu non seulement en enlevant des inégalites du permutaèdre standard Perm_n, mais aussi à partir de n'importe quel polytope P dont l'éventail normal est l'éventail de tresses. Nous montrons que toute congruence de permutarbre est fortement enlèvoédrale. Cela implique que tout congruence enlèvoédrale est en fait fortement enlèvoédrale, ce qui permet de construire des quotientopes non seulement à partir de la fonction de hauteur de Perm_n, mais aussi à partir de n'importe quelle fonction de hauteur strictement sous-modulaire.

Dans la partie 2.4, nous utilisons nos découvertes sur les rayons de l'éventail de permutarbre pour décrire le cône de type d'un éventail de permutarbre. Nous donnons une déscription des facettes du cône de type, nous déterminons son nombre de facettes et nous déduisons un critère pour savoir si le cône de type d'un certain éventail de permutarbre est simplicial. Les éventails de permutarbre dont le cône de type associé est simplicial sont particulièrement intéressants parce qu'ils permettent une représentation canonique du permutarbrèdre comme la somme de Minkowski des polytopes induits par les fonctions de hauteur correspondantes aux rayons du cône de type. Nous terminons ce chapitre en décrivant l'ensemble de tous les quotientopes pour un tel éventail de permutarbre dans l'espace cinématique (voir [AHBHY18]).

3. Polytopes de tessons pour l'arrangement de tresses. Le chapitre 3 est basé sur la partie I de la prépublication suivante :

- [PPR20] Arnau Padrol, Vincent Pilaud, and Julian Ritter. Shard polytopes. Preprint, arXiv:2007.01008, 2020.

Une version courte de l'article apparaît dans les actes de la 33rd International Conference on Formal Power Series and Algebraic Combinatorics (voir https://www.mat.univie.ac.at/~slc/wpapers/FPSAC2021/11.html).

Dans ce chapitre, nous établissons une construction de quotientopes pour n'importe quelle congruence de treillis de l'ordre faible sur $\mathfrak{S}_n$. Ces nouveux quotientopes, appelés shardsumotopes, sont construits comme la somme de Minkowski de nouveaux polytopes élémentaires pour chacun des tessons de l'arrangement, appelés les polytopes de tessons.

Nous commençons dans la partie 3.1 par généraliser les tessons de l'arrangement de tresses orienté pour obtenir ce que l'on appelle pseudo-tessons, une classe plus large de cônes polyédraux avec une représentation combinatoire similaire. Nous introduisons quelques nouveaux objets reliés aux tessons, à la fois inspirés par et compatibles avec la représentation schématique des tessons établie dans [Rea15]. En particular, nous introduisons les couplages d'un tesson, qui peuvent être

vus d'un point de vue géométrique comme certaines sommes de vecteurs $\mathbf{e}_i - \mathbf{e}_j$ normaux aux hyperplanes de l'arrangement de tresses qui sont étroitement liés au tesson.

Nous utilisons alors ces couplages de tesson pour définir le polytope de tesson $\mathsf{SP}(\Sigma)$ dans la partie 3.2. Il y a un tel polytope pour chaque tesson de l'arrangement de tresses. Nous donnons une description par inégalités et une description par sommets et démontrons que ces deux descriptions sont équivalentes. Nous déterminons la dimension, le nombre de facettes et le nombre de sommets du polytope de tesson. En particulier, nous observons que les polytopes de tessons sont des simplexes pour la classe des tessons supérieurs et que le nombre de sommets des polytopes de tesson sont les nombres de Fibonacci pour la classe des tessons alternants. Nous poursuivons en décrivant les faces d'un polytope de tesson. Nous déterminons ses arêtes en utilisant des propriétés combinatoires des couplages de tesson associés. De plus, nous montrons que toute face d'un polytope de tesson est isomorphe à un produit cartesien de polytopes de tessons. Pour conclure cette section, nous établissons quelques symétries des polytopes de tessons.

Dans la partie 3.3, nous examinons les éventails normaux des polytopes de tessons, appelés éventails de tessons et dénotés par $\mathcal{SF}(\Sigma)$. Ils présentent un intérêt particulier comme nous visons à reconstruire un éventail quotient comme l'éventail normal d'une somme de Minkowski de polytopes de tessons, donc l'éventail normal de cette somme de Minkowski sera le raffinement commun de tous les éventails de tessons associés. Nous décrivons les murs et quelques cônes des éventails de tessons. Le résultat principal de cette section garantit que l'union des murs de l'éventail de tesson $\mathcal{SF}(\Sigma)$ à la fois contient le tesson Σ comme sous-ensemble et est contenu dans l'union de tous les tessons Σ' qui forcent Σ au sens introduit dans la partie 1.5.3.

Cette propriété des éventails de tessons nous permet de construire des shardsumotopes dans la partie 3.4. Étant donné une congruence de treillis $\equiv$ sur l'ordre faible, le shardsumotope $\mathsf{SP}_+(\equiv)$ est la somme de Minkowski de tous les polytopes de tessons $\mathsf{SP}(\Sigma)$ pour les tessons Σ qui apparaissent dans l'éventail quotient $\mathcal{F}_\equiv$. L'éventail normal du shardsumotope est alors égal à l'éventail quotient, où chaque polytope de tesson $\mathsf{SP}(\Sigma)$ qui a été sommé dans le processus introduit le tesson Σ dans l'éventail résultant sans ajouter aucun mur non présent dans $\mathcal{F}_\equiv$. Parmi les exemples les plus marquants, citons le parallélépipède induit par les normales de l'arrangement de tresses, un permutaèdre non-standard et une translation de l'associaèdre standard (voir [Lod04]) obtenue comme le shardsumotope de la congruence sylvestre. Nous terminons cette section par une discussion sur les sommets et facettes des shardsumotopes et un moyen de les construire efficacement.

Dans la partie 3.5, nous examinons le rôle que jouent les polytopes de tessons dans le cône de type de l'arrangement de tresses. Nous montrons que les polytopes de tessons ne sont pas décomposables comme sommes de Minkowski, de sorte que leurs fonctions de hauteur se trouvent dans les rayons du cône de type de l'éventail de tresses. Nous visualisons le cône de type de l'éventail de tresses, mettant en relation la structure polyédrale du cône, les polytopes induits par certaines fonctions de hauteur et les tessons de l'arrangement de tresses dans une seule image.

4. Polytopes de tessons pour l'arrangement de type B. Le chapitre 4 est basé sur la partie II de la prépublication suivante :

- [PPR20] Arnau Padrol, Vincent Pilaud, and Julian Ritter. Shard polytopes. Preprint, arXiv:2007.01008, 2020.

Une version courte de l'article apparaît dans les actes de la 33rd International Conference on Formal Power Series and Algebraic Combinatorics (voir https://www.mat.univie.ac.at/~slc/wpapers/FPSAC2021/11.html).

Dans ce chapitre, nous adaptons nos découvertes du chapitre 3 à une autre classe d'arrangements d'hyperplans. Tandis que le chapitre 3 couvre les congruences de treillis sur l'ordre des régions de l'arrangement de tresses $\vec{\mathcal{A}}_n$ (qui est isomorphe au treillis de l'ordre faible sur $\mathfrak{S}_n$), dans le chapitre 4, nous considérons les congruences de treillis sur l'ordre des régions de l'arrangement $\vec{\mathcal{B}}_n$

(qui est isomorphe au treillis de l'ordre faible sur $\mathfrak{S}_n^{\mathcal{B}}$). Le nom de cet arrangement vient de sa relation au groupe de Coxeter de type B (voir [Rea16a]), également appelé le groupe hyperoctaédrique (voir [You30]).

Dans la partie 4.1, nous introduisons l'arrangement de type $\mathcal{B}$ et son ordre des régions isomorphe à l'ordre faible sur le groupe $\mathfrak{S}_n^{\mathcal{B}}$ des permutations signées. Nous déterminons le cône de type de l'arrangement de type $\mathcal{B}$. Nous décrivons le zonotope canonique de l'arrangement de type $\mathcal{B}$, connu comme le $\mathcal{B}$-permutaèdre. Chaque permutation signée sur $[n]$ peut également être décrite comme une permutation de $[\pm n] := \{-n, \ldots, -1, 1, \ldots, n\}$ qui est centralement symétrique. Cela peut être traduit en une relation géométrique des arrangements associés via le sous-espace $\mathcal{H}_n^{\mathcal{B}}$ centralement symétrique. L'arrangement $\vec{\mathcal{B}}_n$ peut être obtenu comme l'intersection d'un arrangement de tresses avec $\mathcal{H}_n^{\mathcal{B}}$. Le $\mathcal{B}$-permutaèdre peut être obtenu comme la projection du permutaèdre standard sur $\mathcal{H}_n^{\mathcal{B}}$.

Dans la partie 4.2, nous examinons les tessons de l'arrangement de type $\mathcal{B}$. Nous montrons qu'ils peuvent être obtenus en intersectant les tessons de l'arrangement de tresses par $\mathcal{H}_n^{\mathcal{B}}$. Nous utilisons alors la géometrie de l'arrangement pour établir soigneusement la relation de forçage parmi les tessons de $\vec{\mathcal{B}}_n$. Il serait commode de supposer que l'ordre de forçage sur les tessons de type $\mathcal{B}$ coïncide avec l'ordre de forçage sur les tessons de l'arrangement de tresses intersectés avec $\mathcal{H}_n^{\mathcal{B}}$. Cependant, nous démontrons que ce n'est pas le cas. En particulier, la plupart des ensembles de tessons de type $\mathcal{B}$ fermés par forçage dans $\vec{\mathcal{B}}_n$ ne peuvent pas être obtenus en intersectant $\mathcal{H}_n^{\mathcal{B}}$ avec les éléments d'un ensemble de tessons de l'arrangement de tresses fermé par forçage dans $\vec{\mathcal{A}}_n$.

Il est connu (voir [Rea16a]) que les congruences de treillis sur l'ordre faible sur $\mathfrak{S}_n^{\mathcal{B}}$ sont en bijection avec les ensembles de tessons de type $\mathcal{B}$ fermés par forçage dans $\vec{\mathcal{B}}_n$ et qu'il définissent des éventails quotients comme le font celles sur l'ordre faible sur $\mathfrak{S}_n$. Dans la partie 4.3, nous décrivons ces éventails quotients. En utilisant les polytopes de tessons pour l'arrangement de tresses construits au chapitre 3 et leurs projections sur $\mathcal{H}_n^{\mathcal{B}}$, nous définissons des polytopes de tessons pour tous les tessons de type $\mathcal{B}$. À nouveau, nous montrons que les éventails normaux de chacun de ces polytopes de tessons de type $\mathcal{B}$ à la fois contient le tesson lui-même et est contenu dans l'union de tous les tessons qui le forcent. Avec ce resultat, nous terminons ce chapitre en construisant des quotientopes pour toute congruence de treillis de l'ordre faible sur $\mathfrak{S}_n^{\mathcal{B}}$.

Logiciel. Au cours de la préparation de cette thèse, j'ai beaucoup utilisé le logiciel libre SageMath [SD19] pour travailler avec de nombreux objets mentionnés jusqu'ici. J'ai écrit du code pour implémenter certaines définitions et algorithmes qui n'étaient pas encore présents dans le logiciel. Cela nous a permis, à mes collaborateurs et à moi-même, d'expérimenter les concepts, de visualiser des exemples et de former une intuition des objets sur lesquels nous travaillions. Des graphiques obtenus grâce à cet effort peuvent être vus dans quelques-unes des figures de cette thèse. Ce soutien informatique a été très utile pour obtenir les résultats présentés dans les chapitres suivants.

1 Preliminaries

Notation

We will use $\mathbb{R}^n$ to denote the standard n-dimensional Euclidian vector space. We will think of points and vectors $\mathbf{v} \in \mathbb{R}^n$ as column vectors. They will be written in boldface (like $\mathbf{x}, \mathbf{y}, \mathbf{z}$), to distinguish them better from scalars and integers (like i, j, k).

In particular, $\mathbf{0}$ will represent the all-zeros vector and $\mathbf{1}$ will represent the all-ones vector. For an integer $i \in [n]$, we use $\mathbf{e}_i$ to denote the unit vector $(0, \ldots, 0, 1, 0, \ldots, 0)$ in dimension n. For any set of integers $X \subseteq [n]$, we use $\mathbf{1}_X$ to denote its characteristic vector, so that $\mathbf{1}_X = \sum_{i \in X} \mathbf{e}_i$. In particular, we have $\mathbf{1}_{[n]} = \sum_{i=1}^{n} \mathbf{e}_i = \mathbf{1}$. We will denote sets by uppercase letters and vectors by lowercase letters. For integers ℓ, r and n, we use

- $[\ell, r] := \{z \in \mathbb{Z} \mid \ell \leq z \leq r\}$,
- $]\ell, r[:= \{z \in \mathbb{Z} \mid \ell < z < r\}$,
- $[n] := [1, n]$,
- $[\pm n] := [-n, n] \setminus \{0\}$.

The definitions and theorems in this chapter are well-known, so in general we do not give proofs. We make exceptions for some statements which are less prominent than others.

1.1 Discrete Geometry

1.1.1 Combinations and Hulls

We first recall some basic ways of geometrically combining given points to obtain others.

Definition 1.1.1 (Linear, Conical, Affine and Convex Combination)**.** Let $\mathbf{x}_1, \ldots, \mathbf{x}_k$ be finitely many points in $\mathbb{R}^n$. Then the weighted sum $\sum_{i=1}^{k} \lambda_i \mathbf{x}_i = \mathbf{x} \in \mathbb{R}^n$ is called

- a **linear combination** of the $\mathbf{x}_i$, if $\lambda_i \in \mathbb{R}$ for all $i \in [n]$,
- a **conical combination** of the $\mathbf{x}_i$, if $\lambda_i \in \mathbb{R}_{\geq 0}$ for all $i \in [n]$,
- an **affine combination** of the $\mathbf{x}_i$, if $\lambda_i \in \mathbb{R}$ for all $i \in [n]$ and $\sum_{i=1}^{n} \lambda_i = 1$,
- a **convex combination** of the $\mathbf{x}_i$, if $\lambda_i \in \mathbb{R}_{\geq 0}$ for all $i \in [n]$ and $\sum_{i=1}^{n} \lambda_i = 1$.

We remark that every affine, conical or convex combination is a linear combination. Furthermore, a combination of the $\mathbf{x}_i$ is convex if and only if it is both conical and affine. For a given subset of $\mathbb{R}^n$, we give a name to the set of all such combinations.

Definition 1.1.2 (Linear, Conical, Affine and Convex Hull)**.** Let $K \subseteq \mathbb{R}^n$ be a non-empty set. The **linear** (resp. **conical**, **affine**, **convex**) **hull** of K is the set of all linear (resp. conical, affine, convex) combinations of elements of K. We also refer to the linear hull (resp. affine hull) as the **linear span** (resp. **affine span**). We denote the hulls by $\operatorname{span}(K), \operatorname{cone}(K), \operatorname{aff}(K)$ and $\operatorname{conv}(K)$, respectively. As a convention, we fix $\operatorname{span}(\emptyset) = \operatorname{cone}(\emptyset) = \{\mathbf{0}\}$ and $\operatorname{aff}(\emptyset) = \operatorname{conv}(\emptyset) = \emptyset$.

Example 1.1.3. Given the unit vectors $\mathbf{e}_1, \ldots, \mathbf{e}_n$ in $\mathbb{R}^n$,

- their linear hull is the entire space $\mathbb{R}^n$: the linear combinations $\sum_{i=1}^{n} \lambda_i \mathbf{e}_i$ for unrestricted choice of scalars $\lambda_i \in \mathbb{R}$ are precisely all vectors in $\mathbb{R}^n$,
- their conical hull is the closed positive orthant $\{\mathbf{x} \in \mathbb{R}^n \mid \forall i \in [n] : x_i \geq 0\}$, as the conical combinations of the unit vectors are exactly those points with nonnegative entries,
- their affine hull is the minimal affine subspace containing all unit vectors, which is equal to the point set $\{\mathbf{x} \in \mathbb{R}^n \mid \sum_{i=1}^{n} x_i = 1\}$,

- their convex hull is the intersection of that affine subspace with the closed positive orthant, equal to the point set $\{\mathbf{x} \in \mathbb{R}^n \mid \sum_{i=1}^n x_i = 1, \forall i \in [n] : x_i \geq 0\}$.

We will use the objects in this example from time to time, so we will illustrate them in Figure 1.1 and give them names and symbols:

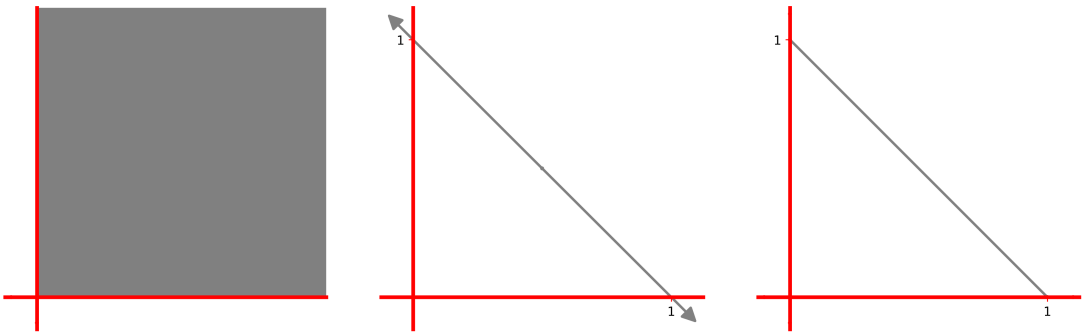

Figure 1.1: The positive orthant $\mathbb{R}^2_{\geq 0}$ (left), the sum-one-hyperplane $\mathcal{H}^2_1$ (center), and the standard simplex Δ_1 (right), all in $\mathbb{R}^2$.

Definition 1.1.4 (Standard Hulls)**.** Let n be a positive integer.

- We denote the (closed) **positive orthant** by $\mathbb{R}^n_{\geq 0} := \{\mathbf{x} \in \mathbb{R}^n \mid \forall i \in [n] : x_i \geq 0\}$.
- We denote the **sum-one-hyperplane** by $\mathcal{H}^n_1 := \{\mathbf{x} \in \mathbb{R}^n \mid \sum_{i=1}^n x_i = 1\}$.
- We denote the **standard simplex** by $\Delta_{n-1} := \{\mathbf{x} \in \mathbb{R}^n \mid \sum_{i=1}^n x_i = 1, \forall i \in [n] : x_i \geq 0\}$.

We note that as every convex combination is both an affine combination and a conical combination, the convex hull is a subset of both the affine hull and the conical hull and therefore a subset of their intersection. But while equality with that intersection holds in our unit vector example ($\Delta_{n-1} = \mathbb{R}^n_{\geq 0} \cap \mathcal{H}^n_1$), it is not true in general. In fact, it fails as soon as the points $\mathbf{x}_1, \ldots, \mathbf{x}_n$ are linearly dependent.

Example 1.1.5. We consider the points $\mathbf{0}$ and $\mathbf{e}_1 + \mathbf{e}_2$ in some $\mathbb{R}^n$ for $n \geq 2$. Their conical hull contains the point $0 \cdot \mathbf{0} + 2 \cdot (\mathbf{e}_1 + \mathbf{e}_2) = 2\mathbf{e}_1 + 2\mathbf{e}_2$. Their affine hull contains that point $-1 \cdot \mathbf{0} + 2 \cdot (\mathbf{e}_1 + \mathbf{e}_2) = 2\mathbf{e}_1 + 2\mathbf{e}_2$ as well. But while there are different conical or affine combinations to obtain that point, none of them is a convex combination, so $2\mathbf{e}_1 + 2\mathbf{e}_2$ is not contained in the convex hull of $\mathbf{0}$ and $\mathbf{e}_1 + \mathbf{e}_2$. See Figure 1.2 for an illustration.

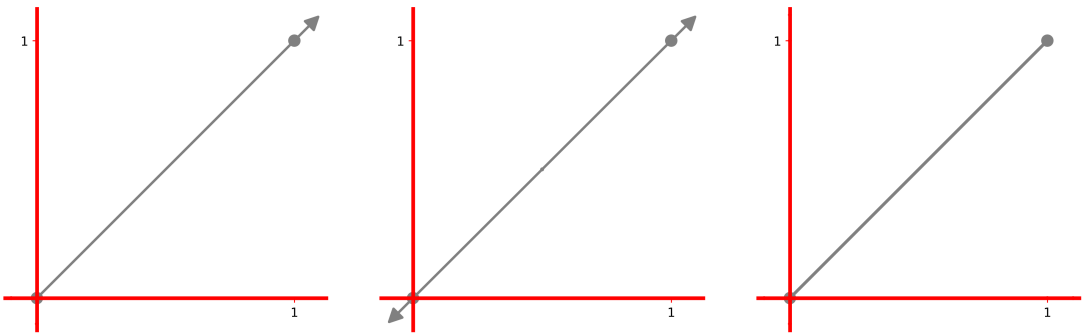

Figure 1.2: The conical hull $\mathrm{cone}(\{\mathbf{0}, \mathbf{e}_1 + \mathbf{e}_2\})$ (left), the affine hull $\mathrm{aff}(\{\mathbf{0}, \mathbf{e}_1 + \mathbf{e}_2\})$ (center), and the convex hull $\mathrm{conv}(\{\mathbf{0}, \mathbf{e}_1 + \mathbf{e}_2\})$ (right) of the points $\mathbf{0}$ and $\mathbf{e}_1 + \mathbf{e}_2$ in $\mathbb{R}^2$.

There are some other standard hulls that are built similarly. The sum-one-hyperplane $\mathcal{H}^n_1$ is defined to contain exactly those $\mathbf{x} \in \mathbb{R}^n$ with $\sum_{i=1}^n x_i = 1$.

Definition 1.1.6 (Standard Hyperplanes)**.** Similarly to the sum-one-hyperplane, we define

- the **sum-zero-hyperplane** $\mathcal{H}_0^n := \{\mathbf{x} \in \mathbb{R}^n \mid \sum_{i=1}^n x_i = 0\}$,
- the **sum-count-hyperplane** $\mathcal{H}_\Sigma^n := \left\{\mathbf{x} \in \mathbb{R}^n \;\middle|\; \sum_{i=1}^n x_i = \sum_{i=1}^n i = \binom{n+1}{2}\right\}$.

The sum-zero-hyperplane contains, in particular, all vectors of the form $\mathbf{e}_i - \mathbf{e}_j$ for two (not necessarily distinct) indices $i, j \in [n]$. The sum-count-hyperplane is useful when dealing with incidence vectors of permutations: Any standard permutation $\sigma \in \mathfrak{S}_n$ can be written as a vector $(\sigma_1, \sigma_2, \ldots, \sigma_n)$ (equivalently, $\sum_{i=1}^n \sigma_i \mathbf{e}_i$), whose sum of entries is $\sum_{i=1}^n i = \binom{n+1}{2}$. Therefore, the sum-count-hyperplane contains all such incidence vectors of permutations.

Definition 1.1.7 (Convex Set)**.** Let n be a nonnegative integer. A set of points $K \subseteq \mathbb{R}^n$ is **convex** if for any two points $\mathbf{x}, \mathbf{y} \in K$, any convex combination of $\mathbf{x}$ and $\mathbf{y}$ (and therefore the entire straight line segment $[\mathbf{x}, \mathbf{y}]$) is also contained in K. Equivalently, K is convex if and only if it is equal to its own convex hull $\mathrm{conv}(K)$.

Example 1.1.8. Both the empty set and a set containing a single point are convex, as they do not contain two points whose interval would have to be contained as well. On the other hand, the entire Euclidian space $\mathbb{R}^n$ is a convex set as the convex combination $\lambda\mathbf{x} + (1-\lambda)\mathbf{y}$ is a real vector for any choice of $\mathbf{x}, \mathbf{y} \in \mathbb{R}^n$ and $\lambda \in \mathbb{R}$ with $0 \leq \lambda \leq 1$.

An intersection of two convex sets is always convex, while their union may fail to be convex. For example, both sets $K_1 := \left\{\mathbf{x} \in \mathbb{R}^3 \;\middle|\; x_1 \geq 0, x_3 = 0\right\}$ and $K_2 := \left\{\mathbf{x} \in \mathbb{R}^3 \;\middle|\; x_2 \geq 0, x_3 = 0\right\}$ are convex. If we pick $-\mathbf{e}_2 \in K_1$ and $-\mathbf{e}_1 \in K_2$, we observe that for any $\lambda \in]0, 1[$, we obtain a convex combination $\mathbf{y} = \lambda(-\mathbf{e}_2) + (1-\lambda)(-\mathbf{e}_1) = (\lambda - 1, -\lambda, 0)$, which has $y_1, y_2 < 0$ and is therefore contained in neither K_1 nor K_2. Their convex hull $K := \mathrm{conv}(K_1 \cup K_2)$ is given by $K = \left\{\mathbf{x} \in \mathbb{R}^3 \;\middle|\; x_3 = 0\right\}$.

A set such as $\left\{\mathbf{x} \in \mathbb{R}^3 \;\middle|\; x_3 = 0\right\}$ is called a hyperplane in $\mathbb{R}^n$, which we will now define more formally along with some associated concepts.

1.1.2 Hyperplanes

We already saw three affine subspaces of $\mathbb{R}^n$ constructed in a similar way. We will now formally introduce this class of subspaces.

Definition 1.1.9 (Hyperplanes and Halfspaces)**.** In the n-dimensional Euclidian space $\mathbb{R}^n$, a **hyperplane** H is an $(n-1)$-dimensional affine subspace of $\mathbb{R}^n$. Any hyperplane can be written as $H = \{\mathbf{x} \in \mathbb{R}^n \mid \langle \mathbf{v} \,|\, \mathbf{x} \rangle = b\}$ for some scalar $b \in \mathbb{R}$ and a nonzero vector $\mathbf{v} \in \mathbb{R}^n$, which is called a **normal vector** of H. The hyperplane H is a **linear** hyperplane if $b = 0$. The two **(closed) halfspaces** induced by H are $H^+ := \{\mathbf{x} \in \mathbb{R}^n \mid \langle \mathbf{v} \,|\, \mathbf{x} \rangle \geq b\}$ and $H^- := \{\mathbf{x} \in \mathbb{R}^n \mid \langle \mathbf{v} \,|\, \mathbf{x} \rangle \leq b\}$. (Analogously, H induces two **open halfspaces** obtained by replacing the weak inequalities with strict ones.) These halfspaces are called **linear** if the associated hyperplane H is linear (equivalently, if $b = 0$).

Definition 1.1.10 (Support and Separation)**.** The hyperplane H is **supporting** for a set $K \subseteq \mathbb{R}^n$ if $H \cap K \neq \emptyset$ and K is contained in one of the closed halfspaces induced by H. Given two convex sets $A, B \subseteq \mathbb{R}^n$, the hyperplane H **separates** A from B if $A \subseteq H^-$ and $B \subseteq H^+$ or vice versa. It **strictly separates** A from B if it separates A from B and $A \cap H = \emptyset = B \cap H$.

Example 1.1.11. Given the hyperplane $H = \left\{\mathbf{x} \in \mathbb{R}^3 \;\middle|\; \mathbf{x}_3 = 1\right\}$, its normal vectors are all nonzero multiples of $\mathbf{e}_3$ (including all negative multiples). H does not contain the origin, so $b \neq 0$ and H is not linear. The halfspaces induced by H are $\{\mathbf{x} \in \mathbb{R}^n \mid \langle \mathbf{e}_3 \,|\, \mathbf{x} \rangle \geq 1\}$ and $\{\mathbf{x} \in \mathbb{R}^n \mid \langle \mathbf{e}_3 \,|\, \mathbf{x} \rangle \leq 1\}$. We note that the assigment of the symbols H^+ and H^- to these

two halfspaces depends on the orientation of the hyperplane determined by the choice of normal vector. The hyperplane H is supporting for the line segment $[0, \mathbf{e}_3]$. It is not supporting for the line segment $[0, 2\mathbf{e}_3]$ (as that one is contained in neither halfspace induced by H) or the line segment $[-\mathbf{e}_3, 0]$ (as that one has an empty intersection with H).

We remark that any closed convex set $K \subseteq \mathbb{R}^n$ is equal to the intersection of the negative halfspaces of all hyperplanes H supporting K. Furthermore, for a closed convex set $K \subseteq \mathbb{R}^n$ and any nonzero direction $\mathbf{v} \in \mathbb{R}^n$, there is a unique $b \in \mathbb{R}$ such that $H := \{\mathbf{x} \in \mathbb{R}^n \mid \langle \mathbf{v} \,|\, \mathbf{x} \rangle = b\}$ is supporting for K.

1.2 Polyhedral Combinatorics

For the basic notions of polyhedral geometry, we start by describing cones. For a both broader and more detailed introduction to polytopes, we refer to the classic textbook [Zie07], whose conventions we largely follow here.

1.2.1 Cones

As a first object of study, we will introduce polyhedral cones. All cones we consider are polyhedral, so we will assume all cones appearing henceforth to be polyhedral and just call them cones.

Definition 1.2.1 ($\mathcal{H}$-Cone and $\mathcal{V}$-Cone)**.** Let n be a nonnegative integer.

- An $\mathcal{H}$-**cone** is the intersection of finitely many closed linear halfspaces of $\mathbb{R}^n$.
- A $\mathcal{V}$-**cone** is the conical hull of finitely many vectors in $\mathbb{R}^n$.

The following statement certifies that $\mathcal{H}$-cones and $\mathcal{V}$-cones are in fact the same objects:

Theorem 1.2.2 (Cone)**.** *A set $C \subseteq \mathbb{R}^n$ is an $\mathcal{H}$-cone if and only if it is a $\mathcal{V}$-cone.*

It is therefore justified to speak of a **cone** whenever we encounter one of these objects, regardless of whether it is given by an $\mathcal{H}$-description or a $\mathcal{V}$-description. We will continue by introducing the principal notion to study the structure of a cone: the notion of a face.

Definition 1.2.3 (Faces of a Cone)**.** Given a cone C, the **dimension** of C is the dimension of the affine hull of C. The **lineality space** of C is the largest linear subspace $L \subseteq \mathbb{R}^n$ such that $\mathbf{l}+\mathbf{x} \in C$ for all $\mathbf{l} \in L$ and $\mathbf{x} \in C$. A **face** of C is the intersection of C with a hyperplane supporting C. Moreover, C is always considered a face of itself. Every face of C is a cone. The **proper faces** of C are all of its faces except for C. A **facet** of C is a face of C whose codimension is 1 (a face of dimension one less than $\dim(C)$). A **ray** of C is a face of C whose dimension is 1. A cone C is called **simplicial** if its dimension equals the number of rays.

This way, we defined a cone as the intersection of *closed* halfspaces. There are analogous definitions arising when intersecting open halfspaces instead.

Definition 1.2.4 (Open Cones and Closures)**.** An **open cone** is the intersection of finitely many open linear halfspaces of $\mathbb{R}^n$. Its **closure** is the cone obtained by the intersection of the closure of each of these halfspaces.

Example 1.2.5 (Orthant)**.** A cone that arises naturally when using the Cartesian coordinate system in three dimensions is the positive orthant $C := \left\{\mathbf{x} \in \mathbb{R}^3 \;\middle|\; x_1, x_2, x_3 \geq 0\right\}$. It is the intersection of the halfspaces $\{\mathbf{x} \in \mathbb{R}^n \mid x_i \geq 0\}$ for $i \in \{1, 2, 3\}$ or equivalently, the conical span of the unit vectors $\mathbf{e}_1, \mathbf{e}_2$ and $\mathbf{e}_3$. The rays of the cone C are the three half-lines from $\mathbf{0}$ in direction $\mathbf{e}_1, \mathbf{e}_2$ and $\mathbf{e}_3$, respectively. Its facets are the three lower-dimensional cones obtained by intersecting C

with one of the three hyperplanes $H_i = \{\mathbf{x} \in \mathbb{R}^n \mid x_i = 0\}$ for $i \in \{1, 2, 3\}$. The faces of C are the origin $\mathbf{0}$ (0-dimensional face), all of its rays (1-dimensional faces), all of its facets (2-dimensional faces) and the entire cone C itself (3-dimensional face).

Any cone is equal to its conical hull and is therefore the set of all conical combinations of its elements (or, more efficiently, of all its rays). This gives us another elegant way of describing a cone.

Observation 1.2.6 (Cones as Images of Orthants)**.** Given a set of vectors $\mathbf{v}_1, \ldots, \mathbf{v}_m \in \mathbb{R}^n$, we can write them as the columns of a matrix $\mathbf{M} \in \mathbb{R}^{n \times m}$. Then the conical hull of the $\mathbf{v}_i$ is the image of the positive orthant in $\mathbb{R}^m$ under the linear map defined by $\phi(\mathbf{x}) = \mathbf{M}\mathbf{x}$. In particular, every cone C is the image of the positive orthant in some $\mathbb{R}^m$ under a linear map. For example, the cone C from Example 1.2.5 is the image of the positive orthant $\mathbb{R}^3_{\geq 0}$ under the identity map defined by the 3-dimensional unit matrix. Moreover, every vector in C can be obtained as a conical combination of the rays.

1.2.2 Polytopes

While cones are based on conical combinations, there is a similar concept based on convex combinations, namely that of polytopes. We will introduce some basic properties and note that many of them are analogous to what we know about cones. Just like cones, polytopes can equivalently be described as the intersection of halfspaces or as the set of combinations (here: convex) of a set of points.

Definition 1.2.7 ($\mathcal{H}$-Polytope and $\mathcal{V}$-Polytope)**.** Let n be a nonnegative integer.

- An **$\mathcal{H}$-polytope** is a bounded intersection of finitely many closed halfspaces of $\mathbb{R}^n$.
- A **$\mathcal{V}$-polytope** is the convex hull of finitely many points in $\mathbb{R}^n$.

As was the case with $\mathcal{H}$-cones and $\mathcal{V}$-cones, the following statement certifies that $\mathcal{H}$-polytopes and $\mathcal{V}$-polytopes are in fact the same objects.

Theorem 1.2.8 (Polytope)**.** *A set $\mathsf{P} \subseteq \mathbb{R}^n$ is an $\mathcal{H}$-polytope if and only if it is a $\mathcal{V}$-polytope.*

Due to this statement, known as the main theorem of polytope theory, it is justified to speak of a **polytope** whenever we encounter one of these objects, regardless of whether it is given by an $\mathcal{H}$-description or a $\mathcal{V}$-description.

An example of an $\mathcal{H}$-description of a polytope defined as the intersection of m halfspaces of $\mathbb{R}^n$ is an $(m \times n)$-matrix $\mathbf{M}$ together with a vector $\mathbf{v} \in \mathbb{R}^m$. Then the polytope $\mathsf{P}(\mathbf{M}, \mathbf{v})$ is defined as $\mathsf{P}(\mathbf{M}, \mathbf{v}) := \{\mathbf{x} \in \mathbb{R}^n \mid \mathbf{M}\mathbf{x} \leq \mathbf{v}\}$. It is the intersection of all the halfspaces defined by the inequalities $\langle \mathbf{M}_i \,|\, \mathbf{x} \rangle \leq v_i$, where $\mathbf{M}_i$ and v_i are the i-th row of the matrix $\mathbf{M}$ and the i-th entry of the vector $\mathbf{v}$, respectively. We remark that while every polytope can be described in this way, not every set of this form is necessarily a polytope as $\mathsf{P}(\mathbf{M}, \mathbf{v})$ might not be bounded.

In Figure 1.1, we saw the three standard hulls (positive orthant for conical combinations, sum-one hyperplane for affine combinations and standard simplex for convex combinations). Just as every cone is the image of an orthant under a linear map built from its rays, every polytope can be given as the image of a standard simplex under a linear map built from its vertices.

Observation 1.2.9 (Polytopes as Images of Simplices)**.** Given a set of vectors $\mathbf{v}_1, \ldots, \mathbf{v}_m \in \mathbb{R}^n$, we can write them as the columns of a matrix $\mathbf{M} \in \mathbb{R}^{n \times m}$. Then the convex hull of the $\mathbf{v}_i$ is the image of the standard simplex $\Delta_{m-1} = \{\mathbf{x} \in \mathbb{R}^m \mid \sum_{i=1}^m \mathbf{x}_i = 1\}$ in $\mathbb{R}^m$ under the linear map defined by $\phi(\mathbf{x}) = \mathbf{M}\mathbf{x}$. In particular, every polytope P is the image of the standard simplex Δ_{m-1} in some dimension m under a linear map. Moreover, every point in P can be obtained as a convex combination of the vertices.

Definition 1.2.10 (Faces of a Polytope)**.** Given a polytope P, the **dimension** of P is the dimension of its affine hull. The **faces** of P are all intersections of P with a hyperplane supporting P, the empty set, and P itself. A **proper face** of P is a face of P that is neither empty nor P itself. Every face of P is a polytope. The **face lattice** of P is the set of its faces, partially ordered by inclusion. Depending on their dimension, a face F of P is called

- a **vertex** of P if $\dim(F) = 0$,
- an **edge** of P if $\dim(F) = 1$,
- a **ridge** of P if $\operatorname{codim}(F) = 2$ (put differently, if $\dim(\mathsf{P}) - \dim(F) = 2$),
- a **facet** of P if $\operatorname{codim}(F) = 1$ (put differently, if $\dim(\mathsf{P}) - \dim(F) = 1$).

A d-dimensional polytope P is called

- **simplicial** if every facet of P contains exactly d vertices of P,
- **simple** if every vertex of P is contained in exactly d facets of P.

We denote by $V(\mathsf{P})$ the set of all vertices of P. A polytope P is called a **simplex** if its dimension is equal to the number of vertices minus one.

Example 1.2.11 (3-Cube)**.** We exemplify these basic notions by the well-known example of the 3-dimensional cube $\mathsf{C}_3 := \left\{\mathbf{x} \in \mathbb{R}^3 \;\middle|\; 0 \leq x_1, x_2, x_3 \leq 1\right\}$. It is the intersection of the three halfspaces $\left\{\mathbf{x} \in \mathbb{R}^3 \;\middle|\; x_i \geq 0\right\}$ and the three halfspaces $\left\{\mathbf{x} \in \mathbb{R}^3 \;\middle|\; x_i \leq 1\right\}$ for $i \in \{1, 2, 3\}$. Equivalently, C_3 is the convex hull of its vertices $\{0, 1\}^3$. We can describe the vertices as the incidence vectors of all subsets of $[3]$, so that $V(\mathsf{C}_3) = \{\mathbf{1}_I \mid I \subseteq [3]\}$. The edges of C_3 are the segments $[\mathbf{1}_A, \mathbf{1}_B]$ for all pairs of sets $A, B \subseteq [3]$ with $|A \Delta B| = 1$. As C_3 is 3-dimensional, its ridges are its edges. The facets of C_3 are the six polytopes obtained by intersecting C_3 with one of the six hyperplanes $\left\{\mathbf{x} \in \mathbb{R}^3 \;\middle|\; x_i = k\right\}$ for $i \in \{1, 2, 3\}$ and $k \in \{0, 1\}$.

Example 1.2.12 (Faces of the Simplex)**.** The standard simplex $\Delta_{n-1} = \operatorname{conv}\{\mathbf{e}_i \mid i \in [n]\}$ has faces Δ_I for each subset $I \subseteq [n]$, where $\Delta_I := \operatorname{conv}\{\mathbf{e}_i \mid i \in I\}$. In particular, we obtain the empty face as $\Delta_\emptyset$ and the entire simplex as $\Delta_{[n]}$.

Definition 1.2.13 (Equivalence of Polytopes)**.** Two polytopes P, Q are **combinatorially equivalent** if their face lattices are isomorphic. The **combinatorial type** of a polytope is its equivalence class with respect to this equivalence relation. In particular, two polytopes are of the same combinatorial type if and only if they are combinatorially equivalent.

Integer Polytopes

Integer polytopes are a class of polytopes of particular interest in optimization. They often appear when combinatorial objects are translated into geometric objects, as will be the case for some classes of polytopes introduced later.

Definition 1.2.14 (Integer Polytope)**.** A polytope $\mathsf{P} \subseteq \mathbb{R}^n$ is an **integer polytope** if every vertex $\mathbf{v}$ of P is an integer vector $\mathbf{v} \in \mathbb{Z}^n$.

To certify that a certain polytope of the form $\{\mathbf{x} \in \mathbb{R}^n \mid \mathbf{M}\mathbf{x} \leq \mathbf{b}\}$ is an integer polytope, one can use special properties of the matrix $\mathbf{M}$.

Definition 1.2.15 (Total Unimodularity, Consecutive Ones)**.** A matrix $\mathbf{M}$ is **totally unimodular** if each square submatrix of $\mathbf{M}$ has determinant equal to $-1, 0$ or $+1$. A matrix $\mathbf{M}$ has the **consecutive ones property** if every row of $\mathbf{M}$ is of the form $(0, \ldots, 0, 1, \ldots, 1, 0, \ldots, 0)$.

The following statement on the relation between these two properties can be attributed to folklore. We give a proof for the sake of completeness.

Lemma 1.2.16 (Consecutive One Matrices Are Totally Unimodular)**.** *If a matrix $\mathbf{M}$ has the consecutive ones property, then $\mathbf{M}$ is totally unimodular.*

Proof. Let $\mathbf{M}$ be a matrix with the consecutive ones property. We fix an arbitrary square $n \times n$ submatrix $\mathbf{A}$ of $\mathbf{M}$. We want to show that $\det(\mathbf{A}) \in \{-1, 0, +1\}$.

We first remark that $\mathbf{A}$ has the consecutive ones property as well. If $\mathbf{A}$ has an all-zero row, then $\det(\mathbf{A}) = 0$ and we are done. Otherwise, let $\mathbf{a}_1, \ldots, \mathbf{a}_n$ be the columns of $\mathbf{A}$. We introduce a new matrix $\mathbf{B}$, whose columns $\mathbf{b}_1, \ldots, \mathbf{b}_n$ are defined by $\mathbf{b}_1 := \mathbf{a}_1$ and $\mathbf{b}_i := \mathbf{a}_i - \mathbf{a}_{i-1}$ for $1 < i \leq n$. As $\mathbf{B}$ is obtained from $\mathbf{A}$ by adding multiples of other columns to each column, we know that $\det(\mathbf{B}) = \det(\mathbf{A})$. Let $\mathbf{a}^r$ be the r-th row of $\mathbf{A}$. As we may asssume $\mathbf{a}^r$ is not all-zero, we have $\mathbf{a}^r = \mathbf{1}_{[k,\ell]}$ for some $1 \leq k \leq \ell \leq n$. If $\ell < n$, then $\mathbf{b}^r = \mathbf{e}_k - \mathbf{e}_{\ell+1}$. If $\ell = n$, then $\mathbf{b}^r = \mathbf{e}_k$. We deduce that every row of $\mathbf{B}$ either has a single nonzero entry $+1$ or it has two nonzero entries adding up to zero.

To determine $\det(\mathbf{B})$, we perform a Laplace expansion along every row that has exactly one nonzero entry. Every such step introduces a factor of ± 1 to the determinant. If this exhausts all rows of $\mathbf{B}$, we deduce that $\det(\mathbf{A}) = \det(\mathbf{B}) \in \{-1, +1\}$. Otherwise, we are left with a submatrix $\mathbf{B}'$ of $\mathbf{B}$. If $\mathbf{B}'$ has a zero row, then $\det(\mathbf{B}') = 0$. Otherwise, every row of $\mathbf{B}'$ has exactly one $+1$ entry and exactly one -1 entry, so $\mathbf{B}' \cdot \mathbf{1} = \mathbf{0}$, which certifies that $\mathbf{B}'$ is singular. In either case, $\det(\mathbf{A}) = \det(\mathbf{B}) = \det(\mathbf{B}') = 0$. As $\mathbf{A}$ was an arbitrary submatrix of $\mathbf{M}$, we conclude that $\mathbf{M}$ is totally unimodular. □

The following lemma about totally unimodular matrices is a special case of a well-known statement due to [HK10].

Lemma 1.2.17 (Totally Unimodular Matrices Give Integer Polytopes)**.** *Let* P *be a polytope in* $\mathbb{R}^n$*. If* $\mathsf{P} = \{\mathbf{x} \in \mathbb{R}^n \mid \mathbf{M}\mathbf{x} \leq \mathbf{b}\}$ *for a totally unimodular matrix* M *and an integer vector* $\mathbf{b}$*, then* P *is an integer polytope.*

Example 1.2.18. Take for example the following totally unimodular matrix $\mathbf{M} \in \mathbb{Z}^{6\times 3}$ together with an integer vector $\mathbf{b} \in \mathbb{Z}^6$:

$$\mathbf{M} = \begin{pmatrix} 1 & 0 & 0 \\ -1 & 0 & 0 \\ 0 & 1 & 0 \\ 0 & -1 & 0 \\ 0 & 0 & 1 \\ 0 & 0 & -1 \end{pmatrix} \quad \mathbf{b} = \begin{pmatrix} 1 \\ 1 \\ 1 \\ 1 \\ 1 \\ 1 \end{pmatrix}$$

Then $\mathsf{P} = \mathsf{P}(\mathbf{M}, \mathbf{b})$ is the 3-dimensional cube with vertex set $V(\mathsf{P}) = \{-1, +1\}^3$, so every vertex of P is an integer vector.

1.2.3 Fans

A concept of particular interest in combinatorial geometry is that of a fan. It is a collection of cones closed under intersections and taking faces.

Definition 1.2.19 (Fan)**.** A **fan** $\mathcal{F}$ in $\mathbb{R}^n$ is a collection of cones such that

- if F is a face of a cone $C \in \mathcal{F}$, then $F \in \mathcal{F}$,
- if $C, C' \in \mathcal{F}$, then $C \cap C'$ is a face of C and of C'.

The fan $\mathcal{F}$ is **complete** if the union of its cones is $\mathbb{R}^n$. The fan $\mathcal{F}$ is **pointed** if $\{\mathbf{0}\} \in \mathcal{F}$ (equivalently, if $\{\mathbf{0}\}$ is a face of every cone in $\mathcal{F}$). The fan $\mathcal{F}$ is **simplicial** if all its cones are simplicial.

The **dimension** of $\mathcal{F}$ is the dimension of the affine hull of the union of its cones. A **chamber** of $\mathcal{F}$ is a cone of $\mathcal{F}$ of codimension 0. A **wall** of $\mathcal{F}$ is a cone of $\mathcal{F}$ of codimension 1. A **ray** of $\mathcal{F}$ is a cone of $\mathcal{F}$ of dimension 1.

We will almost exclusively consider pointed fans, as any complete fan can be obtained as the product of a pointed fan with its lineality space. Complete fans arise naturally from polytopes in the following way:

Definition 1.2.20 (Normal Vector, Normal Cone and Normal Fan)**.** Given a polytope P, a **normal vector** of a facet F of P is a vector $\mathbf{v} \in \mathbb{R}^n$ such that the hyperplane $H := \{\mathbf{x} \in \mathbb{R}^n \mid \langle \mathbf{v} \,|\, \mathbf{x} \rangle \leq b\}$ is supporting for F for some $b \in \mathbb{R}$. It is called an **outer normal vector** if $\mathsf{P} \subseteq H^-$ or an **inner normal vector** if $\mathsf{P} \subseteq H^+$. The **(outer) normal cone** of a non-empty face F of P is the conical hull of all outer normal vectors of the facets containing F. In particular, the normal cone of the empty face of P is the orthogonal complement of P in its ambient space. In the case where P is full-dimensional, this is the conical hull of the empty set, which is $\{\mathbf{0}\}$. The **normal fan** $\mathcal{N}(\mathsf{P})$ of P is the complete fan obtained as the set of all normal cones of all faces of P.

Observation 1.2.21 (Correspondence Between Faces of P and $\mathcal{N}(\mathsf{P})$)**.** We observe that

- the vertices of P correspond to the chambers of $\mathcal{N}(\mathsf{P})$,
- the edges of P correspond to the walls of $\mathcal{N}(\mathsf{P})$,
- the facets of P correspond to the rays of $\mathcal{N}(\mathsf{P})$.

If $\mathsf{P} \subseteq \mathbb{R}^n$ is full-dimensional, then the d-dimensional faces of the polytope P correspond to the $(n-d)$-dimensional faces of its normal fan $\mathcal{N}(\mathsf{P})$.

Definition 1.2.22 (Refinement and Coarsening)**.** Given two fans $\mathcal{F}, \mathcal{G}$ in $\mathbb{R}^n$, the fan $\mathcal{F}$ **refines** $\mathcal{G}$ (equivalently, the fan $\mathcal{G}$ **coarsens** $\mathcal{F}$) if every cone of $\mathcal{G}$ is a union of cones of $\mathcal{F}$. Given two fans $\mathcal{F}_1, \mathcal{F}_2$ in $\mathbb{R}^n$, their **common refinement** is $\mathcal{F}_1 \wedge \mathcal{F}_2 := \{C_1 \cap C_2 \mid C_1 \in \mathcal{F}_1, C_2 \in \mathcal{F}_2\}$.

We remark that for any fan $\mathcal{F}$ in $\mathbb{R}^n$, there is a simplicial fan that refines $\mathcal{F}$.

1.2.4 Type Cones

We saw how a polytope induces a fan. In fact, many different polytopes induce the same fan. We will now study under which circumstances different polytopes have the same normal fan. Given a certain fan $\mathcal{F}$, it turns out that the set of all polytopes with $\mathcal{F}$ as normal fan can be seen geometrically as a cone, which is called the type cone of $\mathcal{F}$ and was introduced in [McM73]. In this section, we will introduce the necessary notions for that result.

We first recall that a ray of $\mathcal{F}$ is a cone of dimension 1. Every ray of a pointed fan can be written as the conical hull of a single vector. To simplify notation, we will often represent a ray by a ray vector, which is a fixed nonzero vector such that the set of nonnegative multiples of this vector equals the ray we started with. Moreover, given a fan $\mathcal{F}$, we fix a ray matrix that can be derived from the fan by choosing one representative ray vector for each of its rays.

Definition 1.2.23 (Ray Matrix)**.** Let $\mathcal{F}$ be a pointed complete simplicial fan in $\mathbb{R}^n$ whose number of rays is N. A **ray matrix** $\mathbf{M}_\mathcal{F}$ for $\mathcal{F}$ is any $(N \times n)$-matrix whose rows are representative vectors for the rays of $\mathcal{F}$.

With these fixed ray vectors, we can define polytopes such that each of their facets is orthogonal to one of these row vectors and thus orthogonal to one of the rays of the fan. We describe such a polytope by describing how far it stretches out in the direction of each of the rays.

Definition 1.2.24 (Height Function)**.** Given a ray matrix $\mathbf{M}_\mathcal{F} \in \mathbb{R}^{N \times n}$, a **height function** with respect to that ray matrix is any vector $\mathbf{h} \in \mathbb{R}^N$, interpreted in the following way: The vector $\mathbf{h} \in \mathbb{R}^N$ induces a polytope $\mathsf{P}(\mathbf{M}_\mathcal{F}, \mathbf{h}) = \{\mathbf{x} \in \mathbb{R}^n \mid \mathbf{M}_\mathcal{F} \cdot \mathbf{x} \leq \mathbf{h}\}$. This polytope $\mathsf{P}(\mathbf{M}_\mathcal{F}, \mathbf{h})$ has an inequality of the form $\langle \mathbf{r} \,|\, \mathbf{x} \rangle \leq \mathbf{h}_\mathbf{r}$ for each ray vector $\mathbf{r}$ appearing as a row of $\mathbf{M}_\mathcal{F}$, where $\mathbf{h}_\mathbf{r}$ denotes the entry of $\mathbf{h}$ corresponding to that row.

We remark that while every facet of $\mathsf{P}(\mathbf{M}_\mathcal{F}, \mathbf{h})$ must have a ray of $\mathcal{F}$ as its outer normal vector, the converse is not true. It follows that given a height function $\mathbf{h}$ for a fan $\mathcal{F}$, that fan $\mathcal{F}$ is not necessarily the normal fan of $\mathsf{P}(\mathbf{M}_\mathcal{F}, \mathbf{h})$, as can be seen in the following example:

Example 1.2.25. Let $\mathcal{F}$ be the 2-dimensional fan generated by $N = 5$ rays in the directions $(0, -1), (-1, 0), (0, 1), (1, 1)$ and $(1, 0)$. It is pointed (as the intersection of all its cones contains nothing but the origin), complete (as the cones spanned by these rays cover $\mathbb{R}^2$) and simplicial (as all maximal cones are simplicial). It can be represented by the following (5×2)-matrix.

$$\mathbf{M}_\mathcal{F} := \begin{pmatrix} 0 & -1 \\ -1 & 0 \\ 0 & 1 \\ 1 & 1 \\ 1 & 0 \end{pmatrix}$$

Given the height function $\mathbf{h} = (1, 1, 1, 2, 1) \in \mathbb{R}^5$ for that ray matrix $\mathbf{M}_\mathcal{F}$, the polytope $\mathsf{P}(\mathbf{M}_\mathcal{F}, \mathbf{h}) = \{\mathbf{x} \in \mathbb{R}^n \mid \mathbf{M}_\mathcal{F} \cdot \mathbf{x} \leq \mathbf{h}\}$ can be obtained as the intersection of the halfspaces defined by $-1 \leq x_1 \leq 1$ (second and fifth row), $-1 \leq x_2 \leq 1$ (first and third row), and $x_1 + x_2 \leq 2$ (fourth row). For an illustration, see Figure 1.3 (center). As the inequality induced by the fourth row is redundant, we obtain $\mathsf{P}(\mathbf{M}_\mathcal{F}, \mathbf{h})$ to be the 2-dimensional cube with vertices $\{-1, +1\}^2$. Therefore, the normal fan $\mathcal{N}(\mathsf{P}(\mathbf{M}_\mathcal{F}, \mathbf{h}))$ only has four rays and is thus different from $\mathcal{F}$.

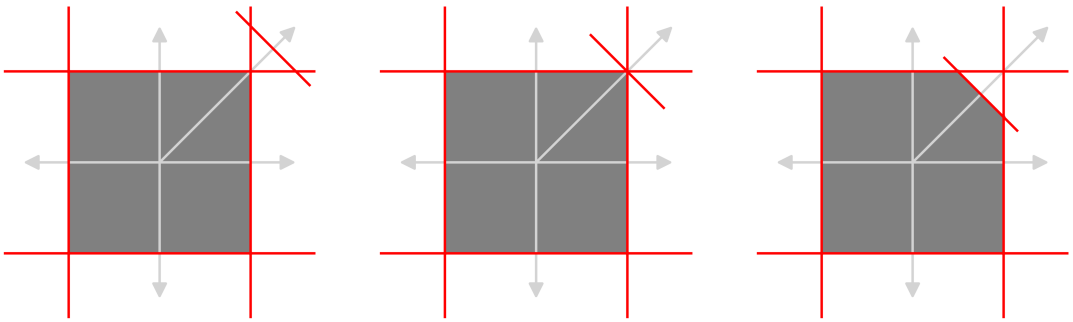

Figure 1.3: The polytope $\mathsf{P}(\mathbf{M}_\mathcal{F}, \mathbf{h})$ with $\mathbf{h} = (1, 1, 1, \lambda, 1)$ for the values $\lambda = 2.5$ (left), $\lambda = 2$ (center) and $\lambda = 1.5$ (right). The ray vectors of $\mathbf{M}_\mathcal{F}$ are drawn in light gray (the rows correspond to the rays in clockwise order, starting with the bottom ray). The boundaries of the half-spaces are indicated in red, the resulting polytope is colored in dark gray. Note that in the examples on the left and in the center, the normal fan of the resulting polytope is different from the fan $\mathcal{F}$ we started with.

We want to describe the set of height functions for which the resulting normal fan is the fan we started with. In this example, the inequality induced by the fourth row was made redundant by the inequalities induced by rows three and five. These are the inequalities coming from the two rays that are adjacent to the fourth ray. If our height vector were $\mathbf{h} = (1, 1, 1, 1.5, 1)$ instead, the fourth row would induce the inequality $x_1 + x_2 \leq 1.5$, which is not redundant and changes the combinatorial type of the polytope $\mathsf{P}(\mathbf{M}_\mathcal{F}, \mathbf{h})$. For an illustration, see Figure 1.3 (right).

In fact, this relation between rays of adjacent maximal cones can be used to describe the situations in which one of the inequalities is made redundant and thus changes the normal fan of the resulting polytope. We will now generalize this approach. First, we exploit that pointed complete simplicial fans admit a special relationship between its neighboring maximal cones.

Definition 1.2.26 (Adjacent Cones)**.** Let $\mathcal{F}$ be a pointed complete simplicial fan in $\mathbb{R}^n$ and let $\mathbf{M}_\mathcal{F} \in \mathbb{R}^{N\times n}$ be a ray matrix for $\mathcal{F}$. Any maximal cone of $\mathcal{F}$ is the conical hull $\mathrm{cone}(R)$ for some set R which contains exactly n rows of $\mathbf{M}_\mathcal{F}$. We denote by $\mathsf{Adj}(\mathcal{F})$ the set of unordered pairs $\{R, S\}$ where $\mathrm{cone}(R)$ and $\mathrm{cone}(S)$ are adjacent maximal cones in $\mathcal{F}$. As the fan $\mathcal{F}$ is simplicial, any such sets of rays R and S satisfy the relation $R \setminus \{\mathbf{r}\} = S \setminus \{\mathbf{s}\}$ for two ray vectors $\mathbf{r}$ and $\mathbf{s}$ that appear as rows of the ray matrix $\mathbf{M}_\mathcal{F}$.

For any such pair of adjacent maximal cones, their generating rays have a linear dependency that can be turned into a criterion to evaluate height functions on the fan.

Definition 1.2.27 (Wall-Crossing Inequality)**.** Let $\mathcal{F}$ be a pointed complete simplicial fan in $\mathbb{R}^n$ with ray matrix $\mathbf{M}_\mathcal{F}$ and let $\mathbf{h} \in \mathbb{R}^N$ be a height function with respect to $\mathbf{M}_\mathcal{F}$. For any pair of adjacent maximal cones $\{R, S\} \in \mathsf{Adj}(\mathcal{F})$, there are ray vectors $\mathbf{r}$ and $\mathbf{s}$ of $\mathcal{F}$ such that $R \setminus \{\mathbf{r}\} = S \setminus \{\mathbf{s}\}$. Then there is a unique (up to rescaling) linear dependence of the form

$$\alpha \cdot \mathbf{r} + \beta \cdot \mathbf{s} + \sum_{\mathbf{t}\in R\cap S} \gamma_\mathbf{t} \cdot \mathbf{t} = 0, \text{ with } \alpha, \beta > 0.$$

The **wall-crossing inequality** associated to these cones is the following inequality on entries of $\mathbf{h}$.

$$\alpha \cdot \mathbf{h}_\mathbf{r} + \beta \cdot \mathbf{h}_\mathbf{s} + \sum_{\mathbf{t}\in R\cap S} \gamma_\mathbf{t} \cdot \mathbf{h}_\mathbf{t} > 0.$$

Without loss of generality, we can always rescale these coefficients such that $\alpha + \beta = 2$. We denote by $\alpha_{R,S}(\mathbf{t})$ the coefficient of $\mathbf{t}$ in the unique linear dependence rescaled in this way. This allows us to rewrite the wall-crossing inequality as

$$\sum_{\mathbf{t}\in R\cup S} \alpha_{R,S}(\mathbf{t}) \cdot \mathbf{h}_\mathbf{t} > 0.$$

These wall-crossing inequalities for a height function are precisely what determines whether or not $\mathcal{F}$ is the normal fan of the polytope induced by that height function, as was pointed out by [CFZ02].

Theorem 1.2.28 (Normal Fans and Wall-Crossing Inequalities)**.** *Let $\mathcal{F}$ be a pointed complete simplicial fan in $\mathbb{R}^n$ and $\mathbf{M}_\mathcal{F} \in \mathbb{R}^{N\times n}$ be a ray matrix for $\mathcal{F}$. Then the following are equivalent for a height function $\mathbf{h} \in \mathbb{R}^N$:*

- *The fan $\mathcal{F}$ is the normal fan of the polytope $P(\mathbf{M}_\mathcal{F}, \mathbf{h})$.*
- *The height function $\mathbf{h}$ satisfies all wall-crossing inequalities of $\mathcal{F}$.*

We can therefore describe all height functions $\mathbf{h}$ that induce polytopes with the same normal fan by a set of linear inequalities on $\mathbf{h}$. The set of all such vectors $\mathbf{h}$ is the intersection of finitely many closed linear halfspaces and therefore a polyhedral cone, which is called the type cone.

Definition 1.2.29 (Type Cone)**.** Let $\mathcal{F}$ be a pointed complete simplicial fan in $\mathbb{R}^n$ with ray matrix $\mathbf{M}_\mathcal{F} \in \mathbb{R}^{N\times n}$. The **type cone** $\mathsf{TC}(\mathcal{F})$ is the set of all height functions $\mathbf{h} \in \mathbb{R}^N$ such that $\mathcal{F}$ is the normal fan of $\mathsf{P}(\mathbf{M}_\mathcal{F}, \mathbf{h})$.

With our knowledge about the wall-crossing inequalities from Definition 1.2.27 and Theorem 1.2.28, we can provide a concise description of the type cone for a given ray matrix.

Corollary 1.2.30 (An $\mathcal{H}$-Description of the Type Cone)**.** Let $\mathcal{F}$ be a pointed complete simplicial fan in $\mathbb{R}^n$ and $\mathbf{M}_\mathcal{F} \in \mathbb{R}^{N\times n}$ be a ray matrix for $\mathcal{F}$. Then the type cone of $\mathcal{F}$ is

$$\mathsf{TC}(\mathcal{F}) = \left\{ \mathbf{h} \in \mathbb{R}^N \;\middle|\; \sum_{\mathbf{t}\in R\cup S} \alpha_{R,S}(\mathbf{t}) \cdot \mathbf{h}_\mathbf{t} > 0 \text{ for all } \{R, S\} \in \mathsf{Adj}(\mathcal{F}) \right\}.$$

We observe that translating a polytope $\mathsf{P}(\mathbf{M}_\mathcal{F}, \mathbf{h})$ in any direction in $\mathbb{R}^n$ preserves its normal fan, but moves its height function along an infinite line contained in the type cone. Therefore, the type cone of a complete simplicial fan in $\mathbb{R}^n$ has an n-dimensional lineality space.

Observation 1.2.31 (Closed Type Cone and Deformation Cone)**.** All the wall-crossing inequalities are strict inequalities. Therefore, the halfspaces containing all their solutions are open halfspaces. As the type cone $\mathsf{TC}(\mathcal{F})$ is the intersection of all of them, it is an open cone. We denote its closure, called the **closed type cone**, by $\overline{\mathsf{TC}(\mathcal{F})}$. An $\mathcal{H}$-description of the closed type cone can simply be obtained by replacing the strict inequality $>$ by a weak inequality $\geq$ in Corollary 1.2.30. If $\mathcal{F}$ is obtained as the normal fan of the polytope P, then $\overline{\mathsf{TC}(\mathcal{F})}$ is also known as the **deformation cone** of P (see [Pos09] and [PRW08]).

We remark that all the constructions in this section depended not only on the fan $\mathcal{F}$, but also on the chosen ray matrix $\mathbf{M}_\mathcal{F}$. We argue that this choice has only minor consequences on the resulting type cone.

Observation 1.2.32 (Type Cone is Independent of Ray Matrix)**.** Let $\mathcal{F}$ be a fan in $\mathbb{R}^n$. Given two ray matrices $\mathbf{M}_1, \mathbf{M}_2$ for $\mathcal{F}$, the type cone $\mathsf{TC}(\mathcal{F})$ constructed from either of them depends only loosely on the choice of ray matrix. Exchanging the order of the rays as rows of the matrix corresponds to exchanging the corresponding entries of the height functions or the type cone. Scaling a ray by a positive factor corresponds to scaling the corresponding entry in the height functions or the type cone. Any two type cones constructed from different ray matrices for the same fan are therefore isomorphic. As we are mainly interested in the combinatorial structure of the type cone, in particular its face lattice, we speak of the type cone of a fan, regardless of the choice of ray matrix.

There are pointed complete simplicial fans whose type cone is empty, meaning that no polytope with this normal fan exists. The following example is so well-known that it has been named **the mother of all examples** in [DLRS10].

Example 1.2.33 (The Mother of All Examples)**.** The fan $\mathcal{F}$ of the mother of all examples can be constructed in $\mathbb{R}^3$ using the following ray matrix:

$$\mathbf{M}_\mathcal{F} = \begin{pmatrix} 4 & 0 & 0 \\ 0 & 4 & 0 \\ 0 & 0 & 4 \\ 2 & 1 & 1 \\ 1 & 2 & 1 \\ 1 & 1 & 2 \\ -1 & -1 & -1 \end{pmatrix}$$

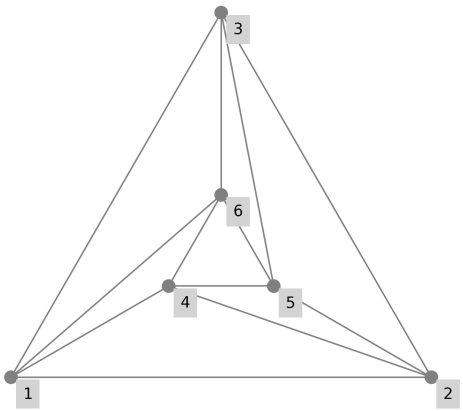

The illustration on the right side shows the intersection of the cones of $\mathcal{F}$ with the hyperplane $H := \left\{ \mathbf{x} \in \mathbb{R}^3 \;\middle|\; \sum_{i=1}^3 x_i = 4 \right\}$. The six numbered points represent the rays in the first six rows of $\mathbf{M}_\mathcal{F}$, while the seventh ray can be imagined to be on the back side of the picture, pointing stright away from the viewpoint. The lines in the illustration are the intersections of the 2-dimensional cones of $\mathcal{F}$ with H. This example is interesting because it is quite easy to construct, yet there is no polytope P whose normal fan $\mathcal{N}(\mathsf{P})$ is the mother of all examples fan $\mathcal{F}$.

1.2.5 Minkowski Sums

We started our introduction to geometry by combining points to obtain other points. We continue now by recalling a basic way to geometrically combine sets of points to obtain other sets of points.

Definition 1.2.34 (Minkowski Sum)**.** The **Minkowski sum** of two sets $A, B \subseteq \mathbb{R}^n$ is denoted by $A + B := \{a + b \mid a \in A, b \in B\}$.

We remark that the Minkowski sum of an arbitrary set and the empty set is the empty set. Moreover, we note that the Minkowski sum of any two convex sets is convex. Even more is true if we sum two convex sets that are polytopes.

Theorem 1.2.35 (Minkowski Sum of Polytopes)**.** *Let* $\mathsf{P}, \mathsf{Q} \subseteq \mathbb{R}^n$ *be two polytopes. Then their Minkowski sum* $\mathsf{P} + \mathsf{Q}$ *is a polytope as well.*

In particular, given a polytope $\mathsf{P} \subseteq \mathbb{R}^n$ and a vector $\mathbf{v} \in \mathbb{R}^n$, then the set containing nothing but the vector $\mathbf{v}$ is a 0-dimensional polytope in $\mathbb{R}^n$. The sum of $\{\mathbf{v}\}$ and P is the set of all points $\{\mathbf{v} + \mathbf{p} \mid \mathbf{p} \in \mathsf{P}\}$. The resulting polytope is refered to as the **translation of** P **by** $\mathbf{v}$ and simply denoted by $\mathbf{v} + \mathsf{P}$.

Observation 1.2.36 (Faces of a Minkowski Sum of Polytopes)**.** Let $\mathsf{P}, \mathsf{Q} \subseteq \mathbb{R}^n$ be two polytopes and let $\mathbf{v} \in \mathbb{R}^n \setminus \{\mathbf{0}\}$ be a nonzero vector. There is a unique scalar $b_\mathsf{P} := \max_{\mathbf{x} \in \mathsf{P}} \langle \mathbf{v} \mid \mathbf{x} \rangle$ with b_Q and $b_{\mathsf{P}+\mathsf{Q}}$ defined analogously. Then $H_\mathsf{P} := \{\mathbf{x} \in \mathbb{R}^n \mid \langle \mathbf{v} \mid \mathbf{x} \rangle \leq b_\mathsf{P}\}$ is a supporting hyperplane for P, so there is an associated face $F_\mathsf{P} := H_\mathsf{P} \cap \mathsf{P}$. We can now define such hyperplanes and faces for the two other polytopes analogously and remark that $F_\mathsf{P} + F_\mathsf{Q} = F_{\mathsf{P}+\mathsf{Q}}$ holds for any nonzero direction, so every face of $\mathsf{P} + \mathsf{Q}$ is the Minkowski sum of a face of P and a face of Q obtained in this way.

Observation 1.2.37 (Normal Fan of a Minkowski Sum of Polytopes)**.** The normal fan of the polytope $\mathsf{P} + \mathsf{Q}$ is the common refinement of the normal fans of P and Q. In particular, every vertex of $\mathsf{P} + \mathsf{Q}$ is the Minkowski sum of a vertex of P and a vertex of Q.

Example 1.2.38. The line segment $\mathsf{P} := \operatorname{conv}\{\mathbf{0}, \mathbf{e}_1\}$ and the triangle $\mathsf{Q} := \operatorname{conv}\{\mathbf{0}, \mathbf{e}_1, \mathbf{e}_2\}$ are two polytopes in $\mathbb{R}^2$ (see Figure 1.4 for an illustration). Their Minkowski sum $\mathsf{P} + \mathsf{Q}$ can be computed as the convex hull $\operatorname{conv}\{\mathbf{p} + \mathbf{q} \mid \mathbf{p} \in \mathsf{P}, \mathbf{q} \in \mathsf{Q}\}$. As every point of P (resp. Q) is a convex combination of its vertices, it suffices to build the convex hull over all Minkowski sums of vertices from $V(\mathsf{P})$ and $V(\mathsf{Q})$. The points obtained in this way are $\mathbf{0}+\mathbf{0}$, $\mathbf{0}+\mathbf{e}_1$, $\mathbf{0}+\mathbf{e}_2$, $\mathbf{e}_1+\mathbf{0}$, $\mathbf{e}_1+\mathbf{e}_1$ and $\mathbf{e}_1+\mathbf{e}_2$. We observe that some of these points are redundant for a $\mathcal{V}$-description of $\mathsf{P}+\mathsf{Q}$ as they can be described as a convex combination of others. For example, $\mathbf{0}+\mathbf{e}_1 = \mathbf{e}_1+\mathbf{0}$ is the center of $\mathbf{0}$ and $2\mathbf{e}_1$. We obtain the $\mathcal{V}$-description $\mathsf{P} + \mathsf{Q} = \operatorname{conv}\{\mathbf{0}, 2\mathbf{e}_1, \mathbf{e}_2, \mathbf{e}_1 + \mathbf{e}_2\}$. We emphasize that the sum of vertices of two polytopes P and Q is not necessarily a vertex of $\mathsf{P} + \mathsf{Q}$.

We observe that $\mathsf{P} + \mathsf{Q}$ has a facet in direction $\mathbf{e}_2$ containing the two vertices $\mathbf{e}_2$ and $\mathbf{e}_1 + \mathbf{e}_2$. It is not the Minkowski sum of a facet of P and a facet of Q, but the Minkowski sum of the entire polytope P with the vertex $\mathbf{e}_2 \in \mathsf{Q}$. We keep in mind that a facet of $\mathsf{P}+\mathsf{Q}$ is not necessarily the sum of facets of P and Q. On the other hand, the vertex $\mathbf{0}$ is a facet of P while the line segment $[\mathbf{e}_1, \mathbf{e}_2]$ is a facet of P. Their Minkowski sum is the line segment $[\mathbf{e}_1, \mathbf{e}_2]$, which is not a face of $\mathsf{P}+\mathsf{Q}$. We keep in mind that the sum of facets of two polytopes P and Q is not necessarily a facet of $\mathsf{P} + \mathsf{Q}$.

Observation 1.2.39 (Sums of Height Functions)**.** Let $\mathcal{F}$ be a fan in $\mathbb{R}^n$ with a ray matrix $\mathbf{M}_\mathcal{F}$ and let $\mathbf{h}, \mathbf{h}' \in \mathsf{TC}(\mathcal{F})$ be two height functions in the type cone. They induce two polytopes $\mathsf{P}(\mathbf{M}_\mathcal{F}, \mathbf{h})$ and $\mathsf{P}(\mathbf{M}_\mathcal{F}, \mathbf{h}')$, respectively. As $\mathsf{TC}(\mathcal{F})$ is a cone, any conical combination of these height vectors, for example $\mathbf{h}^* = \lambda \cdot \mathbf{h} + \mu \cdot \mathbf{h}'$ (where $\lambda, \mu \geq 0$), lies in the type cone as well. Therefore,

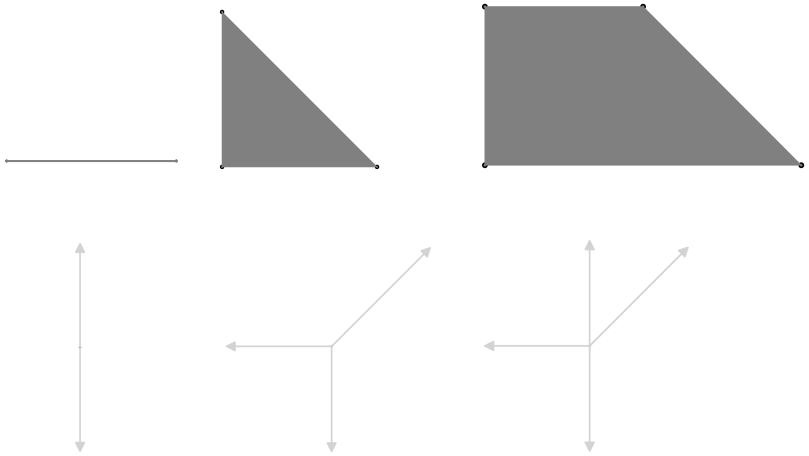

Figure 1.4: The three polytopes $\mathsf{P} = \operatorname{conv}\{\mathbf{0}, \mathbf{e}_1\}$ (top left), $\mathsf{Q} = \operatorname{conv}\{\mathbf{0}, \mathbf{e}_1, \mathbf{e}_2\}$ (top center) and $\mathsf{P} + \mathsf{Q} = \operatorname{conv}\{\mathbf{0}, 2\mathbf{e}_1, \mathbf{e}_2, \mathbf{e}_1 + \mathbf{e}_2\}$ (top right) from Example 1.2.38, together with their normal fans in the bottom row.

all three polytopes $\mathsf{P}_1 = \mathsf{P}(\mathbf{M}_{\mathcal{F}}, \mathbf{h})$ and $\mathsf{P}_2 = \mathsf{P}(\mathbf{M}_{\mathcal{F}}, \mathbf{h}')$ and $\mathsf{P}_3 = \mathsf{P}(\mathbf{M}_{\mathcal{F}}, \mathbf{h}^*)$ have the same normal fan $\mathcal{N}(\mathsf{P}_1) = \mathcal{N}(\mathsf{P}_2) = \mathcal{N}(\mathsf{P}_3) = \mathcal{F}$. Moreover, they are related through a weighted Minkowski sum with coefficients λ and μ, such that $\lambda \cdot \mathsf{P}_1 + \mu \cdot \mathsf{P}_2 = \mathsf{P}_3$.

Example 1.2.40. The normal fan of the polytope $\mathsf{P} + \mathsf{Q}$, as used before and illustrated on the right side in Figure 1.4, can be described by the following ray matrix:

$$\mathbf{M}_{\mathcal{F}} := \begin{pmatrix} 0 & -1 \\ -1 & 0 \\ 0 & 1 \\ 1 & 1 \end{pmatrix}, \ \mathbf{h}(\mathsf{P}) = \begin{pmatrix} 0 \\ 0 \\ 0 \\ 1 \end{pmatrix}, \ \mathbf{h}(\mathsf{Q}) = \begin{pmatrix} 0 \\ 0 \\ 1 \\ 1 \end{pmatrix}, \ \mathbf{h}(\mathsf{P}+\mathsf{Q}) = \mathbf{h}(\mathsf{P}) + \mathbf{h}(\mathsf{Q}) = \begin{pmatrix} 0 \\ 0 \\ 1 \\ 2 \end{pmatrix}$$

We remark that the order of the rows is such that the first row corresponds to the bottom ray, with the other rows following in clockwise order. Then

- the polytope P (on the left side of Figure 1.4) is induced by the height function $\mathbf{h}(\mathsf{P})$,
- the polytope Q (in the center) comes from the height function $\mathbf{h}(\mathsf{Q})$,
- and the polytope $\mathsf{P} + \mathsf{Q}$ (on the right side) comes from the height function $\mathbf{h}(\mathsf{P} + \mathsf{Q})$.

We note that neither $\mathbf{h}(\mathsf{P})$ nor $\mathbf{h}(\mathsf{Q})$ is contained in the type cone. This translates into the fact that neither of the polytopes they induce has $\mathcal{F}$ as their normal fan. We can also argue that they are not in the type cone as they each violate at least one wall-crossing inequality as introduced in Definition 1.2.27. Let $\mathbf{r}_1, \ldots, \mathbf{r}_4$ denote the four row vectors of $\mathbf{M}_{\mathcal{F}}$.

- Between the bottom left cone spanned by $\{\mathbf{r}_1, \mathbf{r}_2\}$ and the top left cone spanned by $\{\mathbf{r}_2, \mathbf{r}_3\}$, the unique linear dependence is $\mathbf{r}_1 + \mathbf{r}_3 = 0$, so the wall-crossing inequality is $\mathbf{h}_1 + \mathbf{h}_3 > 0$. The height function $\mathbf{h}(\mathsf{P})$ violates this inequality, so P does not have the normal fan $\mathcal{F}$.
- Between the top left cone spanned by $\{\mathbf{r}_2, \mathbf{r}_3\}$ and the top right cone spanned by $\{\mathbf{r}_3, \mathbf{r}_4\}$, the linear dependence is $\mathbf{r}_2 + \mathbf{r}_4 - \mathbf{r}_3 = 0$, so the wall-crossing inequality is $\mathbf{h}_2 + \mathbf{h}_4 - \mathbf{h}_3 > 0$. The height function $\mathbf{h}(\mathsf{Q})$ violates this inequality, so Q does not have the normal fan $\mathcal{F}$.

1.2.6 Indecomposability

In this section, we focus on polytopes which cannot be obtained as the Minkowski sum of different polytopes in a non-trivial way. We remark that any polytope P is equal to the Minkowski sum of

itself and the 0-dimensional polytope $\{\mathbf{0}\}$ containing only the origin. We are therefore interested in a suitable definition for being indecomposable.

Definition 1.2.41 (Weak Minkowski Summand)**.** A **weak Minkowski summand** of a polytope P is a polytope Q such that there are a scalar $\lambda \geq 0$ and a third polytope R such that $\mathsf{Q} + \mathsf{R} = \lambda\mathsf{P}$.

For a discussion of several characterizations of weak Minkowski summands of P, we refer to the appendix of [PRW08]. We remark that Q is a weak Minkowki summand of P if and only if the normal fan of Q coarsens the normal fan of P. Moreover, the set of weak Minkowski summands of P is equal to the closed type cone of its normal fan $\mathcal{N}(\mathsf{P})$.

We recall from Observation 1.2.39 that conical combinations of height functions in the type cone correspond to Minkowski sums of the associated polytopes. We remark that the rays of the closed type cone represent Minkowski summands of P that cannot be decomposed further. Such polytopes are called (Minkowski) indecomposable.

Definition 1.2.42 (Indecomposable Polytope)**.** A polytope P is called **indecomposable** if every weak Minkowski summand of P is of the form $\lambda\mathsf{P} + \mathbf{t}$ for some scalar $\lambda \geq 0$ and a vector $\mathbf{t} \in \mathbb{R}^n$.

The following criterion is a special case of a more elaborate statement in [McM87]. We give a modified proof adapted to our case.

Theorem 1.2.43 (Indecomposability Criterion)**.** *Let P be a polytope. If there is an indecomposable face F of P such that every facet of P has a vertex in common with F, then P is indecomposable.*

Proof. We fix an $\mathcal{H}$-representation of the polytope $\mathsf{P} = \mathsf{P}(\mathbf{M}, \mathbf{v}) := \{\mathbf{x} \in \mathbb{R}^n \mid \mathbf{M}\mathbf{x} \leq \mathbf{v}\}$, where we denote the rows of $\mathbf{M}$ and thus the outer normal vectors of the facets of P by $\mathbf{n}_1, \ldots, \mathbf{n}_m$. Then any Minkowki summand Q of P can be written as $\mathsf{Q} = \mathsf{P}(\mathbf{M}, \mathbf{w})$ for some vector $\mathbf{w} \leq \mathbf{v}$, where we choose $\mathbf{w}$ such that all the inequalities are tight for Q.

Let F be an indecomposable face of P whose vertices are $\mathbf{p}_1, \ldots, \mathbf{p}_k$. Let G be a face of Q that maximizes a normal vector of F. Moreover, for each vertex $\mathbf{p}_i$ of F, let $\mathbf{q}_i$ be a vertex of Q that is maximal in direction $\mathbf{p}_i$.

Then the face G is a Minkowski summand of F and therefore of the form $\lambda\mathsf{F} + \mathbf{t}$ for some $\lambda \geq 0$ and $\mathbf{t} \in \mathbb{R}^n$. We deduce that $\mathbf{q}_j = \lambda\mathbf{p}_j + \mathbf{t}$ holds for all $j \in [k]$. If the facet of P that maximizes the direction $\mathbf{n}_i$ contains the vertex $\mathbf{p}_j$, then the facet of Q that is maximal in direction $\mathbf{n}_i$ has to contain the vertex $\mathbf{q}_j$, which leads us to confirm that $w_i = \langle \mathbf{n}_i \mid \mathbf{q}_j \rangle = \lambda v_i + \langle \mathbf{n}_i \mid \mathbf{t} \rangle$. We conclude that $\mathsf{Q} = \lambda\mathsf{P} + \mathbf{t}$. □

1.2.7 Cartesian Products

We look at another classical way of constructing a new polytope based on two existing ones.

Definition 1.2.44 (Product of Polytopes)**.** The **(Cartesian) product** of two polytopes $\mathsf{P} \in \mathbb{R}^n$ and $\mathsf{Q} \in \mathbb{R}^m$ is defined as $\mathsf{P} \times \mathsf{Q} := \{(\mathbf{p}, \mathbf{q}) \in \mathbb{R}^{n+m} \mid \mathbf{p} \in \mathsf{P}, \mathbf{q} \in \mathsf{Q}\}$.

Observation 1.2.45 (Faces of a Cartesian Product of Polytopes)**.** The polytope $\mathsf{P} \times \mathsf{Q}$ has dimension $\dim(\mathsf{P}) + \dim(\mathsf{Q})$ and its non-empty faces are all the products of a non-empty face of P with a non-empty face of Q. In particular, its vertices are the points $(\mathbf{v}, \mathbf{v}')$ for each pair of vertices $\mathbf{v} \in V(\mathsf{P})$ and $\mathbf{v}' \in V(\mathsf{Q})$.

Example 1.2.46. The n-dimensional cube $\mathsf{C}_n := \{\mathbf{x} \in \mathbb{R}^n \mid 0 \leq x_i \leq 1 \text{ for all } i \in [n]\}$ can easily be decomposed into one-dimensional polytopes. On one hand, it is the Minkowski sum of the line segments $[\mathbf{0}, \mathbf{e}_i] \subset \mathbb{R}^n$ for all $i \in [n]$. On the other hand, it is the Cartesian product of n one-dimensional line segments $[0, 1] \subset \mathbb{R}$.

It is not a coincidence that these decompositions of the cube are very similar. In fact, the Cartesian product of any two polytopes $\mathsf{P} \in \mathbb{R}^n$ and $\mathsf{Q} \in \mathbb{R}^m$ is equal to the Minkowski sum of the two polytopes $\mathsf{P}' = \mathsf{P} \times \{0\}^m$ and $\mathsf{Q}' = \{0\}^n \times \mathsf{Q}$. In consequence, the normal fan of $\mathsf{P} \times \mathsf{Q}$ is the common refinement of the normal fans of P' and Q', so its cones are all sets of the form $C_\mathsf{P} \times C_\mathsf{Q}$ for cones $C_\mathsf{P} \in \mathcal{N}(\mathsf{P})$ and $C_\mathsf{Q} \in \mathcal{N}(\mathsf{Q})$.

On the other hand, the Minkowski sum of any two polytopes $\mathsf{P}, \mathsf{Q} \in \mathbb{R}^n$ is the projection of their Cartesian product $\mathsf{P} \times \mathsf{Q} \in \mathbb{R}^{n+n}$ under the linear map defined by $\varphi(\mathbf{e}_i) = \mathbf{e}_i$ for $i \in [1, n]$ and $\varphi(\mathbf{e}_i) = \mathbf{e}_{i-n}$ for $i \in]n, 2n]$.

1.3 Hyperplane Arrangements

We will now study arrangements of hyperplanes. For an introduction to hyperplane arrangements with a focus on their posets of regions, we refer to [Rea16b] and [BEZ90]. We first introduce the basic notions, before focusing on some cones, polytopes and fans associated with hyperplane arrangements and then introducing orientations and orders on them.

1.3.1 Basics

Definition 1.3.1 (Hyperplane Arrangement)**.** Let n be a positive integer. A **(real) hyperplane arrangement** $\mathcal{A}$ is a collection of finitely many hyperplanes in $\mathbb{R}^n$.

We will only consider real hyperplane arrangements, so we omit the term and assume every hyperplane arrangement mentioned henceforth to be real. We will use $\mathcal{A}$ as a set sometimes, so that we can denote a hyperplane of the arrangement by $H \in \mathcal{A}$.

Definition 1.3.2 (Center, Rank, Essential)**.** The **center** of an arrangement $\mathcal{A}$ is the intersection of all hyperplanes $H \in \mathcal{A}$. The arrangement $\mathcal{A}$ is called **central** if its center is non-empty. The **rank** of an arrangement is the dimension of the ambient vector space $\mathbb{R}^n$ minus the dimension of the center. An arrangement is called **essential** if its center has dimension 0 or equivalently, if its rank equals its dimension.

In arrangements of linear hyperplanes, the center of an arrangement $\mathcal{A}$ is always a linear subspace. The **esssentialization** is obtained by restricting all hyperplanes to the orthogonal complement of the center.

Definition 1.3.3 (Arrangement Matrix)**.** An **arrangement matrix** $\mathrm{M}_\mathcal{A} \in \mathbb{R}^{n \times m}$ of an arrangement $\mathcal{A}$ containing m hyperplanes in $\mathbb{R}^n$ is a matrix whose columns are normal vectors $\mathbf{v}_1, \ldots, \mathbf{v}_m$ of the arrangement hyperplanes $H_1, \ldots, H_m \in \mathcal{A}$.

We remark that this definition leaves several degrees of freedom in choosing an arrangement matrix. In particular, any matrix that is obtained through nonzero scaling of column vectors or exchanging column vectors of an arrangement matrix is still an arrangement matrix of the same arrangement.

Example 1.3.4 (Braid Arrangement)**.** We fix a positive integer n. For any pair of distinct integers $i < j \in [n]$, we introduce the hyperplane $H_n(i, j) := \{\mathbf{x} \in \mathbb{R}^n \mid x_i = x_j\}$. The arrangement $\mathcal{A}_n := \{H_n(i, j) \mid 1 \leq i < j \leq n\}$ of all such hyperplanes is called the **braid arrangement**. Its center is the line $\mathbb{R}\mathbf{1}$ containing all points $\{\mathbf{x} \in \mathbb{R}^n \mid \forall i, j \in [n] : x_i = x_n\}$. Therefore, the arrangement $\mathcal{A}_n$ is central, but not essential, as its rank is $n - 1$. Its essentialization is the

intersection with the orthogonal complement of the vector $\mathbf{1}$, which is given by the linear subspace $\mathcal{H}_0^n = \{\mathbf{x} \in \mathbb{R}^n \mid \sum_{i=1}^n x_i = 0\}$. See Figure 1.5 (center) for an illustration of this arrangement. An arrangement matrix for $n = 3$ is the following:

$$\mathbf{M}_{\mathcal{A}} := \begin{pmatrix} 1 & 1 & 0 \\ -1 & 0 & 1 \\ 0 & -1 & -1 \end{pmatrix}$$

The hyperplane arrangements we are interested in will only contain linear hyperplanes. We remark that any such arrangement is central, as the origin $\mathbf{0}$ lies on every linear hyperplane. As all hyperplane arrangements we consider will be real, central hyperplane arrangements of linear hyperplanes, we will omit these terms and assume every arrangement to be real and central and to contain only linear hyperplanes.

1.3.2 Regions, Fan and Faces

We will now study some geometric objects that arise naturally in hyperplane arrangements.

Definition 1.3.5 (Complement and Regions)**.** The **complement** of an arrangement $\mathcal{A}$ is the set $\mathbb{R}^n \setminus \left(\bigcup_{H \in \mathcal{A}} H\right)$ of all points not contained in any hyperplane of $\mathcal{A}$. It is the disjoint union of connected components which are unbounded open polyhedral cones. The **regions** of $\mathcal{A}$ are the closures of these connected components. We denote the set of all regions by $\mathcal{R}(\mathcal{A})$.

Observation 1.3.6 (Regions are Cones)**.** Every hyperplane H of $\mathcal{A}$ slices the space $\mathbb{R}^n$ into two open halfspaces on either side of H. Therefore, every region of $\mathcal{A}$ is the closure of the intersection of finitely many open halfspaces of $\mathbb{R}^n$, making every region a closed polyhedral cone in $\mathbb{R}^n$.

The regions of an arrangement are closed polyhedral cones. We will use the term **open region** whenever we want to denote the interior of a region without its boundary. The following statement certifies that the (closed) regions of an arrangement induce a complete fan in $\mathbb{R}^n$.

Theorem 1.3.7 (Regions and Fan)**.** *The regions of $\mathcal{A}$ are the maximal cones of a complete fan.*

This motivates the following definitions for the objects in the context of that fan.

Definition 1.3.8 (Arrangement Fan)**.** Given an arrangement $\mathcal{A}$, the **arrangement fan** $\mathcal{F}(\mathcal{A})$ is the complete fan whose maximal cones are the regions of $\mathcal{A}$. The **faces** of $\mathcal{A}$ are the cones of $\mathcal{F}(\mathcal{A})$, which are the regions of $\mathcal{A}$ and all their faces. In particular,

- the **chambers** of $\mathcal{F}(\mathcal{A})$ are all regions of $\mathcal{A}$,
- the **walls** of $\mathcal{F}(\mathcal{A})$ are all facets of the regions of $\mathcal{A}$,
- the **rays** of $\mathcal{F}(\mathcal{A})$ are all rays of the regions of $\mathcal{A}$.

The arrangement $\mathcal{A}$ is called **simplicial** if $\mathcal{F}(\mathcal{A})$ is simplicial (equivalently, if every region of $\mathcal{A}$ is a simplicial cone).

We note that the fan of the arrangement is independent of the choice of normal vectors or orientations of the hyperplanes, it is uniquely determined by the arrangement itself. Conversely, the arrangement fan uniquely defines the arrangement.

Observation 1.3.9 (Fans of Essential Arrangements)**.** We remark that the arrangement $\mathcal{A}$ is essential if and only $\{\mathbf{0}\}$ is its center, which is a face of every region and therefore a cone in $\mathcal{F}(\mathcal{A})$. In particular, the arrangement fan $\mathcal{F}(\mathcal{A})$ is pointed if and only if $\mathcal{A}$ is essential.

Example 1.3.10 (Regions and Rays of the Braid Arrangement)**.** The braid arrangement is not essential, as all its hyperplanes contain the line $\mathbb{R}\mathbf{1}$. To obtain a simplicial and essential arrangement fan, the **braid fan** $\mathcal{F}_n$ is defined to be the fan obtained as the intersection of the regions of $\mathcal{A}_n$ with the sum-zero hyperplane $\mathcal{H}_0^n = \{\mathbf{x} \in \mathbb{R}^n \mid \sum_{i=1}^n x_i = 0\}$. We remark that the intersections with the sum-one hyperplane $\mathcal{H}_1^n$ or the sum-count-hyperplane $\mathcal{H}_\Sigma^n$ yield isomorphic fans, but the one intersected with $\mathcal{H}_0^n$ is the most convenient one because the hyperplane normals $\mathbf{e}_j - \mathbf{e}_i$ are all contained in this subspace.

- The chambers of the braid fan (corresponding to the regions of $\mathcal{A}_n$) are in bijection with the permutations in $\mathfrak{S}_n$. The permutation $\sigma = (\sigma_1, \sigma_2, \ldots, \sigma_n)$ corresponds to the $(n-1)$-dimensional cone $C(\sigma) := \{\mathbf{x} \in \mathcal{H}_0^n \mid \mathbf{x}_{\sigma_1} \leq \mathbf{x}_{\sigma_2} \leq \cdots \leq \mathbf{x}_{\sigma_n}\}$. A representative point in the interior of that region is $\mathbf{p}(\sigma) := \sigma^{-1}((1, 2, \ldots, n)) = (\sigma^{-1}(1), \sigma^{-1}(2), \ldots, \sigma^{-1}(n))$.
- The rays of the braid fan (corresponding to the 2-dimensional faces of $\mathcal{A}_n$) are in bijection with the proper subsets of $[n]$. A proper subset $\emptyset \subsetneq I \subsetneq [n]$ corresponds to the 1-dimensional cone $C(I) := \left\{\mathbf{x} \in \mathcal{H}_0^n \;\middle|\; \mathbf{x}_{i_1} = \cdots = \mathbf{x}_{i_p} \leq \mathbf{x}_{j_1} = \cdots = \mathbf{x}_{j_{n-p}}\right\}$, where $I = \{i_1, \ldots, i_p\}$ and $[n] \setminus I = \{j_1, \ldots, j_{n-p}\}$. A representative vector for that ray is $\mathbf{r}(I) := |I| \cdot \mathbf{1} - n \cdot \mathbf{1}_I$, which has an entry $|I| - n$ for every index $i \in I$ and an entry $|I|$ for every index $j \notin I$.
- The rays of the chamber $C(\sigma)$ are the sets $C(\sigma([k]))$ for all $k \in [n-1]$. In particular, the rays of the chamber $C(\mathsf{id}_n)$ associated to the identity permutation are the sets $C([k])$ for all $k \in [n-1]$.

See Figure 1.5 (center) for an illustration of the braid fan $\mathcal{F}_4$.

To represent a rank 3 arrangement in a planar illustration, a **stereographic projection** is commonly used. For this, the arrangement hyperplanes are intersected with a unit ball centered in the origin and the resulting great circles are stereographically projected to the plane. The arrangement hyperplanes are then represented by circles, its rays are the points where two or more circles intersect and its regions are the closed faces of the drawing. See Figure 1.13 (left) for a stereographic projection of the $\vec{\mathcal{A}}_4$ arrangement.

Observation 1.3.11 (Type Cone of an Arrangement)**.** Given a hyperplane arrangement $\mathcal{A}$, the type cone of the arrangement is the type cone of the arrangement fan $\mathcal{F}(\mathcal{A})$. We therefore just write $\mathsf{TC}(\mathcal{A})$ to denote that type cone $\mathsf{TC}(\mathcal{F}(\mathcal{A}))$. We remark that it is independent of any orientation of the arrangement and any choice of base region (both of which we will introduce later). Any height function $\mathbf{h} \in \mathsf{TC}(\mathcal{A})$ induces a polytope whose normal fan is the arrangement fan.

We will now introduce a special class of polytopes whose normal fan is an arrangement fan.

1.3.3 Zonotopes

Zonotopes are a class of polytopes that are closely related to hyperplane arrangements. As every line segment in real space is a one-dimensional polytope, the Minkowski sum of a finite set of line segments is a polytope as well.

Definition 1.3.12 (Zonotope)**.** A **zonotope** is any polytope that can be obtained as the Minkowski sum of finitely many line segments. Equivalently, a zonotope is any polytope that is the image of a cube under an affine map.

Theorem 1.3.13 (Zonotopes and Arrangements)**.** *Let the zonotope $\mathsf{Z} \subseteq \mathbb{R}^n$ be the Minkowski sum of the line segments $[0, \mathbf{v}_i]$ for $i \in [m]$. Then its normal fan $\mathcal{N}(\mathsf{Z})$ is equal to the fan of the arrangement of all hyperplanes $\{\mathbf{x} \in \mathbb{R}^n \mid \langle \mathbf{x} \,|\, \mathbf{v}_i \rangle = 0\}$ for $i \in [m]$.*

We remark that the zonotope $\mathsf{Z} = \sum_{i=1}^m [0, \mathbf{v}_i]$ is the image of the standard m-dimensional cube $\mathsf{C}_m := \mathrm{conv}(\{0,1\}^m)$ under the linear map $\phi(\mathbf{x}) := \mathbf{M}_{\mathcal{A}} \cdot \mathbf{x}$ defined by the arrangement

matrix whose columns are the normal vectors $\mathbf{v}_i$. Any zonotope that can be obtained in this way is called a **zonotope of** $\mathcal{A}$.

Observation 1.3.14 (Arrangement and Zonotope)**.** The structure of an arrangement zonotope is closely related to the structure of the arrangement: The zonotope vertices correspond to the regions of the arrangement, and its edges correspond to the walls of the arrangement. If the arrangement is essential, then the k-dimensional faces of the zonotope correspond to the $(n-k)$-dimensional faces of the arrangement and its facets correspond to the rays of the arrangement. We emphasize that the normal fan of the arrangement zonotope is the arrangement fan and an essential arrangement is simplicial if and only if the corresponding zonotope is simple.

We already saw some of the relations between the braid arrangement and the symmetric group. Unsurprisingly, there is a well-known polytope constructed from permutations that is a zonotope of the braid arrangement.

Example 1.3.15 (Permutahedron)**.** The **permutahedron** Perm_n is defined equivalently as

- the convex hull of the points $\sum_{i=1}^{n} i \cdot \mathbf{e}_{\sigma_i}$ for all permutations $\sigma \in \mathfrak{S}_n$,
- the intersection of the sum-count-hyperplane $\mathcal{H}^n_\Sigma = \left\{\mathbf{x} \in \mathbb{R}^n \;\middle|\; \sum_{i=1}^n x_i = \sum_{i=1}^n i = \binom{n+1}{2}\right\}$ with the halfspaces $\left\{\mathbf{x} \in \mathbb{R}^n \;\middle|\; \sum_{i\in I} \mathbf{x}_i \geq \binom{|I|+1}{2}\right\}$ for all proper subsets $\emptyset \subsetneq I \subsetneq [n]$,
- the translation of the zonotope $\mathsf{Z} = \sum_{1\leq i<j\leq n}[0, \mathbf{e}_i - \mathbf{e}_j]$ by the vector $(1, 2, \ldots, n)$.

In particular, the permutahedron is a zonotope of the braid arrangement, translated from the sum-zero hyperplane to the sum-count-hyperplane. See Figure 1.5 (right) for an illustration of the permutahedron Perm_4. Each $\mathcal{A}_n$ hyperplane $\{\mathbf{x} \in \mathbb{R}^n \mid x_i = x_j\}$ is perpendicular to the line segment $[0, \mathbf{e}_i - \mathbf{e}_j]$, which are exactly the edge directions of the permutahedron.

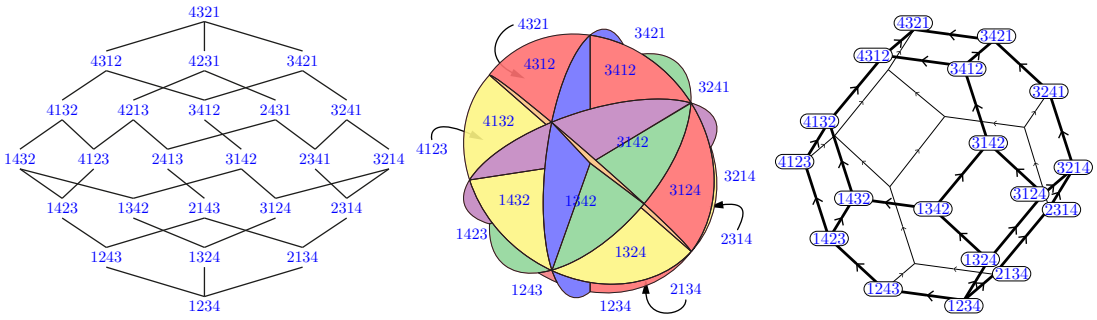

Figure 1.5: The Hasse diagram of the weak order on $\mathfrak{S}_4$ (left) is the poset of regions of the oriented braid arrangement $\vec{\mathcal{A}}_4$ (center), where the regions are labeled by permutations. The permutahedron Perm_4 (right) is a zonotope of the oriented braid arrangement. Its normal fan is the braid fan $\mathcal{F}_4$. The choice of base region 1234 induces an acyclic orientation on the edges of the permutahedron corresponding to the cover relations of the weak order directed upwards. [Picture from [PS19]]

1.3.4 Oriented Arrangements

The following definitions depend on a choice of a **base region** B among the regions $\mathcal{R}(\mathcal{A})$ of the arrangement $\mathcal{A}$. This choice induces an orientation on each hyperplane $H \in \mathcal{A}$, as it now has one halfspace containing B and one halfspace not containing B. Furthermore, the choice of a base region in the arrangement translates into a choice of a base vertex in any zonotope of the arrangement, thereby inducing an acyclic orientation on the edges of the zonotope.

Definition 1.3.16 (Oriented Arrangement)**.** An **oriented arrangement** $\vec{\mathcal{A}}$ is a hyperplane arrangement $\mathcal{A}$ together with a fixed base region $B \in \mathcal{R}(\mathcal{A})$.

To work with an oriented arrangement, we fix an order of the hyperplanes $H_1, \dots, H_m$ of $\vec{\mathcal{A}}$ with associated normal vectors $\mathbf{v}_1, \dots, \mathbf{v}_m$ oriented away from the base region B so that we have $B \subseteq H_i^- = \{\mathbf{x} \in \mathbb{R}^n \mid \langle \mathbf{v}_i \,|\, \mathbf{x} \rangle \leq 0\}$ for every $H_i \in \vec{\mathcal{A}}$. An **oriented arrangement matrix** of $\vec{\mathcal{A}}$ is any arrangement matrix of $\mathcal{A}$ where the column vectors are oriented away from the base region.

Definition 1.3.17 (Sign Vector)**.** Let $\vec{\mathcal{A}}$ be an oriented arrangement in $\mathbb{R}^n$ and $\mathbf{p} \in \mathbb{R}^n$ be a point.

- The **sign** of $\mathbf{p}$ with respect to a hyperplane H_i of $\vec{\mathcal{A}}$ is $\operatorname{sgn}_{H_i}(\mathbf{p}) := \operatorname{sgn} \langle \mathbf{v}_i \,|\, \mathbf{p} \rangle$.
- The **sign vector** of $\mathbf{p}$ in $\vec{\mathcal{A}}$ is $\operatorname{sgn}_{\vec{\mathcal{A}}}(\mathbf{p}) := (\operatorname{sgn}_{H_1}(\mathbf{p}), \dots, \operatorname{sgn}_{H_m}(\mathbf{p}))$.

Informally, the sign $\operatorname{sgn}_H(\mathbf{p})$ tells us on which side of H the point $\mathbf{p}$ is located. It is

- 0 if $\mathbf{p}$ lies on H,
- $+1$ if $\mathbf{p}$ lies in the positive open halfspace $H^+ \setminus H$,
- -1 if $\mathbf{p}$ lies in the negative open halfspace $H^- \setminus H$.

We emphasize that the notions of positive and negative halfspace depend on the orientation of the arrangement via the orientation of the hyperplane normal vector.

Observation 1.3.18 (Sign Vector of a Region)**.** As the open regions of $\vec{\mathcal{A}}$ are not intersected by any hyperplane of $\vec{\mathcal{A}}$, all points in their interior have the same sign vector. We denote the sign vector of a region $R \in \mathcal{R}(\vec{\mathcal{A}})$ by $\operatorname{sgn}_{\vec{\mathcal{A}}}(R)$. We remark that for every region $R \in \mathcal{R}(\vec{\mathcal{A}})$, we have $\operatorname{sgn}_{\vec{\mathcal{A}}}(R) \in \{-1, +1\}^m$ as the open region is contained in the complement of $\vec{\mathcal{A}}$ and therefore does not lie on any of the hyperplanes. A point in the boundary of a region R lies on one or more of the hyperplanes of $\vec{\mathcal{A}}$, so its sign vector has one or more corresponding zero entries and is otherwise identical with the sign vector of the region. We remark that in this way, the interior of every cone of the arrangement fan (not just the chambers) has a unique sign vector.

We recall from Definition 1.1.10 that a hyperplane H separates two regions $R_1, R_2 \in \mathcal{R}(\vec{\mathcal{A}})$ if they are in opposite closed halfspaces induced by H. We will use this notion to establish a partial order on $\mathcal{R}(\vec{\mathcal{A}})$.

Definition 1.3.19 (Separating Set)**.** Given a region $R \in \mathcal{R}(\vec{\mathcal{A}})$ of an oriented arrangement $\vec{\mathcal{A}}$ with base region B, the **separating set** $\operatorname{Sep}(R)$ is the set of hyperplanes in $\vec{\mathcal{A}}$ that separate R from B.

We remark that we can equivalently define the set $\operatorname{Sep}(R)$ from sign vectors. The set $\operatorname{Sep}(R)$ contains exactly those hyperplanes $H \in \vec{\mathcal{A}}$ for which $\operatorname{sgn}_H(R) \neq \operatorname{sgn}_H(B)$, which holds if and only if $\operatorname{sgn}_H(R) = +1$.

Definition 1.3.20 (Basic Hyperplanes)**.** Let $\vec{\mathcal{A}}$ be an oriented arrangement in $\mathbb{R}^n$. The **basic hyperplanes** of $\vec{\mathcal{A}}$ are those that intersect the base region B in dimension $(n-1)$.

Equivalently, a hyperplane $H_i \in \vec{\mathcal{A}}$ is basic if and only if there is a region $R \in \mathcal{R}(\vec{\mathcal{A}})$ whose separating set is $\{H_i\}$ or, yet equivalently, whose sign vector has -1 in each entry except for the i-th one, where it has $+1$. We emphasize that the notion of a basic hyperplane depends entirely on the orientation: For every hyperplane $H \in \mathcal{A}$, we can choose a chamber of the arrangement fan on which H induces a facet and define an orientation on $\mathcal{A}$ with that chamber as the base region, then H is basic in this oriented arrangement.

To give examples for these notions in the braid arrangement, we introduce some notation for permutations of the symmetric group. Every permutation of $[n]$ is uniquely determined by the pairs of numbers that do not occur in increasing order. This concept can be formalized as follows:

Definition 1.3.21 (Inversion of a Permutation)**.** Given a permutation $\pi \in \mathfrak{S}_n$, an **inversion** of π is a pair of values (π_a, π_b) such that $1 \leq a < b \leq n$ but $\pi_a > \pi_b$. The **inversion set** of a permutation is the set of all its inversions $\mathrm{Inv}(\pi) := \{(\pi_a, \pi_b) \mid 1 \leq a < b \leq n \text{ and } \pi_a > \pi_b\}$.

We note that the identity permutation has an empty inversion set, as the integers $1, 2, \ldots, n$ appear in order, while the opposite permutation $\pi = (n, \ldots, 2, 1)$ has $\binom{[n]}{2}$ as its inversion set, because every pair of integers is in reverse order.

Example 1.3.22 (The Oriented Braid Arrangement)**.** In the braid arrangement $\mathcal{A}_n$, the canonical choice of base region is $B = \{\mathbf{x} \in \mathbb{R}^n \mid \mathbf{x}_1 \leq \mathbf{x}_2 \leq \cdots \leq \mathbf{x}_n\}$. In terms of permutations, it corresponds to the identity permutation id, so $B = C(\mathsf{id}_n)$. It is spanned by the rays $C([k])$ for all $k \in [n]$. This is equivalent to orienting all hyperplanes $H_n(i, j)$ away from the point $(1, 2, \ldots, n)$ in B by setting the normal vectors $\mathbf{e}_j - \mathbf{e}_i$ whenever $i < j$.

We denote the oriented braid arrangement with this choice of base region by $\vec{\mathcal{A}}_n$. This choice induces an acyclic orientation on the edges of the permutahedron Perm_n, equivalent to ordering them along the direction $(1, 2, \ldots, n)$. Its basic hyperplanes are $H_n(k, k+1)$ for all $k \in [n-1]$.

Given a permutation $\sigma \in \mathfrak{S}_n$, the corresponding region $C(\sigma)$ of the braid arrangement has the representative point $\mathbf{p} = (\sigma^{-1}(1), \sigma^{-1}(2), \ldots, \sigma^{-1}(n))$. It is on the positive side of a hyperplane $H_n(i, j)$ if and only if $\mathbf{p}_i > \mathbf{p}_j$, which occurs exactly if $\sigma^{-1}(i) > \sigma^{-1}(j)$ or put differently, exactly if j occurs before i in σ, which was the definition of (j, i) being an inversion of σ. Therefore, the separation set of the region $C(\sigma)$ contains exactly the hyperplanes $H_n(i, j)$ for all inversions (j, i) of σ.

The orientation of an arrangement through the choice of a base region allows us to compare its regions and partially order them in the following way.

Definition 1.3.23 (Poset of Regions)**.** The **poset of regions** $\mathrm{Pos}(\vec{\mathcal{A}})$ of an oriented arrangement $\vec{\mathcal{A}}$ is the set of regions $\mathcal{R}(\mathcal{A})$ partially ordered by inclusion of separating sets, meaning that $R_1 \leq R_2$ if and only if $\mathrm{Sep}(R_1) \subseteq \mathrm{Sep}(R_2)$.

We note that the Hasse diagram of $\mathrm{Pos}(\vec{\mathcal{A}})$ is the vertex graph of any arrangement zonotope $\mathsf{Zono}(\mathcal{A})$. Furthermore, any choice of base region for $\mathcal{A}$ induces an acyclic orientation on the edges of $\mathsf{Zono}(\mathcal{A})$.

To determine the poset of regions of the braid arrangement, we first remark that the inversion sets defined above can be used to introduce a partial order on the symmetric group $\mathfrak{S}_n$ for a fixed n.

Definition 1.3.24 (Weak Order)**.** The **weak order** on the permutations of $\mathfrak{S}_n$ is the partial order defined by $\sigma \leq \sigma' \iff \mathrm{Inv}(\sigma) \subseteq \mathrm{Inv}(\sigma')$.

As we saw in Example 1.3.22, the inversion sets of permutations in $\mathfrak{S}_n$ are in bijection with the separating sets of regions in the oriented braid arrangement. In consequence, the poset of regions $\mathrm{Pos}(\vec{\mathcal{A}}_n)$ of the oriented braid arrangement is isomorphic to the weak order on $\mathfrak{S}_n$. See Figure 1.5 (left) for an illustration.

We will introduce one last concept connected to arrangement regions and separating sets. As every linear hyperplane is centrally symmetric with respect to $\mathbf{0}$, the same holds for an entire arrangement of linear hyperplanes. In consequence, the centrally reflected image of a region of $\mathcal{A}$ is another region of $\mathcal{A}$.

Definition 1.3.25 (Opposite Region)**.** Let $\mathcal{A}$ be an arrangement in $\mathbb{R}^n$. Given a region $R \in \mathcal{R}(\mathcal{A})$, the **opposite region** of R is the region $-R := \{\mathbf{x} \in \mathbb{R}^n \mid -\mathbf{x} \in R\}$.

Many properties of $-R$ are closely related to the properties of R. In particular, its sign vector is $\mathrm{sgn}_{\vec{\mathcal{A}}}(-R) = -\mathrm{sgn}_{\vec{\mathcal{A}}}(R)$ and its separating set is $\mathrm{Sep}(-R) = \mathcal{A} \backslash \mathrm{Sep}(R)$. In the oriented braid arrangement, the region opposite to $C(\sigma)$ is the region labeled by the permutation $(\sigma_n, \ldots, \sigma_2, \sigma_1)$ and its inversion set contains all pairs (j, i) with $1 \leq i < j \leq n$ such that $(j, i) \notin \mathrm{Inv}(\sigma)$.

1.4 Posets and Lattices

We will study the posets of regions of oriented hyperplane arrangements. For a more detailed overview of this topic, we refer to the survey [Rea16b], which we will largely follow in this section. We therefore introduce a number of definitions and concepts used to describe partially ordered sets. As any arrangement of finitely many hyperplanes has finitely many regions, any poset of regions we will encounter will have finitely many elements. This allows us to consider only partial orders on finite sets.

1.4.1 Posets

Definition 1.4.1 (Partial Order and Total Order)**.** Given a finite set S, a **partial order** on S is a binary relation $\leq$ which is

- reflexive ($x \leq x$ for every $x \in S$),
- transitive (if $x \leq y$ and $y \leq z$, then $x \leq z$),
- and antisymmetric (if $x \leq y$ and $y \leq x$, then $x = y$).

A partial order is called a **total order** if $\leq$ also is a total relation ($\forall x, y \in S : x \leq y$ or $y \leq x$).

- A **partially ordered set** (also called **poset**) $(S, \leq)$ is a set S with a partial order $\leq$ on S.
- A **totally ordered set** (also called **chain**) $(T, \leq')$ is a set T with a total order $\leq'$ on T.

We now define some key concepts for partially ordered sets.

Definition 1.4.2 (Poset Terminology)**.** Let $(S, \leq)$ be a finite poset. For $x, y \in S$ with $x \leq y$, the **interval** between x and y is $[x, y] := \{s \in S \mid x \leq s \leq y\}$. The **cover relations** of the poset are all intervals where $[x, y] = \{x, y\}$. We then write $x \prec y$ and say that y **covers** x. A poset is **bounded** if it has a unique minimal element $\hat{0}$ and a unique maximal element $\hat{1}$. A **chain** of the poset is a subset of S on which $\leq$ is a total order. The **length** of a chain is the number of its elements minus one (equivalently, its number of cover relations). A poset is **graded** if it is bounded and every maximal chain from $\hat{0}$ to $\hat{1}$ has the same length. The **rank** of a graded poset is the length of a chain from $\hat{0}$ to $\hat{1}$.

There is a canonical way to illustrate a poset by its cover relations, called the Hasse diagram. See Figure 1.5 (left) for an example, illustrating the weak order on $\mathfrak{S}_4$.

Definition 1.4.3 (Hasse Diagram)**.** A **Hasse diagram** of a finite poset $(S, \leq)$ is a drawing of the oriented graph with one vertex for each element of S and an edge from x to y directed upwards whenever y covers x.

The structure of permutations together with the definition of inversions allows us to describe the cover relations in the weak order.

Observation 1.4.4 (Cover Relations in the Weak Order)**.** The cover relations $\sigma \prec \pi$ of the weak order on $\mathfrak{S}_n$ are those pairs of permutations $\sigma, \pi \in \mathfrak{S}_n$ that differ only in two consecutive positions k and $k+1$, such that $\pi_{k+1} = \sigma_k < \sigma_{k+1} = \pi_k$. Then the inversion sets of σ and π differ only by the inversion of these entries, so that $\mathrm{Inv}(\pi) = \mathrm{Inv}(\sigma) \cup \{(\pi_k, \pi_{k+1})\}$.

With this partial order on permutations of $\mathfrak{S}_n$, we say that two permutations $\pi, \sigma \in \mathfrak{S}_n$ are **adjacent** if one covers the other in the weak order.

Definition 1.4.5 (Subposets and Superposets)**.** Let $(S, \leq)$ be a finite poset. Another poset $(S', \leq')$ is called a **subposet** of $(S, \leq)$ if $S' \subseteq S$ and $\leq' \subseteq \leq$ as relations (so that $x \leq' y$ implies $x \leq y$). In that case, $(S, \leq)$ is also called a **superposet** of $(S', \leq')$. If $\leq' = \leq \cap (S' \times S')$ (so $\leq'$ preserves all relations between elements of S'), then $(S', \leq')$ is called an **induced subposet** of $(S, \leq)$. A **linear extension** of a finite poset $(S, \leq)$ is any superposet of $(S, \leq)$ on the same set S that is a total order.

Example 1.4.6. The lexicographic order on the permutations of $\mathfrak{S}_n$ is a linear extension of the weak order: it is transitive, antisymmetric and a total relation and whenever $\pi \leq \pi'$ in the weak order, then $\pi \leq \pi'$ in lexicographic order, so the weak order is a subset of the lexicographic order.

Definition 1.4.7 (Upper Set and Lower Set)**.** Let $(S, \leq)$ be a partially ordered set. An **upper set** of $(S, \leq)$ is a subset $U \subseteq S$ such that whenever $x \in U$ and $x \leq y$, then $y \in U$ as well. Analogously, a **lower set** of $(S, \leq)$ is a subset $L \subseteq S$ such that whenever $x \in L$ and $z \leq x$, then $z \in L$ as well.

Such a set is also known as an upward closed set (resp. downward closed set). We remark that the complement of an upper set in a poset is a lower set and vice versa.

1.4.2 Lattices

We now introduce lattices as a special kind of posets. We remark that these lattices are not to be confused with lattices in the sense of grids (for example when looking at integer points in real space).

Definition 1.4.8 (Lattice)**.** A **lattice** is a finite poset $(L, \leq)$ where every two elements $x, y \in L$ have a unique minimal upper bound in L (called the **join** $x \vee y$) and a unique maximal lower bound in L (called the **meet** $x \wedge y$).

Figure 1.6: A mnemonic to tell join and meet apart. The join is associated to the symbol $\vee$ and is found somewhere above the elements in the Hasse diagram, while the meet is associated to the symbol $\wedge$ and is found somewhere below the elements in the Hasse diagram.

In particular, every lattice is bounded, as the meet of all elements is the unique minimal element and the join of all elements is the unique maximal element. The weak order on $\mathfrak{S}_n$ we introduced in the previous section is a lattice whose minimal element is the identity permutation and whose maximal element is the reverse permutation.

Definition 1.4.9 (Join-Irreducibles and Meet-Irreducibles)**.** Given a lattive $(L, \leq)$, an element $j \in L$ is called **join-irreducible** if it covers exactly one element. An element $m \in L$ is called **meet-irreducible** if it is covered by exactly one element.

To describe the join-irreducible elements in the weak order on $\mathfrak{S}_n$, we first need to define special pairs of entries of a permutation that are a special case of inversions of a permutation.

Definition 1.4.10 (Descent of a Permutation)**.** Given a permutation $\pi \in \mathfrak{S}_n$, a **descent** of π is a pair of consecutive entries (π_k, π_{k+1}) such that $\pi_k > \pi_{k+1}$. The descent set of a permutation is the set of all its descents $\mathrm{Desc}(\pi) := \{(\pi_k, \pi_{k+1}) \mid k \in [n-1] \text{ and } \pi_k > \pi_{k+1}\}$.

We can use a special notation for permutations with a single descent that will have further applications later.

Observation 1.4.11 (Permutations with a Single Descent)**.** A permutation $\sigma = (\sigma_1, \sigma_2, \ldots, \sigma_n)$ that has exactly one descent (σ_k, σ_{k+1}) can be written in the form $\pi_n(\ell, r, A, B)$, where we set $\ell = \sigma_{k+1}$ and $r = \sigma_k$, while $A = \{\sigma_i \mid 1 \leq i < k \text{ and } \sigma_i \in]\ell, r[\}$ is the set of all integers between ℓ and r that appear in σ before the descent , and $B = \{\sigma_j \mid k+1 < j \leq n \text{ and } \sigma_j \in]\ell, r[\}$ is the set of all integers between ℓ and r that appear in σ after the descent.

This notation can be used to introduce an illustration of a permutation with a unique descent, called an arc.

Definition 1.4.12 (Arc)**.** Given a permutation $\pi = \pi_n(\ell, r, A, B)$ with a unique descent, the **arc** associated to π is an x-monotone continuous curve from ℓ to r, wiggling around the horizontal axis and passing above the points of A and below the points of B.

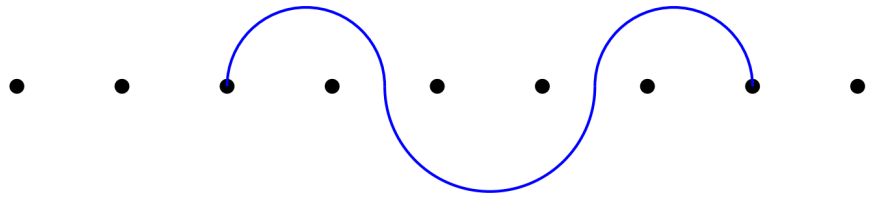

Figure 1.7: The arc corresponding to $\sigma = 124783569 \in \mathfrak{S}_9$. The nine dots represent the integers $1, 2, \ldots, 9$. The permutation σ has a single descent $(8, 3)$, (so the arc connects the dots 3 and 8), with 4 and 7 appearing before the descent (so the arc passes above the corresponding dots) and 5 and 6 appearing after the descent (so the arc passes below the corresponding dots).

Example 1.4.13. For example, the permutation $\sigma = 124783569 \in \mathfrak{S}_9$ has the unique descent $(8, 3)$. Here, the sets $A = \{4, 7\}$ and $B = \{5, 6\}$ contain those integers between 3 and 8 that appear in σ before resp. after the descent. Therefore, we can write $\sigma = \pi_9(3, 8, \{4, 7\}, \{5, 6\})$. See Figure 1.7 for an illustration of the associated arc.

Conversely, given $1 \leq \ell < r \leq n$ and disjoint sets $A, B \subseteq [n]$ such that $A \dot\cup B =]\ell, r[$, we can reconstruct a permutation $\pi_n(\ell, r, A, B)$ in the following way: It starts with entries $1, 2, \ldots, \ell - 1$, followed by the elements of A in increasing order, then by r and ℓ, next by the elements of B in increasing order and finally the numbers $r + 1, \ldots, n - 1, n$. A permutation constructed in this way always has exactly one descent, namely (r, ℓ).

These permutations with a single descent do not only have a special notation and illustration, they are in fact exactly the join-irreducible elements in the weak order on $\mathfrak{S}_n$.

Theorem 1.4.14 (Join-Irreducible Elements in the Weak Order)**.** *The join-irreducible elements of the weak order on $\mathfrak{S}_n$ are exactly those permutations that have a single descent.*

1.4.3 Join Representations

Join and meet of elements in a lattice can be used to describe an element of that lattice, stating that it is the join (resp. meet) of a certain set of other elements.

Definition 1.4.15 (Join and Meet Representations)**.** Given a lattice $(L, \leq)$ and an element $x \in L$, a **join representation** of x is a subset $J \subseteq L$ such that $x = \bigvee(J)$. The join representation is **irredundant** if for every strict subset $J' \subseteq J$, we have $x \neq \bigvee(J')$. A **meet representation** of x is a subset $M \subseteq L$ such that $x = \bigwedge(M)$. Irredundancy is defined analogously.

Every element x of a lattice L admits some trivial join representations: The set $\{y \in L \mid y \leq x\}$ of all elements of the lattice below x is a join representation of x. In general, this join representation is not irredundant, as the smaller set $\{x\}$ is another join representation of x. A more interesting kind of join representation occurs when it is irredundant but at the same time, the elements of the representation are as low in the lattice as possible.

Definition 1.4.16 (Canonical Join and Meet Representations)**.** The **canonical join representation** of x is an irredundant join representation $x = \bigvee(J)$ such that for any other irredundant join representation $x = \bigvee(J')$ and any element $j \in J$, there is some $j' \in J'$ such that $j \leq j'$. The **canonical meet representation** is defined analogously.

The elements in a canonical join representation of an element $x \in L$ are join-irreducible elements of L. In particular, the canonical join representation of x has only one element if and only if x is join-irreducible in L, in which case the canonical join representation is $x = \bigvee\{x\}$. Canonical representations do not exist in all lattices. In fact, the class of lattices which guarantees their existence has a dedicated name.

Definition 1.4.17 (Semidistributive Lattice)**.** A lattice is **semidistributive** if every element has a canonical join representation and a canonical meet representation.

The following statement certifies that canonical meet and join representations always exist in a poset of regions as soon as the underlying arrangement is simplicial.

Theorem 1.4.18 (Semidistributive Lattice of Regions)**.** *Let $\vec{\mathcal{A}}$ be an oriented simplicial arrangement. Then the poset of regions $\mathrm{Pos}(\vec{\mathcal{A}})$ is a semidistributive lattice.*

The braid arrangement is a simplicial arrangement. Together with the orientation induced by choosing the region of the identity permutation as base region, its poset of regions is the weak order. We can describe the canonical join representation of any permutation in $\mathfrak{S}_n$.

Observation 1.4.19 (Canonical Join Representations in the Weak Order)**.** The canonical join representation of any permutation σ is obtained by joining, for all descents (σ_k, σ_{k+1}) of σ, the permutations $\pi_n(\sigma_{k+1}, \sigma_k, A_k, B_k)$, where $A_k = \{\sigma_i \mid 1 \leq i < k \text{ and } \sigma_{k+1} < \sigma_i < \sigma_k\}$ is the set of integers between σ_{k+1} and σ_k that appear in σ before the descent (σ_k, σ_{k+1}) and where $B_k = \{\sigma_j \mid k+1 < j \leq n \text{ and } \sigma_{k+1} < \sigma_j < \sigma_k\}$ is the set of integers between σ_{k+1} and σ_k that appear after the descent (σ_k, σ_{k+1}).

In fact, multiple arcs as introduced in the previous section can be combined to give a unique representation of a permutation that allows us to directly read off its canonical join representation.

Definition 1.4.20 (Noncrossing Arc Diagram)**.** The arcs of two permutations $\pi_n(\ell_1, r_1, A_1, B_1)$ and $\pi_n(\ell_2, r_2, A_2, B_2)$ **cross** if the two associated curves cross in their interior. That is the case if and only if neither $A_1 \cap (\{\ell_2, r_2\} \cup B_2)$ nor $A_2 \cap (\{\ell_1, r_1\} \cup B_1)$ are empty. A **noncrossing arc diagram** is a collection of arcs such that no two of them cross, no two of them have the same left endpoint ℓ and no two of them have the same right endpoint r. We emphasize that the left endpoint of one arc may be the right endpoint of another arc in the same noncrossing arc diagram.

Example 1.4.21. The permutation $\sigma = 395284176 \in \mathfrak{S}_9$ has the five descents $(9,5)$, $(5,2)$, $(8,4)$, $(4,1)$ and $(7,6)$. Its canonical join representation is therefore $\sigma = 123495687 \vee 135246789 \vee 123584679 \vee 234156789 \vee 123457689$. See Figure 1.8 for an illustration of the associated arc diagram.

1.4.4 Lattice Congruences

Lattices allow a special kind of equivalence relation that respect the structure of meets and joins in the lattice.

Definition 1.4.22 (Lattice Congruence)**.** Given a lattice $(L, \leq)$ a **lattice congruence** on L is an equivalence relation $\equiv$ on L that preserves meets and joins. More formally, if $x_1 \equiv x_2$ and $y_1 \equiv y_2$, then $x_1 \wedge y_1 \equiv x_2 \wedge y_2$ and $x_1 \vee y_1 \equiv x_2 \vee y_2$.

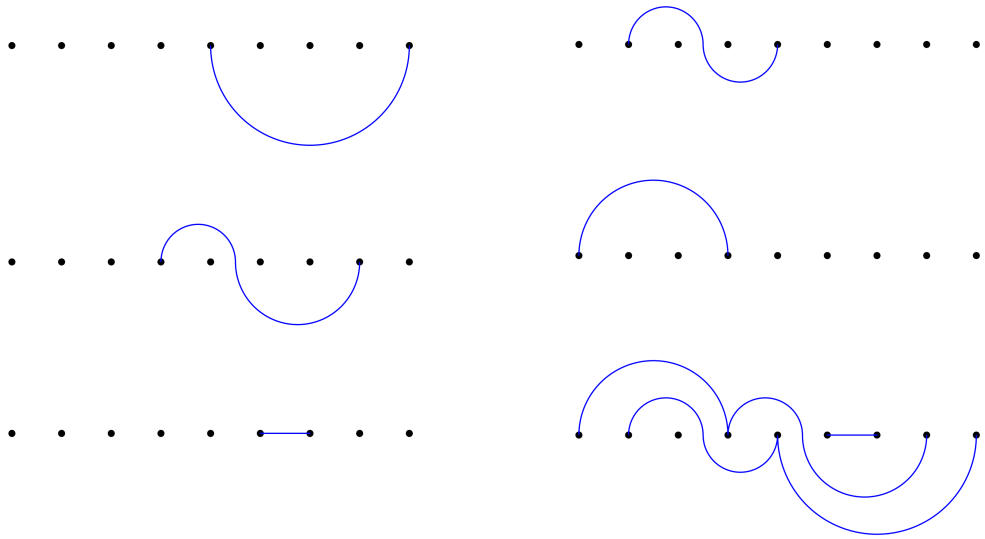

Figure 1.8: The arcs corresponding to 123495687 (top left), 135246789 (top right), 123584679 (center left), 234156789 (center right) and 123457689 (bottom left), all combined in the noncrossing arc diagram for $\sigma = 395284175$ (bottom right). We emphasize that no two arcs in a noncrosing arc diagram have the same left endpoint or the same right endpoint, but the left endpoint of one arc can be the right endpoint of another. This occurs whenever the permutation has two consecutive descents. In this example, the arcs representing the descents $(9, 5)$ and $(5, 2)$ touch in 5, and the arcs representing the descents $(8, 4)$ and $(4, 1)$ touch in 4.

Example 1.4.23 (Sylvester Congruence)**.** A well-known congruence on the weak order on $\mathfrak{S}_n$ is the **sylvester congruence**. It has one equivalence class for every binary tree with internal nodes labeled $1, 2, \ldots, n$ from left to right in inorder notation. Then each binary tree is interpreted as a partial order on $[n]$ where $x \leq y$ if and only if the node labeled x is below the node labeled y in the binary tree. The equivalence classes of the sylvester congruence are the sets of linear extensions of each of the binary trees. See Figure 1.9 for an illustration.

We remark that the equivalence classes of any lattice congruence are intervals in the lattice. Furthermore, the set of all congruences on the same lattice can be partially ordered by inclusion of their equivalence classes.

Definition 1.4.24 (Congruence Lattice)**.** Given a lattice $(L, \leq)$, the **congruence lattice** ConL is the set of all lattice congruences on L, partially ordered by $\equiv_1 \leq \equiv_2$ if and only if $\equiv_1 \subseteq \equiv_2$ as relations (or equivalently, if $x \equiv_1 y$ implies $x \equiv_2 y$ for any choice of elements $x, y \in L$).

Observation 1.4.25 (Top and Bottom Element of the Congruence Lattice)**.** The top and bottom element of the congruence lattice ConL are trivial equivalence relations on the elements of L: The top element is the trivial equivalence relation where there is only a single equivalence class containing all elements of L. The bottom element is the trivial equivalence relation where each element of L is the only element of its equivalence class.

So far, we only introduced ConL as a poset, but the following statement tells us that it is in fact a lattice, and provides the rules to construct meet and join of elements in ConL, which are congruences in L.

Theorem 1.4.26 (Meet and Join of Congruences)**.** *Given a lattice $(L, \leq)$, the congruence lattice* ConL *is a lattice. The meet of two congruences in* ConL *is their intersection. The join of two congruences in* ConL *is the transitive closure of their union.*

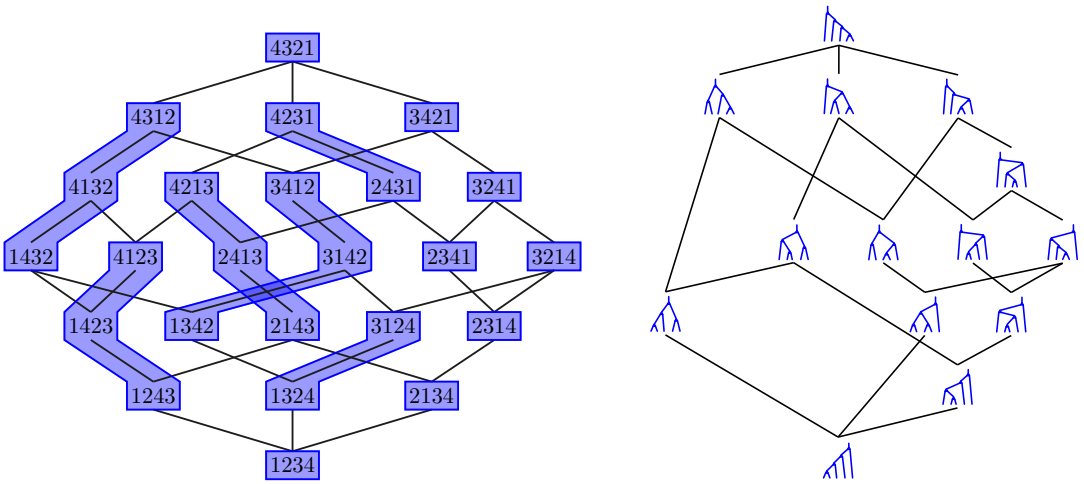

Figure 1.9: The sylvester congruence, illustrated by its equivalence classes on the weak order on $\mathfrak{S}_4$ (left), and the associated quotient lattice, which is known as the Tamari lattice, partially ordering the binary trees with 4 internal nodes (right). [Picture from [PS19]]

Definition 1.4.27 (Contraction)**.** Given a lattice $(L, \leq)$, and a join-irreducible $j \in L$, we denote by j_* the unique element of L covered by j. We say that a congruence $\equiv \in \mathrm{ConL}$ **contracts** j if $j \equiv j_*$. The **minimal congruence contracting** j is denoted by $\mathrm{con}(j)$. It is the meet in ConL of all those congruences $\equiv$ on L with $j \equiv j_*$.

As ConL is a lattice itself, it has join-irreducible elements. We will now see that these join-irreducibles of ConL are closely connected to the join-irreducibles of L.

Theorem 1.4.28 (Join-Irreducible Congruences)**.** *Given a lattice $(L, \leq)$, the join-irreducible elements of* ConL *are exactly the congruences of the form* $\mathrm{con}(j)$ *for some join-irreducible element $j \in L$.*

We remark that there is not necessarily a bijection as there might be distinct join-irreducible elements $j, j' \in L$ with the same minimal contracting congruence $\mathrm{con}(j) = \mathrm{con}(j')$. Neverthelesss, any lattice congruence is completely determined by the set of join-irreducibles it contracts.

Theorem 1.4.29 (Canonical Join Representation of a Congruence)**.** *Let $\equiv \in \mathrm{ConL}$ be a congruence on the lattice $(L, \leq)$ and let J be the set of join-irreducibles of L that are contracted by $\equiv$. Then the canonical join representation of $\equiv$ in* ConL *is* $\bigvee_{j \in J} \mathrm{con}(j)$.

Definition 1.4.30 (Forcing in ConL)**.** Given a lattice $(L, \leq)$, we call join-irreducibles $j, j' \in L$ **forcing-equivalent** if $\mathrm{con}(j) = \mathrm{con}(j')$. We say that j **forces** j' and write $j \to j'$, if we have $\mathrm{con}(j) \geq \mathrm{con}(j')$ in ConL. The **forcing order** $\geq_f$ is a partial order on forcing-equivalence classes of join-irreducible elements defined such that $j \geq_f j'$ if and only if $\mathrm{con}(j) \geq \mathrm{con}(j')$ in ConL. The lattice $(L, \leq)$ is called **congruence uniform** if no two distinct join-irreducibles of L are forcing-equivalent, so there is a bijection between the join-irreducible elements $j \in L$ and the join-irreducible congruences $\mathrm{con}(j) \in \mathrm{ConL}$.

We can view the forcing order as the subposet of ConL induced by join-irreducible congruences. The lower sets of this subposet completely determine the congruence lattice ConL.

Theorem 1.4.31 (Congruences and Forcing)**.** *Let $(L, \leq)$ be a lattice. Its congruence lattice* ConL *is isomorphic to the poset of lower sets in the forcing order, partially ordered by inclusion.*

In Section 1.5, we will apply all these notions and statements to the poset of regions of simplicial hyperplane arrangements in general and the braid arrangement in particular. For now, we will introduce one last lattice-theoretic concept: What happens if we use the partial order on L to partially order the equivalence classes of a lattice congruence $\equiv$ on L?

1.4.5 Quotient Lattices

Definition 1.4.32 (Quotient Lattice)**.** Given a lattice $(L, \leq)$ and a lattice congruence $\equiv$ on L, the **quotient lattice** $L/\equiv$ is the set of equivalence classes of $\equiv$, partially ordered by $C \leq C'$ if and only if there exist $x \in C$ and $x' \in C'$ with $x \leq x'$ in L. The meet $C \wedge C'$ (resp. join $C \vee C'$) of two $\equiv$-classes is the unique $\equiv$-class C^* that contains all the meets $x \wedge x'$ (resp. all the joins $x \vee x'$) for all $x \in C$ and $x' \in C'$.

The following theorem states that this partial order is not only well-defined, but that it is even a lattice with canonical join and meet representations (if the original lattice L had canonical join and meet representations).

Theorem 1.4.33 (Semidistributive Quotient Lattice)**.** *For a semidistributive lattice $(L, \leq)$ and a lattice congruence $\equiv$ on L, the quotient lattice $L/\equiv$ is a semidistributive lattice.*

The following statement tells us what the cover relations of the quotient lattice (equivalently, the edges of its Hasse diagram) look like.

Lemma 1.4.34 (Cover Relations of a Quotient Lattice)**.** *The cover relations of the quotient lattice $L/\equiv$ are $C \prec C'$ wherever there are $x \in C$ and $x' \in C'$ with $x \prec x'$ in L.*

Example 1.4.35 (Tamari Lattice)**.** For the lattice L of the weak order on $\mathfrak{S}_n$ and the sylvester congruence $\equiv$ on L, the quotient lattice $L/\equiv$ is the **Tamari lattice**. Its elements are the equivalence classes of $\equiv$, which are the binary trees with n internal nodes. Its cover relations are rotations in binary trees. See Figure 1.9 for an illustration of the Hasse diagram of the Tamari lattice labeled by the binary trees.

1.5 Quotients on the Poset of Regions

We will now apply the concepts of the previous section to the posets of regions of simplicial hyperplane arrangements. Once again, we follow the survey [Rea16b]. We already saw in Theorem 1.4.18 that any poset of regions of such an arrangement is a semidistributive lattice, guaranteeing the existence of canonical join representations. As these depend on join-irreducible elements of the lattice, we will first identify the geometric objects in an oriented arrangement corresponding to join-irreducible elements in the poset of regions. As we will see, these join-irreducibles are closely related to certain parts of the arrangement hyperplanes, called the shards of an oriented arrangement.

1.5.1 Shards

The name »shard« reminds us that we are »breaking the hyperplane, like a pane of glass, into pieces«, as remarked in [Rea16b]. See Figure 1.12 (center) for an illustration of the shards that the hyperplanes of the $\vec{\mathcal{A}}_3$ arrangement are broken into. To know how to construct these pieces in order to obtain meaningful objects, we need some further notions related to an oriented arrangement.

Definition 1.5.1 (Rank-Two Subarrangement)**.** Let $\vec{\mathcal{A}}$ be an oriented arrangement with base region B. Let $H_1, H_2 \in \mathcal{A}$ be two hyperplanes. The **rank-two subarrangement** induced by H_1 and H_2 is the oriented arrangement $\vec{\mathcal{A}}' := \left\{ H \in \vec{\mathcal{A}} \;\middle|\; H_1 \cap H_2 \subseteq H \right\}$ containing all hyperplanes of $\vec{\mathcal{A}}$ that contain the codimension-2 subspace $H_1 \cap H_2$. The **base region** of $\vec{\mathcal{A}}'$ is the unique region B' of $\vec{\mathcal{A}}'$ which is a superset of the base region B. The **basic hyperplanes** of $\vec{\mathcal{A}}'$ are those that are basic with respect to B'.

Definition 1.5.2 (Cutting Hyperplanes)**.** Let $\vec{\mathcal{A}}$ be an oriented arrangement. For two hyperplanes $H_1, H_2 \in \vec{\mathcal{A}}$, let $\vec{\mathcal{A}}'$ be their common rank-two subarrangement. We say that H_1 **cuts** H_2 if and only if H_1 is basic in $\vec{\mathcal{A}}'$ and H_2 is not basic in $\vec{\mathcal{A}}'$.

We are now ready to define the shards of an oriented hyperplane arrangement. Every hyperplane H is cut into pieces along each intersection with another hyperplane H' that cuts H.

Definition 1.5.3 (Shards)**.** Let $H \in \vec{\mathcal{A}}$ be a hyperplane. We denote by $\mathrm{Cut}(H)$ the set of all hyperplanes in $\vec{\mathcal{A}}$ that cut H. The **shards** of H are the closures of the connected complements of $H \setminus \bigcup \mathrm{Cut}(H)$. The shards of the arrangement $\vec{\mathcal{A}}$ are the shards of all the hyperplanes in $\vec{\mathcal{A}}$. Given a shard Σ, we denote by $H(\Sigma)$ the hyperplane that Σ is a shard of. Moreover, we denote the set of all shards of the arrangement $\vec{\mathcal{A}}$ by the symbol $\mathbf{\Sigma}(\vec{\mathcal{A}})$ and just write $\mathbf{\Sigma}$ whenever it is clear which oriented arrangement we are discussing.

To get a better understanding of these concepts, we will describe them in the oriented braid arrangement $\vec{\mathcal{A}}_n$.

Example 1.5.4 (Shards of the Braid Arrangement)**.** We recall that the hyperplanes of the braid arrangement are of the form $H_n(i,j) := \{\mathbf{x} \in \mathbb{R}^n \mid x_i = x_j\}$ for all $1 \leq i < j \leq n$. In the canonically oriented braid arrangement $\vec{\mathcal{A}}_n$, for any two hyperplanes $H_n(i_1, j_1)$ and $H_n(i_2, j_2)$,

- their rank-two subarrangement does not contain any other hyperplane if $|\{i_1, j_1, i_2, j_2\}| = 4$. In this case, both hyperplanes are basic, so neither of them cuts the other.
- If $i_1 = j_2$ (resp. $i_2 = j_1$), then the rank-two subarrangement also contains the hyperplane $H_n(i_2, j_1)$ (resp. $H_n(i_1, j_2)$), but this one is not basic in the subarrangement, while the two we started with are. Therefore, neither of them cuts the other.
- If $i_1 = i_2$ and $j_1 < j_2$ (resp. $i_2 < i_1$ and $j_1 = j_2$), then the rank-two subarrangement also contains the hyperplane $H_n(j_1, j_2)$ (resp. $H_n(i_2, i_1)$) which is basic in the subarrangement, while $H_n(i_2, j_2)$ is not. Therefore, the hyperplane $H_n(i_1, j_1)$ cuts the hyperplane $H_n(i_2, j_2)$.

In consequence, the hyperplane $H_n(i,j)$ is cut by all hyperplanes $H_n(i,k)$ and all hyperplanes $H_n(k,j)$ for all $k \in]i,j[$. The shards of $H_n(i,j)$ are the closures of the connected components that remain after removing the intersections with all these cutting hyperplanes. This means that for each cutting hyperplane, every shard of $H_n(i,j)$ is entirely contained in one of the two closed halfspaces induced by that cutting hyperplane. In particular, either $x_k \leq x_i = x_j$ or $x_i = x_j \leq x_k$ holds for each $k \in]i,j[$ and the shard is uniquely determined by the set of these decisions for all k.

The shards of the oriented braid arrangement $\vec{\mathcal{A}}_n$ are therefore all sets of the form $\Sigma_n(\ell, r, A, B)$ for all $1 \leq \ell < r \leq n$ and $A \dot\cup B =]\ell, r[$. We denote the set of all the shards of $\vec{\mathcal{A}}_n$ by the symbol $\mathbf{\Sigma}_n := \{\Sigma_n(\ell, r, A, B) \mid 1 \leq \ell < r \leq n \text{ and } A \dot\cup B =]\ell, r[\}$.

This notation for $\vec{\mathcal{A}}_n$ shards is very similar to the one we used previously to describe permutations with a single descent and their associated arcs. We will see their relation to the shards of the oriented braid arrangement in the following section. Before, we briefly mention that this notation allows us to concisely describe which rays of the braid arrangement lie on a certain shard. As shards are cut only along hyperplanes of the arrangement, any $\vec{\mathcal{A}}_n$ shard is equal to the convex hull of all the arrangement rays it contains.

1.5.2 Shards and Congruences

In this section, we examine the connection between the shards of an oriented arrangement and the lattice congruences on the poset of regions. The first step to achieve this is to associate to each shard a certain set of regions of the arrangement.

Definition 1.5.5 (Upper and Lower Regions and Shards)**.** Given an oriented arrangement $\vec{\mathcal{A}}$,

- an **upper region** of a shard Σ is a region $R \in \mathcal{R}(\mathcal{A})$ that intersects Σ in dimension $n-1$ and has $H_\Sigma \in \mathrm{Sep}(R)$. In that case, the shard Σ is called a **lower shard** of R.
- Analogously, a **lower region** of Σ is a region $R \in \mathcal{R}(\mathcal{A})$ that intersects Σ in dimension $n-1$ and has $H_\Sigma \notin \mathrm{Sep}(R)$. In that case, the shard Σ is called an **upper shard** of R.

The set of all upper regions of a shard Σ is denoted by $\mathrm{Upper}(\Sigma)$, while the set of all lower regions of Σ is denoted by $\mathrm{Lower}(\Sigma)$.

To provide some examples for these definitions, we return to the oriented braid arrangement $\vec{\mathcal{A}}_n$ We recall that the regions of that arrangement are in bijection with the permutations in $\mathfrak{S}_n$.

Example 1.5.6 (Lower Shards of a Braid Arrangement Region)**.** We set $\sigma = 395284176 \in \mathfrak{S}_9$ as in Example 1.4.21. Its five descents are $(9,5)$, $(5,2)$, $(8,4)$, $(4,1)$ and $(7,6)$. Let $R(\sigma) \in \mathcal{R}(\vec{\mathcal{A}}_9)$ be the region associated to σ in the poset of regions of $\vec{\mathcal{A}}_9$. The regions covered by $R(\sigma)$ are exactly those associated to a permutation in $\mathfrak{S}_9$ that can be obtained from σ by exchanging one of the descents of σ by the same two entries in ascending order.

For the descent $(8,4)$, the adjacent permutation π without that descent is $\pi = 395248176$. The facet separating $R(\sigma)$ from $R(\pi)$ is a part of the hyperplane $H_9(4,8)$. More precisely, the shard we cross is $\Sigma_9(4,8,\{5\},\{6,7\})$ as 5 appears before 4 and 8, while 6 and 7 appear after 4 and 8 in both σ and π. Therefore, the lower shards of $R(\sigma)$ are:

- $\Sigma_9(5,9,\emptyset,\{6,7,8\})$,
- $\Sigma_9(2,5,\{3\},\{4\})$,
- $\Sigma_9(4,8,\{5\},\{6,7\})$,
- $\Sigma_9(1,4,\{2,3\},\emptyset)$,
- $\Sigma_9(6,7,\emptyset,\emptyset)$.

Example 1.5.7 (Upper Regions of a Braid Arrangement Shard)**.** Given a shard $\Sigma := \Sigma_n(\ell, r, A, B)$ of the oriented braid arrangement $\vec{\mathcal{A}}_n$, the upper regions of Σ are given by all permutations with a descent (r,ℓ) such that all entries of A appear before it and all entries of B appear after it.

The following result connects the shards of an oriented arrangement to the join-irreducible regions of its poset of regions.

Theorem 1.5.8 (Shards and Join-Irreducibles)**.** *Let $\vec{\mathcal{A}}$ be an oriented simplicial arrangement and Σ be a shard of $\vec{\mathcal{A}}$. Then $\mathrm{Upper}(\Sigma)$ is a connected subposet of $\mathrm{Pos}(\vec{\mathcal{A}})$ whose unique minimal element is a join-irreducible of $\mathrm{Pos}(\vec{\mathcal{A}})$ denoted by J_Σ. Every join-irreducible region of $\mathrm{Pos}(\vec{\mathcal{A}})$ is J_Σ for a unique shard Σ of $\vec{\mathcal{A}}$.*

Example 1.5.9 (Shards and Arcs of the Braid Arrangement)**.** In the oriented braid arrangement $\vec{\mathcal{A}}_n$, the join-irreducible regions are exactly those regions associated to a permutation with a single descent. In Observation 1.4.11, we denoted such a permutation by $\pi_n(\ell, r, A, B)$ and subsequently illustrated such a permutation by a single arc.

In Example 1.5.4, we saw that we can describe all the shards of the arrangement by sets of the form $\Sigma_n(\ell, r, A, B)$, with the identical conditions $1 \leq \ell < r \leq n$ and $A \dot\cup B =]\ell, r[$. Now Theorem 1.5.8 explains the reason behind this: Every permutation $\pi_n(\ell, r, A, B)$ with a single descent is the unique minimal element among the upper regions of a shard and that shard is just obtained by using $\Sigma_n(\ell, r, A, B)$ with the same parameters n, ℓ, r, A, B.

Definition 1.5.10 (On Shards of the Braid Arrangement)**.** Let $\Sigma = \Sigma_n(\ell, r, A, B)$ be a shard of the braid arrangement. The **left endpoint** of Σ is ℓ and the **right endpoint** of Σ is r. The **length** of Σ is the difference $r - \ell$. The shard Σ is called an **up shard**, if $B = \emptyset$ (equivalently, if the associated arc passes above all points in between ℓ and r). It is called a **down shard**, if $A = \emptyset$ (equivalently, if the associated arc passes below all points in between ℓ and r). It is called a **mixed shard**, if it is neither an up shard nor a down shard (equivalently, if the associated arc crosses the axis).

In particular, the basic hyperplanes of the oriented braid arrangement are exactly its shards of length 1, namely all sets of the form $\Sigma_n(k, k+1, \emptyset, \emptyset)$ for all $k \in [n-1]$, which are equal to the hyperplanes $H_n(k, k+1)$.

Theorem 1.5.11 (Shards and Join Representations)**.** *Let $\vec{\mathcal{A}}$ be an oriented simplicial arrangement. The canonical join representation of a region $R \in \mathcal{R}(\mathcal{A})$ is $R = \bigvee \{J_\Sigma \mid R \in \mathrm{Upper}(\Sigma)\}$.*

Example 1.5.12 (Arcs in an Arc Diagram)**.** Theorem 1.5.11 explains why the lower shards of the region associated with the permutation $\sigma = 395284176$ in Example 1.5.6 are so similar to the arcs used in the join representation of the same permutation in Example 1.4.21. The canonical join representation of a region contains exactly those join-irreducibles whose corresponding shards are lower shards of the region.

Lemma 1.5.13 (Rays in an $\vec{\mathcal{A}}_n$ Shard)**.** *For any index set $\emptyset \subsetneq I \subsetneq [n]$, any $1 \leq \ell < r \leq n$ and any partition $A \dot\cup B =]\ell, r[$, the ray $C(I)$ lies in the shard $\Sigma_n(\ell, r, A, B)$ if and only if*

- *either $\ell, r \in I$ and $A \subseteq I$,*
- *or $\ell, r \notin I$ and $B \subseteq [n] \setminus I$.*

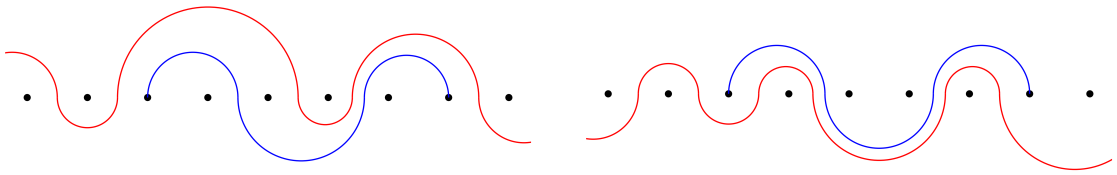

Figure 1.10: The shard $\Sigma_9(3, 8, \{4, 7\}, \{5, 6\})$, visualized by the arc in blue, together with two rays it contains, labeled by the index sets $I_1 = \{1, 3, 4, 5, 7, 8\}$ (visualized in red on the left) and $I_2 = \{2, 4, 7\}$ (visualized in red on the right).

The statement of Lemma 1.5.13 has a straightforward visualisation, given in Figure 1.10. We saw that every $\vec{\mathcal{A}}_n$ shard can be visualized by an arc. Similarly, we can represent an $\mathcal{A}_n$ ray labeled by an index set I by an arc from 0 to $n+1$ passing above all dots in I and below all dots in $[n] \setminus I$. Then the ray lies in the $\vec{\mathcal{A}}_n$ shard if and only if this line does not cross the arc associated to the shard.

1.5.3 Shards and Forcing

We will now analyze how we can describe forcing among congruences on the poset of regions of an oriented arrangement through its shards.

Definition 1.5.14 (Shard Digraph)**.** Let Σ_1, Σ_2 be two shards of $\vec{\mathcal{A}}$. We say that the shard Σ_2 **arrows** Σ_1 and write $\Sigma_2 \to \Sigma_1$ if and only if $H(\Sigma_2)$ cuts $H(\Sigma_1)$ and $\Sigma_1 \cap \Sigma_2$ has dimension $n-2$. The **shard digraph** for $\vec{\mathcal{A}}$ is the directed graph whose vertices are $\boldsymbol{\Sigma}(\vec{\mathcal{A}})$ with directed edges from Σ_2 to Σ_1 whenever Σ_2 arrows Σ_1.

These arrows allow us to describe forcing among the congruences in the following way.

Theorem 1.5.15 (Forcing Among Shards)**.** *Let $\vec{\mathcal{A}}$ be an oriented simplicial arrangement whose poset of regions is L. Let $\Sigma_1, \Sigma_2 \in \mathbf{\Sigma}(\vec{\mathcal{A}})$ be two distinct $\vec{\mathcal{A}}$ shards. Then $\mathrm{con}(J_{\Sigma_1}) \leq \mathrm{con}(J_{\Sigma_2})$ in the congruence lattice ConL if and only if there is a directed path from Σ_2 to Σ_1 in the shard digraph. In this case, we say that Σ_2 **forces** Σ_1.*

We will now exemplify these notions on the braid arrangement.

Example 1.5.16 (Forcing in the Braid Arrangement)**.** We introduced the shards of the braid arrangement $\vec{\mathcal{A}}_n$ in Example 1.5.4. We saw that the hyperplane $H_n(i,j)$ is cut by all hyperplanes $H_n(i,k)$ and $H_n(k,j)$ for all $k \in]i,j[$. For a shard $\Sigma_n(i,j,A,B)$ on the hyperplane $H_n(i,j)$, the only shard on $H_n(i,k)$ that intersects it in dimension $n-2$ is the shard $\Sigma_n(i,k,A \cap]i,k[\,, B \cap]i,k[)$. In consequence, the shard $\Sigma := \Sigma_n(\ell_1, r_1, A_1, B_1)$ forces the shard $\Sigma' := \Sigma_n(\ell_2, r_2, A_2, B_2)$ if and only if $\ell_2 \leq \ell_1 < r_1 \leq r_2$ and both $A_1 \subseteq A_2$ and $B_1 \subseteq B_2$. The special case where Σ arrows Σ' occurs if and only if additionally, they agree in either the left or the right endpoint.

We can visualise this through arcs: The $\vec{\mathcal{A}}_n$ shard $\Sigma := \Sigma_n(\ell_1, r_1, A_1, B_1)$ forces another $\vec{\mathcal{A}}_n$ shard $\Sigma' := \Sigma_n(\ell_2, r_2, A_2, B_2)$ if the endpoints of Σ are inside the endpoints of Σ' and the two arcs *agree* in between, meaning that for every dot in $]\ell_1, r_1[$, they either both pass above or both pass below. See Figure 1.11 (left) for an example of this visualisation.

The **shard poset** on $\vec{\mathcal{A}}_n$ is the set of all $\vec{\mathcal{A}}_n$ shards, partially ordered by forcing. Its minimal elements are the shards of the hyperplane $H_n(1,n)$ and its maximal elements are the basic hyperplanes $H_n(k,k+1)$ for all $k \in [n-1]$. See Figure 1.11 (right) for an illustration of the shard poset on $\vec{\mathcal{A}}_4$.

The weak order on $\mathfrak{S}_n$ (equivalently, the poset of regions of the braid arrangement) is a congruence uniform lattice. The congruences on that lattice are in bijection with the lower sets in the shard poset, as described in Theorem 1.4.31.

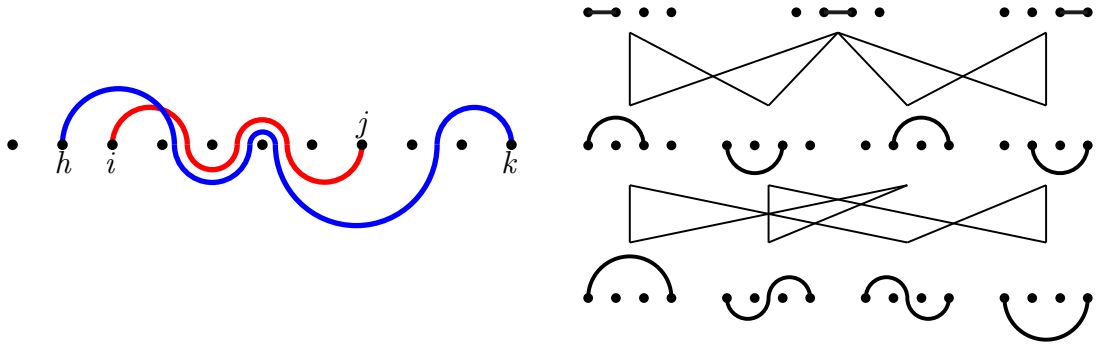

Figure 1.11: An example of forcing among shards of $\vec{\mathcal{A}}_n$ (left), illustrated by the red shard of the hyperplane $H_n(i,j)$ and the blue shard of $H_n(h,k)$. As $h \leq i < j \leq k$ and both arcs agree on $]i,j[$, the red shard forces the blue shard. On the right, the shard poset of the braid arrangement $\vec{\mathcal{A}}_4$. [Picture from [PS19]]

We recall from Definition 1.4.27 that a congruence $\equiv$ is said to contract a join-irreducible element j if $j \equiv j_*$. We introduce a similar term for the shard associated to that join-irreducible.

Definition 1.5.17 (Removing and Retaining Shards)**.** Given an oriented simplicial arrangement $\vec{\mathcal{A}}$ and a shard $\Sigma \in \mathbf{\Sigma}(\vec{\mathcal{A}})$, a congruence $\equiv$ on $\mathrm{Pos}(\vec{\mathcal{A}})$ **removes** the shard Σ, if $\equiv$ contracts J_Σ. Otherwise, $\equiv$ **retains** Σ. We denote the set of shards that $\equiv$ removes by $\mathbf{\Sigma}^{\times}_{\equiv}$ and the set of shards that $\equiv$ retains by $\mathbf{\Sigma}^{\checkmark}_{\equiv}$.

We remark that for any lattice congruence $\equiv$ on $\mathrm{Pos}(\vec{\mathcal{A}})$, the set $\mathbf{\Sigma}^{\times}_{\equiv}$ is a lower set in the forcing order and the set $\mathbf{\Sigma}^{\checkmark}_{\equiv}$ is an upper set in the forcing order. They are disjoint and their union is $\mathbf{\Sigma}(\vec{\mathcal{A}})$. We recall from Theorem 1.4.31 that the congruences on $\mathrm{Pos}(\vec{\mathcal{A}})$ are in bijection with the lower sets of shards they remove in the forcing order. Equivalently, the congruences on $\mathrm{Pos}(\vec{\mathcal{A}})$ are in bijection with the upper sets of shards they retain in the forcing order.

We now have assembled some translations between the geometry of the shards in an oriented simplicial arrangement and the combinatorics of a congruence in its lattice of regions. Next, we will study the geometric counterpart of a quotient lattice of the lattice of regions.

1.5.4 Quotient Fans

Theorem 1.5.18 (Quotient Fan)**.** *Let $\vec{\mathcal{A}}$ be an oriented simplicial arrangement and $\equiv$ be a congruence on $\mathrm{Pos}(\vec{\mathcal{A}})$. Then the closures of the connected components of $\mathbb{R}^n \setminus (\bigcup \Sigma)$ (where the union runs over all shards of $\vec{\mathcal{A}}$ retained by $\equiv$) are the maximal cones of a fan. We denote that fan by $\mathcal{F}_{\equiv}$ and call it the $\equiv$-**quotient fan** of $\vec{\mathcal{A}}$. Equivalently, the maximal cones of $\mathcal{F}_{\equiv}$ are each obtained by uniting all the regions contained in one equivalence class of $\equiv$.*

In particular, any quotient fan $\mathcal{F}_{\equiv}$ coarsens the arrangement fan $\mathcal{F}(\mathcal{A})$ (equivalently, the arrangement fan $\mathcal{F}(\mathcal{A})$ refines each quotient fan $\mathcal{F}_{\equiv}$).

We can describe the quotient fan $\mathcal{F}_{\equiv}$ by what we know about the congruence $\equiv$. We already learned about its chambers and we will later examine the rays of quotient fans derived from the braid arrangement. Here, we will describe the walls of a quotient fan built from any oriented simplicial arrangement.

Lemma 1.5.19 (Walls of the Quotient Fan)**.** *Every wall of the quotient fan $\mathcal{F}_{\equiv}$ is a subset of some shard $\Sigma \in \mathbf{\Sigma}^{\checkmark}_{\equiv}$ retained by $\equiv$.*

Proof. It follows from Theorem 1.5.18 that the union of the walls of the quotient fan is the union of all shards retained by $\equiv$. Assume for a contradiction that there is a wall w of $\mathcal{F}_{\equiv}$ that is not the subset of any retained shard. Then w is the union of multiple facets of $\mathcal{F}$ that are part of at least two different adjacent shards Σ_1, Σ_2 on the same hyperplane H. As these shards are adjacent, there has to be a hyperplane H' which cuts H and there is at least one shard Σ' on H' that intersects w in dimension $n-2$. Then Σ' forces at least one of Σ_1 and Σ_2 and therefore is retained in the quotient fan. But then w cannot be a wall of the quotient fan as its intersection with Σ' lies in the relative interior of w and is not a face of w, which is impossible as $\mathcal{F}_{\equiv}$ is a fan. □

To give an example of a quotient fan, we examine the fan that arises from the sylvester congruence that we introduced in Example 1.4.23.

Example 1.5.20 (Sylvester Fan)**.** For the sylvester congruence $\equiv$ and the associated quotient lattice $L/\equiv$ that is the Tamari lattice, the quotient fan $\mathcal{F}_{\equiv}$ is called the **sylvester fan**. It has

- a **chamber** $C(T)$ for each binary tree T on the nodes $[n]$, given by an $\mathcal{H}$-description as the set $C(T) = \{\mathbf{x} \in \mathcal{H}^n_\Sigma \mid \mathbf{x}_i \leq \mathbf{x}_j \text{ if } i \text{ is a descendant of } j \text{ in } T\}$,
- a **ray** $C(I)$ for each proper interval $I = [i, j] \subsetneq [n]$.

1.5.5 Quotientopes

We know that for every real central hyperplane arrangement, the arrangement fan is the normal fan of the arrangement zonotope $\mathsf{Zono}(n)$. For some quotient lattices $L/\equiv$ on the poset of regions L, the quotient fan $\mathcal{F}_{\equiv}$ is the normal fan of a polytope as well.

Example 1.5.21 (Associahedron)**.** There is a well-known polytope whose normal fan is the sylvester fan $\mathcal{F}_{\equiv}$, called the **associahedron** Asso_n. To give a suitable $\mathcal{V}$-description, we first introduce a notation for some numbers of leaves in a binary tree T, where the internal nodes are labeled in inorder (see [Lod04]).

- $\ell(T, j)$ denotes the number of leaves in the left subtree of the node j in T.
- $r(T, j)$ denotes the number of leaves in the right subtree of the node j in T.

Now the associahedron Asso_n can be defined equivalently as

- a $\mathcal{V}$-polytope that is the convex hull of the points $\sum_{j=1}^{n} \ell(T, j) \cdot r(T, j) \cdot \mathbf{e}_j$ for all binary trees T on n nodes (see [Lod04]),
- an $\mathcal{H}$-polytope that is the intersection of the sum-count hyperplane $\mathcal{H}_{\Sigma}^{n}$ with the halfspaces $\left\{ \mathbf{x} \in \mathbb{R}^n \;\middle|\; \sum_{k=i}^{j} \mathbf{x}_k \geq \binom{j-i+2}{2} \right\}$ for all intervals $[i, j] \subseteq [n]$ (see [SS93]),
- a translation of the Minkowski sum of the faces $\Delta_{[a,b]}$ (as introduced in Example 1.2.12) of the standard simplex Δ_{n-1} for all $1 \leq a \leq b \leq n$ (see [Pos09]).

We have seen one introductory example where the quotient fan is the normal fan of a polytope. The central question that arises in this context is the following: Given an oriented simplicial hyperplane arrangement and a quotient lattice of the poset of regions, is the resulting quotient fan the normal fan of a polytope? We will first give such polytopes a dedicated name.

Definition 1.5.22 (Quotientope)**.** Let $\vec{\mathcal{A}}$ be an oriented simplicial hyperplane arrangement and let $\equiv$ be a lattice congruence on $\mathrm{Pos}(\vec{\mathcal{A}})$. A polytope Q is called a **quotientope** for $\equiv$ if its normal fan $\mathcal{N}(\mathsf{Q})$ is equal to the quotient fan $\mathcal{F}_{\equiv}$.

We will now briefly introduce the results of [PS19] on quotientopes in the oriented braid arrangement $\vec{\mathcal{A}}_n$. They first defined a class of real-valued functions on the set of shards $\mathbf{\Sigma}_n$ of the $\vec{\mathcal{A}}_n$ arrangement.

Definition 1.5.23 (Forcing Dominant Function)**.** A function $f : \mathbf{\Sigma}_n \to \mathbb{R}_{>0}$ is called **forcing dominant** if $f(\Sigma) > \sum_{\Sigma'} f(\Sigma')$ (where the sum runs over all Σ' that force Σ) holds for any shard $\Sigma \in \mathbf{\Sigma}_n$.

We remark that such a forcing dominant function always exists, an explicit example for f being the function defined by $f(\Sigma) = n^{-(r-\ell)^2}$. Next, we define a function γ that takes as arguments an $\vec{\mathcal{A}}_n$ shard and a set representing an $\mathcal{A}_n$ ray and maps them to either zero or one.

Definition 1.5.24 (Shard Contribution)**.** Given a shard $\Sigma = \Sigma_n(\ell, r, A, B)$ and a set $\emptyset \subsetneq I \subsetneq [n]$, the **shard contribution** $\gamma(\Sigma, I)$ is defined to be 1 if both $|I \cap \{\ell, r\}| = 1$ and $A = I \cap]\ell, r[$, and 0 otherwise.

With these two definitions, one can construct a height function $\mathbf{h}$ for any fixed lattice congruence $\equiv$ on the lattice of regions of $\vec{\mathcal{A}}_n$ in the following way.

Definition 1.5.25 (f-Height)**.** Let $\equiv$ be a lattice congruence of the poset of regions $\mathrm{Pos}(\vec{\mathcal{A}}_n)$ and let $f : \mathbf{\Sigma}_n \to \mathbb{R}_{>0}$ be a forcing dominant function. Then $\mathbf{h}_f$ is the height function defined by $\mathbf{h}_f(I) := \sum_{\Sigma \in \mathbf{\Sigma}_n} f(\Sigma)\gamma(\Sigma, I)$ for any proper subset $\emptyset \subsetneq I \subsetneq [n]$.

This class of height functions satisfies all the wall-crossing inequalities of the quotient fan. In consequence, any such $\mathbf{h}_f$ induces a polytope whose normal fan is the quotient fan.

Theorem 1.5.26 (Quotientopes in the Braid Arrangement)**.** *Let $\equiv$ be a lattice congruence of the poset of regions $\mathrm{Pos}(\vec{\mathcal{A}}_n)$ and $\mathbf{h}_f$ be a height function constructed as above. Then the polytope $\mathsf{P}_{\mathbf{h}_f} := \{\mathbf{x} \in \mathbb{R}^n \mid \langle \mathbf{r}(I) \,|\, \mathbf{x} \rangle \leq \mathbf{h}_f(I)$ for all $\emptyset \subsetneq I \subsetneq [n]\}$ is a quotientope for $\equiv$.*

We will keep their result in mind, but aim to find a different approach to constructing quotientopes that is less dependent on the structure of the braid arrangement and can be generalized to other arrangement. For now, we will focus on the structure of the braid arrangement for a little longer.

1.6 Deformed Permutahedra and Removahedra

In this section, we will discuss the closed type cone of the braid fan $\mathcal{F}_n$. As the permutahedron is a zonotope of the braid arrangement, this type cone is also known as the deformation cone of the permutahedron. We will first describe the linear dependences that define the closed braid fan in Section 1.6.1. Next, we will use this to give a concise description of the deformation cone in Section 1.6.2. Then we will introduce a name for polytopes induced by the height functions in the boundary of the closed type cone in Section 1.6.3. In the final Section 1.6.4, we are particularly interested in those deformed permutahedra that are obtained by deleting facets from the permutahedron.

1.6.1 Linear Dependences in the Braid Fan

We recall that the rays of the braid fan $\mathcal{F}_n$ are labeled by all proper subsets $\emptyset \subsetneq I \subsetneq [n]$ and represented by ray vectors $\mathbf{r}(I) = |I|\,\mathbf{1} - n\mathbf{1}_I$. Furthermore, we set $\mathbf{r}(\emptyset) = \mathbf{r}([n]) = \mathbf{0}$ for convenience in notation. We recall that to describe the inequalities of the type cone, it is crucial to know the linear dependences that occur among the rays of adjacent chambers.

Lemma 1.6.1 (Linear Dependence Among Braid Fan Rays)**.** *Let $\emptyset \subsetneq I, J \subsetneq [n]$ be two proper subsets of $[n]$. Then ray vectors of the braid arrangement labeled by these sets satisfy the linear dependence $\mathbf{r}(I) + \mathbf{r}(J) = \mathbf{r}(I \cap J) + \mathbf{r}(I \cup J)$.*

With this knowledge, it is possible to describe the desired linear dependence for any pair of adjacent chambers of the braid fan.

Lemma 1.6.2 (Linear Dependence Among Braid Fan Chambers)**.** *Let σ, π be two adjacent permutations in $\mathfrak{S}_n$. Then their chambers $C(\sigma)$ and $C(\pi)$ in the braid fan $\mathcal{F}_n$ have $n-2$ rays in common. We fix $\emptyset \subsetneq I \subsetneq [n]$ and $\emptyset \subsetneq J \subsetneq [n]$ such that $C(I)$ is the ray of $C(\sigma)$ not in $C(\pi)$ and $C(J)$ is the ray of $C(\pi)$ not in $C(\sigma)$. Then the unique linear dependence among the ray vectors of the cones $C(\sigma)$ and $C(\pi)$ is $\mathbf{r}(I) + \mathbf{r}(J) = \mathbf{r}(I \cap J) + \mathbf{r}(I \cup J)$.*

Example 1.6.3. In $\mathcal{A}_3$, the permutations $\mathsf{id} = 123$ and $\pi = 213$ are adjacent. We know from Example 1.3.10 that the rays of the region $C(123)$ are labeled by the index sets $\{1\}$ and $\{1,2\}$, while the rays of the region $C(213)$ are labeled by the index sets $\{2\}$ and $\{1,2\}$. In particular, the ray of $C(\mathsf{id})$ not in $C(\pi)$ is labeled by $I = \{1\}$ and the ray of $C(\pi)$ not in $C(\mathsf{id})$ is labeled by $J = \{2\}$. Their linear dependence is $\mathbf{r}(\{1\}) + \mathbf{r}(\{2\}) = \mathbf{r}(\{1,2\}) + \mathbf{0}$, which checks out as $(-2,1,1) + (1,-2,1) = (-1,-1,2)$.

Another permutation adjacent to $\mathsf{id} = 123$ is $\sigma = 132$. There, we obtain $\{1,2\}$ as label of the ray of $C(\mathsf{id})$ not in $C(\sigma)$ and $\{1,3\}$ as label of the ray of $C(\sigma)$ not in $C(\mathsf{id})$. This gives us $\mathbf{r}(\{1,2\}) + \mathbf{r}(\{1,3\}) = \mathbf{r}(\{1\})$ (see Figure 1.12). We remark that in both these examples, either $I \cap J$ or $I \cup J$ is not a proper subset. The first cases which are not degenerate in this sense appear in the braid fan $\mathcal{F}_4$. As an example, the cones $C(4132)$ and $C(4312)$ are adjacent and their linear dependence is given by $\mathbf{r}(\{3,4\}) + \mathbf{r}(\{1,4\}) = \mathbf{r}(\{4\}) + \mathbf{r}(\{1,3,4\})$ (see Figure 1.13).

1.6.2 Submodular Functions

The closed type cone of the braid fan, also known as the deformation cone of the permutahedron, has been studied in detail in [Pos09] and [PRW08]. We use our knowledge about the linear dependences in the braid fan from the previous section to give a concise description.

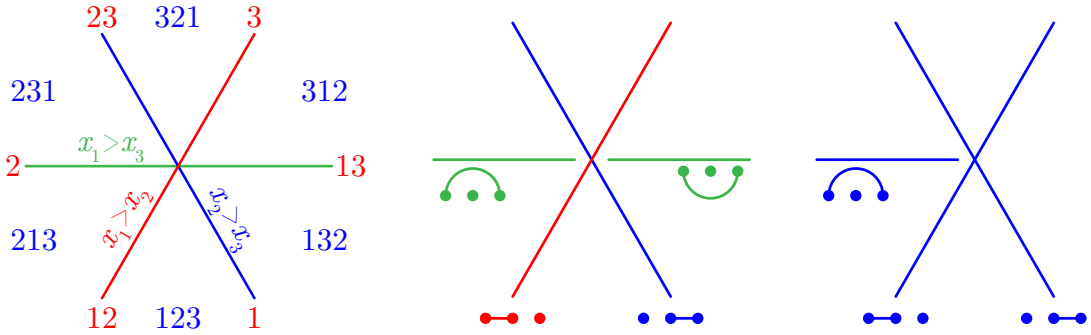

Figure 1.12: The braid fan $\mathcal{F}_3$ with rays labeled in red, chambers labeled in blue and hyperplanes labeled with inequalities (left), the four shards of the oriented arrangement (with base region 123) labeled by their arcs (center), and the quotient fan for the sylvester congruence (right). [Picture from [PS19]]

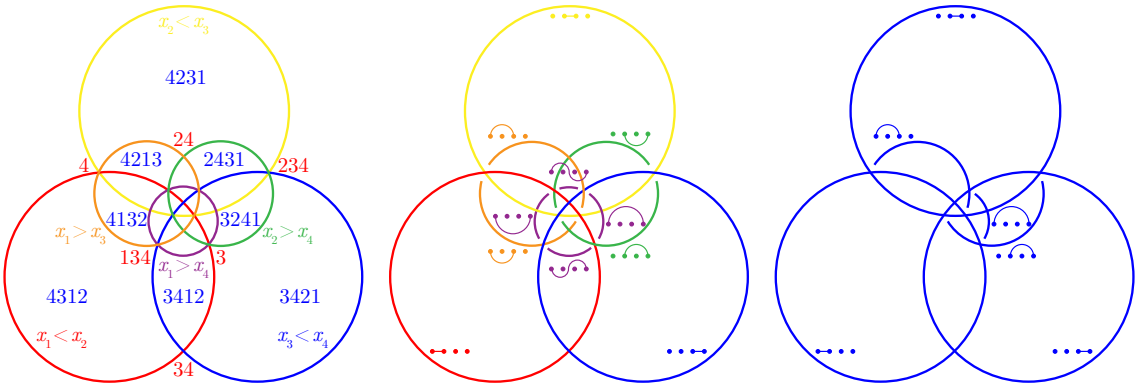

Figure 1.13: A stereographic projection of the braid fan $\mathcal{F}_4$ from a point opposite to the region labeled 1234, with some rays labeled in red, some chambers labeled in blue and some hyperplanes labeled with inequalities (left), all 11 shards of the oriented arrangement (with base region 1234) labeled by their arcs (center), and the quotient fan for the sylvester congruence (right). [Picture from [PS19]]

Definition 1.6.4 (Submodular Inequalities and Functions)**.** Let $n \in \mathbb{N}$ and $X, Y \subseteq [n]$ be subsets of $[n]$. The **submodular inequality** for X and Y is $f(X) + f(Y) \geq f(X \cup Y) + f(X \cap Y)$. A real-valued function $f : 2^{[n]} \to \mathbb{R}$ on subsets of $[n]$ is called a **submodular function** if it satisfies the submodular inqualities for all $X, Y \subseteq [n]$. It is called **strictly submodular** if it satisfies all the corresponding strict inequalities.

The following classical statement follows from Theorem 1.2.28 and Lemma 1.6.2. We recall that we can naturally identify a vector $\mathbf{h}$ in the type cone, whose entries correspond to ray vectors of the braid fan $\mathcal{F}_n$, with a function $\mathbf{h} : 2^{[n]} \to \mathbb{R}_{\geq 0}$ with $\mathbf{h}(\emptyset) = \mathbf{h}([n]) = 0$.

Theorem 1.6.5 (Closed Type Cone of the Braid Fan)**.** *The closed type cone of the braid fan $\mathcal{F}_n$ is the set of functions $\mathbf{h} : 2^{[n]} \to \mathbb{R}_{\geq 0}$ which are submodular and satisfy $\mathbf{h}(\emptyset) = \mathbf{h}([n]) = 0$. The facets of $\overline{\mathsf{TC}(\mathcal{F}_n)}$ correspond to those submodular inequalities where $|I \setminus J| = |J \setminus I| = 1$.*

As the normal fan of the permutahedron (as we constructed it in Example 1.3.15) is the braid fan, it is induced by a height function which lies in this type cone. We will now introduce its height function and show that it is indeed submodular.

Example 1.6.6 (Height Function of the Permutahedron)**.** The permutahedron Perm_n was defined in Example 1.3.15 as a $\mathcal{V}$-polytope. Therefore, it is induced by the height function which, given a ray vector $\mathbf{r}(I)$ of the braid fan, asks which of the vertices has the largest scalar product with that ray vector. As the ray vector $\mathbf{r}(I)$ is of the form $|I|\,\mathbf{1} - n\mathbf{1}_I$, this scalar product is maximized at any vertex where σ has its $|I|$ smallest entries in those coordinates indexed by I. In any such vertex, the scalar product $\langle \mathbf{r}(I) \,|\, \sigma \rangle$ adds a $|I|$ for every integer from 1 to n and subtracts an n for every integer from 1 to $|I|$. We deduce the following explicit height function denoted by $\mathbf{h}_\circ$:

$$\mathbf{h}_\circ(I) = \max_{\sigma \in \mathfrak{S}_n} \langle \mathbf{r}(I) \,|\, \sigma \rangle = |I| \binom{n+1}{2} - n\binom{|I|+1}{2} = \tfrac{n}{2} \cdot |I|\,(n - |I|).$$

To verify that this height function is submodular, we observe that

$$\mathbf{h}_\circ(I) + \mathbf{h}_\circ(J) - \mathbf{h}_\circ(I \cup J) - \mathbf{h}_\circ(I \cap J) = n \cdot |J \setminus I| \cdot |I \setminus J| \geq 0.$$

1.6.3 Deformed Permutahedra

With the help of submodular functions, we described the closed type cone of the permutahedron. We recall that only the height functions in the open type cone yield a polytope with the desired normal fan, while those in the boundary yield polytopes with different normal fans that coarsen the normal fan of the permutahedron. We will give this class of polytopes a dedicated name.

Definition 1.6.7 (Deformed Permutahedron)**.** A polytope P whose normal fan $\mathcal{N}(\mathsf{P})$ coarsens the braid fan $\mathcal{F}_n$ for some $n \in \mathbb{N}$ is called a **deformed permutahedron**.

We remark that in particular, any quotientope on the braid arrangement is a deformed permutahedron since the quotient fan $\mathcal{F}_{\equiv}$ coarsens the braid fan $\mathcal{F}_n$ by definition.

Observation 1.6.8 (Deformed Permutahedra and Submodular Functions)**.** Up to translation, any deformed permutahedron is given by $\mathsf{Defo}_{\mathbf{h}} := \left\{ \mathbf{x} \in \mathcal{H}^n_\Sigma \;\middle|\; \sum_{i \in I} \mathbf{x}_i \leq \mathbf{h}(I) \text{ for all } \emptyset \subsetneq I \subsetneq [n] \right\}$ for some submodular function $\mathbf{h} : 2^{[n]} \to \mathbb{R}_{\geq 0}$.

We use the term *deformed permutahedron* instead of the term *generalized permutahedron* as used by A. Postnikov in [Pos09] and [PRW08]. There are different ways to generalize a class of polytopes, and the expression *deformed permutahedron* is more precise to describe the special kind of generalization obtained by coarsening the normal fan.

1.6.4 Removahedra

We will now see a particular class of deformed permutahedra. We characterize these polytopes by the way we obtain their fan which coarsens the braid fan, as is the case for all deformed pemutahedra, but does so in a special way.

Definition 1.6.9 (Removahedron)**.** A deformed permutahedron P which can be obtained by deleting inequalities in an $\mathcal{H}$-description of the permutahedron Perm_n is called a **removahedron**.

We can use the following convenient notation for removahedra.

Observation 1.6.10 ($\mathcal{H}$-Description for Removahedra)**.** Any removehedron can be written as $\mathsf{Remo}_{\mathcal{I}} := \left\{ \mathbf{x} \in \mathcal{H}^n_\Sigma \;\middle|\; \sum_{i \in I} \mathbf{x}_i \leq \mathbf{h}_\circ(I) \text{ for all } I \in \mathcal{I} \right\}$ for the height function $\mathbf{h}_\circ$ of the permutahedron Perm_n and some family $\mathcal{I}$ of proper subsets $\emptyset \subsetneq I \subsetneq [n]$ for some $n \in \mathbb{N}$.

We remark that the combinatorial type of the removahedron depends not only on the choice of family $\mathcal{I}$, but also on the choice of height function, where choosing an arbitrary $\mathbf{h} \in \mathsf{TC}(\mathcal{F}_n)$

would not necessarily yield the same polytope as the one obtained by removing inequalities from the standard permutahedron Perm_n. While the term removahedron is used to describe a polytope, we will also give a special name to normal fans and lattice congruences appearing in the context of a removahedron.

Definition 1.6.11 (Removahedral Fans and Congruences)**.** A fan $\mathcal{G}$ with rays $\{\mathbf{r}(I) \mid I \in \mathcal{I}\}$ is called **removahedral** if it is the normal fan of the removahedron $\mathsf{Remo}_{\mathcal{I}}$. A lattice congruence $\equiv$ of the weak order is called **removahedral** if its quotient fan $\mathcal{F}_{\equiv}$ is a removahedral fan.

We remark that while removahedra and removahedral fans are in bijection, not all removahedral fans (and thus not all removahedra) are induced by a removahedral congruence on the poset of regions of the braid arrangement.

Example 1.6.12. For example, in the permutahedron Perm_4 illustrated in Figure 1.5 (right), the vertices corresponding to the permutations $1324, 1342, 3124$ and 3142 span a facet. Removing the inequality that defines this facet yields a removahedron, and its normal fan is a removahedral fan. On the other hand, any lattice congruence $\equiv$ of the poset of regions of $\vec{\mathcal{A}}_n$ (and thus of the weak order on $\mathfrak{S}_n$) that considers 1324 and 3124 to be equivalent (they are separated by the down shard connecting 1 and 3) has to consider 1423 and 3123 to be equivalent as well (they are separated by the down shard connecting 1 and 4) due to the rules of forcing. Therefore, the removahedral fan we just constructed cannot be obtained as the quotient fan of any removahedral congruence.

This motivates the name **quotientopal removahedron** for those removahedra that are quotientopes of some removahedral congruence. As we just saw, not all removahedra are quotientopal, and this is the case in particular for all unbounded removahedra as the definition of a removahedron does not require the resulting polyhedron to be a polytope.

Example 1.6.13 (Removahedra)**.** We already know some examples of removahedra.

- The permutahedron Perm_n itself is a trivial removahedron obtained by removing none of the inequalities at all.
- The associahedron Asso_n can be obtained as a removahedron by removing exactly those inequalities that do not correspond to an interval $[i, j] \subseteq [n]$.
- The graph associahedron Asso_G (as described in [CD06, Dev09]) is a removahedron if and only if the graph G is chordful (meaning that every cycle induces a clique, see [Pil17]).

We remark that there are lattice congruences of the weak order on $\mathfrak{S}_n$ which are not removahedral congruences.

Example 1.6.14 (Non-Removahedral Congruence)**.** We consider the congruence $\equiv$ of $\mathfrak{S}_4$ which removes only one shard, namely $\Sigma_4(1, 4, \{2\}, \{3\})$. This removed shard does not contain any ray in its interior, so the rays of the associated quotient fan $\mathcal{F}_{\equiv}$ are exactly the rays of the original braid fan $\mathcal{F}_n$. In consequence, the removahedron corresponding to this quotient fan is the permutahedron Perm_4 whose normal fan is different from $\mathcal{F}_{\equiv}$.

We will move on to another class of removahedra in the next section.

1.7 Permutrees

Permutrees are combinatorial objects introduced in [PP17] that generalize and interpolate between permutations and binary trees. They appear naturally in the context of congruences on the weak order.

1.7.1 Basics

To define permutrees, we start with some definitions on oriented trees.

Definition 1.7.1 (Ancestry in Trees)**.** Let T be an oriented tree and j be a node of T.
- A **parent** of j is an outgoing neighbor of j.
- A **child** of j is an incoming neighbor of j.
- An **ancestor subtree** of j is a connected components of $T \setminus \{j\}$ containing a parent of j.
- A **descendant subtree** of j is a connected components of $T \setminus \{j\}$ containing a child of j.

These definitions allow us to define permutrees in the following way:

Definition 1.7.2 (Permutree)**.** A **permutree** is an oriented tree T with nodes $[n]$ such that
- every node has exactly one or two parents and exactly one or two children,
- if node $j \in [n]$ has two parents, then
  - all nodes in the left ancestor subtree of j are smaller than j,
  - all nodes in the right ancestor subtree of j are larger than j,
- and if node $j \in [n]$ has two children, then
  - all nodes in the left descendant subtree of j are smaller than j,
  - all nodes in the right descendant subtree of j are larger than j.

The definition of permutrees allow us to enforce the following conventions when drawing them:
- The edges are oriented from bottom to top (so children are below and parents are above).
- The nodes in $[n]$ appear from left to right in ascending order.
- We draw an auxiliary vertical red wall
  - below each node with two children (separating the left and right descendant subtrees),
  - above each node with two children (separating the left and right ancestor subtrees).

Definition 1.7.3 (Permutree Decorations)**.** In a drawing of a permutree, we represent a node by one of the following symbols, depending on the number of parents and children of a node.
- the symbol ⏀ for a node with one parent and one child,
- the symbol ☮ for a node with one parent and two children,
- the symbol ⚲ for a node with two parents and one child,
- the symbol ⊗ for a node with two parents and two children.

The sequence of these symbols for the nodes $1, \dots, n$ is called the **decoration** δ of T. The **length** of the decoration δ is n. For a given permutree T,
- the set $\delta^- := \{j \in [n] \mid \delta_j = ☮ \text{ or } ⊗\}$ contains all nodes with exactly two children,
- the set $\delta^+ := \{j \in [n] \mid \delta_j = ⚲ \text{ or } ⊗\}$ contains all nodes with exactly two parents.

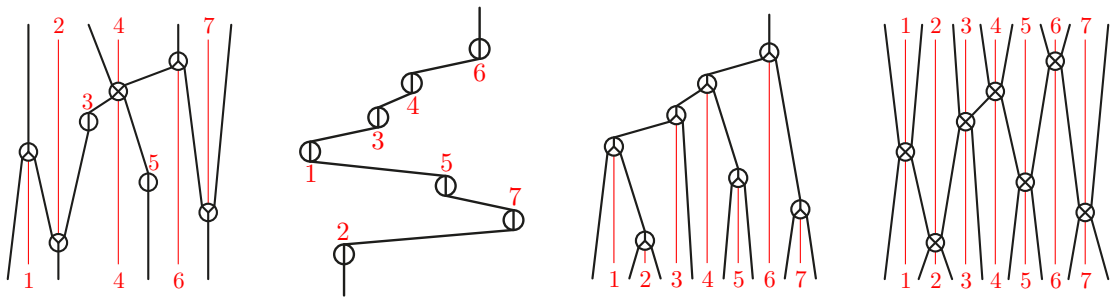

Figure 1.14: Four examples of permutrees. While the left one is a generic one for the decoration ☮⚲⏀⊗⏀☮⚲, the other three use specific decorations corresponding to permutations ($⏀^7$), binary trees ($☮^7$), and binary sequences ($⊗^7$). [Picture from [APR20]]

Observation 1.7.4 (Special Permutrees)**.** Permutrees generalize several combinatorial concepts.
- Permutrees with decoration $\delta = \textcircled{\scriptsize I}^n$ correspond to permutations on $\mathfrak{S}_n$.
- Permutrees with decoration $\delta = \textcircled{\scriptsize /}^n$ correspond to binary trees with n internal nodes.
- Permutrees with decoration $\delta = \otimes^n$ correspond to binary sequences of length n.

Examples for these three special cases as well as the general case are illustrated in Figure 1.14.

Definition 1.7.5 (Permutree Edge Cut)**.** Let T be a permutree and $i \to j$ be an oriented edge of T. An **edge cut** $(I \parallel J)$ in T is a partition of the nodes $[n]$ of T into the two connected components I and $J := [n] \setminus I$ obtained after removing the edge from $i \in I$ to $j \in J$.

These edge cuts will prove useful to describe the geometry of the permutree fan defined later.

1.7.2 Permutree Lattices

Similarly to the standard rotation on binary trees, there is a local operation on δ-permutrees which reverses the orientation of one edge and rearranges the endpoints of two other edges.

Definition 1.7.6 (Permutree Rotation)**.** Let T be a permutree with decoration δ. Fix an edge $i \to j$ in T. We label a descendant subtree D and an ancestor subtree U as follows:
- We set D to be the descendant subtree of node i (the **right** one if $i \in \delta^-$).
- We set U to be the ancestor subtree of node j (the **left** one if $j \in \delta^+$).

We obtain a new oriented tree S from T by reversing the orientation of $i \to j$, attaching the subtree U to i and attaching the subtree D to j. This transformation from T to S is called the **rotation** of the edge $i \to j$.

The following statement shows that the result of a rotation is always another δ-permutree. Put differently, the set of δ-permutrees is closed under permutree rotations.

Theorem 1.7.7 (Edge Cuts of Adjacent Permutrees)**.** *Let T be δ-permutree and let $i \to j$ be an edge in T. Then the tree S resulting from the rotation of $i \to j$ is a δ-permutree as well. Moreover, S has the same edge cuts as T except for the cut defined by $i \to j$, and S is the unique δ-permutree with that property.*

For a fixed decoration δ, we can define an orientation on the δ-permutree rotations, which yields a directed graph on the set of δ-permutrees.

Definition 1.7.8 (Increasing Permutree Rotations)**.** Let T and S be two δ-permutrees which differ only by a single rotation of an edge with endpoints $i < j$. If that edge is directed $i \to j$ in T and $j \to i$ in S, then the rotation from T to S is called an **increasing rotation**. The **increasing rotation graph** for δ is the directed graph whose vertices are the δ-permutrees and whose directed edges are increasing rotations.

The following statement shows that the transitive closure of this directed graph is not only a partial order on the set of δ-permutrees, but even a lattice. Two examples of such permutree lattices are illustrated in Figure 1.15.

Theorem 1.7.9 (Permutree Lattice)**.** *Let δ be a permutree decoration. The transitive closure of the increasing rotation graph on δ-permutrees is a lattice. It is called the δ-**permutree lattice**.*

Observation 1.7.10 (Special Permutree Lattices)**.** Just as permutrees generalize permutations, binary trees and binary sequences, the permutree lattices obtained from certain permutree decorations generalize some well-known lattices.
- For $\delta = \textcircled{\scriptsize I}^n$, the δ-permutree lattice is the lattice of the weak order.
- For $\delta = \textcircled{\scriptsize /}^n$, the δ-permutree lattice is the Tamari lattice.
- For $\delta = \otimes^n$, the δ-permutree lattice is the Boolean lattice.
- For $\delta \in \{\textcircled{\scriptsize /}, \textcircled{\scriptsize \reflectbox{/}}\}^n$, the δ-permutree lattice is a Cambrian lattice (see [Rea06]).

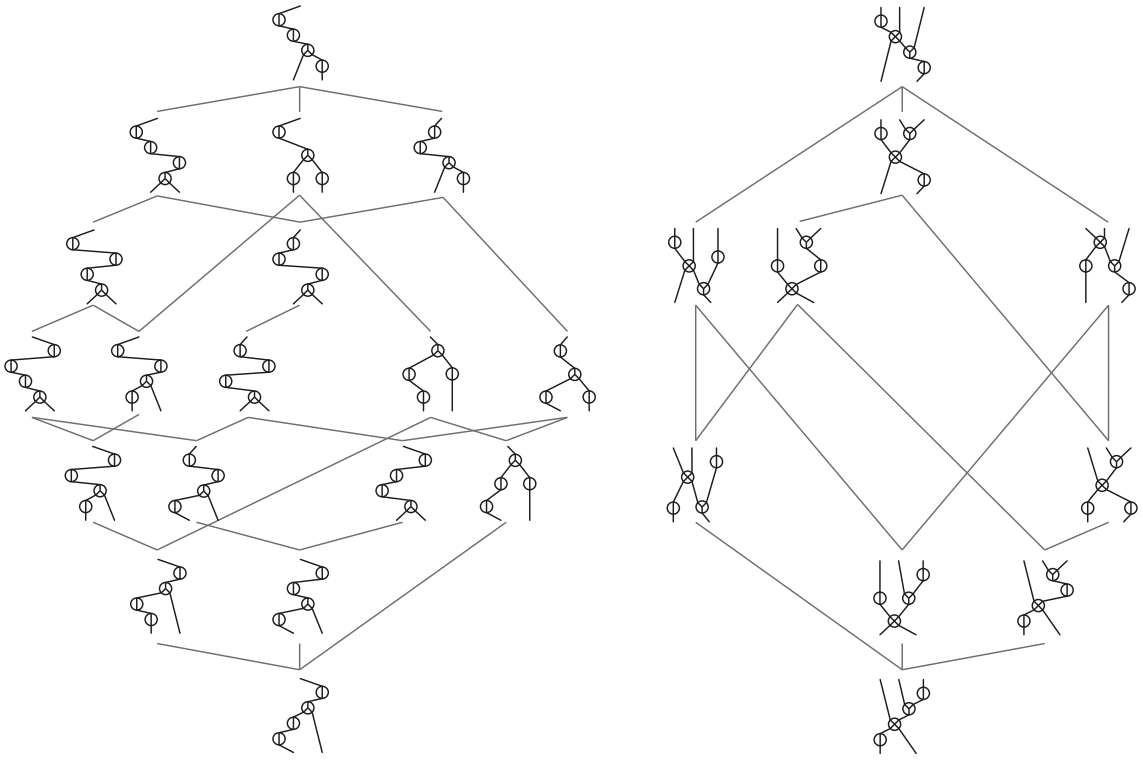

Figure 1.15: The δ-permutree lattices, for two decorations of length 4, namely $\delta = ⦶⦶⦶⦶$ (left) and $\delta = ⦶⊗⊗⦶$ (right). [Picture from [PP17]]

All these examplary δ-permutree lattices are quotient lattices of the weak order. In fact, every permutree lattice for a decoration of length n is a quotient lattice of the weak order on $\mathfrak{S}_n$, as we will see in the following section.

1.7.3 Permutree Congruences

The δ-permutree lattices form a special subclass of quotient lattices of the weak order. They can be described in the following way:

Definition 1.7.11 (Permutree Congruence)**.** Let $\delta \in \{⦶, ⦵, ⊗, ⊗\}^n$ be a permutree decoration. The **δ-permutree congruence** $\equiv_\delta$ is the equivalence relation on the weak order on $\mathfrak{S}_n$ whose equivalence classes are the sets of linear extensions of the δ-permutrees (similar to the construction in Example 1.4.23).

The following statement tells us that these equivalence relations are in fact lattice congruences.

Theorem 1.7.12 (Permutree Quotient)**.** *Let δ be a permutree decoration of length n. Then the δ-permutree congruence is a lattice congruence of the weak order on $\mathfrak{S}_n$ and the associated quotient lattice $\mathfrak{S}_n/\equiv_\delta$ is isomorphic to the δ-permutree lattice.*

Futher equivalent definitions of permutree congruences, using tree insertions or rewriting rules on words, can be found in [PP17]. For now, we are more interested in describing a permutree congruence by the shards $\mathbf{\Sigma}^{\checkmark}_{\equiv_\delta}$ it retains.

Observation 1.7.13 (Shards of a Permutree Congruence)**.** We know that every lattice congruence on the weak order is defined uniquely by the set of shards that it retains. Given a permutree decoration δ, the set of shards retained by $\equiv_\delta$ are those shards $\Sigma_n(\ell, r, A, B)$ with $1 \leq \ell < r \leq n$ and $\delta^- \cap]\ell, r[\subseteq A$ and $\delta^+ \cap]\ell, r[\subseteq B$.

The arcs corresponding to these shards are those with left endpoint ℓ and right endpoint r that do not pass below any $k \in \delta^-$ and do not pass above any $k \in \delta^+$, as can be visualised through the impenetrable vertical red walls below all $k \in \delta^-$ and above all $k \in \delta^+$.

Observation 1.7.14 (Special Permutree Congruences)**.** Regardless of the description we use, these permutree congruences generalize other well-known congruences on the weak order.

- For $\delta = \text{◫}^n$, the congruence $\equiv_\delta$ is the trivial congruence.
- For $\delta = \text{✇}^n$, the congruence $\equiv_\delta$ is the sylvester congruence (see [HNT05]).
- For $\delta = \otimes^n$, the congruence $\equiv_\delta$ is the hypoplactic congruence (see [KT97], [Nov00]).
- For $\delta \in \{\text{✇}, \text{⍒}\}^n$, the congruence $\equiv_\delta$ is a Cambrian congruence (see [Rea06]).

See Figure 1.16 for illustrations of the sets of retained shards for some permutree congruences.

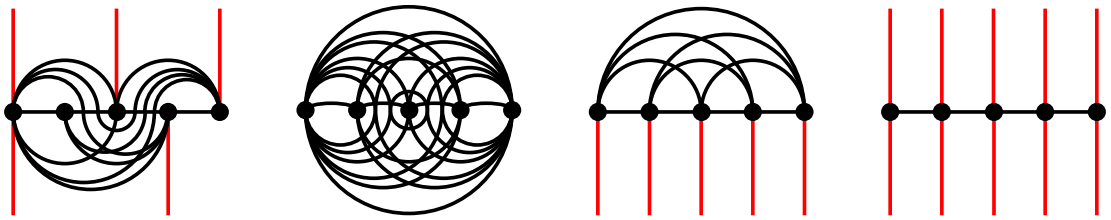

Figure 1.16: Four sets of retained shards of a permutree congruence, illustrated by their arcs. The leftmost one is generic and corresponds to the permutree decoration ⊗◫⍒✇⍒. The three others illustrate the decoration ◫^5 (corresponding to permutations) the decoration ✇^5 (corresponding to binary trees) and the decoration $\otimes^5$ (corresponding to binary sequences). [Picture from [APR20]]

We can use the retained shards to determine whether a congruence is induced by a permutree.

Theorem 1.7.15 (Generators of a Permutree Congruence)**.** *Let $\equiv$ be a lattice congruence on the weak order on $\mathfrak{S}_n$. The following are equivalent:*

- *$\equiv$ is a permutree congruence.*
- *All forcing-maximal removed shards in $\mathbf{\Sigma}^\times_\equiv$ are of length 2 (so all of them are shards of the form $\Sigma_n(i-1, i+1, \emptyset, \{i\})$ or $\Sigma_n(i-1, i+1, \{i\}, \emptyset)$ for some $1 < i < n$).*

There is a straightforward partial order on the decoration symbols which allows us to partially order permutree decorations.

Definition 1.7.16 (Refinement of Permutree Decorations)**.** There is a natural partial order on the symbols $\{\text{◫}, \text{✇}, \text{⍒}, \otimes\}$ that is induced by increasing number of parents and children and is denoted by $\preccurlyeq$. The cover relations are $\text{◫} \preccurlyeq \text{✇}, \text{⍒}$ and $\text{✇}, \text{⍒} \preccurlyeq \otimes$. Let $\delta, \delta' \in \{\text{◫}, \text{✇}, \text{⍒}, \otimes\}^n$ be two decorations of the same length. Then δ **refines** δ' (written: $\delta \preccurlyeq \delta'$) if for all $i \in [n]$, the symbols of δ and δ' in position i satisfy $\delta_i \preccurlyeq \delta'_i$.

We can use this partial order on decorations to partially order the associated congruences.

Observation 1.7.17 (Refinement of Permutree Congruences)**.** Let $\delta, \delta' \in \{\text{◫}, \text{✇}, \text{⍒}, \otimes\}^n$ be two decorations of the same length. Then the refinement relation on decorations implies inclusion of the associated lattice congruences on the weak order L. If δ refines δ', then $\delta \leq \delta'$ in $\mathrm{Con}L$, so for any two permutations $\sigma, \pi \in \mathfrak{S}_n$, the equivalence $\sigma \equiv_\delta \pi$ implies $\sigma \equiv_{\delta'} \pi$.

1.7.4 Permutree Fans

In the previous subsection, we have seen that every permutree decoration of length n induces a quotient lattice of the weak order on $\mathfrak{S}_n$. As seen in section Section 1.5.4, every quotient lattice induces a polyhedral fan called the quotient fan. We can now describe this fan:

Definition 1.7.18 (Permutree Fan)**.** Let δ be a permutree decoration. The **δ-permutree fan** $\mathcal{F}_\delta$ is the quotient fan associated to the δ-permutree lattice congruence $\equiv_\delta$.

To describe the rays and chambers of the permutree fan $\mathcal{F}_\delta$, we first recall the description of braid fan chambers and rays from Example 1.3.10. As the rays are labeled by proper subsets of $[n]$, we will determine which of them are rays of the permutree fan through the index sets they are labeled with.

Definition 1.7.19 (Index Sets Compatible with a Permutree)**.** Let $\delta \in \{\textcircled{\scriptsize /}, \textcircled{\scriptsize \backslash}, \textcircled{\scriptsize Y}, \otimes\}^n$ be a permutree decoration of length n. A proper subset $\emptyset \subsetneq I \subsetneq [n]$ is called **compatible** with δ if both of the following hold for all $k \in [n]$.

- If $k \in \delta^- \setminus I$, then $k < \min(I)$ or $\max(I) < k$.
- If $k \in \delta^+ \cap I$, then $k < \min([n] \setminus I)$ or $\max([n] \setminus I) < k$.

We denote by $\mathcal{I}_\delta$ the collection of all index sets compatible with δ.

The following result connecting compatible index sets and permutree rays is a consequence of Corollary 2.2.6, which we will prove later.

Corollary 1.7.20 (Rays of a Permutree Fan)**.** The rays of the permutree fan $\mathcal{F}_\delta$ are the rays $r(I)$ for all index sets I compatible with δ.

Next, we will describe the chambers of the permutree fan. As the fan coarsens the braid fan, each chamber is a union of chambers of the braid fan. The following statement helps us determine which chambers of the braid fan are united to obtain the permutree fan for a fixed decoration δ.

Observation 1.7.21 (Chambers of a Permutree Fan)**.** The chambers of $\mathcal{F}_\delta$ are in bijection with the δ-permutrees. The chamber corresponding to a δ-permutree T can be equivalently described

- as the union of the chambers $C(\sigma)$ for all permutations σ that are linear extensions of T,
- as the intersection of the halfspaces defined by $x_i \leq x_j$ for all edges $i \to j$ of T,
- as the conical hull of the rays $|I| \cdot \mathbf{1}_J - |J| \cdot \mathbf{1}_I$ for all edge cuts $(I \parallel J)$ of T.

See Figure 1.17 for an illustration of two exemplary permutree fans and their chambers.

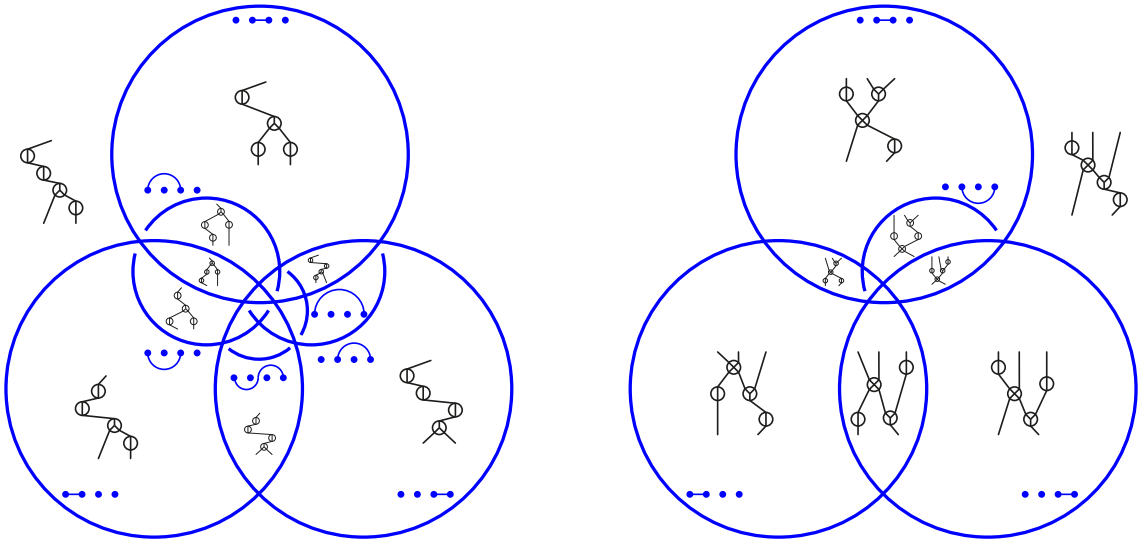

Figure 1.17: The permutree fans $\mathcal{F}_{\textcircled{\scriptsize /}\textcircled{\scriptsize /}\otimes\textcircled{\scriptsize \backslash}}$ (left) and $\mathcal{F}_{\textcircled{\scriptsize /}\otimes\textcircled{\scriptsize Y}\textcircled{\scriptsize \backslash}}$ (right). Each shard is labeled with its corresponding arc, and some chambers are labeled with their corresponding permutree. [Picture from [APR20]]

As was the case with permutree congruences and permutree lattices, some special cases of permutree fans turn out to be well-known fans or ones that are particularly easy to construct.

Observation 1.7.22 (Special Permutree Fans)**.** The permutree fans include some well-known fans for particular decorations:

- If $\delta = ⦶^n$, the permutree fan $\mathcal{F}_\delta$ is the braid fan $\mathcal{F}_n$.
- If $\delta \in \{⦵, ⊘\}^n$, the permutree fans $\mathcal{F}_\delta$ are the type A Cambrian fans (see [RS09]).
- If $\delta \in \{⦶, ⊗\}^n$, the permutree fan $\mathcal{F}_\delta$ is the fan of the arrangement defined by the hyperplanes $\{\mathbf{x} \in \mathbb{R}^n \mid x_i = x_j\}$ for those $1 \le i < j \le n$ where $\delta_k = ⦶$ for all $k \in]i, j[$.
- If $\delta = ⊗^n$, then $\mathcal{F}_\delta$ is the fan of the arrangement of $\{\mathbf{x} \in \mathbb{R}^n \mid x_i = x_{i+1}\}$ for all $i \in [n-1]$.

Finally, we observe that refinement of permutree decorations as defined in Definition 1.7.16 translates to refinement of permutree fans.

Observation 1.7.23 (Refinement of Permutree Fans)**.** Let $\delta, \delta' \in \{⦶, ⦵, ⊘, ⊗\}^n$ be two decorations of the same length. If $\delta \preccurlyeq \delta'$, then the δ-permutree fan $\mathcal{F}_\delta$ refines the δ'-permutree fan $\mathcal{F}_{\delta'}$.

1.7.5 Permutreehedra

Following the established path from a congruence to a quotient lattice to a quotient fan to a quotientope, we will now describe the quotientopes for permutree congruences, called permutreehedra. We first introduce some numbers for a δ-permutree that are useful to describe these polytopes.

Definition 1.7.24 (Subtree Numbers for a Permutree)**.** Let T be a δ-permutree and j be a node of T. The following numbers describe the number of nodes in certain subtrees of j in T:

- $d(T, j)$ is the number of nodes in the descendant subtrees of j in T,
- $\overline{\ell}(T, j)$ is the number of nodes in the left ancestor subtree of j in T,
- $\overline{r}(T, j)$ is the number of nodes in the right ancestor subtree of j in T,
- $\underline{\ell}(T, j)$ is the number of nodes in the left descendant subtree of j in T,
- $\underline{r}(T, j)$ is the number of nodes in the right descendant subtree of j in T,
- $n(T, j) := 1 + d(T, j) + \underline{\ell}(T, j)\underline{r}(T, j) - \overline{\ell}(T, j)\overline{r}(T, j)$ is calculated from these numbers.

With the help of these numbers, we give two equivalent definitions of the δ-permutreehedron.

Definition 1.7.25 (Permutreehedron)**.** Let $\delta \in \{⦶, ⦵, ⊘, ⊗\}^n$ be a permutree decoration of length n. The **δ-permutreehedron** PT_δ is the polytope defined equivalently as

- the convex hull of the points $\sum_{j=1}^n n(T, j)\mathbf{e}_j$ for all δ-permutrees T,
- the intersection of the sum-count hyperplane $\mathcal{H}^n_\Sigma = \left\{\mathbf{x} \in \mathbb{R}^n \;\middle|\; \sum_{i=1}^n x_i = \binom{n+1}{2}\right\}$ with the halfspaces $\left\{\mathbf{x} \in \mathbb{R}^n \;\middle|\; \sum_{i \in I} x_i \ge \binom{|I|+2}{2}\right\}$ for all index sets $I \in \mathcal{I}_\delta$ compatible with δ.

We find illustrations for two examples of permutreehedra in Figure 1.18. The following statement tells us that a δ-permutreehedron is a quotientope for the δ-permutree congruence on the weak order.

Theorem 1.7.26 (Permutreehedra are Quotientopes)**.** *Let δ be a permutree decoration. The δ-permutree fan $\mathcal{F}_\delta$ is the normal fan of the δ-permutreehedron PT_δ.*

Observation 1.7.27 (Special Permutreehedra)**.** The permutreehedra Perm_n include some well-known polytopes for particular decorations.

- If $\delta = ⦶^n$, then PT_δ is the permutahedron Perm_n.
- If $\delta = ⦵^n$, then PT_δ is J.-L. Loday's associahedron Asso_n (see [SS93, Lod04]).
- If $\delta \in \{⦵, ⊘\}^n$, then PT_δ is a Hohlweg-Lange associahedron Asso_δ (see [HL07, LP18]).
- If $\delta = ⊗^n$, then PT_δ is the parallelpiped with directions $\mathbf{e}_i - \mathbf{e}_{i+1}$ for all $i \in [n-1]$.
- If $\delta \in \{⦶, ⊗\}^n$, then PT_δ is the graphical zonotopes $\mathsf{Zono}(n)_\delta$ generated by those vectors $\mathbf{e}_i - \mathbf{e}_j$ where $1 \le i < j \le n$ with $\delta_k = ⦶$ for all $k \in]i, j[$.

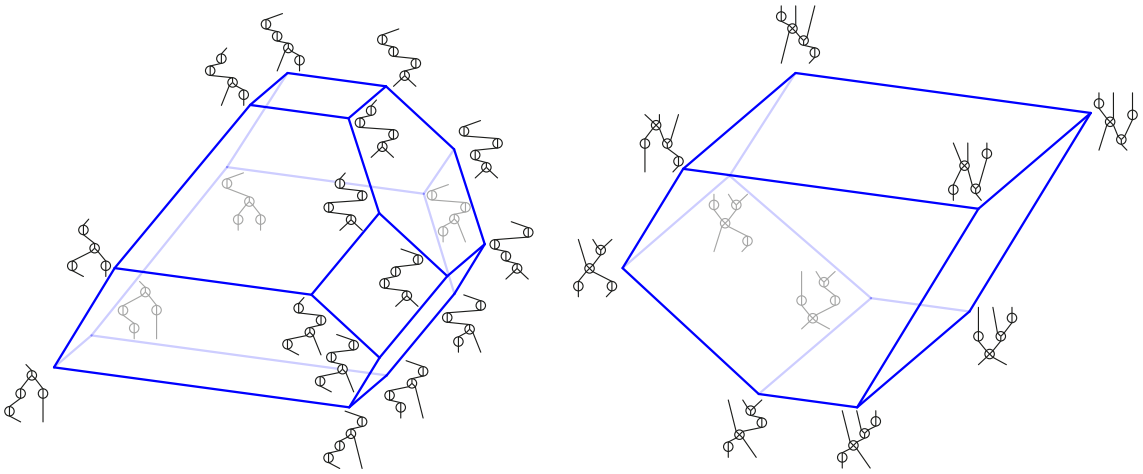

Figure 1.18: The permutreehedra $\mathsf{PT}_{\text{◐◐◑◐}}$ (left) and $\mathsf{PT}_{\text{◐⊗◒◐}}$ (right). The vertices are labeled by the permutrees for the respective decoration. [Picture from [PP17]]

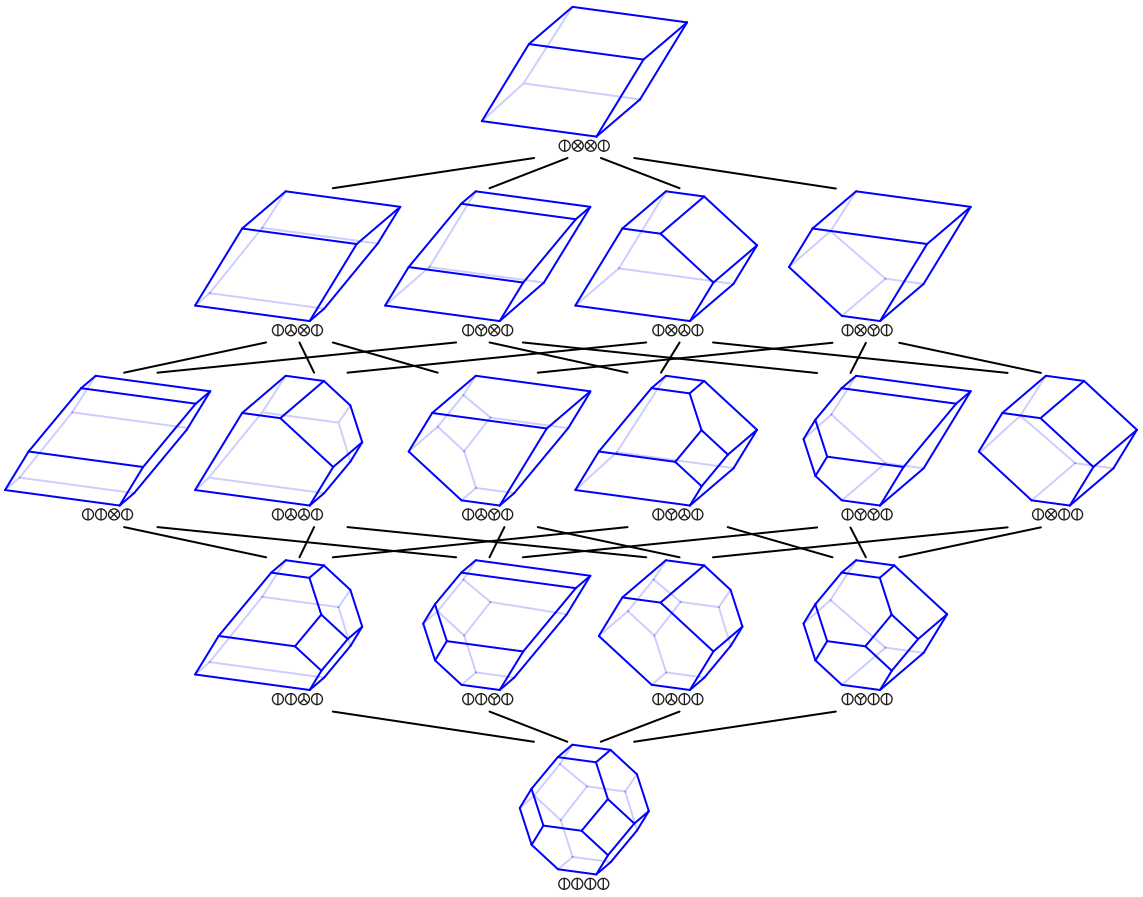

Figure 1.19: The δ-permutreehedra, for all decorations $\delta \in \{◐\} \times \{◐, ◒, ◒, ⊗\}^2 \times \{◐\}$. [Picture from [PP17]]

Finally, refinement of permutree decorations as defined in Definition 1.7.16 also translates to a kind of refinement among permutreehedra.

Observation 1.7.28 (Refinement of Permutreehedra)**.** Let $\delta, \delta' \in \{\textcircled{\scriptsize I}, \textcircled{\scriptsize /}, \textcircled{\scriptsize Y}, \otimes\}^n$ be two decorations of the same length. If $\delta \preccurlyeq \delta'$, then the δ'-permutreehedron $\mathsf{PT}_{\delta'}$ is obtained from the δ-permutreehedron PT_δ by deleting inequalities in the facet description of PT_δ.

We recall that $\textcircled{\scriptsize I}^n$ is the finest among the permutree decorations of length n. The associated permutree congruence is the trivial congruence where every element is a singleton in its equivalence class. The associated permutree lattice is the weak order on $\mathfrak{S}_n$ itself. Therefore, the permutree fan is the braid fan $\mathcal{F}_n$ and the associated permutreehedron is the permutahedron Perm_n. As any permutree decoration of length n is refined by $\textcircled{\scriptsize I}^n$, any permutreehedron can be obtained from the permutahedron by deleting inequalities. See Figure 1.19 for an illustration of the permutreehedra, partially ordered by refinement of the underlying permutree decorations, or equivalently, by inclusion of the sets of facet inequalities of the permutahedron to be deleted. This can be rephrased in the following way:

Corollary 1.7.29 (Permutree Congruences are Removahedral)**.** All permutree congruences are removahedral congruences.

2 Quotientopes and Removahedra

In this chapter, we will make some observations about congruences of the weak order on $\mathfrak{S}_n$ (or equivalently, on the lattice of regions of the braid arrangement $\vec{\mathcal{A}}_n$). We will describe the rays and chambers of a quotient fan, using the established notation and illustration through arcs. We will use these results to describe the rays of a permutree fan and prove that all permutree congruences are removahedral congruences. Finally, we will describe the type cone of a permutree fan.

To prepare these results, we first argue that we can restrict our analysis to a certain kind of congruences that cannot be described as the combination of simpler congruences in lower dimensional arrangements.

2.1 Essential Congruences

We first introduce the notion of polygons in a lattice. They are intervals with a special property. We first review in Section 2.1.1 their definition and two results established in [Rea16b] before proving some new results in Section 2.1.2.

2.1.1 Basics

Definition 2.1.1 (Polygonal Lattices)**.** Let L be a finite lattice. A **polygon** in L is an interval $[x, y]$ that is equal to the union of two maximal chains C_1 and C_2 from x to y such that $C_1 \cap C_2 = \{x, y\}$. The **bottom edges** of a polygon are the cover relations in the interval that are adjacent to x. The **top edges** of a polygon are the cover relations in the interval that are adjacent to y. The **side edges** of a polygon are the cover relations that are neither top nor bottom edges. A lattice L is called a **polygonal lattice** if both of the following hold.

- Whenever $x \prec y_1$ and $x \prec y_2$, then $[x, y_1 \vee y_2]$ is a polygon,
- whenever $x_1 \prec y$ and $x_2 \prec y$, then $[x_1 \wedge x_2, y]$ is a polygon.

The posets of regions we are dealing with are always polygonal lattices. Moreover, the following statement tells us that certain sets of regions defined geometrically have the combinatorial structure of a polygonal interval in the poset of regions.

Lemma 2.1.2 (Polygonal Lattice of Regions)**.** *Let $\vec{\mathcal{A}}$ be an oriented simplicial arrangement. Its poset of regions is a polygonal lattice. Moreover, given a $(d-2)$-dimensional face F of $\vec{\mathcal{A}}$, the set of regions containing F is a polygon in* $\mathrm{Pos}(\vec{\mathcal{A}})$.

Polygonal lattices have some simple rules of forcing, describing which equivalences among its elements imply other equivalences.

Lemma 2.1.3 (Polygonal Forcing)**.** *Let L be a polygonal lattice, let $[x, y]$ be a polygon in L and let $\equiv$ be a congruence on L. If $x \prec a$ is a bottom edge of the polygon such that $x \equiv a$, then $b \equiv c$ holds for every side edge $b \prec c$ of the polygon.*

2.1.2 Polygons in the Lattice of Regions

Given a quotient of such a polygonal lattice, we are particularly interested in those equivalence classes that cover the minimal congruence class $[0] \in L/\equiv$. These equivalence classes have the following property in any polygonal lattice.

Lemma 2.1.4 (Congruence Classes in Quotients of Polygonal Lattices)**.** *Let L be a polygonal lattice and $\equiv$ be a congruence on L. Let C be an $\equiv$-class that covers the minimal congruence class $[0] \in L/\equiv$. Then the minimal element j of C is join-irreducible in L and $b \in [0]$ for all $b < j$.*

Proof. Let C be an $\equiv$-class with $[0] \prec C$ in $L/\equiv$. We know that each $\equiv$-class is an interval in L. Let $j, k \in L$ be the minimal and maximal element of C such that $C = [j, k] \subset L$.

We first observe that all elements strictly below j are equivalent to $0 \pmod{\equiv}$. Assume there exists an element $b \in L$ with $0 \leq b < j$ which is not equivalent to $0 \pmod{\equiv}$. Then $[0] < [b] < [j] = C$, in contradiction to C covering $[0]$ in $L/\equiv$.

Now assume for a contradiction that j is not join-irreducible in L. Then we may fix two distinct elements x_1, x_2 both covered by j. Let $x := x_1 \wedge x_2$ be their meet in L. We observed above that the elements x, x_1 and x_2 are all in the $\equiv$-class $[0]$. As L is a polygonal lattice, the interval $[x, j]$ is a polygon. Let a be the element covering x in the chain from x to x_1. Then $j = a \vee x_2 = j$ in L. As lattice congruences preserve joins, we obtain $j \equiv a \vee x_2 \equiv 0$, in contradiction to the choice of $j \in C$. □

We recall from Definition 1.4.27 that for any join-irreducible element $j \in L$, there is a unique smallest congruence, denoted by $\mathrm{con}(j)$, that contracts j and its lower neighbor j_*. Similarly, for any pair of elements $a, b \in L$ in a lattice, we denote the unique smallest congruence relation $\equiv$ on L such that $a \equiv b$ by $\mathrm{con}(a, b)$. We now study the minimal congruence that contracts the base region with one of its neighbors and its behavior regarding the other neighbors of the base region.

Lemma 2.1.5 (Minimal Regions in a Quotient Lattice of Regions)**.** *Let $\vec{\mathcal{A}}$ be an oriented simplicial hyperplane arrangement with base region B. Let $R_1, \ldots, R_k$ be the regions of $\vec{\mathcal{A}}$ that cover B in $\mathrm{Pos}(\vec{\mathcal{A}})$. If $\equiv_1$ is the lattice congruence $\mathrm{con}(B, R_1)$, then $B \not\equiv_1 R$ for all $R \in R_2, \ldots, R_k$.*

Proof. For $i \in [k]$, let H_i be the hyperplane separating B from R_i. Then $\{H_i \mid i \in [k]\}$ is the set of basic hyperplanes of $\vec{\mathcal{A}}$. Then the set of all shards of $\vec{\mathcal{A}}$ except for those H_j with $j > 1$ is a lower set in the forcing poset, as no shard can arrow a basic hyperplane. This lower set corresponds to a lattice congruence $\equiv$ on $\mathrm{Pos}(\vec{\mathcal{A}})$. It removes all shards except for $H_2, \ldots, H_k$. In particular, we obtain $R_1 \equiv B \not\equiv R_j$ for all $j > 1$. As $\equiv_1 := \mathrm{con}(B, R_1)$ is minimal among all congruences contracting $B \prec R_1$, this asserts that $B \not\equiv_1 R_2, \ldots, R_k$ as well. □

With all these preparations, we can now prove that for each of the join-irreducible regions neighboring the base region, there exists a congruence that removes the basic hyperplanes that separates it from the base region while retaining all other basic hyperplanes. In the induced quotient fan, the number of chambers adjacent to the new base region decreases by 1.

Proposition 2.1.6 (Upper Covers in a Non-Essential Congruence)**.** *Let $\vec{\mathcal{A}}$ be an oriented simplicial hyperplane arrangement with base region B and lattice of regions L. Let $R_1, R_2, \ldots, R_k$ be the upper covers of B in L. Let $\equiv := \mathrm{con}(R_1)$ be the smallest congruence contracting R_1. The upper covers of the $\equiv$-class $[B]$ in the quotient lattice $L/\equiv$ are exactly the $k - 1$ distinct congruence classes $[R_2], [R_3], \ldots, [R_k]$.*

Proof. We prove the statement in two steps: First we show that $[R_2], \ldots, [R_k]$ are distinct and each cover $[B]$, then we show that there is no other congruence class covering $[B]$.

1. Claim: For $2 \leq i < j \leq k$, the $\equiv$-classes $[R_i]$ and $[R_j]$ are distinct and each cover $[B]$.
   Let $2 \leq i \leq k$. From Lemma 2.1.5, we know that $\equiv$ does not contract $B \prec R_i$. Denote by C_i be the $\equiv$-class containing R_i. As $B \prec R_i$ in L, we obtain $[B] \prec C_i$ in $L/\equiv$. From Lemma 2.1.4. we know that every C_i contains only elements $\geq J_i$ for some join-irreducible $J_i \in L$. As there is no join-irreducible below R_i, this gives us $J_i = R_i$. In particular, for $i \neq j$, we obtain $J_i \neq J_j$ and therefore $[R_i] \neq [R_j]$.

2. Claim: There is no other $\equiv$-class covering $[B]$.
   Let C be an $\equiv$-class with $[B] \prec C$ in $L/\equiv$. From Lemma 2.1.4, we know that there is a join-irreducible J contained in C such that all lattice elements below J are in $[B]$. Denote by J_* the unique region covered by J in L. If $J_* = B$, we obtain $J = R_i$ for some $2 \leq i \leq k$.
   Assume that C, unlike the equivalence classes considered so far, has $J_* \neq B$. Then we can fix a region R covered by J_*. Let F be the intersection of $J \cap J_*$ and $J_* \cap R$, two facets of the region J_*. Since A is a simplicial arrangement, F is a $d-2$-dimensional face. By Lemma 2.1.2 the set of regions containing F is a polygonal interval in L. The region J cannot be the top element of that polygon because it is join-irreducible in L. The region J_* cannot be the bottom element of the polygon because the region $R \prec J_*$ contains F and is therefore an element of the polygon. We deduce that the edge $J_* \prec J$ is a side edge of the polygon. Let $S \prec T$ be the bottom edge of the chain in the polygon containing J_* and J. As the regions $S \prec T$ are strictly below J in L, they are both in $[B]$ and $\equiv$ has contracted the bottom edge $S \prec T$. Due to Lemma 2.1.3, then $J_* \equiv J$ as well. This is impossible as $J \in C$ was chosen such that all lattice elements below it are in $[B]$. Therefore, all $\equiv$-classes covering [B] in $L/\equiv$ are of the form $[R_i]$ for $2 \leq i \leq k$. □

2.1.3 Essential Quotientopes

With the help of Proposition 2.1.6, we can characterize those congruences that yield quotientopes whose dimension is equal to that of an arrangement zonotope. We will give these congruences a dedicated name.

Definition 2.1.7 (Essential Congruences)**.** Let $\vec{\mathcal{A}}$ be an oriented simplicial arrangement. A lattice congruence $\equiv$ on $\mathrm{Pos}(\vec{\mathcal{A}})$ is called **essential** if it does not remove any basic hyperplane.

Corollary 2.1.8 (Essential Quotientopes)**.** Let $\vec{\mathcal{A}}$ be an oriented simplicial arrangement and let $\equiv$ be a lattice congruence on $\mathrm{Pos}(\vec{\mathcal{A}})$. A quotientope Q whose normal fan is the quotient fan $\mathcal{F}_{\equiv}$ has the same dimension as an arrangement zonotope if and only if $\equiv$ is essential.

Proof. If $\equiv$ does not remove any basic hyperplane, then none of the join-irreducibles covering the base region in the lattice of regions is contracted. Therefore, each of their respective congruence classes is an upper cover of the new base region in the quotient lattice. By the same argument used in the first part of the proof for Proposition 2.1.6, these upper covers are distinct. Therefore, the base chamber of the quotient fan is equal to the base chamber of the original fan, so its quotientope has the same edge directions around the vertex corresponding to the base region. In particular, the dimension of the quotientope is the same as the dimension of any arrangement zonotope.

Conversely, if $\equiv$ does remove at least one of the basic hyperplanes, then Proposition 2.1.6 tells us that the base chamber of the quotient fan has one neighbor less than the base chamber of the arrangement fan. As the arrangement is simplicial, the number of upper covers of the base region is equal to the rank of the arrangement. Equivalently, the zonotope is simple, so its dimension is equal to the number of neighbors of any given vertex. As any $\equiv$-quotientope has to have fewer neighbors for the vertex corresponding to the base region, its dimension has to be lower as well. □

2.1.4 Products of Quotientopes

We will now take a look at the consequences that these statements have for quotientopes in the braid arrangement, associated with lattice congruences of the weak order. In particular, we can describe a way to construct a quotientope for a non-essential congruence from quotientopes of lower-dimensional braid arrangements.

A non-essential congruence $\equiv$ on the poset of regions of $\vec{\mathcal{A}}_n$, removes at least one basic hyperplane $H_n(k, k+1)$ for some $k \in [n-1]$. Therefore, any shard retained by $\equiv$ is part of a

hyperplane $H_n(i,j)$ with either $1 \leq i < j \leq k$ or $k+1 \leq i < j \leq n$. The set of retained shards of either type each form an upper set in the forcing order, so each is the set of retained shards of a lattice congruence on the weak order on $\mathfrak{S}_n$, which we call $\equiv_1$ and $\equiv_2$, respectively.

Now any two permutations where the integers $[1,k]$ appear in the same order are $\equiv_1$-equivalent, while any two permutations where the integers $[k+1,n]$ appear in the same order are $\equiv_2$-equivalent. Therefore, the congruence $\equiv_1$ is isomorphic to a congruence on the weak order of permutations of length k, while the congruence $\equiv_2$ is isomorphic to a congruence on the weak order of permutations of length $n-k$. Furthermore, the quotient fan $\mathcal{F}_{\equiv_1}$ only has cones of the form $C \times \mathbb{R}^{n-k}$ while the quotient fan $\mathcal{F}_{\equiv_2}$ only has cones of the form $\mathbb{R}^k \times C$.

All the hyperplanes of shards retained by $\equiv_1$ contain the line $\mathrm{cone}(\sum_{i=1}^{k} \mathbf{e}_i)$ and all the hyperplanes of shards retained by $\equiv_2$ contain the line $\mathrm{cone}(\sum_{i=k+1}^{n} \mathbf{e}_i)$. Therefore, the center of the quotient fan $\mathcal{F}_{\equiv}$ will contain all multiples of the vector $\sum_{i=1}^{k} \mathbf{e}_i - \sum_{i=k+1}^{n} \mathbf{e}_i$.

Observation 2.1.9 (Minkowski Sum of Quotientopes)**.** Let $\vec{\mathcal{A}}$ be an oriented simplicial arrangement, let $\equiv_1$ and $\equiv_2$ be two lattice congruences on $\mathrm{Pos}(\vec{\mathcal{A}})$ and let $\equiv \; := \; \equiv_1 \vee \equiv_2$ be the join of the two congruences in ConL. The common refinement of the quotient fans $\mathcal{F}_{\equiv_1}$ and $\mathcal{F}_{\equiv_2}$ is the quotient fan $\mathcal{F}_{\equiv}$. Therefore, given an $\equiv_1$-quotientope Q_1 and an $\equiv_2$-quotientope Q_2, their Minkowski sum $\mathsf{Q}_1 + \mathsf{Q}_2$ is an $\equiv$-quotientope.

Therefore, if the lattice congruence $\equiv$ is not essential, we can just combine an $\equiv_1$-quotientope and an $\equiv_2$-quotientope into an $\equiv$-quotientope by building their Cartesian product. The resulting quotientope is supposed to have one vertex for each $\equiv$-class. It does so as these equivalence classes are obtained by independently combining one class of $\equiv_1$ (determining the order of $[1,k]$) with a class of $\equiv_2$ (determining the order of $[k+1,n]$) and ignoring how these two parts are interlaced, as all hyperplanes connecting two integers $i \leq k$ and $j > k$ were removed in the quotient fan $\mathcal{F}_{\equiv}$. This corresponds geometrically to combining vertices $\mathbf{v}_1$ and $\mathbf{v}_2$ of either smaller quotientope into vertices $(\mathbf{v}_1, \mathbf{v}_2)$ of the new quotientope.

As a consequence of this shortcut, we only need to consider essential congruences in our analysis of quotientopes for lattice congruences.

2.2 Removing and Retaining Rays

In this section, we will take a closer look at the structure of a quotient fan induced by a lattice congruence on the weak order on $\mathfrak{S}_n$. We will begin by examining its rays.

2.2.1 Rays of the Quotient Fan

We recall from Lemma 1.5.13 the criterion describing which rays lie on an $\vec{\mathcal{A}}_n$ shard. We now give an aditional criterion. For a given ray, it tells us which $\vec{\mathcal{A}}_n$ shards contain that ray in their relative interior. We will say that those are shards **around** that ray. We recall from Definition 1.5.10 the definition of up shards and down shards in the braid arrangement and introduce the following definition of special up and down shards for a certain ray index set.

Definition 2.2.1 (I-Conformal shards)**.** Let $\emptyset \subsetneq I \subsetneq [n]$ be an index set for the $\mathcal{A}_n$ ray $C(I)$, where $I = \{i_1, i_2, \ldots, i_a\}$ and $J := [n] \setminus I = \{j_1, j_2, \ldots, j_b\}$.

- An **I-consecutive down shard** is a shard $\Sigma_n(i_k, i_{k+1}, \emptyset,]i_k, i_{k+1}[)$ for any $k \in [a-1]$.
- A **J-consecutive up shard** is a shard $\Sigma_n(j_k, j_{k+1},]j_k, j_{k+1}[, \emptyset)$ for any $k \in [b-1]$.

Informally, each of these shards has two consecutive indices from its index set as endpoints and has all integers in between as part of its B-set (for a down shard) resp. its A-set (for an

up shard). The set of all I**-conformal shards** $\mathbf{\Sigma}_{I,n}$ is the set of all I-consecutive down shards and all J-consecutive up shards:

$$\begin{aligned}\mathbf{\Sigma}_{I,n} := &\{\Sigma_n(i_k, i_{k+1}, \emptyset,]i_k, i_{k+1}[) \mid k \in [|I|-1]\} \\ &\cup \{\Sigma_n(j_k, j_{k+1},]j_k, j_{k+1}[, \emptyset) \mid k \in [|J|-1]\}\,.\end{aligned}$$

We remark that for an index set I, there are $n-2$ distinct I-conformal shards, of which $|I|-1$ are I-consecutive down shards and $n-|I|-1$ are J-consecutive up shards.

Example 2.2.2. We examine the ray of the $\mathcal{A}_9$ arrangement labeled by the set $I = \{1,4,5,6,8\}$. We can illustrate that $\mathcal{A}_9$ ray by a red arc from 0 to 10 passing above the entries of I and below the entries of $J := [n] \setminus I = \{2,3,7,9\}$. See Figure 2.1 (left) for an illustration. The I-consecutive down shards are $\Sigma_9(1,4,\emptyset,\{2,3\})$, $\Sigma_9(4,5,\emptyset,\emptyset)$, $\Sigma_9(5,6,\emptyset,\emptyset)$ and $\Sigma_9(6,8,\emptyset,\{7\})$. The J-consecutive up shards are $\Sigma_9(2,3,\emptyset,\emptyset)$, $\Sigma_9(3,7,\{4,5,6\},\emptyset)$ and $\Sigma_9(7,9,\{8\},\emptyset)$.

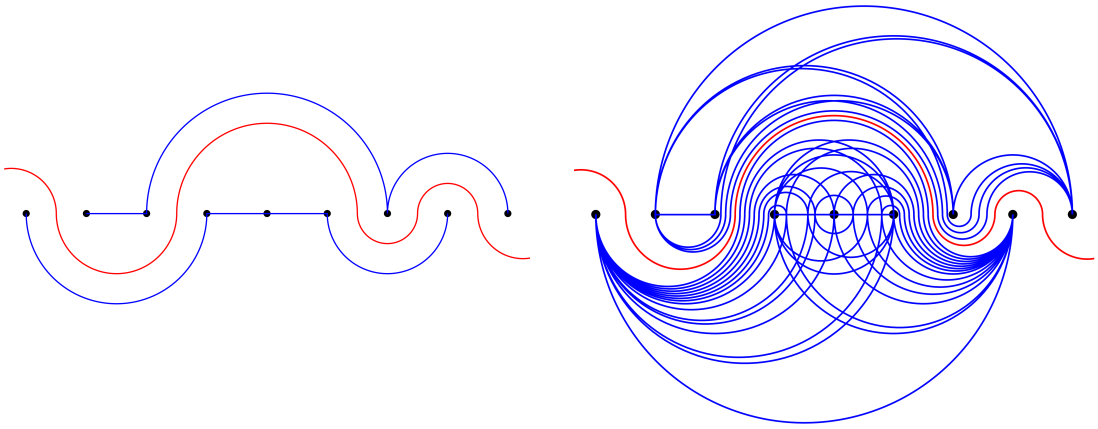

Figure 2.1: The $\vec{\mathcal{A}}_9$ ray indexed by $I = \{1,4,5,6,8\}$ is illustrated by the red arc passing above 1, 4, 5, 6 and 8 and below 2, 3, 7 and 9. The left pictures shows this ray together with all I-conformal shards $\Sigma_{I,9}$, illustrated by the blue arcs. These are the shards that contain $C(I)$ in their interior. The right pictures shows this ray together with all shards that contain the ray $C(I)$ (in their interior or in their boundary), illustrated by the blue arcs. These are the arcs that are entirely below or entirely above the red arc. We remark that neither of these sets of blue shards is an upper or lower set in the forcing order. For example, the blue shard $\Sigma_9(6,8,\emptyset,\{7\})$ is included in both sets. It forces the shard $\Sigma_9(6,9,\emptyset,\{7,8\})$ and is forced by the shard $\Sigma_9(6,7,\emptyset,\emptyset)$, both of which are clearly absent from both sets, as their arcs cross the red arc corresponding to the ray.

This helps us in describing the rays of the quotient fan as these I-conformal shards turn out to be exactly the $\vec{\mathcal{A}}_n$ shards which contain the ray labelled by I in their relative interior.

Proposition 2.2.3 (Shards with $\mathcal{A}_n$ Ray in the Interior)**.** *Given an index set $\emptyset \subsetneq I \subsetneq [n]$, the $\vec{\mathcal{A}}_n$ shards containing $\mathbf{r}(I)$ in their relative interior are exactly the $(n-2)$ I-conformal shards $\mathbf{\Sigma}_{I,n}$.*

Proof. We recall from Example 1.3.10 that the ray vector labelled by I is $\mathbf{r}(I) = |I| \cdot \mathbf{1} - n \cdot \mathbf{1}_I$, which has an entry $|I| - n$ for every $i \in I$ and an entry $|I|$ for every $j \in [n] \setminus I$. Moreover, the relative interior of an $\vec{\mathcal{A}}_n$ shard $\Sigma_n(\ell, r, A, B)$ is the set of all $\mathbf{x} \in \mathbb{R}^n$ with $x_a < x_\ell = x_r < x_b$ for all $a \in A$ and $b \in B$. Therefore, $\mathbf{r}(I)$ lies in the relative interior of the shard if and only if

- either $x_a = |I| - n$ for all $a \in A$ and $x_\ell = x_r = |I|$ and $B = \emptyset$,
- or $A = \emptyset$ and $x_\ell = x_r = |I| - n$ and $x_b = |I|$ for all $b \in B$.

These cases are equivalent to the following choices of ℓ, r, A and B:

- either $]\ell, r[= A \subseteq I$ and $\ell, r \in [n] \setminus I$,
- or $\ell, r \in I$ and $]\ell, r[= B \subseteq [n] \setminus I$,

where the first case is equivalent to being an I-consecutive down shard and the second case is equivalent to being an $([n] \setminus I)$-consecutive up shard. □

We can directly deduce a little result on shards that are neither up shards nor down shards:

Observation 2.2.4 (Rays Inside Mixed Shards)**.** As a mixed shard (equivalently, a shard whose arc crosses the axis) can have neither $A =]\ell, r[$ and $B = \emptyset$ nor $A = \emptyset$ and $B =]\ell, r[$, the relative interior of any mixed shard never contains any $\mathcal{A}_n$ ray.

Next, we describe the rays of a quotient fan $\mathcal{F}_\equiv$. As any quotient fan $\mathcal{F}_\equiv$ coarsens the arrangement fan $\mathcal{F}(\mathcal{A}_n)$, the set of rays of $\mathcal{F}_\equiv$ is a subset of the set of rays of $\mathcal{F}(\mathcal{A}_n)$. The following statement tells us which rays are preserved for a fixed congruence $\equiv$ on the weak order on $\mathfrak{S}_n$.

Proposition 2.2.5 (Rays of a Quotient Fan)**.** *Let $\equiv$ be an essential congruence on $\mathrm{Pos}(\vec{\mathcal{A}}_n)$ and $\emptyset \subsetneq I \subsetneq [n]$ be an index set. Then $C(I)$ is a ray of $\mathcal{F}_\equiv$ if and only if $\mathbf{\Sigma}_{I,n} \subseteq \mathbf{\Sigma}_\equiv^\checkmark$.*

Proof. If $\mathbf{\Sigma}_{I,n} \subseteq \mathbf{\Sigma}_\equiv^\checkmark$, we examine the intersection of all I-conformal shards $\Sigma \in \mathbf{\Sigma}_{I,n}$. We distinguish two cases.

- If I is an initial interval $[1, k]$, then $C(I)$ is a ray of the basic chamber of the braid fan. If I is a final interval $[k+1, n]$, then $C(I)$ is a ray of the opposite of the basic chamber of the braid fan. As $\equiv$ is an essential congruence, the basic chamber of the braid fan and its opposite are chambers of the quotient fan $\mathcal{F}_\equiv$ as well, and so are their rays.
- If I is neither an initial nor a final interval, there are indices $1 \le a < b < c \le n$ with either $a, c \in I$ and $b \notin I$ or $a, c \notin I$ and $b \in I$. Then the intersection of the shards in $\mathbf{\Sigma}_{I,n}$ is the set of all $\mathbf{x} \in \mathcal{H}_0^n$ with $x_i \le x_j$ for all $i \in I$ and $j \notin I$, which coincides with the definition of the cone $C(I)$. As all these shards intersect along this ray, we can replace each of them with a wall of the quotient fan such that their intersection still equals this way. The quotient fan $\mathcal{F}_\equiv$ is closed under intersection of its cones, so this ray $C(I)$ is a cone of $\mathcal{F}_\equiv$ as desired.

Conversely, if $\mathbf{\Sigma}_{I,n} \not\subseteq \mathbf{\Sigma}_\equiv^\checkmark$, then we can fix an I-conformal shard $\Sigma = \Sigma_n(\ell, r, A, B) \in \mathbf{\Sigma}_{I,n}$ that is not retained by $\equiv$. Without loss of generality, let Σ be an I-consecutive down shard (if Σ is an $([n] \setminus I)$-consecutive up shard, an analogous argument holds). We assume for a contradiction that $C(I)$ is a ray of the quotient fan $\mathcal{F}_\equiv$. Then $C(I)$ is a cone of the fan and therefore an intersection of some of its maximal cones. In particular, there is a set of walls of $\mathcal{F}_\equiv$ whose intersection is $C(I)$. By Lemma 1.5.19, this can be rewritten as a set of retained shards $\Sigma_1, \Sigma_2, \dots, \Sigma_k$ such that their intersection $S = \bigcap_{i=1}^k \Sigma_i$ equals $C(I)$. If we set $I' := I \cap [1, \ell]$ (which is distinct from $C(I)$ as $r \in I$), then the intersection S does not include the ray $C(I')$. Then there is at least one of the shards we intersect to obtain S, say $\Sigma_j = \Sigma_n(\ell', r', A', B')$, such that $r(I')$ does not lie in Σ_j. As S contains $r(I)$, so does Σ_j. We first observe that either $\ell', r' \in I$ or $\ell', r' \notin I$ as otherwise, Σ_j would intersect $C(I)$ in the origin only.

- If $\ell', r' \notin I$, then $\ell', r' \notin I'$. As $r(I')$ does not lie in Σ_j, Lemma 1.5.13 tells us that there is some $\ell' < p < r'$ with $p \in B'$ and $p \in I'$. Then S has $x_{\ell'} \le x_p$ (due to Σ_j), while $r(I)$ has $x_p < x_{\ell'}$ (as $p \in I$ and $\ell' \notin I$), which contradicts our assumption that $r(I)$ lies in Σ_j.
- If $\ell', r' \in I$ and $\ell', r' \in I'$, then Lemma 1.5.13 tells us that there is some $\ell' < p < r'$ with $p \in A'$ and $p \notin I'$ (and therefore $p \notin I$). Then S has $x_p \le x_{\ell'}$ (due to Σ_j) while $r(I)$ has $x_{\ell'} < x_p$ (as $\ell' \in I$ and $p \notin I$), which contradicts our assumption that $r(I)$ lies in Σ_j.

- If $\ell', r' \in I$ while $\ell' \in I'$ and $r' \notin I'$, then we have $\ell' \leq \ell < r \leq r'$. If Σ and Σ_j agree on $]\ell, r[$ (meaning that for every index in this interval, they agree on whether it is in their A or B set), then Σ forces Σ_j. As Σ is not an element of $\Sigma_\equiv$ (which is an upper set in the forcing poset), this implies that Σ_j cannot be an element of $\Sigma_\equiv$ either, in contradiction to our choice of Σ_j. We conclude that Σ and Σ_j do not agree on $]\ell, r[$.
  As we chose Σ to be an I-consecutive down shard, it can only disagree with Σ_j if there is some $\ell < p < r$ such that $p \in A'$. But then S has $x_{\ell'} \geq x_p$ (due to Σ_j) while $r(I)$ has $x_{\ell'} < x_p$ (as $\ell < p < r$ and Σ is I-consecutive), which contradicts our assumption that $r(I)$ lies in Σ_j.
- If $\ell', r' \in I$ and $\ell', r' \notin I'$, then Lemma 1.5.13 tells us that there is some $\ell' < p < r'$ with $p \in B'$ and $p \in I'$. This would mean that I contains both ℓ' and p while I' contains only p, which is impossible due to the construction of I'. □

2.2.2 Rays of the Permutree Fan

In this section, we specialize Proposition 2.2.5 to δ-permutree congruences. We obtain the following description of the rays of the δ-permutree fan $\mathcal{F}_\delta$. This result was already mentioned in Corollary 1.7.20, which is a consequence of it.

Corollary 2.2.6 (Rays of the Permutree Fan)**.** Let δ be a decoration of length n and $\emptyset \subsetneq I \subsetneq [n]$ be an index set. Then $C(I)$ is a ray of $\mathcal{F}_\delta$ if and only if both of the following hold.
- If $k \in \delta^- \setminus I$, then $k < \min(I)$ or $\max(I) < k$.
- If $k \in \delta^+ \cap I$, then $k < \min([n] \setminus I)$ or $\max([n] \setminus I) < k$.

Equivalently, $C(I)$ is a ray of $\mathcal{F}_\delta$ if and only if for all $a < b < c$, both of the following hold.
- If $a, c \in I$, then $b \notin \delta^- \setminus I$.
- If $a, c \in [n] \setminus I$, then $b \notin \delta^+ \cap I$.

Proof. We recall from Observation 1.7.13 that the shards retained by $\equiv_\delta$ are exactly those shards $\Sigma_n(\ell, r, A, B)$ with $\delta^- \cap]\ell, r[\subseteq A$ and $\delta^+ \cap]\ell, r[\subseteq B$. Conversely, the shards removed by $\equiv_\delta$ are those where there is some $k \in]\ell, r[$ with $k \in \delta^- \setminus A$ or $k \in \delta^+ \setminus B$.

By Proposition 2.2.5, the 1-dimensional cone $C(I)$ is a ray of the permutree fan $\mathcal{F}_\delta$ if and only if $\equiv_\delta$ removes no I-conformal shard. Therefore, $C(I)$ is a ray of $\mathcal{F}_\delta$ if and only if
- no I-consecutive down shard $\Sigma_n(i_k, i_{k+1}, \emptyset,]i_k, i_{k+1}[)$ has a $k \in \delta^- \setminus I$
- and no $([n] \setminus I)$-consecutive up shard $\Sigma_n(j_k, j_{k+1},]j_k, j_{k+1}[, \emptyset)$ has a $k \in \delta^+ \cap I$.

I-consecutive down shards are I-compatible if $\ell, r \in I$ are consecutive elements of I and $([n] \setminus I)$-consecutive up shards are I-compatible if $\ell, r \in I$ are consecutive elements of $[n] \setminus I$. Such consecutive elements exist if and only if there is a pair of indices in I (resp. $[n] \setminus I$) such that k lies in between. This proves our claim. □

Example 2.2.7. For the decorations of Figure 1.15, Figure 1.17 and Figure 1.18, the rays of $\mathcal{F}_{\mathbb{O}\mathbb{O}\otimes\mathbb{O}}$ correspond to the subsets 1, 2, 3, 4, 12, 13, 23, 34, 123, 134, 234. The rays of $\mathcal{F}_{\mathbb{O}\otimes\otimes\mathbb{O}}$ correspond to the subsets 1, 4, 12, 34, 123, 124, 234.

Example 2.2.8. As examples of Corollary 2.2.6, we find the following classic descriptions.
- When $\delta = \mathbb{O}^n$, the fan $\mathcal{F}_\delta = \mathcal{F}_{\mathbb{O}^n}$ is the braid fan and its rays are labeled by all proper subsets $\emptyset \subsetneq I \subsetneq [n]$.
- When $\delta = \mathbb{A}^n$, the rays of $\mathcal{F}_{\mathbb{A}^n}$ are labeled by those proper subsets of $[n]$ that are intervals $[i, j]$ for $1 \leq i \leq j \leq n$. These intervals can also be visualised as internal diagonals of a polygon with vertices $0, 1, \ldots, n+1$, where $[i, j]$ represents the diagonal $(i-1, j+1)$.
- When $\delta = \otimes^n$, the rays of $\mathcal{F}_{\otimes^n}$ are all initial intervals $[1, k]$ and all final intervals $[k, n]$ distinct from $[1, n]$.

We can use our results on the rays of the δ-permutree fan to count them.

Corollary 2.2.9 (Number of Rays of a Permutree Fan)**.** Let δ be a permutree decoration of length n. The number $\rho(\delta)$ of rays of the δ-permutree fan $\mathcal{F}_\delta$ is

$$\rho(\delta) = n - 1 + \sum_{\substack{1 \leq i < j \leq n \\ \forall k \in]i,j[:\ \delta_k \neq \otimes}} 2^{|\{k \in]i,j[\ |\ \delta_k = \oplus\}|}.$$

Proof. We count the number of different possibilities to pick a proper subset $\emptyset \subsetneq I \subsetneq [n]$ such that the induced ray $C(I)$ is a ray of the quotient fan $\mathcal{F}_\delta$. In order to do so, we first choose two positions $i, j \in [n]$.

- We fix i to be the last position such that $\{1, \dots, i\}$ is a subset of either I or $[n] \setminus I$.
- We fix j to be the first position such that $\{j, \dots, n\}$ is a subset of either I of $[n] \setminus I$.

As I has to be a proper subset of $[n]$, we require that $i < j$. With these positions fixed, we have to decide for every $k \in]i, j[$, if $k \in I$. We remark that the choice for $k = i + 1$ uniquely determines whether $1, \dots, i$ are all in I or all in $[n] \setminus I$ (analogously with the choice for $k = j - 1$). We will deal with the case where $]i, j[= \emptyset$ later.

Now Corollary 2.2.6 tells us that if $k \in \delta^-$, then $k \notin I$ is a necessary condition for $C(I)$ to be a ray. Similarly, if $k \in \delta^+$, then $k \in I$ has to hold. In the case where there is some $k \in]i, j[$ with $\delta_k = \otimes$, there is no valid choice and $C(I)$ cannot be a ray. We therefore have to restrict to those choices of i and j that have $\delta_k \neq \otimes$ for all $k \in]i, j[$.

For any valid choice of i and j meeting these conditions, we have to set $k \in I$ whenever $\delta_k = \circledcirc$ and $k \notin I$ whenever $\delta_k = \circledast$. This leaves us a choice between 2 options for each $k \in]i, j[$ with $\delta_k = \oplus$, which gives us $2^{|\{k \in]i,j[\ |\ \delta_k = \oplus\}|}$ choices in total for fixed valid i and j. We can sum up these powers of 2 for all valid choices of $1 \leq i < j \leq n$ with $\delta_k \neq \otimes$ for all $k \in]i, j[$.

The cases where $i + 1 = j$ have $]i, j[= \emptyset$ and therefore each contribute $2^0 = 1$ to this sum. In these cases, it is not determined whether $I = \{1, \dots, i\}$ or $I = \{j, \dots, n\}$. Both are possible and both induce a ray $C(I)$ which is a ray of the permutree fan according to Corollary 2.2.6. As we only counted each of these cases once, we have to add $n - 1$ to our sum. □

Example 2.2.10. For the decorations of Figure 1.15, Figure 1.17 and Figure 1.18, we obtain $\rho(\oplus\oplus\circledast\oplus) = 11$ and $\rho(\oplus\otimes\circledcirc\oplus) = 7$.

Example 2.2.11. As examples of Corollary 2.2.9, we find the following classic numbers.

- When $\delta = \oplus^n$, the braid fan $\mathcal{F}_{\oplus^n}$ has $\rho(\oplus^n) = 2^n - 2$ rays.
- When $\delta = \circledast^n$, the fan $\mathcal{F}_{\circledast^n}$ has $\binom{n+1}{2} - 1$ rays. This equals the number of internal diagonals of an $(n + 2)$-gon.
- When $\delta = \otimes^n$, the fan $\mathcal{F}_{\otimes^n}$ has $2n - 2$ rays.

In the sum formula given in Corollary 2.2.9, the powers of 2 vary depending on the number of $\oplus$ symbols in the decoration. If there is no such symbol in δ, all these powers of 2 collapse to $2^0 = 1$ and the number of rays of the permutree fan is particularly easy to calculate.

Corollary 2.2.12 (Number of Rays of Some Permutree Fans)**.** If $\delta \in \{\circledast, \circledcirc, \otimes\}^n$, we have

$$\rho(\delta) = n - 1 + |\{1 \leq i < j \leq n \mid \forall k \in]i, j[:\ \delta_k \neq \otimes\}|.$$

2.2.3 Rays and Chambers in the Quotient Fan

We make some more small observations on the structure of the quotient fan that we will use to prove statements about removahedral congruences in the following section.

Lemma 2.2.13 (Hyperplane Separating Two Braid Fan Rays)**.** *Let $\emptyset \subsetneq I, J \subsetneq [n]$ be two index sets for the braid fan. The hyperplane $\{\mathbf{x} \in \mathbb{R}^n \mid \mathbf{x}_i = \mathbf{x}_j\}$ strictly separates the ray vectors $\mathbf{r}(I)$ and $\mathbf{r}(J)$ if and only if $i \in I \setminus J$ and $j \in J \setminus I$ (or vice versa).*

Proof. For the ray vector $\mathbf{r} = \mathbf{r}(I)$ to be on a side of the hyperplane, we first need $r_i \neq r_j$, say $r_i < r_j$ without loss of generality. Then $i \in I$ and $j \notin I$. Then $\mathbf{r}' = \mathbf{r}(J)$ is on the other side of that hyperplane if and only if $r'_i > r'_j$, which is equivalent to $j \in J$ and $i \notin J$, as claimed. □

Corollary 2.2.14 (Braid Region Containing Two Specific Rays)**.** Let $\emptyset \subsetneq I, J \subsetneq [n]$ be two index sets for the braid fan. There is a region of the braid arrangement that has both $C(I)$ and $C(J)$ as rays if and only if $I \subseteq J$ or $I \supseteq J$.

Proof. As the regions of the braid arrangement are the closures of the connected components, two rays are faces of the same region if and only if they are not strictly separated by any $\mathcal{A}_n$ hyperplane. By Lemma 2.2.13, such a hyperplane exists if and only if neither of I and J is a subset of the other. □

Corollary 2.2.15 (Number of Braid Regions with Two Specific Rays)**.** Let $\emptyset \subsetneq I \subset J \subsetneq [n]$ be two index sets for the braid fan. The number of regions of the braid arrangement that have both $C(I)$ and $C(J)$ as rays is $|I|! \cdot |J \setminus I|! \cdot |[n] \setminus J|!$.

Proof. We know from Example 1.3.10 that the rays of the chamber $C(\sigma)$ are the one-dimensional cones $C(\sigma([k]))$ for all $k \in [n-1]$. In order to have both $C(I)$ and $C(J)$ as rays, a permutation σ has to have $\sigma([|I|]) = I$ and $\sigma([|J|]) = J$. We note that this is another proof that one of I and J has to be a subset of the other. To fix a suitable permutation $\sigma = (\sigma_1, \sigma_2, \ldots, \sigma_n) \in \mathfrak{S}_n$, we need it to start with all entries of I, followed by those entries of J not in I, and filled up by the entries not in J. Within each of these three blocks, the order in which the values appear is arbitrary. □

Observation 2.2.16 (Wall-Crossing Inequalities in a Quotient Fan)**.** For index sets $\emptyset \subsetneq I, J \subsetneq [n]$, we always have

$$\begin{aligned}\mathbf{r}(I) + \mathbf{r}(J) &= (|I| + |J|)\mathbf{1} - n(\mathbf{1}_I + \mathbf{1}_J) \\ &= (|I \cap J| + |I \cup J|)\mathbf{1} - n(\mathbf{1}_{I\cap J} + \mathbf{1}_{I\cup J}) \\ &= \mathbf{r}(I \cap J) + \mathbf{r}(I \cup J).\end{aligned}$$

To determine whether these rays induce a wall-crossing inequality, the question is just whether the rays labeled I and J are in adjacent chambers whose intersection contains the rays labeled $I \cap J$ and $I \cup J$.

2.3 Removahedral Congruences

We recall that a congruence $\equiv$ is called removahedral if a suitable quotientope can be obtained by deleting facet-defining inequalities of the permutahedron Perm_n as defined in Example 1.3.15. We will now take a look at how removahedral congruences and permutree congruences are related.

2.3.1 Removahedral Congruences are Permutree Congruences

We learned from Corollary 1.7.29 that every permutree congruence is an essential removahedral congruence. In this section, we want to show that the opposite holds as well. We will prove that every essential removahedral congruence is a permutree congruence.

We attempt to prove this by contradiction: We fix a lattice congruence $\equiv$ of the weak order on $\mathfrak{S}_n$ which is an essential removahedral congruence but not a permutree congruence. We will

use our findings from the previous section to describe the quotient fan $\mathcal{F}_{\equiv}$ and reason that it cannot in fact be a removahedral fan, proving that no such congruence can exist.

Given our fixed congruence $\equiv$, the set $\mathbf{\Sigma}^{\times}_{\equiv}$ is the set of shards removed by $\equiv$, which is a lower set in the forcing order on $\vec{\mathcal{A}}_n$. We denote by $\mathcal{S}$ the set of maximal elements of the lower set $\mathbf{\Sigma}^{\times}_{\equiv}$ with respect to the forcing order. Our first result will guarantee that $\mathcal{S}$ must contain a shard of a certain type.

Claim 2.3.1. *The set $\mathcal{S}$ defined above contains a shard of length 3 or more which is not mixed.*

Proof. We first remark that as $\equiv$ is an essential congruence, the set $\mathcal{S}$ does not contain any shard of length 1. We can partition $\mathcal{S}$ into the subsets $\mathcal{S}_2$ and $\mathcal{S}_{\geq 3}$, where the elements of $\mathcal{S}_2$ are those shards in $\mathcal{S}$ that have length 2 and $\mathcal{S}_{\geq 3}$ contains those shards in $\mathcal{S}$ that have a length of 3 or more. Since $\equiv$ is not a permutree congruence, the set $\mathcal{S}$ must contain a shard of length distinct from 2 according to Theorem 1.7.15, so the set $\mathcal{S}_{\geq 3}$ is non-empty. We recall from Theorem 1.7.15 that we can interpret $\mathcal{S}_2$ as a set of forcing-maximal removed shards for some permutree congruence which we shall denote by $\equiv_\delta$. This congruence is distinct from $\equiv$, so the permutree fan $\mathcal{F}_\delta$ is distinct from the quotient fan $\mathcal{F}_{\equiv}$. As $\equiv$ removes some mixed shards which are retained in $\equiv_\delta$, this implies that $\mathcal{F}_{\equiv}$ coarsens $\mathcal{F}_\delta$.

We assume for a contradiction that $\mathcal{S}_{\geq 3}$ contains only mixed shards. As mixed shards force only mixed shards, the up shards and down shards retained by $\equiv$ are the same as those retained by $\equiv_\delta$. Then Proposition 2.2.5 tells us that the quotient fan $\mathcal{F}_{\equiv}$ and the permutree fan $\mathcal{F}_\delta$ have the exact same rays. Equivalently, as both $\equiv$ and $\equiv_\delta$ are removahedral congruences, their corresponding removahedra are obtained from the permutahedron Perm_n by removing the exact same facet inequalities, yielding the exact same quotientope. But as the normal fans $\mathcal{F}_{\equiv}$ and $\mathcal{F}_\delta$ of these two quotientopes are distinct, they cannot both be removahedral congruences, in contradiction to our assumption. Therefore, the set $\mathcal{S}_{\geq 3}$ has to contain some shard that is not mixed, which proves our claim. □

With this result, we can fix an up shard $\Sigma_n(\ell, r,]\ell, r[, \emptyset)$ that is among the maximal elements of the lower set $\mathbf{\Sigma}^{\times}_{\equiv}$. In the case where the shard is a down shard of the form $\Sigma_n(\ell, r, \emptyset,]\ell, r[)$, the proof is symmetric. We now introduce five subsets of $[n]$ given by the intervals

- $I :=]\ell + 1, r[$,
- $J :=]\ell, r - 1[$,
- $K := [1, r[$,
- $L :=]\ell, n]$,
- and $M :=]\ell + 1, r - 1[$.

We observe that for each of these intervals, the left boundary is smaller or equal to the right boundary as the shard we started with has length $r - \ell \geq 3$. We remark that M is the only one of these intervals which is possibly empty (in the case where $\ell+3 = r$). To get a better understanding of how our reasoning for the remainder of this section is meant to work, we will first consider an example.

Example 2.3.2. We consider the lattice congruence $\equiv$ on the weak order of $\mathfrak{S}_4$ whose only removed shard is $\Sigma_4(1, 4, \{2, 3\}, \emptyset)$. This induces the following five subsets:

- $I =]1 + 1, 4[= \{3\}$,
- $J =]1, 4 - 1[= \{2\}$,
- $K = [1, 4[= \{1, 2, 3\}$,
- $L =]1, 4] = \{2, 3, 4\}$,
- $M =]1 + 1, 4 - 1[= \emptyset$.

We remark that our fixed shard $\Sigma_4(1, 4, \{2, 3\}, \emptyset)$ is a join-irreducible in $\mathrm{Pos}(\vec{\mathcal{A}})$, so it corresponds to a permutation σ with a single descent which we can give explicitly as $\sigma = 2341$. The only permutation covered by σ in $\mathrm{Pos}(\vec{\mathcal{A}})$ is $\pi = 2314$. The meaning of the five subsets becomes clearer when we examine the chambers of the braid fan labeled by σ and π.

The rays of the region $C(\sigma)$ are labeled by $\{2\}, \{2, 3\}$ and $\{2, 3, 4\}$, while the rays of the region $C(\pi)$ are labeled by $\{2\}, \{2, 3\}$ and $\{1, 2, 3\}$. These two chambers of the braid fan are part of the same chamber of the quotient fan $\mathcal{F}_{\equiv}$ as the shard $\Sigma_4(1, 4, \{2, 3\}, \emptyset)$ separating them was the one shard removed by $\equiv$. Therefore, $\mathcal{F}_{\equiv}$ has a chamber spanned by the

rays labeled $\{2\}, \{2,3\}, \{1,2,3\}$ and $\{2,3,4\}$. We remark that the ray $C(\{2,3\})$, represented by the ray vector $\mathbf{r}(\{2,3\}) = (2,-2,-2,2)$, lies in the conical span of $C(\{1,2,3\})$ (represented by $\mathbf{r}(\{1,2,3\}) = (-1,-1,-1,3)$) and $C(\{2,3,4\})$ (represented by $\mathbf{r}(\{2,3,4\}) = (3,-1,-1,-1)$), so $C(\{2,3\})$ is a ray of the braid fan $\mathcal{F}_4$, but not a ray of the quotient fan $\mathcal{F}_{\equiv}$ and not a ray of that chamber in particular.

Similarly, we analyze the braid fan regions labeled by $\sigma' = 3241$ and $\pi' = 3214$. They are separated by $\Sigma_4(1,4,\{2,3\},\emptyset)$ as well. Therefore, together they form a chamber of the quotient fan containing the braid fan rays labeled $\{3\}, \{2,3\}, \{1,2,3\}$ and $\{2,3,4\}$. As before, the ray labeled $\{2,3\}$ is not extremal in this chamber. In fact, it is not a ray of the quotient fan $\mathcal{F}_{\equiv}$ according to Proposition 2.2.5 as the removed shard $\Sigma_4(1,4,\{2,3\},\emptyset)$ is an $([n] \setminus \{2,3\})$-consecutive up shard.

Now the chamber spanned by the rays labeled $K = \{1,2,3\}, L = \{2,3,4\}$ and $J = \{2\}$ and the chamber spanned by the rays labeled $K = \{1,2,3\}, L = \{2,3,4\}$ and $I = \{3\}$ are adjacent in the quotient fan $\mathcal{F}_{\equiv}$, separated by the hyperplane $\{\mathbf{x} \in \mathbb{R}^n \mid \mathbf{x}_2 = \mathbf{x}_3\}$, and their ray vectors are related by the equation $\mathbf{r}(I) + \mathbf{r}(J) = (2,-2,-2,2) = \mathbf{r}(K) + \mathbf{r}(L)$. We recall that the height function $\mathbf{h}_\circ$ of the permutahedron Perm_n is given by $\mathbf{h}_\circ(S) = 4\,|S|\,(4 - |S|)$. This height function violates the wall-crossing inequality $\mathbf{h}_\circ(I) + \mathbf{h}_\circ(J) > \mathbf{h}_\circ(K) + \mathbf{h}_\circ(L)$ as $\mathbf{h}_\circ(I) + \mathbf{h}_\circ(J) = 2 \cdot 4 \cdot 1 \cdot 3 = \mathbf{h}_\circ(K) + \mathbf{h}_\circ(L)$. In consequence, the quotient fan $\mathcal{F}_{\equiv}$ is not the normal fan of a removahedron, so the lattice congruence $\equiv$ cannot be removahedral.

We now establish some general statements to extend this reasoning from one example to any essential removahedral congruence $\equiv$ that is assumed not to be a permutree congruence. We begin by making sure the braid fan rays we are dealing with are guaranteed to be rays of the quotient fan as well.

Claim 2.3.3. *All the rays $C(I)$, $C(J)$, $C(K)$, $C(L)$ and $C(M)$ are rays of the quotient fan $\mathcal{F}_{\equiv}$.*

Proof. By using Proposition 2.2.3, we can determine which shards contain the rays labeled by I, J, K, L and M in their interior. As we assumed $\equiv$ to be an essential congruence, it has to retain all basic shards. If we can show that all non-basic shards that contain any of these rays in their relative interior are retained by $\equiv$ as well, then we know that all of these rays are still present in the quotient fan $\mathcal{F}_{\equiv}$.

We know from Proposition 2.2.3 that the shards containing one of these rays in their interior are exactly those that are S-conformal for some $S \in \{I, J, K, L, M\}$. We first remark that as all the index sets are proper intervals, all S-consecutive down shards are basic shards. To find all non-basic S-conformal shards, we only need to search among the $[n] \setminus S$-consecutive up shards for each of the index sets. The complement of any of these index set intervals in $[n]$ is either an initial or a final interval (in which case all $[n] \setminus S$-consecutive up shards are basic) or the disjoint union of an initial and a final interval (in which case the only non-basic one is the up shard connecting $\min(S) - 1$ to $\max(S) + 1$).

- For $I =]\ell + 1, r[$, the only non-basic I-conformal shard is $\Sigma_n(\ell+1, r,]\ell+1, r[\,, \emptyset)$.
- For $J =]\ell, r-1[$, the only non-basic J-conformal shard is $\Sigma_n(\ell, r-1,]\ell, r-1[\,, \emptyset)$.
- For $K = [1, r[$, all K-conformal shards are basic.
- For $L =]\ell, n]$, all L-conformal shards are basic.
- For $M =]\ell+1, r-1[$, the only non-basic M-conformal shard is the $[n] \setminus M$-consecutive up shard $\Sigma_n(\ell+1, r-1,]\ell+1, r-1[\,, \emptyset)$.

We remark that each of these non-basic shards we found is forcing $\Sigma_n(\ell, r,]\ell, r[\,, \emptyset)$. But as we fixed that shard to be maximal in $\mathbf{\Sigma}^{\times}_{\equiv}$, this implies that all these non-basic shards are retained by $\equiv$. Therefore, all the rays $C(I), C(J), C(K), C(L)$ and $C(M)$ are still rays in the quotient fan $\mathcal{F}_{\equiv}$. □

Next, we will see that the rays labeled by I, J, K, L and M are related in a certain way in the quotient fan $\mathcal{F}_{\equiv}$ associated to our fixed congruence $\equiv$.

Claim 2.3.4. *The quotient fan $\mathcal{F}_{\equiv}$ contains adjacent chambers C_1 and C_2 separated by the hyperplane $H_n(\ell+1, r-1)$ such that $\mathbf{r}(I) \in C_1$ and $\mathbf{r}(J) \in C_2$, while $\{\mathbf{r}(K), \mathbf{r}(L), \mathbf{r}(M)\} \subset C_1 \cap C_2$.*

Proof. The index sets are related by $M \subseteq I, J \subseteq K, L$. Following Lemma 2.2.13, two rays cannot be separated by a hyperplane of the braid fan (and therefore of the quotient fan) if one of the index sets contains the other. We deduce that the only ones among them whose rays might be strictly separated by a hyperplane of the braid arrangement are induced by the pair of I and J and induced by the pair of K and L.

- The index sets I and J have $I \setminus J = \{r-1\}$ and $J \setminus I = \{\ell+1\}$. In consequence, the rays $C(I)$ and $C(J)$ are strictly separated only by the hyperplane $\{\mathbf{x} \in \mathbb{R}^n \mid \mathbf{x}_{\ell+1} = \mathbf{x}_{r-1}\}$.
- The index sets K and L have $K \setminus L = [1, \ell]$ and $L \setminus K = [r, n]$. In consequence, the rays $C(K)$ and $C(L)$ are strictly separated by all those hyperplanes $\{\mathbf{x} \in \mathbb{R}^n \mid \mathbf{x}_a = \mathbf{x}_b\}$ where $a \in [1, \ell]$ and $b \in [r, n]$. We remark that the quotient fan $\mathcal{F}_{\equiv}$ is missing all shards of the form $\Sigma_n(i, j,]i, j[, \emptyset)$ for $i \in [1, \ell]$ and $j \in [r, n]$, as they are forced by the removed up shard $\Sigma_n(\ell, r,]\ell, r[, \emptyset)$. Therefore, $C(K)$ and $C(L)$ are not separated by any $\mathcal{F}_{\equiv}$ hyperplane and are in a common chamber of $\mathcal{F}_{\equiv}$.

Alternatively, we can explicitly walk through a sequence of permutations to see whether their associated regions in $\vec{\mathcal{A}}_n$ all are equivalent under $\equiv$ and whether they contain some of the rays $C(I)$, $C(J)$, $C(K)$, $C(L)$ and $C(M)$. We fix the permutation $\sigma := (\ell+2, \dots, r-2, r-1, \ell+1, \ell, \dots, 1, r, \dots, n)$ and the permutation $\pi := (\ell+2, \dots, r-2, r-1, \ell+1, r, \dots, n, \ell, \dots, 1)$. We build a sequence of permutations adjacent in the weak order, starting with σ and ending with π, each of which starts with the block $(\ell+2, \dots, r-2, r-1, \ell+1)$ and ends with a shuffle of $(\ell, \dots, 1)$ with $(r, \dots, n)$. We go from σ to π by transposing in each step two values $i \leq \ell$ and $j \geq r$ in consecutive positions. At each such step, all indices of the interval $]i, j[$ between the two transposed values appear before the position of the transposition. Therefore, the two permutations related by this transposition are separated by the shard $\Sigma_n(i, j,]i, j[, \emptyset)$ which is forced by $\Sigma_n(\ell, r,]\ell, r[, \emptyset)$ and therefore removed by $\equiv$. Therefore, all the permutations of the sequence belong to the same equivalence class of $\equiv$. Regarding the quotient fan $\mathcal{F}_{\equiv}$, in each step of the sequence of adjacent permutations, we cross a shard that has been removed in $\mathcal{F}_{\equiv}$ and therefore, the cones of all these permutations in the braid fan are part of the same cone of $\mathcal{F}_{\equiv}$.

We observe that the sets $I =]\ell+1, r[$ and $M =]\ell+1, r-1[$ are initial intervals of all permutations in our sequence, while $K = [1, r]$ is an initial interval of σ and $L =]\ell, n]$ is an initial interval of π. Therefore, the chamber of $\mathcal{F}_{\equiv}$ associated with our sequence of permutations contains all the rays $C(I)$, $C(K)$, $C(L)$ and $C(M)$.

Analogously, we can build another very similar sequence of permutations starting with the permutation $\sigma' := (\ell+2, \dots, r-2, \ell+1, r-1, \ell, \dots, 1, r, \dots, n)$ and ending with $\pi' := (\ell+2, \dots, r-2, \ell+1, r-1, r, \dots, n, \ell, \dots, 1)$ and using the same steps as before. For the same reason as above, all these permutations in this sequence belong to a common chamber of $\mathcal{F}_{\equiv}$ as well. Furthermore, this chamber is adjacent to the one associated with our first sequence as σ and σ' are adjacent in the weak order in $\mathfrak{S}_n$, differing only by a transposition of $\ell+1$ and $r-1$ and separated by the shard $\Sigma_n(\ell+1, r-1,]\ell+1, r-1[, \emptyset)$ which forces $\Sigma_n(\ell, r,]\ell, r[, \emptyset)$ and is therefore retained by $\equiv$ as $\Sigma_n(\ell, r,]\ell, r[, \emptyset)$ is maximal in $\mathbf{\Sigma}^{\times}_{\equiv}$. In this family of permutations, the index sets $J =]\ell, r-1[$ and $M =]\ell+1, r-1[$ are initial intervals of all the permutations, while $K = [1, r[$ is an initial interval of σ' and $L =]\ell, n]$ is an initial interval of π'. Therefore, this chamber contains all the rays $C(J)$, $C(K)$, $C(L)$ and $C(M)$ and is adjacent to the one studied above. □

We now analyze the linear dependence induced by the rays labeled by I, J, K, L and M.

Claim 2.3.5 (Linear Dependence for IJKLM)**.** *The ray vectors* $\mathbf{r}(I)$, $\mathbf{r}(J)$, $\mathbf{r}(K)$, $\mathbf{r}(L)$ *and* $\mathbf{r}(M)$ *satisfy the equation* $\mathbf{r}(I) + \mathbf{r}(J) = \mathbf{r}(K) + \mathbf{r}(L) + \mathbf{r}(M)$.

Proof. We recall that the ray vectors are given by $\mathbf{r}(S) = |S| \cdot \mathbf{1} - n \cdot \mathbf{1}_S$. The needed cardinalities are $|I| = |J| = r-\ell-2$ and $|K| = r-1$ and $|L| = n-\ell$ and $|M| = r-\ell-3$. so $|K|+|L|+|M| = 2(r-\ell-2)+n$. We deduce the following sums of ray vectors:

$$\begin{aligned}\mathbf{r}(I) + \mathbf{r}(J) &= 2 \cdot (r-\ell-2) \cdot \mathbf{1} - n \cdot \mathbf{1}_I - n \cdot \mathbf{1}_J \\ \mathbf{r}(K) + \mathbf{r}(L) + \mathbf{r}(M) &= 2 \cdot (r-\ell-2) \cdot \mathbf{1} + n \cdot \mathbf{1} - n \cdot \mathbf{1}_K - n \cdot \mathbf{1}_L - n \cdot \mathbf{1}_M\end{aligned}$$

Due to the overlapping intervals, we find that $\mathbf{1}_K + \mathbf{1}_L = \mathbf{1}_{[n]} + \mathbf{1}_I + \mathbf{1}_J - \mathbf{1}_M$, and conclude that $\mathbf{r}(I) + \mathbf{r}(J) = \mathbf{r}(K) + \mathbf{r}(L) + \mathbf{r}(M)$, proving our claim. □

Next, we examine the behaviour of the permutahedron height function with respect to the wall-crossing inequality induced by these linearly dependent rays.

Claim 2.3.6 (Wall-Crossing Inequality for IJKLM)**.** *The height function* $\mathbf{h}_\circ$ *of the permutahedron* Perm_n *satisfies the inequality* $\mathbf{h}_\circ(I) + \mathbf{h}_\circ(J) \leq \mathbf{h}_\circ(K) + \mathbf{h}_\circ(L) + \mathbf{h}_\circ(M)$.

Proof. We recall that the height function of Perm_n is given by $\mathbf{h}_\circ(S) = \frac{n}{2}|S| \cdot (n - |S|)$. For the values of this function, we obtain

$$\begin{aligned}\mathbf{h}_\circ(I) + \mathbf{h}_\circ(J) &= n(r-\ell-2)(n-r+\ell+2) \\ &= n\left(nr - n\ell - 2n - \ell^2 - r^2 - 4\ell + 4r + 2\ell r - 4\right) \\ \mathbf{h}_\circ(K) + \mathbf{h}_\circ(L) + \mathbf{h}_\circ(M) &= \tfrac{n}{2} \cdot ((r-1)(n-r+1) + (n-\ell)\ell) \\ &\quad + \tfrac{n}{2} \cdot (r-\ell-3)(n-r+\ell+3) \\ &= \tfrac{n}{2} \cdot \left(nr - r^2 + r - n + r - 1 + n\ell - \ell^2\right) \\ &\quad + \tfrac{n}{2} \cdot \left(nr - n\ell - 3n - \ell^2 + 2\ell r - 6\ell - r^2 + 6r - 9\right) \\ &= n \cdot \left(nr - \ell^2 - r^2 - 2n + \ell r - 3\ell + 4r - 5\right)\end{aligned}$$

and conclude that

$$\begin{aligned}\mathbf{h}_\circ(I) + \mathbf{h}_\circ(J) - \mathbf{h}_\circ(K) - \mathbf{h}_\circ(L) - \mathbf{h}_\circ(M) &= n\left(-n\ell - \ell + \ell r + 1\right) \\ &= n\ell(r-n) + n(1-\ell) \\ &\leq 0,\end{aligned}$$

where the last inequality holds because neither summand is positive as $1 \leq \ell < r \leq n$. □

This completes our preparations for the proof of Theorem 2.3.7, our main statement in this section.

Theorem 2.3.7 (Removahedral Congruences are Permutree Congruences)**.** *All essential removahedral congruences on the lattice of regions of the braid arrangement are permutree congruences.*

Proof. Combining Claim 2.3.3, Claim 2.3.4, Claim 2.3.5 and Claim 2.3.6, we assumed that there was an essential lattice congruence $\equiv$ of the weak order on $\mathfrak{S}_n$ that was removahedral, but not a permutree congruence. We showed that there are adjacent chambers C_1 and C_2 of the quotient fan $\mathcal{F}_\equiv$, which both contain $\mathbf{r}(K), \mathbf{r}(L)$ and $\mathbf{r}(M)$, with one of them containing $\mathbf{r}(I)$ and the other one containing $\mathbf{r}(J)$. These adjacent chambers of the quotient fan induce a wall-crossing inequality $\mathbf{h}_\circ(I) + \mathbf{h}_\circ(J) > \mathbf{h}_\circ(K) + \mathbf{h}_\circ(L) + \mathbf{h}_\circ(M)$ which is violated by the height function of

the permutahedron Perm_n. Therefore, the quotient fan $\mathcal{F}_\equiv$ cannot be obtained from the braid fan just by deleting inequalities from an $\mathcal{H}$-description of the permutahedron Perm_n. In consequence, the congruence $\equiv$ cannot be removahedral, which contradicts our assumption. □

2.3.2 Permutree Congruences are Strongly Removahedral

We now introduce a stronger criterion for certain congruences on $\mathrm{Pos}(\vec{\mathcal{A}})$ which we call strongly removahedral.

Definition 2.3.8 (Strongly Removahedral Congruence)**.** Let $\equiv$ be a removahedral lattice congruence of the weak order on $\mathfrak{S}_n$. The congruence $\equiv$ is called **strongly removahedral** if its quotient fan $\mathcal{F}_\equiv$ can be obtained from any polytope P whose normal fan is the braid fan by deleting inequalities of the $\mathcal{H}$-description of P.

It has been established that every permutree congruence is removahedral. In the rest of this section, we will show that every permutree congruence is in fact strongly removahedral. We start by describing the combinatorial structure behind any two adjacent chambers of the permutree fan.

Proposition 2.3.9 (Rays of Adjacent Chambers of the Permutree Fan)**.** *Let δ be a permutree decoration with associated permutree fan $\mathcal{F}_\delta$. Let R and S be two sets of standard ray vectors of the braid fan such that the two associated chambers $\mathrm{cone}(R)$ and $\mathrm{cone}(S)$ of $\mathcal{F}_\delta$ are adjacent. Let $\emptyset \subsetneq I, J \subsetneq [n]$ be the two index sets such that $R \setminus S = \{\mathbf{r}(I)\}$ and $S \setminus R = \{\mathbf{r}(J)\}$. Then both braid fan rays $C(I \cap J)$ and $C(I \cup J)$ are rays of $\mathcal{F}_\delta$ and both are included in $\mathrm{cone}(R \cap S)$.*

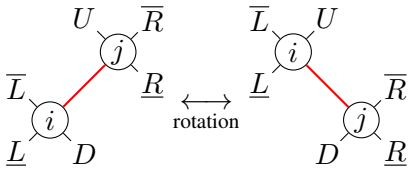

Figure 2.2: The rotation from T_R to T_S. [Picture from [APR20]]

Proof. Let T_R and T_S be the two δ-permutrees whose chambers in the permutree fan $\mathcal{F}_\delta$ are $C(T_R) = \mathrm{cone}(R)$ and $C(T_S) = \mathrm{cone}(S)$. As these chambers are adjacent, there is an edge $i \to j$ of T_R that is rotated to the edge $j \to i$ in T_S. We assume that $i < j$ (otherwise, we swap the roles of I and J in the following argument). We denote by U, D, $\underline{L}$, $\overline{L}$, $\underline{R}$, $\overline{R}$ the subtrees of T_R and T_S as illustrated in Figure 2.2. We remark that not all of the subtrees $\underline{L}$, $\overline{L}$, $\underline{R}$, $\overline{R}$ have to exist if $\delta_i \neq \otimes$ or $\delta_j \neq \otimes$. In this case, we assume the respective subtree to be empty.

We recall from Observation 1.7.21 that the standard ray vectors of the chamber $C(T_R)$ are exactly the vectors $|I| \cdot \mathbf{1}_J - |J| \cdot \mathbf{1}_I$ for all edge cuts $(I \parallel J)$ of T_R. According to Theorem 1.7.7, the edge cuts of T_R and those of T_S are the same except for the one corresponding to the edge between i and j. We obtain that $I = \{i\} \cup D \cup \underline{L} \cup \overline{L}$ and $J = \{j\} \cup D \cup \underline{R} \cup \overline{R}$. We deduce that $I \cap J = D$ and $I \cup J = [n] \setminus U$ (as $I \cup J = \{i, j\} \cup D \cup \underline{L} \cup \overline{L} \cup \underline{R} \cup \overline{R}$).

But both $(D \parallel [n] \setminus D)$ and $([n] \setminus U \parallel U)$ are edge cuts in both δ-permutrees T_R and T_S. Therefore, the corresponding rays $C(I \cap J)$ and $C(I \cup J)$ are rays of the δ-permutree fan $\mathcal{F}_\delta$ and both ray vectors $\mathbf{r}(I \cap J)$ and $\mathbf{r}(I \cup J)$ are elements of the intersection $R \cap S$. □

We deduce that the wall-crossing-inequalities used to describe a permutree fan $\mathcal{F}_\delta$ are all of a certain form.

Corollary 2.3.10 (Wall-Crossing Inequalities of a Permutree Fan)**.** All wall-crossing inequalities of the δ-permutree fan $\mathcal{F}_\delta$ are of the form $\mathbf{h}(I) + \mathbf{h}(J) > \mathbf{h}(I \cap J) + \mathbf{h}(I \cup J)$ with the usual convention that $\mathbf{h}(\emptyset) = \mathbf{h}([n]) = 0$.

Proof. We saw that any two adjacent chambers of the δ-permutree fan $\mathcal{F}_\delta$ satisfy a linear dependence of the form $\mathbf{r}(I)+\mathbf{r}(J) = \mathbf{r}(I\cap J)+\mathbf{r}(I\cup J)$. The corresponding wall-crossing inequality then is of the form $\mathbf{h}(I) + \mathbf{h}(J) > \mathbf{h}(I \cap J) + \mathbf{h}(I \cup J)$. As this holds for any pair of adjacent chambers, all wall-crossing inequalities of the δ-permutree fan $\mathcal{F}_\delta$ are of this form. □

We are now ready to deduce the main result of this section. We can start from any polytope whose normal fan is the braid fan (equivalently, any strict submodular function as stated in Theorem 1.6.5) and build a permutreehedron for any decoration δ just by removing the inequalities corresponding to those rays of the braid fan that are not rays of the permutree fan.

Corollary 2.3.11 (Permutreehedra from Strictly Submodular Functions)**.** Let $\mathbf{h} : 2^{[n]} \to \mathbb{R}_{\geq 0}$ be a strictly submodular function with $\mathbf{h}(\emptyset) = \mathbf{h}([n]) = 0$ and let $\delta \in \{\textcircled{\scriptsize /}, \textcircled{\scriptsize \backslash}, \textcircled{\scriptsize \cdot}, \textcircled{\scriptsize -}\}^n$ be a decoration of length n. Then the δ-permutree fan $\mathcal{F}_\delta$ is the normal fan of the polytope

$$\mathsf{PT}^{\mathbf{h}}_\delta := \left\{ \mathbf{x} \in \mathcal{H}^n_\Sigma \;\middle|\; \sum_{i \in I} \mathbf{x}_i \leq \mathbf{h}(I) \text{ for all } I \in \mathcal{I}_\delta \right\},$$

where $\mathcal{I}_\delta := \{\emptyset \subsetneq I \subsetneq [n] \mid \mathbf{r}(I) \text{ is a ray of } \mathcal{F}_\delta\}$ is characterized by Corollary 2.2.6. In particular, any permutree congruence $\equiv_\delta$ is strongly removahedral.

By combining this result with Theorem 2.3.7, we may conclude that every essential removahedral congruence is in fact a strongly removahedral congruence. This does not mean that we can construct every removahedron by deleting inequalities from the $\mathcal{H}$-description of an arbitrary polytope whose normal fan is the braid fan, as our new statements only concern those removahedra that are associated with a lattice congruence.

2.4 Type Cones of Permutree Fans

This section is dedicated to giving a complete facet description of the type cone $\mathsf{TC}(\mathcal{F}_\delta)$ associated to the permutree fan $\mathcal{F}_\delta$. We start by analyzing the pairs of rays that induce wall-crossing inequalities.

2.4.1 Exchangeable Rays

Proposition 2.3.9 implies that any two adjacent chambers $\mathrm{cone}(R)$ and $\mathrm{cone}(S)$ of the permutree fan $\mathcal{F}_\delta$ with $R \setminus S = \{\mathbf{r}(I)\}$ and $S \setminus R = \{\mathbf{r}(J)\}$ have a linear dependence that does not depend on R and S, but only on $\mathbf{r}(I)$ and $\mathbf{r}(J)$. This property of a fan is called the **unique exchange property** in [PPPP19]. We call a pair of rays **exchangeable** if their ray vectors $\mathbf{r}(I)$ and $\mathbf{r}(J)$ are associated in this way. It allows us to completely describe the type cone using only inequalities associated with exchangeable rays.

We therefore first identify the pairs of exchangeable rays of $\mathcal{F}_\delta$. We consider two index sets $\emptyset \subsetneq I, J \subsetneq [n]$ such that $C(I)$ and $C(J)$ are rays of the δ-permutree fan $\mathcal{F}_\delta$, as we characterized them in Corollary 2.2.6.

Proposition 2.4.1 (Exchangeable Rays in the Permutree Fan)**.** *The pair $\{C(I), C(J)\}$ of rays in the permutree fan $\mathcal{F}_\delta$ is exchangeable if and only if all of the following hold.*

(i) $i := \max(I \setminus J) < \min(J \setminus I) =: j$,
(ii) $I \setminus J = \{i\}$ *or* $\delta_i \neq \text{◁}$,
(iii) $J \setminus I = \{j\}$ *or* $\delta_j \neq \text{◁}$,
(iv) $]i, j[\cap \delta^- \subseteq (I \cap J)$,
(v) $]i, j[\cap \delta^+ \cap (I \cap J) = \emptyset$.

We first look at the pairs of exchangeable rays in an example.

Example 2.4.2. For the decorations of Figure 1.15, Figure 1.17 and Figure 1.18, the pairs of exchangeable rays of $\mathcal{F}_{\text{◁◁⊗◁}}$ are labeled by the following pairs of subsets.

- $\{\{1\},\{2\}\}$,
- $\{\{1\},\{3\}\}$,
- $\{\{1\},\{3,4\}\}$,
- $\{\{1,2\},\{1,3\}\}$,
- $\{\{1,2\},\{1,3,4\}\}$,
- $\{\{1,2\},\{2,3\}\}$,
- $\{\{1,2\},\{2,3,4\}\}$,
- $\{\{1,2,3\},\{1,3,4\}\}$,
- $\{\{1,2,3\},\{2,3,4\}\}$,
- $\{\{1,2,3\},\{4\}\}$,
- $\{\{1,3\},\{2,3\}\}$,
- $\{\{1,3\},\{3,4\}\}$,
- $\{\{1,3\},\{4\}\}$,
- $\{\{1,3,4\},\{2,3,4\}\}$,
- $\{\{2\},\{3\}\}$,
- $\{\{2\},\{3,4\}\}$,
- $\{\{2,3\},\{3,4\}\}$,
- $\{\{2,3\},\{4\}\}$,
- $\{\{3\},\{4\}\}$.

The pairs of exchangeable rays of $\mathcal{F}_{\text{◁⊗⊗◁}}$ are labeled by the following pairs of subsets.

- $\{\{1\},\{2,3,4\}\}$,
- $\{\{1,2\},\{3,4\}\}$,
- $\{\{1,2\},\{4\}\}$,
- $\{\{1,2,3\},\{1,2,4\}\}$,
- $\{\{1,2,3\},\{4\}\}$,
- $\{\{1,2,4\},\{3,4\}\}$.

Example 2.4.3. In special cases of Proposition 2.4.1, we obtain the following pairs of exchangeable rays in $\mathcal{F}_\delta$ labeled by pairs of proper subsets $\{I, J\}$ which have the following properties:

- If $\delta = \text{◁}^n$, the pairs of exchangeable rays are all the pairs of $I = K \cup \{i\}$ and $J = K \cup \{j\}$ for some $1 \leq i < j \leq n$ and $K \subseteq [n] \setminus \{i, j\}$.
- If $\delta = \text{⊗}^n$, the pairs are of the form $I = [h, j[$ and $J =]i, k]$ for $1 \leq h \leq i < j \leq k \leq n$. These pairs correspond to the pairs of intersecting internal diagonals of the $(n+2)$-gon labeled by $(h-1, j)$ and $(i, k+1)$.
- If $\delta = \text{▷}^n$, the pairs are of the form $I = [1, i]$ and $J =]i, n]$ for $1 \leq i < n$.

We now proceed by proving Proposition 2.4.1. We recall from Section 1.7.1 that a red wall is drawn above the nodes of δ^+ to separate their left and right ancestor subtrees and below the nodes of δ^- to separate their left and right descendant subtrees.

Proof of Proposition 2.4.1. In the first part of the proof, we show that the conditions in Proposition 2.4.1 are necessary for the rays $C(I)$ and $C(J)$ to be exchangeable in the δ-permutree fan $\mathcal{F}_\delta$. We follow the notation introduced in the proof of Proposition 2.3.9.

(i) We recall that we had set $I = \{i\} \cup D \cup \underline{L} \cup \overline{L}$ and $J = \{j\} \cup D \cup \underline{R} \cup \overline{R}$. As we know that $\max(\underline{L} \cup \overline{L}) < i < j < \min(\underline{R} \cup \overline{R})$, we obtain $i = \max(I \setminus J)$ and $j = \min(J \setminus I)$.
(ii) If $\delta_i = \text{◁}$, both subtrees $\underline{L}$ and $\overline{L}$ are empty. We obtain $I \setminus J = \{i\} \cup \underline{L} \cup \overline{L} = \{i\}$.
(iii) If $\delta_j = \text{◁}$, both subtrees $\underline{R}$ and $\overline{R}$ are empty. We obtain $J \setminus I = \{j\} \cup \underline{R} \cup \overline{R} = \{j\}$.
(iv) If there is some index $k \in]i, j[$ with $k \in \delta^-$ and $k \notin I \cap J$, then the δ-permutree edge connecting i and j crosses the red wall below k.
(v) If there is some index $k \in]i, j[$ with $k \in \delta^+$ and $k \in I \cap J$, then the δ-permutree edge connecting i and j crosses the red wall above k.

For the opposite direction of the proof, we assume that I and J satisfy the conditions of both Corollary 2.2.6 and Proposition 2.4.1. We will construct two δ-permutrees T and S which are related by the rotation of the edge connecting i and j, whose edge cut in T is $(I \parallel [n] \setminus I)$ and whose edge cut in S is $(J \parallel [n] \setminus J)$.

In a first step, we fix permutrees that follow the decoration δ on certain sets of indices.

- D on the restriction of δ to $I \cap J$,
- U on the restriction of δ to $[n] \setminus (I \cup J)$,
- L on the restriction of δ to $(I \setminus \{i\}) \setminus J$,
- R on the restriction of δ to $(J \setminus \{j\}) \setminus I$.

We use these smaller permutrees to construct an oriented tree T on $[n]$. We start with a directed edge $i \to j$ and place the small permutrees around it in the following way.

- If $i \in \delta^-$, we make L the left descendant subtree of i and D the right descendant subtree of i.
- If $i \notin \delta^-$, we make L the left ancestor subtree of i and D the only descendant subtree of i.
- We make U an ancestor subtree of j (the left one if $j \in \delta^+$).
- We make R the right descendant subtree of j if $j \in \delta^-$, else the right ancestor subtree of j.

We remark that there is only one way to place these subtrees. To place D if $i \in \delta^-$, we have to connect the leftmost upper blossom of D to the right lower blossom of i (to the only lower blossom if $i \notin \delta^-$.

Next, we will show that the conditions of Corollary 2.2.6 and Proposition 2.4.1 make sure that T is a δ-permutree. First of all, we remark that T is indeed a tree as L is empty if $\delta_i = \circlearrowleft$ and R is empty if $\delta_j = \circlearrowleft$ due to the second condition of Proposition 2.4.1. We therefore need to show that the edges of T neither cross any red wall below a node $k \in \delta^-$ nor any red wall above any node $k \in \delta^+$.

First of all, the nodes in L are all smaller than i and the nodes in R are all larger than j by the first condition. Therefore, there is no red wall below those nodes of U between i and j due to the fourth condition and no red wall above those nodes of D between i and j due to the fifth condition. We deduce that the edge from i to j does not cross any red wall.

We now consider an edge from ℓ to ℓ', both elements of $L \cup \{i\}$ with $\ell < \ell'$. This edge does not cross any red wall induced by a node r of $R \cup \{j\}$ since $\ell' \leq i < j \leq r$. It does not cross any red wall induced by a node u of U since otherwise, we would have $\ell < u < \ell'$ with $\ell, \ell' \in I$ and $u \in \delta^- \setminus I$, in contradiction to Corollary 2.2.6 Similarly, it does not cross any red wall induced by a node d of D since otherwise, we would have $\ell < d < \ell'$ with $\ell, \ell' \notin J$ and $d \in \delta^+ \cap J$, in contradiction to Corollary 2.2.6 Similarly, we can prove that no edge in $D \cup \{i\}$ or $U \cup \{j\}$ or $R \cup \{j\}$ crosses any red wall. Therefore, T is a δ-permutree.

We finally denote by S the δ-permutree obtained by rotating the edge $i \to j$ of T. As a result of this construction, the edge $i \to j$ induces the edge cut $(I \parallel [n] \setminus I)$ in T, while the edge $j \to i$ induces the edge cut $(J \parallel [n] \setminus J)$ in S. In consequence, the δ-permutrees T and S correspond to adjacent chambers of the δ-permutree fan $\mathcal{F}_\delta$ and the rays $C(I)$ and $C(J)$ are exchangeable in these chambers. □

We want to calculate the number of pairs of exchangeable rays in the δ-permutree fan $\mathcal{F}_\delta$. We first introduce an auxiliary function Ω.

Definition 2.4.4 (Omega Function)**.** For a sequence $(\delta_1 \dots \delta_k)$ of decoration symbols $\circlearrowleft, \circledcirc, \circledcirc, \otimes$, we define the function Ω inductively by $\Omega() = 1$ for the empty sequence and

$$\Omega(\delta_1 \dots \delta_k) := \begin{cases} 2 \cdot \Omega(\delta_1 \dots \delta_{k-1}) & \text{if } \delta_k = \circlearrowleft, \\ 1 + \Omega(\delta_1 \dots \delta_{k-1}) & \text{if } \delta_k \in \{\circledcirc, \circledcirc\}, \\ 2 & \text{if } \delta_k = \otimes. \end{cases}$$

We then define the functions $\Omega^\otimes$ and $\Omega^\circlearrowleft$ for a sequence $(\delta_1 \dots \delta_i)$ by

$$\Omega^\otimes(\delta_1 \dots \delta_i) := \begin{cases} 1 & \text{if } \delta_i = \otimes, \\ \Omega(\delta_1 \dots \delta_{i-1}) & \text{if } \delta_i \neq \otimes, \end{cases}$$

$$\Omega^\circlearrowleft(\delta_1 \dots \delta_i) := \begin{cases} \Omega(\delta_1 \dots \delta_{i-1}) & \text{if } \delta_i = \circlearrowleft, \\ 1 & \text{if } \delta_i \neq \circlearrowleft. \end{cases}$$

We can visualize the mechanism behind the function Ω in the following way: We start with a trivial binary tree containing nothing but a root node. Then each step of the construction can be visualized as the construction of a new binary tree based on the one obtained in the previous step.

- If $\delta_k = \textcircled{\scriptsize |}$, the root node has two copies of the previous tree as children.
- If $\delta_k \in \{\textcircled{\scriptsize /}, \textcircled{\scriptsize \backslash}\}$, one child of the root is a leaf while the other is a copy of the previous tree.
- If $\delta_k = \otimes$, both children of the root are leafs.

Then Ω equals the number of leafs of the binary tree obtained after the last step, while for $\Omega^{\otimes}$, we either keep this number or replace it by one if the last symbol is $\otimes$ and for $\Omega^{\textcircled{\scriptsize |}}$, we either keep this number or replace it by one if the last symbol is different from $\textcircled{\scriptsize |}$.

Regardless of this illustration, we can use the function to count all pairs of exchangeable rays for a given permutree decoration δ.

Corollary 2.4.5 (Number of Pairs of Exchangeable Rays)**.** Let δ be a permutree decoration of length n. The number $\boldsymbol{\chi}(\delta)$ of pairs of exchangeable rays in the permutree fan $\mathcal{F}_\delta$ is

$$\boldsymbol{\chi}(\delta) = \sum_{\substack{1 \le i < j \le n \\ \forall k \in]i,j[\colon \delta_k \neq \otimes}} \Omega^{\otimes}(\delta_1 \dots \delta_i) \cdot 2^{|\{k \in]i,j[\mid \delta_k = \textcircled{\scriptsize |}\}|} \cdot \Omega^{\otimes}(\delta_n \dots \delta_j).$$

Example 2.4.6. For the decorations of Figure 1.15, Figure 1.17 and Figure 1.18, we obtain $\boldsymbol{\chi}(\textcircled{\scriptsize |}\textcircled{\scriptsize |}\textcircled{\scriptsize /}\otimes\textcircled{\scriptsize |}) = 19$ and $\boldsymbol{\chi}(\textcircled{\scriptsize |}\otimes\otimes\textcircled{\scriptsize |}) = 6$.

Example 2.4.7. We study the consequences of Corollary 2.4.5 for certain simple decorations.

- If $\delta = \textcircled{\scriptsize |}^n$, then the associated permutree fan $\mathcal{F}_{\textcircled{\scriptsize |}^n} = \mathcal{F}_n$ is the braid fan, and its number of pairs of exchangeable rays is $2^{n-1} \cdot \binom{n}{2}$.
- If $\delta = \textcircled{\scriptsize /}^n$, then the asociated permutree fan $\mathcal{F}_{\textcircled{\scriptsize /}^n}$ has $\binom{n+2}{4}$ pairs of exchangeable rays. This equals the number of quadruples of vertices of the $(n+2)$-gon.
- If $\delta = \otimes^n$, then the associated permutree fan $\mathcal{F}_{\otimes^n}$ has $n-1$ pairs of exchangeable rays.

After looking at these examples, we will now prove the statement about the number of pairs of exchangeable rays in a permutree fan as stated in Corollary 2.4.5.

Proof of Corollary 2.4.5. We recall from Corollary 2.2.6 that the rays of the δ-permutree fan $\mathcal{F}_\delta$ are labeled by those index sets $\emptyset \subsetneq I \subseteq [n]$ where for all $1 \le a < b < c \le n$, whenever $a, c \in I$, then $b \notin \delta^- \setminus I$ and whenever $a, c \notin I$, then $b \notin \delta^+ \cap I$. Furthermore, Proposition 2.4.1 gives us a condition for when two such index sets labeling rays of the permutree fan form a pair of exchangeable rays of $\mathcal{F}_\delta$. We count the number of ways to build two index sets I and J that both label rays of the permutree fan $\mathcal{F}_\delta$ that are exchangeable.

- First, we choose two indices $1 \le i < j \le n$. We will shape I and J such that $i = \max(I \setminus J)$ and $j = \min(J \setminus I)$. This ensures that they satisfy Corollary 2.2.6 (i).
- For each $k \in]i,j[$, the aforementioned condition $\max(I \setminus J) = i < k < j = \min(J \setminus I)$ implies that either $k \in I \cap J$ or $k \in [n] \setminus (I \cup J)$. We have two restrictions: If $k \in \delta^-$, we need $k \in I \cap J$ due to Proposition 2.4.1 (iv). If $k \in \delta^+$, we need $k \in [n] \setminus (I \cup J)$ due to Proposition 2.4.1 (v). Depending on the decoration δ, the following cases are possible.
  - If $\delta_k = \otimes$, there is no such pair of index sets. This explains the condition on the sum.
  - If $\delta_k = \textcircled{\scriptsize /}$, we need $k \in I \cap J$, leaving us no choice.
  - If $\delta_k = \textcircled{\scriptsize \backslash}$, we need $k \in [n] \setminus (I \cup J)$, leaving us no choice.
  - If $\delta_k = \textcircled{\scriptsize |}$, we are free to choose either $k \in I \cap J$ or $k \in [n] \setminus (I \cup J)$.

  Combining these choices over all $k \in]i,j[$, the number of choices is obtained by multiplying a 2 for each $k \in]i,j[$ that has $\delta_k = \textcircled{\scriptsize |}$, giving a us $2^{|\{k \in]i,j[\mid \delta_k = \textcircled{\scriptsize |}\}|}$ choices.
- For each $k \in [1,i[$, we first note that we cannot have $k \in J \setminus I$ as $k < i < j = \min(J \setminus I)$. Furthermore, if $\delta_i = \textcircled{\scriptsize |}$, then we cannot have $k \in I \setminus J$ due to Proposition 2.4.1 (ii).

We take a look at the conditions imposed by Corollary 2.2.6. If $i \in \delta^+$, then we need that $i < \min([n]\setminus I)$ as the alternative $\max([n]\setminus I) < i$ is impossible due to $i < j \in [n]\setminus I$. Therefore, if $i \in \delta^+$, we are forced to have $k \in I$ for all $k \in [1, i[$. Analogously, if $i \in \delta^-$, we are forced to have $k \notin J$. This narrows down our choices as follows, depending on the symbol δ_i.

- If $\delta_i = \otimes$, we are forced to have $k \in I \setminus J$.
- If $\delta_i = \circledcirc$, we are forced to have $k \notin J$ with either $k \in I$ or $k \notin I$.
- If $\delta_i = \circledast$, we are forced to have $k \in I$ with either $k \in J$ or $k \notin J$.
- If $\delta_i = \oplus$, we have either $k \in I \cap J$ or $k \in [n] \setminus (I \cup J)$.

Therefore, if $\delta_i = \otimes$, this determines the assignment of all indices in $[1, i[$ to the sets I and J. Otherwise, our choices are limited further by the conditions imposed by Corollary 2.2.6.

- If $k \in \delta^-$ with $k \notin I$, then $k < \min(I)$, so all indices $< k$ have to be excluded from I.
- If $k \in \delta^-$ with $k \notin J$, then $k < \min(J)$, so all indices $< k$ have to be excluded from J.
- If $k \in \delta^+$ with $k \in I$, then $k < \min([n] \setminus I)$, so all indices $< k$ have to be included in I.
- If $k \in \delta^+$ with $k \in J$, then $k < \min([n] \setminus J)$, so all indices $< k$ have to be included in J.

Then the Omega function from Definition 2.4.4 counts the number of ways in which we can decide for each index $k \in [1, i[$ whether it should be included in I or J or both or none. We recall that as $\delta_i \in \{\oplus, \circledcirc, \circledast\}$, we have exactly two valid choices for each of these positions, which are not independent.

- Whenever $\delta_k = \oplus$, we double the number of valid combinations on the smaller indices as neither of our choices imposes a constraint.
- Whenever $\delta_k \in \{\circledcirc, \circledast\}$, one of our choices keeps up all the previous combinations, while the other choice forces us to use one specific combination on the smaller indices.
- Whenever $\delta_k = \otimes$, each of our choices forces us to use one specific combination on the smaller indices.

Therefore, the function $\Omega(\delta_1 \dots \delta_{i-1})$ gives the number of valid assignments of the indices in $[1, i[$ to the sets I and J. The function $\Omega^{\otimes}(\delta_1 \dots \delta_i)$ either keeps this value or replaces it by 1 in the case where $\delta_i = \otimes$.

- The choices for $k \in]j, n]$ are counted analogously to those for $k \in [1, i[$. □

2.4.2 Facets of the Type Cone

Due to the unique exchange property of the δ-permutree fan $\mathcal{F}_\delta$, every pair of exchangeable rays of $\mathcal{F}_\delta$ yields a wall-crossing inequality for the type cone $\mathsf{TC}(\mathcal{F}_\delta)$. When collecting all these inequalities, some of them are redundant. Regarding the geometry of the type cone, this means that these inequalities do not define facets of $\mathsf{TC}(\mathcal{F}_\delta)$. We can characterize those pairs of exchangeable rays that do define a facet of $\mathsf{TC}(\mathcal{F}_\delta)$ by criteria similar to those given in Proposition 2.4.1. In fact, conditions (i), (iv) and (v) are identical, only conditions (ii) and (iii) are slightly stricter.

Proposition 2.4.8 (Facets of the Permutree Type Cone)**.** *The pair $\{C(I), C(J)\}$ of rays in the permutree fan $\mathcal{F}_\delta$ is exchangeable and defines a facet of the type cone $\mathsf{TC}(\mathcal{F}_\delta)$ if and only if all of the following hold.*

(i) $i := \max(I \setminus J) < \min(J \setminus I) =: j$,
(ii) $I \setminus J = \{i\}$ *or* $\delta_i = \otimes$,
(iii) $J \setminus I = \{j\}$ *or* $\delta_j = \otimes$,
(iv) $]i, j[\cap \delta^- \subseteq (I \cap J)$,
(v) $]i, j[\cap \delta^+ \cap (I \cap J) = \emptyset$.

Example 2.4.9. For the decorations of Figure 1.15, Figure 1.17 and Figure 1.18, the facets of the type cone $\mathsf{TC}(\mathcal{F}_{\oplus\circledcirc\otimes\circledast})$ correspond to rays labeled by the pairs of subsets

- $\{\{1\},\{2\}\}$,
- $\{\{1\},\{3\}\}$,
- $\{\{1,2\},\{1,3\}\}$,
- $\{\{1,2\},\{2,3\}\}$,
- $\{\{1,2,3\},\{1,3,4\}\}$,
- $\{\{1,2,3\},\{2,3,4\}\}$,
- $\{\{1,3\},\{2,3\}\}$,
- $\{\{1,3\},\{3,4\}\}$,
- $\{\{1,3,4\},\{2,3,4\}\}$,
- $\{\{2,3\},\{3,4\}\}$,
- $\{\{3\},\{4\}\}$.

The facets of the type cone $\mathsf{TC}(\mathcal{F}_{\textcircled{1}\otimes\textcircled{1}})$ correspond to rays labeled by the subsets

- $\{\{1\},\{2,3,4\}\}$,
- $\{\{1,2\},\{4\}\}$,
- $\{\{1,2,3\},\{1,2,4\}\}$,
- $\{\{1,2,4\},\{3,4\}\}$.

Example 2.4.10. As special cases of Proposition 2.4.8, we find that the pairs of echangeable rays of $\mathcal{F}_\delta$ described in Example 2.4.3 define facets of the type cone $\mathsf{TC}(\mathcal{F}_\delta)$ when $\delta = \textcircled{1}^n$ or $\delta = \otimes^n$. If $\delta = \textcircled{\scriptsize{$\otimes$}}^n$, the facets of the type cone $\mathsf{TC}(\mathcal{F}_{\textcircled{\scriptsize{$\otimes$}}^n})$ are induced by pairs of rays labeled $[i,j[$ and $]i,j]$ for some $1 \leq i < j \leq n$. These pairs correspond to intersecting internal diagonals $(i-1,j)$ and $(i,j+1)$ of the $(n+2)$-gon, which differ only by a shift.

Observation 2.4.11 (Index Set Intervals and Type Cone Facets)**.** By combining Corollary 2.2.6 and Proposition 2.4.8 (ii)-(iii), we can say something more about pairs of index sets that induce facets of the type cone.

- The interval $[1,i[$ is included
  - in $I \setminus J$ if $\delta_i = \otimes$,
  - in $[n] \setminus (I \cup J)$ if $\delta_i = \textcircled{\scriptsize{$\otimes$}}$,
  - in $I \cap J$ if $\delta_i = \textcircled{\scriptsize{$\otimes$}}$.
- The interval $]j,n]$ is included
  - in $J \setminus I$ if $\delta_j = \otimes$,
  - in $[n] \setminus (I \cup J)$ if $\delta_j = \textcircled{\scriptsize{$\otimes$}}$,
  - in $I \cap J$ if $\delta_j = \textcircled{\scriptsize{$\otimes$}}$.

In particular, we obtain that $I \setminus J$ is either $\{i\}$ or $[1,i]$, and $J \setminus I$ is either $\{j\}$ or $[j,n]$. However, these conditions are not sufficient, as for example $I = \{1,2\}$ and $J = \{3\}$ do not label a pair of rays that induces a facet of the type cone.

Proof of Proposition 2.4.8. We consider two index sets I, J that satisfy the conditions of Corollary 2.2.6 and label a pair of exchangeable rays as stated in Proposition 2.4.1. We will show that they satisfy the stronger conditions of Proposition 2.4.8 (ii)-(iii) if and only if the wall-crossing inequality corresponding to the exchange of $C(I)$ and $C(J)$ defines a facet of the permutree type cone $\mathsf{TC}(\mathcal{F}_\delta)$. This gives us two statements to prove:

1. If I, J do not satisfy Proposition 2.4.8 (ii)-(iii), then the wall-crossing inequality induced by I and J can be expressed as the sum of wall-crossing inequalities induced by other pairs of exchangeable rays.
2. If I, J satisfy Proposition 2.4.8 (ii)-(iii), then there is a point in the ambient space of the type cone that satisfies all wall-crossing inequalities induced by pairs of exchangeable rays of $\mathcal{F}_\delta$ except for the one induced by the pair $\{I, J\}$.

We start by proving the first of these two statements. Let I, J be two index sets that label a pair of exchangeable rays of the permutree fan (thus satisfying the conditions of Corollary 2.2.6 and Proposition 2.4.1 (ii)-(iii)), but fail to satisfy Proposition 2.4.8 (ii)-(iii). Then at least one of the following holds:

- $|I \setminus J| > 1$ and $\delta_i \neq \otimes$,
- or $|J \setminus I| > 1$ and $\delta_j \neq \otimes$.

As I and J satisfy Proposition 2.4.1 (ii)-(iii), in both these cases, $\delta_i \neq \otimes$ (resp. $\delta_j \neq \otimes$) has to hold. Therefore, at least one of the following holds:

- $|I \setminus J| > 1$ and $\delta_i \in \{\textcircled{\scriptsize{$\otimes$}}, \textcircled{\scriptsize{$\otimes$}}\}$,
- or $|J \setminus I| > 1$ and $\delta_j \in \{\textcircled{\scriptsize{$\otimes$}}, \textcircled{\scriptsize{$\otimes$}}\}$.

We will examine the consequences of the case where $|I \setminus J| > 1$ and $\delta_i = \textcircled{\scriptsize{$\otimes$}}$, while the other cases are symmetric. We first set, as usual,

- $i := \max(I \setminus J)$,
- $j := \min(J \setminus I)$,
- $D := I \cap J$,
- $U := [n] \setminus (I \cup J)$,
- $L := (I \setminus J) \setminus \{i\}$,
- $R := (J \setminus I) \setminus \{j\}$.

As done in the proof of Proposition 2.4.1, we choose a suitable permutree on D, U, L and R and construct δ-permutrees T and S such that the rotation from T to S exchanges the rays labeled by I

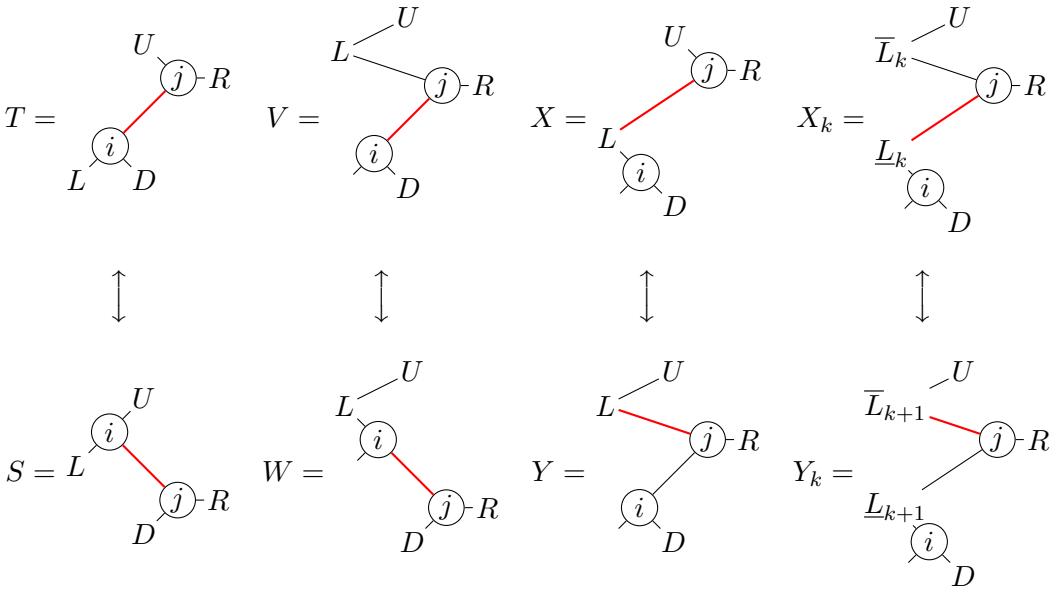

Figure 2.3: Some rotations in δ-permutrees. The third column is a combination of rotations of the form given in the fourth column. [Picture from [APR20]]

and J. See Figure 2.3 for an illustration of S, T and the δ-permutrees V, W, X and Y constructed similarly. Note that the subtree R is drawn at the same level as the node j, and can be the right ancestor or right descendant subtree of j, depending on whether $\delta_j = ☮$ or $\delta_j = ☹$. We will now examine the rotations in Figure 2.3 and see which wall-crossing inequalities they induce.

- The trees S and T.
  We already know that the inequality induced by the pair $\{I, J\}$ is
  $$\mathbf{h}(I) + \mathbf{h}(J) > \mathbf{h}(I \cap J) + \mathbf{h}(I \cup J).$$
- The trees V and W.
  We first note that both have $\delta_i = ☮$, so both V and W are δ-permutrees as well. In the tree V, the leftmost lower blossom of L is connected to j. In the tree W, the leftmost lower blossom of L is connected to i. The rightmost upper blossom of L is connected to the blossom of U which used to be connected to j in the tree T. If we set $I' := D \cup \{i\} = (I \cap J) \cup \{i\}$, then the edge cut induced by $i \to j$ in V is $(I' \parallel [n] \setminus I')$ and the edge cut induced by $j \to i$ in W is $(J \parallel [n] \setminus J)$ as $D \cup R \cup \{j\} = J$. This gives us the inequality
  $$\mathbf{h}(I') + \mathbf{h}(J) > \mathbf{h}(I \cap J) + \mathbf{h}(I \cup J).$$
- The trees X and Y.
  Clearly, Y is a δ-permutree as it is equal to V. By the same arguments, X is a δ-permutree as well. If both i and j are connected to the same node of L, then rotating the edge joining L and j relates X and Y. Otherwise, this rotation moves a part of L in between j and U and leaves the remaining part of L between i and j. This yields a sequence of rotations between the δ-permutrees X_k and Y_k as illustrated in Figure 2.3, where we set $X_1 := X$ and $X_{k+1} := Y_k$ in every step. Each of these is a δ-permutree where we have a partition of L into the lower part $\underline{L}_k$ and the upper part $\overline{L}_k$. Then $\underline{L}_{k+1}$ is obtained from $\underline{L}_k$ by deleting the node connected to j in X_k and all its left ancestors and descendants. This way, we will finally end up with $Y_p = Y$.
  We set $J' := J \cup \{i\} = R \cup D \cup \{j\} \cup \{i\}$ and recall that $I' = D \cup \{i\}$. Each of the

above rotations relates the ray labeled by $I' \cup \underline{L}_k$ to the ray labeled by $J' \cup \underline{L}_{k+1}$, where the intersection of these two sets is $I' \cup \underline{L}_{k+1}$ and their union is $J' \cup \underline{L}_k$. This gives us one wall-crossing inequality per step, each of the form

$$\mathbf{h}(I' \cup \underline{L}_k) + \mathbf{h}(J' \cup \underline{L}_{k+1}) \;>\; \mathbf{h}(I' \cup \underline{L}_{k+1}) + \mathbf{h}(J' \cup \underline{L}_k)$$

in each step. Summing up all these inequalities, due to the fact that $\underline{L}_1 = L$ and $\underline{L}_p = \emptyset$, as well as $I' = I \cap J'$ and $J' \cup L = I \cup J'$, we obtain the inequality

$$\begin{aligned}
\sum_{k=1}^{p-1} \mathbf{h}(I' \cup \underline{L}_k) + \sum_{k=2}^{p} \mathbf{h}(J' \cup \underline{L}_k) \;&>\; \sum_{k=2}^{p} \mathbf{h}(I' \cup \underline{L}_k) + \sum_{k=1}^{p-1} \mathbf{h}(J' \cup \underline{L}_k) \\
\mathbf{h}(I' \cup \underline{L}_1) + \mathbf{h}(J' \cup \underline{L}_p) \;&>\; \mathbf{h}(I' \cup \underline{L}_p) + \mathbf{h}(J' \cup \underline{L}_1) \\
\mathbf{h}(I) + \mathbf{h}(J') \;&>\; \mathbf{h}(I \cap J') + \mathbf{h}(I \cup J').
\end{aligned}$$

If we sum up the wall-crossing inequality induced by the pair $\{I', J\}$ and the wall-crossing inequality induced by the pair $\{I, J'\}$, recalling that $I \cap J' = I'$ and $I' \cup J = J'$, we obtain

$$\begin{aligned}
\mathbf{h}(I') + \mathbf{h}(J) + \mathbf{h}(I) + \mathbf{h}(J') \;&>\; \mathbf{h}(I \cap J) + \mathbf{h}(I \cup J) + \mathbf{h}(I \cap J') + \mathbf{h}(I \cup J') \\
\mathbf{h}(I) + \mathbf{h}(J) \;&>\; \mathbf{h}(I \cap J) + \mathbf{h}(I \cup J).
\end{aligned}$$

We have therefore shown that the wall-crossing inequality $\mathbf{h}(I) + \mathbf{h}(J) > \mathbf{h}(I \cap J) + \mathbf{h}(I \cup J)$ induced by the pair $\{I, J\}$ is nothing but the sum of the wall-crossing inequalities induced by the rotation from V to W and the stepwise rotation from X to Y. In consequence, the pair of I and J does not define a facet of the type cone $\mathsf{TC}(\mathcal{F}_\delta)$. This concludes our proof for the first statement.

It is left to show that if the pair $\{I, J\}$ satisfies Proposition 2.4.8 (ii)-(iii), then there is a point in the ambient space of the type cone that satisfies all wall-crossing inequalities induced by pairs of exchangeable rays of $\mathcal{F}_\delta$ except for the one induced by the pair $\{I, J\}$.

We first introduce some notations and definitions. For any finite set S, we denote its power set (the set containing all subsets of S) by $\mathcal{P}(S) := \{X \subseteq S\}$. For two finite sets A, B, we define $\nabla(A, B) := \mathcal{P}(A \cup B) \setminus (\mathcal{P}(A) \cup \mathcal{P}(B))$ to be the set of all subsets that contain at least one element of both $A \setminus B$ and $B \setminus A$. We write $A \between B$ if neither $A \setminus B$ not $B \setminus A$ are empty. If $A \between B$, we observe that

- $A \cup B$ is the inclusion-maximal element of $\nabla(A, B)$,
- A and B are inclusion-maximal among the subsets of $A \cup B$ not included in $\nabla(A, B)$,
- the two-element sets contained in $\nabla(A, B)$ are precisely the unordered pairs $\{a, b\}$ for any combination of $a \in A \setminus B$ and $b \in B \setminus A$.

Moreover, given two pairs of finite sets $\{A, B\}$ and $\{C, D\}$ with $A \between B$ and $C \between D$, we obtain the following statements.

- If $\nabla(A, B) = \nabla(C, D)$, then $A \cup B = C \cup D$ and $\{A \setminus B, B \setminus A\} = \{C \setminus D, D \setminus C\}$, so $\{A, B\} = \{C, D\}$ are in fact the same pair of sets.
- If $\nabla(A, B) \subseteq \nabla(C, D)$, then $A \cup B \subseteq C \cup D$, and up to exchanging C and D, we have $A \setminus B \subseteq C \setminus D$ and $B \setminus A \subseteq D \setminus C$.

Furthermore, we will build the type cone $\mathsf{TC}(\mathcal{F}_\delta)$ in the space $\mathbb{R}^{\mathcal{I}_\delta}$ indexed by those index sets $I \in \mathcal{I}_\delta$ that label rays of the permutree fan $\mathcal{F}_\delta$. We denote by $(\mathbf{g}_M)_{M \in \mathcal{I}_\delta}$ the standard basis of this space. Given our pair of subsets $\{I, J\}$ labeling a pair of exchangeable rays, we set $\mathbf{n}(I, J) := \mathbf{g}_I + \mathbf{g}_J - \mathbf{g}_{I \cap J} - \mathbf{g}_{I \cup J}$ to be the normal vector of the wall-crossing inequality associated to that pair. Our task now is to find a point $\mathbf{p} \in \mathbb{R}^{\mathcal{I}_\delta}$ such that

- $\langle \mathbf{p} \,|\, \mathbf{n}(I, J) \rangle < 0$ for our pair $\{I, J\}$,
- $\langle \mathbf{p} \,|\, \mathbf{n}(K, L) \rangle \geq 0$ for any other pair $\{K, L\}$ satisfying the conditions of Proposition 2.4.8.

To achieve this, we define three auxiliary vectors $\mathbf{x}, \mathbf{y}, \mathbf{z} \in \mathbb{R}^{\mathcal{I}_\delta}$ as follows:

$$\begin{aligned}\mathbf{x} &:= -\sum_{M \in \mathcal{I}_\delta} |\mathcal{P}(M) \setminus \nabla(I,J)| \cdot \mathbf{g}_M,\\ \mathbf{y} &:= -\sum_{M \in \mathcal{I}_\delta} |\mathcal{P}(M) \cap \nabla(I,J)| \cdot \mathbf{g}_M,\\ \mathbf{z} &:= -\mathbf{n}(I,J).\end{aligned}$$

We construct the point $\mathbf{p} \in \mathbb{R}^{\mathcal{I}_\delta}$ as $\mathbf{p} := \lambda\mathbf{x} + \mu\mathbf{y} + \mathbf{z}$, where $\lambda \in \mathbb{R}$ is an arbitrary scalar such that $\lambda > |\langle \mathbf{z} \,|\, \mathbf{n}(K,L)\rangle|$ for any pair $\{K,L\}$ of subsets and $\mu \in \mathbb{R}$ is an arbitrary scalar such that $0 < \mu\,|\nabla(I,J)| < \langle \mathbf{z} \,|\, \mathbf{z}\rangle$. We will prove that this point $\mathbf{p}$ satisfies the desired inequalities.

For this, let $\{K,L\}$ be a pair of index sets satisfying Proposition 2.4.8 (ii)-(iii). We analyze the scalar product of the point $\mathbf{p}$ with the normal vector $\mathbf{n}(K,L)$ associated to the pair $\{K,L\}$. We do so by analyzing the scalar products of $\mathbf{x}$, $\mathbf{y}$ and $\mathbf{z}$ with $\mathbf{n}(K,L)$. We first note that due to inclusion-exclusion, we have $|\nabla(K,L)| = |\mathcal{P}(K \cup L)| - |\mathcal{P}(K)| - |\mathcal{P}(L)| + |\mathcal{P}(K \cap L)|$. This helps us with the following calculations.

$$\begin{aligned}\langle \mathbf{x} \,|\, \mathbf{n}(K,L)\rangle =& \mathbf{x}_K + \mathbf{x}_L - \mathbf{x}_{K\cap L} - \mathbf{x}_{K\cup L}\\ =& -|\mathcal{P}(K) \setminus \nabla(I,J)| - |\mathcal{P}(L) \setminus \nabla(I,J)|\\ &+ |\mathcal{P}(K\cup L) \setminus \nabla(I,J)| + |\mathcal{P}(K\cap L) \setminus \nabla(I,J)|\\ =& |\nabla(K,L) \setminus \nabla(I,J)|\\ \langle \mathbf{y} \,|\, \mathbf{n}(K,L)\rangle =& \mathbf{y}_K + \mathbf{y}_K - \mathbf{y}_{K\cap L} - \mathbf{y}_{K\cup L}\\ =& -|\mathcal{P}(K) \cap \nabla(I,J)| - |\mathcal{P}(L) \cap \nabla(I,J)|\\ &+ |\mathcal{P}(K\cup L) \cap \nabla(I,J)| + |\mathcal{P}(K\cap L) \cap \nabla(I,J)|\\ =& |\nabla(K,L) \cap \nabla(I,J)|\\ \langle \mathbf{z} \,|\, \mathbf{n}(K,L)\rangle =& -\langle \mathbf{n}(I,J) \,|\, \mathbf{n}(K,L)\rangle\\ =& -\langle \mathbf{g}_I + \mathbf{g}_J - \mathbf{g}_{I\cup J} - \mathbf{g}_{I\cap J} \,|\, \mathbf{g}_K + \mathbf{g}_L - \mathbf{g}_{K\cup L} - \mathbf{g}_{K\cap L}\rangle\end{aligned}$$

We can now evaluate the scalar product of $\mathbf{p}$ with the normal vector associated to the facet defined by a pair of index sets $\{K,L\}$ and, in particular, the pair of index sets $\{I,J\}$.

$$\begin{aligned}\langle \mathbf{p} \,|\, \mathbf{n}(K,L)\rangle &= \lambda \cdot |\nabla(K,L) \setminus \nabla(I,J)| + \mu \cdot |\nabla(K,L) \cap \nabla(I,J)| + \langle \mathbf{z} \,|\, \mathbf{n}(K,L)\rangle\\ \langle \mathbf{p} \,|\, \mathbf{n}(I,J)\rangle &= \lambda \cdot |\nabla(I,J) \setminus \nabla(I,J)| + \mu \cdot |\nabla(I,J) \cap \nabla(I,J)| + \langle \mathbf{z} \,|\, \mathbf{n}(I,J)\rangle\\ &= 0 + \mu \cdot |\nabla(I,J)| - \langle \mathbf{z} \,|\, \mathbf{z}\rangle \;<\; 0,\end{aligned}$$

where the final inequality is due to the definition of μ (which implies $\mu \cdot |\nabla(I,J)| < \langle \mathbf{z} \,|\, \mathbf{z}\rangle$). To evaluate $\langle \mathbf{p} \,|\, \mathbf{n}(K,L)\rangle$, we distinguish the cases where $\nabla(K,L)$ is a subset of $\nabla(I,J)$ or not:

- If $\nabla(K,L) \not\subseteq \nabla(I,J)$, then $\nabla(K,L) \setminus \nabla(I,J)$ is non-empty, so $\lambda \cdot |\nabla(K,L) \setminus \nabla(I,J)| \geq \lambda$. By definition, $\lambda > |\langle \mathbf{z} \,|\, \mathbf{n}(K,L)\rangle|$, so

$$\begin{aligned}\langle \mathbf{p} \,|\, \mathbf{n}(K,L)\rangle =& \lambda \cdot |\nabla(K,L) \setminus \nabla(I,J)| + \mu \cdot |\nabla(K,L) \cap \nabla(I,J)| + \langle \mathbf{z} \,|\, \mathbf{n}(K,L)\rangle\\ >& \mu \cdot |\nabla(K,L) \cap \nabla(I,J)| \;\geq\; 0.\end{aligned}$$

- If $\nabla(K,L) \subsetneq \nabla(I,J)$, then $\lambda \cdot |\nabla(K,L) \setminus \nabla(I,J)| = 0$. Furthermore, $\nabla(K,L)$ is guaranteed to contain $K \cup L$, so $\mu \cdot |\nabla(K,L) \cap \nabla(I,J)| > 0$. All we need to show is that $\langle \mathbf{z} \,|\, \mathbf{n}(K,L)\rangle = 0$ which can be reformulated as

$$\langle \mathbf{g}_I + \mathbf{g}_J - \mathbf{g}_{I\cup J} - \mathbf{g}_{I\cap J} \,|\, \mathbf{g}_K + \mathbf{g}_L - \mathbf{g}_{K\cup L} - \mathbf{g}_{K\cap L}\rangle = 0,$$

which is equivalent to $\{I,\ J,\ I \cup J,\ I \cap J\}$ and $\{K,\ L,\ K \cup L,\ K \cap L\}$ being disjoint. Up to reversing the roles of I and J, we can set $i := \max(I \setminus J) < \min(J \setminus I) =: j$. We do the same for $k := \max(K \setminus L) < \min(L \setminus K) =: \ell$. As demonstrated when we introduced the ∇-notation, the fact that $\nabla(K, L) \subseteq \nabla(I, J)$ implies that $K \setminus L \subseteq I \setminus J$ and $L \setminus K \subseteq J \setminus I$, from which we deduce that $k \leq i < j \leq \ell$. As we know that the pair $\{I, J\}$ satisfies the condition Proposition 2.4.8 (ii), there are two possibilities.

- If $I \setminus J = \{i\}$, then $\emptyset \subsetneq K \setminus L \subsetneq I \setminus J$ implies that $K \setminus L = \{i\}$ as well.
- If $\delta_i = \otimes$, then $k \leq i$ implies that $k = i$ (otherwise, there would be $i \in]k, \ell[$ with $i \in \delta^- \cap \delta^+$, contradicting Proposition 2.4.8 (iv)-(v)). We know from Observation 2.4.11 that $[1, i[\subseteq I \setminus J$, so $I \setminus J = [1, i]$ and, for the same reason, $K \setminus L = [1, i]$ as well.

As a symmetric proof holds for the sets $J \setminus I$ and $L \setminus K$, we conclude that $K \setminus L = I \setminus J$ and $L \setminus K = J \setminus I$, where in particular, $k = i$ and $j = \ell$. We are now ready to prove that $\{I, J, I \cup J, I \cap J\}$ and $\{K, L, K \cup L, K \cap L\}$ are disjoint.

- As $i \in I \setminus L$ and $j \in L \setminus I$, we have $I \notin \{L, K \cup L, K \cap L\}$. Similarly, we obtain $J \notin \{K, K \cup L, K \cap L\}$ and $K \notin \{J, I \cup J, I \cap J\}$ and $L \notin \{J, I \cup J, I \cap J\}$. If $I = K$, then $J = (J \setminus I) \cup (I \setminus (I \setminus J)) = (L \setminus K) \cup (K \setminus (K \setminus L)) = L$. Similarly, if $J = L$, then $I = K$, but we assumed the pair $\{I, J\}$ to be distinct from $\{K, L\}$,
- It is left to show that $\{I \cup J, I \cap J\}$ and $\{K \cup L, K \cap L\}$ are not disjoint.
  - Clearly, $I \cup J \neq K \cap L$ as $i \in I \setminus L$.
  - Similarly, $I \cap J \neq K \cup L$ as $j \in L \setminus I$.
  - If $I \cup J = K \cup L$, then $I = (I \cup J) \setminus (J \setminus I) = (K \cup L) \setminus (L \setminus K) = K$, contradiction.
  - And if $I \cap J = K \cap L$, then $I = (I \cap J) \cup (I \setminus J) = (K \cap L) \cup (K \setminus L) = K$ again.

  This completes our argument that the two sets are disjoint.

So as $\{I, J, I \cup J, I \cap J\}$ and $\{K, L, K \cup L, K \cap L\}$ are disjoint, we have $\langle \mathbf{z} \,|\, \mathbf{n}(K, L) \rangle = 0$ and therefore, $\langle \mathbf{p} \,|\, \mathbf{n}(K, L) \rangle > 0$.

So the point $\mathbf{p}$ we picked proves that any pair of index sets $\{I, J\}$ that satisfies the conditions of Proposition 2.4.8 does indeed induce a facet of the type cone of the permutree fan. □

2.4.3 Number of Facets of the Type Cone

Similarly to Corollary 2.4.5, we can count the number of facets of the type cone with the help of the Ω function. The proof is almost identical to that of Corollary 2.4.5.

Corollary 2.4.12 (Number of Facets of the Permutree Fan Type Cone)**.** The number $\phi(\delta)$ of facets of the type cone $\mathsf{TC}(\mathcal{F}_\delta)$ of the δ-permutree fan $\mathcal{F}_\delta$ is

$$\phi(\delta) := \sum_{\substack{1 \leq i < j \leq n \\ \forall k \in]i,j[:\ \delta_k \neq \otimes}} \Omega^{\circlearrowleft}(\delta_1 \dots \delta_i) \cdot 2^{|\{i<k<j \,|\, \delta_k = \circlearrowleft\}|} \cdot \Omega^{\circlearrowleft}(\delta_n \dots \delta_j).$$

Example 2.4.13. For the decorations of Figure 1.15, Figure 1.17 and Figure 1.18, we obtain $\phi(\circlearrowleft\circlearrowleft\otimes\circlearrowleft) = 12$ and $\phi(\circlearrowleft\otimes\otimes\circlearrowleft) = 4$.

Example 2.4.14. Specializing Corollary 2.4.12, we obtain the following well-known numbers:

- If $\delta = \circlearrowleft^n$, then the type cone $\mathsf{TC}(\mathcal{F}_{\circlearrowleft^n})$ has $2^{n-2} \cdot \binom{n}{2}$ facets.
- If $\delta = \otimes^n$, then the type cone $\mathsf{TC}(\mathcal{F}_{\otimes^n})$ has $\binom{n}{2}$ facets. This equals the number of quadrilaterals of the form $(i-1, i, j, j+1)$ in the $(n+2)$-gon.
- If $\delta = \otimes^n$, then the type cone $\mathsf{TC}(\mathcal{F}_{\otimes^n})$ has $(n-1)$ facets.

The following is an immediate corollary of Corollary 2.4.12 for the case where the symbol $\circlearrowleft$ does not appear in the decoration.

Corollary 2.4.15 (Number of Facets of Some Permutree Fan Type Cones)**.** If $\delta \in \{⦻, ⊖, ⊗\}^n$, we have $\phi(\delta) = |\{1 \leq i < j \leq n \mid \forall k \in]i,j[: \ \delta_k \neq ⊗\}|$.

2.4.4 Simplicial Type Cone

As we now know the number of facets of the type cone, we can determine when it is simplicial.

Corollary 2.4.16 (Simplicial Type Cone of the Permutree Fan)**.** The type cone $\mathsf{TC}(\mathcal{F}_\delta)$ is simplicial if and only if $\delta_j \neq ⊕$ for all $k \in]1,n[$.

Proof. The type cone $\mathsf{TC}(\mathcal{F}_\delta)$ is simplicial if and only if the number $\rho(\delta)$ of rays of the fan $\mathcal{F}_\delta$ and the number $\phi(\delta)$ of facets of the type cone $\mathsf{TC}(\mathcal{F}_\delta)$ satisfy the equality $\rho(\delta) = \phi(\delta) + n - 1$. We find formulas for $\rho(\delta)$ in Corollary 2.2.9 and for $\phi(\delta)$ in Corollary 2.4.12:

$$\rho(\delta) - n + 1 = \sum_{\substack{1 \leq i < j \leq n \\ \forall k \in]i,j[: \ \delta_k \neq ⊗}} 2^{|\{k \in]i,j[\mid \delta_k = ⊕\}|}$$

$$\phi(\delta) = \sum_{\substack{1 \leq i < j \leq n \\ \forall k \in]i,j[: \ \delta_k \neq ⊗}} 2^{|\{k \in]i,j[\mid \delta_k = ⊕\}|} \cdot \Omega^{⊕}(\delta_1 \dots \delta_i) \cdot \Omega^{⊕}(\delta_n \dots \delta_j)$$

As we know that the function $\Omega^{⊕}$ is ≥ 1 for any sequence of decoration symbols, the equality $\rho(\delta) = \phi(\delta) + n - 1$ holds if and only if all factors $\Omega^{⊕}(\delta_1 \dots \delta_i)$ and $\Omega^{⊕}(\delta_n \dots \delta_j)$ are one. This is clearly the case if $\delta_k \neq ⊕$ for all $k \in]1,n[$. Conversely, as soon as $\delta_k = ⊕$ for a $k \in]1,n[$, then $\Omega^{⊕}(\delta_1 \dots \delta_k) > 1$, so the equality does not hold. □

2.4.5 All Permutreehedra

We can now apply Corollary 1.2.30 to obtain all realizations of the δ-permutree fan in the kinematic space (see [AHBHY18]) for the case where $\delta \in \{⦻, ⊖, ⊗\}^n$. We assume that $\delta_1 = \delta_n = ⊗$. We remark that the decorations δ_1 and δ_n are irrelevant in all decorations, so this assumption does not lose generality.

Definition 2.4.17 (Sets for Permutreehedra in Kinematic Space)**.** Given a permutree decoration δ of length n, we define the set $\mathfrak{F}_\delta := \{1 \leq i < j \leq n \mid \forall k \in]i,j[: \ \delta_k = ⊗\}$. Moreover, we set $\mathfrak{R}_n := \{0,1\} \times [n]^2 \times \{0,1\}$. For each pair $(i,j) \in \mathfrak{F}_\delta$ and sign $\varepsilon \in \{+,-\}$, we define the following numbers:

$$p^\varepsilon_\delta(i,j) := \begin{cases} \min\left(\{j\} \cup (]i,j[\cap \delta^\varepsilon)\right) - 1 & \text{if } i \in \delta^\varepsilon, \\ i - 1 & \text{if } i \notin \delta^\varepsilon, \end{cases}$$

$$q^\varepsilon_\delta(i,j) := \begin{cases} \max\left(\{i\} \cup (]i,j[\cap \delta^\varepsilon)\right) + 1 & \text{if } j \in \delta^\varepsilon, \\ j + 1 & \text{if } j \notin \delta^\varepsilon, \end{cases}$$

$$s^\varepsilon_\delta(k) := \begin{cases} 1 & \text{if } k \in \delta^+, \\ 0 & \text{if } k \notin \delta^+. \end{cases}$$

With these notations, we can fix a vector $\mathbf{u} \in \mathbb{R}^{\mathfrak{F}_\delta}_{>0}$ and define a polytope $\mathsf{Q}_\delta(\mathbf{u})$.

Definition 2.4.18 (Permutreehedron in Kinematic Space)**.** Let $\delta \in \{⦻, ⊖, ⊗\}^n$ be a permutree decoration with $\delta_1 = \delta_n = ⊗$ and let $\mathbf{u} \in \mathbb{R}^{\mathfrak{F}_\delta}_{>0}$. We define the polytope $\mathsf{Q}_\delta(\mathbf{u})$ to contain all $\mathbf{z} \in \mathbb{R}^{\mathfrak{F}_\delta}_{\geq 0}$ that satisfy all of the following conditions.

- If $(p,q) \notin \mathfrak{F}_\delta$, then $\mathbf{z}_{(\ell,p,q,r)} = 0$ for all $\ell, r \in \{0,1\}$.

- If $p+1 \neq q$, then $\mathbf{z}_{(\ell,p,q,r)} = \mathbf{z}_{(\ell',p,q,r')}$ for all $\ell, \ell', r, r' \in \{0,1\}$.
- If $(i,j) \in \mathfrak{F}_\delta$, then $\mathbf{z}_{(1,\, p_\delta^+(i,j),\, q_\delta^-(i,j),\, 0)} + \mathbf{z}_{(0,\, p_\delta^-(i,j),\, q_\delta^+(i,j),\, 1)}$ $- \mathbf{z}_{(1-s_\delta^-(i),\, p_\delta^-(i,j+1),\, q_\delta^-(i-1,j),\, 1-s_\delta^-(j))} - \mathbf{z}_{(s_\delta^+(i),\, p_\delta^+(i,j+1),\, q_\delta^+(i-1,j),\, s_\delta^+(j))} = \mathbf{u}_{(i,j)}$.

We obtain the following complete set of realizations of the δ-permutree fan $\mathcal{F}_\delta$.

Proposition 2.4.19 (Quotientopes for the Permutree Fan)**.** *Let $\delta \in \{\circledcirc, \circledcirc, \otimes\}^n$ be a permutree decoration with $\delta_1 = \delta_n = \otimes$. Then the polytopes whose normal fan is equal to the δ-permutree fan $\mathcal{F}_\delta$ are exactly the polytopes $\mathsf{Q}_\delta(\mathbf{u})$ for all $\mathbf{u} \in \mathbb{R}^{\mathfrak{F}_\delta}_{>0}$.*

Example 2.4.20. For special decorations, we get the following special cases of Proposition 2.4.19.

- If $\delta = \otimes^n$, then $p_\delta^+(i,j) = p_\delta^-(i,j) = i$ and $q_\delta^+(i,j) = q_\delta^-(i,j) = j$. Then the polytope $\mathsf{Q}_\delta(\mathbf{u})$ is equivalent to the kinematic cube (see [AHBHY18])

$$\left\{ \mathbf{y} \in \mathbb{R}^{\{0,1\}\times[n-1]} \;\middle|\; \mathbf{y} \geq 0 \text{ and } \forall i \in [n-1] :\ \mathbf{y}_{(0,i)} + \mathbf{y}_{(1,i)} = \mathbf{u}_{(i,i+1)} \right\}.$$

  The map is given by $\mathbf{y}_{(0,i)} = \mathbf{z}_{(0,i,i+1,1)}$ and $\mathbf{y}_{(1,i)} = \mathbf{z}_{(1,i,i+1,0)}$.
- If $\delta = \otimes\circledcirc^{n-1}\otimes$, then $p_\delta^+(i,j) = i$ and $q_\delta^+(i,j) = j$ and

$$p_\delta^-(i,j) = \begin{cases} j-1 & \text{if } i = 1, \\ i-1 & \text{if } i \neq 1, \end{cases} \qquad \text{as well as} \qquad q_\delta^-(i,j) = \begin{cases} i+1 & \text{if } j = n, \\ j+1 & \text{if } j \neq n. \end{cases}$$

  Then the polytope $\mathsf{Q}_\delta(\mathbf{u})$ is equivalent to the kinematic associahedron (see [AHBHY18])

$$\left\{ \mathbf{y} \in \mathbb{R}^{\binom{[0,n+1]}{2}} \;\middle|\; \begin{array}{l} \mathbf{y} \geq 0 \\ \mathbf{y}_{(0,n+1)} = 0 \\ \mathbf{y}_{(i,j)} = 0 \text{ if } i+1 = j \\ \mathbf{y}_{(i,j+1)} + \mathbf{y}_{(i-1,j)} - \mathbf{y}_{(i-1,j+1)} - \mathbf{y}_{(i,j)} = \mathbf{u}_{(i,j)} \text{ for all } (i,j) \in \binom{[n]}{2} \end{array} \right\}.$$

  The map is given by $\mathbf{y}_{(0,j)} = \mathbf{z}_{(1,j-1,j,0)}$ and $\mathbf{y}_{(i,n+1)} = \mathbf{z}_{(0,i,i+1,1)}$ and $\mathbf{y}_{(i,j)} = \mathbf{z}_{(\ell,i,j,r)}$ for any $\ell, r \in \{0,1\}$.

Proof of Proposition 2.4.19. We will parametrize the rays of the permutree fan $\mathcal{F}_\delta$ by $\mathfrak{R}_n$ and the facets of its type cone $\mathsf{TC}(\mathcal{F}_\delta)$ by $\mathfrak{F}_\delta$. For any sequence $(\ell,p,q,r) \in \mathfrak{R}_n$, we build a subset $R(\ell,p,q,r) \subseteq [n]$ as follows:

- If $(p,q) \notin \mathfrak{F}_\delta$, then we set
  - $R(0,p,q,0) := \emptyset$,
  - $R(1,p,q,0) := \emptyset$,
  - $R(0,p,q,1) := \emptyset$,
  - $R(1,p,q,1) := [n]$.
- If $(p,q) \in \mathfrak{F}_\delta$ and $p+1 = q$, then we set
  - $R(0,p,q,0) := \emptyset$,
  - $R(1,p,q,0) := [1,p]$,
  - $R(0,p,q,1) := [q,n]$,
  - $R(1,p,q,1) := [n]$.
- If $(p,q) \in \mathfrak{F}_\delta$ and $p+1 < q$, then we ignore the values of ℓ and r and make the set $R(\ell,p,q,r)$ the unique proper subset $\emptyset \subsetneq R \subsetneq [n]$ which satisfies the conditions of Corollary 2.2.6 and has the property that i is the last position such that $[1,i]$ either all belong to R or belong to $[n] \setminus R$ and j is the last position such that $[j,n]$ either all belong to R or belong to $[n] \setminus R$. There is one unique set R with these properties, as we showed in the proof of Corollary 2.2.9 (We emphasize that we are in the case where $\delta \in \{\circledcirc, \circledcirc, \otimes\}^n$).

This way, we parametrize the rays of the permutree fan $\mathcal{F}_\delta$ by the set $\mathfrak{R}_n$, where we ignore (ℓ,p,q,r) whenever $(p,q) \notin \mathfrak{F}_\delta$ and identify all sequences (a,p,q,b) for all $a,b \in \{0,1\}$ whenever $(p,q) \in \mathfrak{F}_\delta$ and $p+1 = q$.

We will now associate to every pair $(i,j) \in \mathfrak{F}_\delta$ a pair of subsets $(I(i,j), J(i,j))$ that label a pair of rays that defines a facet of the type cone as elaborated in Corollary 2.2.6 and Proposition 2.4.8. As usual, we want to have $i = \max(I(i,j) \setminus J(i,j))$ and $j = \min(J(i,j) \setminus I(i,j))$. As $\delta \in \{⊘, ⊖, ⊗\}^n$), that pair of subsets is unique due to Observation 2.4.11. We claim that these sets, their intersection and union are given by

$$\begin{aligned}
I(i,j) &= R(1\ ,\ p_\delta^+(i,j)\ ,\ q_\delta^-(i,j)\ ,\ 0),\\
J(i,j) &= R(0\ ,\ p_\delta^-(i,j)\ ,\ q_\delta^+(i,j)\ ,\ 1),\\
I(i,j) \cap J(i,j) &= R(1_{i\notin\delta^-}\ ,\ p_\delta^-(i,j+1)\ ,\ q_\delta^-(i-1,j)\ ,\ 1_{j\notin\delta^-}),\\
I(i,j) \cup J(i,j) &= R(1_{i\in\delta^+}\ ,\ p_\delta^+(i,j+1)\ ,\ q_\delta^+(i-1,j)\ ,\ 1_{j\in\delta^+}).
\end{aligned}$$

We will now prove these four claims.

- We recall from Proposition 2.4.8 that $]i,j[\cap \delta^- \subseteq I(i,j)$ and $[i,j[\cap \delta^+ \subseteq [n] \setminus I(i,j)$. Moreover, Observation 2.4.11 tells us that
  - If $i \in \delta^+$, then $[1,i] \subseteq I(i,j)$, and the maximal position p such that $[1,p]$ all belong to $I(i,j)$ is the position just before the first element of $]i,j[\cap \delta^+$, or $p = j$ if there is no such element.
  - If $i \notin \delta^+$, then $[1,i[\subseteq [n] \setminus I(i,j)$, while $i \in I(i,j)$, and therefore the maximal position p such that $[1,p]$ all belong to $[n] \setminus I(i,j)$ is $p = i-1$.

  We remark that in all these cases, that position p is equal to $p_\delta^+(i,j)$. By a symmetric argument, we find that the smallest position q such that the interval $[q,n]$ entirely belongs to $I(i,j)$ or entirely belongs to $[n] \setminus I(i,j)$ is equal to $q_\delta^-(i,j)$. These properties also ensure that $1 \leq p_\delta^+(i,j) < q_\delta^-(i,j) \leq n$. We have $i-1 \leq p_\delta^+(i,j)$ with equality only when $i \notin \delta^+$ and $q_\delta^-(i,j) \leq j+1$ with equality only when $j \notin \delta^-$. Together with $\delta_k \neq ⊗$ for all $k \in]i,j[$, this implies that $\delta_k \neq ⊗$ for all $k \in \left]p_\delta^+(i,j), q_\delta^-(i,j)\right[$. We conclude that $(p_\delta^+(i,j), q_\delta^-(i,j)) \in \mathfrak{F}_\delta$. In the case where $i \notin \delta^+$, we have the equality $p_\delta^+(i,j) = i-1$, implying that $q_\delta^-(i,j) \geq i+1 > p_\delta^+(i,j)+1$. We therefore obtain
  - If $p_\delta^+(i,j)+1 = q_\delta^-(i,j)$, then $i \in \delta^+$, so $[1,i] \subseteq I(i,j)$ and we deduce the equality $I(i,j) = \left[1, p_\delta^+(i,j)\right] = R(1,\ p_\delta^+(i,j),\ q_\delta^-(i,j),\ 0)$.
  - If $p_\delta^+(i,j)+1 < q_\delta^-(i,j)$, then these two values fully determine $I(i,j)$ and we have $I(i,j) = R(1,\ p_\delta^+(i,j),\ q_\delta^-(i,j),\ 0)$.

  This concludes our proof for the claimed form of $I(i,j)$.
- The argument for $J(i,j)$ is symmetric.
- To determine the intersection of $I(i,j)$ and $J(i,j)$, we distinguish the cases where that intersection is either empty or not.
  - If $I(i,j) \cap J(i,j) = \emptyset$, then Observation 2.4.11 tells us that $i,j \in \delta^-$ and Proposition 2.4.8 (v) gives us $]i,j[\subseteq \delta^+$. We deduce the two equalities $p_\delta^-(i,j+1) = j-1$ and $q_\delta^-(i-1,j) = i+1$. This implies that $p_\delta^-(i,j+1) \not< q_\delta^-(i-1,j)$, so that the pair $(p_\delta^-(i,j+1)\ ,\ q_\delta^-(i-1,j))$ cannot be an element of $\mathfrak{F}_\delta$ except for the case where $p_\delta^-(i,j+1)+1 = q_\delta^-(i-1,j)$. Since $i,j \in \delta^-$, this yields in both situations that $R(1_{i\notin\delta^-}\ ,\ p_\delta^-(i,j+1)\ ,\ q_\delta^-(i-1,j)\ ,\ 1_{j\notin\delta^-}) = \emptyset = I(i,j) \cap J(i,j)$.
  - If $I(i,j) \cap J(i,j) \neq \emptyset$, we examine separately the cases where $i \in \delta^+$ or $i \notin \delta^+$. Then Observation 2.4.11 gives us the following results:
    - If $i \in \delta^+$, then $[1,i[\subseteq [n] \setminus (I(i,j) \cap J(i,j))$ and the largest position p such that the entire interval $[1,p]$ is contained in $[n] \setminus (I(i,j) \cap J(i,j))$ is the position just before the smallest element of $]i,j[\cap \delta^-$, or $j+1$ if there is no such element.
    - If $i \notin \delta^+$, then $[1,i[\subseteq I(i,j) \cap J(i,j)$ while $i \notin I(i,j) \cap J(i,j)$. We deduce that the largest position p such that the entire interval $[1,p]$ is contained in $I(i,j) \cap J(i,j)$ is the position $i-1$.

We conclude that the position $p^-_\delta(i, j+1)$ is in fact the largest position p such that the interval $[1, p]$ is entirely contained in either $I(i, j) \cap J(i, j)$ or $[n] \setminus (I(i, j) \cap J(i, j))$. A symmetric argument shows that $q^-_\delta(i-1, j)$ is the smalles position q such that the interval $[q, n]$ is entirely contained in either $I(i, j) \cap J(i, j)$ or $[n] \setminus (I(i, j) \cap J(i, j))$. This ensures that the pair $\big(p^-_\delta(i, j+1)\ ,\ q^-_\delta(i-1, j)\big) \in \mathfrak{F}_\delta$.
We can now distinguish the following three cases:

- If $p^-_\delta(i, j+1) + 1 < q^-_\delta(i-1, j)$, then

$$I(i, j) \cap J(i, j) = R(1_{i \notin \delta^-}\ ,\ p^-_\delta(i, j+1)\ ,\ q^-_\delta(i-1, j)\ ,\ 1_{j \notin \delta^-}),$$

  as they are both fully determined by $p^-_\delta(i, j+1)$ and $q^-_\delta(i-1, j)$.
- If $p^-_\delta(i, j+1)+1 = q^-_\delta(i-1, j)$ and $[1, i[\subseteq I(i, j) \cap J(i, j)$, then $i \in \delta^+$ and $j \in \delta^-$ by Observation 2.4.11, so we get

$$\begin{aligned} I(i, j) \cap J(i, j) &= \big[1, p^-_\delta(i, j+1)\big] \\ &= R(1\ ,\ p^-_\delta(i, j+1)\ ,\ q^-_\delta(i-1, j)\ ,\ 0) \\ &= R(1_{i \notin \delta^-}\ ,\ p^-_\delta(i, j+1)\ ,\ q^-_\delta(i-1, j)\ ,\ 1_{j \notin \delta^-}). \end{aligned}$$

- If $p^-_\delta(i, j+1) + 1 = q^-_\delta(i-1, j)$ and $[1, i] \subseteq [n] \setminus (I(i, j) \cap J(i, j))$, then $i \in \delta^-$ and $j \in \delta^+$ by Observation 2.4.11, so we get

$$\begin{aligned} I(i, j) \cap J(i, j) &= \big[q^-_\delta(i-1, j), n\big] \\ &= R(0\ ,\ p^-_\delta(i, j+1)\ ,\ q^-_\delta(i-1, j)\ ,\ 1) \\ &= R(1_{i \notin \delta^-}\ ,\ p^-_\delta(i, j+1)\ ,\ q^-_\delta(i-1, j)\ ,\ 1_{j \notin \delta^-}). \end{aligned}$$

  This concludes the proof for all cases of the intersection $I(i, j) \cap J(i, j)$: It is always equal to $R(1_{i \notin \delta^-}\ ,\ p^-_\delta(i, j+1)\ ,\ q^-_\delta(i-1, j)\ ,\ 1_{j \notin \delta^-})$.
- The proof for the union $I(i, j) \cup J(i, j) = R(1_{i \in \delta^+}\ ,\ p^+_\delta(i, j+1)\ ,\ q^+_\delta(i-1, j)\ ,\ 1_{j \in \delta^+})$ is identical.

Now we have listed these pairs $(I(i, j), J(i, j))$ for all $(i, j) \in \mathfrak{F}_\delta$. Then Proposition 2.3.9 tells us that the wall-crossing inequalities of the δ-permutree fan $\mathcal{F}_\delta$ are of the form described in Definition 2.4.18. Now Corollary 1.2.30 certifies that the polytope $\mathsf{Q}_\delta(\mathbf{u})$ is made up of all the height vectors that realize the permutree fan. □

3 Shard Polytopes for the Braid Arrangement

In this chapter, we will have a closer look at the shards of the oriented braid arrangement $\vec{\mathcal{A}}_n$. We will define a polytope for each $\vec{\mathcal{A}}_n$ shard, using some newly introduced concepts. We will describe these polytopes, in particular give explicit $\mathcal{H}$- and $\mathcal{V}$-descriptions, determine when two of their vertices form an edge and give some more information on the shape of their faces. We will then analyze the normal fans of shard polytopes and see that they have suitable properties that allow us to create any $\vec{\mathcal{A}}_n$ quotientope as the Minkowski sum of certain shard polytopes.

3.1 Shard Matchings, Climbs and Falls

We will first prepare our results by introducing some notions revolving around $\vec{\mathcal{A}}_n$ shards.

3.1.1 Pseudoshards

We introduce a generalization of shards in the braid arrangement, which can be expressed by abusing the notation introduced for shards. Pseudoshards are denoted just like shards, but the union of the disjoint above- and below-sets is not necessarily the entire interval in between the endpoints of the shard.

Definition 3.1.1 (Pseudoshards)**.** Let $1 \leq \ell < r \leq n$ and let A and B be a pair of disjoint subsets of the open interval $]\ell, r[$ (where $A \dot\cup B$ may or may not equal to that interval). We define the $\vec{\mathcal{A}}_n$ **pseudoshard** $\Sigma_n(\ell, r, A, B) := \{\mathbf{x} \in \mathbb{R}^n \mid \forall a \in A, b \in B : x_a \leq x_\ell = x_r \leq x_b\}$. It is an $\tilde{\mathcal{A}}_\mathbf{n}$ **shard** if and only if $A \dot\cup B =]\ell, r[$.

For any pair of integers $1 \leq \ell < r \leq n$, we may partially order all pseudoshards $\Sigma_n(\ell, r, A, B)$ by inclusion of their sets A and B. The unique minimal pseudoshard with respect to this order is $\Sigma_n(\ell, r, \emptyset, \emptyset)$, which is equal to the entire hyperplane $H_n(\ell, r)$. On the other hand, the maximal pseudoshards with respect to this order are the pseudoshards where $A \dot\cup B =]\ell, r[$, which are precisely the $\vec{\mathcal{A}}_n$ shards of $H_n(\ell, r)$. It is therefore justified to say that pseudoshards interpolate between $\vec{\mathcal{A}}_n$ hyperplanes and their shards. We say that a pseudoshard $\Sigma_n(\ell, r, A, B)$ **skips** an integer $i \in]\ell, r[$ if i is an element of neither A nor B. The $\vec{\mathcal{A}}_n$ shards are precisely those $\vec{\mathcal{A}}_n$ pseudoshards that do not skip any integer.

While $\vec{\mathcal{A}}_n$ shards have a gentle illustration as arcs on the dots from 1 to n, pseudoshards cannot be drawn as easily, as it is not clear how the arc should behave at those positions that are contained in neither A nor B. However, there is a straightforward way of mapping a pseudoshard to a proper $\vec{\mathcal{A}}_c$ shard of the hyperplane $H_c(1, c)$, where $c < n$.

Observation 3.1.2 (From Pseudoshard to Shard)**.** Every $\vec{\mathcal{A}}_n$ pseudoshard can be mapped to an $\vec{\mathcal{A}}_c$ shard in the following way: Given a pseudoshard $\Sigma = \Sigma_n(\ell, r, A, B)$, we fix the set $C = \{\ell, r\} \cup A \cup B$ and its cardinality $c := |C|$. We can then use the order preserving bijection $\varphi : C \to [c]$. We observe that $\varphi(\ell) = 1$ and $\varphi(r) = c$. We abuse notation to denote the effect of that map to an entire pseudoshard Σ to be $\varphi(\Sigma) := \Sigma_c(\varphi(\ell), \varphi(r), \varphi(A), \varphi(B))$.

3.1.2 Climbs and Falls

To each $\vec{\mathcal{A}}_n$ shard, we can associate a characteristic vector in $\{-1, 0, +1\}^n$ that describes for each index in $[\ell, r]$ whether it lies in A or B.

Definition 3.1.3 (Characteristic Vector of a Shard)**.** Let $\Sigma = \Sigma_n(\ell, r, A, B)$ be an $\vec{\mathcal{A}}_n$ shard. We define the **characteristic vector** (or **direction**) of the shard Σ to be $\boldsymbol{\chi}(\Sigma) := \mathbf{1}_{\{\ell\}\cup A} - \mathbf{1}_{B\cup\{r\}}$.

We remark that a characteristic vector of a pseudshard can be constructed in the exact same way. While the characteristic vector of a shard has zero entries precisely in the coordinates of $[n] \setminus [\ell, r]$, the characteristic vector of a pseudshard has zeros for those indices $i \in]\ell, r[$ where $i \notin A$ and $i \notin B$.

Any $\vec{\mathcal{A}}_n$ shard $\Sigma_n(\ell, r, A, B)$ is a part of an $\vec{\mathcal{A}}_n$ hyperplane $H_n(\ell, r)$, so the associated arc connects the dot labeled ℓ to the one labeled r. The behavior of the arc with respect to the dots in between ℓ and r is entirely determined by the sets A and B. We will keep this illustration in mind and introduce some names for certain indices between ℓ and r.

Definition 3.1.4 (Climbs, Falls and Turns)**.** Let $\Sigma := \Sigma_n(\ell, r, A, B)$ be an $\vec{\mathcal{A}}_n$ shard. We define

- a **Σ-climb** to be a position $j \in [\ell, r[$ where $j \in \{\ell\} \cup B$ and $j + 1 \in A \cup \{r\}$,
- a **Σ-fall** to be a position $j \in [\ell, r[$ where $j \in \{\ell\} \cup A$ and $j + 1 \in B \cup \{r\}$,
- a **Σ-turn** to be any position distinct from ℓ and $r - 1$ which is a Σ-climb or a Σ-fall,
- the **number of Σ-turns** to be $t(\Sigma) := |\{j \in [\ell + 1, r - 2] \mid j \text{ is a } \Sigma\text{-turn}\}|$.

Example 3.1.5. Both positions ℓ and $r - 1$ are always Σ-climbs or Σ-falls: If $\ell = r - 1$, then the position $\ell = r - 1$ is both a Σ-climb and a Σ-fall. Otherwise, ℓ is a Σ-climb if $\ell + 1 \in A$ and a Σ-fall if $\ell + 1 \in B$. Analogously, $r - 1$ is a Σ-climb if $r - 1 \in B$ and a Σ-fall if $r - 1 \in A$.

We can extend the notions of climbs and falls to a pseudoshard $\Sigma = \Sigma_n(\ell, r, A, B)$, where we recall that $A \dot\cup B$ is contained in (but not necessarily equal to) the interval $]\ell, r[$. Once more, we use the set $C := A \cup B \cup \{\ell, r\}$ of all positions occuring in the pseudoshard.

Observation 3.1.6 (Climbs, Falls and Turns for Pseudoshards)**.** For a fixed $j \in [\ell, r[$, the position $j + 1$ might not be contained in $A \dot\cup B$. We define the successor of j in the pseudoshard by setting $s(j) := \min\{i \in C \mid i > j\}$. Using this generalized notation, a Σ-climb is a position $j \in [\ell, r[$ with $j \in \{\ell\} \cup B$ and $s(j) \in A \cup \{r\}$. A Σ-fall is a position $j \in [\ell, r[$ with $j \in \{\ell\} \cup A$ and $s(j) \in B \cup \{r\}$. We note that these definitions are equivalent to the ones given in Definition 3.1.4 in the case where Σ is a shard.

Observation 3.1.7 (Climbs and Falls, Left and Right)**.** Let $\Sigma := \Sigma_n(\ell, r, A, B)$ be an $\vec{\mathcal{A}}_n$ shard. For every $a \in A$, we observe that there is at least one climb in $[\ell, a[$ and at least one fall in $[a, r[$. Analogously, for every $b \in B$, there is at least one fall in $[\ell, b[$ and at least one climb in $[b, r[$.

Observation 3.1.8 (Number of Turns)**.** We can deduce from Example 3.1.5 that the number of Σ-climbs plus the number of Σ-falls is equal to the number of Σ-turns plus two. This implies that the number of Σ-climbs plus the number of Σ-falls is at least 2. Furthermore, the arc of Σ crosses the horizontal axis between the dots j and $j + 1$ if and only if j is a Σ-turn. In particular, the number of Σ-turns is equal to the number of times arc crosses the horizontal axis.

Example 3.1.9. We have a look at two examples of shards, illustrated in Figure 3.1.

- The shard $\Sigma_9(4, 8, \{5\}, \{6, 7\})$ (illustrated by the left arc) has the characteristic vector $\boldsymbol{\chi}(\Sigma) = (0, 0, 0, +, +, -, -, -, 0)$. It has climbs in positions 4 and 7 and a fall in position 5. Its only turn is in position 5, where its arc crosses the horizontal axis.
- The shard $\Sigma_9(1, 4, \{2, 3\}, \emptyset)$ (illustrated by the right arc) has the characteristic vector $\boldsymbol{\chi}(\Sigma) = (+, +, +, -, 0, 0, 0, 0, 0)$. It has a climb in position 1 and a fall in position 3. It does not have any turns and its arc does not cross the horizontal axis.

Figure 3.1: The arcs of $\Sigma_9(4, 8, \{5\}, \{6, 7\})$ (left) and $\Sigma_9(1, 4, \{2, 3\}, \emptyset)$ (right).

3.1.3 Shard Matchings

The notation of $\vec{\mathcal{A}}_n$ shards as $\Sigma_n(\ell, r, A, B)$, partitioning an interval in between two endpoints into two disjoint sets A and B, allows us to think about matchings between these two sets. We will impose a number of conditions on how to match positions in one set with positions in the other one and introduce a handy notation in accordance with the ones for shards. These shard matchings will then be used to describe shard polytopes.

Definition 3.1.10 (Shard Matching)**.** Let $\Sigma = \Sigma_n(\ell, r, A, B)$ be an $\vec{\mathcal{A}}_n$ shard. We define

- a **Σ-matching** to be a (possibly empty) set $M = \{a_1, b_1, \ldots, a_k, b_k\} \subseteq [\ell, r]$, where
  - $\ell \leq a_1 < b_1 < \cdots < a_k < b_k \leq r$,
  - $a_i \in \{\ell\} \cup A$ and $b_i \in B \cup \{r\}$ for $i \in [k]$,
- the **pairs** of a non-empty Σ-matching to be (a_i, b_i) for $i \in [k]$,
- the **semi-length** of a Σ-matching to be k,
- the **characteristic vector** of a Σ-matching to be $\boldsymbol{\chi}(M) := \sum_{i\in[k]} \mathbf{e}_{a_i} - \mathbf{e}_{b_i}$,
- the **set of all Σ-matchings** to be $\mathcal{M}(\Sigma) := \{M \subseteq [\ell, r] \mid M \text{ is a } \Sigma\text{-matching}\}$.

We observe that the characteristic vector of any Σ-matching agrees in all its nonzero entries with the characteristic vector of the shard Σ, so that $\langle \boldsymbol{\chi}(M) \,|\, \boldsymbol{\chi}(\Sigma)\rangle = |M|$.

Example 3.1.11. For every $\vec{\mathcal{A}}_n$ shard Σ, there are two trivial Σ-matchings.

- $M = \emptyset$ is a Σ-matching with no pairs. Its characteristic vector is $\boldsymbol{\chi}(M) = \mathbf{0}$.
- $M = \{\ell, r\}$ is a Σ-matching with one pair (ℓ, r) and characteristic vector $\boldsymbol{\chi}(M) = \mathbf{e}_\ell - \mathbf{e}_r$.

The following are other simple examples of Σ-matchings for a shard $\Sigma = \Sigma_n(\ell, r, A, B)$.

- Given any position $a \in A$, the set $\{a, r\}$ is a Σ-matching.
- Given any position $b \in B$, the set $\{\ell, b\}$ is a Σ-matching.

Extending the diagrams used to represent $\vec{\mathcal{A}}_n$ shards by arcs, we can illustrate a Σ-matching using a simple visualisation where

- solid dots ● represent the elements $a_1, a_2, \ldots, a_k$ (the positive entries of $\boldsymbol{\chi}(M)$),
- hollow dots ○ represent the elements $b_1, b_2, \ldots, b_k$ (the negative entries of $\boldsymbol{\chi}(M)$),
- tiny dots • represent elements not part of the matching (the zero entries of $\boldsymbol{\chi}(M)$).

In particular, all solid dots are on or below the arc illustrating the shard Σ, while all hollow dots are on or above the arc. This visualisation allows a rather symbolic interpretation: If we imagine the arc to depict the water surface between the solid shore on the left and an object floating in the sea on the right, then the solid elements in between are below the sea level as they sink, the hollow elements float above it.

Example 3.1.12. The shard $\Sigma_4(1, 4, \{3\}, \{2\})$ illustrated by  has the matchings

- $M = \emptyset$, illustrated by • • • •, characteristic vector $\boldsymbol{\chi}(M) = (0, 0, 0, 0)$,
- $M = \{1, 4\}$, illustrated by ● • • ○, characteristic vector $\boldsymbol{\chi}(M) = (+1, 0, 0, -1)$,
- $M = \{1, 2\}$, illustrated by ● ○ • •, characteristic vector $\boldsymbol{\chi}(M) = (+1, -1, 0, 0)$,
- $M = \{3, 4\}$, illustrated by • • ● ○, characteristic vector $\boldsymbol{\chi}(M) = (0, 0, +1, -1)$,
- $M = \{1, 2, 3, 4\}$, illustrated by ● ○ ● ○, characteristic vector $\boldsymbol{\chi}(M) = (+1, -1, +1, -1)$.

We remark that we can partially order the Σ-matchings by inclusion as sets. We will give this partial order a name:

Definition 3.1.13 (Poset of Matchings)**.** Given an $\vec{\mathcal{A}}_n$ shard Σ, the **poset of Σ-matchings** is the set of all Σ-matchings partially ordered by set inclusion.

We note that the poset of Σ-matchings is not ordering Σ-matchings by the inclusion of pairs. To give an example for the shard $\Sigma = \Sigma_n(1, 4, \{2\}, \{3\})$, the matching $M = \{1, 4\}$ is included in the Σ- matching $M' = \{1, 2, 3, 4\}$ as a set, but its only pair $(1, 4)$ is not a pair of the matching M'.

We will now discuss the circumstances under which every single matching for one shard is a matching for another shard as well.

Lemma 3.1.14 (Common Matchings)**.** *Let $\Sigma_1 = \Sigma_n(\ell_1, r_1, A_1, B_1)$ and $\Sigma_2 = \Sigma_n(\ell_2, r_2, A_2, B_2)$ be two $\vec{\mathcal{A}}_n$ shards. Then $\mathcal{M}(\Sigma_2) \subseteq \mathcal{M}(\Sigma_1)$ if and only if Σ_2 forces Σ_1 and $\ell_2 \notin B_1$ and $r_2 \notin A_1$.*

Proof. We prove the two directions of the statement separately.

- If $\mathcal{M}(\Sigma_2) \subseteq \mathcal{M}(\Sigma_1)$, we exploit that certain Σ_2-matchings are Σ_1-matchings:
  - The Σ_2-matching $M = \{\ell_2, r_2\}$ always exists. As it has to be a Σ_1-matching, we deduce that $\ell_2 \in \{\ell_1\} \cup A_1$ and $r_2 \in B_1 \cup \{r_1\}$. This implies that $\ell_1 \leq \ell_2$ and $r_2 \leq r_1$.
  - For every $b \in B_2$, there is the Σ_2-matching $M = \{\ell_2, b\}$. As this has to be a Σ_1-matching, we deduce that $b \in B_1$, so $B_2 \subseteq B_1$ (as $\max(B_2) < r_2 \leq r_1$ implies $b < r_1$).
  - For every $a \in A_2$, there is the Σ_2-matching $M = \{a, r_2\}$. As it has to be a Σ_1-matching, we deduce that $a \in A_1$, so $A_2 \subseteq A_1$ (as $\ell_1 \leq \ell_2 < \min(A_2)$ implies $\ell_1 < a$).

  These inequalities and set inclusions certify that Σ_2 forces Σ_1. Moreover, $\ell_2 \in \{\ell_1\} \cup A_1$ implies that $\ell_2 \notin B_1$ and an analogous argument gives us $r_2 \notin A_1$.
- If Σ_2 does force Σ_1, then we have $A_2 \subseteq A_1$ and $B_2 \subseteq B_1$ and $\ell_1 \leq \ell_2 < r_2 \leq r_1$ by definition of forcing in $\vec{\mathcal{A}}_n$. If additionally, $\ell_2 \notin B_1$, then we have $\ell_2 = \ell_1$ or $\ell_2 \in A_1$, so in either case, $\{\ell_2\} \cup A_2 \subseteq \{\ell_1\} \cup A_1$, and analogously, $B_2 \cup \{r_2\} \subseteq B_1 \cup \{r_1\}$. We conclude that by Definition 3.1.10, every Σ_2-matching is a Σ_1-matching as desired. □

Definition 3.1.15 (Compatible Pairs)**.** Given an $\vec{\mathcal{A}}_n$ shard Σ, we call two Σ-pairs (a_1, b_1) and (a_2, b_2) **compatible** if $b_1 < a_2$ or $b_2 < a_1$. We say that a Σ-pair (a, b) is **compatible** with a Σ-matching M if (a, b) is compatible with every pair of M.

We first note that compatibility of pairs depends only on the positions, not on the shard. We remark that if a Σ-pair (a, b) is compatible with a Σ-matching M, then every pair of M is either completely to the left of completely to the right of the interval $[a, b]$. Therefore, we can add (a, b) to the existing Σ-matching and the resulting set $M \cup \{a, b\}$ is a Σ-matching as well.

Example 3.1.16. Given the $\vec{\mathcal{A}}_6$ shard $\Sigma = \Sigma_6(1,\ 6,\ \{3, 5\},\ \{2, 4\})$, the set $M = \{1, 2, 5, 6\}$ is a Σ-matching (illustrated by ●○ • • ●○) and the Σ-pair $(3, 4)$ is compatible with M, therefore the set $M \cup \{3, 4\} = \{1, 2, 3, 4, 5, 6\}$ is a Σ-matching as well (illustrated by ●○●○●○).

Observation 3.1.17 (Pseudoshard Matchings)**.** We remark that we can use matchings as defined in Definition 3.1.10 on pseudoshards without any restriction. The set M will not contain any integer that is skipped by the pseudoshard and pairs, semi-length and characteristic vector can be used in the exact same way.

Every Σ-matching is uniquely defined by the Σ-pairs it contains. In this sense, every Σ-matching can be written as a vector in $\{0, 1\}^P$, where P is the set of all Σ-pairs. Their convex hull forms a polytope in $\mathbb{R}^P$, which can equivalently be described by the inequalities

- $0 \leq x_p \leq 1$ for every $p \in P$,
- $x_p + x_{p'} \leq 1$ for any two pairs p and p' that are not compatible.

This polytope is easy to construct, but might have very high dimension. We can project it into $\mathbb{R}^n$ by mapping every unit vector $\mathbf{e}_{(a,b)} \in \mathbb{R}^P$ to the difference of unit vectors $\mathbf{e}_a - \mathbf{e}_b \in \mathbb{R}^n$. We note that as every matching is uniquely defined by its pairs, this projection is injective on the set of vertices: We obtain exactly the characteristic vectors of all Σ-matchings. We will focus on the lower-dimensional projection of this polytope which has very interesting properties. We have completed our preparations and introduced all terminology necessary to define shard polytopes.

3.2 Shard Polytopes

3.2.1 Construction

We introduce a polytope for every $\vec{\mathcal{A}}_n$ shard Σ. We will give both a $\mathcal{V}$-description and an $\mathcal{H}$-description and prove later that they are equivalent. Our first definition uses the characteristic vectors of Σ-matchings as defined in Definition 3.1.10 to describe the vertices of the polytope.

Definition 3.2.1 (Shard Polytope by $\mathcal{V}$-Description)**.** Let Σ be an $\vec{\mathcal{A}}_n$ shard. The **shard polytope** $\mathsf{SP}(\Sigma)$ is the convex hull of the characteristic vectors $\boldsymbol{\chi}(M)$ of all Σ-matchings M.

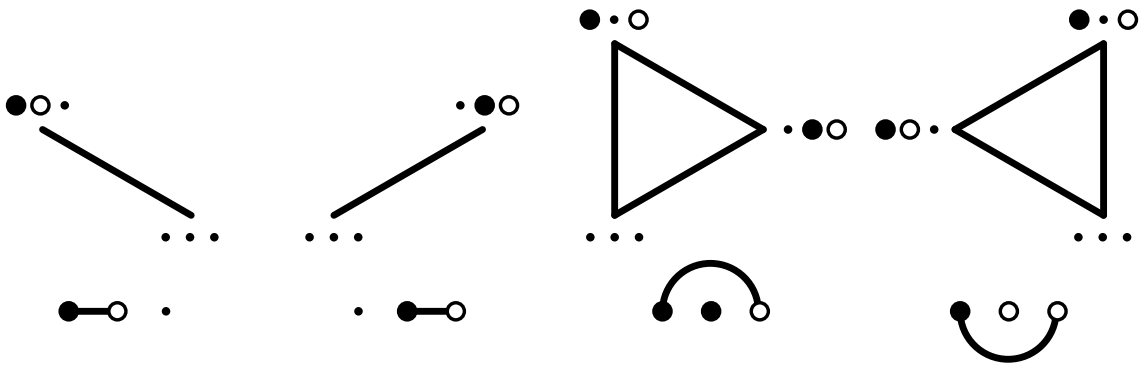

Figure 3.2: Shard polytopes for all $\vec{\mathcal{A}}_3$ shards. [Picture from [PPR20]]

Our second definition uses climbs and falls of the shard Σ as defined in Definition 3.1.4 to describe the facets of the polytope.

Definition 3.2.2 (Shard Polytope by $\mathcal{H}$-Description)**.** Let $\Sigma = \Sigma_n(\ell, r, A, B)$ be an $\vec{\mathcal{A}}_n$ shard. The **shard polytope** $\mathsf{SP}(\Sigma)$ is the intersection of the sum-zero hyperplane $\mathcal{H}_0^n$ with the linear subspace $\{\mathbf{x} \in \mathbb{R}^n \mid \forall i \notin [\ell, r] : x_i = 0\}$ and the halfspaces defined by

- $x_a \geq 0$ for every $a \in A$,
- $x_b \leq 0$ for every $b \in B$,
- $\sum_{i \leq f} x_i \leq 1$ for every Σ-fall f,
- $\sum_{i \leq c} x_i \geq 0$ for every Σ-climb c.

Before we prove the equivalence of these two definitions, we will take a closer look at the inequalities of shard polytopes, based solely on the $\mathcal{H}$-description of Definition 3.2.2.

Lemma 3.2.3 (Some Inequalities for the Shard Polytope)**.** *Let $\Sigma = \Sigma_n(\ell, r, A, B)$ be an $\vec{\mathcal{A}}_n$ shard. For every point $\mathbf{x} \in \mathsf{SP}(\Sigma)$ in the shard polytope $\mathsf{SP}(\Sigma)$, we have*

- $0 \leq x_j \leq 1$ *for every* $j \in \{\ell\} \cup A$,
- $-1 \leq x_j \leq 0$ *for every* $j \in B \cup \{r\}$,
- $0 \leq \sum_{i \leq k} x_i \leq 1$ *for every* $k \in [n]$.

Proof. We fix an arbitrary point $\mathbf{x} \in \mathsf{SP}(\Sigma)$. For ease of notation, we introduce the vector $\mathbf{y} \in \mathbb{R}^n$ with entries $y_j := \sum_{i \leq j} x_i$. By definition of the shard polytope, this vector $\mathbf{y}$ has

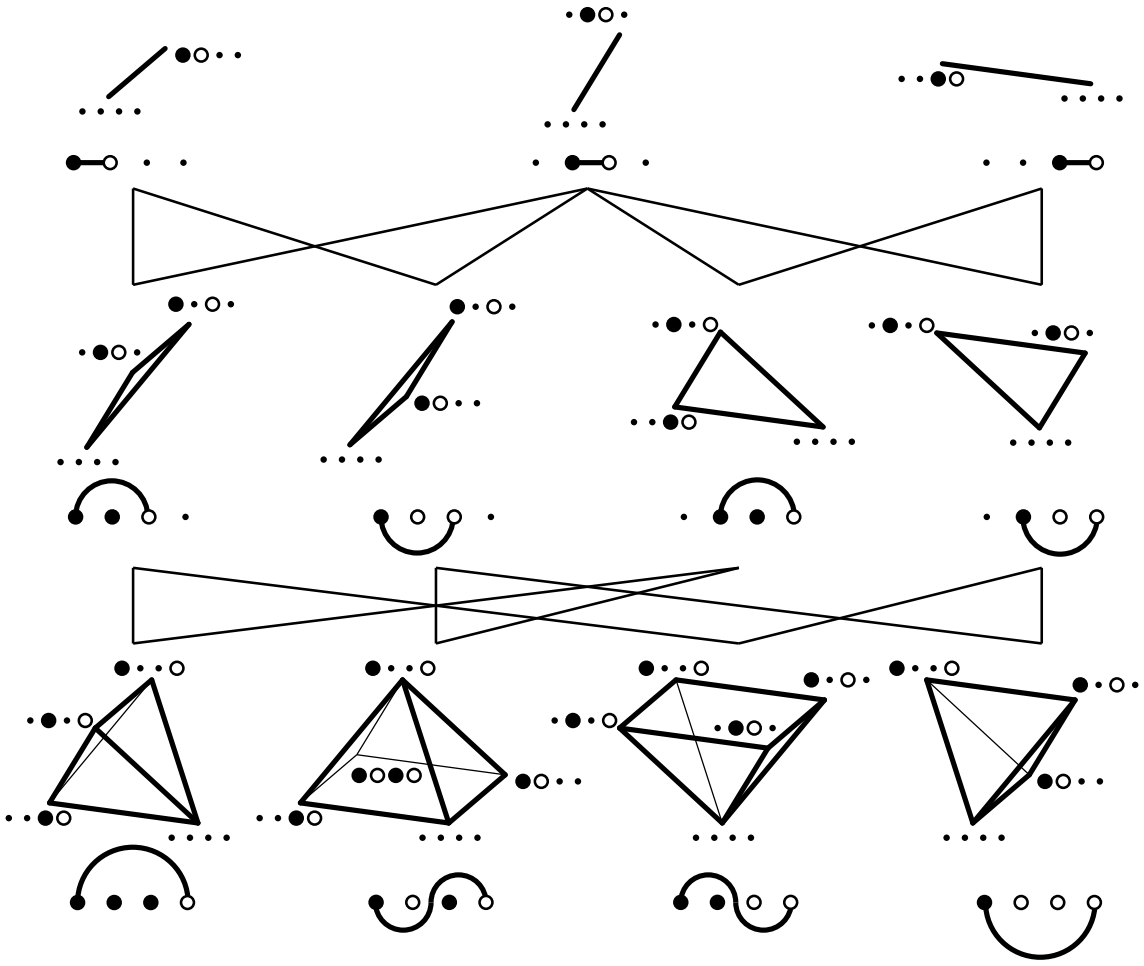

Figure 3.3: Shard polytopes for all $\vec{\mathcal{A}}_4$ shards, arranged to illustrate the forcing order among them. [Picture from [PPR20]]

- $y_f \leq 1$ for every Σ-fall f,
- $y_c \geq 0$ for every Σ-climb c,
- $y_r \leq y_s$ for every $1 \leq r \leq s \leq n$ with $]r, s] \subseteq A$,
- $y_r \geq y_s$ for every $1 \leq r \leq s \leq n$ with $]r, s] \subseteq B$,
- $y_n = 0$ as $\mathbf{x}$ lies on the sum-zero hyperplane $\mathcal{H}_0^n$.

We examine the entries of $\mathbf{x}$ and $\mathbf{y}$ and distinguish cases by the position of j relative to ℓ and r.

- If $j < \ell$, then $x_j = 0$ and $y_j = \sum_{i \leq j} x_i = 0$ by definition.
- If $j = \ell$, we set c to be the first Σ-climb in $[\ell, r[$ and f to be the first Σ-fall in $[\ell, r[$. We deduce that $]\ell, c] \subseteq B$ and $]\ell, f] \subseteq A$ and conclude that $0 \leq y_c \leq y_\ell \leq y_f \leq 1$. Furthermore, we know $y_\ell = y_{\ell-1} + x_\ell = 0 + x_\ell$, so $0 \leq x_\ell \leq 1$ holds as well.
- If $j \in A$, we set c to be the last Σ-climb in $[\ell, j[$ and f to be the first Σ-fall in $[j, r[$. As we noted in Observation 3.1.7, both do exist. We deduce $]c, j] \subseteq A$ and $]j, f] \subseteq A$ and conclude that $0 \leq y_c \leq y_j \leq y_f \leq 1$. This also implies that $x_j = y_j - y_{j-1} \leq 1 - y_c \leq 1$ and we already know $0 \leq x_j$ holds as $j \in A$.
- If $j \in B$, we proceed analogously by setting f to be the last Σ-fall in $[\ell, j[$ and c to be the first Σ-climb in $[j, r[$. We conclude that on one hand, $0 \leq y_c \leq y_j \leq y_f \leq 1$ while on the other hand, $x_j = y_j - y_{j-1} \geq 0 - y_f \geq -1$ and $x_j \leq 0$ holds as $j \in B$.
- If $j = r$, then all x_i with $j < i$ are zero, so $y_r + 0 = y_n = 0$. Furthermore, we obtain the equality $x_r = y_r - y_{r-1} = 0 - y_{r-1}$, where y_{r-1} lies in between 0 and 1 as shown before.

- If $j > r$, then $x_j = 0$ and $\sum_{i \leq j} x_i = y_n - \sum_{k=j+1}^{n} x_k = 0 - 0 = 0$.

In particular, we showed that $\mathsf{SP}(\Sigma)$ is a subset of the n-cube $[-1, +1]^n \subseteq \mathbb{R}^n$. □

Now that we know a number of additional inequalities that are valid for the shard polytope $\mathsf{SP}(\Sigma)$, we proceed by proving that none of the inequalities used in Definition 3.2.2 can be left out: They are in fact irredundant.

Lemma 3.2.4 (Shard Polytope Facets)**.** *Let Σ be an $\vec{\mathcal{A}}_n$ shard. The facets of $\mathsf{SP}(\Sigma)$ correspond to the inequalities in Definition 3.2.2.*

Proof. To prove irredundancy, we provide one vector in $\mathbb{R}^n$ for each of the inequalities. That vector violates this particular inequality while satisfying all the others. We list them explicitly.

- For every $a \in A$, the inequality $x_a \geq 0$ is violated by $\mathbf{e}_\ell - \mathbf{e}_a$.
- For every $b \in B$, the inequality $x_b \leq 0$ is violated by $\mathbf{e}_b - \mathbf{e}_r$.
- For every Σ-climb c, the inequality $\sum_{i \leq c} x_i \geq 0$ is violated by $\mathbf{e}_{c+1} - \mathbf{e}_c$.
- For every Σ-fall f, the inequality $\sum_{i \leq f} x_i \leq 1$ is violated by $2\mathbf{e}_f - 2\mathbf{e}_{f+1}$.

We conclude that each inequality in Definition 3.2.2 defines a facet of $\mathsf{SP}(\Sigma)$. Clearly, every facet is defined by a supporting inequality of the polytope and distinct inequalities define distinct facets, so the facets of $\mathsf{SP}(\Sigma)$ correspond to these inequalities. □

We now prove that the definitions of the shard polytope as a $\mathcal{V}$-polytope in Definition 3.2.1 and as an $\mathcal{H}$-polytope in Definition 3.2.2 are in fact equivalent.

Proposition 3.2.5 (Equivalence of Shard Polytope Descriptions)**.** *Let $\Sigma := \Sigma_n(\ell, r, A, B)$ be an $\vec{\mathcal{A}}_n$ shard. The polytope defined by the inequalities of Definition 3.2.2 is equal to the polytope defined as convex hull of the characteristic vectors of all Σ-matchings as stated in Definition 3.2.1.*

Proof. We fix an arbitrary $\vec{\mathcal{A}}_n$ shard Σ. We define P to be the convex hull of the characteristic vectors of all Σ-matchings as in Definition 3.2.1 and Q to be the intersection of halfspaces described in Definition 3.2.2. We will prove the equality $\mathsf{P} = \mathsf{Q}$ by showing that either polytope is contained in the other.

1. We fix an arbitrary Σ-matching M. Then its characteristic vector $\mathbf{x} = \boldsymbol{\chi}(M)$ satisfies all the equalities and inequalities that define the polytope Q:
   - M only contains elements in the range $[\ell, r]$, so $x_i = 0$ wherever $i < \ell$ or $i > r$.
   - For any $a \in A$, either $a \in M$ (so $x_a = 1$), or $a \notin M$ (so $x_a = 0$). Either way, $x_a \geq 0$.
   - For any $b \in B$, either $b \in M$ (so $x_b = -1$), or $b \notin M$ (so $x_b = 0$). Either way, $x_b \leq 0$.
   - For the remaining criteria, we note that for an arbitrary position $j \in [0, n]$, we can define the set $M_j := M \cap [0, j]$. If M_j has an even number of elements, then $\mathbf{x}$ has equally many positive and negative entries up to j, so $\sum_{i \leq j} x_i = 0$. In particular, for $j = n$, we obtain that $\sum_{i \leq n} x_i = 0$ as M has even cardinality. If M_j has an odd number of elements, then the number of positive entries of $\mathbf{x}$ up to j exceeds the number of negative entries of $\mathbf{x}$ up to j by exactly one, so that $\sum_{i \leq j} x_i = 1$. We conclude that $0 \leq \sum_{i \leq j} x_i \leq 1$ for every $j \in [\ell, r]$. In particular, this holds for every Σ-climb and every Σ-fall.

   We proved that every vertex of P satisfies all the inequalities of Q. As both P and Q are convex, this implies that P is a subset of Q.
2. To prove that Q is a subset of P, We will first show that Q is an integer polytope. We can rewrite Q in the form $\{\mathbf{x} \in \mathbb{R}^n \mid \mathbf{M}\mathbf{x} \leq \mathbf{b}\}$ for a matrix $\mathbf{M} \in \mathbb{R}^{m \times n}$ and an integer vector $\mathbf{b} \in \mathbb{R}^m$. The rows of $\mathbf{M}$ and scalars in $\mathbf{b}$ correspond to the conditions in Definition 3.2.2.
   - For every $i \in [n] \setminus [\ell, r]$, we write row with $\mathbf{e}_i$ in $\mathbf{M}$ and 0 in $\mathbf{b}$.
   - For every $i \in [n] \setminus [\ell, r]$, we write row with $-\mathbf{e}_i$ in $\mathbf{M}$ and 0 in $\mathbf{b}$.

- We write a row with $\mathbf{1}$ in $\mathbf{M}$ and 0 in $\mathbf{b}$.
- We write a row with $-\mathbf{1}$ in $\mathbf{M}$ and 0 in $\mathbf{b}$.
- For every $a \in A$, we write a row with $-\mathbf{e}_a$ in $\mathbf{M}$ and 0 in $\mathbf{b}$.
- For every $b \in B$, we write a row with $\mathbf{e}_b$ in $\mathbf{M}$ and 0 in $\mathbf{b}$.
- For every Σ-fall f, we write a row with $\mathbf{1}_{[1,f]}$ in $\mathbf{M}$ and 1 in $\mathbf{b}$.
- For every Σ-climb c, we write a row with $-\mathbf{1}_{[1,c]}$ in $\mathbf{M}$ and 0 in $\mathbf{b}$.

We construct another matrix $\mathbf{M}'$ which is identical to $\mathbf{M}$ except that every row of $\mathbf{M}$ which has negative entries gets multiplied by -1. Then $\mathbf{M}'$ has the consecutive ones property as defined in Definition 1.2.15. We observe that every square submatrix of $\mathbf{M}'$ can be obtained from a square submatrix of $\mathbf{M}$ by multiplying some rows by -1. We deduce that $\mathbf{M}$ has the consecutive ones property as well, so by Lemma 1.2.16, we conclude that $\mathbf{M}$ is totally unimodular. As $\mathbf{b}$ is an integer vector, we can apply Lemma 1.2.17 and deduce that all vertices of Q have integer coordinates.

Let $\mathbf{w}$ now be one of the vertices of Q. We define the set $M(\mathbf{w}) := \{j \in [n] \mid w_j \neq 0\}$ and show that it is in fact a Σ-matching.

- We first note that if $\mathbf{w} = \mathbf{0}$, then $M(\mathbf{w}) = \emptyset$ is a trivial Σ-matching.
- By Definition 3.2.2, all nonzero entries of $\mathbf{w}$ appear in between ℓ and r, so $M \subseteq [\ell, r]$.
- We denote the smallest element of $M(\mathbf{w})$ by a_1. Assume $a_1 \in B \cup \{r\}$ for a contradiction. Then $\sum_{i \leq a_1} w_i \leq -1$, in contradiction to Lemma 3.2.3 valid for Q.
- We denote the second smallest element of $M(\mathbf{w})$ by b_1. Assume $b_1 \in \{\ell\} \cup A$ for a contradiction. Then $\sum_{i \leq b_1} w_i \geq 2$, in contradiction to Lemma 3.2.3 valid for Q.
- These two arguments can be continued up to the last element of $M(\mathbf{w})$.

We deduce that $M(\mathbf{w})$ is a Σ-matching. This implies that every vertex of Q is the characteristic vector of a Σ-matching and therefore contained in P. As both Q and P are convex, we deduce that Q is a subset of P.

We conclude that $\mathsf{P} = \mathsf{Q}$, so the two definitions of shard polytopes are equivalent. □

Observation 3.2.6 (Pseudoshard Polytopes)**.** As remarked in Observation 3.1.17, we can define Σ-matchings for pseudoshards in the exact same way as for ordinary shards. The skipped positions (described by the set $]\ell, r[\setminus (A \dot\cup B)$) will never appear in any Σ-matching. On the other hand, we saw a way to use climbs and falls for pseudoshards in Observation 3.1.6. We may therefore define the **pseudoshard polytope** $\mathsf{SP}(\Sigma)$ equivalently

- as the convex hull of the characteristic vectors of all Σ-matchings,
- by the equalities and inequalities given in Definition 3.2.2, with the additional requirement that $x_j = 0$ for every j that is skipped by Σ (that is, every $j \in]\ell, r[\setminus (A \dot\cup B)$).

We recall that we can map the pseudoshard Σ to a shard $\varphi(\Sigma)$ through the map φ given in Observation 3.1.2. Then the pseudoshard polytope $\mathsf{SP}(\Sigma)$ is affinely isomorphic to the shard polytope $\mathsf{SP}(\varphi(\Sigma))$.

3.2.2 Basic Properties

We now know how to construct a shard polytope for any $\vec{\mathcal{A}}_n$ shard. We already know its facets (we showed in Lemma 3.2.4 that the inequalities in the $\mathcal{H}$-description given in Definition 3.2.2 are irredundant). In this section, we will examine shard polytopes for some more basic polytope properties, such as their dimension, number of facets and vertices, before learning more about the shape of their faces, their edges and edge directions.

Lemma 3.2.7 (Shard Polytope Dimension)**.** *Let $\Sigma = \Sigma_n(\ell, r, A, B)$ be an $\vec{\mathcal{A}}_n$ shard. Its shard polytope $\mathsf{SP}(\Sigma)$ has dimension $r - \ell$.*

Proof. We first recall that every vertex $\mathbf{v}$ of $\mathsf{SP}(\Sigma)$ has $\sum_{i=1}^{n} v_i = 0$ and $v_j = 0$ for all $j \in [n] \setminus [\ell, r]$. As these equalities define an $(r-\ell)$-dimensional linear subspace of $\mathbb{R}^n$ containing all vertices of $\mathsf{SP}(\Sigma)$, the dimension of their convex hull $\mathsf{SP}(\Sigma)$ cannot be larger than $r-\ell$. On the other hand, we know that every Σ-matching yields a point in $\mathsf{SP}(\Sigma)$.

- The empty Σ-matching $\emptyset$ yields the point $\mathbf{0}$.
- The Σ-matching $\{\ell, r\}$ yields the point $\mathbf{e}_\ell - \mathbf{e}_r$.
- For every $a \in A$, the Σ-matching $\{a, r\}$ yields the point $\mathbf{e}_a - \mathbf{e}_r$.
- For every $b \in B$, the Σ-matching $\{\ell, b\}$ yields the point $\mathbf{e}_\ell - \mathbf{e}_b$.

These are $1+1+|A|+|B| = \ell - r + 1$ distinct points in $\mathsf{SP}(\Sigma)$. As they are affinely independent, we deduce that the dimension of $\mathsf{SP}(\Sigma)$ is at least $r-\ell$. □

Lemma 3.2.8 (Shard Polytope Facet Number)**.** *Let $\Sigma = \Sigma_n(\ell, r, A, B)$ be an $\vec{\mathcal{A}}_n$ shard and let t be the number of Σ-turns. The number of facets of $\mathsf{SP}(\Sigma)$ is $r - \ell + 1 + t$. The polytope $\mathsf{SP}(\Sigma)$ is a simplex if and only if Σ does not have any turns.*

Proof. We know by Lemma 3.2.4 that the facets of $\mathsf{SP}(\Sigma)$ are in bijection with the inequalities of Definition 3.2.2. There, we have one inequality for each element of A or B, which gives us a total of $r - \ell - 1$ inequalities, plus one more inequality for each Σ-climb and each Σ-fall. We recall that the number of Σ-climbs plus the number of Σ-falls equals the number of Σ-turns plus 2. We deduce that the number of facets of $\mathsf{SP}(\Sigma)$ is $r - \ell - 1 + 2 + t$.

As we saw that the dimension of $\mathsf{SP}(\Sigma)$ is $r - \ell$, we know it is a simplex if and only if it has $r - \ell + 1$ facets, which is the case if and only if Σ does not have any turns. □

Lemma 3.2.9 (Shard Polytope Vertices)**.** *Let $\Sigma := \Sigma_n(\ell, r, A, B)$ be an $\vec{\mathcal{A}}_n$ shard. The vertices of the shard polytope $\mathsf{SP}(\Sigma)$ are exactly the characteristic vectors of all Σ-matchings.*

Proof. We already know that $\mathsf{SP}(\Sigma)$ is the convex hull of the characteristic vectors of all Σ-matchings. It is left to show that all of them are extremal points in $\mathsf{SP}(\Sigma)$. We fix a Σ-matching M and define the direction $\mathbf{d}(M) \in \mathbb{R}^n$ by $\mathbf{d}(M) := 2\boldsymbol{\chi}(M) - \boldsymbol{\chi}(\Sigma)$, where $\boldsymbol{\chi}(\Sigma)$ and $\boldsymbol{\chi}(M)$ are the characteristic vectors of the shard and the matching as introduced in Definition 3.1.3 and Definition 3.1.10, respectively. Then for any Σ-matching M', we obtain

$$\begin{aligned}
\big\langle \mathbf{d}(M) \,\big|\, \boldsymbol{\chi}(M') \big\rangle &= \big\langle 2\boldsymbol{\chi}(M) \,\big|\, \boldsymbol{\chi}(M') \big\rangle - \big\langle \boldsymbol{\chi}(\Sigma) \,\big|\, \boldsymbol{\chi}(M') \big\rangle \\
&= 2 \cdot \big|M \cap M'\big| - \big|M'\big| \\
&= \big|M \cap M'\big| - \big|M' \setminus M\big| \\
&\leq |M| \,.
\end{aligned}$$

We deduce that M is the only Σ-matching whose scalar product with $\mathbf{d}(M)$ is $|M|$, while the scalar product for any other Σ-matching is smaller. Therefore, $\boldsymbol{\chi}(M)$ cannot be a convex combination of characteristic vectors of other Σ-matchings. We conclude that every characteristic vector $\boldsymbol{\chi}(M)$ of a Σ-matching M is a vertex of $\mathsf{SP}(\Sigma)$. □

We now count the number of vertices of a shard polytope, equal to the number of shard matchings. We first introduce two auxiliary functions counting certain sets which can be completed to a matching. We use binary variables $\delta_{x \in Y}$ that are 1 if the index condition is satisfied, otherwise 0.

Definition 3.2.10 (Counting Matching Prefixes)**.** Let $\Sigma := \Sigma_n(\ell, r, A, B)$ be an $\vec{\mathcal{A}}_n$ shard. We define two integer functions $v_\Sigma, w_\Sigma : [\ell, r] \to \mathbb{N}$ by

1. $v_\Sigma(\ell), w_\Sigma(\ell) := 1$,
2. $v_\Sigma(i) := v_\Sigma(i-1) + \delta_{i \in \{\ell\} \cup A} \cdot w_\Sigma(i-1)$ for $i \in]\ell, r[$,
3. $w_\Sigma(i) := w_\Sigma(i-1) + \delta_{i \in B \cup \{r\}} \cdot v_\Sigma(i-1)$ for $i \in]\ell, r[$.

We observe that $w_\Sigma(i)$ counts the number of Σ-matchings that only contain values in $[\ell, i]$. Similarly, $v_\Sigma(i)$ counts the number of subsets of $[\ell, i]$ that become a Σ-matching when adding r. More formally, we can describe $v_\Sigma(i)$ (resp. $w_\Sigma(i)$) as the number of odd (resp. even) subsets of $[\ell, i]$ that are of the form $M \cap [\ell, i]$ for some Σ-matching M.

In particular, $w_\Sigma(\ell) = 1$ because the only Σ-matching using only values in $[\ell, \ell]$ is the empty one and $v_\Sigma(\ell) = 1$ as the only subset of $[\ell, \ell]$ that becomes a Σ-matching by adding r is the set $\{\ell\}$. Moreover, $w_\Sigma(r)$ is the total number of Σ-matchings. This gives us the following result:

Corollary 3.2.11 (Shard Polytope Vertex Number)**.** Let $\Sigma := \Sigma_n(\ell, r, A, B)$ be an $\vec{\mathcal{A}}_n$ shard. The number of vertices of its shard polytope $\mathsf{SP}(\Sigma)$ is $w_\Sigma(r)$.

Example 3.2.12. For two examples of $\vec{\mathcal{A}}_n$ shards, we obtain the following numbers of vertices:

- Given the up shard $\Sigma = \Sigma_n(1,\, n,\,]1, n[\,, \emptyset)$ with endpoints 1 and n, its shard polytope $\mathsf{SP}(\Sigma)$ has n vertices. This result can also be obtained by combining that the dimension of $\mathsf{SP}(\Sigma)$ is $n - 1$ (see Lemma 3.2.7) and that $\mathsf{SP}(\Sigma)$ is a simplex as Σ does not have any turns (see Lemma 3.2.8).
- Given a shard $\Sigma = \Sigma_n(1, n, A, B)$ of the hyperplane $H_n(1, n)$, where the positions in $]1, n[$ alternate between A and B (for example, $\Sigma = \Sigma_6(1,\, 6,\, \{3, 5\}, \{2, 4\})$). Then v_Σ and w_Σ increase alternatingly, so the number of vertices of $\mathsf{SP}(\Sigma)$ is the Fibonacci number F_{n+1}.

3.2.3 Edges

In this section, we will analyze the edges of a shard polytope. As every edge is a one-dimensional face of the polytope, no convex combinations of its two endpoints can be represented as a convex combination of the remaining vertices of the polytope. For our shard polytope, this condition translates into a condition on the sum of the characteristic vectors of two Σ-matchings. To understand these sums, we examine the different ways to obtain a sum of two characteristic vectors.

Lemma 3.2.13 (Combining Σ-Matchings)**.** *Let $\Sigma = \Sigma_n(\ell, r, A, B)$ be an $\vec{\mathcal{A}}_n$ shard and let M_1 and M_2 be two distinct Σ-matchings. Exactly one of the following holds.*

- *Either there exist two Σ-matchings M_3 and M_4 both distinct from M_1 and M_2 such that $\boldsymbol{\chi}(M_1) + \boldsymbol{\chi}(M_2) = \boldsymbol{\chi}(M_3) + \boldsymbol{\chi}(M_4)$,*
- *or there exist two Σ-matchings H and T with $h := \sup(H)$ and $t := \inf(T)$ and some positions $a_i \in \{\ell\} \cap A$ and $b_i \in B \cup \{r\}$, such that $\{M_1, M_2\}$ is one of the following pairs:*
  1. *$\{H \cup \{a_0, b_0\} \cup T,\ H \cup T\}$ with $h < a_0 < b_0 < t$,*
  2. *$\{H \cup \{a_0, b_1\} \cup T,\ H \cup \{a_0, b_2\} \cup T\}$ with $h < a_0 < b_1, b_2 < t$,*
  3. *$\{H \cup \{a_1, b_0\} \cup T,\ H \cup \{a_2, b_0\} \cup T\}$ with $h < a_1, a_2 < b_0 < t$,*
  4. *$\{H \cup \{a_1, b_1, a_2, b_2\} \cup T,\ H \cup \{a_1, b_2\} \cup T$ with $h < a_1 < b_1 < a_2 < b_2 < t$.*

Proof. We fix two Σ-matchings M_1 and M_2 and set H to be the unique maximal common initial Σ-matching of M_1 and M_2. More formally, H is the maximal subset of $M_1 \cap M_2$ such that H is a Σ-matching and $H = \{i \in M_1 \cap M_2 \mid i \leq \sup(H)\}$. Analogously, we set T to be the unique maximal common final Σ-matching of M_1 and M_2 (so that T is a Σ-matching with the property that $T = \{i \in M_1 \cap M_2 \mid \inf(T) \leq i\}$). As the two Σ-matchings M_1 and M_2 are distinct, at least one of the sets $M_1 \setminus (H \dot\cup T)$ and $M_2 \setminus (H \dot\cup T)$ is non-empty.

For any vector $\mathbf{w} \in \mathbb{R}^n$, we denote its support (the set of coordinates where it has nonzero entries) by $\mathrm{Supp}(\mathbf{w}) := \{i \in [n] \mid \mathbf{w}_i \neq 0\}$. We define the sequence $\delta(\mathbf{w}) := (\delta(\mathbf{w})_j)_{j \in \mathrm{Supp}(\mathbf{w})}$ with entries $\delta(\mathbf{w})_j := \sum_{i \leq j} \mathbf{w}_i$ for every position $j \in \mathrm{Supp}(\mathbf{w})$. Given a Σ-matching M of semi-length k, the sequence $\delta(\boldsymbol{\chi}(M))$ has length $2k$ and is alternating between a 1 for every element of $(\{\ell\} \cup A) \cap M$ and a 0 for every element of $(B \cup \{r\}) \cap M$, as it sums up the entries of the

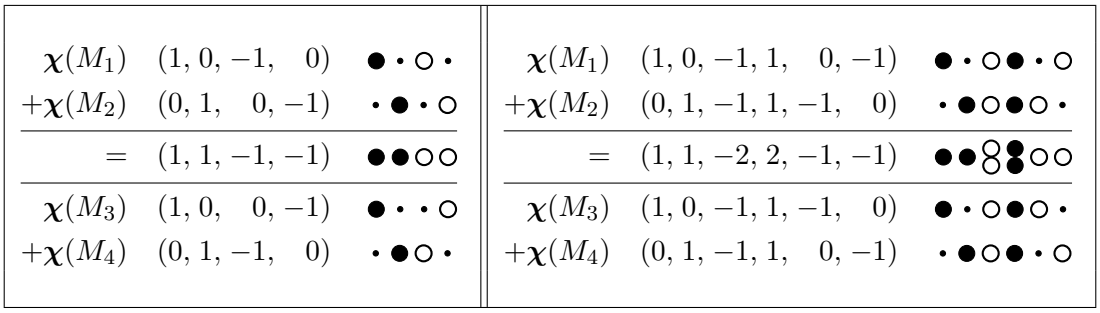

Figure 3.4: Two examples of the standard case of Lemma 3.2.13. In each of these, the vector $\boldsymbol{\chi}(M_1) + \boldsymbol{\chi}(M_2)$ can equivalently be obtained as the sum of characteristic vectors of two matchings M_3 and M_4 distinct from M_1 and M_2. This remains true if we add matchings H to the left and T to the right of all of them.

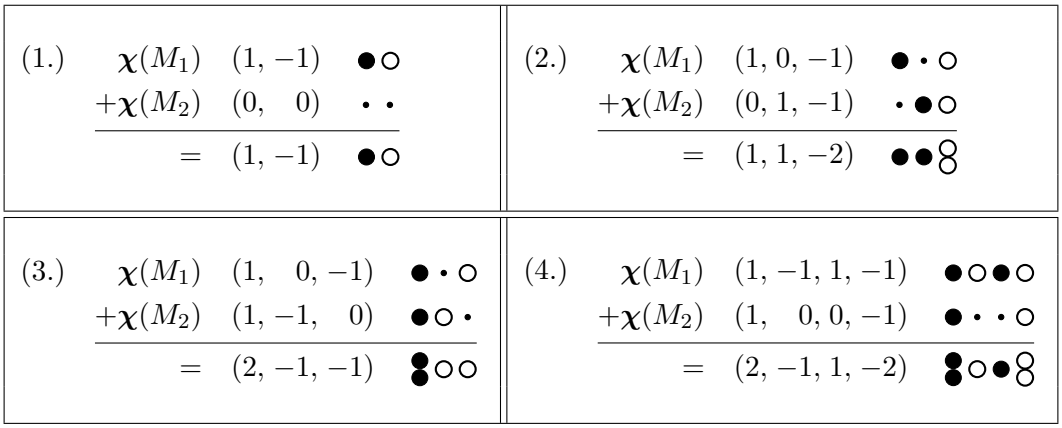

Figure 3.5: The four special cases of Lemma 3.2.13. In each of these, it is impossible to obtain the vector $\boldsymbol{\chi}(M_1) + \boldsymbol{\chi}(M_2)$ as the sum of characteristic vectors of two matchings distinct from M_1 and M_2. This remains true if we add matchings H to the left and T to the right of both M_1 and M_2.

characteristic vector up to that position. In particular, the sequence $\delta(\boldsymbol{\chi}(M_1)+\boldsymbol{\chi}(M_2))$ is alternating between 2 and 0 in the entries corresponding to H and T, with $\delta(\boldsymbol{\chi}(M_1)+\boldsymbol{\chi}(M_2))_{\sup(H)} = 0$ and $\delta(\boldsymbol{\chi}(M_1) + \boldsymbol{\chi}(M_2))_{\inf(T)} = 2$ (if H and T are non-empty so that $\sup(H)$ and $\inf(T)$ are integers).

Looking at the two Σ-matchings M_1 and M_2, we have $\delta(\boldsymbol{\chi}(M_1) + \boldsymbol{\chi}(M_2))_j \in \{0, 1, 2\}$ for every $j \in M_1 \cup M_2$. We will examine that sequence $\delta(\boldsymbol{\chi}(M_1) + \boldsymbol{\chi}(M_2))$ in more detail, and we focus on the central positions included in neither H nor T, which can equivalently be defined as $C := (M_1 \cup M_2) \cap]\sup(H), \inf(T)[$ or $C := (M_1 \cup M_2) \setminus (H \dot\cup T)$. We note that M_1 and M_2 do not differ outside of the positions in C. As we assumed M_1 and M_2 to be distinct, we deduce that C is not empty. We define the subsequence $d := \delta(\boldsymbol{\chi}(M_1)+\boldsymbol{\chi}(M_2))_{j\in C}$ and observe that $d \in \{0, 1, 2\}^C$.

We note that the first entry of d corresponds to an element of $\{\ell\} \cup A$, as H is either empty or its maximal element corresponds to an element of $B \cup \{r\}$ contained in both M_1 and M_2. Analogously, the last entry of d corresponds to an element of $B \cup \{r\}$, as T is either empty or its first element corresponds to an element of $\{\ell\} \cup A$ contained in both M_1 and M_2. Each position $j \in C \subseteq [\ell, r]$ either has $j \in \{\ell\} \cup A$, so the entry d_j equals the previous one minus 1 or 2, or $j \in B \cup \{r\}$, so the entry d_j equals the previous one plus 1 or 2. In particular, the first

entry of d is nonzero while the last entry has to be zero. We now distinguish cases by the position of zeros in d.

We first consider the case where there is a zero in d apart from the last position. Then there are three positions $i < j < k \in C$ such that $d_i, d_k > 0 = d_j$. This implies that we obtain Σ-matchings from each of the constructions

- $L_1 := M_1 \cap [\ell, j]$,
- $L_2 := M_2 \cap [\ell, j]$,
- $R_1 := M_1 \cap]j, r]$,
- $R_2 := M_2 \cap]j, r]$.

Note that they are all distinct. If two of them were identical, they would have to be part of H resp. T. We know that $M_1 = L_1 \dot\cup R_1$ and $M_2 = L_2 \dot\cup R_2$ have to hold. Therefore, the sets $M_3 := L_1 \dot\cup R_2$ and $M_4 := L_2 \dot\cup R_1$ are two new matchings distinct from M_1 and M_2 such that $\boldsymbol{\chi}(M_1) + \boldsymbol{\chi}(M_2) = \boldsymbol{\chi}(M_3) + \boldsymbol{\chi}(M_4)$ as desired. We remark that in this case, none of the four special cases listed in the lemma may occur.

We now consider the cases where the only zero in d is in the last position. There are four special cases to consider, in which there only is a single way to decompose into Σ-matchings.

1. If $d = (10)$, then $\mathrm{Supp}(d)$ is of the form $\{a_0, b_0\}$,
   so one of the matchings has to contain $\{a_0, b_0\}$, and the other one contains neither.
2. If $d = (210)$, then $\mathrm{Supp}(d)$ is of the form $\{a_0, b_1, b_2\}$,
   so one of the matchings has to contain $\{a_0, b_1\}$, and the other has to contain $\{a_0, b_2\}$.
3. If $d = (120)$, then $\mathrm{Supp}(d)$ is of the form $\{a_1, a_2, b_0\}$,
   so one of the matchings has to contain $\{a_1, b_0\}$, and the other has to contain $\{a_2, b_0\}$.
4. If $d = (2120)$, then $\mathrm{Supp}(d)$ is of the form $\{a_1, b_1, a_2, b_2\}$,
   so one of the matchings has to contain $\{a_1, b_2\}$, and the other has to contain $\{a_1, b_1, a_2, b_2\}$.

We distinguish the remaining cases by their first entry of d. We first recall that d cannot start with a 0. If d starts with a 1, then we may assume that it neither starts with 10 nor with 120 (as we have already considered these cases), so it has to start with 121. We recall that the first entry of d always corresponds to an element of $\{\ell\} \cup A$. As the second entry is larger than the first one, it corresponds to an element of A. We denote the two positions by $a_1 < a_2$.

- We first consider the subcase where $d = 1210$. Then $C = \{a_1 < a_2 < b_1 < b_2\}$, and we can decompose C in two distinct ways: Either as $\{\{a_1, b_1\}, \{a_2, b_2\}\}$ or as $\{\{a_1, b_2\}, \{a_2, b_1\}\}$. Appending H and T yields the desired decompositions of $\boldsymbol{\chi}(M_1) + \boldsymbol{\chi}(M_2)$.
- We now consider the other subcase where d starts with 1212. Then those first four entries of C are of the form $a_1 < a_2 < b_1 < a_3$. We can decompose this part in two different ways, independently of the rest of d, either as $\{\{a_1, b_1, a_3\}, \{a_2\}\}$ or as $\{\{a_1\}, \{a_2, b_1, a_3\}\}$. With H and T appended, this also guarantees that there are at least two distinct decompositions of $\boldsymbol{\chi}(M_1) + \boldsymbol{\chi}(M_2)$.

If d starts with a 2, then we first remark that it cannot start with 20: This would mean that the first two entries of d correspond to positions that should be part of H, as they are contained in both M_1 and M_2. We may also assume that it neither starts with 210 not with 2120. So d starts with 2121.

- We first consider the subcase where $d = 21210$. Then $C = \{a_1 < b_1 < a_2 < b_2 < b_3\}$, and we can decompose C in two distinct ways: Either as $\{\{a_1 < b_1 < a_2 < b_2\}, \{a_1 < b_3\}\}$ or as $\{\{a_1 < b_1 < a_2 < b_3\}, \{a_1 < b_2\}\}$.
- We are left with the case where d starts with 21212. Then those first five entries of C are of the form $a_1 < b_1 < a_2 < b_2 < a_3$. We can decompose this part in two different ways, namely as $\{\{a_1 < b_1 < a_2 < b_2 < a_3\}, \{a_1\}\}$ or as $\{\{a_1 < b_1 < a_2\}, \{a_1 < b_2 < a_3\}\}$. □

To illustrate this proof, Figure 3.4 gives examples of pairs of matchings where the sum of the characteristic vectors can be obtained from other matchings as well, while Figure 3.5 shows the special cases where it is impossible. We can deduce a simple sufficient criterion to decide whether two Σ-matchings can be recombined into two new Σ-matchings.

Corollary 3.2.14 (Decomposable Σ-Matchings)**.** Let Σ be an $\vec{A}_n$ shard. Let M_1, M_2 be two distinct Σ-matchings with $|M_1 \Delta M_2| > 2$. Then there exist two Σ-matchings M_3 and M_4 both distinct from M_1 and M_2 such that $\boldsymbol{\chi}(M_1) + \boldsymbol{\chi}(M_2) = \boldsymbol{\chi}(M_3) + \boldsymbol{\chi}(M_4)$.

Proof. We observe that in each of the four special cases of Lemma 3.2.13, we have $|M_1 \Delta M_2| = 2$. We conclude that we are in the other one of the two exlusive cases. □

This leads us to the following characterization of all edges of the shard polytope.

Lemma 3.2.15 (Shard Polytope Edges)**.** *Let $\Sigma := \Sigma_n(\ell, r, A, B)$ be an $\vec{A}_n$ shard. The edges of its shard polytope $\mathsf{SP}(\Sigma)$ are exactly those pairs of characteristic vectors of Σ-matchings M and M' where $|M \Delta M'| = 2$.*

Proof. We fix two Σ-matchings M and M' and define the direction $\mathbf{d} := \boldsymbol{\chi}(M) + \boldsymbol{\chi}(M') - \boldsymbol{\chi}(\Sigma)$. For any matching M'', we first observe that we can partition the set to rewrite its cardinality as $|M''| = |M'' \setminus (M \cup M')| + |(M'' \cap M) \setminus M'| + |(M'' \cap M') \setminus M| + |M'' \cap M \cap M'|$. This leads us to the following expression for the scalar product of $\mathbf{d}$ and $\boldsymbol{\chi}(M'')$: we obtain

$$\begin{aligned}
\langle \mathbf{d} \,|\, \boldsymbol{\chi}(M'') \rangle &= \langle \boldsymbol{\chi}(M) \,|\, \boldsymbol{\chi}(M'') \rangle + \langle \boldsymbol{\chi}(M') \,|\, \boldsymbol{\chi}(M'') \rangle - \langle \boldsymbol{\chi}(\Sigma) \,|\, \boldsymbol{\chi}(M'') \rangle \\
&= \big|M \cap M''\big| + \big|M' \cap M''\big| - \big|M''\big| \\
&= 2\big|M \cap M' \cap M''\big| + \big|(M \cap M'') \setminus M'\big| + \big|(M' \cap M'') \setminus M\big| - \big|M''\big| \\
&= 2\big|M \cap M' \cap M''\big| + \big|M'' \cap (M \setminus M')\big| + \big|M'' \cap (M' \setminus M)\big| - \big|M''\big| \\
&= \big|M \cap M' \cap M''\big| - \big|M'' \setminus (M \cup M')\big|.
\end{aligned}$$

In particular, we note that $\langle \mathbf{d} \,|\, \boldsymbol{\chi}(M'') \rangle \leq |M \cap M' \cap M''| \leq |M \cap M'|$. The first inequality is tight if and only if $M'' \subseteq M \cup M'$ while the second inequality is tight if and only if $M \cap M' \subseteq M''$. We deduce that $\langle \mathbf{d} \,|\, \boldsymbol{\chi}(M'') \rangle = |M \cap M'|$ holds if and only if $M \cap M' \subseteq M'' \subseteq M \cup M'$. If $|M \Delta M'| = 2$, these conditions are satisfied if and only if $M'' = M$ or $M'' = M'$. In this case, there are exactly two vertices of $\mathsf{SP}(\Sigma)$ that are maximal along the direction $\mathbf{d}$, so their convex hull is a face of $\mathsf{SP}(\Sigma)$, implying that $\mathsf{SP}(\Sigma)$ has an edge connecting $\boldsymbol{\chi}(M)$ and $\boldsymbol{\chi}(M')$ as soon as $|M \Delta M'| = 2$.

It is left to show that all edges of $\mathsf{SP}(\Sigma)$ are of this form. We fix an arbitrary edge e of $\mathsf{SP}(\Sigma)$. We recall that the vertices of $\mathsf{SP}(\Sigma)$ are exactly the characteristic vectors of Σ-matchings, so there are Σ-matchings M_1 and M_2 such that e connects $\boldsymbol{\chi}(M_1)$ to $\boldsymbol{\chi}(M_2)$. We assume for a contradiction that $|M_1 \Delta M_2| > 2$. Then Corollary 3.2.14 states that there are Σ-matchings M_3 and M_4 both distinct from M_1 and M_2 such that $\boldsymbol{\chi}(M_1) + \boldsymbol{\chi}(M_2) = \boldsymbol{\chi}(M_3) + \boldsymbol{\chi}(M_4)$. This means that the center of $\boldsymbol{\chi}(M_1)$ and $\boldsymbol{\chi}(M_2)$ is equal to the center of $\boldsymbol{\chi}(M_3)$ and $\boldsymbol{\chi}(M_4)$, so e cannot be an edge of $\mathsf{SP}(\Sigma)$. □

We now know all the edges of the shard polytope and are able to determine when two of its vertices are adjacent. We extend this notion of adjacency to the matchings that such vertices correspond to.

Definition 3.2.16 (Adjacent Matchings)**.** We call two Σ-matchings **adjacent** if their characteristic vectors are adjacent vertices of $\mathsf{SP}(\Sigma)$. Equivalently, Σ-matchings M and M' are adjacent if and only if $|M \Delta M'| = 2$.

Now that we characterized the edges of the shard polytope, we can examine all the edge directions appearing in $\mathsf{SP}(\Sigma)$.

Corollary 3.2.17 (Shard Polytope Edge Directions)**.** The edge directions of $\mathsf{SP}(\Sigma)$ are exactly the $\binom{r-\ell+1}{2}$ directions $\mathbf{e}_j - \mathbf{e}_i$ for $\ell \leq i < j \leq r$.

Proof. We fix an $\vec{\mathcal{A}}_n$ shard $\Sigma = \Sigma_n(\ell, r, A, B)$ and examine its shard polytope $\mathsf{SP}(\Sigma)$. As the empty matching and the matching $\{\ell, r\}$ are always Σ-matchings, the shard polytope has at least two vertices and therefore at least one edge. We fix an edge connecting $\boldsymbol{\chi}(M)$ and $\boldsymbol{\chi}(M')$. By Lemma 3.2.15, the set $M \Delta M'$ contains exactly two elements which we denote by $i < j$. Without loss of generality, we may assume that $i \in M \setminus M'$. We can quickly cover all cases.

- If $i, j \in \{\ell\} \cup A$, then $j \in M' \setminus M$, so $\boldsymbol{\chi}(M) - \mathbf{e}_i = \boldsymbol{\chi}(M') - \mathbf{e}_j$.
- If $i, j \in B \cup \{r\}$, then $j \in M' \setminus M$, so $\boldsymbol{\chi}(M) + \mathbf{e}_i = \boldsymbol{\chi}(M') + \mathbf{e}_j$.
- If $i \in \{\ell\} \cup A$ and $j \in B \cup \{r\}$, then $j \in M \setminus M'$, so $\boldsymbol{\chi}(M') + \mathbf{e}_i - \mathbf{e}_j = \boldsymbol{\chi}(M)$.
- If $i \in B \cup \{r\}$ and $j \in \{\ell\} \cup A$, then $j \in M \setminus M'$, so $\boldsymbol{\chi}(M') - \mathbf{e}_i + \mathbf{e}_j = \boldsymbol{\chi}(M)$.

In each of these cases, $\boldsymbol{\chi}(M) - \boldsymbol{\chi}(M') \in \{\mathbf{e}_i - \mathbf{e}_j, \mathbf{e}_j - \mathbf{e}_i\}$, so all edge directions of $\mathsf{SP}(\Sigma)$ have the form we claimed. We now fix $i < j \in [\ell, r]$. It is left to show that every direction $\mathbf{e}_j - \mathbf{e}_i$ is the direction of an $\mathsf{SP}(\Sigma)$ edge.

- If $i, j \in \{\ell\} \cup A$, we set $M := \{i, r\}$ and $M' := \{j, r\}$.
- If $i, j \in B \cup \{r\}$, we set $M := \{\ell, i\}$ and $M' := \{\ell, j\}$.
- If $i \in \{\ell\} \cup A$ and $j \in B \cup \{r\}$, we set $M := \{i, j\}$ and $M' := \emptyset$.
- If $i \in B \cup \{r\}$ and $j \in \{\ell\} \cup A$, we set $M := \{\ell, i, j, r\}$ and $M' := \{\ell, r\}$.

In each of these cases, M and M' are distinct Σ-matchings with $|M \Delta M'| = 2$, so their characteristic vectors share an edge in $\mathsf{SP}(\Sigma)$ according to Lemma 3.2.15. Moreover, the direction of this edge is $\boldsymbol{\chi}(M) - \boldsymbol{\chi}(M') \in \{\mathbf{e}_i - \mathbf{e}_j, \mathbf{e}_j - \mathbf{e}_i\}$ as desired. □

Observation 3.2.18 (Cover Relations in the Poset of Matchings)**.** We recall that the poset of Σ-matchings as introduced in Definition 3.1.13 is the set of all Σ-matchings partially ordered by set inclusion. The cover relations in this poset are all pairs of Σ-matchings $M < M'$ such that both $|M| + 2 = |M'|$ and $M \subset M'$. The latter condition is not necessarily the case for any two adjacent matchings, so not all of them form a cover relation. Therefore, the edges of the Hasse diagram of this poset correspond to those edges of $\mathsf{SP}(\Sigma)$ connecting the characteristic vectors of two Σ-matchings where one is included in the other, so they correspond to the edge directions $\mathbf{e}_a - \mathbf{e}_b$ for all positions $a \in \{\ell\} \cup A$ and $b \in B \cup \{r\}$. Equivalently, the cover relations of the Hasse diagram correspond to those edges of $\mathsf{SP}(\Sigma)$ whose endpoints have different scalar products with the characteristic vector $\boldsymbol{\chi}(\Sigma)$ of the shard, as $\langle \boldsymbol{\chi}(\Sigma) \,|\, \boldsymbol{\chi}(M) \rangle = |M|$ holds for any Σ-matching M. Therefore, different values in this scalar product ensure different cardinalities of the matchings and thus different ranks in the poset of Σ-matchings.

For edges in direction $\mathbf{e}_i - \mathbf{e}_j$ with i, j both in $\{\ell\} \cup A$ or both in $B \cup \{r\}$, both endpoints of the edge correspond to matchings with the same cardinality. Therefore, in general we cannot use $\boldsymbol{\chi}(\Sigma)$ or the poset of Σ-matchings to induce an orientation on all edges of $\mathsf{SP}(\Sigma)$.

We are now ready to answer the following question about the graph of the polytope $\mathsf{SP}(\Sigma)$. Given some Σ-matching M, what is the neighborhood of its vertex in $\mathsf{SP}(\Sigma)$?

Observation 3.2.19 (Shard Polytope Edge Types)**.** We know that for any fixed Σ-matching M, every adjacent Σ-matching M' as defined in Definition 3.2.16 has $|M \Delta M'| = 2$ by Lemma 3.2.15. We can distinguish cases by the shape of $M \Delta M'$, as we know that we are in one of the four cases described by Lemma 3.2.13.

1. For every Σ-pair (a, b) compatible with M, there is an adjacent Σ-matching $M \cup \{a, b\}$. Conversely, for every pair (a_i, b_i) of M, there is an adjacent Σ-matching $M \setminus \{a_i, b_i\}$.
2. For every Σ-pair (a, b) of M, every distinct Σ-pair (a, b') compatible with $M \setminus \{a, b\}$ induces an adjacent Σ-matching $(M \cup \{b'\}) \setminus \{b\}$. Clearly, the pair (a, b') is compatible with $M \setminus \{a, b\}$ if and only if $a < b' < \min(M \cap]b, r])$.
3. For every Σ-pair (a, b) of M, every distinct Σ-pair (a', b) compatible with $M \setminus \{a, b\}$ induces an adjacent Σ-matching $(M \cup \{a'\}) \setminus \{a\}$. Clearly, the pair (a', b) is compatible with $M \setminus \{a, b\}$ if and only if $\max(M \cap [\ell, a[) < a' < b$.

4. For every Σ-pair (a, b) of M, whenever there are positions $a < b' < a' < b$ with $a' \in A$ and $b' \in B$, they induce an adjacent Σ-matching $M \cup \{b', a'\}$, replacing the pair (a, b) by the consecutive pairs (a, b') and (a', b). Conversely, for every two consecutive Σ-pairs $(a_i, b_i), (a_{i+1}, b_{i+1})$ of M, there is an adjacent Σ-matching $M \setminus \{b_i, a_{i+1}\}$, replacing the two consecutive pairs by the new pair (a_i, b_{i+1}).

This gives us a rough lower bound on the number of neighbors of a vertex $\boldsymbol{\chi}(M)$ of $\mathsf{SP}(\Sigma)$: It has at least one neighbor for every pair of M and one neighbor for any two pairs consecutive in M, so the number of neighbors is at least twice the number of pairs of M minus one. In particular, we can state that the number of neighbors of the zero vector is equal to the number of Σ-pairs.

3.2.4 Faces

Next, we will examine the faces of shard polytopes. As every pseudoshard polytope is affinely isomorphic to a shard polytope, many statements can easily be reformulated to hold for all pseudoshard polytopes as well. For a given shard Σ, we first introduce a class of shards on different hyperplanes that force Σ.

Definition 3.2.20 (Restriction of a Shard)**.** Let $\Sigma = \Sigma_n(\ell, r, A, B)$ be an $\vec{\mathcal{A}}_n$ shard. For positions i, j with $\ell \leq i < j \leq r$, we denote by $\Sigma^{[i,j]}$ the **restriction of Σ to** $[i, j]$ defined as

- $\Sigma^{[i,j]} := \Sigma_n(i,\ j,\ A \cap]i, j[\ ,\ B \cap]i, j[)$.

It is the unique shard on the $\mathcal{A}_n$ hyperplane $H_n(i, j)$ that forces Σ. Similarly, we introduce two more restrictions of Σ which both force Σ.

- $\Sigma^{\leq i} := \Sigma_n(\ell,\ i,\ A \cap]\ell, j[,\ B \cap]\ell, i[)$ is a shard of $H_n(\ell, i)$.
- $\Sigma^{>j} := \Sigma_n(j+1,\ r,\ A \cap]j+1, r[,\ B \cap]j+1, r[)$ is a shard of $H_n(j+1, r)$.

Moreover, we introduce a pseudoshard obtained by omitting one of the positions $k \in]\ell, r[$.

- $\Sigma^{\setminus i} := \Sigma_n(\ell,\ r,\ A \setminus \{i\},\ B \setminus \{i\})$ is an $\vec{\mathcal{A}}_n$ pseudoshard of the hyperplane $H_n(\ell, r)$.

We remark that this statement remains valid for pseudoshards as well if we replace $j + 1$ by the successor $s(j)$ of j in the notation for $\Sigma^{>j}$ and the associated hyperplane. We use these restrictions to prove that all faces of a shard polytope are (affinely isomorphic to) Cartesian products of other shard polytopes of lower dimension.

Proposition 3.2.21 (Shard Polytope Faces as Cartesian Products of Pseudoshard Polytopes)**.** *Let $\Sigma = \Sigma_n(\ell, r, A, B)$ be an $\vec{\mathcal{A}}_n$ shard. Then every face of $\mathsf{SP}(\Sigma)$ is a Cartesian product of pseudoshard polytopes.*

Proof. We first recall that the proper faces of a Cartesian product of polytopes are the Cartesian products of the proper faces of the individual polytopes. As every proper i-dimensional face is the facet of an $i + 1$-dimensional face, it is sufficient to prove the statement for the facets of $\mathsf{SP}(\Sigma)$. We obtained the description of all facets of $\mathsf{SP}(\Sigma)$ in Lemma 3.2.4. We prove the statement for both types of facets:

1. The facet defined by the equality $x_i = 0$ is equal to the pseudoshard polytope $\mathsf{SP}(\Sigma^{\setminus i})$.
2. We remark that by definition of pseudoshard polytopes, the polytope $\mathsf{SP}(\Sigma^{\leq j})$ lies in a linear subspace of $\mathbb{R}^n$ defined as $\{\mathbf{x} \in \mathbb{R}^n \mid x_i = 0 \text{ for all } j < i\}$, while the polytope $\mathsf{SP}(\Sigma^{\geq j})$ lies in the subspace $\{\mathbf{x} \in \mathbb{R}^n \mid x_i = 0 \text{ for all } i \leq j\}$. We deduce that their Cartesian product $\mathsf{SP}(\Sigma^{\leq j}) \times \mathsf{SP}(\Sigma^{\geq j})$ can naturally be understood as a polytope in $\mathbb{R}^n$.
   - If j is a Σ-climb, then the facet defined by the equality $\sum_{i \leq j} x_i = 0$ is spanned by the characteristic vectors of those Σ-matchings whose restriction to the interval $[\ell, j]$ is a Σ-matching itself. This implies that their restriction to the interval $[s(j), r]$ is a Σ-matching as well. The facet is therefore equal to the Cartesian product of the pseudoshard polytopes $\mathsf{SP}(\Sigma^{\leq j}) \times \mathsf{SP}(\Sigma^{>j})$.

- Analogously, for every Σ-fall $j \in [\ell, r[$, the facet defined by the equality $\sum_{i \leq j} x_i = 1$ is spanned by the characteristic vectors of those Σ-matchings whose restriction to the interval $[\ell, j]$ contains one more element of $\{\ell\} \cup A$ than of B. Let M be such a matching. We find new matchings depending on whether j and $s(j)$ are elements of M.
  - If $j \in M$, then $M \cap [\ell, j[$ is a $\Sigma^{\leq j}$-matching.
  - If $j \notin M$, then $(M \cap [\ell, j[) \cup \{j\}$ is a $\Sigma^{\leq j}$-matching.
  - If $s(j) \in M$, then $M \cap]s(j), r]$ is a $\Sigma^{>j}$-matching.
  - If $s(j) \notin M$, then $\{s(j)\} \cup (M \cap]s(j), r])$ is a $\Sigma^{>j}$-matching.

  The facet is therefore equal to the Cartesian product $\mathsf{SP}(\Sigma^{\leq j}) \times \mathsf{SP}(\Sigma^{>j})$ of two pseudoshard polytopes, translated by $\mathbf{e}_j - \mathbf{e}_{s(j)}$. □

Next, we will have a closer look at some faces that are particularily easy to describe. For every pair of a Σ-matching, the shard polytope $\mathsf{SP}(\Sigma)$ has a face for which we can give a $\mathcal{V}$-description.

Lemma 3.2.22 (Face for a Σ-Pair)**.** *Let Σ be an $\vec{\mathcal{A}}_n$ shard. For every Σ-matching pair (a, b), there is a face of $\mathsf{SP}(\Sigma)$ which is the convex hull of the characteristic vectors of those Σ-matchings that contain (a, b) as a pair.*

Proof. Given a Σ-pair (a, b), we introduce the direction $\mathbf{d} := \mathbf{e}_a - \mathbf{e}_b - \mathbf{1}_{A \cap]a,b[} + \mathbf{1}_{B \cap]a,b[}$. We remark that $\langle \mathbf{d} \,|\, \boldsymbol{\chi}(M) \rangle \leq 2$ for every Σ-matching M, where equality holds if and only if M contains both a and b and no position in between, which is precisely the case when M contains (a, b) as a pair. Those Σ-matchings that do have characteristic vectors that are maximal in direction $\mathbf{d}$, so their convex hull is a face of $\mathsf{SP}(\Sigma)$. □

Each such face is isomorphic to the Cartesian product of two shard polytopes.

Observation 3.2.23 (Face for a Σ-Pair as Cartesian Product)**.** Every Σ-matching M containing (a, b) as a pair can be split up into three parts:

- The left part $M_{<a} := M \cap [\ell, a[$ has to be a matching for the shard $\Sigma^{\leq b^*}$ as denoted in Definition 3.2.20, where $b^* := \max\{b' \in B \mid b' < a\}$ as the last element of $M_{<a}$ cannot be in A.
- The central part $M \cap [a, b]$ contains exactly a and b.
- Analogously, the right part $M_{>b} := M \cap]b, r]$ has to be a matching for the shard $\Sigma^{\geq a^*}$, where $a^* := \min\{a' \in A \mid b < a'\}$.

Therefore, the characteristic vector of any Σ-matching M containing (a, b) as a pair is of the form $\boldsymbol{\chi}(M_{<a}) + \mathbf{e}_a - \mathbf{e}_b + \boldsymbol{\chi}(M_{>b})$. Put differently, the face of $\mathsf{SP}(\Sigma)$ induced by the pair (a, b) is isomorphic to the Cartesian product of the shard polytopes $\mathsf{SP}(\Sigma^{\leq b^*})$ and $\mathsf{SP}(\Sigma^{\geq a^*})$.

In the proof of Lemma 3.2.22, we used certain directions to talk about faces of $\mathsf{SP}(\Sigma)$. Before, we saw that shard polytopes sometimes appear as faces of other shard polytopes. To investigate some more connections of this kind, we introduce a number of vectors in $\mathbb{R}^n$ related to a pair of $\vec{\mathcal{A}}_n$ shards.

Definition 3.2.24 (Vectors for Two Shards)**.** Given two $\vec{\mathcal{A}}_n$ shards $\Sigma_1 := \Sigma_n(\ell_1, r_1, A_1, B_1)$ and $\Sigma_2 := \Sigma_n(\ell_2, r_2, A_2, B_2)$, we define

- the **direction** $\mathbf{d}(\Sigma_1, \Sigma_2) := \boldsymbol{\chi}(\Sigma_2) - \boldsymbol{\chi}(\Sigma_1) = \mathbf{1}_{\{\ell_2\} \cup A_2} - \mathbf{1}_{\{\ell_1\} \cup A_1} - \mathbf{1}_{B_2 \cup \{r_2\}} + \mathbf{1}_{B_1 \cup \{r_1\}}$,
- the **translation** $\mathbf{t}(\Sigma_1, \Sigma_2) := \delta_{\ell_2 \in B_1}(\mathbf{e}_{\ell_1} - \mathbf{e}_{\ell_2}) + \delta_{r_2 \in A_1}(\mathbf{e}_{r_2} - \mathbf{e}_{r_1})$,
- the **translated direction** $\mathbf{v}(\Sigma_1, \Sigma_2) := \mathbf{d}(\Sigma_1, \Sigma_2) + 2\mathbf{t}(\Sigma_1, \Sigma_2)$.

While translation and translated direction will appear later, we will first make ourselves a little more familiar with the direction vector $\mathbf{d}(\Sigma_1, \Sigma_2)$ in the case where the shard Σ_2 forces Σ_1. We recall that this implies that $\ell_1 \leq \ell_2 < r_2 \leq r_1$ and $A_2 \subseteq A_1$ and $B_2 \subseteq B_1$. If additionally, $\ell_2 \in \{\ell_1\} \cup A_1$ and $r_2 \in B_1 \cup \{r_1\}$ hold, then $\boldsymbol{\chi}(\Sigma_1)$ and $\boldsymbol{\chi}(\Sigma_2)$ agree on all the entries

labelled by $[\ell_2, r_2]$. In particular, for any Σ_1-matching M, we have $\langle \boldsymbol{\chi}(\Sigma_1) \,|\, \boldsymbol{\chi}(M) \rangle = |M|$ and $\langle \boldsymbol{\chi}(\Sigma_2) \,|\, \boldsymbol{\chi}(M) \rangle = |M \cap [\ell_2, r_2]|$. We deduce that $\langle \mathbf{d}(\Sigma_1, \Sigma_2) \,|\, \boldsymbol{\chi}(M) \rangle \leq 0$ with equality if and only if $M \subseteq [\ell_2, r_2]$ which is equivalent to M being a Σ_2-matching. This motivates the following statement.

Lemma 3.2.25 (Faces from Forcing)**.** *Let $\Sigma_1 := \Sigma_n(\ell_1, r_1, A_1, B_1)$ and $\Sigma_2 := \Sigma_n(\ell_2, r_2, A_2, B_2)$ be two $\vec{\mathcal{A}}_n$ shards. Then the shard polytope $\mathsf{SP}(\Sigma_2)$ is a face of the shard polytope $\mathsf{SP}(\Sigma_1)$ if and only if Σ_2 forces Σ_1 and both $\ell_2 \notin B_1$ and $r_2 \notin A_1$.*

Proof. We first assume that Σ_1 and Σ_2 meet these requirements. Then every Σ_2-matching is a Σ_1-matching according to Lemma 3.1.14, so the vertex set of $\mathsf{SP}(\Sigma_2)$ is a subset of the vertex set of $\mathsf{SP}(\Sigma_1)$. Furthermore, as argued above, we know that for every Σ_1-matching, we have $\langle \mathbf{d}(\Sigma_1, \Sigma_2) \,|\, \boldsymbol{\chi}(M) \rangle \leq 0$ with equality if and only if M is a Σ_2-matching. As $\mathsf{SP}(\Sigma_2)$ is precisely the convex hull of the characteristic vectors of those matchings which maximize the polytope $\mathsf{SP}(\Sigma_1)$ in the direction $\mathbf{d}(\Sigma_1, \Sigma_2)$, so we conclude that $\mathsf{SP}(\Sigma_2)$ is a face of $\mathsf{SP}(\Sigma_1)$.

It is left to show the opposite direction. We assume that $\mathsf{SP}(\Sigma_2)$ is a face of $\mathsf{SP}(\Sigma_1)$. Then every vertex of $\mathsf{SP}(\Sigma_2)$ is a vertex of $\mathsf{SP}(\Sigma_1)$. In particular, every Σ_2-matching is a Σ_1-matching, so Lemma 3.1.14 implies all of the requested properties. □

We will see that there are some more relations between one shard polytope and the faces of another one. For a shard Σ_2 forcing a shard Σ_1, we can make a statement about $\mathsf{SP}(\Sigma_2)$ being related to a face of $\mathsf{SP}(\Sigma_1)$ even if they do not meet the requirements of Lemma 3.2.25, meaning that $\ell_2 \in B_1$ or $r_2 \in A_1$. To prepare this, we examine the effect of the translation vector $\mathbf{t}(\Sigma_1, \Sigma_2)$, defined in Definition 3.2.24, on the characteristic vector of a Σ_2-matching. We first define a subclass of Σ_1-matchings.

Definition 3.2.26 (Inspired Matching)**.** Let $\Sigma_1 = \Sigma_n(\ell_1, r_1, A_1, B_1)$ and $\Sigma_2 = \Sigma_n(\ell_2, r_2, A_2, B_2)$ be two $\vec{\mathcal{A}}_n$ shards such that Σ_2 forces Σ_1. A **Σ_2-inspired Σ_1-matching** M is a Σ_1-matching with the additional properties

- if $\ell_1 < \ell_2$, then $\ell_1 \in M$ if and only if $\ell_2 \in B_1$,
- if $r_2 < r_1$, then $r_1 \in M$ if and only if $r_2 \in A_1$,
- $M \setminus \{\ell_1, r_1\} \subseteq [\ell_2, r_2]$.

We note that every Σ_2-inspired Σ_1-matching is a Σ_1-matching by definition, but the converse holds only if both are the same shard. Furthermore, if $\ell_2 \notin B_1$ and $r_2 \notin A_1$, then Σ_2-matchings and Σ_2-inspired Σ_1-matchings are the same, while if $\ell_2 \in B_1$ or $r_2 \in A_1$, then no Σ_2-matching is a Σ_2-inspired Σ_1-matching. But even in this case, they are in bijection, as we will see in the following statement.

Lemma 3.2.27 (Bijection with Inspired Matchings)**.** *Given $\vec{\mathcal{A}}_n$ shards Σ_1 and Σ_2 such that Σ_2 forces Σ_1, the equation $\boldsymbol{\chi}(M_1) = \boldsymbol{\chi}(M_2) + \mathbf{t}(\Sigma_1, \Sigma_2)$ induces a natural bijection between all Σ_2-matchings and all Σ_2-inspired Σ_1-matchings.*

Proof. From a fixed Σ_2-matching M_2, we derive a Σ_2-inspired Σ_1-matching by modifying M_2.

- If $\ell_2 \in B_1 \cap M_2$, we replace ℓ_2 by ℓ_1 in M_2.
- If $\ell_2 \in B_1 \setminus M_2$, we add the pair (ℓ_1, ℓ_2) to M_2.
- If $r_2 \in A_1 \cap M_2$, we replace r_2 by r_1 in M_2.
- If $r_2 \in A_1 \setminus M_2$, we add the pair (r_2, r_1) to M_2.

We note that this corresponds to adding $(\mathbf{e}_{\ell_1} - \mathbf{e}_{\ell_2})$ to the characteristic vector of M_2 if and only if $\ell_2 \in B_1$ and adding $(\mathbf{e}_{r_2} - \mathbf{e}_{r_1})$ to the characteristic vector of M_2 if and only if $r_2 \in A_1$. Therefore, the characteristic vector of the resulting matching is $\boldsymbol{\chi}(M_2) + \mathbf{t}(\Sigma_1, \Sigma_2)$.

Conversely, we can modify a Σ_2-inspired Σ_1-matching M_1 to obtain a Σ_2-matching:
- If $\{\ell_1 < \ell_2\} \subseteq M_1$, we remove both ℓ_1 and ℓ_2 from M_1.
- If $\ell_1 \in M_1$ and $\ell_2 \notin M_1$ we replace ℓ_1 by ℓ_2.
- If $\{r_2 < r_1\} \subseteq M_1$, we remove both r_2 and r_1 from M_1.
- If $r_1 \in M_1$ and $r_2 \notin M_1$, we replace r_1 by r_2.

This corresponds to subtracting $(\mathbf{e}_{\ell_1} - \mathbf{e}_{\ell_2})$ from the characteristic vector of M_2 if and only if we have $\ell_2 \in B_1$ and subtracting $(\mathbf{e}_{r_2} - \mathbf{e}_{r_1})$ if and only if $r_2 \in A_1$, so that the characteristic vector of the resulting matching is $\boldsymbol{\chi}(M_1) - \mathbf{t}(\Sigma_1, \Sigma_2)$. □

We saw that there is a bijection between Σ_2-matchings and Σ_2-inspired Σ_1-matchings, such that their characteristic vectors differ by $\mathbf{t}(\Sigma_1, \Sigma_2)$. We can use this knowledge to derive some more statements about the faces of $\mathsf{SP}(\Sigma_1)$.

Lemma 3.2.28 (Faces from Forcing and Translation)**.** *Let Σ_1 and Σ_2 be two $\vec{\mathcal{A}}_n$ shards such that Σ_2 forces Σ_1. Then the translated shard polytope $\mathbf{t}(\Sigma_1, \Sigma_2) + \mathsf{SP}(\Sigma_2)$ is a face of $\mathsf{SP}(\Sigma_1)$.*

Proof. To prove this statement, we introduce a direction in $\mathbb{R}^n$ such that certain vertices of $\mathsf{SP}(\Sigma_1)$ are maximal in that direction, meaning that they span a face of $\mathsf{SP}(\Sigma_1)$. We describe the Σ_1-matchings whose characteristic vectors lie in this face and give a bijection between them and the set of all Σ_2-matchings. That bijection defined by manipulating sets then geometrically corresponds to adding $\mathbf{t}(\Sigma_1, \Sigma_2)$ to their characeristic vectors. We recall the vector $\mathbf{v}(\Sigma_1, \Sigma_2)$ from Definition 3.2.24. As Σ_2 forces Σ_1, we have $A_2 \subseteq A_1$ and $B_2 \subseteq B_1$ and therefore

$$\mathbf{v}(\Sigma_1, \Sigma_2) = (2\delta_{\ell_2 \in B_1} - 1)(\mathbf{e}_{\ell_1} - \mathbf{e}_{\ell_2}) + (2\delta_{r_2 \in A_1} - 1)(\mathbf{e}_{r_2} - \mathbf{e}_{r_1}) - \mathbf{1}_{A_1 \setminus A_2} + \mathbf{1}_{B_1 \setminus B_2}.$$

We want to find those vertices of $\mathsf{SP}(\Sigma_1)$ whose scalar product with $\mathbf{v}(\Sigma_1, \Sigma_2)$ is maximal. We fix an arbitrary Σ_1-matching M_1 and take a close look at the scalar product $x = \langle \mathbf{v}(\Sigma_1, \Sigma_2) \,|\, \boldsymbol{\chi}(M_1) \rangle$ by going through all nonzero entries of $\boldsymbol{\chi}(M_1)$.
- If $\ell_1 \in M_1$, it contributes 1 to x if $\ell_2 \in B_1$, and 0 if $\ell_2 = \ell_1$, and -1 if $\ell_2 \in A_1$.
- Any position in $M_1 \cap]\ell_1, \ell_2[$ is in $A_1 \setminus A_2$ or $B_1 \setminus B_2$, so it contributes -1 to x.
- If $\ell_1 < \ell_2 \in M_1$, it contributes 0 to x regardless of whether $\ell_2 \in A_1$ or $\ell_2 \in B_1$.
- Any position in $M_1 \cap]\ell_2, r_2[$ is in $A_1 \cap A_2$ or $B_1 \cap B_2$, so it contributes 0 to x.
- If $r_1 > r_2 \in M_1$, it contributes 0 to x regardless of whether $r_2 \in A_1$ or $r_2 \in B_1$.
- Any position in $M_1 \cap]r_2, r_1[$ is in $A_1 \setminus A_2$ or $B_1 \setminus B_2$, so it contributes -1 to x.
- If $r_1 \in M_1$, it contributes 1 to x if $r_2 \in A_1$, and 0 if $r_2 = r_1$, and -1 if $r_2 \in B_1$.

We deduce that for any Σ_1-matching M_1, we have $\langle \mathbf{v}(\Sigma_1, \Sigma_2) \,|\, \boldsymbol{\chi}(M_1) \rangle \leq \delta_{\ell_2 \in B_1} + \delta_{r_2 \in A_1}$, where equality holds if and only if the Σ_1-matching M_1 is Σ_2-inspired. It follows that the characteristic vectors of all Σ_2-inspired Σ_1-matchings span a face of $\mathsf{SP}(\Sigma_1)$. But as we saw in Lemma 3.2.27, these are exactly the characteristic vectors of all Σ_2-matchings, translated by $\mathbf{t}(\Sigma_1, \Sigma_2)$. Therefore, the shard polytope $\mathsf{SP}(\Sigma_2)$ translated by $\mathbf{t}(\Sigma_1, \Sigma_2)$ is a face of the shard polytope $\mathsf{SP}(\Sigma_1)$. □

We have seen how shard polytopes translate into faces of another shard polytope. Next, we will study how this works vertex by vertex, and have a closer look at when a matching is inspired.

Lemma 3.2.29 (All Non-Trivial Matchings are Inspired)**.** *Let $\Sigma_1 = \Sigma_n(\ell_1, r_1, A_1, B_1)$ be an $\vec{\mathcal{A}}_n$ shard and let M_1 be a Σ_1-matching. If $M_1 \cap]\ell_1, r_1[\neq \emptyset$, there is an $\vec{\mathcal{A}}_n$ shard Σ_2 distinct from Σ_1 such that Σ_2 forces Σ_1 and M_1 is a Σ_2-inspired Σ_1-matching.*

Proof. We introduce the set $J := M_1 \cap]\ell_1, r_1[$ containing the elements of M_1 apart from the endpoints of the shard. For each case, we define a new shard $\Sigma_2 = \Sigma_n(\ell_2, r_2, A_2, B_2)$.
- If $|J| = 1$, we denote its only element by j. Then
  - either $j \in B_1$, so $M_1 = \{\ell_1, j\}$ and we set $\Sigma_2 := \Sigma_n(\ell_1,\ j,\ A_1 \cap]\ell_1, j[,\ B_1 \cap]\ell_1, j[)$,

- or $j \in A_1$, so $M_1 = \{j, r_1\}$ and we set $\Sigma_2 := \Sigma_n(j,\, r_1,\, A_1 \cap]j, r_1[\,,\, B_1 \cap]j, r_1[)$.

In either case, Σ_2 forces Σ_1 and M_1 is Σ_2-inspired.

- If $|J| \geq 2$, we set the endpoints $\ell_2 := \min(J)$ and $r_2 := \max(J)$. Then we define the $\vec{\mathcal{A}}_n$ shard $\Sigma_2 := \Sigma_n(\ell_2,\, r_2,\, A_1 \cap]\ell_2, r_2[\,,\, B_1 \cap]\ell_2, r_2[)$. We observe that Σ_2 is distinct from Σ_1 and forces Σ_1. Moreover, we recall that the smallest element of a Σ_1-matching cannot be an element of B_1. Therefore, if $\ell_2 \in B_1$, it is not the smallest element of M_1, so $\ell_1 \in M_1$. Conversely, if $\ell_1 \in M_1$, then $\ell_2 \in B_1$ is guaranteed because it is the second smallest element of the Σ_1-matching M_1. Analogously, $r_1 \in M_1$ if and only if $r_2 \in A_1$. All the other elements of M_1 are in $[\ell_2, r_2]$ by definition. We conclude that M_1 is Σ_2-inspired. □

This allows us to recursively define the vertex set of a shard polytope depending on the vertex sets of the shard polytopes for all shards that force our fixed shard.

Corollary 3.2.30 (Vertices of the Shard Polytope from Forcing)**.** Let $\Sigma_1 := \Sigma_n(\ell_1, r_1, A_1, B_1)$ be an $\vec{\mathcal{A}}_n$ shard. The vertices of the shard polytope $\mathsf{SP}(\Sigma_1)$ are $\mathbf{0}$, $\mathbf{e}_{\ell_1} - \mathbf{e}_{r_1}$, and the vertices of the translated shard polytopes $\mathbf{t}(\Sigma_1, \Sigma_2) + \mathsf{SP}(\Sigma_2)$ for every shard Σ_2 forcing Σ_1.

Proof. We first recall from Lemma 3.2.9 that the vertices of $\mathsf{SP}(\Sigma_1)$ are exactly the characteristic vectors of Σ_1-matchings. As $\emptyset$ and $\{\ell_1, r_1\}$ are trivial Σ_1-matchings, their characteristic vectors $\mathbf{0}$ and $\mathbf{e}_{\ell_1} - \mathbf{e}_{r_1}$ are always vertices of $\mathsf{SP}(\Sigma_1)$.

Every nontrivial Σ_1-matching M_1 has $M_1 \cap]\ell_1, r_1[\neq \emptyset$. Then Lemma 3.2.29 guarantees that there is a shard Σ_2 forcing Σ_1 such that M_1 is Σ_2-inspired. According to Lemma 3.2.27, this implies that there is a Σ_2-matching M_2 such that $\boldsymbol{\chi}(M_2) + \mathbf{t}(\Sigma_1, \Sigma_2) = \boldsymbol{\chi}(M_1)$. Therefore, the characteristic vector of M_1 is a vertex of the translated shard polytope $\mathbf{t}(\Sigma_1, \Sigma_2) + \mathsf{SP}(\Sigma_2)$.

On the other hand, Lemma 3.2.28 certifies that if Σ_2 forces Σ_1, then every vertex of the translated shard polytope $\mathbf{t}(\Sigma_1, \Sigma_2) + \mathsf{SP}(\Sigma_2)$ is a vertex of $\mathsf{SP}(\Sigma_1)$ as well. □

3.2.5 Symmetries

Shards admit multiple types of symmetry, which we can rediscover in their shard polytopes. We will first introduce some terminology to describe these symmetries. We will use ρ (lowercase rho) to denote maps on integers, sets of integers and vectors. We will use P (uppercase Rho) to introduce an associated operation on shards.

Definition 3.2.31 (Shard Polytope Symmetry Maps)**.** Given $n \in \mathbb{N}$, we define involutive maps.

- For an integer $i \in [n]$, we define $\rho_n^{\leftrightarrow}(i) := n + 1 - i$.
- For a set of positions $T \subseteq [n]$, we define $\rho_n^{\leftrightarrow}(T) := \{n + 1 - j \mid j \in T\}$.
- We define the linear map $\rho_n^{\leftrightarrow} : \mathbb{R}^n \to \mathbb{R}^n$ by $\rho_n^{\leftrightarrow}(\mathbf{e}_i) := \mathbf{e}_{n+1-i}$.
- We define the linear map $\rho^{\updownarrow} : \mathbb{R}^n \to \mathbb{R}^n$ by $\rho^{\updownarrow}(\mathbf{e}_i) := -\mathbf{e}_i$.

We introduce two more maps $\mathrm{P}_n^{\leftrightarrow}$ and $\mathrm{P}^{\updownarrow}$, each acting as an involution on the set $\boldsymbol{\Sigma}_n$ of all $\vec{\mathcal{A}}_n$ shards, defined by their effect on an $\vec{\mathcal{A}}_n$ shard $\Sigma = \Sigma_n(\ell, r, A, B)$.

- A vertically mirrored shard is given by $\mathrm{P}_n^{\leftrightarrow}(\Sigma) := \Sigma_n(\rho_n^{\leftrightarrow}(r),\, \rho_n^{\leftrightarrow}(\ell),\, \rho_n^{\leftrightarrow}(A),\, \rho_n^{\leftrightarrow}(B))$.
- A horizontally mirrored shard is given by $\mathrm{P}^{\updownarrow}(\Sigma) := \Sigma_n(\ell, r, B, A)$.

We note that the definitions of $\rho_n^{\leftrightarrow}$ on integers, sets of integers and vectors are compatible. For a set $T \subseteq [n]$, we have $\rho_n^{\leftrightarrow}(T) = \{\rho_n^{\leftrightarrow}(j) \mid j \in T\}$, for an integer $i \in [n]$, we have $\rho_n^{\leftrightarrow}(\mathbf{e}_i) = \mathbf{e}_{\rho_n^{\leftrightarrow}(i)}$. Geometrically, the map $\rho_n^{\leftrightarrow}$ is a rotation mapping any coordinate $i \in [n]$ to coordinate $n + 1 - i$, while the map $\rho^{\updownarrow}$ corresponds to the reflection through the origin $\mathbf{0}$.

With the help of these maps, we can describe the interplay between shard polytopes of mirrored shards and rotated and reflected shard polytopes.

Lemma 3.2.32 (Shard Polytope Symmetries)**.** *Let* $\Sigma := \Sigma_n(\ell, r, A, B)$ *be an* $\vec{\mathcal{A}}_n$ *shard. Then*

$$\begin{aligned}
\mathsf{SP}(\mathrm{P}^{\updownarrow}(\Sigma)) &= \rho^{\updownarrow}(\mathsf{SP}(\Sigma) - \mathbf{e}_\ell + \mathbf{e}_r) &&= \rho^{\updownarrow}(\mathsf{SP}(\Sigma)) + \mathbf{e}_\ell - \mathbf{e}_r,\\
\mathsf{SP}(\mathrm{P}_n^{\leftrightarrow}(\Sigma)) &= \rho_n^{\leftrightarrow}(\mathsf{SP}(\Sigma) - \mathbf{e}_\ell + \mathbf{e}_r) &&= \rho_n^{\leftrightarrow}(\mathsf{SP}(\Sigma)) + \mathbf{e}_{n+1-r} - \mathbf{e}_{n+1-\ell},\\
\mathsf{SP}(\mathrm{P}_n^{\leftrightarrow} \circ \mathrm{P}^{\updownarrow}(\Sigma)) &= \rho_n^{\leftrightarrow} \circ \rho^{\updownarrow}(\mathsf{SP}(\Sigma)).
\end{aligned}$$

Proof. The shard polytopes $\mathsf{SP}(\mathrm{P}^{\updownarrow}(\Sigma))$ and $\mathsf{SP}(\mathrm{P}_n^{\leftrightarrow}(\Sigma))$ can be described as the convex hull of the characteristic vectors of all $\mathrm{P}^{\updownarrow}(\Sigma)$-matchings (resp. all $\mathrm{P}_n^{\leftrightarrow}(\Sigma)$-matchings). We therefore have a closer look at $\mathrm{P}^{\updownarrow}(\Sigma)$-matchings and $\mathrm{P}_n^{\leftrightarrow}(\Sigma)$-matchings.

- Given a Σ-matching M, we can turn it into a $\mathrm{P}^{\updownarrow}(\Sigma)$-matching M' in the following way:
  - If $\ell \in M$, we remove it.
  - If $\ell \notin M$, we add it.
  - If $r \in M$, we remove it.
  - If $r \notin M$, we add it.

  This way, the empty matching turns into $\{\ell, r\}$ and vice versa. If M contains at least one element from $]\ell, r[$, these rules ensure that the elements of the resulting set alternate between elements of $\{\ell\} \cup B$ and $A \cup \{r\}$ as desired. We deduce that $M \mapsto M\Delta\{\ell, r\}$ injectively maps a Σ-matching to an $\mathrm{P}^{\updownarrow}(\Sigma)$-matching. As this map is involutive, it can also be used to map an $\mathrm{P}^{\updownarrow}(\Sigma)$-matching to a Σ-matching, inducing a bijection between these sets.
  For the $\mathrm{P}^{\updownarrow}(\Sigma)$-matching $M\Delta\{\ell, r\}$, its characteristic vector $\boldsymbol{\chi}(M\Delta\{\ell, r\})$ is therefore equal to $\boldsymbol{\chi}(M\Delta\{\ell, r\}) = -\boldsymbol{\chi}(M) + \mathbf{e}_\ell - \mathbf{e}_r$. This way, the signs on all positions in $]\ell, r[$ are flipped (reflecting the exchange of A and B by $\mathrm{P}^{\updownarrow}$), while the entries at the endpoints are adjusted accordingly. Now we can describe the vertices of the shard polytope $\mathsf{SP}(\mathrm{P}^{\updownarrow}(\Sigma))$ as the vertices of $-\mathsf{SP}(\Sigma) = \mathrm{P}^{\updownarrow}(\mathsf{SP}(\Sigma))$, translated by $\mathbf{e}_\ell - \mathbf{e}_r$.
- Analogously, if M is a Σ-matching, then $\rho_n^{\leftrightarrow}(M\Delta\{\ell, r\})$ is a $\mathrm{P}_n^{\leftrightarrow}(\Sigma)$-matching and vice versa. Therefore, the vertices of the shard polytope $\mathsf{SP}(\mathrm{P}_n^{\leftrightarrow}(\Sigma))$ are exactly the vectors of the form $\boldsymbol{\chi}(\rho_n^{\leftrightarrow}(M\Delta\{\ell, r\})) = \rho_n^{\leftrightarrow}(\boldsymbol{\chi}(M) - \mathbf{e}_\ell + \mathbf{e}_r)$, and the shard polytope $\mathsf{SP}(\mathrm{P}_n^{\leftrightarrow}(\Sigma))$ is equal to the polytope $\rho_n^{\leftrightarrow}(\mathsf{SP}(\Sigma))$ translated by $\mathbf{e}_{\rho_n^{\leftrightarrow}(r)} + \mathbf{e}_{\rho_n^{\leftrightarrow}(\ell)}$.
- For the last part of the statement, we compute the shard polytope $\mathsf{SP}(\mathrm{P}_n^{\leftrightarrow} \circ \mathrm{P}^{\updownarrow}(\Sigma))$ using the above equalities. As desired, we obtain

$$\begin{aligned}
\mathsf{SP}(\mathrm{P}_n^{\leftrightarrow} \circ \mathrm{P}^{\updownarrow}(\Sigma)) &= \rho_n^{\leftrightarrow}(\mathsf{SP}(\mathrm{P}^{\updownarrow}(\Sigma)) - \mathbf{e}_\ell + \mathbf{e}_r)\\
&= \rho_n^{\leftrightarrow}(\rho^{\updownarrow}(\mathsf{SP}(\Sigma)) + \mathbf{e}_\ell - \mathbf{e}_r - \mathbf{e}_\ell + \mathbf{e}_r)\\
&= \rho_n^{\leftrightarrow} \circ \rho^{\updownarrow}(\mathsf{SP}(\Sigma)).
\end{aligned}$$

□

3.3 Shard Fans

The reason we introduced shard polytopes in the first place is that their normal fans exhibit a behaviour that is compatible with the forcing poset on shards. We first define these fans properly and have a closer look at the normal fan of $\mathsf{SP}(\Sigma)$.

Definition 3.3.1 (Shard Fan)**.** Given an $\vec{\mathcal{A}}_n$ shard Σ, the **shard fan** $\mathcal{SF}(\Sigma)$ is the normal fan of the shard polytope $\mathsf{SP}(\Sigma)$, formed by the normal cones of all facets of $\mathsf{SP}(\Sigma)$.

Observation 3.3.2 (Basic Correspondences of Shard Polytope and Shard Fan)**.** We observe that

- the chambers of $\mathcal{SF}(\Sigma)$ correspond to the vertices of $\mathsf{SP}(\Sigma)$,
- the walls of $\mathcal{SF}(\Sigma)$ correspond to the edges of $\mathsf{SP}(\Sigma)$,
- the rays of $\mathcal{SF}(\Sigma)$ correspond to the facets of $\mathsf{SP}(\Sigma)$.

We will be especially interested in the union of all walls of $\mathcal{SF}(\Sigma)$. It can be described equivalently as the union of the normal cones of all edges of $\mathsf{SP}(\Sigma)$ or as the union of the boundaries of

the normal cones of all vertices of $\mathsf{SP}(\Sigma)$. In particular, a vector lies in the normal cone of more than one vertex of $\mathsf{SP}(\Sigma)$ if and only if it lies in the union of all walls of $\mathcal{SF}(\Sigma)$.

As the vertices of $\mathsf{SP}(\Sigma)$ are in bijection with the Σ-matchings, so are the chambers of $\mathcal{SF}(\Sigma)$. A vector $\mathbf{t} \in \mathbb{R}^n$ lies in the chamber associated to the Σ-matching M if and only if the inequality $\langle \mathbf{t} \,|\, \boldsymbol{\chi}(M) \rangle \geq \langle \mathbf{t} \,|\, \boldsymbol{\chi}(M') \rangle$ holds for every Σ-matching M' distinct from M. It lies in the interior of the chamber if and only if that inequality is always strict. Conversely, if there is more than one Σ-matching whose characteristic vector maximizes this scalar product with $\mathbf{t}$, then $\mathbf{t}$ cannot be contained in the interior of any of the chambers of $\mathcal{SF}(\Sigma)$ and is therefore contained in the union of the walls of $\mathcal{SF}(\Sigma)$. For a fixed $\mathbf{t}$, we will use the notation $\tau(M) := \langle \mathbf{t} \,|\, \boldsymbol{\chi}(M) \rangle$ to denote the scalar product of $\mathbf{t}$ with the characteristic vector $\boldsymbol{\chi}(M)$ throughout this section.

3.3.1 Walls

We can gather some information on this union of walls by giving both a subset which it contains and a superset which it is contained in.

Proposition 3.3.3 (Shard Fan Walls)**.** *For any $\vec{\mathcal{A}}_n$ shard Σ, the union of the walls of $\mathcal{SF}(\Sigma)$ is a superset of the shard Σ and a subset of the union of all shards Σ' that force Σ.*

Proof. We fix an $\vec{\mathcal{A}}_n$ shard $\Sigma = \Sigma_n(\ell, r, A, B)$ and a real vector $\mathbf{t} \in \mathbb{R}^n$. To prove one direction of the statement, we fix a vector $\mathbf{t} \in \Sigma$ on the shard itself. By definition of an $\vec{\mathcal{A}}_n$ shard, the vector $\mathbf{t}$ then satisfies the inequalities $t_a \leq t_\ell = t_r \leq t_b$ for all $a \in A$ and $b \in B$. As any matching M can be rewritten as $M = \{a_1 < b_1 < \cdots < a_k < b_k\}$, we have $\tau(M) = \sum_{i=1}^{k} t_{a_i} - t_{b_i}$. For any pair $\{a_i, b_i\}$ of M, we have $a_i \in \{\ell\} \cup A$ and $b_i \in B \cup \{r\}$, so $t_{a_i} - t_{b_i} \leq 0$. This implies that $\tau(M) \leq 0$ with equality if and only if $t_{a_i} = t_{b_i}$ for every $i \in [k]$. In particular, $\tau(M) = 0$ holds for both $M = \emptyset$ and $M = \{\ell < r\}$. As $\mathbf{t}$ is maximized by these two vertices (and possibly others) of $\mathsf{SP}(\Sigma)$, it lies in the normal cone of both vertices and thus in their intersection. We conclude that it is contained in the union of the walls of $\mathcal{SF}(\Sigma)$.

To prove the second part of the statement, we fix a vector $\mathbf{t} \in \mathbb{R}^n$ that lies in the union of the walls of $\mathcal{SF}(\Sigma)$. As walls of $\mathcal{SF}(\Sigma)$ correspond to edges of $\mathsf{SP}(\Sigma)$, there is at least one edge e of $\mathsf{SP}(\Sigma)$ such that $\mathbf{t}$ lies in the normal cone of e. Let M_1 and M_2 be the two Σ-matchings whose characteristic vectors are connected by e. Then the normal cone of e is the intersection of normal cones of the $\mathsf{SP}(\Sigma)$-vertices $\boldsymbol{\chi}(M_1)$ and $\boldsymbol{\chi}(M_2)$. As e is an edge of $\mathsf{SP}(\Sigma)$, its center cannot be rewritten as a convex combination of the remaining vertices of $\mathsf{SP}(\Sigma)$. In particular, no Σ-matchings M_3 and M_4 distinct from M_1 and M_2 can have characteristic vectors that satisfy $\boldsymbol{\chi}(M_1) + \boldsymbol{\chi}(M_2) = \boldsymbol{\chi}(M_3) + \boldsymbol{\chi}(M_4)$. This implies that M_1 and M_2 are related in one of four very special ways, as described in Lemma 3.2.13.

As done there, we first set H (resp. T) to be the unique maximal common initial (resp. final) Σ-matching of M_1 and M_2. We recall that as $\mathbf{t}$ belongs to the normal cones of both $\boldsymbol{\chi}(M_1)$ and $\boldsymbol{\chi}(M_2)$, we have $\tau(M_1) = \tau(M_2)$. Futhermore, $\tau(M') \leq \tau(M_1)$ (resp. $\tau(M_2)$) holds for all Σ-matchings M'. We will go through the four special cases of Lemma 3.2.13 and introduce for each of them a new shard $\Sigma' := \Sigma_n(\ell', r', A', B')$ with $A' := A \cap]\ell', r'[$ and $B' := B \cap]\ell', r'[$, where the variables ℓ' and r' will by defined separately in each case. We will show that Σ' forces Σ. Moreover, we introduce two families of Σ-matchings M_a and M_b for each case. We emphasize that these are Σ-matchings, not Σ'-matchings. They will help us prove that the vector $\mathbf{t}$ is an element of the shard Σ'.

1. If $M_1 = H \cup \{a_0 < b_0\} \cup T$ and $M_2 = H \cup T$, we set
   - $\ell' := a_0$ and $r' := b_0$,
   - $M_a := H \cup \{a < b_0\} \cup T$ for $a \in A'$,
   - $M_b := H \cup \{a_0 < b\} \cup T$ for $b \in B'$.
2. If $M_1 = H \cup \{a_0 < b_2\} \cup T$ and $M_2 = H \cup \{a_0 < b_1\} \cup T$ with $b_1 < b_2$, we set
   - $\ell' := b_1$ and $r' := b_2$,
   - $M_a := H \cup \{a_0 < b_1 < a < b_2\} \cup T$ for $a \in A'$,
   - $M_b := H \cup \{a_0 < b\} \cup T$ for $b \in B'$.
3. If $M_1 = H \cup \{a_1 < b_0\} \cup T$ and $M_2 = H \cup \{a_2 < b_0\} \cup T$ with $a_1 < a_2$, we set
   - $\ell' := a_1$ and $r' := a_2$,
   - $M_a := H \cup \{a < b_0\} \cup T$ for $a \in A'$,
   - $M_b := H \cup \{a_1 < b < a_2 < b_0\} \cup T$ for $b \in B'$.
4. If $M_1 = H \cup \{a_1 < b_2\} \cup T$, and $M_2 = H \cup \{a_1 < b_1 < a_2 < b_2\} \cup T$ we set
   - $\ell' := b_1$ and $r' := a_2$,
   - $M_a := H \cup \{a_1 < b_1 < a < b_2\} \cup T$ for $a \in A'$,
   - $M_b := H \cup \{a_1 < b < a_2 < b_2\} \cup T$ for $b \in B'$.

We first observe that in each of the four cases, the new shard $\Sigma' := \Sigma_n(\ell', r', A', B')$ satisfies the inequalities $\ell \leq \ell' < r' \leq r$ and has $A' \subseteq A$ and $B' \subseteq B$ as well as $A' \dot\cup B' =]\ell', r'[$. We conclude that Σ' is an $\vec{\mathcal{A}}_n$ shard that forces Σ.

It is left to show that the vector $\mathbf{t}$ is contained in the shard Σ'. For this, we need to ensure that in all four cases, $t_a \leq t_{\ell'} = t_{r'} \leq t_b$ holds for any $a \in A'$ and $b \in B'$.

- In each case, we defined ℓ' and r' in such a way that $\tau(M_1) - \tau(M_2) = t_{\ell'} - t_{r'}$. We already noted that $\tau(M_1) = \tau(M_2)$, and this implies that $t_{\ell'} = t_{r'}$.
- In each case, we defined Σ-matchings M_a in such a way that $\tau(M_1) - \tau(M_a) = t_{\ell'} - t_a$. Then $\tau(M_a) \leq \tau(M_1)$ implies that $t_a \leq t_{\ell'}$. for each $a \in A'$.
- In each case, we defined Σ-matchings M_b in such a way that $\tau(M_1) - \tau(M_b) = t_b - t_{r'}$. Then $\tau(M_b) \leq \tau(M_1)$ implies that $t_{r'} \leq t_b$ for each $b \in B'$.

We conclude that $\mathbf{t}$ is contained in the shard Σ' which forces Σ, so $\mathbf{t}$ is contained in the union of all shards that force Σ. □

3.3.2 Cones for Matchings

In this section, we will describe some of the cones of $\mathcal{SF}(\Sigma)$. We do this by applying our knowledge about the neighbors of a given $\mathsf{SP}(\Sigma)$ vertex $\boldsymbol{\chi}(M)$ to describe the inequalities bounding the corresponding chamber of $\mathcal{SF}(\Sigma)$. We recall our notation $\tau(M) = \langle \mathbf{t} \,|\, \boldsymbol{\chi}(M) \rangle$ so that the vector $\mathbf{t} \in \mathbb{R}^n$ lies in the chamber corresponding to the Σ-matching M if and only if $\tau(M) \geq \tau(M')$ holds for every Σ-matching M'. Equivalently, $\mathbf{t}$ lies in the chamber of M if this inequality holds for every matching M' such that $\boldsymbol{\chi}(M)$ and $\boldsymbol{\chi}(M')$ are adjacent in $\mathsf{SP}(\Sigma)$. We can now define one inequality for each neighbor of M, in each case drawing conclusions from the condition $\tau(M) \geq \tau(M')$. We know all possible neighbors of M from Lemma 3.2.15 via Observation 3.2.19 and use the same numbering of cases.

1. If $M' = M \cup \{a < b\}$ for some Σ-pair (a, b), then $\tau(M) \geq \tau(M')$ is equivalent to $0 \geq \langle \mathbf{t} \,|\, \boldsymbol{\chi}(M') - \boldsymbol{\chi}(M) \rangle = t_a - t_b$. We obtain the inequality $t_a \leq t_b$ for every M-compatible Σ-pair (a, b). Conversely, if $M' = M \setminus \{a < b\}$ for some Σ-pair (a, b), then we obtain $0 \leq \langle \mathbf{t} \,|\, \boldsymbol{\chi}(M) - \boldsymbol{\chi}(M') \rangle = t_a - t_b$ and deduce the inequality $t_a \geq t_b$ for every pair (a, b) of M.
2. If $M \setminus \{b\} = M' \setminus \{b'\}$, where b belongs to the Σ-pair (a, b) of M, then we obtain $t_b \leq t_{b'}$ for every Σ-pair (a, b') compatible with $M \setminus \{a, b\}$.
3. If $M \setminus \{a\} = M' \setminus \{a'\}$, where a belongs to the Σ-pair (a, b) of M, then we obtain $t_a \geq t_{a'}$ for every Σ-pair (a', b) compatible with $M \setminus \{a, b\}$.

4. If $M' = M \cup \{b' < a'\}$, then there is a Σ-pair (a, b) of M such that $a < b' < a' < b$. We obtain $t_{b'} \geq t_{a'}$. Conversely, if $M' = M \setminus \{b' < a'\}$, then there are two consecutive Σ-pairs (a, b') and (a', b) of M. We obtain $t_{b'} \leq t_{a'}$.

We can use this information to describe some cones of the shard fan $\mathcal{SF}(\Sigma)$. In particular, we will describe the normal cone associated to the vertex of $\mathsf{SP}(\Sigma)$ corresponding to a Σ-matching and the normal cone associated to the face of $\mathsf{SP}(\Sigma)$ corresponding to a Σ-pair.

Lemma 3.3.4 (Shard Fan Cone for Matching)**.** *Let $\Sigma = \Sigma_n(\ell, r, A, B)$ be an $\vec{\mathcal{A}}_n$ shard and M be a Σ-matching. The cone of $\mathcal{SF}(\Sigma)$ corresponding to M contains exactly the vectors $\mathbf{t} \in \mathbb{R}^n$ with*

1. *$t_a \leq t_b$ for every Σ-pair (a, b) compatible with M,*
2. *$t_a \geq t_b$ for every Σ-pair (a, b) of M,*
3. *$t_b \leq t_{b'}$ for every Σ-pair (a, b) of M and every Σ-pair (a, b') compatible with $M \setminus \{a, b\}$,*
4. *$t_a \geq t_{a'}$ for every Σ-pair (a, b) of M and every Σ-pair (a', b) compatible with $M \setminus \{a, b\}$,*
5. *$t_{b'} \geq t_{a'}$ for every Σ-pair (a, b) of M such that (a, b') and (a', b) are compatible Σ-pairs,*
6. *$t_b \leq t_{a'}$ for every two Σ-pairs (a, b) and (a', b') consecutive in M.*

Proof. We first show that all of these conditions are necessary. For each of the conditions, we assume that $\mathbf{t}$ violates it and introduce a modified Σ-matching M' with $\tau(M') > \tau(M)$, which certifies that $\boldsymbol{\chi}(M)$ is not maximal in the direction $\mathbf{t}$ among the vertices of $\mathsf{SP}(\Sigma)$.

(i) If $t_a > t_b$ for a Σ-pair (a, b) compatible with M,
then we set $M' := M \cup \{a, b\}$.

(ii) If $t_a < t_b$ for a Σ-pair (a, b) of M,
then we set $M' := M \setminus \{a, b\}$.

(iii) If $t_b > t_{b'}$ for a Σ-pair (a, b) of M and a Σ-pair (a, b') compatible with $M \setminus \{a, b\}$,
then we set $M' := M \cup \{b'\} \setminus \{b\}$.

(iv) If $t_a < t_{a'}$ for a Σ-pair (a, b) of M and a Σ-pair (a', b) compatible with $M \setminus \{a, b\}$,
then we set $M' := M \cup \{a'\} \setminus \{a\}$.

(v) If $t_{b'} < t_{a'}$ for a Σ-pair (a, b) of M such that (a, b') and (a', b) are compatible Σ-pairs,
then we set $M' := M \cup \{b', a'\}$.

(vi) If $t_b > t_{a'}$ for two Σ-pairs (a, b) and (a', b') consecutive in M,
then we set $M' := M \setminus \{b, a'\}$.

In each of these cases, M' is a Σ-matching such that $\tau(M') > \tau(M)$, so $\mathbf{t}$ does not lie in the cone of $\mathcal{SF}(\Sigma)$ corresponding to M.

For the second part of the statement, we assume for a contradiction that these conditions are not sufficient. Then we can fix a vector $\mathbf{t} \in \mathbb{R}^n$ and a Σ-matching M such that $\mathbf{t}$ satisfies all conditions, but is not included in the chamber of $\mathcal{SF}(\Sigma)$ corresponding to M. This implies that there is an adjacent chamber of $\mathcal{SF}(\Sigma)$ corresponding to a Σ-matching M' such that $\tau(M') > \tau(M)$. As the chamber of M' is adjacent in $\mathcal{SF}(\Sigma)$, the vertex is adjacent to that of M in $\mathsf{SP}(\Sigma)$, so Lemma 3.2.15, implies that $|M \Delta M'| = 2$. We can now go through all forms of adjacent Σ-matchings as described by Observation 3.2.19.

1. If $M' = M \cup \{a, b\}$ for an M-compatible Σ-pair (a, b), we have $0 < \tau(M') - \tau(M) = t_a - t_b$ and deduce that $t_a > t_b$, violating 1. Conversely, if $M' = M \setminus \{a, b\}$ for a Σ-pair (a, b) of M, we have $0 < \tau(M') - \tau(M) = t_b - t_a$, so that $t_a < t_b$ violates 2.
2. If $M' = (M \cup \{b'\}) \setminus \{b\}$ for a Σ-pair (a, b) of M such that the Σ-pair (a, b') is compatible with $M \setminus \{a, b\}$, we have $0 < \tau(M') - \tau(M) = t_b - t_{b'}$, now $t_b > t_{b'}$ violates 3.
3. If $M' = (M \cup \{a'\}) \setminus \{a\}$ for a Σ-pair (a, b) of M such that the Σ-pair (a', b) is compatible with $M \setminus \{a, b\}$, we have $0 < \tau(M') - \tau(M) = t_{a'} - t_a$, now $t_a < t_{a'}$ violates 4.
4. If $M' = M \cup \{b', a'\}$ such that $a < b' < a' < b$, where (a, b') and (a', b) are Σ-pairs of M', we have $0 < \tau(M') - \tau(M) = t_{a'} - t_{b'}$, and $t_{b'} < t_{a'}$ violates 5. Conversely, if $M' = M \setminus \{b, a'\}$ for two Σ-pairs (a, b) and (a', b') consecutive in M, we have $0 < \tau(M') - \tau(M) = t_b - t_{a'}$, and $t_b > t_{a'}$ violates 6.

In each of these cases, we showed that $\mathbf{t}$ violates one of the conditions, contradicting our assumption. Therefore, $\mathbf{t}$ does lie in the chamber of M in $\mathcal{SF}(\Sigma)$ if it satisfies all of the conditions. □

This result can be used to describe some other cones in the shard fan as well.

3.3.3 Cones for Pairs

We recall that any polyhedral cone can equivalently be described as the positive linear span of its rays or as the intersection of the halfspaces defined by its inequalities. For the normal cone of the face of $\mathsf{SP}(\Sigma)$ corresponding to a Σ-pair, the rays correspond to the facets of $\mathsf{SP}(\Sigma)$ that contain this face. On the other hand, the normal cone of a face of $\mathsf{SP}(\Sigma)$ can be described as the intersection of those chambers of $\mathcal{SF}(\Sigma)$ associated to the vertices of the polytope that are contained in the face. Therefore, to describe the normal cone corresponding to a Σ-pair, it is sufficient to collect all inequalities that are used to describe one of these chambers.

We remark that in $\mathsf{SP}(\Sigma)$, a vertex associated to a Σ-matching M is contained in each of the faces of $\mathsf{SP}(\Sigma)$ associated to a Σ-pair contained in M. Conversely, the normal cone of the face of a Σ-pair is contained in all normal cones of Σ-matchings containing that pair. Therefore, all inequalities bounding the normal cone of a Σ-matching must hold for the normal cone of any of its Σ-pairs as well. To describe the cone of $\mathcal{SF}(\Sigma)$ corresponding to the face of $\mathsf{SP}(\Sigma)$ induced by all Σ-matchings containing a fixed Σ-pair (a, b), we can collect all inequalities for all normal cones associated to Σ-matchings containing that pair.

The wall-defining inequalities of the chambers of the shard fan are exactly those corresponding to the edges of the shard polytope. We know that those are of a certain form connecting two matchings that differ by exactly two positions. In particular, the normal cone of any face of the shard fan can be described using only inequalities between two entries of the vector.

Corollary 3.3.5 (Shard Fan Cone for Pair)**.** Let $\Sigma := \Sigma_n(\ell, r, A, B)$ be an $\vec{\mathcal{A}}_n$ shard and (a, b) be a Σ-pair. If $A \cap]b, r]$ is non-empty, we set a^* to be its minimal element. If $B \cap [\ell, a[$ is non-empty, we set b^* to be its maximal element. A vector $\mathbf{t} \in \mathbb{R}^n$ lies in the cone of $\mathcal{SF}(\Sigma)$ corresponding to the Σ-pair (a, b) if and only if it satisfies

- $t_a \geq t_b$,
- $t_i \leq t_a$ for every $i \in [\ell, a[$,
- $t_b \leq t_j$ for every $j \in]b, r]$,
- $t_a \geq t_{a'}$ for every $a' \in A \cap]a, b[$,
- $t_{b'} \geq t_b$ for every $b' \in B \cap]a, b[$,
- $t_{b'} \geq t_{a'}$ for all compatible Σ-pairs (a, b') and (a', b).
- If a^* exists, then $t_j = t_r$ for every $j \in [a^*, r]$.
- If b^* exists, then $t_\ell = t_i$ for every $i \in [\ell, b^*]$.

Proof. We collect the inequalities of Lemma 3.3.4 where we go through all Σ-matchings containing (a, b) as a pair. □

So far, we described cones of the fan $\mathcal{SF}(\Sigma)$. There is another polyhedral cone in the same space that we want to describe, which is not a cone of $\mathcal{SF}(\Sigma)$, but the union of some of its chambers. In Corollary 3.3.5, we described the vectors in the normal cone of a given Σ-pair, which is the intersection of all cones of $\mathcal{SF}(\Sigma)$ associated to Σ-matchings with that pair. Now, we will describe the vectors in the union of all these cones, which will give us a description of all vectors that lie in the normal cone of some Σ-matching containing that pair.

Corollary 3.3.6 (Cone for all Matchings Containing a Pair)**.** Let $\Sigma := \Sigma_n(\ell, r, A, B)$ be an $\vec{\mathcal{A}}_n$ shard and (a, b) be a Σ-pair. A vector $\mathbf{t} \in \mathbb{R}^n$ lies in a chamber of $\mathcal{SF}(\Sigma)$ corresponding to some Σ-matching containing the pair (a, b) if and only if all of the following conditions hold:

1. $t_a \geq t_b$,
2. $t_{b'} \geq t_b$ for every $b' \in B \cap]a, b[$,
3. $t_a \geq t_{a'}$ for every $a' \in A \cap]a, b[$ with $a < b' < a' < b$,
4. whenever $t_{a'} > t_a$ with $a' \in \{\ell\} \cup A$ and $a' < a$, there is a $b' \in B \cap]a', a[$ with $t_{b'} < t_a$,
5. whenever $t_b > t_{b'}$ with $b' \in B \cup \{r\}$ and $b < b'$, there is an $a' \in A \cap]b, b'[$ with $t_b < t_{a'}$,
6. $t_{b'} \geq t_{a'}$ for all $b' \in B$ and $a' \in A$.

Proof. We collect all inequalities of Lemma 3.3.4 that separate a Σ-matching M containing (a, b) as a pair from a Σ-matching M' not containing (a, b) as a pair. We go through them in the numbering used in Lemma 3.3.4.

(i) We ignore inequalities $t_{a'} \leq t_{b'}$ for compatible Σ-pairs (a', b') as we only care about (a, b).
(ii) We keep the inequality $t_a \geq t_b$ for our pair (a, b).
(iii) We keep the inequalities $t_b \leq t_{b'}$ for our pair (a, b) and every distinct Σ-pair (a, b').
(iv) We keep the inequalities $t_a \geq t_{a'}$ for our pair (a, b) and every distinct Σ-pair (a', b).

For positions a' or b' outside of $[a, b]$ in these two cases, we rewrite the conditions to reflect that the inequality only matters if M' contains (a', b) or (b, a') not only as a subset, but as a pair.

(v) We keep the inequalities $t_{b'} \geq t_{a'}$ for all compatible Σ-pairs (a, b') and (a', b).
(vi) We keep the inequalities $t_{b_1} \leq t_{a_2}$ for any two Σ-pairs (a_1, b_1) and (a_2, b_2) consecutive in M such that (a, b) is one of them.

We find that this last type of conditions is redundant: Assume there is a $b_1 \in B \cap]\ell, a[$ such that $t_{b_1} > t_a$. If $\mathbf{t}$ is contained in the chamber of M, the pair (a_1, b_1) has to give a non-negative contribution to $\tau(M)$, so $t_{a_1} \geq t_{b_1} > t_a$. Therefore, by condition 4, there has to be some position $b' \in B \cap]a_1, a[$ with $t_{b'} < t_a$ and thus there is a Σ-matching $M' := (M \cup \{b'\}) \setminus \{b_1\}$ adjacent to M with $\tau(M') > \tau(M)$, which contradicts the assumption that $\mathbf{t}$ lies in the chamber of M. An analogous argument holds for the case where (a, b) is the first of the two consecutive pairs in M. Therefore, the inequality $t_{b_1} \leq t_{a_2}$ is already guaranteed to hold by the conditions written up so far. □

3.3.4 Cones for Edges

We conclude our analysis of some cones of the shard fan $\mathcal{SF}(\Sigma)$ with the normal cone of an edge in the shard polytope $\mathsf{SP}(\Sigma)$.

Corollary 3.3.7 (Shard Fan Cone for an Edge in a Certain Direction)**.** Let $\Sigma := \Sigma_n(\ell, r, A, B)$ be an $\vec{\mathcal{A}}_n$ shard and $\ell \leq i < j \leq r$ be two positions. Then a vector $\mathbf{t} \in \mathbb{R}^n$ is in the normal cone of an edge of $\mathsf{SP}(\Sigma)$ in the direction $\mathbf{e}_i - \mathbf{e}_j$ if and only if $t_i = t_j$ and

- If $i \in \{\ell\} \cup A$ and $j \in B \cup \{r\}$, there are two Σ-matchings M and $M' = M \cup \{i, j\}$ such that $\mathbf{t}$ lies in the normal cone of both. Equivalently, $\mathbf{t}$ lies in the normal cone of a Σ-matching containing the pair (i, j).
- If $i \in B \cup \{r\}$ and $j \in \{\ell\} \cup A$, there are $a < i < j < b$ such that M is a Σ-matching containing the pairs (a, i) and (j, b) and $M' = M \setminus \{i, j\}$ is a Σ-matching containing the pair (a, b) such that $\mathbf{t}$ lies in the normal cone of both. Equivalently, $\mathbf{t}$ lies in the normal cone of a Σ-matching containing the pairs (a, i) and (j, b).
- If $i, j \in \{\ell\} \cup A$, there is some $b > j$ with $b \in B \cup \{r\}$ such that M is a Σ-matching containing the pair (j, b) and $M' = (M \cup \{i\}) \setminus \{j\}$ is a Σ-matching containing the pair (i, b) such that $\mathbf{t}$ lies in the normal cone of both. Equivalently, $\mathbf{t}$ lies in the normal cone of a Σ-matching containing the pair (i, b).

- If $i, j \in B \cup \{r\}$, there is some $a < i$ with $a \in \{\ell\} \cup A$ such that M is a Σ-matching containing the pair (a, i) and $M' = (M \cup \{j\}) \setminus \{i\}$ is a Σ-matching containing the pair (a, j) such that $\mathbf{t}$ lies in the normal cone of both. Equivalently, $\mathbf{t}$ lies in the normal cone of a Σ-matching containing the pair (a, j).

Proof. We first show that these conditions are necessary. To prove this, we assume that $\mathbf{t}$ is in the $\mathcal{SF}(\Sigma)$ cone corresponding to an edge e connecting two $\mathsf{SP}(\Sigma)$ vertices, where e is in direction $\mathbf{e}_i - \mathbf{e}_j$. We denote the two endpoints by $\boldsymbol{\chi}(M)$ and $\boldsymbol{\chi}(M')$, where M and M' are two distinct Σ-matchings with $\boldsymbol{\chi}(M') - \boldsymbol{\chi}(M) = \mathbf{e}_i - \mathbf{e}_j$. As $\mathbf{t}$ lies in the normal cone of this edge, we have $\tau(M) = \tau(M')$ and thus $t_i = t_j$. The four cases follow by distinguishing cases based on the positions i and j.

It is left to show that the conditions are sufficient. In each of the four cases, there are two adjacent Σ-matchings M and M' such that $\mathbf{t}$ lies in the normal cone of both. They are connected by a $\mathsf{SP}(\Sigma)$ edge in direction $\mathbf{e}_i - \mathbf{e}_j$ which we denote by e. We deduce that $\tau(M) = \tau(M')$ and there is no Σ-matching M^* with $\tau(M^*) > \tau(M)$. Then $\mathbf{t}$ is maximized by a face F of $\mathsf{SP}(\Sigma)$ that contains e. As $e \subseteq F$, we have $\mathbf{t} \in \mathcal{N}(F) \subseteq \mathcal{N}(e)$, so $\mathbf{t}$ is contained in the normal cone of the edge e in direction $\mathbf{e}_i - \mathbf{e}_j$. □

3.4 Shardsumotopes

We will now describe the polytopes and normal fans that are obtained by building the Minkowski sum of multiple shard polytopes. In particular, we will sum up shard polytopes for sets of shards that are upper sets in the forcing order. We will call such a set a **upper set of shards** and recall from Theorem 1.4.31 that the lattice congruences on $\mathrm{Pos}(\vec{\mathcal{A}}_n)$ are in bijection with the upper sets of $\vec{\mathcal{A}}_n$ shards, so any upper set of $\vec{\mathcal{A}}_n$ shards can be written as $\mathcal{S} = \boldsymbol{\Sigma}^{\checkmark}_{\equiv}$ for some lattice congruence $\equiv$ and vice versa.

3.4.1 Construction

Definition 3.4.1 (Shardsumotopes)**.** Given an upper set of shards $\mathcal{S} \subseteq \boldsymbol{\Sigma}$, we define

- The **summed shard polytope** or **shardsumotope** $\mathsf{SP}_+(\mathcal{S})$ to be the Minkowski sum of all shard polytopes for shards in $\mathcal{S}$, written as $\mathsf{SP}_+(\mathcal{S}) := \sum_{\Sigma \in \mathcal{S}} \mathsf{SP}(\Sigma)$
- The **summed shard fan** or **shardsumofan** $\mathcal{SF}_+(\mathcal{S})$ to be the normal fan of the shardsumotope $\mathsf{SP}_+(\mathcal{S})$ or equivalently, the common refinement of all shard fans $\mathcal{SF}(\Sigma)$ for $\Sigma \in \mathcal{S}$.

Given a latttice congruence $\equiv$ on the poset of regions of $\vec{\mathcal{A}}_n$, we define $\mathsf{SP}_+(\equiv) := \mathsf{SP}_+(\boldsymbol{\Sigma}^{\checkmark}_{\equiv})$ to be the shardsumotope for the upper set of shards retained by $\equiv$ (and do the same for $\mathcal{SF}_+(\equiv)$).

Proposition 3.4.2 (Shardsumotopes are Quotientopes)**.** *For any lattice congruence $\equiv$ on the poset of regions of $\vec{\mathcal{A}}_n$, the quotient fan $\mathcal{F}_{\equiv}$ is equal to the summedsumofan $\mathcal{SF}_+(\equiv)$. Therefore, the shardsumotope $\mathsf{SP}_+(\equiv)$ is a quotientope for $\equiv$.*

Proof. The statement is a consequence of Proposition 3.3.3. The walls of every single shard fan $\mathcal{SF}(\Sigma)$ for a shard Σ retained by $\equiv$ is a superset of that shard, so $\mathcal{SF}_+(\boldsymbol{\Sigma}^{\checkmark}_{\equiv})$ contains all walls of $\mathcal{F}_{\equiv}$. On the other hand, all walls contained in one of the shard fans $\mathcal{SF}(\Sigma)$ are a subset of the union of all shards Σ' that force Σ. As $\boldsymbol{\Sigma}^{\checkmark}_{\equiv}$ is an upper set of shards, the set of walls is also a subset of the union of all shards of $\boldsymbol{\Sigma}^{\checkmark}_{\equiv}$, so $\mathcal{SF}_+(\boldsymbol{\Sigma}^{\checkmark}_{\equiv})$ only contains walls of $\mathcal{F}_{\equiv}$. □

Observation 3.4.3 (Weighted Shardsumotopes)**.** We remark that the statement can be generalized to weighted Minkowski sums of the shard polytopes. For any choice of strictly positive weight function $\omega : \boldsymbol{\Sigma}^{\checkmark}_{\equiv} \to \mathbb{R}_{>0}$, the weighted Minkowski sum $\sum_{\Sigma \in \boldsymbol{\Sigma}^{\checkmark}_{\equiv}} \omega(\Sigma)\mathsf{SP}(\Sigma)$ always has the normal fan $\mathcal{F}_{\equiv}$.

These results reward our effort in constructing shard polytopes: Summing them up, we have found a new way to construct quotientopes in the $\vec{\mathcal{A}}_n$ arrangement. In contrast to the approach of [PS19], these quotientopes can be explicitly constructed from their vertices. This allows us to examine them quite closely and to describe some of their properties.

We can reformulate the symmetries of shard polytopes stated in Lemma 3.2.32 to apply to shardsumotopes as well:

Corollary 3.4.4 (Shardsumotope Symmetries)**.** Let $\mathcal{S}$ be an upper set of $\vec{\mathcal{A}}_n$ shards that is invariant under the map $\mathrm{P}^{\updownarrow}$ (resp. $\mathrm{P}_n^{\leftrightarrow}$) as defined in Definition 3.2.31. Then the shardsumotope $\mathsf{SP}_+(\mathcal{S})$ is invariant under the map $\mathrm{P}^{\updownarrow}$ (resp $\mathrm{P}_n^{\leftrightarrow}$) up to a translation. In particular, if $\mathcal{S}$ is centrally symmetric (in other words, the set is invariant under the map $\mathrm{P}_n^{\leftrightarrow} \circ \mathrm{P}^{\updownarrow}$), then $\mathsf{SP}_+(\mathcal{S}) = \rho_n^{\leftrightarrow} \circ \rho^{\updownarrow}(\mathsf{SP}_+(\mathcal{S}))$.

3.4.2 Examples

We will now construct shardsumotopes for some well-known congruences and upper sets of shards.

Example 3.4.5. Given a basic shard $\Sigma := \Sigma_n(i,\, i+1,\, \emptyset,\, \emptyset)$ for some $i \in [n-1]$, the only Σ-matchings are $\emptyset$ and $\{i, i+1\}$. Therefore, the shard polytope $\mathsf{SP}(\Sigma)$ of any basic shard is the line segment between the vertices $\mathbf{0}$ and $\mathbf{e}_i - \mathbf{e}_{i+1}$. We denote the upper set of shards consisting of all basic shards by $\mathcal{S}_{\text{rec}} := \{\Sigma_n(i,\, i+1,\, \emptyset,\, \emptyset) \mid i \in [n-1]\}$. The associated shardsumotope is the parallelotope $\mathsf{SP}_+(\mathcal{S}_{\text{rec}}) = \sum_{i=1}^{n-1} [\mathbf{0},\, \mathbf{e}_i - \mathbf{e}_{i+1}]$.

Example 3.4.6. Let $\equiv$ be the sylvester congruence (see Example 1.4.23) on the lattice of regions of $\vec{\mathcal{A}}_n$. The shards retained by $\equiv$ are precisely the up shards (see Definition 1.5.10). For any up shard $\Sigma = \Sigma_n(\ell,\, r,\,]\ell, r[\,,\, \emptyset)$ with $1 \le \ell < r \le n$, the Σ-matchings are the empty matching and the 2-element sets $\{i, r\}$ for all $\ell \le i < r$. Therefore, each shard polytope $\mathsf{SP}(\Sigma)$ can be viewed as the convex hull of the points $\mathbf{e}_j$ for all $j \in [\ell, r]$, translated by the vector $-\mathbf{e}_r$. This convex hull is a face of the standard simplex Δ which can be denoted by $\Delta_{[\ell,r]}$, indicating that it is the convex hull of all $\mathbf{e}_k$ for $k \in [\ell, r]$.

We can therefore describe the shardsumotope $\mathsf{SP}_+(\equiv)$ as a translate of the associahedron Asso_n (as seen in Example 1.5.21) by the vector $\sum_{j=1}^{n} (1-j)\mathbf{e}_j$. Our construction as a shardsumotope corresponds to the Minkowski decomposition of this polytope into faces of the standard simplex indexed by the intervals of $[n]$ that was described in [Pos09].

An illustration of this shardsumotope in $\vec{\mathcal{A}}_3$ can be found among all shardsumotopes for essential congruences in Figure 3.6, where it is the second picture from the left. The 3-dimensional case is illustrated in Figure 3.7 (left).

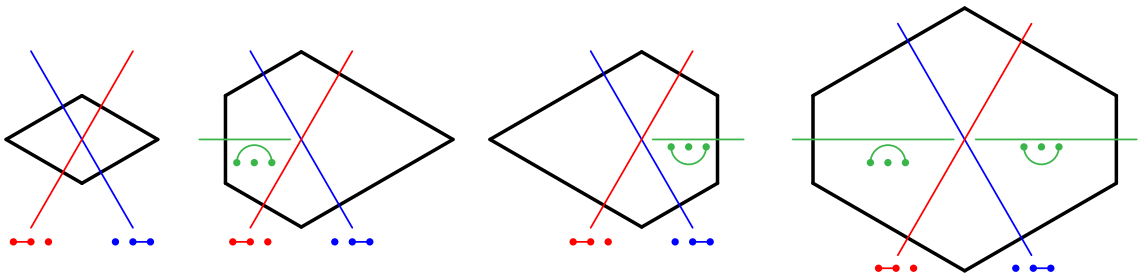

Figure 3.6: The shardsumotopes $\mathsf{SP}_+(\equiv)$ for all essential congruences $\equiv$ on the poset of regions of $\vec{\mathcal{A}}_3$. These are precisely those congruences that retain at least the two basic shards $\Sigma_3(1,2,\emptyset,\emptyset)$ (illustrated by the red arc) and $\Sigma_3(2,3,\emptyset,\emptyset)$ (illustrated by the blue arc). [Picture from [PPR20]]

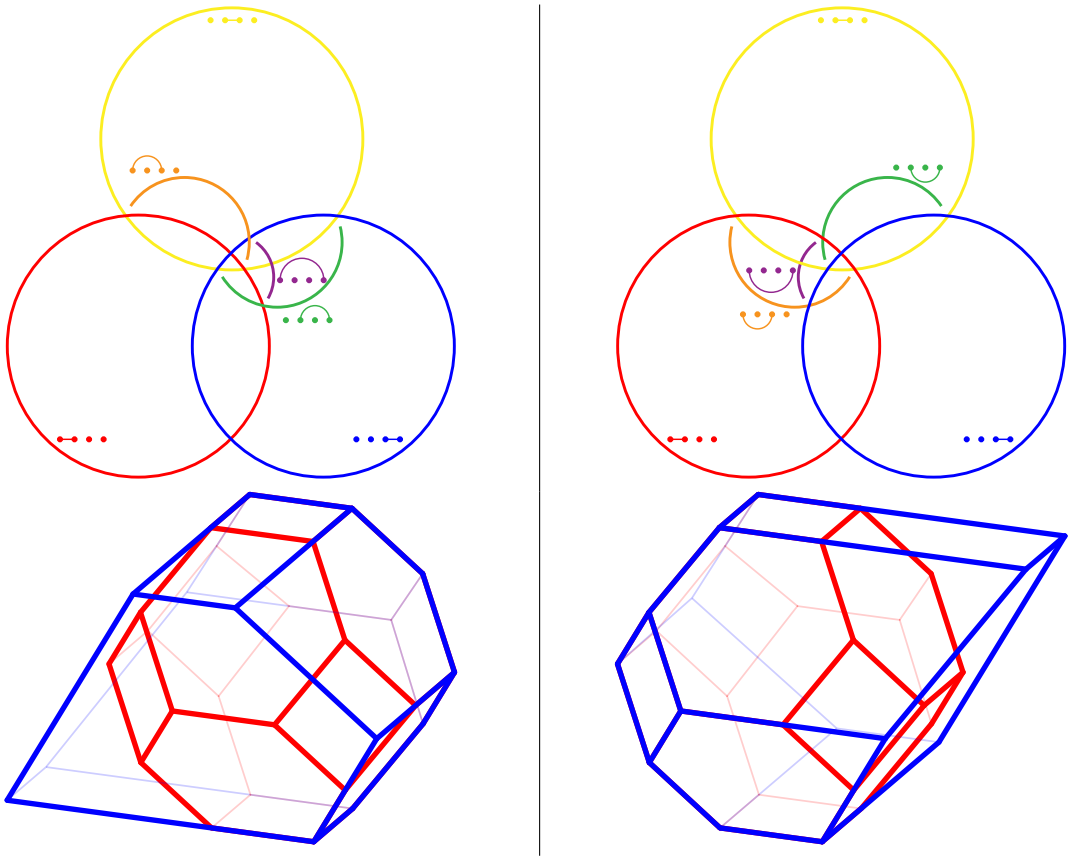

Figure 3.7: The classic associahedron obtained as a shardsumotope from the sylvester congruence retaining exactly the up shards (left) and the centrally reflected shardsumotope built from the congruence retaining exactly the down shards (right). Both these shardsumotopes drawn in blue can equivalently described by removing inequalities from the $\mathcal{H}$-description of the permutahedron Perm_4 (visualized inside the shardsumotopes, colored in red), as they were constructed in [HL07]. [Picture from [PPR20]]

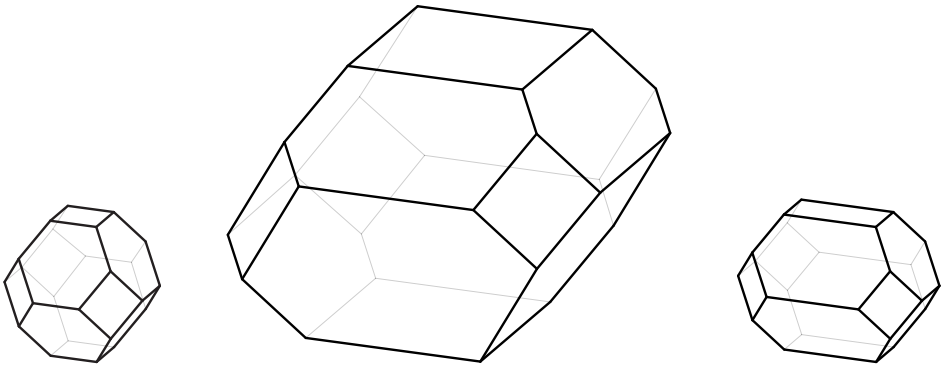

Figure 3.8: The permutahedron Perm_4 (left) as defined in Example 1.3.15. The shardsumotope $\mathsf{SP}_+(\mathbf{\Sigma}_4)$ (center) obtained by summing the shard polytopes for all shards in $\vec{\mathcal{A}}_4$ or equivalently, the shard polytopes of all shards retained by the trivial lattice congruence that does not contract anything. The shardsumotope $\mathsf{SP}_+(\mathcal{S})$ (right) obtained by summing the shard polyoptes of all minimal shards in the forcing order of $\vec{\mathcal{A}}_4$. [Picture from [PPR20]]

Example 3.4.7. The set of all shards of $\vec{\mathcal{A}}_n$, denoted by $\mathbf{\Sigma}_n$, is an upper set of shards. It corresponds to the trivial lattice congruence on the poset of regions of $\vec{\mathcal{A}}_n$ that assigns each region to its own equivalence class. In consequence, the shardsumotope $\mathsf{SP}_+(\mathbf{\Sigma}_n)$ has as its normal fan the braid fan $\mathcal{F}_n$ itself. See Figure 3.8 for an illustration of the shardsumotope in $\vec{\mathcal{A}}_4$.

It exhibits both symmetries introduced in Corollary 3.4.4, but it does not have all the symmetries of the classical permutahedron Perm_n.

3.4.3 Vertices

We can use our knowledge about the chambers of the shard fan to associate to any vector $\mathbf{t} \in \mathbb{R}^n$ a Σ-matching M, chosen such that the normal cone of the shard polytope vertex $\boldsymbol{\chi}(M)$ contains the vector $\mathbf{t}$. Put differently, $\mathbf{t}$ lies the normal cone of the shard fan corresponding to the matching M. This map will then be useful to determine the vertices of a shardsumotope, as each vertex is a Minkowski sum of vertices of the individual shard polytopes.

We first introduce a map that sends a vector $\mathbf{t}$ to the characteristic vector of a Σ-matching in the following way.

Definition 3.4.8 (Artificial Matching Vector)**.** Given an $\vec{\mathcal{A}}_n$ shard $\Sigma := \Sigma_n(\ell, r, A, B)$ and a vector $\mathbf{t} \in \mathbb{R}^n$, we define the point $\mathbf{v}(\mathbf{t}, \Sigma) \in \{-1, 0, 1\}^n$ where the j-th coordinate is

- 1 if and only if all of the following hold.
  - $j \in \{\ell\} \cup A$.
  - For every $a \in \{\ell\} \cup A$ with $a < j$ and $t_a > t_j$, there is some $b \in B \cap]a, j[$ with $t_b < t_j$.
  - There is a $b \in B \cup \{r\}$ with $j < b$ such that $t_j > t_b$ and $t_j > t_a$ for every $a \in A \cap]j, b[$.
- -1 if and only if all of the following hold.
  - $j \in B \cup \{r\}$
  - For every $b \in B \cup \{r\}$ with $j < b$ and $t_j > t_b$, there is some $a \in A \cap]j, b[$ with $t_j < t_a$.
  - There is an $a \in \{\ell\} \cup A$ with $a < j$ such that $t_a > t_j$ and $t_b > t_j$ for every $b \in B \cap]a, j[$.

For an upper set of shards $\mathcal{S}$, we define $\mathbf{v}(\mathbf{t}, \mathcal{S}) := \sum_{\Sigma \in \mathcal{S}} \mathbf{v}(\mathbf{t}, \Sigma)$.

The following two lemmas demonstrate that a point constructed this way is always the characteristic vector of a Σ-matching (in Lemma 3.4.9) and that every characteristic vector of a Σ-matching can be obtained with this construction for some vector $\mathbf{t} \in \mathbb{R}^n$ (in Lemma 3.4.10).

Lemma 3.4.9 (Artificial Matching Vectors are Characteristic Vectors of Matchings)**.** *For any vector $\mathbf{t} \in \mathbb{R}^n$ and any $\vec{\mathcal{A}}_n$ shard Σ, the vector $\mathbf{v}(\mathbf{t}, \Sigma)$ is the characteristic vector of a Σ-matching.*

Proof. We fix an arbitrary vector $\mathbf{t} \in \mathbb{R}^n$ and set $\mathbf{v} := \mathbf{v}(\mathbf{t}, \Sigma)$. If $\mathbf{v} = \mathbf{0}$, it is the characteristic vector of the empty Σ-matching. Otherwise, we need to show that the nonzero entries alternate in sign, starting with a positive entry and ending with a negative entry. We first observe that the j-th entry of $\mathbf{v}$ can be positive only if $j \in \{\ell\} \cup A$ and negative only if $j \in B \cup \{r\}$.

We assume for a contradiction that there are two positions $a < a'$ with positive entries in $\mathbf{v}$ such that there is no negative entry of $\mathbf{t}$ in between. We choose a position $j \in B \cap]a, a'[$ such that t_j is minimal among all candidates. If multiple candidates have the same minimal value t_j, we choose the unique smallest position among them. We distinguish cases by comparing t_a and $t_{a'}$ to demonstrate that j exists (implying that $B \cap]a, a'[$ is nonempty) and has $t_j < t_a$ and $t_j < t_{a'}$.

- If $t_a > t_{a'}$, then $v_{a'} = 1$ implies through the second condition that there is at least one position $b \in B \cap]a, a'[$ with $t_b < t_{a'}$. Therefore, j exists and $t_j \leq t_b < t_{a'} < t_a$.
- If $t_a \leq t_{a'}$, then $v_a = 1$ implies through the third condition that there is at least one position $b \in B \cup \{r\}$ with $a < b$ such that $t_a > t_b$ and $t_a > t_{a^*}$ for every $a^* \in A \cap]a, b[$. As $a' < b$ would imply $t_a > t_{a'}$, we deduce that $b < a'$. In particular, j exists and $t_j < t_b < t_a \leq t_{a'}$.

We will now show that this j satisifies all three conditions for having a negative entry in $\mathbf{v}(\mathbf{t}, \Sigma)$:

- Clearly, $j \in B \cup \{r\}$.
- Every $b \in B \cup \{r\}$ with $j < b$ and $t_j > t_b$ has to have $a' < b$ as we chose j in such a way that there cannot be any $b \in B \cap]a, a'[$ with $t_j > t_b$. Therefore, a' gives us $t_j < t_{a'}$ to satisfy the second condition.
- Moreover, we have $a < j$ with $t_a > t_j$ and $t_b > t_j$ for every $b \in B \cap]a, j[$ through our choice of b, which certifies that the third condition is satisfied as well.

We deduce that $v_b = -1$, which contradicts our assumption that a and a' do not have any negative entry in between. An analogous argument shows that there cannot be two negative entries consecutive among the nonzero entries of $\mathbf{v}(\mathbf{t}, \Sigma)$ either.

It is left to show that the first nonzero entry is positive and the last nonzero entry is negative. We set m to be the smallest position such that $v_m \neq 0$ and assume for a contradiction that $m \in B \cup \{r\}$. As the entry in position m is nonzero, it satisfies the third condition, so there has to be at least one $a \in \ell \cup A$ with $a < m$ such that $t_a > t_m$ and $t_b > t_m$ for every $b \in B \cap]a, m[$. We fix a to be the position with maximal value t_a among all positions with these properties (If there are multiple candidates with the same value, we choose the unique largest position among them).

As m was assumed to be the first nonzero entry of $\mathbf{v}$, the position a has to have a zero entry, so it has to violate one of the conditions. It clearly satisfies $a \in \ell \cup A$. It satisfies the third condition as $m \in B \cup \{r\}$ provides $a < m$ and $t_a > t_m$, while for every $a' \in A \cap]a, m[$, we have $t_a > t_{a'}$ by our choice of a. So a has to violate the second condition. We deduce that there is an $a^* \in \{\ell\} \cup A$ with $a^* < a$ and $t_{a^*} > t_a$ such that all $b \in B \cap]a^*, a[$ have $t_b \geq t_a$. This implies that a^* has the properties $t_{a*} > t_m$ and $t_b \geq t_m$ for all $b \in B \cap]a^*, m[$. But this contradicts our choice of a as we have $a^* < a$. We conclude that the first nonzero entry cannot be negative. An analogous argument shows that the last nonzero entry cannot be positive. □

Lemma 3.4.10 (Every Characteristic Vector of a Matching is an Artificial Matching Vector)**.** *Let Σ be an $\vec{\mathcal{A}}_n$ shard. For every Σ-matching M, we have $\boldsymbol{\chi}(M) = \mathbf{v}(\boldsymbol{\chi}(M), \Sigma)$.*

Proof. For the shard $\Sigma = \Sigma_n(\ell, r, A, B)$, we fix a Σ-matching M and a position $a \in \{\ell\} \cup A$. We set the two vectors $\mathbf{t} := \boldsymbol{\chi}(M) \in \{-1, 0, 1\}^n$ and $\mathbf{v} := \mathbf{v}(\mathbf{t}, \Sigma)$.

We first assume that $a \in M$. Then $t_a = 1$. We want to show that $v_a = 1$ holds as well. We fix $b := M \cap]a, r]$ to be the partner of a in M (so that (a, b) is a pair of M). Clearly, a meets the first two conditions of Definition 3.4.8 as $a \in \{\ell\} \cup A$ and there is no entry of $\mathbf{t}$ larger than $t_a = 1$. Moreover, we have $a < b$ and $1 = t_a > t_b = -1$ and for every $a' \in A \cap]a, b[$, we have $a' \notin M$ by our choice of b, so we obtain $1 = t_a > t_{a'} = 0$. We conclude that $v_a = 1$.

We now assume $a \notin M$. To show that $v_a = 0$, we distinguish cases based on the position of a with respect to our matching M.

- If $a > \max(M)$, every $j \in]a, r]$ has $t_j = 0$, so there cannot be any $b \in B \cup \{r\}$ with $a < b$ and $0 = t_a > t_b$, so a violates the third condition.
- If $a < \min(M)$, we set $a' = \min(M)$. Any $b \in B \cup \{r\}$ has $0 = t_a > t_b$ if and only if $b \in M$, which implies $a' < b$, so we have $a' \in A \cap]a, b[$ with $t_a < t_{a'}$, which violates the third condition.
- If $a' < a < b'$ for some M-pair (a', b'), then $a' \in \{\ell\} \cup A$ has $a' < a$ with $1 = t_{a'} > t_a$ and there cannot be any $b \in B \cap]a', a[$ with $t_b < t_a = 0$ as that would contradict (a', b') being an M-pair. Therefore, a violates the second condition.
- If $b' < a < a^*$ for two consecutive M-pairs (a', b') and (a^*, b^*), then for every $b \in B \cup \{r\}$ with $a < b$ and $0 = t_a > t_b$, we have to have $t_b = -1$ and thus $b \in M$, which implies that $a^* < b$. In particular, there is $a^* \in A \cap]a, b[$ with $0 = t_a \leq t_{a^*} = 1$, violating the third condition.

We conclude that $v_a = 0$. Analogous arguments show that $v_b = -1$ holds if and only if $b \in M$ with $b \in B \cup \{r\}$. This proves that $\mathbf{v} = \mathbf{v}(\boldsymbol{\chi}(M), \Sigma)$ and $\boldsymbol{\chi}(M)$ are equal. □

We have seen that the vectors $\mathbf{v}(\mathbf{t}, \Sigma)$ are precisely the characteristic vectors of Σ-matchings. Put differently, we have seen that the vertex set of the shard polytope $\mathsf{SP}(\Sigma)$ is equal to the set of vectors $\mathbf{v}(\mathbf{t}, \Sigma)$ obtained from all $\mathbf{t} \in \mathbb{R}^n$. Moreover, we will see that each vector of the form $\mathbf{v}(\mathbf{t}, \Sigma)$ maximizes the shard polytope $\mathsf{SP}(\Sigma)$ in the direction given by $\mathbf{t}$.

Corollary 3.4.11 (Artificial Matching Vectors Maximize a Direction)**.** Let Σ be an $\vec{\mathcal{A}}_n$ shard and let $\mathbf{t} \in \mathbb{R}^n$ be a nonzero vector. Then $\mathbf{v}(\mathbf{t}, \Sigma)$ is maximal in direction $\mathbf{t}$ among all vertices of $\mathsf{SP}(\Sigma)$.

Proof. The vector $\mathbf{v}(\mathbf{t}, \Sigma)$ is the characteristic vector of some Σ-matching M, as we learned in Lemma 3.4.9. We verify that the vector $\mathbf{t}$ lies in the normal cone of this matching by going through the inequalities provided by Corollary 3.3.6 for each pair of M. This implies the desired statement. □

We are now prepared to characterize the vertices of a shardsumotope.

Proposition 3.4.12 (Vertices of Shardsumotopes)**.** *For an $\vec{\mathcal{A}}_n$ shard Σ, the vertices of $\mathsf{SP}(\Sigma)$ are precisely the points $\mathbf{v}(\mathbf{t}, \Sigma)$ for all $\mathbf{t} \in \mathbb{R}^n$. For an upper set of $\vec{\mathcal{A}}_n$ shards $\mathcal{S} \subseteq \mathbf{\Sigma}_n$, the vertices of the shardsumotope $\mathsf{SP}_+(\mathcal{S})$ are precisely the points $\mathbf{v}(\mathbf{t}, \mathcal{S})$ for all $\mathbf{t} \in \mathbb{R}^n$.*

Proof. The two lemmas 3.4.9 and 3.4.10 showed that every vector $\mathbf{t} \in \mathbb{R}^n$ yields a characteristic vector $\mathbf{v}(\mathbf{t}, \Sigma)$ and every characteristic vector is of the form $\mathbf{v}(\mathbf{t}, \Sigma)$ for some vector $\mathbf{t} \in \mathbb{R}^n$. Therefore, the points we obtain in this way are precisely the vertices of the shard polytope.

For the shardsumotope, we know that each summand of $\mathbf{v}(\mathbf{t}, \mathcal{S}) := \sum_{\Sigma \in \mathcal{S}} \mathbf{v}(\mathbf{t}, \Sigma)$ is a vertex of the respective shard polytope, but not every Minkowski sum of vertices is necessarily a vertex of the resulting Minkowski sum polytope. But we learned in Corollary 3.4.11 that the vector $\mathbf{t}$ lies in the normal cone of the vertex $\mathbf{v}(\mathbf{t}, \Sigma)$ for each of the shards $\Sigma \in \mathcal{S}$. We deduce that $\mathbf{v}(\mathbf{t}, \mathcal{S})$ lies in the intersection of all these normal cones, which is the normal cone of the vertex of $\mathsf{SP}_+(\mathcal{S})$ maximal in direction $\mathbf{t}$. □

While the preceding statement precisely describes the vertices of a shardsumotope, the following statement gives us a more efficient way to construct it.

Corollary 3.4.13 (Constructing Shardsumotopes)**.** Let $\equiv$ be a lattice congruence on the poset of regions of $\vec{\mathcal{A}}_n$. Let $\Pi_\equiv$ be a set of permutations $\pi \in \sigma_n$ representing the congruence classes of $\equiv$. Then the vertices of the shardsumotope $\mathsf{SP}_+(\equiv)$ are exactly the points $\mathbf{v}(\pi^{-1}, \mathbf{\Sigma}^{\checkmark}_{\equiv})$ for all $\pi \in \Pi_\equiv$.

Proof. We saw in Proposition 3.4.12 that every point constructed in this way is a vertex of the shardsumope $\mathsf{SP}_+(\equiv)$. It is left to show that every vertex of $\mathsf{SP}_+(\equiv)$ can be obtained in this way. We recall that for any permutation $\pi \in \sigma_n$, the direction π^{-1} as a vector in $\mathbb{R}^n$ lies in the cone of the braid fan associated to the permutation π. Therefore, in the quotient fan $\mathcal{F}_\equiv$, the direction π^{-1} lies in the maximal cone associated to the $\equiv$-congruence class containing π.

Due to Corollary 3.4.11, the vector $\mathbf{v}(\pi^{-1}, \mathbf{\Sigma}^{\checkmark}_{\equiv})$ is the vertex of the shardsumotope corresponding to the congruence class containing π. By going through $\Pi_\equiv$, we obtain one vertex for every $\equiv$-congruence class and thus all vertices of the quotientope. □

We remark that one straightforward choice for $\Pi_\equiv$ is obtained by collecting the unique minimal permutation (in weak order) of every congruence class of $\mathrm{Pos}(\vec{\mathcal{A}}_n)/\equiv$.

3.4.4 Facets

Now that we know a straightforward way to describe a shardsumotope by its vertices, we will take a closer look at its facets. We first introduce some notation.

Definition 3.4.14 (I-Minimal Σ-Pairs)**.** Given an $\vec{\mathcal{A}}_n$ shard $\Sigma := \Sigma_n(\ell, r, A, B)$ and a proper subset $\emptyset \subsetneq I \subsetneq [n]$, we define an **I-minimal Σ-pair** to be a Σ-pair (a, b) where $a \in I$ and $b \notin I$ with the property that $(B \Delta I) \cap]a, b[= \emptyset$. We define $h(I, \Sigma)$ to be the number of I-minimal Σ-pairs. For an upper set of shards $\mathcal{S} \subseteq \mathbf{\Sigma}_n$, we define $h(I, \mathcal{S}) := \sum_{\Sigma \in \mathcal{S}} h(I, \Sigma)$.

We remark that given $\ell \leq a < k < b \leq r$, the condition $k \notin B \Delta I$ means that either $k \in B \cap I$ or $k \in A \setminus I$. Therefore, a Σ-pair (a, b) has this property if and only if there is no other Σ-pair (a', b') with $a \leq a' < b' \leq b$ satisfying the condition.

Lemma 3.4.15 (Shard Polytope Heights)**.** *Given an $\vec{\mathcal{A}}_n$ shard Σ and a proper subset $\emptyset \subsetneq I \subsetneq [n]$, the maximum of the scalar product $\langle \mathbf{1}_I \,|\, \mathbf{x} \rangle$ over all points $\mathbf{x}$ of the shard polytope $\mathsf{SP}(\Sigma)$ is $h(I, \Sigma)$.*

Proof. We know that for any direction, the maximum over a polytope in that direction can be obtained in a vertex of the polytope. We learned in Corollary 3.4.11 that any direction $\mathbf{t}$ is maximized in $\mathsf{SP}(\Sigma)$ by $\mathbf{v}(\mathbf{t}, \Sigma)$. In particular, the direction $\mathbf{1}_I$ is maximized by the vertex $\mathbf{v}(\mathbf{1}_I, \Sigma)$. That maximal scalar product is $s := \langle \mathbf{1}_I \,|\, \mathbf{v}(\mathbf{1}_I, \Sigma) \rangle = \sum_{k \in I} v(\mathbf{1}_I, \Sigma)_k$.

We first observe that for any $k \in I \cap (B \cup \{r\})$, Definition 3.4.8 certifies that $v(\mathbf{1}_I, \Sigma)_k = 0$ as there cannot exist any $a \in \{\ell\} \cup A$ with an entry higher than the one of k. We deduce from the definition that $v(\mathbf{1}_I, \Sigma)_k = 1$ if and only if $k \in I \cap (\{\ell\} \cup A)$ and there is some $b \in (B \cup \{r\}) \setminus I$ with $k < b$ and $a \notin I$ for every $a \in A \cap]k, b[$.

We observe that the second condition is equivalent to there being a minimal such $b \in B \cup \{r\}$ with $k < b$ such that $(B \Delta R) \cap]k, b[= \emptyset$. We deduce that s counts the number of Σ-pairs (k, b) with $(B \Delta R) \cap]k, b[= \emptyset$ which by Definition 3.4.14 equals $h(R, S)$. □

The following corollary follows by the properties of a Minkowski sum of polytopes:

Corollary 3.4.16 (Shardsumotope Heights)**.** Given an upper set of $\vec{\mathcal{A}}_n$ shards $\mathcal{S} \subseteq \mathbf{\Sigma}_n$ and a proper subset $\emptyset \subsetneq I \subsetneq [n]$, the maximum of the scalar product $\langle \mathbf{1}_I \,|\, \mathbf{x} \rangle$ over all points $\mathbf{x}$ of the shardsumotope $\mathsf{SP}_+(\mathcal{S})$ is $h(I, \mathcal{S})$.

This allows us to give the following $\mathcal{H}$-description of the shardsumotope $\mathsf{SP}_+(\mathcal{S})$.

Corollary 3.4.17 ($\mathcal{H}$-Description of a Shardsumotope)**.** Given an upper set of $\vec{\mathcal{A}}_n$ shards $\mathcal{S} \subseteq \mathbf{\Sigma}_n$, the shardsumotope $\mathsf{SP}_+(\mathcal{S})$ is given by

$$\mathsf{SP}_+(\mathcal{S}) \;=\; \{\mathbf{x} \in \mathbb{R}^n \mid \langle \mathbf{1} \,|\, \mathbf{x} \rangle = 0 \text{ and } \langle \mathbf{1}_I \,|\, \mathbf{x} \rangle \leq h(I, \mathcal{S}) \text{ for every } \emptyset \subsetneq I \subsetneq [n]\}\,.$$

Given a lattice congruence $\equiv$, we recall from Proposition 2.2.5 that the rays of the quotient fan $\mathcal{F}_\equiv$ are precisely those labelled by index sets $\emptyset \subsetneq I \subsetneq [n]$ which satisfy $\mathbf{\Sigma}_{I,n} \subseteq \mathbf{\Sigma}_\equiv^\checkmark$ as introduced in Definition 2.2.1. This allows us to describe the facets of a shardsumotope in the following way.

Corollary 3.4.18 (Facets of a Shardsumotope)**.** Let $\equiv$ be a lattice congruence on the poset of $\vec{\mathcal{A}}_n$ regions. Then the facets of the shardsumotope $\mathsf{SP}_+(\equiv)$ are the intersections with the hyperplanes given by $\langle \mathbf{1}_I \,|\, \mathbf{x} \rangle = -h([n] \setminus I,\ \mathbf{\Sigma}_\equiv^\checkmark)$ for all index sets $\emptyset \subsetneq I \subsetneq [n]$ which satisfy $\mathbf{\Sigma}_{I,n} \subseteq \mathbf{\Sigma}_\equiv^\checkmark$ as defined in Definition 2.2.1.

3.4.5 Examples of Vertices and Facets

We will now look at the vertices and facets of some specific shardsumotopes that we already looked at in Section 3.4.2.

Example 3.4.19. We first analyze the shardsumotope $\mathsf{SP}_+(\mathcal{S}_{\text{rec}})$ as seen in Example 3.4.5, where the upper set of shards $\mathcal{S}_{\text{rec}}$ contains all basic $\vec{\mathcal{A}}_n$ shards. Let $\Sigma = \Sigma_n(i, i+1, \emptyset, \emptyset)$ be a basic $\vec{\mathcal{A}}_n$ shard for some $i \in [n-1]$. We obtain

- $\mathbf{v}(\mathbf{t}, \Sigma) = \mathbf{e}_i - \mathbf{e}_{i+1}$ if $t_i > t_{i+1}$, and $\mathbf{0}$ otherwise.
- $h(I, \Sigma) = 1$ if $i \in I$ and $i+1 \notin I$, and 0 otherwise.

The shardsumotope $\mathsf{SP}_+(\mathcal{S}_{\text{rec}})$ has

- one vertex $\mathbf{v}(\mathbf{t}, \mathcal{S}_{\text{rec}}) = \sum_{i=1}^{n-1} \delta_{t_i > t_{i+1}} (\mathbf{e}_i - \mathbf{e}_{i+1})$ for each possible pattern of ascents and descents of a vector $\mathbf{t} \in \mathbb{R}^n$, or put differently, for each binary sequence of length $n-1$,
- two facets defined by $0 \le \langle \mathbf{1}_{[i]} \,|\, \mathbf{x} \rangle \le 1$ for each $i \in [n-1]$.

Example 3.4.20. Next, we take a look at the sylvester congruence $\equiv$ (introduced in Example 1.4.23), where the set $\mathbf{\Sigma}^{\checkmark}_{\equiv}$ of retained shards contains all up shards (introduced in Definition 1.5.10). Let $\Sigma = \Sigma_n(\ell, r,]\ell, r[\,, \emptyset)$ be an $\vec{\mathcal{A}}_n$ up shard. We obtain

- $\mathbf{v}(\mathbf{t}, \Sigma) = \mathbf{e}_j - \mathbf{e}_r$, where j is the position where $\mathbf{t}$ is maximal among all entries in the interval $[\ell, r]$ (if there is more then one such position, we choose the rightmost one of them),
- $h(I, \Sigma) = 1$ if $r \notin I$ and there is some $j \in [\ell, r[$ with $j \in I$.

The shardsumotope $\mathsf{SP}_+(\equiv)$ has

- a vertex $\mathbf{v} = \mathbf{v}(\mathbf{t}, \mathbf{\Sigma}^{\checkmark}_{\equiv})$ for each $\equiv$-class, whose coordinates are $v_j = (j-i)(k-j) - j$, with $i = \max(\{0\} \cup \{p \in [1, j[\mid t_p > t_j\})$ and $k = \min(\{p \in]j, n] \mid t_j < t_p\} \cup \{n+1\})$.
- a facet defined by $\langle \mathbf{1}_{[i,j]} \,|\, \mathbf{x} \rangle \ge (1-i)(j-1+1)$ for each interval $1 \le i \le j \le n$.

We remark that this vertex description can be directly linked to binary trees. We know that the sylvester congruence classes on the poset of regions of $\vec{\mathcal{A}}_n$ correspond to binary trees. Given a vector $\mathbf{t} \in \mathbb{R}^n$, we can say that it belongs to the binary tree T if and only if $t_i < t_j$ holds whenever i is a descendant of j in T (using infix labeling). In the j-th coordinate of $\mathbf{v}$, given by $(j-i)(k-j) - j$, we can then intrepret the factors $(j-i)$ and $(k-j)$ as the number of leaves in the left and right subtrees of j in T. This agrees with the vertex description of the associahedron Asso_n given in [Lod04], translated by the vector $-(1, 2, \ldots, n)$.

Moreover, we can use this same translation to recover the facet description from [Lod04] given by $\langle \mathbf{1}_{[i,j]} \,|\, \mathbf{x} \rangle \ge (1-i)(j-1+1) + \sum_{k=i}^{j} k = \binom{j-i+2}{2}$ for all intervals $[i, j]$, where the endpoints have to satisfy $1 \le i \le j \le n$.

Example 3.4.21. Finally, we examine the shardsumotope for the upper set of shards $\mathbf{\Sigma}_n$ containing all $\vec{\mathcal{A}}_n$ shards. The shardsumotope $\mathsf{SP}_+(\mathbf{\Sigma}_n)$ has

- a vertex $\mathbf{v}(\mathbf{t}, \mathbf{\Sigma}_n)$ for each permutation, where

$$v_j = 2^{n-1} \left(\sum_{\substack{i<j \\ t_i > t_j}} 2^{i-j} - \sum_{\substack{j<k \\ t_j > t_k}} 2^{j-k} \right).$$

  We remark that the sums go over all inversions of the vector $\mathbf{t}$ involving the position j,
- a facet for each index set $\emptyset \subsetneq I \subsetneq [n]$ defined by

$$\langle \mathbf{1}_I \,|\, \mathbf{x} \rangle \le \sum_{\substack{i<j \\ i \in I, j \notin I}} 2^{n+i-j}.$$

3.4.6 Shard Polytope Minkowski Identity

We observed in Example 3.4.7 that the permutahedron we constructed as a shardsumotope (illustrated in Figure 3.8) is not the classical permutahedron Perm_n as introduced in Example 1.3.15. There raises the question if there are some positive weights such that Perm_n can be obtained as a weighted Minkowski sum of shard polytopes. We will see in Corollary 3.4.25 that this is not the case.

To prepare this result, we will establish a Minkowski identity on shard polytopes. We recall the definitions of restricted shards from Definition 3.2.20 and introduce two more shards that can be obtained from a shard.

Definition 3.4.22 (Shards With Flipped Position)**.** Given an $\vec{\mathcal{A}}_n$ shard $\Sigma := \Sigma_n(\ell, r, A, B)$ and a position $k \in]\ell, r[$, we define

- $\Sigma^{k\to A} := \Sigma_n(\ell,\ r,\ A \cup \{k\},\ B \setminus \{k\})$,
- $\Sigma^{k\to B} := \Sigma_n(\ell,\ r,\ A \setminus \{k\},\ B \cup \{k\})$.

Proposition 3.4.23 (Shard Polytope Minkowski Identity)**.** *Given an $\vec{\mathcal{A}}_n$ shard $\Sigma := \Sigma_n(\ell, r, A, B)$ and a position $k \in]\ell, r[$, we have* $\mathsf{SP}(\Sigma^{k\to A}) + \mathsf{SP}(\Sigma^{k\to B}) = \mathsf{SP}(\Sigma^{\setminus k}) + \mathsf{SP}(\Sigma^{\leq k}) + \mathsf{SP}(\Sigma^{\geq k})$.

Proof. We first remark that both sides of the equation describe a Minkowski sum of (pseudo)shard polytopes, which makes both sides of the equation a polytope. It therefore suffices to show that every vertex of the left-hand side polytope is contained in the right-hand side polytope and vice versa. We know every vertex of a Minkowski sum of polytopes is a sum of vertices of the summands, so in this case, a sum of characteristic vectors of (pseudo)shard matchings. We fix an $\vec{\mathcal{A}}_n$ shard Σ and a position $k \in]\ell, r[$ and set the left-hand side polytope $\mathsf{P} := \mathsf{SP}(\Sigma^{k\to A}) + \mathsf{SP}(\Sigma^{k\to B})$ and the right-hand side polytope $\mathsf{Q} := \mathsf{SP}(\Sigma^{\setminus k}) + \mathsf{SP}(\Sigma^{\leq k}) + \mathsf{SP}(\Sigma^{\geq k})$.

We fix a vertex $\mathbf{v}$ of P. Then there are a $\Sigma^{k\to A}$-matching M_A and a $\Sigma^{k\to B}$-matching M_B such that $\mathbf{v} = \boldsymbol{\chi}(M_A) + \boldsymbol{\chi}(M_B)$. We distinguish cases by the inclusion of k in M_A and M_B and introduce three matchings M, $M_\leq$ and $M_\geq$ for the three (pseudo)shards $\Sigma^{\setminus k}$, $\Sigma^{\leq}$ and $\Sigma^{\geq}$.

- If $k \in M_A \cap M_B$,
  we set $M := (M_A \cap [\ell, k[) \cup (M_B \cap]k, r])$ and $M_\leq := M_B \cap [\ell, k]$ and $M_\geq := M_A \cap [k, r]$.
- If $k \in M_A \setminus M_B$,
  we set $M := M_B$ and $M_\leq := M_A \cap [\ell, k[$ and $M_\geq := M_A \cap [k, r]$.
- If $k \in M_B \setminus M_A$,
  we set $M := M_A$. and $M_\leq := M_B \cap [\ell, k]$ and $M_\geq := M_B \cap]k, r]$.
- If $k \notin M_A \cup M_B$ and $|M_B \cap [\ell, k[|$ is even,
  we set $M := M_A$ and $M_\leq := M_B \cap [\ell, k[$ and $M_\geq := M_B \setminus M_\leq$.
- If $k \notin M_A \cup M_B$ and $|M_B \cap [\ell, k[|$ is odd,
  we set $M := M_A$ and $M_\leq := (M_B \cap [\ell, k[) \cup \{k\}$ and $M_\geq := \{k\} \cup (M_B \cap]k, r])$

In each of these cases, $M_\leq$ is a $\Sigma^{\leq k}$-matching and $M_\geq$ is a $\Sigma^{\geq k}$-matching, while the matching denoted by M is a $\Sigma^{\setminus k}$-matching with the property that $\mathbf{v} = \boldsymbol{\chi}(M_\leq) + \boldsymbol{\chi}(M_\geq) + \boldsymbol{\chi}(M)$, so $\mathbf{v} \in \mathsf{Q}$. We deduce that $\mathsf{P} \subseteq \mathsf{Q}$.

To prove the opposite inclusion, we fix $\mathbf{w}$ to be a vertex of Q. Then there are a Σ-matching M not containing k, an $\Sigma_{\leq k}$-matching $M_\leq$ and an $\Sigma_{\geq k}$-matching $M_\geq$ that together satisfy the equation $\mathbf{w} = \boldsymbol{\chi}(M) + \boldsymbol{\chi}(M_\leq) + \boldsymbol{\chi}(M_\geq)$. We distinguish cases by the shape of M.

- If $|M \cap [\ell, k[|$ is even, then $M \cap [\ell, k[$ and $M \cap]k, r]$ are two Σ-matchings. We define the sets $M_A := (M \cap [\ell, k[) \cup M_\geq$ and $M_B := M_\leq \cup (M \cap]k, r])$.
- If $|M \cap [\ell, k[|$ is odd, we distinguish cases by the inclusion of k in $M_\leq$ and $M_\geq$.
  - If $k \notin M_\leq \cup M_\geq$, we set $M_A := M$ and $M_B := M_\leq \cup M_\geq$.
  - If $k \in M_\leq \cap M_\geq$, we note that $\mathbf{w}_k = 0$, so we can set $M_A := (M_\leq \setminus \{k\}) \cup (M \cap]k, r])$ and $M_B := (M \cap]\ell, k[) \cup (M_\geq \setminus \{k\})$.

- If $k \in M_{\leq} \setminus M_{\geq}$, we note $\mathbf{w}_k = -1$ and set $M_A := M$ and $M_B := M_{\leq} \cup M_{\geq}$.
- If $k \in M_{\geq} \setminus M_{\leq}$, we note $\mathbf{w}_k = +1$ and set $M_A := M_{\leq} \cup M_{\geq}$ and $M_B := M$.

In each of these cases, M_A is a $\Sigma^{k \to A}$-matching and M_B is a $\Sigma^{k \to B}$-matching with the property that $\mathbf{w} = \boldsymbol{\chi}(M_A) + \boldsymbol{\chi}(M_B)$, so $\mathbf{w} \in \mathsf{P}$. We deduce that $\mathsf{Q} \subseteq \mathsf{P}$ and conclude $\mathsf{P} = \mathsf{Q}$, proving our statement. □

This identity, illustrated in Figure 3.9, allows us to describe any shard polytope as a Minkowski sum and difference of shard polytopes of up shards. We recall from Example 3.4.6 that those shard polytopes are simplices. This rediscovers a formula that first appeared in [ABD10].

We will now use the Minkowski identity to decribe the polytope shown on the right side of Figure 3.8, where we built the sum of shard polytopes of all forcing minimal shards of $\vec{\mathcal{A}}_n$, which are precisely the shards of the $\mathcal{A}_n$ hyperplane $H_n(1, n)$.

Proposition 3.4.24 (Sum of Forcing Minimal Shard Polytopes)**.** *The Minkowski sum of the shard polytopes* $\mathsf{SP}(\Sigma)$ *for all forcing minimal shards* Σ *of* $\vec{\mathcal{A}}_n$ *is a zonotope that is combinatorially equivalent to the permutahedron* Perm_n*. It can be described as*

$$\sum_{A \subseteq]1,n[} \mathsf{SP}(\Sigma_n(1,\ n,\ A,\ ]1,n[\setminus A)) = \sum_{1 \leq i < j \leq n} 2^{f(i,j)} \cdot [\mathbf{0},\ \mathbf{e}_i - \mathbf{e}_j],$$

where $f(i,j) := |\{p \in]1,n[\mid p \notin [i,j]\}| = \max(i-2,\ 0) + \max(n-j-1,\ 0)$.

Proof. We will prove a statement for a broader class of sums of pseudoshard polytopes. We fix an arbitrary set $X \subseteq [n]$, fix the variables $\ell := \min(X)$ and $r := \max(X)$, the set $Y := X \setminus \{\ell, r\}$ of intermediate positions, the leftmost intermediate position $k := \min(Y)$ and the sets $X' := X \setminus \{k\}$ and $Y' := Y \setminus \{k\} = X \setminus \{\ell, k, r\}$, which each have k removed. We then have a look at a Minkowski sum of shard polytopes defined by $\mathsf{P}(X) := \sum_{A \subseteq Y} \mathsf{SP}(\Sigma_n(\ell,\ r,\ A,\ Y \setminus A))$. We note that the Minkowski sum in Proposition 3.4.24 is a special case of this form if we set $X = [n]$.

In the general case, whenever $|X| > 2$, then Y is non-empty, so k exists. Then we can pair up all the subsets $A \subseteq Y$ such that each pair differs only by whether $k \in A$ or not. This way, we can group all the summands of $\mathsf{P}(X)$ into $2^{|Y'|} = 2^{|X|-3}$ pairs. For each such pair of shard polytopes, Proposition 3.4.23 allows us to rewrite their sum. If we do that for all the summands of $\mathsf{P}(X)$ simultaneously, we obtain the equality

$$\begin{aligned}
\mathsf{P}(X) &= \sum_{A \subseteq Y} \mathsf{SP}(\Sigma_n(\ell,\ r,\ A,\ Y \setminus A)) \\
&= \sum_{A \subseteq Y'} \mathsf{SP}(\Sigma_n(\ell,\ r,\ A,\ Y' \setminus A)) \\
&\quad + \sum_{A \subseteq Y'} \mathsf{SP}(\Sigma_n(k,\ r,\ A,\ Y' \setminus A)) \\
&\quad + 2^{|Y'|} \mathsf{SP}(\Sigma_n(\ell,\ k,\ \emptyset,\ \emptyset)) \\
&= \mathsf{P}(X \setminus \{k\}) + \mathsf{P}(X \setminus \{\ell\}) + 2^{|X|-3} [\mathbf{0},\ \mathbf{e}_\ell - \mathbf{e}_k]\,.
\end{aligned}$$

Using this reformulation, we claim that for any choice of $X \subseteq [n]$ with $|X| \geq 2$, the polytope $\mathsf{P}(X)$ is a Minkowski sum of line segments of the form $[\mathbf{0},\ \mathbf{e}_i - \mathbf{e}_j]$. We prove this claim by induction on the cardinality of X.

- For $|X| = 2$, we obtain a pseudoshard of the form $\Sigma_n(\ell, r, \emptyset, \emptyset)$, where the only pseudoshard matchings are $\emptyset$ and $\{\ell, r\}$, so that its pseudoshard polytope is of the desired form.
- For the induction step, we may assume that the polytopes $\mathsf{P}(X \setminus \{k\})$ and $\mathsf{P}(X \setminus \{\ell\})$ can be expressed as Minkowski sums of line segments, so the above recursion proves our claim.

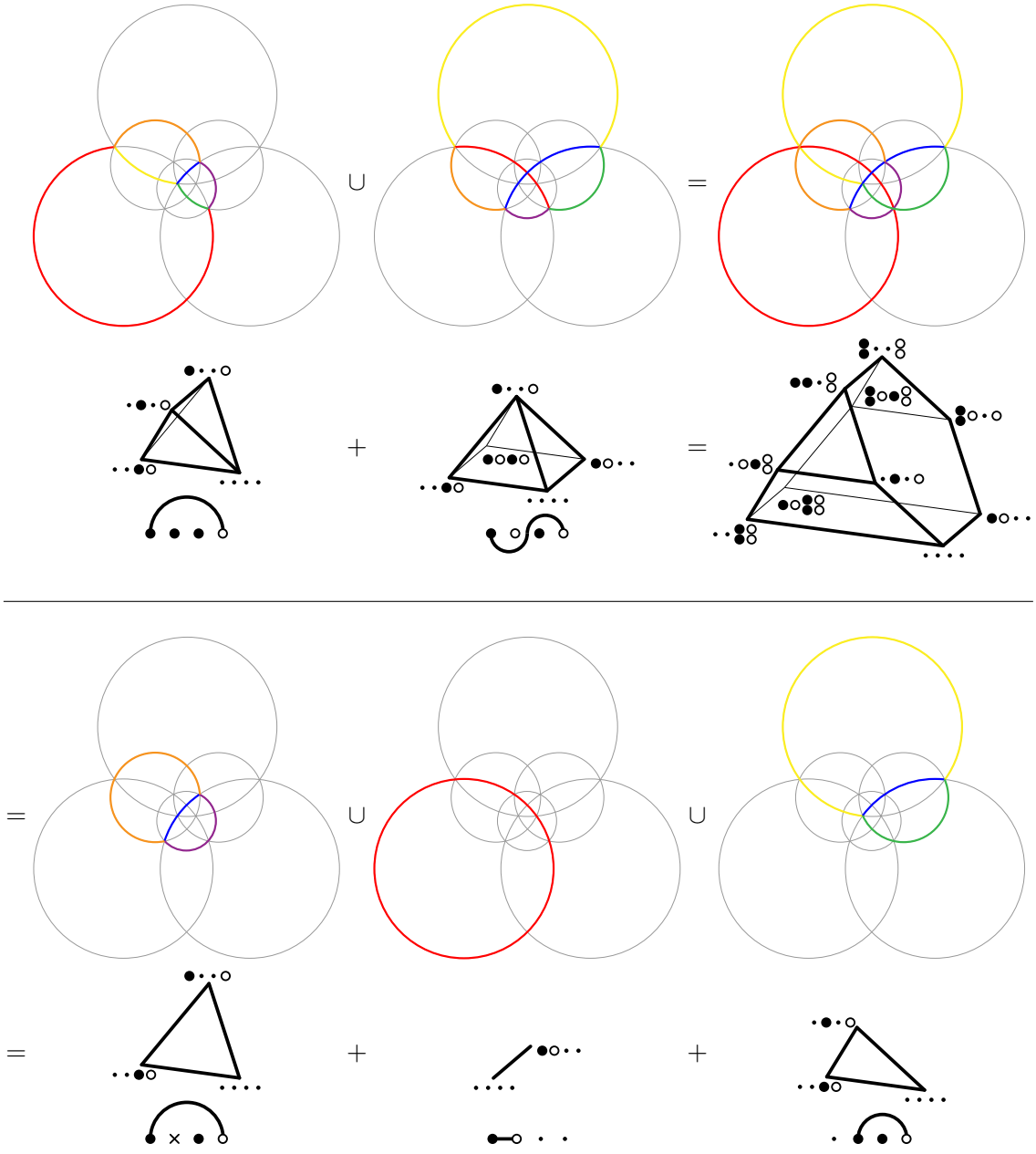

Figure 3.9: An example of the Minkowski identity given in Proposition 3.4.23, exemplified for the shard $\Sigma_4(1, 4, \{2, 3\}, \emptyset)$ or the shard $\Sigma_4(1, 4, \{3\}, \{2\})$ and the position $k = 2$. [Picture from [PPR20]]

To find the appropriate coefficients for the line segments summed up to obtain $\mathsf{P}([n])$, we oberve that the line segment $[\mathbf{0}, \mathbf{e}_i - \mathbf{e}_j]$ appears explicitly in the recursion if and only if i and j are the two minimal elements of X. Starting the recursion with $\mathsf{P}([n])$, this gives us a factor of 2 for each integer strictly in between 1 and i, while the segment's muliplicity of $2^{|X|-3}$ gives us as many factors of 2 as there are positions strictly in between j and n, making the total number of factors of 2 equal to the function $f(i, j)$ introduced above. □

Corollary 3.4.25 (Permutahedra as Weighted Shardsumotopes)**.** For $n \geq 4$, the standard permutahedron Perm_n cannot be written as a weighted Minkowski sum of shard polytopes.

Proof. We recall from Proposition 3.3.3 that for any $\vec{\mathcal{A}}_n$ shard Σ^*, the union of the walls of $\mathcal{SF}(\Sigma^*)$ is a subset of the union of all shards Σ' that force Σ^*. It follows that for any forcing-minimal shard Σ, there is no other shard whose shard fan contains Σ in its union of walls. In particular, edges in direction $\mathbf{e}_1 - \mathbf{e}_n$ and thus normal to the hyperplane $H_n(1, n)$ appear only as edges of the shard polytopes $\mathsf{SP}(\Sigma)$ for all minimal shards Σ (which are precisely the shards of $H_n(1, n)$).

The normal fan of Perm_n is the braid fan $\mathcal{F}_n$ and contains all these walls, so the permutahedron contains all the corresponding edges. If we want to write Perm_n as a weighted sum $\mathsf{Perm}_n = \sum_{\Sigma \in \mathbf{\Sigma}_n} w_\Sigma \mathsf{SP}(\Sigma)$ of shard polytopes, it is therefore necessary that all polytopes of forcing-minimal shards are included with a strictly positive weight $w_\Sigma > 0$. As the edge connecting $\mathbf{0}$ and $\mathbf{e}_1 - \mathbf{e}_n$ has the same length $\sqrt{2}$ in all shard polytopes $\mathsf{SP}(\Sigma)$ for minimal shards Σ and all edges of Perm_n have the same length, the weights w_Σ have to coincide for all minimal shards $\Sigma \in \mathbf{\Sigma}_n$.

But if all these weights coincide, we can deduce from Proposition 3.4.24 that for $n \geq 4$, the sum of all the minimal shard polytopes has edges of length at least $2 \cdot \sqrt{2}$. In particular, the permutahedron Perm_n would have edges of length at least $2 \cdot \sqrt{2}$, in contradiction to the fact that all its edges have the same length. □

We have seen that while every quotient fan of the braid arrangement appears as the normal fan of some shardsumotope, not every polytope whose normal fan is a quotient fan can be obtained as a Minkowski sum of shard polytopes. In the following section, we will have a closer look at shard polytopes in the type cone of the braid fan and the role their Minkowski sums play.

3.5 Type Cones and Shard Polytopes

We have found a way to build quotientopes by adding shard polytopes. It is natural to ask whether this is the end of the road or if shard polytopes can themselves be built as Minkowski sums of even more elementary polytopes. We will see that this is not the case, which mean that shard polytopes are in some sense elementary objects. We use the definition of (Minkowski) indecomposability introduced in Section 1.2.6 and show that shard polytopes are indecomposable in this regard.

Proposition 3.5.1 (Shard Polytopes are Indecomposable)**.** *For any $\vec{\mathcal{A}}_n$ shard Σ, the shard polytope $\mathsf{SP}(\Sigma)$ is indecomposable.*

Proof. We fix a shard $\Sigma = \Sigma_n(\ell, r, A, B)$ and recall the $\mathbf{H}$-description of its shard polytope $\mathsf{SP}(\Sigma)$ provided in Definition 3.2.2 and go through all its facets to check whether they contain the two vertices $\mathbf{0}$ (which is the characteristic vector of the empty Σ-matching $\{\}$) and $\mathbf{e}_\ell - \mathbf{e}_r$ (which is the characteristic vector of the Σ-matching $\{\ell, r\}$).

- All facets defined by an inequality $x_a \geq 0$ for some $a \in A$ contains both $\mathbf{0}$ and $\mathbf{e}_\ell - \mathbf{e}_r$.
- The same holds for all facets defined by inequalities $x_b \leq 0$.
- Each facet defined by an inequality $\sum_{i \leq f} x_i \leq 1$ for a Σ-fall f contains the vertex $\mathbf{e}_\ell - \mathbf{e}_r$.

- Each facet defined by an inequality $\sum_{i \leq c} x_i \geq 0$ for a Σ-climb c contains the vertex $\mathbf{0}$.

The empty matching and the matching $\{\ell, r\}$ differ in exactly two of their entries. We learned in Lemma 3.2.15 that this means that their characteristic vectors share an edge in $\mathsf{SP}(\Sigma)$. We just saw that this edge shares at least one vertex with every facet of the polytope. We conclude from Theorem 1.2.43 that $\mathsf{SP}(\Sigma)$ is indecomposable. □

We have seen that shard polytopes are indecomposable, so each of them corresponds to a ray of the type cone. This does not imply that all rays of the type cone correspond to shard polytopes or that all indecomposable deformed permutahedra are shard polytopes. We will now have a closer look at the type cone of the braid fan $\mathcal{F}_3$.

Example 3.5.2 (Type Cone of the Braid Fan)**.** The braid fan $\mathcal{F}_3$ is a 2-dimensional fan with 6 rays. Its type cone lies in the space of height functions on those 6 rays and is therefore naturally embedded in $\mathbb{R}^6$. This means that type cones are difficult to visualize even for low-dimensional arrangements with few rays such as $\mathcal{A}_3$.

We can nevertheless visualise the closed type cone $\overline{\mathsf{TC}(\mathcal{F}_3)}$ in three dimensions in the following way. The cone has a two-dimensional lineality space corresponding to translations of the resulting polytopes in $\mathbb{R}^2$. We can therefore intersect the type cone with the orthogonal complement of this lineality space without losing any information. We obtain a 4-dimensional cone in a 4-dimensional linear subspace of $\mathbb{R}^6$.

We remark that this cone still contains all dilations of each of the polytopes defined by its height functions. We can therefore concentrate on the intersection of the cone with another hyperplane that throws out all but one scalar multiple of each height function. We choose that hyperplane in such a way that it contains the height functions of all shard polytopes. We obtain a polytope that we call the **type polytope** $\mathsf{TP}(\mathcal{F})$. In the case of $\mathcal{F}_3$, the type polytope $\mathsf{TP}(\mathcal{F}_3)$ is a bipyramid over a triangle. See Figure 3.10 for an illustration.

Proposition 3.5.3 (Shard Polytopes Span a Simplex within the Type Polytope)**.** *The height functions of the shard polytopes* $\mathsf{SP}(\Sigma)$ *for all shards* Σ *of the oriented braid arrangement* $\vec{\mathcal{A}}_n$ *span a simplex that is a full-dimensional subset of the type polytope* $\mathsf{TP}(\mathcal{F}_n)$.

Proof. We first observe that the dimension of the type polytope is $2^n - n - 2$, as the braid fan $\mathcal{F}_n$ has $2^n - 2$ rays, the lineality space of the type cone has dimension $n - 1$ and the dimension decreases by one more through the intersection with a hyperplane to turn the cone into a polytope.

Furthermore, we observe that the number of $\vec{\mathcal{A}}_n$ shards of the hyperplane $H_n(\ell, r)$ is $2^{r-\ell-1}$ due to the number of ways to distribute the positions in $]\ell, r[$ into disjoint sets A and B. Summing these up over all $\mathcal{A}_n$ hyperplanes, we deduce the total number of $\vec{\mathcal{A}}_n$ shards to be equal to $\sum_{1 \leq \ell < r \leq n} 2^{r-\ell-1} = 2^n - n - 1$. This is the number of $\vec{\mathcal{A}}_n$ shard polytopes.

It now suffices to prove that the set of shard polytopes is affinely independent in the type polytope or equaivalently, linearly independent in the type cone. Asumme for a contradiction that there are coefficients $\lambda : \mathbf{\Sigma}_n \to \mathbb{R}$ such that $0 = \sum_{\Sigma \in \mathbf{\Sigma}_n} \lambda(\Sigma)\mathsf{SP}(\Sigma)$ is a linear dependence in the type cone $\mathsf{TC}(\mathcal{F}_n)$. We can then fix two subsets of shards defined by $\mathcal{S}^+ := \{\Sigma \in \mathbf{\Sigma}_n \mid \lambda(\Sigma) > 0\}$ and $\mathcal{S}^- := \{\Sigma \in \mathbf{\Sigma}_n \mid \lambda(\Sigma) < 0\}$. This enables us to rewrite the linear dependence of the height functions as the equality $\mathsf{P}^+ = \mathsf{P}^-$ of the two Minkowski decomposable polytopes defined by $\mathsf{P}^+ := \sum_{\Sigma \in \mathcal{S}^+} \lambda(\Sigma)\mathsf{SP}(\Sigma)$ and $\mathsf{P}^- := \sum_{\Sigma \in \mathcal{S}^-} \lambda(\Sigma)\mathsf{SP}(\Sigma)$.

Let Σ^* be a forcing minimal shard in $\mathcal{S}^+ \cup \mathcal{S}^-$. According to Proposition 3.3.3, the shard polytope $\mathsf{SP}(\Sigma^*)$ is the only shard polytope for a shard in $\mathcal{S}^+ \cup \mathcal{S}^-$ whose normal fan contains the shard Σ^*. This implies that this shard is contained in one of the normal fans of P^+ and P^- but not in both, which contradicts our assumption that $\mathsf{P}^+ = \mathsf{P}^-$. □

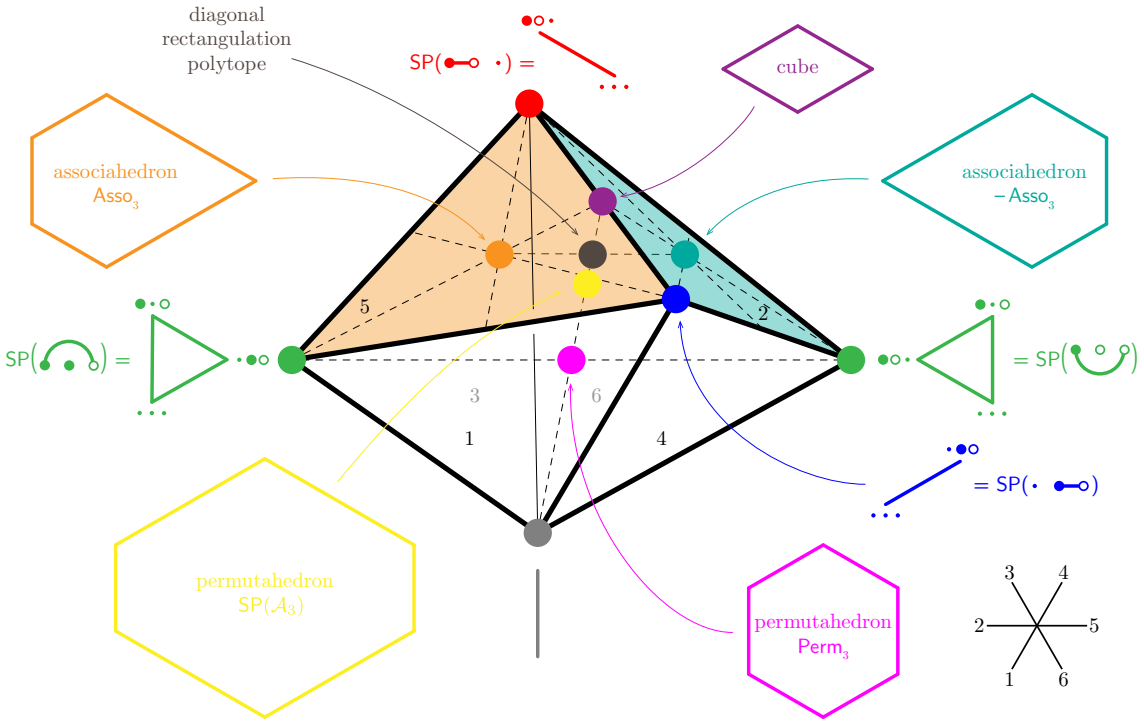

Figure 3.10: The type polytope $\mathsf{TP}(\mathcal{F}_3)$ of the braid fan $\mathcal{F}_3$. Its facets are labeled from 1 to 6, where facets 3 and 6 are labeled in grey as they are on the opposite side of the viewpoint. The diagram on the bottom to the right shows the $\mathcal{A}_3$ arrangement, where the walls are labeled from 1 to 6 as well and correspond to the facets of $\mathsf{TP}(\mathcal{F}_3)$. The bold dots indicate the position of several polytopes we discussed. We emphasize that all shard polytopes $\mathsf{SP}(\Sigma)$ corresponding to the four shards of $\vec{\mathcal{A}}_3$ are vertices of the type polytope. [Picture from [PPR20]]

We remark that this result does not contradict Proposition 3.4.23, which gives an equality of different Minkowski sums of pseudoshard polytopes, as the equalities described there always contain at least one pseudoshard polytope, whereas Proposition 3.5.3 implies that no equality of different Minkowski sums using only shard polytopes can exist.

The result of Proposition 3.5.3 can be used to describe any quotientope (not just the ones obtained as shardsumotopes) in this basis of shard polytopes. Such an expression might have negative coefficients, which requires using so-called Minkowski differences and working in the space of virtual polytopes as described in [PK92]. In particular, this approach can be used to describe the quotientopes constructed in [PS19] as Minkowski sums of dilated shard polytopes.

4 Shard Polytopes for the Type B Arrangement

In this chapter, we adapt our findings from Chapter 3 to a different class of hyperplane arrangements. In Section 4.1, we will have a look at shards of the oriented type $\mathcal{B}$ arrangement $\vec{\mathcal{B}}_n$. We define the arrangement, have a look at its regions and rays, its canonical zonotope and type cone. We will then analyze the shards of the type $\mathcal{B}$ arrangement in Section 4.2. We use the geometry of the arrangement to describe forcing among $\vec{\mathcal{B}}_n$ shards. In Section 4.3, we describe lattice congruences and quotient lattices of the poset of regions. We use shard polytopes for $\vec{\mathcal{A}}_n$ shards to introduce shard polytopes for $\vec{\mathcal{B}}_n$ shards with similar properties. We use them to construct quotientopes for all lattice congruences of the weak order on $\mathfrak{S}_n^{\mathcal{B}}$.

Notation We recall the following conventions on notation for an integer n:

- $[n] := [1, n]$ denotes the set of integers from 1 to n,
- $[\pm n] := [-n, n] \setminus \{0\}$ denotes the integers from 1 to n and their additive inverses.

We start using some more special notation in this chapter. For any vector $\mathbf{x} \in \mathbb{R}^n$, we introduce additional virtual coordinates $x_{-i} := -x_i$ for $i \in [-n, n]$. In particular, this implies $x_0 = 0$. Moreover, for a set of indices $X \subseteq [-n, n]$, we use

- $X^+ := \{i \in [n] \mid i \in X\}$ for the subset of positive integers contained in X,
- $X^- := \{i \in [n] \mid -i \in X\}$ for those positive integers whose additive inverse is in X,
- $-X := \{-i \in \mathbb{Z} \mid i \in X\}$ for the additive inverses of the elements of X,
- $X^\pm := X \cap -X$ for those integers which appear in X with both signs.

4.1 The Type B Arrangement

We will first introduce signed permutations and then the $\mathcal{B}_n$ hyperplane arrangement whose combinatorics can be described using them. For a more detailed introduction to the combinatorics of type $\mathcal{B}$ Coxeter groups and therefore the combinatorics behind the type $\mathcal{B}$ arrangement, we refer to the classic textbooks [Hum90] and [BB05].

4.1.1 Signed Permutations

Definition 4.1.1 ($\mathcal{B}$-Permutation)**.** Let $\sigma : [-n, +n] \to [-n, +n]$ be a bijection on the set of integers $[-n, +n]$. It is called **centrally symmetric** if $\sigma(-a) = -\sigma(a)$ holds for all $a \in [-n, +n]$. A centrally symmetric bijection on $[-n, n]$ is called a **$\mathcal{B}$-permutation**. The **type $\mathcal{B}$ Coxeter group** denoted by $\mathfrak{S}_n^{\mathcal{B}}$ is the group of all $\mathcal{B}$-permutations on $[-n, +n]$.

Central symmetry implies in particular that $\sigma(0) = -\sigma(0) = 0$, so the $\mathcal{B}$-permutations in $\mathfrak{S}_n^{\mathcal{B}}$ can equivalently be viewed as bijections acting on $\pm[n]$ instead of $[-n, +n]$. Any $\mathcal{B}$-permutation $\sigma \in \mathfrak{S}_n^{\mathcal{B}}$ is uniquely determined by its values for the arguments $1, \ldots, n$. This allows for the compact notation $\sigma = \sigma(1)\sigma(2)\cdots\sigma(n)$, using $\overline{x}$ to denote a negative value $-x$. For example, we write $2\overline{1}$ for the bijection $\sigma : [\pm 2] \to [\pm 2]$ with values $\sigma(1) = 2$ and $\sigma(2) = -1$. For compactness, this notation will be used in illustrations throughout this chapter. We can interpret σ as a **signed permutation** on $[n]$, combining a regular permutation from $\mathfrak{S}_n$ and a sequence of

signs in $\{-,+\}^n$. This implies in particular that the number of $\mathcal{B}$-permutations and therefore the number of elements of $\mathfrak{S}_n^{\mathcal{B}}$ is equal to $2^n n!$.

Just like for permutations in the symmetric group $\mathfrak{S}_n$ (see Definition 1.3.21), we can define inversions on the $\mathcal{B}$-permutations in $\mathfrak{S}_n^{\mathcal{B}}$.

Definition 4.1.2 (Inversion of a $\mathcal{B}$-Permutation)**.** An **inversion** of a $\mathcal{B}$-permutation $\sigma \in \mathfrak{S}_n^{\mathcal{B}}$ is
- either a pair of values (σ_a, σ_b) such that $1 \leq a < b \leq n$ but $\sigma_a > \sigma_b$,
- or a pair of values (σ_{-a}, σ_b) such that $1 \leq a \leq b \leq n$ but $\sigma_{-a} > \sigma_b$.

The **inversion set** of a $\mathcal{B}$-permutation σ is the set of all its inversions

$$\begin{aligned}\mathrm{Inv}^{\mathcal{B}}(\sigma) := \quad & \{(\sigma_a, \sigma_b) \mid 1 \leq a < b \leq n \text{ and } \sigma_a > \sigma_b\} \\ & \cup \{(\sigma_{-a}, \sigma_b) \mid 1 \leq a \leq b \leq n \text{ and } \sigma_{-a} > \sigma_b\}.\end{aligned}$$

These inversion sets enable us to partially order $\mathcal{B}$-permutations just like standard permutations.

Definition 4.1.3 (Weak Order on $\mathfrak{S}_n^{\mathcal{B}}$)**.** The **weak order** on the $\mathcal{B}$-permutations of $\mathfrak{S}_n^{\mathcal{B}}$ is the partial order defined by $\sigma \leq \sigma' \iff \mathrm{Inv}^{\mathcal{B}}(\sigma) \subseteq \mathrm{Inv}^{\mathcal{B}}(\sigma')$.

We remark that the weak order on $\mathfrak{S}_n^{\mathcal{B}}$ is a lattice. Its cover relations are all those pairs of signed permutations which differ only by the sign of $\sigma(1)$ and all those pairs of signed permutations which differ only by swapping two consecutive positions $\sigma(i)$ and $\sigma(i+1)$ for some $i \in [n-1]$. See Figure 4.1 (left) for an illustration of the Hasse diagram of the weak order on $\mathfrak{S}_3^{\mathcal{B}}$.

4.1.2 Hyperplanes

We will now introduce the $\mathcal{B}_n$ hyperplane arrangement, which is a geometric realization for the weak order on $\mathfrak{S}_n^{\mathcal{B}}$, just as the $\mathcal{A}_n$ arrangement is for the weak order on $\mathfrak{S}_n$.

Definition 4.1.4 (The $\mathcal{B}_n$ Arrangement)**.** The **type $\mathcal{B}$ arrangement** denoted by $\mathcal{B}_n$ is the arrangement of all hyperplanes of the form $\{\mathbf{x} \in \mathbb{R}^n \mid x_a = x_b\}$ for some $a, b \in [\pm n]$.

This compact description uses the virtual coordinates $x_{-i} = -x_i$. To describe all $\mathcal{B}_n$ hyperplanes, we can use the notation $H_n(\ell, r) = \{\mathbf{x} \in \mathbb{R}^n \mid x_\ell = x_r\}$ introduced in Example 1.3.4 to denote $\mathcal{A}_n$ hyperplanes. This time, we allow the first index ℓ to be zero or negative, with the restriction that $|\ell| < r$.

To better understand the hyperplanes of the $\mathcal{B}_n$ arrangement, we introduce three families of hyperplanes in $\mathbb{R}^n$ by their normal vectors, each of which is oriented such that the point $(1, 2, \ldots, n)$ is on their positive side. This will be useful when introducing an orientation to construct the poset of regions of $\mathcal{B}_n$ where the canonical choice of base region will again be the one corresponding to the identity permutation id.

Observation 4.1.5 ($\mathcal{B}_n$ Hyperplane Normals)**.** The $\mathcal{B}_n$ hyperplanes are:
1. the first family of hyperplanes $H_n(0, i)$ normal to $\mathbf{e}_i$ for some $1 \leq i \leq n$,
2. the second family of hyperplanes $H_n(i, j)$ normal to $\mathbf{e}_j - \mathbf{e}_i$ for some $1 \leq i < j \leq n$,
3. the third family of hyperplanes $H_n(-i, j)$ normal to $\mathbf{e}_i + \mathbf{e}_j$ for some $1 \leq i < j \leq n$.

Given a $\mathcal{B}_n$ hyperplane H, we denote by $\mathrm{family}(H) \in \{1, 2, 3\}$ the family it belongs to. We remark that these three families can be distinguished by the sign of the first value in the $H_n(\cdot, \cdot)$ notation. We deduce that the $\mathcal{B}_n$ arrangement contains $n + \binom{n}{2} + \binom{n}{2} = n^2$ hyperplanes. We can give a simple bijection from $[n] \times [n]$ to the set of $\mathcal{B}_n$ hyperplanes.

Observation 4.1.6 (Numbering $\mathcal{B}_n$ Hyperplanes)**.** Picking $a, b \in [n]$ independently,
- we assign the first family hyperplane $H_n(0, a)$ normal to $\mathbf{e}_a$ if $a = b$,
- or the second family hyperplane $H_n(a, b)$ normal to $\mathbf{e}_b - \mathbf{e}_a$ if $a < b$,
- or the third family hyperplane $H_n(-b, a)$ normal to $\mathbf{e}_a + \mathbf{e}_b$ if $a > b$.

4.1.3 Regions

Just like the regions of the $\mathcal{A}_n$ arrangement correspond to standard permutations in $\mathfrak{S}_n$, the regions of the $\mathcal{B}_n$ arrangement correspond to $\mathcal{B}$-permutations in $\mathfrak{S}_n^{\mathcal{B}}$.

Observation 4.1.7 (Regions of the $\mathcal{B}_n$ Arrangement)**.** The regions of the $\mathcal{B}_n$ arrangement are in bijection with the $\mathcal{B}$-permutations in $\mathfrak{S}_n^{\mathcal{B}}$. The $\mathcal{B}$-permutation $\sigma \in \mathfrak{S}_n^{\mathcal{B}}$ corresponds to the $\mathcal{B}_n$ region defined by

$$C(\sigma) := \left\{ \mathbf{x} \in \mathbb{R}^n \;\middle|\; x_{\sigma(1)} \leq x_{\sigma(2)} \leq \cdots \leq x_{\sigma(n)} \right\}.$$

We remark that this assigns to each $\mathcal{B}$-permutation σ the unique the region of the arrangement containing the point $(\sigma^{-1}(1), \sigma^{-1}(2), \ldots, \sigma^{-1}(n))$. The canonical choice of base region is $C(\mathsf{id}_n)$, which is labeled by the identity permutation id_n and contains the point $(1, 2, \ldots, n)$. See Figure 4.1 (center) for an illustration of the $\mathcal{B}_3$ arrangement with their regions labelled by signed permutations.

4.1.4 Rays

The rays of the $\mathcal{B}_n$ arrangement correspond to the non-trivial faces of the n-dimensional cube C_n in the following way: $\mathcal{B}_n$ is the arrangement of reflection hyperplanes of C_n. This is illustrated in Figure 4.1 (center), which shows the intersection of the $\mathcal{B}_n$ hyperplanes with the C_n cube. Every non-empty face F of the cube has a unique canonical outer normal vector $\mathbf{v}(\mathsf{F}) \in \{-1, 0, +1\}^n$. For the entire cube as a trivial face of itself, we set $\mathbf{v}(\mathsf{C}_n) = (0, \ldots, 0)$, which is the only vector in $\{-1, 0, +1\}^n$ that is not a $\mathcal{B}_n$ ray. This allows us to count the rays of $\mathcal{B}_n$ without much effort and with an equality to the number of non-trivial cube faces.

Observation 4.1.8 (Number of $\mathcal{B}_n$ Rays)**.** The number of $\mathcal{B}_n$ rays is $3^n - 1 = \sum_{d=1}^{n} 2^d \binom{n}{d}$.

We can also represent such a vector by the corresponding subset $I(\mathsf{F}) \subset [\pm n]$ containing the non-zero coordinates of the vector, signed accordingly. For example, the cube face with outer normal vector $(0, 1, 0, -1)$ corresponds to the set $2\overline{4}$. For an i-dimensional face F_i, the vector $\mathbf{v}(\mathsf{F}_i)$ has exactly i zeros and $|I(\mathsf{F}_i)| = n - i$.

Conversely, to every non-empty signed index set $\emptyset \subsetneq I \subsetneq [\pm n]$ with $\{-i, i\} \not\subseteq I$ for all $i \in [n]$, we assign the ray vector $\mathbf{r}(I) := \sum_{i \in I} \mathbf{e}_i$ and the ray cone $C(I) := \mathrm{cone}(\mathbf{r}(I))$. This construction gives us a bijection between $\mathcal{B}_n$ rays and proper signed index sets in the above sense.

As the arrangement is n-dimensional and simplicial, every region has exactly n rays. We will collect the tools necessary to describe the rays of a region in more detail in Section 4.1.7. Let us just remark here that the $\mathcal{B}_n$ region $C(\sigma)$ is the polyhedral cone spanned by the rays $C(\sigma([k, n]))$ for all $k \in [n]$.

4.1.5 Type Cone

We briefly discuss the fan of the type $\mathcal{B}$ arrangement and its type cone, containing all height functions that induce polytopes whose normal fan is that arrangement fan.

Definition 4.1.9 (The $\mathcal{B}_n$ Fan)**.** The fan of $\mathcal{B}_n$ is called the **type $\mathcal{B}$ fan** and denoted by $\mathcal{F}_n^{\mathcal{B}}$.

For an illustration of $\mathcal{F}_3^{\mathcal{B}}$, see Figure 4.2. We will now construct the type cone of the fan $\mathcal{F}_n^{\mathcal{B}}$. As the rays of $\mathcal{B}_n$ are in bijection with the proper faces of C_n, we will have a closer look at their combinatorial structure first.

Definition 4.1.10 (Maximal Flag of a Polytope)**.** A **maximal flag** of a polytope P is a chain of faces $\mathsf{F}_{-1} \subset \mathsf{F}_0 \subset \cdots \subset \mathsf{F}_{n-1} \subset \mathsf{F}_n$ such that each F_i is an i-dimensional face of P. The maximal flags of a polytope are in bijection with the maximal chains from bottom to top in the polytope's face lattice.

Observation 4.1.11 (Regions of $\mathcal{B}_n$ as Cube Faces)**.** The regions of the $\mathcal{B}_n$ arrangement are in bijection with the maximal flags of the n-cube. The set differences $I(\mathsf{F}_{i-1}) \setminus I(\mathsf{F}_i)$ of any maximal flag are singletons for $i \in [n]$. They can be used to recover the associated signed permutation by setting $\sigma(i) := I(\mathsf{F}_{i-1}) \setminus I(\mathsf{F}_i)$ for $i \in [n]$. Conversely, the rays of a region corresponding to the maximal chain $\mathsf{F}_{-1} \subset \mathsf{F}_0 \subset \cdots \subset \mathsf{F}_{n-1} \subset \mathsf{F}_n$ are exactly the vectors $\mathbf{v}(\mathsf{F}_0), \ldots, \mathbf{v}(\mathsf{F}_{n-1})$.

We recall the definition of wall-crossing inequalities as described in Definition 1.2.27. We can use the description of $\mathcal{B}_n$ regions as maximal flags to determine these inequalities for the $\mathcal{B}_n$ fan.

Lemma 4.1.12 ($\mathcal{B}_n$ Ray Exchanges)**.** *The equalities between the rays of adjacent regions of $\mathcal{B}_n$ are of one of the following shapes:*

- $\mathbf{v}(\mathsf{F}_0) + \mathbf{v}(\mathsf{F}'_0) = 2\mathbf{v}(\mathsf{F}_1)$ *for all* $\mathsf{F}_0, \mathsf{F}'_0 \subset \mathsf{F}_1$
- $\mathbf{v}(\mathsf{F}_i) + \mathbf{v}(\mathsf{F}'_i) = \mathbf{v}(\mathsf{F}_{i-1}) + \mathbf{v}(\mathsf{F}_{i+1})$ *for all* $\mathsf{F}_{i-1} \subset \mathsf{F}_i, \mathsf{F}'_i \subset \mathsf{F}_{i+1}$*, where* $0 < i < n$.

Proof. Let R be a $\mathcal{B}_n$ region with associated signed permutation $\sigma \in \mathfrak{S}_n^{\mathcal{B}}$ and associated maximal flag $\mathsf{F}_{-1} \subset \cdots \subset \mathsf{F}_n$. Recall from Section 4.1.1 that the signed permutations of all regions neighboring to R are obtained by either changing the sign of $\sigma(1)$ or exchanging $\sigma(i)$ and $\sigma(i+1)$ for some $i \in [n-1]$.

Changing the sign of $\sigma(1)$ corresponds to replacing the vertex F_0 by the unique other endpoint of the edge F_1. This gives the equation $\mathbf{v}(\mathsf{F}_0) + \mathbf{v}(\mathsf{F}'_0) = 2\mathbf{v}(\mathsf{F}_1)$. It is independent of the choices of higher-dimensional faces in the flag. Exchanging $\sigma(i)$ and $\sigma(i+1)$ for $0 < i < n$ corresponds to replacing the face F_i by the unique other face F'_i with the properties $\mathsf{F}_{i-1} \subset \mathsf{F}'_i \subset \mathsf{F}_{i+1}$. That exchange is unique due to the diamond property of polytope face lattices. The exchange of the faces gives the equation $\mathbf{v}(\mathsf{F}_i) + \mathbf{v}(\mathsf{F}'_i) = \mathbf{v}(\mathsf{F}_{i-1}) + \mathbf{v}(\mathsf{F}_{i+1})$. This equation is the same for all pairs of adjacent regions with rays $\mathbf{v}(\mathsf{F}_{i-1})$ and $\mathbf{v}(\mathsf{F}_{i+1})$. □

Given a lattice L, a subposet P of L is commonly known as a **diamond** if it consists exactly of elements a, b, c, d, whose only cover relations are $a \prec b, c$ and $b, c \prec d$. The exchangeable pairs of rays of the $\mathcal{B}_n$ arrangement are in bijection with the diamonds in the face lattice of the n-cube. We are now ready to describe and count all pairs of exchangeable rays and the geometric object that these exchanges form: The type cone of the $\mathcal{B}_n$ arrangement fan $\mathcal{F}_n^{\mathcal{B}}$.

Corollary 4.1.13 ($\mathcal{B}_n$ Type Cone)**.** Let $\mathsf{C}_n^{\mathsf{F}}$ be the set of proper faces of the n-cube C_n. The type cone $TC(\mathcal{B}_n)$ is the set of all height functions $h : \mathsf{C}_n^{\mathsf{F}} \to \mathbb{R}_{\geq 0}$ with

- $h(\mathsf{F}_0) + h(\mathsf{F}'_0) < 2h(\mathsf{F}_1)$ for all $\mathsf{F}_0, \mathsf{F}'_0 \subset \mathsf{F}_1$,
- $h(\mathsf{F}_i) + h(\mathsf{F}'_i) < h(\mathsf{F}_{i-1}) + h(\mathsf{F}_{i+1})$ for all $\mathsf{F}_{i-1} \subset \mathsf{F}_i, \mathsf{F}'_i \subset \mathsf{F}_{i+1}$, where $0 < i < n$.

We can now use a simple counting argument in the face lattice of the n-dimensional cube to deduce information on the type cone of the $\mathcal{B}_n$ arrangement fan.

Lemma 4.1.14 (Counting Diamonds)**.** *The number of diamonds in the face lattice of C_n is*

$$2^{n-1}n + 3^{n-2}n(n-1).$$

Proof. We count those diamonds whose bottom element is F_{-1} separately: Their number equals the number of edges of the n-cube, which is $2^{n-1}n$. For diamonds with bottom element F_{i-1}, where $0 < i < n$, we note that the number of $(i-1)$-faces of the n-cube is $2^{n-i+1}\binom{n}{i-1}$. The number of $(i+1)$-faces containing a given F_{i-1}-face is $\binom{n-i+1}{2}$. So for a given i, the number of face pairs $\mathsf{F}_{i-1} \subset \mathsf{F}_{i+1}$ is $2^{n-i+1}\binom{n}{i-1}\binom{n-i+1}{2} = 2^{n-i}n(n-1)\binom{n-2}{i-1}$. Summing up, we get a total of $2^{n-1}n + n(n-1)\sum_{i=1}^{n-1} 2^{n-i}\binom{n-2}{i-1} = 2^{n-1}n + n(n-1)3^{n-2}$. □

As we saw in Lemma 4.1.12, the diamonds in the face lattice of C_n are in bijection with the ray exchanges in the arrangement fan $\mathcal{F}_n^{\mathcal{B}}$. However, a ray exchange may be associated with multiple walls of the $\mathcal{B}_n$ arrangement, so we have to count them separately.

Lemma 4.1.15 (Number of $\mathcal{B}_n$ Walls)**.** *The number of walls in the $\mathcal{B}_n$ arrangement is $2^{n-1}n! \cdot n$.*

Proof. We can count the number of walls of the arrangement directly: Every region has n adjacent regions, so the number of walls is $n/2$ times the number of regions. This gives $2^n n! \cdot n/2$.

The number of pairs of adjacent regions can also be obtained by summing for each diamonds in the face lattice the number of maximal flags containing the diamond's top and bottom point.

- For fixed $\mathsf{F}_0 \subset \mathsf{F}_1$, there are $(n-1)!$ maximal flags containing them.
- For fixed $\mathsf{F}_{i-1} \subset \mathsf{F}_{i+1}$ with $i \in [n-1]$, we look at both sides of the remaining flag separately.
  - There are $2^{i-1}(i-1)!$ maximal flags $\mathsf{F}_0 \subset \cdots \subset \mathsf{F}_{i-1}$.
  - There are $(n-i-1)!$ maximal flags $\mathsf{F}_{i+1} \subset \cdots \subset \mathsf{F}_n$.

So in total, there are $2^{i-1}(i-1)!(n-i-1)!$ maximal flags containing fixed $\mathsf{F}_{i-1} \subset \mathsf{F}_{i+1}$. This way, we obtain the same number of walls as a result of the computation
$2^{n-1}n \cdot (n-1)! + \sum_{i=1}^{n-1} 2^{n-i+1}\binom{n}{i-1}\binom{n-i+1}{2} \cdot 2^{i-1}(i-1)!(n-i-1)! = 2^{n-1}n! \cdot n.$ □

4.1.6 B-Permutahedron

Just as the standard permutahedron (see Example 1.3.15) whose graph is the Hasse diagram of the weak order on $\mathfrak{S}_n$ is a zonotope of the $\mathcal{A}_n$ arrangement, there is a type $\mathcal{B}$ permutahedron associated to the weak order on $\mathfrak{S}_n^{\mathcal{B}}$ that is a zonotope of the $\mathcal{B}_n$ arrangement.

Definition 4.1.16 (Type $\mathcal{B}$ Permutahedron)**.** The **$\mathcal{B}$-Permutahedron** $\mathsf{Perm}_n^{\mathrm{B}}$ is a polytope defined equivalently as

- the convex hull of the points $\sum_{i=1}^n i\mathbf{e}_{\sigma(i)}$ for all $\mathcal{B}$-permutations $\sigma \in \mathfrak{S}_n^{\mathcal{B}}$,
- the intersection of the halfspaces $\left\{\mathbf{x} \in \mathbb{R}^n \;\middle|\; \sum_{i\in I} x_i \leq \binom{n+1}{2} - \binom{|I|+1}{2}\right\}$ for all signed index sets $\emptyset \subsetneq I \subsetneq [\pm n]$ with $\{-j, j\} \not\subseteq I$ for all $j \in [n]$,
- a translation of the Minkowski sum $\sum_{-n\leq a<b\leq n} [\mathbf{e}_a, \mathbf{e}_b]$ of all $\mathcal{B}_n$ hyperplane normals.

We can immediately deduce the number of $\mathcal{B}$-permutahedron faces of certain dimensions.

- It has $2^n \cdot n!$ vertices as $\mathcal{B}_n$ has that many regions.
- It has $2^{n-1} \cdot n \cdot n!$ edges as $\mathcal{F}_n^{\mathcal{B}}$ has that many walls.
- It has $3^n - 1$ facets as $\mathcal{B}_n$ has that many rays.

Moreover, the normal fan of the $\mathcal{B}$-permutahedron is the arrangement fan $\mathcal{F}_n^{\mathcal{B}}$ of the $\mathcal{B}_n$ arrangement. The graph of the $\mathcal{B}$-permutahedron is the Hasse diagram of the weak order on $\mathfrak{S}_n^{\mathcal{B}}$, oriented in the direction $-\sum_{i=1}^n i \cdot \mathbf{e}_i$.

Both $\mathcal{A}_n$ and $\mathcal{B}_n$ arrangements and their associated standard permutahedron Perm_n and $\mathcal{B}$-permutahedron $\mathsf{Perm}_n^{\mathrm{B}}$ are closely connected not only in a combinatorial sense, but also through geometric operations. In general, [Zie07, Lemma 7.11] states that for a polytope $\mathsf{P} \in \mathbb{R}^a$ and a projection $\varphi : \mathbb{R}^a \to \mathbb{R}^b$, the dual map $\varphi^* : \mathbb{R}^b \to \mathbb{R}^a$ gives an isomorphism between the normal fan of the projected polytope $\varphi(\mathsf{P}) \in \mathbb{R}^b$ and the section of $\mathcal{N}(\mathsf{P})$ by the image of φ^*. We can use this to relate $\mathcal{A}_{[\pm n]}$ and $\mathcal{B}_n$ arrangements and zonotopes.

Definition 4.1.17 (Centrally Symmetric Subspace)**.** Let $(\mathbf{e}_i)_{i\in[n]}$ denote the canonical basis of $\mathbb{R}^n$ (where the $\mathcal{B}_n$ arrangement and $\mathcal{B}$-permutahedron $\mathsf{Perm}_n^{\mathrm{B}}$ are defined) and let $(\mathbf{f}_j)_{j\in[\pm n]}$ denote the canonical basis of $\mathbb{R}^{[\pm n]}$ (where for the $\mathcal{A}_{[\pm n]}$ arrangement and its zonotope isomorphic to Perm_{2n} are defined). We consider the linear projection $\varphi^{\mathcal{B}} : \mathbb{R}^{[\pm n]} \to \mathbb{R}^n$ defined by $\varphi^{\mathcal{B}}(\mathbf{f}_j) := \mathbf{e}_j$ and $\varphi^{\mathcal{B}}(\mathbf{f}_{-j}) := -\mathbf{e}_j$ for all $j \in [n]$. The dual map of $\varphi^{\mathcal{B}}$ is $\varphi^{\mathcal{B}*} : \mathbb{R}^n \to \mathbb{R}^{[\pm n]}$ defined by $\varphi^{\mathcal{B}*}(\mathbf{e}_i) := \mathbf{f}_i - \mathbf{f}_{-i}$. The **centrally symmetric subspace** of $\mathbb{R}^{[\pm n]}$ is the image of the dual map $\varphi^{\mathcal{B}*}$, denoted by $\mathcal{H}_n^{\mathcal{B}} := \left\{\mathbf{x} \in \mathbb{R}^{[\pm n]} \;\middle|\; x_{-i} = -x_i \text{ for all } i \in [\pm n]\right\}$.

With this centrally symmetric subspace and the projection $\varphi^{\mathcal{B}}$, we can relate the $\mathcal{B}_n$ arrangement and its zonotope with their counterparts from $\mathcal{A}_n$.

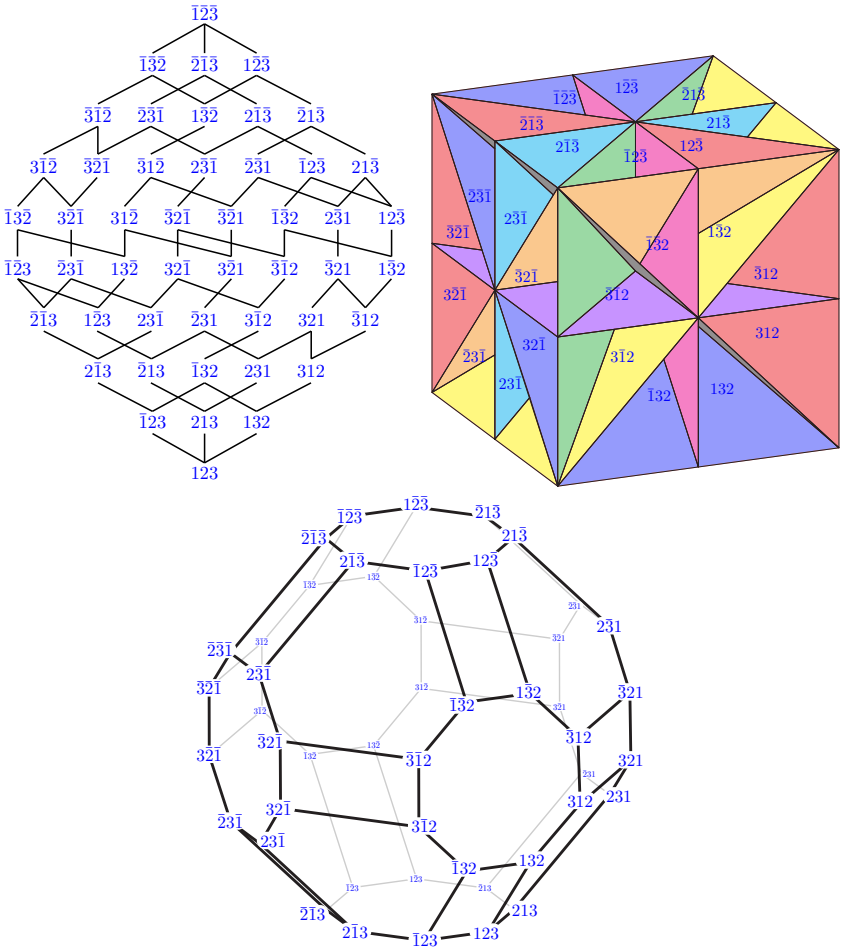

Figure 4.1: The Hasse diagram of the weak order on $\mathfrak{S}_3^{\mathcal{B}}$ (left) is isomorphic to the poset of regions of $\vec{\mathcal{B}}_3$. The arrangement fan $\mathcal{F}_3^{\mathcal{B}}$ (right) is illustrated by its intersection with the C_3 cube to indicate the correspondence between $\mathcal{B}_3$ rays and C_3 faces and the $\mathcal{B}_n$ hyperplanes being the reflection hyperplanes of C_3. The $\mathcal{B}$-permutahedron $\mathsf{Perm}_3^{\mathsf{B}}$ (bottom) is a polytope whose normal fan is the $\mathcal{F}_3^{\mathcal{B}}$ arrangement fan and whose vertex graph is the Hasse diagram of the weak order on $\mathfrak{S}_3^{\mathcal{B}}$. [Picture from [PPR20]]

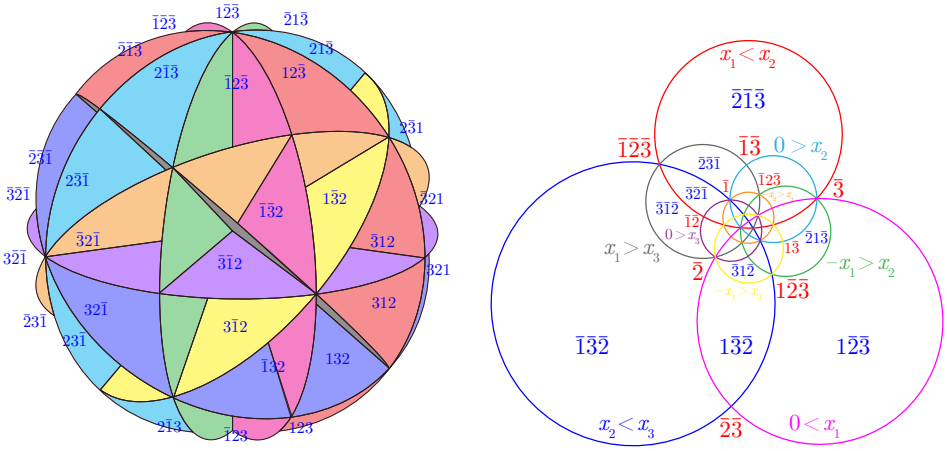

Figure 4.2: The arrangement fan $\mathcal{F}_3^{\mathcal{B}}$, intersected with a unit ball in $\mathbb{R}^3$ (left) and as a stereographic projection of the great circles to a 2-dimensional plane (right). [Picture from [PPR20]]

Observation 4.1.18 (Connecting $\mathcal{B}_n$ and $\mathcal{A}_n$ Arrangements)**.** The $\mathcal{B}_n$ arrangement is the section of the $\mathcal{A}_{[\pm n]}$ arrangement by the centrally symmetric subspace $\mathcal{H}_n^{\mathcal{B}}$. The $\mathcal{B}$-permutahedron $\mathsf{Perm}_n^{\mathrm{B}}$ is the image of the standard permutahedron Perm_n by the projection map $\varphi^{\mathcal{B}}$.

4.1.7 The Poset of Rays

We will now examine a partial order on the rays of $\mathcal{B}_n$ that will help us to understand the combinatorial structure of the regions and, later, the shards of $\mathcal{B}_n$.

Definition 4.1.19 (Poset of $\mathcal{B}_n$ Rays)**.** The **poset of rays** of $\mathcal{B}_n$ is the set of all nonzero vectors $\mathbf{r} \in \{-1, 0, +1\}^n$, partially ordered by inclusion of their associated n-cube faces. Equivalently, $\mathbf{r} \leq \mathbf{r}'$ if and only if every entry r'_i is either zero or equal to r_i for $i \in [n]$.

We observe that the maximal rays in the poset are all positive and negative unit vectors $\pm\mathbf{e}_i$ for $i \in [n]$. The minimal rays in the poset are the vectors $\{-1, +1\}^n$. We recall some definitions revolving around posets and introduce a notation for one of them.

Definition 4.1.20 (Lower Sets)**.** Let $(P, \leq)$ be a poset. A subset $S \subseteq P$ is called a **lower set** in P if $x \in S$ and $y \in P$ with $y \leq x$ imply that $y \in S$. A lower set S is called a **principal lower set** if it has a unique maximum element $m \in S$ such that $s \leq m$ for all $s \in S$. Given an antichain of poset elements $\{a_1, \ldots, a_k\} \subseteq P$, we denote by $\downarrow(\{a_1, \ldots, a_k\})$ the unique lower set in which the maximal elements are $a_1, \ldots, a_k$. Whenever it is clear that $a_1, \ldots, a_k$ are poset elements, not sets, we omit the curly brackets and just write $\downarrow(a_1, \ldots, a_k)$. As a convention, we fix $\downarrow(\mathbf{0}) = P$ and $\downarrow(\emptyset) = \emptyset$.

Observation 4.1.21. The principal lower set $\downarrow(\mathbf{e}_i)$ contains 3^{n-1} rays for every $i \in [n]$. The principal lower set of one ray of the form $\pm\mathbf{e}_i \pm \mathbf{e}_j$ contains 3^{n-2} rays.

Observation 4.1.22. As we denote indices and vectors by lower case and sets by upper case, we will carefully use the notations $-E(X) := \{-\mathbf{e}_i : i \in X\}$ and $E(-Y) := \{\mathbf{e}_i : -i \in Y\}$.

For the remainder of this section, we introduce some rather technical lemmas to deal with lower sets in the poset of rays. They will be used later in our proofs for the geometry of $\vec{\mathcal{B}}_n$ shards.

Lemma 4.1.23 (Arithmetics in the Poset of $\mathcal{B}_n$ Rays)**.** *Let A, B be disjoint subsets of $[n]$. Then*

- $\downarrow(E_A) \cup \downarrow(E_B) = \downarrow(E_{A \cup B})$,
- $\downarrow(\sum_{k \in A} \mathbf{e}_k) \cap \downarrow(\sum_{k \in B} \mathbf{e}_k) = \downarrow(\sum_{k \in A \cup B} \mathbf{e}_k)$,
- $\bigcup_{J \subseteq A} (\downarrow(\sum_{k \in J} \mathbf{e}_k) \setminus \downarrow(E_{A \setminus J})) = \{-1, 0, +1\}^n \setminus \{\mathbf{0}\}$.

Proof. For the first two statements, we repeatedly apply the simple facts

- $\downarrow(\mathbf{e}_a) \cup \downarrow(\mathbf{e}_b) = \downarrow(\mathbf{e}_a, \mathbf{e}_b)$
- and $\downarrow(\mathbf{e}_a) \cap \downarrow(\mathbf{e}_b) = \downarrow(\mathbf{e}_a + \mathbf{e}_b)$

for distinct indices $a, b \in [n]$. In the last statement, the left-hand side clearly is a subset of the right-hand side. To prove the converse, we fix a nonzero vector $\mathbf{x} \in \{-1, 0, +1\}^n$ and use the set $J_{\mathbf{x}} := \{a \in A \mid x_a = 1\}$. Then $\mathbf{x} \in \downarrow(\sum_{k \in J_x} \mathbf{e}_k)$ and $\mathbf{x} \notin \downarrow(E_{A \setminus J_x})$. Therefore, $\mathbf{x}$ is contained in the left-hand side set. □

We will need some more set-theoretic tools, that are simple, yet not immediately clear. We prove them here for the sake of completeness.

Lemma 4.1.24 (technical)**.** *Let I be a finite set of indices such that there are finite sets of $\mathcal{B}_n$ rays $T_i \subseteq S_i$ for all $i \in I$. For an index set $J \subseteq I$, let $\overline{J}$ denote its complement $I \setminus J$, let $S(J)$ denote the union $\bigcup_{j \in J} S_j$ and let $T(J)$ denote the intersection $\bigcap_{j \in J} T_j$, where $T(\emptyset) := \bigcup_{i \in I} S_i$. Then*

$$\bigcup_{i \in I} (S_i \setminus T_i) = \bigcup_{i \in I} S_i \setminus \bigcup_{J \subseteq I} (T(J) \setminus S(\overline{J})).$$

Proof. Let $\mathbf{x} \in \bigcup_{i \in I} S_i$. Then $\mathbf{x}$ is contained in $\bigcup_{i \in I}(S_i \setminus T_i)$ if and only if there is at least one index $k \in I$ such that $x \in S_k$, but $\mathbf{x} \notin T_k$.

First assume there is such a $k \in I$. Let $J \subseteq I$ be an arbitrary subset of indices. If $k \in J$, then $\mathbf{x} \notin T(J)$. If $k \notin J$, the index k is in $\overline{J}$, so $\mathbf{x} \in S(\overline{J})$. In any case, x is not contained in $T(J) \setminus S(\overline{J})$. Therefore, $\mathbf{x}$ is not contained in their union over all $J \subseteq I$ and thus contained in the right-hand side set.

Now assume there is no such k. Let $J_{\mathbf{x}} \subseteq I$ denote the index set (possibly empty) of all $j \in I$ such that $x \in T_j$. Then by assumption, $\mathbf{x} \notin S_i$ for all $i \in \overline{J_{\mathbf{x}}}$. Therefore, $\mathbf{x} \in T(J_x) \setminus S(\overline{J_{\mathbf{x}}})$, so it is among the elements of $\bigcup_{i \in I} S_i$ that are excluded from the right-hand side set. □

Corollary 4.1.25 (technical)**.** For finite sets $T_1 \subseteq S_1$ and $T_2 \subseteq S_2$, we obtain

$$(S_1 \setminus T_1) \cup (S_2 \setminus T_2) = (S_1 \cup S_2) \setminus \Big((T_1 \cap T_2) \cup (T_1 \setminus S_2) \cup (T_2 \setminus S_1)\Big).$$

In particular, if $T_1 = T_2$, we obtain $(S_1 \setminus T) \cup (S_2 \setminus T) = (S_1 \cup S_2) \setminus T$.

Lemma 4.1.26 (technical)**.** *The set of rays violating a given inequality among the entries of a ray vector can be described as a set difference of lower sets in the poset of rays. Let $i, j \in [n]$ be distinct integers.*

1. *The set of rays violating $r_i \leq 0$ is $\downarrow(\mathbf{e}_i) \setminus \emptyset$.*
   The set of rays violating $r_i \geq 0$ is $\downarrow(-\mathbf{e}_i) \setminus \emptyset$.
   The set of rays violating $r_i = 0$ is $\downarrow(\{\pm\mathbf{e}_i\}) \setminus \emptyset$.
2. *The set of rays violating $r_i \leq r_j$ is $\downarrow(\mathbf{e}_i, -\mathbf{e}_j) \setminus \downarrow(\mathbf{e}_i + \mathbf{e}_j, -\mathbf{e}_i - \mathbf{e}_j)$.*
   The set of rays violating $r_i = r_j$ is $\downarrow(\{\pm\mathbf{e}_i, \pm\mathbf{e}_j\}) \setminus \downarrow(\mathbf{e}_i + \mathbf{e}_j, -\mathbf{e}_i - \mathbf{e}_j)$.
3. *The set of rays violating $r_i \leq -r_j$ is $\downarrow(\mathbf{e}_i, \mathbf{e}_j) \setminus \downarrow(\mathbf{e}_i - \mathbf{e}_j, \mathbf{e}_j - \mathbf{e}_i)$.*
   The set of rays violating $-r_i \leq r_j$ is $\downarrow(-\mathbf{e}_i, -\mathbf{e}_j) \setminus \downarrow(\mathbf{e}_i - \mathbf{e}_j, \mathbf{e}_j - \mathbf{e}_i)$.
   The set of rays violating $-r_i = r_j$ is $\downarrow(\{\pm\mathbf{e}_i, \pm\mathbf{e}_j\}) \setminus \downarrow(\mathbf{e}_i - \mathbf{e}_j, \mathbf{e}_j - \mathbf{e}_i)$.

Proof. In each case, the set of rays violating the equality is equal to the union of the sets of rays violating either inequality.

1. The rays violating $r_i \leq 0$ are exactly the rays with $r_i = 1$. By definition of the poset of rays, these are exactly the rays $\leq \mathbf{e}_i$. An analogous argument holds for $r_i \geq 0$.
2. The rays violating $r_i \leq r_j$ are the rays with $r_i = 1$ (hence below $\mathbf{e}_i$) or $r_j = -1$ (hence below $-\mathbf{e}_j$) except for those rays with $r_i = r_j \in \{\pm 1\}$ (which are exactly the ones below $\mathbf{e}_i + \mathbf{e}_j$ or below $-\mathbf{e}_i - \mathbf{e}_j$).
3. The rays violating $r_i \leq -r_j$ are the rays with $r_i = 1$ (hence below $\mathbf{e}_i$) or $-r_j = -1$ (hence below $\mathbf{e}_j$) except for those rays with $-r_i = r_j \in \{\pm 1\}$ (which are exactly the ones below $\mathbf{e}_i - \mathbf{e}_j$ or below $\mathbf{e}_j - \mathbf{e}_i$). An analogous argument holds for $-r_i \leq r_j$. □

Example 4.1.27. The above lemma gives us a more formal way to state simple properties of $\mathcal{B}_n$ rays and $\mathcal{B}_n$ hyperplanes. For example, let us take a look at the halfspace defined by $x_i \leq x_j$. The set $\downarrow(\mathbf{e}_i, -\mathbf{e}_j) \setminus \downarrow(\mathbf{e}_i + \mathbf{e}_j, -\mathbf{e}_i - \mathbf{e}_j)$ can be described as follows: If $x_i = 1$ or $x_j = -1$, then $\mathbf{r}$ does not comply with the restriction except for the cases where $x_i = x_j = 1$ or $x_i = x_j = -1$.

4.2 Type B Shards

We will now examine the oriented arrangement $\vec{\mathcal{B}}_n$ induced by the choice of a base region of $\mathcal{B}_n$. By convention, we designate the region containing $(1, 2, \ldots, n)$ as base region. To analyze the poset of regions $\mathrm{Pos}(\vec{\mathcal{B}}_n)$, we recall that the join-irreducibles in the poset of regions of any oriented simplicial arrangement are in bijection with the shards of the arrangement. We will construct them geometrically from first principles of shards and carefully analyze their forcing relation.

4.2.1 Rank-Two Subarrangements

We start our discussion of $\vec{\mathcal{B}}_n$ shards with an overview of rank-two subarrangements of $\vec{\mathcal{B}}_n$ as defined in Definition 1.5.1. We recall that if a rank-two subarrangement contains only two hyperplanes, neither of them cuts the other. We will call such a subarrangement **trivial**.

Lemma 4.2.1 (Subarrangements of $\vec{\mathcal{B}}_n$)**.** *There are three classes of non-trivial subarrangements of $\vec{\mathcal{B}}_n$. In each of them, the first two are basic hyperplanes, written in **boldface**.*

1. $\{\mathbf{e_i},\ \mathbf{e_j}-\mathbf{e_i},\ e_j,\ e_i+e_j\}$ *(where $i<j$),*
2. $\{\mathbf{e_j}-\mathbf{e_i},\ \mathbf{e_k}-\mathbf{e_j},\ e_k-e_i\}$ *(where $i<j<k$),*
3. $\{\mathbf{e_j}-\mathbf{e_i},\ \mathbf{e_i}+\mathbf{e_p},\ e_j+e_p\}$ *(where $i<j$ and $p\in[n]\setminus\{i,j\}$).*

Observation 4.2.2 (Number of Subarrangements of $\vec{\mathcal{B}}_n$)**.** There are $\binom{n}{2}$ subarrangements of the first type and $\binom{n}{3}$ of the second type and $\binom{n}{2}(n-2)$ of the third type. In total, the number of non-trivial rank-two subarrangements is $\frac{1}{6}n(n-1)(4n-5)$. Note that each rank-two subarrangements of the first type is isomorphic to the $\mathcal{B}_2$ arrangement, while the ones of the second and third type are isomorphic to the $\mathcal{A}_2$ arrangement.

We can rewrite the list of subarrangements using the $H_n(a,b)$ notation as follows:

Observation 4.2.3 (Subarrangements of $\vec{\mathcal{B}}_n$)**.** The rank-two subarrangements of $\vec{\mathcal{B}}_n$ are the following subarrangements for all $i,j\in[n]$ with $i<j$.

1. $\{\mathbf{H_n(0,i)},\mathbf{H_n(i,j)},H_n(0,j),H_n(-i,j)\}$,
2. $\{\mathbf{H_n(i,j)},\mathbf{H_n(j,k)},H_n(i,k)\}$ for each $k\in]j,n]$,
3. $\{\mathbf{H_n(i,j)},\mathbf{H_n(-k,i)},H_n(-k,j)\}$ for each $k\in[1,i[$,
4. $\{\mathbf{H_n(i,j)},\mathbf{H_n(-i,k)},H_n(-k,j)\}$ for each $k\in]i,j[$,
5. $\{\mathbf{H_n(i,j)},\mathbf{H_n(-i,k)},H_n(-j,k)\}$ for each $k\in]j,n]$.

We recall the notion of hyperplane cutting from Definition 1.5.2. We can now deduce all cutting relations in the $\vec{\mathcal{B}}_n$ arrangement from the rank-two subarrangements we just introduced.

Lemma 4.2.4 (Hyperplane Cutting Table for $\vec{\mathcal{B}}_n$)**.** *Let $a,b,\ell,r\in[-n,n]$ with $|\ell|<r$ and $|a|<b$. Then the following are all cases where $H_n(a,b)$ cuts $H_n(\ell,r)$:*

	$\ell=0$	$\ell>0$	$\ell<0$
$a=0$	*if* $0=\ell=a<b<r$	—	*if* $\ell=-b<-a=0<r$
$a>0$	*if* $0=\ell<a<b=r$	*if* $0<\ell=a<b<r$ *or* $0<\ell<a<b=r$	*if* $\ell=-b<-a<0<r$ *or* $\ell<0<+a<+b=r$
$a<0$	—	—	*if* $\ell=+a<0<+b<r$ *or* $\ell<+a<0<+b=r$ *or* $\ell=-b<0<-a<r$

We can rephrase this statement in a more compact way.

Corollary 4.2.5 (Hyperplane Cutting in $\vec{\mathcal{B}}_n$)**.** Let $a,b,\ell,r\in[-n,n]$ with $|\ell|<r$ and $|a|<b$. Then $H_n(a,b)$ cuts $H_n(\ell,r)$ exactly in the following three cases.

- $\ell=a$ and $b<r$,
- $\ell<a\neq 0$ and $b=r$,
- $\ell=-b$ and $-a<r$

In particular, if we set $I=\{|a|,|b|,|\ell|,|r|\}$, then $|I|<4$ whenever $H_n(a,b)$ cuts $H_n(\ell,r)$.

4.2.2 Preparing Shards

In this rather technical section, we make some preparations to determine the shards of the $\vec{\mathcal{B}}_n$ arrangement. We do so by introducing a class of polyhedral cones that generalize $\mathcal{B}_n$ hyperplanes and $\mathcal{B}_n$ halfspaces.

Definition 4.2.6 ($S_n(U,V)$)**.** Given two signed index sets $U, V \subseteq [-n,n]$, we define the set $S_n(U,V) := \{\mathbf{x} \in \mathbb{R}^n \mid \forall u \in U, v \in V : x_u \leq x_v\}$ with the usual conventions $x_{-i} := -x_i$ and $x_0 := 0$.

Observation 4.2.7. $S_n(U,V)$ is contained in the subspace $\{x \in \mathbb{R}^n \mid \forall i,j \in U \cap V : x_i = x_j\}$.

We observe that $S_n(U,V)$ is a closed polyhedral cone. We can prove this in two different ways: Firstly, for every $\mathbf{x} \in S_n(U,V)$ and $\lambda \in \mathbb{R}_{\geq 0}$, the scalar multiple λx is contained in $S_n(U,V)$ as well. Secondly, we observe that $S_n(U,V)$ is the intersection of halfspaces induced by $\mathcal{B}_n$ hyperplanes.

Observation 4.2.8 (Nested $S_n(U,V)$)**.** Given sets $U_1, U_2, V_1, V_2 \subset [-n,n]$ with $U_1 \subseteq U_2$ and $V_1 \subseteq V_2$, we have $S_n(U_1,V_1) \supseteq S_n(U_2,V_2)$.

We will make heavy use of the notions of Section 4.1.7 and the notation introduced right at the beginning of Chapter 4.

Lemma 4.2.9 ($\mathcal{B}_n$ Rays not in $S_n(U,V)$)**.** *The set of all $\mathcal{B}_n$ rays not contained in $S_n(U,V)$ is given by $\downarrow\big(E(U^+ \cup -V^-) \cup -E(V^+ \cup -U^-)\big) \setminus T$, where T is the minimal set containing*

1. *$\downarrow(\sum_{k\in V^+} \mathbf{e}_k - \sum_{k\in -V^-} \mathbf{e}_k) \subseteq T$ if $V^\pm = \emptyset$, and*
2. *$\downarrow(\sum_{k\in -U^-} \mathbf{e}_k - \sum_{k\in U^+} \mathbf{e}_k) \subseteq T$ if $U^\pm = \emptyset$,*

and T is empty if $U^\pm \neq \emptyset \neq V^\pm$.

Proof. We give a non-constructive proof. We first show that every $\mathcal{B}_n$ ray vector not in $S_n(U,V)$ is in the set. Then we will show that no $\mathcal{B}_n$ ray vector contained in $S_n(U,V)$ is in the set.

1. Let $\mathbf{x}$ be a $\mathcal{B}_n$ ray vector that is not in $S_n(U,V)$. Then there are $u \in U, v \in V$ such that $x_u > x_v$. Therefore, either $x_u = 1$ or $x_v = -1$ or both.
   - If $x_u = 1$ and $u > 0$, then $u \in U^+$, so $x \in E(U^+ \cup -V^-)$.
   - If $x_u = 1$ and $u < 0$, then $u \in -U^-$, so $x \in -E(V^+ \cup -U^-)$.
   - If $x_v = -1$ and $v > 0$, then $v \in V^+$, so $x \in -E(V^+ \cup -U^-)$.
   - If $x_v = -1$ and $v < 0$, then $v \in -V^-$, so $x \in E(U^+ \cup -V^-)$.

   It is left to show that $\mathbf{x} \notin T$. As $x_u > x_v$, we know that
   - $x_u \neq -1$ (thus $x \not\leq \sum_{k\in -U^-} \mathbf{e}_k - \sum_{k\in U^+} \mathbf{e}_k$ if $U^\pm = \emptyset$),
   - and $x_v \neq 1$ (thus $x \not\leq \sum_{k\in V^+} \mathbf{e}_k - \sum_{k\in -V^-} \mathbf{e}_k$ if $V^\pm = \emptyset$),

   so we can conclude that $\mathbf{x} \notin T$.
2. Let $\mathbf{x}$ be a $\mathcal{B}_n$ ray that is contained in $S_n(U,V)$. Then $x_u \leq x_v$ for all $u \in U$ and $v \in V$. Assume $\mathbf{x} \in \downarrow\big(E(U^+ \cup -V^-) \cup -E(V^+ \cup -U^-)\big)$. It is left to show that $\mathbf{x} \in T$. We observe that least one of the following has to hold:
   - Given an $i \in U^+$ such that $x_i = 1$ or an $i \in -U^-$ such that $x_i = -1$, we know that $x_v = 1$ for all $v \in V$, in particular, $0 \notin V$. Therefore, if $V^\pm = \emptyset$, we have $x \leq \sum_{k\in V^+} \mathbf{e}_k - \sum_{k\in -V^-} \mathbf{e}_k$.
   - Given an $i \in -V^-$ such that $x_i = 1$ or an $i \in V^+$ such that $x_i = -1$, we know that $x_u = -1$ for all $u \in U$, in particular $0 \notin U$. Therefore, if $U^\pm = \emptyset$, we have $x \leq \sum_{k\in -U^-} \mathbf{e}_k - \sum_{k\in U^+} \mathbf{e}_k$.

   We conclude that $\mathbf{x} \in T$ as desired. □

Observation 4.2.10. Given $U, V \subseteq [-n,n]$, we define three auxiliary sets of indices:

- $J_{UV} := (U^+ \cap V^+) \cup (-U^- \cap -V^-)$
- $J_U := (U^+ \cap -U^-) \setminus (V^+ \cup -V^-)$
- $J_V := (V^+ \cap -V^-) \setminus (U^+ \cup -U^-)$

Then J_{UV}, J_U and J_V are pairwise disjoint and their union is $(U^+ \cup -V^-) \cap (V^+ \cup -U^-)$.

Proposition 4.2.11 (Dimension of $S_n(U,V)$)**.** *Let $U, V \subset [-n,n]$. Then*

$$\dim S_n(U,V) = \begin{cases} n - |J_{UV}| - |J_U| - |J_V| & \text{if } U^{\pm} \neq \emptyset \neq V^{\pm}, \\ n - |J_{UV}| + 1 & \text{if } \big(U^{\pm} = \emptyset \text{ or } V^{\pm} = \emptyset\big) \text{ and } J_{UV} \neq \emptyset, \\ n & \text{if } \big(U^{\pm} = \emptyset \text{ or } V^{\pm} = \emptyset\big) \text{ and } J_{UV} = \emptyset. \end{cases}$$

Proof. We will prove the statement in two steps. First, we will show that the $\geq$ direction of these equalities hold. Then, we will give a proof for their $\leq$ direction.

To show that the given expressions are lower bounds for $\dim S_n(U,V)$, we will collect a set of linearly independent rays contained in $S_n(U,V)$. As it is a linear cone, it contains the positive linear span of these rays, so its dimension has to be at least the number of these rays.

1. We set $I := [n] \setminus (J_{UV} \dot\cup J_U \dot\cup J_V)$. Then for every $k \in I$, either $k \notin U^+ \cup -V^-$ or $k \notin V^+ \cup -U^-$ or both. In the first case, the ray $\mathbf{e}_k$ is contained in $S_n(U,V)$. In the second case, the ray $-\mathbf{e}_k$ is contained in $S_n(U,V)$. In this way, the indices in I induce a set of distinct linearly independent rays contained in $S_n(U,V)$, so its dimension is at least $|I| = n - |J_{UV}| - |J_U| - |J_V|$.
2. If $U^{\pm} = \emptyset$, then $|J_U| = 0$ and for every $\ell \in J_V$, the ray $\mathbf{e}_\ell + \sum_{k \in -U^-} \mathbf{e}_k - \sum_{k \in U^+} \mathbf{e}_k$ is contained in $S_n(U,V)$. All these $|J_V|$ rays together with the ones constructed from I are distinct, linearly independent and contained in $S_n(U,V)$. Therefore, the dimension is at least $|I| + |J_V| = n - |J_{UV}|$. If J_{UV} is empty, this is equal to n. If it is not empty, then for every $\ell \in J_{UV}$, neither $\mathbf{e}_\ell$ nor $-\mathbf{e}_\ell$ is contained in $S_n(U,V)$, so the sum $\sum_{k \in -U^-} \mathbf{e}_k - \sum_{k \in U^+} \mathbf{e}_k$ itself is not only contained in $S_n(U,V)$, but also distinct and linearly independent from all the other rays collected so far, increasing the lower bound by one. An analogous argument holds if $V^{\pm} = \emptyset$.

It remains to show that the expressions are valid upper bounds for $\dim S_n(U,V)$. We will collect a set of vectors that are orthogonal to everything in $S_n(U,V)$. If the vectors in our collection are linearly independent, then the dimension of $S_n(U,V)$ is at most n minus the size of our collection.

1. For the first case, assume $U^{\pm} \neq \emptyset \neq V^{\pm}$. We distinguish cases by the shape of J_U and J_V.
   a) If $J_U \neq \emptyset \neq J_V$, then for every pair of $u \in J_U$ and $v \in J_V$, the four inequalities $\pm x_u \leq \pm x_v$ are valid on $S_n(U,V)$, and they imply $\pm x_u = \pm x_v = 0$. Therefore, we have $x_k \leq 0 \leq x_k$ valid for every $k \in J_{UV}$ and thus $x_k = 0$. Therefore, $S_n(U,V)$ is orthogonal to $\mathbf{e}_k$ for every $k \in J_{UV} \dot\cup J_U \dot\cup J_V$.
   b) If $J_U \neq \emptyset = J_V$, then $V^{\pm} = \{0\}$ by our assumption. For every $k \in J_{UV}$, the inequalities $x_k \leq 0 \leq x_k$ are valid, and for every $k \in J_U$, the inequalities $\pm x_k \leq 0$ are valid for $S_n(U,V)$. In either case, $S_n(U,V)$ is orthogonal to the unit vector $\mathbf{e}_k$ for all $k \in J_{UV} \dot\cup J_U \dot\cup J_V$ (as $J_V = \emptyset$). An analogous argument holds if $J_U = \emptyset \neq J_V$.
   c) If $J_U = \emptyset = J_V$, then by assumption, $U^{\pm} = \{0\} = V^{\pm}$, so $0 \in U \cap V$. Then for every $k \in (U^+ \cup -V^-) \cap (V^+ \cup -U^-)$, the inequalities $x_k \leq 0$ and $0 \leq x_k$ are valid for $S_n(U,V)$. Therefore, $S_n(U,V)$ is orthogonal to $\mathbf{e}_k$ for every $k \in J_{UV} \dot\cup J_U \dot\cup J_V$.

   We conclude that the dimension of the subspace orthogonal to $S_n(U,V)$ is greater than or equal to $|J_{UV}| + |J_U| + |J_V|$.
2. If $J_{UV} \neq \emptyset$, we can fix $i = \min(J_{UV})$. Then $x_i \leq x_j \leq x_i$ are valid on $S_n(U,V)$ for every $j \in J_{UV} \setminus \{i\}$. Therefore, $S_n(U,V)$ is orthogonal to $\mathbf{e}_j - \mathbf{e}_i$ for every $j \in J_{UV} \setminus \{i\}$. We conclude that the dimension of the subspace orthogonal to $S_n(U,V)$ is at least $|J_{UV}| - 1$.
3. The third case holds with equality as $\dim S_n(U,V) \leq \dim \mathbb{R}^n = n$. □

Observation 4.2.12. As a byproduct, we determined the orthogonal complement of $S_n(U,V)$:

1. In the first case, it is generated by $\{\mathbf{e}_k \mid k \in J_{UV} \dot\cup J_U \dot\cup J_V\}$.
2. In the second case, it is generated by $\{\mathbf{e}_j - \mathbf{e}_i \mid i,j \in J_{UV}, i < j\}$.
3. In the third case, it contains nothing but the origin.

Corollary 4.2.13 (Dimension of $S_n(T,T)$)**.** Let $T \subset [-n,n]$. Set $I := \{|t| \mid t \in T\}$. Then

$$\dim(S_n(T,T)) = \begin{cases} n-|I| & \text{if } 0 \notin I \text{ and } |I| < |T|i, \\ n-|I|+1 & \text{else.} \end{cases}$$

Proof. We set $U = V = T$ and apply Proposition 4.2.11. Note that $J_{UV} = I \setminus \{0\}$, while both J_U and J_V are empty. We observe that $U^{\pm} = V^{\pm} = \{i \in I : -i, i \in T\}$.

- If $0 \in I$, then $0 \in U^{\pm}, V^{\pm}$, so $\dim(S_n(U,V)) = n - |J_{UV}| = n - |I| + 1$.
- If $0 \notin I$ and $|I| = |T|$, then $U^{\pm} = V^{\pm} = \emptyset$, so $\dim(S_n(U,V)) = n - |J_{UV}| + 1 = n - |I| + 1$.
- If $0 \notin I$ and $|I| < |T|$, then two elements of T add up to zero. They are both contained in $U^{\pm} \cap V^{\pm}$, so $\dim(S_n(U,V)) = n - |J_{UV}| = n - |I|$. □

4.2.3 Shard Basics

We will introduce a special case of sets of the form $S_n(U,V)$ that are defined very similarly to $\vec{\mathcal{A}}_n$ shards. We then study their properties and show that they are exactly the $\vec{\mathcal{B}}_n$ shards.

Definition 4.2.14 ($S_n(\ell, r, A, B)$)**.** Let $-n \le \ell < r \le n$. Let A, B be a pair of sets partitioning the interval $]\ell, r[$, that is, $A \cup B =]\ell, r[$ and $A \cap B = \emptyset$. We then define

$$S_n(\ell, r, A, B) := \{\mathbf{x} \in \mathbb{R}^n \mid \forall a \in A, b \in B : x_a \le x_\ell = x_r \le x_b\}.$$

Observation 4.2.15. Including ℓ and r in the notation is often redundant, but very convenient.

1. We set $\overline{A} := A \cup \{\ell, r\}$ and $\overline{B} := B \cup \{\ell, r\}$. Then $S_n(\ell, r, A, B) = S_n(\overline{A}, \overline{B})$.
2. Note that 0 is an element of $A \cup B$ if and only if $\ell < 0 < r$.
3. Assume $r + \ell \neq 0$. The set $S = S_n(\ell, r, A, B)$ is orthogonal to $\mathbf{e}_r - \mathbf{e}_\ell$. Therefore, we observe that S is contained in the hyperplane $H_n(\ell, r)$ if $|\ell| < r$ (and contained in $H_n(-r, -\ell)$ otherwise). We denote by $\mathrm{family}(S)$ the family of that hyperplane.

Definition 4.2.16 (Sherds)**.** We call $S = S_n(\ell, r, A, B)$ an **n-sherd** if the following hold.

1. $-n \le \ell < r \le n$,
2. $A \cup B =]\ell, r[$ and $A \cap B = \emptyset$,
3. if $0 \in A$, then $\overline{B} \cap -\overline{B} = \emptyset$ and if $0 \in B$, then $\overline{A} \cap -\overline{A} = \emptyset$.

We call the n-sherd **dexter** if $\ell + r > 0$ and we call it **sinister** if $\ell + r < 0$. We note that the third condition implies in particular that $\ell + r \neq 0$.

Observation 4.2.17 (Sherd Arithmetic)**.** Given a set $S_n(\ell, r, A, B)$, the following are equal:

1. $S_n(\ell, r, A, B)$
2. $S_n(-r, -\ell, -B, -A)$ (reciprocal notation)
3. $-S_n(\ell, r, B, A)$ (geometric opposite)
4. $-S_n(-r, -\ell, -A, -B)$ (geometric opposite)

In consequence, every dexter n-sherd has a reciprocal notation as a sinister n-sherd and vice versa, so dexter n-sherds and sinister n-sherds are the same objects.

Lemma 4.2.18 (Sherd Dimension)**.** *Every n-sherd is $(n-1)$-dimensional.*

Proof. Let S be an n-sherd. Let $S_n(\ell, r, A, B)$ be a dexter notation for S. To apply Proposition 4.2.11, we define $U := \overline{A} = \{\ell, r\} \cup A$ and $V := \overline{B} = \{\ell, r\} \cup B$ and set J_{UV}, J_U and J_V as in Observation 4.2.10

1. If $\ell = 0$, then $U^{\pm} = \{0\} = V^{\pm}$. We therefore find ourselves in the first case of Proposition 4.2.11. As $J_U = \emptyset = J_V$ and $J_{UV} = \{r\}$, we obtain $\dim(S) = n - 1 - 0 - 0$.

2. If $\ell \neq 0$, then $J_{UV} = \{|\ell|, r\}$. If $\ell > 0$, then $U, V \subset [n]$. Therefore, both $U^{\pm}$ and $V^{\pm}$ are empty. If $\ell < 0$, then $\ell < 0 < r$ as S is dexter and therefore, $0 \in A$ or $0 \in B$. By the definition of n-sherds, this means that $U^{\pm} = \overline{A} \cap -\overline{A} = \emptyset$ or $V^{\pm} = \overline{B} \cap -\overline{B} = \emptyset$. We conclude by using the second case of Proposition 4.2.11, giving us $\dim(S) = n-2+1$. □

Lemma 4.2.19 (Sherd Union)**.** *Every $\vec{\mathcal{B}}_n$ hyperplane is equal to the union of all n-sherds on it.*

Proof. Let H be a $\mathcal{B}_n$ hyperplane. As every n-sherd on H is a subset of H, their union is a subset of H as well. It remains to show that H is a subset of their union. We fix an arbitrary point $\mathbf{x} \in H$ and prove that there is an n-sherd on H containing x. We distinguish cases by the family of H.

1. If $\text{family}(H) = 1$, then $H = H_n(0, r)$ for some $r \in [n]$. We set $A := \{k \in]0, r[\mid x_k \leq 0\}$ and $B := \{k \in]0, r[\mid x_k > 0\}$. Then $\mathbf{x} \in S_n(0, r, A, B)$, a valid n-sherd.
2. If $\text{family}(H) = 2$, then $H = H_n(\ell, r)$ for some positions $0 < \ell < r \leq n$. We fix the sets $A := \{k \in]\ell, r[\mid x_k \leq x_i\}$ and $B := \{k \in]\ell, r[\mid x_k > x_i\}$. Then $\mathbf{x} \in S_n(\ell, r, A, B)$, a valid n-sherd.
3. If $\text{family}(H) = 3$, then $H = H_n(\ell, r)$ for some $0 < -\ell < r \leq n$. Recall that $x_{-k} = -x_k$ and $x_0 = 0$ and set $A := \{k \in]\ell, r[\mid x_k \leq x_r\}$ and $B := \{k \in]\ell, r[\mid x_k > x_r\}$. Then we have $\mathbf{x} \in S_n(\ell, r, A, B)$. We check that this is indeed a valid n-sherd: Clearly, $A \cup B =]\ell, r[$ and $A \cap B = \emptyset$ hold as well as $-n \leq \ell < r \leq n$. We check the third condition:
   - If $0 \in A$, then $0 \leq x_r$. No k with $\pm x_k > x_r \geq 0$ can exist, so $\overline{B} \cap -\overline{B} = \emptyset$.
   - If $0 \in B$, then $0 > x_r$. No k with $\pm x_k \leq x_j < 0$ can exist, so $\overline{A} \cap -\overline{A} = \emptyset$. □

Lemma 4.2.20 (Sherd Intersection)**.** *Let H be a $\mathcal{B}_n$ hyperplane and let S_1, S_2 be two distinct n-sherds on H. Then $S_1 \cap S_2 \subseteq \check{H}$ for some $\mathcal{B}_n$ hyperplane $\check{H}$ that cuts H.*

Proof. Let $H = H_n(i, j)$. Let $S_1 = S_n(i, j, A_1, B_1)$ and $S_2 = S_n(i, j, A_2, B_2)$ be two shards. Note that they are in dexter notation. As they are distinct, we can assume without loss of generality that $A_1 \setminus A_2$ is non-empty. Set $k := \max(A_1 \setminus A_2)$. Then $x_k \leq x_j$ is valid on S_1 and $x_k \geq x_j$ is valid on S_2. Therefore, $S_1 \cap S_2 \subseteq \{x \in \mathbb{R}^n \mid x_k = x_j\} = H_n(k, j)$.

It is left to show that $H_n(k, j)$ cuts H. We first assume $k = 0$. Then $0 \in A_1 \setminus A_2$, so $0 \leq x_j = x_i$ is valid on S_1, therefore $-x_i \leq x_j$ on S_1 and analogously, $-x_i \geq x_j$ on S_2. Note that $k = 0$ implies $i < 0 < j$, therefore $-i \in A_1 \setminus A_2$, which contradicts the fact that k was chosen to be maximal. But if $k \neq 0$, we see from Lemma 4.2.4 that $H_n(k, j)$ cuts $H_n(i, j)$. □

Lemma 4.2.21 (Sherd in Shard)**.** *Every n-sherd is part of a $\vec{\mathcal{B}}_n$ shard.*

Proof. Let $S = S_n(\ell, r, A, B)$ be an n-sherd in dexter notation. Then $H = H_n(\ell, r)$ is the hyperplane containing S. We need to show that for every hyperplane $\check{H}$ cutting $H_n(\ell, r)$, the set S is entirely contained in one of the closed halfspaces induced by $\check{H}$. We recall that we can find all cutting relations between hyperplanes in Lemma 4.2.4. Let $\check{H}$ be a hyperplane that cuts H.

1. If $H_n(\ell, r)$ is of the first family, then $0 = \ell < r$.
   - If $\check{H}$ is normal to $\mathbf{e}_i$ for some $i \in]0, r[$, then $i \in A \dot{\cup} B$ and S is contained in a halfspace induced by $\mathbf{e}_i$: the positive one if $i \in B$ or the negative one if $i \in A$.
   - If $\check{H}$ is normal to $\mathbf{e}_r - \mathbf{e}_i$ for some $i \in]0, r[$, then $i \in A \dot{\cup} B$ and S is contained in a halfspace induced by $\mathbf{e}_r - \mathbf{e}_i$: the positive one if $i \in A$ or the negative one if $i \in B$.
2. If $H_n(\ell, r)$ is of the second family, then $0 < \ell < r$.
   - If $\check{H}$ is normal to $\mathbf{e}_r - \mathbf{e}_k$ for some $k \in]\ell, r[$, then $k \in A \dot{\cup} B$. S is contained in a halfspace induced by $\mathbf{e}_r - \mathbf{e}_k$: the positive one if $k \in A$ or the negative one if $k \in B$.
   - If $\check{H}$ is normal to $\mathbf{e}_k - \mathbf{e}_\ell$ for some $k \in]\ell, r[$, then $k \in A \dot{\cup} B$. S is contained in a halfspace induced by $\mathbf{e}_k - \mathbf{e}_\ell$: the positive one if $k \in B$ or the negative one if $k \in A$.
3. If $H_n(\ell, r)$ is of the third family, then $\ell < 0 < r$ with $|\ell| < r$.

- If $\check{H}$ is normal to $\mathbf{e}_{|\ell|}$, we note that on H, we have $x_{-\ell} \geq 0$ if and only if $x_{-\ell} \geq x_\ell$. The sherd S is contained in a halfspace induced by $\mathbf{e}_{|\ell|}$: In the positive one if $-\ell \in B$ or in the negative one if $-\ell \in A$.
- If $\check{H}$ is normal to $\mathbf{e}_{|\ell|} - \mathbf{e}_k$ for some $k \in]0, -\ell[$, then $-k \in A \dot{\cup} B$. Note that we have $x_{-\ell} - x_k \geq 0$ if and only if $x_{-k} \geq x_\ell$. The sherd S is contained in a halfspace induced by the normal vector $\mathbf{e}_{|\ell|} - \mathbf{e}_k$: the positive one if $-k \in B$ or the negative one if $-k \in A$.
- If $\check{H}$ is normal to $\mathbf{e}_r - \mathbf{e}_k$ for some $k \in]0, r[$, then $k \in A \dot{\cup} B$. S is contained in a halfspace induced by $\mathbf{e}_r - \mathbf{e}_k$: the positive one if $k \in A$ or the negative one if $k \in B$.
- If $\check{H}$ is normal to $\mathbf{e}_{|\ell|} + \mathbf{e}_k$ for some $k \in] - \ell, r[$, then $k \in A \dot{\cup} B$. Note that we have $x_k + x_{-\ell} \geq 0$ if and only if $x_k \geq x_\ell$. S is contained in a halfspace induced by $\mathbf{e}_k + \mathbf{e}_{|\ell|}$: the positive one if $k \in B$ or the negative one if $k \in A$.
- If $\check{H}$ is normal to $\mathbf{e}_k + \mathbf{e}_r$ for some $k \in]0, -\ell[$, then $-k \in A \dot{\cup} B$. Note that we have $x_k + x_r \geq 0$ if and only if $x_{-k} \leq x_\ell$. S is contained in a halfspace induced by $\mathbf{e}_k + \mathbf{e}_r$: the positive one if $-k \in A$ or the negative one if $-k \in B$.
- If $\check{H}$ is normal to $\mathbf{e}_k + \mathbf{e}_{|\ell|}$ for some $k \in]0, -\ell[$, then $k \in A \dot{\cup} B$. Note that we have $x_k + x_{-\ell} \geq 0$ if and only if $x_k \geq x_\ell$. S is contained in a halfspace induced by $\mathbf{e}_k + \mathbf{e}_{|\ell|}$: the positive one if $k \in B$ or the negative one if $k \in A$. □

Proposition 4.2.22 (Shards of $\vec{\mathcal{B}}_n$)**.** *The set $\mathbf{\Sigma}^{\mathcal{B}}$ of all shards of $\vec{\mathcal{B}}_n$ contains exactly the n-sherds.*

Proof. We know from Lemma 4.2.19 that every $\mathcal{B}_n$ hyperplane H is the union of all n-sherds on H. Therefore, every $\vec{\mathcal{B}}_n$ shard intersects at least one n-sherd. We know from Lemma 4.2.21 that every n-sherd is part of a $\vec{\mathcal{B}}_n$ shard. Therefore, no n-sherd belongs to more than one $\vec{\mathcal{B}}_n$ shard. Still, there could be multiple n-sherds in one $\vec{\mathcal{B}}_n$ shard. But we know from Lemma 4.2.18 that every n-sherd is $(n-1)$-dimensional and Lemma 4.2.20 tells us that any two n-sherds of the same hyperplane intersect only in a bounding hyperplane of the shard. Therefore, no two n-sherds belong to the same $\vec{\mathcal{B}}_n$ shard. □

Observation 4.2.23. Every basic hyperplane of $\vec{\mathcal{B}}_n$ is a shard. The basic hyperplanes of $\vec{\mathcal{B}}_n$ are exactly the sets $S_n(i-1, i, \emptyset, \emptyset)$ for $i \in [n]$.

Now that we have found $\vec{\mathcal{B}}_n$ shards and a way to describe them using two endpoints and a partition of the positions in between as was the case for $\vec{\mathcal{A}}_n$ shards. To continue to work our way towards quotientopes, we need to analyze the forcing relation of $\vec{\mathcal{B}}_n$ shards. We will now prepare to describe this relation with our notation for sherds.

4.2.4 $\vec{\mathcal{B}}_n$ Arcs

Now that we exhaustively described $\vec{\mathcal{B}}_n$ shards, we will try to illustrate them in the same way we illustrated $\vec{\mathcal{A}}_n$ shards, using arcs. We recall from Observation 4.1.18 the concept of the $\vec{\mathcal{A}}_{[\pm n]}$ arrangement and its intersection with the centrally symmetric subspace $\mathcal{H}_n^{\mathcal{B}}$. Just as every $\vec{\mathcal{B}}_n$ hyperplane is the intersection of an $\vec{\mathcal{A}}_{[\pm n]}$ hyperplane with that subspace, every $\vec{\mathcal{B}}_n$ shard is the intersection of an $\vec{\mathcal{A}}_{[\pm n]}$ shard with that subspace.

We will therefore assign to each $\vec{\mathcal{B}}_n$ shard S a canonical (dexter) **representative** $\vec{\mathcal{A}}_{[\pm n]}$ shard Σ in the space $\mathbb{R}^{[\pm n]}$. We define this representative using the notation $\Sigma = \Sigma_{[\pm n]}(\ell, r, A, B) := \left\{\mathbf{x} \in \mathbb{R}^{[\pm n]} \;\middle|\; x_a \leq x_\ell = x_r \leq x_b \text{ for all } a \in A, b \in B\right\}$ for endpoints $\ell < r \in [\pm n]$ such that $A \dot{\cup} B = [\ell, r] \setminus \{0\}$. We emphasize that shards in $\vec{\mathcal{A}}_{[\pm n]}$ do not use the index zero, but only the nonzero integers in $[\pm n]$. Therefore, the set of $\vec{\mathcal{A}}_{[\pm n]}$ shards we can describe in this way are just shards of the $\mathcal{A}_{2n}$ arrangement with a shifted notation.

Definition 4.2.24 (Representative Shard)**.** Given a $\vec{\mathcal{B}}_n$ shard $S = S_n(\ell, r, A, B)$ in dexter notation, we associate an $\vec{\mathcal{A}}_{[\pm n]}$ shard Σ in the following way.

- If $\mathrm{family}(S) = 1$ (so $\ell = 0$), we set $\Sigma = \Sigma_{[\pm n]}(-r,\ r,\ -A \cup A,\ -B \cup B)$.
- If $\mathrm{family}(S) = 2$ (so $\ell > 0$), we set $\Sigma = \Sigma_{[\pm n]}(\ell, r, A, B)$.
- If $\mathrm{family}(S) = 3$ (so $\ell < 0$), we set $\Sigma = \Sigma_{[\pm n]}(\ell,\ r,\ A \setminus \{0\},\ B \setminus \{0\})$.

These choices of representative shards correspond to $\vec{\mathcal{A}}_{[\pm n]}$ arcs. As every representative shard is full-dimensional in the centrally symmetric subspace $\mathcal{H}_n^{\mathcal{B}}$ of $\mathbb{R}^{[\pm n]}$, its arcs are centrally symmetric, too.

Definition 4.2.25 ($\vec{\mathcal{B}}_n$ Arcs)**.** Given a $\vec{\mathcal{B}}_n$ shard S, the associated $\vec{\mathcal{B}}_n$ **arc** is the arc of the representative $\vec{\mathcal{A}}_{[\pm n]}$ shard Σ of S. In the case of $\mathrm{family}(S) > 1$, it is usually shown together with its centrally symmetric image. We call the $\vec{\mathcal{B}}_n$ **arc**

- **singular** if $\mathrm{family}(S) = 1$, where the representative arc is centrally symmetric in itself,
- **separated** if $\mathrm{family}(S) = 2$, where the representative arc and its centrally symmetric image are strictly separated by the position 0,
- **overlapped** if $\mathrm{family}(S) = 3$, where the representative arc and its centrally symmetric image overlap around the position 0.

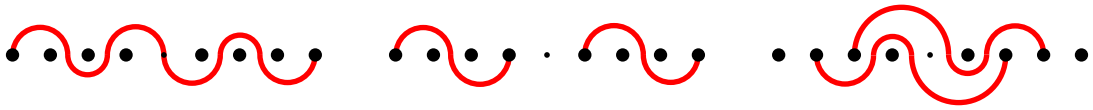

Figure 4.3: The $\vec{\mathcal{B}}_4$ arcs for the shard $S_4(0, 4, \{2\}, \{1, 3\})$ of the first family (with a singular arc, on the left), for the shard $S_4(1, 4, \{2\}, \{3\})$ of the second family (with a separated arc, in the middle), and for the shard $S_4(-2, 3, \{-1, 0, 2\}, \{1\})$ of the third family (with an overlapped arc, on the right). [Picture from [PPR20]]

See Figure 4.4 for an illustration of the $\vec{\mathcal{B}}_2$ arrangement and its shards labeled by $\vec{\mathcal{B}}_n$ arcs and see Figure 4.5 for a stereographic projection of the $\vec{\mathcal{B}}_3$ arrangement.

If $\mathrm{family}(S) = 3$ and the representative $\vec{\mathcal{B}}_n$ arc is overlapped, we call the $\vec{\mathcal{B}}_n$ arc **upper** if it passes above its centrally symmetric image or **lower** if it passes below. This is well-defined as the arc and its centrally symmetric image are non-crossing. As $\vec{\mathcal{A}}_{[\pm n]}$ arcs are in bijection with $\vec{\mathcal{A}}_{[\pm n]}$ shards, we call an $\vec{\mathcal{A}}_{[\pm n]}$ shard upper (resp. lower) if the corresponding $\vec{\mathcal{A}}_{[\pm n]}$ arc is.

These $\vec{\mathcal{B}}_n$ arcs give us a way to enumerate $\vec{\mathcal{B}}_n$ shards: We count pairs of $\vec{\mathcal{A}}_{[\pm n]}$ arcs centrally symmetric to each other (or pairs of an arc with itself in the case of a singular $\vec{\mathcal{B}}_n$ arc).

Lemma 4.2.26 (Number of $\vec{\mathcal{B}}_n$ Shards)**.** *The number of $\vec{\mathcal{B}}_n$ shards is $3^n - n - 1$.*

Proof. We will prove the statement by induction on n. For $n = 1$, the only $\vec{\mathcal{B}}_n$ arc is the singular one connecting -1 to $+1$. For the induction step, we remark that we can split the pairs of $\vec{\mathcal{A}}_{[\pm n]}$ arcs into those incident to the dots $-n$ and $+n$ and those not indicent to them, which are corresponding to the $\vec{\mathcal{B}}_{n-1}$ shards, whose number we assume to be $3^{n-1} - n$ by induction. We need to count those indicent to $-n$ and $+n$ and we do so by splitting them into the three types discussed above.

- Counting singular arcs, we know that each of them connects $-n$ to $+n$ and they are centrally symmetric, so we have two choices to pass above or below each dot in $[1, n-1]$ and the rest is determined by symmetry. This gives us $f_n^1 := 2^{n-1}$ choices.
- Counting separated arcs, we look at the dexter one connecting some k to n. For each choice of $k \in [1, n-1]$, there are 2^{n-k-1} ways to pass above or below the dots in between. This gives us $f_n^2 := \sum_{k=1}^{n-1} 2^{n-k-1} = 2^{n-1} - 1$ choices.

- Counting overlapped arcs, we look at the dexter one connecting some $-k$ to n. For each choice of $k \in [1, n-1]$, there are
  - 2 choices for every position in $[k, n]$ as the arc can pass above or below it,
  - 3 choices for very position in $[1, k[$, as the dot can lie above both the arc and its centrally symmetric image, below both arcs or in between the two.

  As all these choices are distinct and independent and completely determine the arc due to central symmetry, this gives us $f_n^3 := \sum_{k=1}^{n-1} 2^{n-k} \cdot 3^{k-1} = 2 \cdot 3^{n-1} - 2^n$.

We conclude that the number of $\vec{\mathcal{B}}_n$ shards is

$$\begin{aligned}\left(3^{n-1} - n\right) + f_n^1 + f_n^2 + f_n^3 &= 3^{n-1} - n + 2^{n-1} + 2^{n-1} - 1 + 2 \cdot 3^{n-1} - 2^n \\ &= 3^n - n - 1.\end{aligned}$$

□

4.2.5 Arrows Between Shards

We recall the definition of arrows in an oriented hyperplane arrangement from Definition 1.5.14. To determine whether one shard arrows another, we want to know what the dimension of their intersection is. In some cases, we can easily describe the intersection using the same notation we introduced for shards.

Lemma 4.2.27 ($\vec{\mathcal{B}}_n$ Shard Intersection)**.** *Let $S_1 = S_n(\ell_1, r_1, A_1, B_1)$ and $S_2 = S_n(\ell_2, r_2, A_2, B_2)$ be two $\vec{\mathcal{B}}_n$ shards such that $\{\ell_1, r_1\} \cap \{\ell_2, r_2\} \neq \emptyset$. Then $S_1 \cap S_2 = S_n(\overline{A_1} \cup \overline{A_2}, \overline{B_1} \cup \overline{B_2})$.*

Proof. Let $s \in \{\ell_1, r_1\} \cap \{\ell_2, r_2\}$. We prove one direction of inclusion after the other. Firstly, let $x \in S_1 \cap S_2$. Then $x_a \leq x_s$ for all $a \in \overline{A_1} \cup \overline{A_2}$. On the other hand, $x_s \leq x_b$ for all $b \in \overline{B_1} \cup \overline{B_2}$. Therefore, $x \in S_n(\overline{A_1} \cup \overline{A_2}, \overline{B_1} \cup \overline{B_2})$. Secondly, let $\mathbf{x} \in S_n(\overline{A_1} \cup \overline{A_2}, \overline{B_1} \cup \overline{B_2})$. Then $x_a \leq x_b$ for all $a \in \overline{A_1}, b \in \overline{B_1}$, so $\mathbf{x} \in S_1$. Moreover, $x_a \leq x_b$ for all $a \in \overline{A_2}, b \in \overline{B_2}$, so $\mathbf{x} \in S_2$. □

We introduce a notation that we can use to describe all pairs of shards arrowing another.

Lemma 4.2.28 (Nested $\vec{\mathcal{B}}_n$ Shard Notation)**.** *Let S_1 and S_2 be $\vec{\mathcal{B}}_n$ shards such that S_2 arrows S_1. Then we can write S_1 and S_2 in a way that $S_1 = S_n(\ell_1, r_1, A_1, B_1)$ and $S_2 = S_n(\ell_2, r_2, A_2, B_2)$ with $\ell_1 \leq \ell_2 < r_2 \leq r_1$.*

Proof. Let $S_1 = S_n(a_1, b_1, X_1, Y_1)$ and $S_2 = S_n(a, b_2, X_2, Y_2)$ be two shards in dexter notation. Then $H_n(a_1, b_1)$ and $H_n(a_2, b_2)$ are the two $\mathcal{B}_n$ hyperplanes that contain S_1 and S_2. If S_2 arrows S_1, then $H_n(a_2, b_2)$ cuts $H_n(a_1, b_1)$. By Corollary 4.2.5, we are in one of the following cases.

- If $a_1 \leq a_2$ and $b_2 \leq b_1$,
  then we can denote $S_1 = S_n(a_1, b_1, X_1, Y_1)$ and $S_2 = S_n(a_2, b_2, X_2, Y_2)$.
- If $a_1 \leq -b_2$ and $-a_2 \leq b_1$,
  then we can denote $S_1 = S_n(a_1, b_1, X_1, Y_1)$ and $S_2 = S_n(-b_2, -a_2, -Y_2, -X_2)$.

Either way, we can denote the two shards in such a nested fashion. □

Using this notation of nested shards, we can exclude some cases where S_2 cannot arrow S_1.

Lemma 4.2.29 (Nested $\vec{\mathcal{B}}_n$ Shards Without Arrows)**.** *Let S_1 and S_2 be two $\vec{\mathcal{B}}_n$ shards denoted by $S_1 = S_n(\ell_1, r_1, A_1, B_1)$ and $S_2 = S_n(\ell_2, r_2, A_2, B_2)$. We set $I = \{|\ell_1|, |\ell_2|, |r_1|, |r_2|\}$. If $|I| \neq 3$, then neither of S_1 and S_2 arrows the other.*

Proof. We first observe that $|I| \geq 2$ as $\ell_1 \neq r_1$ and $\ell_1 \neq -r_1$ by definition of $\vec{\mathcal{B}}_n$ shards. Clearly, $|I| \leq 4$. To prove the statement, we show that in the cases $|I| = 2$ and $|I| = 4$, neither of $H_n(S_1)$ and $H_n(S_2)$ cuts the other.

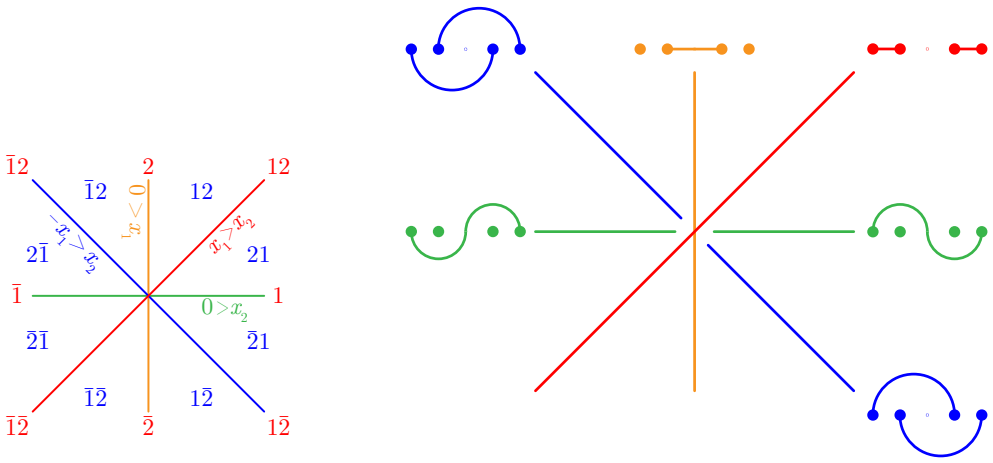

Figure 4.4: The type $\mathcal{B}$ fan $\mathcal{F}_2^{\mathcal{B}}$ (left) and the corresponding $\vec{\mathcal{B}}_n$ shards and $\vec{\mathcal{B}}_n$ arcs (right). The chambers of the fan are labeled by signed permutations in blue, its rays are labeled by signed index sets in red and hyperplanes are labeled by inequalities with different colors for each hyperplane. [Picture from [PPR20]]

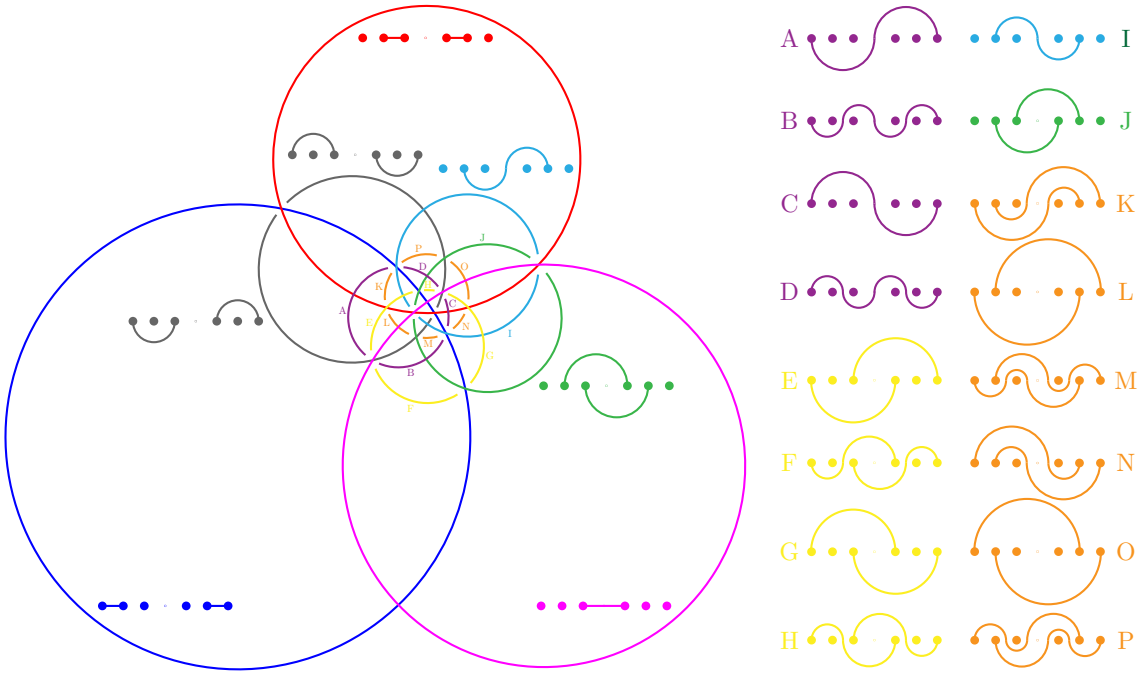

Figure 4.5: The 3-dimensional oriented type $\mathcal{B}$ arrangement $\mathcal{B}_3$, stereographically projected to the plane from a viewpoint opposite of the base region. Each hyperplane is drawn in a different color and the $\vec{\mathcal{B}}_n$ arcs of their shards are colored accordingly and replaced by letters if necessary. [Picture from [PPR20]]

- If $|I| = 4$, then Corollary 4.2.5 certifies that neither $H_n(S_1)$ nor $H_n(S_2)$ cuts the other.
- If $|I| = 2$, then either ($\ell_1 = \ell_2$ and $r_1 = r_2$) or ($\ell_1 = -r_2$ and $r_1 = -\ell_2$). We deduce that S_1 and S_2 are part of the same hyperplane. Therefore, $H_n(S_1) = H_n(S_2)$, but no $\vec{\mathcal{B}}_n$ hyperplane cuts itself.

We conclude that neither of S_1 and S_2 arrows the other. □

We can combine these two statements to describe all pairs of shards where one arrows the other in a way that they share exactly one of their endpoints.

Corollary 4.2.30 (Nested $\vec{\mathcal{B}}_n$ Shards with Common Endpoint)**.** Let S_1 and S_2 be two $\vec{\mathcal{B}}_n$ shards such that S_2 arrows S_1. We can always write them in such a way that $S_1 = S_n(\ell_1, r_1, A_1, B_1)$ and $S_2 = S_n(\ell_2, r_2, A_2, B_2)$ with either ($\ell_1 = \ell_2$ and $r_2 < r_1$) or ($\ell_1 < \ell_2$ and $r_2 = r_1$).

Without loss of generality, for any pair of shards where S_1 arrows S_2, we can use dexter and sinister notation to denote them in a way that $r_1 = r_2$. It therefore suffices to check these cases for arrows. We first determine when the intersection of S_1 and S_2 has dimension $n-2$ in the case where $\ell_2 \neq 0$.

Lemma 4.2.31 (Dimension of Nested $\vec{\mathcal{B}}_n$ Shard Intersection)**.** *Let $S_1 = S_n(\ell_1, r, A_1, B_1)$ and $S_2 = S_n(\ell_2, r, A_2, B_2)$ be two $\vec{\mathcal{B}}_n$ shards with $\ell_1 < \ell_2$ and $\ell_2 \neq 0$. Then $\dim(S_1 \cap S_2) = n-2$ if and only if all of the following hold.*

1. *$A_1 \supseteq A_2$ and $B_1 \supseteq B_2$,*
2. *if $-\ell_2 = \ell_1$, then $A_1^{\pm} \cup B_1^{\pm} = \{0\}$,*
3. *if $-\ell_2 \in A_1$, then $0 \in A_1$,*
4. *if $-\ell_2 \in B_1$, then $0 \in B_1$.*

Proof. We set $LR := \{\ell_1, \ell_2, r\}$ and $U := A_1 \cup A_2 \cup LR$ and $V := B_1 \cup B_2 \cup LR$. Then by Lemma 4.2.27, we have $S_1 \cap S_2 = S_n(U, V)$. As in Observation 4.2.10, we define

- $J_{UV} := (U^+ \cap V^+) \cup (-U^- \cap -V^-)$,
- $J_U := (U^+ \cap -U^-) \setminus (V^+ \cup -V^-)$,
- $J_V := (V^+ \cap -V^-) \setminus (U^+ \cup -U^-)$.

We obtain

- $J_{UV} = (A_1^+ \cap B_2^+) \cup (A_2^+ \cap B_1^+) \cup (-A_1^- \cap -B_2^-) \cup (-A_2^- \cap -B_1^-) \cup (LR^+ \cup -LR^-)$,
- $J_U = \big((A_1^+ \cup A_2^+) \cap (-A_1^- \cup -A_2^-)\big) \setminus (B_1^+ \cup B_2^+ \cup -B_1^- \cup -B_2^-)$,
- $J_V = \big((B_1^+ \cup B_2^+) \cap (-B_1^- \cup -B_2^-)\big) \setminus (A_1^+ \cup A_2^+ \cup -A_1^- \cup -A_2^-)$.

We remark that J_{UV} is non-empty. and recall the results of Proposition 4.2.11.

- If $U^{\pm} \neq \emptyset \neq V^{\pm}$, then $\dim(S_1 \cap S_2) = n - |J_{UV}| - |J_U| - |J_V|$.
- If $U^{\pm} = \emptyset$ or $V^{\pm} = \emptyset$, then $\dim(S_1 \cap S_2) = n + 1 - |J_{UV}|$.

We know that $\ell_1 < \ell_2 < r$ and $-\ell_1, -\ell_2 \neq r$, but possibly, $-\ell_1 = \ell_2$. We distinguish cases by their signs. Note that condition (2) only applies if $\ell_1 < 0 \leq \ell_2$. Conditions (3) and (4) are only meaningful if $\ell_1 < 0 < \ell_2$ or $\ell_2 < 0 < r$. In all other cases, $\dim(S_1 \cap S_2) = n - 2$ will just be shown to be equivalent to $A_1 \cap B_2 = A_2 \cap B_1 = \emptyset$. Note that this is equivalent to condition (1) as we have $A_2 \dot\cup B_2 =]\ell_2, r[\subset]\ell_1, r[= A_1 \dot\cup B_1$.

- If $0 < \ell_1 < \ell_2 < r$, then $U, V \subseteq [n]$, so both $U^{\pm}$ and $V^{\pm}$ are empty. We conclude that the dimension of the intersection is $\dim(S_1 \cap S_2) = n+1-|J_{UV}| = n-2-|A_1 \cap B_2|-|A_2 \cap B_1|$. This is equal to $n-2$ if and only if $A_1 \cap B_2, A_2 \cap B_1 = \emptyset$.
- If $\ell_1 = 0 < \ell_2 < r$, then $0 \in LR$, so $0 \in U^{\pm} \cap V^{\pm}$ and the dimension of the intersection is $\dim(S_1 \cap S_2) = n - |J_{UV}| - |J_U| - |J_V|$. As both sets J_U and J_V are empty while for the third one, we have $J_{UV} = (A_1^+ \cap B_2^+) \cup (A_2^+ \cap B_1^+) \cup \{\ell_2, r\}$, we deduce the intersection dimension $\dim(S_1 \cap S_2) = n - 2 - |A_1 \cap B_2| - |A_2 \cap B_1|$. This is equal to $n-2$ if and only if both $A_1 \cap B_2$ and $A_2 \cap B_1$ are empty.

- If $\ell_1 < 0 < \ell_2 < r$, we assume without loss of generality that $0 \in A_1$. Then by Definition 4.2.16, $B_1^{\pm} = \{0\}$ and furthermore, $U^{\pm} \neq \emptyset$ as it contains 0. We distinguish subcases by the order of $-\ell_1$ and ℓ_2.
  - If $-\ell_1 < \ell_2$, then $V^{\pm} = \emptyset$. Therefore, the dimension of the intersection is given by $\dim(S_1 \cap S_2) = n + 1 - |J_{UV}| = n - 2 - |A_1^+ \cap B_2^+| - |A_2^+ \cap B_1^+|$. We conclude that $\dim(S_1 \cap S_2) = n - 2$ if and only if $A_1 \cap B_2, A_2 \cap B_1 = \emptyset$.
  - If $-\ell_1 = \ell_2$, then $\ell_2 \in V^{\pm}$. Therefore, $\dim(S_1 \cap S_2) = n - |J_{UV}| - |J_U| - |J_V| = n-2-|A_1^+ \cap B_2^+| - |A_2^+ \cap B_1^+| - |A_1^+ \cap -A_1^-|$. We conclude that $\dim(S_1 \cap S_2) = n-2$ if and only if $A_1 \cap B_2, A_2 \cap B_1$ and $A_1^{\pm} \cup B_1^{\pm} = \{0\}$.
  - If $-\ell_1 > \ell_2$, we recall from Definition 4.2.16 that $0 \in A_1$ implies $\overline{B_1} \cap -\overline{B_1} = \emptyset$, so in particular $r \notin -\overline{B_1}$ and $-\ell_1 \notin B_1$ and $-B_1 \cap B_2 = -B_1 \cap A_1 \cap B_2$. Then $V^{\pm} = \emptyset$ if and only if $-\overline{B_1} \cap \overline{B_2} = \emptyset$ or equivalently $(-B_1 \cup \{-\ell_1\}) \cap (\{\ell_2\} \cup B_2) = \emptyset$.
    - If $-\ell_2 \notin B_1$ and $A_1 \cap B_2 = A_2 \cap B_1 = \emptyset$, then $V^{\pm} = \emptyset$. Then the dimension of the intersection is $\dim(S_1 \cap S_2) = n + 1 - |J_{UV}| = n - 2$.
    - If $-\ell_2 \in B_1$, then $-\ell_2 \in V^{\pm}$. Then $\dim(S_1 \cap S_2) = n - |J_{UV}| - |J_U| - |J_V| \leq n-3$ as $\{\ell_2, -\ell_1, r\} \subseteq J_{UV}$.
    - If $(A_1 \cap B_2) \cup (A_2 \cap B_1) \neq \emptyset$, they contain some k.
      - If $k = -\ell_1$, we deduce that $-\ell_1 \in B_2$ as $-\ell_1 \notin B_1$. Then $-\ell_1 \in V^{\pm}$, so that $\dim(S_1 \cap S_2) = n - |J_{UV}| - |J_U| - |J_V| \leq n - 3$.
      - Otherwise, $|J_{UV}| \geq 4$, so we have $\dim(S_1 \cap S_2) \leq n + 1 - |J_{UV}| \leq n - 3$.

    We conclude that $\dim(S_1 \cap S_2) = n - 2$ if and only if both $A_1 \cap B_2$ and $A_2 \cap B_1$ are empty and $-\ell_2 \notin B_1$.
- If $\ell_1 < \ell_2 < 0 < r$, we first observe that if $0 \in A_1 \cap B_2$ or $0 \in A_2 \cap B_1$, then $0 \in U^{\pm} \cap V^{\pm}$, therefore $\dim(S_1 \cap S_2) = n - |J_{UV}| - |J_U| - |J_V| \leq n - |LR| = n - 3$.
  To find the cases where the dimension is $n - 2$, we may assume without loss of generality that $0 \in A_1 \cap A_2$, then $0 \in U^{\pm}$. By Definition 4.2.16, we know that both $\overline{B_1} \cap -\overline{B_1}$ and $\overline{B_2} \cap -\overline{B_2}$ are empty. Firstly, we remark that $-r \notin B_1, B_2$. Secondly, we deduce that the set $V^{\pm} = (\overline{B_1} \cup \overline{B_2}) \cap (-\overline{B_1} \cup -\overline{B_2})$ is empty if and only if $\overline{B_1} \cap -\overline{B_2}$ is empty. As $\overline{B_1} \cap -\overline{B_2} = \overline{B_1} \cap (\{-\ell_2\} \cup -B_2)$, this is the case if and only if both $A_1 \cap B_2 = A_2 \cap B_1 = \emptyset$ and $-\ell_2 \notin B_1$.
  - If $V^{\pm} = \emptyset$, then $\dim(S_1 \cap S_2) = n + 1 - |J_{UV}| = n + 1 - |(LR^+ \cup -LR^-)| = n - 2$.
  - If $V^{\pm} \neq \emptyset$, then $\dim(S_1 \cap S_2) = n - |J_{UV}| - |J_U| - |J_V| \leq n - |(LR^+ \cup -LR^-)| = n - 3$.

  We conclude that $\dim(S_1 \cap S_2) = n - 2$ if and only if $A_1 \cap B_2 = A_2 \cap B_1 = \emptyset$ and $-\ell_2 \notin B_1$. An analogous argument with the roles of A and B exchanged holds if $0 \in B_1 \cap B_2$.
- If $\ell_1 < \ell_2 < 0 = r$, then $0 \in LR$, so $0 \in U^{\pm} \cap V^{\pm}$ and the dimension of the intersection is given by $\dim(S_1 \cap S_2) = n - |J_{UV}| - |J_U| - |J_V|$. As both J_U and J_V are empty and $J_{UV} = (-A_1^- \cap -B_2^-) \cup (-A_2^- \cap -B_1^-) \cup \{-\ell_1, -\ell_2\}$, we obtain $\dim(S_1 \cap S_2) = n - 2 - |A_1 \cap B_2| - |A_2 \cap B_1|$. This is equal to $n - 2$ if and only if $A_1 \cap B_2, A_2 \cap B_1 = \emptyset$.
- If $\ell_1 < \ell_2 < r < 0$, then $U, V \subseteq -[n]$, so $U^{\pm} = V^{\pm} = \emptyset$. We conclude that the dimension of the intersection is $\dim(S_1 \cap S_2) = n + 1 - |J_{UV}| = n - 2 - |A_1 \cap B_2| - |A_2 \cap B_1|$. This is equal to $n - 2$ if and only if $A_1 \cap B_2, A_2 \cap B_1 = \emptyset$. □

Observation 4.2.32. We can give some simpler explanation that the conditions 1 - 4 in the lemma we just discussed are necessary.

1. If $A_1 \not\supseteq A_2$, there is a $k \in A_2$ such that $k \notin A_1$. As $A_2 \subset]\ell_2, r[\subset]\ell_1, r[= A_1 \dot\cup B_1$, we know that k has to be contained in B_1. We fix the three index sets $T := \{\ell_1, \ell_2, k, r\}$ and $I := \{|\ell|, |k|, |r_1|, |r_2|\}$ and $S := S_n(T, T)$. As $S_1 \cap S_2 = S_n(\overline{A_1} \cup \overline{A_2}, \overline{B_1} \cup \overline{B_2})$ by Lemma 4.2.27, we have $S_1 \cap S_2 \subset S$ by Lemma 4.2.7 and deduce $\dim(S_1 \cap S_2) \leq \dim(S)$. We first observe that $|I| \leq 2$ is impossible: r can neither be equal to $-\ell_1$ nor to $-\ell_2$, but if $-k = r$, then $\ell_1 < \ell_2 < k < 0$, so ℓ_1 and ℓ_2 cannot add up to zero. We now

assume that $|I| = 3$ and $0 \in I$. Then exactly two of ℓ_1, ℓ_2, k, r have to add up to zero. We note that $\ell_1 = 0$ or $r = 0$ are impossible as all remaining variables would have the same sign, so no two of them can add up to zero. $\ell_2 = 0$ is forbidden by the conditions of the lemma. But if $k = 0$, then $-r$ would have to be equal to ℓ_1 or ℓ_2, which is impossible by Definition 4.2.16. Therefore, $|I| = 3$ implies that $0 \notin I$.
Corollary 4.2.13 states that if $0 \notin I$ and $|I| < |T|$, then $\dim(S) = n - |I|$, while otherwise, we have $\dim(S) = n - |I| + 1$. We conclude that $\dim(S_1 \cap S_2) \leq \dim(S) \leq n - 3$. An analogous argument holds if $B_1 \not\supseteq B_2$.

2. If $-\ell_2 = \ell_1$ and $A_1^{\pm} \cup B_1^{\pm} \neq \{0\}$, we assume without loss of generality that there is some $0 < k \in A_1^{\pm}$. Note that $x_{\ell_1} = x_{\ell_2}$ is equivalent to $x_{\ell_1} = x_{\ell_2} = 0$. All $\mathbf{x} \in S_1$ have $-x_k, x_k \leq x_r = x_{\ell_1}$ and all $\mathbf{x} \in S_2$ have $x_r = x_{\ell_2} = -x_{\ell_1}$. Therefore, every vector $\mathbf{x} \in S_1 \cap S_2$ has $-x_k, x_k \leq x_{\ell_1} = -x_{\ell_1}$ and thus $x_k = x_{\ell_2} = x_r = 0$. We can conclude that $\dim(S_1 \cap S_2) \leq n-3$. An analogous argument holds if there is a $0 < k \in B_1^{\pm}$.
3. If $-\ell_2 \in A_1$ and $0 \in B_1$, then all $\mathbf{x} \in S_1$ have $-x_{\ell_2} \leq x_r \leq 0$. As all $\mathbf{x} \in S_2$ have the property $x_{\ell_2} = x_r$, we know that all $x \in S_1 \cap S_2$ have $-x_{\ell_2}, x_{\ell_2} \leq x_r \leq 0$. This implies $x_{\ell_2} = 0$, so that all $\mathbf{x} \in S_1 \cap S_2$ have $x_{\ell_1} = x_{\ell_2} = x_r = 0$. We conclude that $\dim(S_1 \cap S_2) \leq n - 3$. An analogous argument holds if $-\ell_2 \in B_1$ and $0 \in A_1$.

Note that the proof of Lemma 4.2.31 showed that these conditions are sufficient as well.

We use our findings to deduce when S_2 arrows S_1 in the case we discussed.

Corollary 4.2.33 (Arrows in Most Cases)**.** Let $S_1 = S_n(\ell_1, r, A_1, B_1)$ and $S_2 = S_n(\ell_2, r, A_2, B_2)$ be $\vec{\mathcal{B}}_n$ shards with $\ell_1 < \ell_2$ and $\ell_2 \neq 0$. Then S_2 arrows S_1 if and only if all of the following hold.

1. $A_1 \supseteq A_2$ and $B_1 \supseteq B_2$,
2. if $-\ell_2 = \ell_1$, then $A_1^{\pm} \cup B_1^{\pm} = \{0\}$,
3. if $-\ell_2 \in A_1$, then $0 \in A_1$,
4. if $-\ell_2 \in B_1$, then $0 \in B_1$.

Proof. We first distinguish cases by dexter and sinister notation of S_1 and S_2:

- If S_2 is in dexter notation, then $H_n(S_2) = H_n(\ell_2, r)$.
  - If S_1 is in dexter notation, then $H_n(S_1) = H_n(\ell_1, r)$.
  - If S_1 is in sinister notation, then $H_n(S_1) = H_n(-r, -\ell_1)$.
- If S_2 is in sinister notation, then $H_n(S_2) = H_n(-r, -\ell_2)$. As $\ell_2 < r$ and $|\ell_2| > r$, we know that $\ell_2 < 0$. Then $\ell_1 < \ell_2$ implies $|\ell_1| > |\ell_2| > r$, so S_1 is in sinister notation as well and $H_n(S_1) = H_n(-r, -\ell_1)$.

For all these cases, Corollary 4.2.5 certifies that $H_n(S_2)$ cuts $H_n(S_1)$. By definition, S_2 arrows S_1 if and only if $\dim(S_1 \cap S_2) = n-2$ and $H_n(S_2)$ cuts $H_n(S_1)$. It is left to show that the dimension of the intersection is $\dim(S_1 \cap S_2) = n - 2$ if and only if all four conditions hold. That is exactly the result of Lemma 4.2.31. □

It is left to determine when the intersection of S_1 and S_2 has dimension $n - 2$ in the case where $\ell_2 = 0$. We immediately combine this question with hyperplane cutting to determine whether S_2 arrows S_1.

Lemma 4.2.34 (Arrows From Family 1 to Family 3)**.** *Let $S_1 = S_n(\ell, r, A_1, B_1)$ with $\ell < 0$ and $S_2 = S_n(0, r, A_2, B_2)$ be two $\vec{\mathcal{B}}_n$ shards. Then S_2 arrows S_1 if and only if $A_2 \subseteq A_1 \cap -B_1$ and $B_2 \subseteq B_1 \cap -A_1$.*

Proof. We first show that $r < -\ell$ holds if S_2 arrows S_1 or if $A_2 \subseteq A_1 \cap -B_1$ and $B_2 \subseteq B_1 \cap -A_1$.

- Assume that S_2 arrows S_1 and $-r < \ell$. Then S_1 is part of the hyperplane $H_n(-\ell, r)$. We know from Lemma 4.2.4 that $H_n(-\ell, r)$ does not cut $H_n(0, r)$, so S_2 does not arrow S_1, which contradicts our asumption. We conclude that $\ell < -r$ as $\ell = -r$ is impossible by Definition 4.2.16.

- Assume that $A_2 \subseteq A_1 \cap -B_1$ and $B_2 \subseteq B_1 \cap -A_1$, then $A_2 \dot\cup B_2 \subseteq -A_1 \dot\cup -B_1$, so $]0,r[\subseteq]-r,-\ell[$, which implies $r \leq -\ell$. As $r = -\ell$ is impossible by Definition 4.2.16, we conclude that $r < -\ell$.

We know that $r < -\ell$ implies that the hyperplane $H_n(-r,-\ell)$ cuts $H_n(0,r)$. It is left to show that if $r < -\ell$, then $\dim(S_1 \cap S_2) = n-2$ if and only if $A_2 \subseteq A_1 \cap -B_1$ and $B_2 \subseteq B_1 \cap -A_1$. We set $LR := \{\ell, 0, r\}$ and $U := A_1 \cup A_2 \cup LR$ and $V := B_1 \cup B_2 \cup LR$. Then by Lemma 4.2.27, we have $S_1 \cap S_2 = S_n(U,V)$.

We recall the result of Proposition 4.2.11: Because of $0 \in LR$, we have $U^\pm \neq \emptyset \neq V^\pm$, so $\dim(S_1 \cap S_2) = n - |J_{UV}| - |J_U| - |J_V| = n - |(U^+ \cup -V^-) \cap (V^+ \cup -U^-)|$. We fix another set $X = (A_1^+ \cup A_2^+ \cup -B_1^-) \cap (B_1^+ \cup B_2^+ \cup -A_1^-)$ and observe that $X \cup \{-\ell, r\} = (U^+ \cup -V^-) \cap (V^+ \cup -U^-)$. As $r < -\ell$, we have $X \subseteq]0,-\ell[$, so $-\ell \notin X$. Furthermore, we remark that $A_1^+, A_2^+, B_1^+, B_2^+ \subseteq]0,r[$ and $r \notin -B_1^- \cap -A_1^-$, so $r \notin X$. We conclude that $X \cap \{-\ell, r\} = \emptyset$, so $\dim(S_1 \cap S_2) = n-2-|X|$. It remains to show that $X = \emptyset$ if and only if both $A_2 \subseteq A_1 \cap -B_1$ and $B_2 \subseteq B_1 \cap -A_1$.

- If $X = \emptyset$, then in particular, $A_2^+ \cap B_1^+ = A_2^+ \cap -A_1^- = \emptyset$. We fix a $k \in A_2 \subseteq]0,r[$.
  - Then $k \notin B_1^+$. As $k \in]0,r[= B_1^+ \dot\cup A_1^+$, we know that $k \in A_1^+$.
  - Furthermore, $k \notin -A_1^-$. As $k \in]0,-\ell[= -A_1^- \dot\cup -B_1^-$, we know that $k \in -B_1^-$.

  We conclude that $A_2 \subseteq A_1 \cap -B_1$. An analogous argument proves that $B_2 \subseteq B_1 \cap -A_1$.
- If $A_2 \subseteq A_1 \cap -B_1$ and $B_2 \subseteq B_1 \cap -A_1$, we use the fact that $A_1 \cap B_1 = \emptyset$. Then $A_2 \subseteq A_1$ implies $A_2 \cap B_1 = \emptyset$. Analogously, we find $A_2 \cap -A_1 = \emptyset$ and $B_2 \cap A_1 = B_2 \cap -A_1 = \emptyset$. We rewrite $X = \big(A_2^+ \cup (A_1^+ \cup -B_1^-)\big) \cap \big(B_2^+ \cup (B_1^+ \cup -A_1^-)\big)$. As $A_2 \cap B_2 = \emptyset$, we deduce that $X = (A_1^+ \cup -B_1^-) \cap (B_1^+ \cup -A_1^-) = (A_1^+ \cap -A_1^-) \cup (B_1^+ \cap -B_1^-)$. Assume there is a $k \in A_1^+ \cap -A_1^- \subseteq]0,r[$. Then $k \notin B_1, -B_1$, so on one hand, $k \notin A_2 \subseteq A_1 \cap -B_1$ and on the other hand, $k \notin B_2 \subseteq B_1 \cap -A_1$. But then $k \notin A_2 \cup B_2 =]0,r[$, a contradiction. An analogous argument shows that $B_1^+ \cap -B_1^- = \emptyset$, so we can conclude that $X = \emptyset$ as desired. □

4.2.6 Forcing of Shards

It is a direct consequence of Lemma 4.2.4 that the cutting relation on the $\vec{\mathcal{B}}_n$ hyperplanes is acylic. In consequence, the arrows on the $\vec{\mathcal{B}}_n$ shards are acyclic, so its reflexive-transitive closure is anti-symmetric. We can therefore adapt the established definition of Theorem 1.5.15 to our case.

Observation 4.2.35 (Chain of Arrows Among $\vec{\mathcal{B}}_n$ Shards)**.** Let S_1 and S_2 be two $\vec{\mathcal{B}}_n$ shards such that S_2 forces S_1. Then by definition of forcing, there has to exist a finite chain of shards such that $S_2 = T_1 \to T_2 \to \cdots \to T_k = S_1$ with $k \geq 2$. Repeated application of Corollary 4.2.30 certifies that we can always write them as $S_1 = S_n(\ell_1, r_1, A_1, B_1)$ and $S_2 = S_n(\ell_2, r_2, A_2, B_2)$ in such a way that for every $i \in [k]$, we have $T_i = S_n(x_i, y_i, X_i, Y_i)$ and for each $i \in [k-1]$, we even have either ($x_i = x_{i+1}$ and $y_i > y_{i+1}$) or ($x_i < x_{i+1}$ and $y_i = y_{i+1}$).

We introduce new binary relations on of $\vec{\mathcal{B}}_n$ shards. They are fairly simple to grasp and will prove to be very useful in describing the forcing relation among $\vec{\mathcal{B}}_n$ shards.

Definition 4.2.36 (Extension and Restriction of Shards)**.** Let S_1 and S_2 be $\vec{\mathcal{B}}_n$ shards denoted by $S_1 = S_n(\ell_1, r_1, A_1, B_1)$ and $S_2 = S_n(\ell_2, r_2, A_2, B_2)$. We say that S_2 **restricts** S_1 (equivalently, S_1 **extends** S_2) if one or both of the following statements hold:

- $A_1 \supseteq A_2$ and $B_1 \supseteq B_2$ and $[\ell_1, r_1] \supseteq [\ell_2, r_2]$,
- $A_1 \supseteq -B_2$ and $B_1 \supseteq -A_2$ and $[\ell_1, r_1] \supseteq [-r_2, -\ell_2]$.

We say that S_2 **doubly restricts** S_1 (equivalently, S_1 **doubly extends** S_2) if both hold. Note that these definitions are independent of the choice of notation for each shard.

Observation 4.2.37. We can easily check several properties of these four binary relations:

1. (Inclusion of Relations): As a relation, double restriction (resp. extension) is a strict subset of simple restriction (resp. extension): If S_1 doubly restricts (resp. extends) S_2, then S_1 restricts (resp. extends) S_2.
2. (Reflexivity): Restriction and extension are reflexive relations: Every $\vec{\mathcal{B}}_n$ shard restricts and extends itself. Double restriction and double extension are irreflexive relations: No $\vec{\mathcal{B}}_n$ shard doubly restricts or doubly extends itself.
3. (Antisymmetry): Both simple and double extension or restriction are antisymmetric relations on the set of shards of $\mathcal{B}_n$: If S_1 restricts (resp. doubly / extends) S_2 and S_2 restricts (resp. doubly / extends) S_1, then $S_1 = S_2$.
4. (Transitivity): Both simple and double extension or restriction are transitive relations on the set of shards of $\mathcal{B}_n$: If S_1 restricts (resp. doubly / extends) S_2 and S_2 restricts (resp. doubly / extends) S_3, then S_1 restricts (resp. doubly / extends) S_3.

Example 4.2.38. Let $S = S_n(-2,\ 3,\ A = \{-1, 0, 2\},\ B = \{1\})$. We note that we can't just intersect A and B with a smaller interval $]\ell_2, r_2[$, even if $\ell_2 + r_2 \neq 0$. For example, we are not allowed to restrict S to $]-1, 2[$. We would obtain $T = S_n(-1, 2, \{0\}, \{1\})$ which has $0 \in A$, but $1 \in \overline{B} \cap -\overline{B}$, so T is not a $\vec{\mathcal{B}}_n$ shard.

We will now give three statements concerning the connection between forcing and restricting.

Lemma 4.2.39 (Restriction if S_2 Forces S_1)**.** *Let S_1 and S_2 be two $\vec{\mathcal{B}}_n$ shards where S_2 forces S_1.*

1. *Then S_2 restricts S_1.*
2. *If $\mathrm{family}(S_1) = 3$ and $\mathrm{family}(S_2) = 1$, then S_2 doubly restricts S_1.*

Proof. As S_2 forces S_1, Observation 4.2.35 certifies that there exists a chain of shards such that $S_2 = T_1 \to T_2 \to \cdots \to T_k = S_1$ with $k \geq 2$, where we can denote $S_1 = S_n(\ell_1, r_1, A_1, B_1)$ and $S_2 = S_n(\ell_2, r_2, A_2, B_2)$ in such a way that for every $i \in [k]$, we have $T_i = S_n(x_i, y_i, X_i, Y_i)$ and for each $i \in [k-1]$, we even have

- either $x_i = x_{i+1}$ and $y_i > y_{i+1}$,
- or $x_i < x_{i+1}$ and $y_i = y_{i+1}$.

We will prove the second case first. We first note that as no hyperplane of family 1 or 3 cuts a hyperplane of family 2, no shard of family 1 or 3 arrows a shard of family 2. Furthermore, no hyperplane of family 3 cuts a hyperplane of family 1, so no shard of family 3 arrows a shard of family 1. We deduce that if T_i is a family 3 shard, then T_{i+1} is a family 3 shard as well. As $\mathrm{family}(T_1) = 1$ and $\mathrm{family}(T_k) = 3$, there is exactly one index $m \in [k]$ such that $\mathrm{family}(T_i) = 1$ for $1 \leq i < m$ and $\mathrm{family}(T_i) = 3$ for $m \leq i \leq k$. In particular, we know that $T_{m-1} \to T_m$. We deduce from Lemma 4.2.34 that $X_m \subseteq X_{m-1} \cap -Y_{m-1}$ and $Y_m \subseteq Y_{m-1} \cap -X_{m-1}$. Furthermore, repeated application of Corollary 4.2.33 certifies that $X_{m-1} \subseteq A_1$ and $Y_{m-1} \subseteq B_1$ and $A_2 \subseteq X_m$ and $B_2 \subseteq Y_m$ on the other side. We deduce that $A_2 \subseteq A_1 \cap -B_1$ and $B_2 \subseteq B_1 \cap -A_1$, so we conclude that S_2 doubly restricts S_1.

We will now consider the case where $\mathrm{family}(S_1) - \mathrm{family}(S_2) < 2$. Then repeated application of Corollary 4.2.33 certifies that $X_1 \subseteq X_k$ and $Y_1 \subseteq Y_k$. We note that this also holds if there is an index $m \in [k-1]$ such that $\mathrm{family}(T_m) = 1$ and $\mathrm{family}(T_{m+1}) = 3$. We conclude that S_2 restricts S_1. □

We will now prove the opposite direction: Restriction implies forcing. We explicitly construct an arrowing chain of shards to deduce that the first one forces the last.

Lemma 4.2.40 (Forcing if S_2 Restricts S_1)**.** *Let S_1 and S_2 be two distinct $\vec{\mathcal{B}}_n$ shards such that $\mathrm{family}(S_1) - \mathrm{family}(S_2) < 2$. If S_2 restricts S_1, then S_2 forces S_1.*

Proof. Denote $S_2 = S_n(\ell_2, r_2, A_2, B_2)$ in dexter notation (so that $|\ell_2| < r_2$). Assume that S_2 restricts S_1. Then we can denote $S_1 = S_n(\ell_1, r_1, A_1, B_1)$, where we choose the notation such that $A_2 \subseteq A_1$ and $B_2 \subseteq B_1$ and $\ell_1 \leq \ell_2 < r_2 \leq r_1$. We set $X := A_1 \cap]\ell_2, r_1[$ and $Y := B_1 \cap]\ell_2, r_1[$ and $T := S_n(\ell_2, r_1, X, Y)$. As S_2 restricts S_1, we observe that as $A_2 = A_1 \cap]\ell_2, r_2[$ and $X = A_1 \cap]\ell_2, r_1[$, we have $A_2 \subseteq X \subseteq A_1$ and analogously, $B_2 \subseteq Y \subseteq B_1$.

We first check the conditions of Definition 4.2.16 to make sure that T is a $\vec{\mathcal{B}}_n$ shard:

1. Clearly, $-n \leq \ell_2 < r_1 \leq n$
2. We have $X \cup Y = (A_1 \cup B_1) \cap]\ell_2, r_1[=]\ell_1, r_1[\cap]\ell_2, r_1[=]\ell_2, r_1[$ as S_1 is a $\vec{\mathcal{B}}_n$ shard itself. For the same reason, we obtain $X \cap Y = A_1 \cap B_1 \cap]\ell_2, r_1[= \emptyset$.
3. If $0 \in X$, then $X \subseteq A_1$ implies $0 \in A_1$, so $\overline{B_1} \cap -\overline{B_1} = \emptyset$ as S_1 is a $\vec{\mathcal{B}}_n$ shard. In particular, $B_1 \cap -B_1 = \emptyset$ and $-r_1 \notin B_1$. As $Y \subseteq B_1$, we deduce that $Y \cap -Y = \emptyset$ and $-r_1 \notin Y$. To prove that $\overline{Y} \cap -\overline{Y} = \emptyset$, it is left to show that $-\ell_2 \notin Y$. This is clear if $-\ell_2 \leq 0$. Assume $\ell_2 < 0$ and $-\ell_2 \in Y$. As S_2 was denoted in dexter notation, we have $\ell_2 < -\ell_2 < r_2$ and $B_2 = B_1 \cap]\ell_2, r_2[$ implies that $-\ell_2 \in B_2$. Then $\overline{B_2} \cap -\overline{B_2} \neq \emptyset$, but $0 \in A_2$, which is impossible because S_2 is a $\vec{\mathcal{B}}_n$ shard. An analogous argument holds if $0 \in Y$.

We confirmed that T is a $\vec{\mathcal{B}}_n$ shard. As S_2 was denoted in dexter notation, we have $|\ell_2| < r_2$, which implies $|\ell_2| < r_1$, so $T = S_n(\ell_2, r_1, X, Y)$ is in dexter notation as well.

We will now show that either $S_2 = T$ or $S_2 \to T$. Clearly, if $r_1 = r_2$, then $T = S_2$. Otherwise, we use the opposite notations $T = S_n(-r_1, -\ell_2, -Y, -X)$ and $S_2 = S_n(-r_2, -\ell_2, -B_2, -A_2)$. As $0 < r_2 < r_1$, we can apply Corollary 4.2.33: We check that T and S_2 meet the conditions. Firstly, $A_2 \subseteq X$ implies that $-X \supseteq -A_2$ and analogously, $-Y \supseteq -B_2$. We remark that $0 < r_2 < r_1$ implies $-r_1 \neq -r_2$. Furthermore, $X \cup Y =]\ell_2, r_1[$ and $|\ell_2| < r_2 < r_1$ imply that neither $r_2 \in -Y$ nor $r_2 \in -X$. We conclude that $S_2 \to T$.

It is left to show that either $T = S_1$ or $T \to S_1$. Clearly, if $\ell_1 = \ell_2$, then $T = S_1$. Otherwise, we have $\ell_1 < \ell_2$. We observe that $\ell_2 = 0$ is impossible as it would imply that $\mathrm{family}(S_1) - \mathrm{family}(S_2) = 2$, contradictory to the condition of the lemma. We distinguish cases by the signs of ℓ_1 and ℓ_2.

- If $0 \leq \ell_1 < \ell_2$, then $T \to S_1$ by Corollary 4.2.33: Firstly, $A_1 \supseteq X$ and $B_1 \supseteq Y$. Secondly, $-\ell_1 \neq \ell_2$. Thirdly, as $-\ell_2 \notin]\ell_1, r_1[$, we have neither $-\ell_2 \in A_1$ nor $-\ell_2 \in B_1$.
- If $\ell_1 < \ell_2 < 0$, then $T \to S_1$ by Corollary 4.2.33: Firstly, $A_1 \supseteq X$ and $B_1 \supseteq Y$. Secondly, $-\ell_1 \neq \ell_2$. Thirdly, we assume for a contradiction that $-\ell_2 \in A_1$ and $0 \in B_1$. Then we recall that the dexter notation of S_2 implied that $|\ell_2| < r_2$. Therefore $-\ell_2, 0 \in]\ell_2, r_2[$, so $-\ell_2 \in A_2$ and $0 \in B_2$. Then $0 \in B_2$ and $\ell_2 \in \overline{A_2} \cap -\overline{A_2}$, which is impossible as S_2 is a $\vec{\mathcal{B}}_n$ shard. An analogous argument forbids the combination of $-\ell_2 \in B_1$ and $0 \in A_1$.
- If $\ell_1 < 0 < \ell_2$, we introduce one more shard. We set $V = A_1 \cap]\ell_3, r_1]$ and $W = B_1 \cap]\ell_3, r_1]$ and $U := S_n(\ell_3, r_1, V, W)$. We set ℓ_3 to -1 or 1 depending on the shard S_1. We distinguish cases by that decision:
  - If 0 and 1 are both in A_1 or both in B_1, then we set $\ell_3 = -1$. We check the conditions of Definition 4.2.16 to make sure that U is a $\vec{\mathcal{B}}_n$ shard:
    1. Clearly, $-n \leq -1 < r_1 \leq n$.
    2. We have $V \cup W = (A_1 \cup B_1) \cap]-1, r_1[=]\ell_1, r_1[\cap]-1, r_1[=]-1, r_1[$ and $V \cap W = (A_1 \cap B_1) \cap]-1, r_1[= \emptyset$ as S_1 is a $\vec{\mathcal{B}}_n$ shard.
    3. If $0 \in V$, we want to show that $\overline{W} \cap -\overline{W} = \emptyset$ or equivalently, $W \cap -W = \emptyset$ and $1 \notin W$ and $-r_1 \notin W$. Firstly, $W \cap -W = \emptyset$ and $-r_1 \notin W$ follow from $\overline{B_1} \cap -\overline{B_1}$ as S_1 is a $\vec{\mathcal{B}}_n$ shard. Secondly, $1 \notin W$ as we assumed that 0 and 1 are either both in A_1 (and thus in W) or both in B_1 (and thus in V).

    We want to prove $T \to S_1$. We first show $T \to U$ by Corollary 4.2.33: Firstly, $V \supseteq X$ and $W \supseteq Y$. Secondly, we note that one of $V^{\pm}$ and $W^{\pm}$ is empty while the other contains only 0. Thirdly, as $V \cup W = [0, r_1[$, we have neither $-\ell_2 \in V$ nor $-\ell_2 \in W$.

As a second step, we show that either $U = S_1$ or $U \to S_1$. Clearly, if $\ell_1 = -1$, then $U = S_1$. Otherwise, we have $\ell_1 < -1$ and want to show that $U \to S_1$. Once more, we apply Corollary 4.2.33: Firstly, $A_1 \supseteq V$ and $B_1 \supseteq W$. Secondly, we note that $1 \neq \ell_1$. Thirdly, assume for a contradiction that $1 \in A_1$ and $0 \in B_1$. Then $1 \in V$ and $0 \in W$, so $0 \in W$ and $1 \in \overline{V} \cap -\overline{V}$, which is impossible as U is a $\vec{\mathcal{B}}_n$ shard. An analogous arugment holds if $1 \in B_1$ and $0 \in A_1$. We conclude that $T \to S_1$ as desired.

- If ($0 \in A_1$ and $1 \in B_1$) or ($0 \in B_1$ and $1 \in A_1$), then we set $\ell_3 = 1$. Then U is a $\vec{\mathcal{B}}_n$ shard of the second family.
  We want to prove $T \to S_1$. As a first step, we show that either $T = U$ or $T \to U$. Clearly, if $1 = \ell_2$, then $T = U$. Otherwise, we have $1 < \ell_2$ and want to show that $T \to U$. As always, we apply Corollary 4.2.33: Firstly, $V \supseteq X$ and $W \supseteq Y$. Secondly, we note that $-1 \neq \ell_2$. Thirdly, as $V \cup W = [2, r_1[$, we have neither $-\ell_2 \in V$ nor $-\ell_2 \in W$.
  As a second step, we show that $U \to S_1$. Of course, we use Corollary 4.2.33: Firstly, $A_1 \supseteq V$ and $B_1 \supseteq W$. Secondly, if $-\ell_3 = \ell_1$, then $\ell_1 = -1$, so one of $A_1^{\pm}$ and $B_1^{\pm}$ is empty while the other one contains only 0. Thirdly, we assume for a contradiction that $-\ell_3 \in A_1$ and $0 \in B_1$. Then $\overline{A_1} \cap -\overline{A_1} = \emptyset$ as S_1 is a $\vec{\mathcal{B}}_n$ shard. But this implies $1 = \ell_3 \notin A_1$ in contradiction to the assumption of the case we are in. An analogous arugment holds if $-\ell_3 \in B_1$ and $0 \in A_1$. We conclude that $T \to S_1$ as desired.

As S_1 and S_2 were presumed to be distinct, we conclude that S_2 forces S_1. □

Lemma 4.2.41 (Forcing from Double Restriction)**.** *Let S_1 and S_2 be two $\vec{\mathcal{B}}_n$ shards such that* $\text{family}(S_1) = 3$ *and* $\text{family}(S_2) = 1$. *If S_2 doubly restricts S_1, then S_2 forces S_1.*

Proof. We denote the shard $S_1 = S_n(\ell_1, r_1, A_1, B_1)$ in sinister notation (so that $r_1 < -\ell_1$) and $S_2 = S_n(0, r_2, A_2, B_2)$ in dexter notation. As S_2 doubly restricts S_1, we obtain the sequence of inequalities $\ell_1 < -r_1 \leq 0 < r_2 \leq r_1 < -\ell_1$ and $A_2 \subseteq A_1 \cap -B_1$ and $B_2 \subseteq B_1 \cap -A_1$. We set $T := S_n(0, r_1, A_1^+, B_1^+)$. Clearly, T is a $\vec{\mathcal{B}}_n$ shard. Then Lemma 4.2.34 certifies that $T \to S_1$.

- If $r_1 = r_2$, then $T = S_2$, so $S_2 \to S_1$, so S_2 forces S_1.
- If $r_1 > r_2$, we can use the sinister notations for the shards $T = S_n(-r_1, 0, -B_1^+, -A_1^+)$ and $S_2 = S_n(-r_2, 0, -B_2, -A_2)$. We note that $-A_2 \subseteq -A_1^+$ and $-B_2 \subseteq -B_1^+$. Then Corollary 4.2.33 certifies that $S_2 \to T$, and we deduce that S_2 forces S_1. □

The following statement is a direct consequence of the three lemmas we just discussed and gives a compact exhaustive criterion to determine whether one $\vec{\mathcal{B}}_n$ shard forces another. We refer to Observation 4.1.5 for the classification of all hyperplanes a $\vec{\mathcal{B}}_n$ shard can lie on into three disjoint families.

Proposition 4.2.42 (Forcing in $\vec{\mathcal{B}}_n$)**.** *A $\vec{\mathcal{B}}_n$ shard S_2 forces another $\vec{\mathcal{B}}_n$ shard S_1 if and only if*

1. $\text{family}(S_1) - \text{family}(S_2) < 2$ *and S_2 restricts S_1 or*
2. $\text{family}(S_1) - \text{family}(S_2) = 2$ *and S_2 doubly restricts S_1.*

See Figure 4.6 for an illustration of the forcing poset on $\vec{\mathcal{B}}_3$ shards. We remark that forcing on $\vec{\mathcal{B}}_n$ shards is not as straightforward as forcing on $\vec{\mathcal{A}}_n$ shards when using arc representations.

Observation 4.2.43 (Forcing on $\vec{\mathcal{B}}_n$ Arcs)**.** A $\vec{\mathcal{B}}_n$ shard S with representative Σ forces another $\vec{\mathcal{B}}_n$ shard S' with representative Σ' if and only if

- S and S' are both of the third family (so they each have overlapped $\vec{\mathcal{B}}_n$ arcs) and the upper arc of S forces the upper arc of S' as arcs of $\vec{\mathcal{A}}_{[\pm n]}$ shards.
- or S is not of the third family and the arc of S or its centrally symmetric image forces the arc of S' as arcs of $\vec{\mathcal{A}}_{[\pm n]}$ shards.

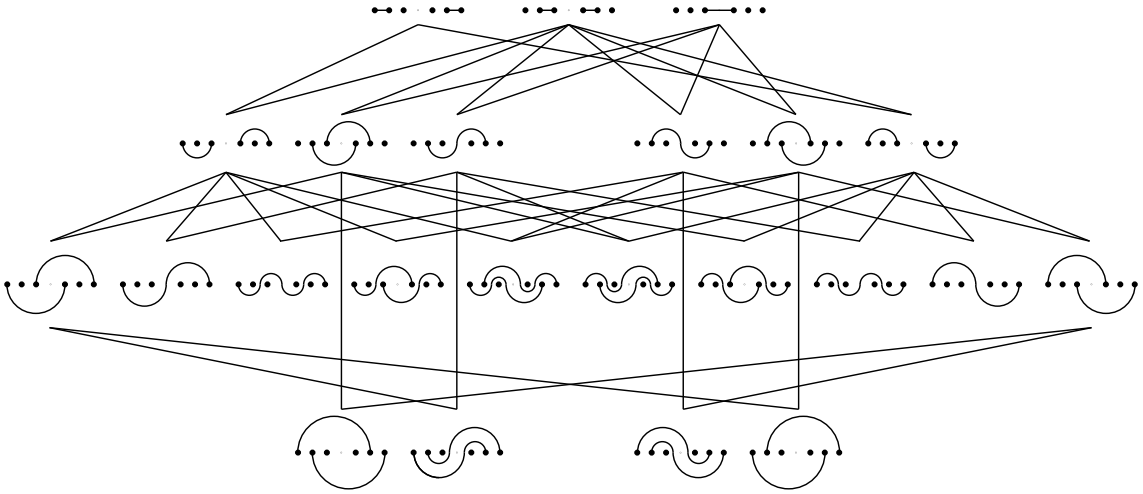

Figure 4.6: The forcing order on $\vec{\mathcal{B}}_3$ shards, illustrated by their $\vec{\mathcal{B}}_n$ arcs. [Picture from [PPR20]]

This has a number of implications.

- A third family shard can only force shards that are of the third family as well. On the other hand, a third family shard might be forced by other shard of any family. For example,  does not force  which forces  .
- For forcing among third family shards (with overlapped arcs), the distinction between upper and lower arcs is important as it determines whether $0 \in A$ or $0 \in B$. For example,  is forced by  , but not by  .

4.3 Type B Quotients

In this section, we will use our knowledge on the shards of $\vec{\mathcal{B}}_n$ and their forcing relation to analyze lattice congruences on the poset of regions $\mathrm{Pos}(\vec{\mathcal{B}}_n)$, the quotient lattices they induce, their quotient fans and quotientopes for them.

4.3.1 Lattice Congruences

Similar to the $\vec{\mathcal{A}}_n$ arrangement, we can see lattice congruences as upper sets in the forcing poset. This is a consequence of the properties of forcing discussed in Section 1.5.3.

Theorem 4.3.1 ($\vec{\mathcal{B}}_n$ Lattice Congruences)**.** *The lattice congruences on* $\mathrm{Pos}(\vec{\mathcal{B}}_n)$ *(equivalently, on the weak order on* $\mathfrak{S}_n^{\mathcal{B}}$*) are in bijection with the upper sets of the poset of* $\vec{\mathcal{B}}_n$ *shards.*

We remark that there are some connections between lattice congruences on the poset of regions of $\vec{\mathcal{B}}_n$ and lattice congruences on the poset of regions of $\vec{\mathcal{A}}_{[\pm n]}$. First, we will take a look at upper sets of $\vec{\mathcal{B}}_n$ shards, translated into upper sets of $\vec{\mathcal{A}}_{[\pm n]}$ shards.

Corollary 4.3.2 (Upper Set without Third Family Shards)**.** If an upper set in the poset of $\vec{\mathcal{B}}_n$ shards has no shard of the third family among its minimal elements, it does not contain any shard of the third family and the corresponding set of $\vec{\mathcal{A}}_{[\pm n]}$ shards is an upper set in the forcing poset of $\vec{\mathcal{A}}_{[\pm n]}$.

We next have a look at upper sets of $\vec{\mathcal{A}}_{[\pm n]}$ shards, trying to translate them back into sets of $\vec{\mathcal{B}}_n$ shards. For some $\vec{\mathcal{A}}_{[\pm n]}$ shards, this is considerably easier than for others.

Definition 4.3.3 (Centrally Symmetrizable Shard)**.** Let $\Sigma_{[\pm n]} = \Sigma_n(\ell, r, A, B)$ be an $\vec{\mathcal{A}}_{[\pm n]}$ shard. It is called **centrally symmetrizable** if $S_n(\ell, r, A, B)$ is a $\vec{\mathcal{B}}_n$ shard as defined in Definition 4.2.16. We then call $S_n(\ell, r, A, B)$ its symmetrized $\vec{\mathcal{B}}_n$ shard. Equivalently, the shard Σ is centrally symmetrizable if its corresponding $\vec{\mathcal{A}}_{[\pm n]}$ arc is either centrally symmetric in itself or if it is not crossing its centrally symmetric image.

Corollary 4.3.4 (Upper Set of Symmetrized Shards)**.** Let $\mathcal{S}$ be an upper set of $\vec{\mathcal{A}}_{[\pm n]}$ shards. The set of symmetrized $\vec{\mathcal{B}}_n$ shards for all centrally symmetrizable shards in $\mathcal{S}$ is an upper set of $\vec{\mathcal{B}}_n$ shards.

4.3.2 Quotient Fans

As in the braid arrangement $\vec{\mathcal{A}}_n$, we are interested in the quotient fans that are obtained by applying lattice congruences of the weak order on $\vec{\mathcal{B}}_n$ to the type $\mathcal{B}$ arrangement fan. The following is a reformulation of Theorem 1.5.18 for the $\vec{\mathcal{B}}_n$ arrangement.

Theorem 4.3.5 ($\vec{\mathcal{B}}_n$ Quotient Fan)**.** *Let $\equiv^{\mathcal{B}}$ be a lattice congruence on $\mathrm{Pos}(\vec{\mathcal{B}}_n)$. It induces a quotient fan $\mathcal{F}^{\mathcal{B}}_{\equiv}$ that coarsens the $\mathcal{B}_n$ fan $\mathcal{F}^{\mathcal{B}}_n$. Its chambers can be described*

- *as the closures of the connected components of the complement in $\mathbb{R}^n$ of the union of all $\vec{\mathcal{B}}_n$ shards $S \in \mathbf{\Sigma}^{\mathcal{B}\checkmark}_{\equiv}$ retained by $\equiv^{\mathcal{B}}$,*
- *or as the unions of chambers $C(\sigma)$ of $\mathcal{F}^{\mathcal{B}}_n$ corresponding to all $\mathcal{B}$-permutations $\sigma \in \mathfrak{S}^{\mathcal{B}}_n$ in each congruence class of $\equiv^{\mathcal{B}}$.*

We can now describe the rays of the quotient fan $\mathcal{F}^{\mathcal{B}}_{\equiv}$.

Lemma 4.3.6 (Rays of the $\vec{\mathcal{B}}_n$ Quotient Fan)**.** *Given a lattice congruence $\equiv^{\mathcal{B}}$ on the poset of regions of $\mathrm{Pos}(\vec{\mathcal{B}}_n)$ and a non-empty signed subset $\emptyset \subsetneq I \subsetneq [\pm n]$, the ray $C(I)$ of the $\mathcal{B}_n$ arrangement fan $\mathcal{F}^{\mathcal{B}}_n$ is a ray of the quotient fan $\mathcal{F}^{\mathcal{B}}_{\equiv}$ if and only if for any $\ell < r \in [\pm n]$, the congruence $\equiv^{\mathcal{B}}$ retains all the shards*

- $S_n(\ell,\ r,\ \emptyset,\ ]\ell, r[)$ *whenever $\ell, r \in I$ with $\ell + r \neq 0$ and $]\ell, r[\cap I = \emptyset$,*
- $S_n(\ell,\ r,\ ]\ell, r[,\ \emptyset)$ *whenever $\ell, r \in -I$ with $\ell + r \neq 0$ and $]\ell, r[\cap -I = \emptyset$,*
- $S_n(0,\ r,\ \emptyset,\ ]0, r[)$ *whenever $\ell, r \in I$ with $\ell + r = 0$ and $]\ell, r[\cap I = \emptyset$,*
- $S_n(0,\ r,\ ]0, r[,\ \emptyset)$ *whenever $\ell, r \in -I$ with $\ell + r = 0$ and $]\ell, r[\cap -I = \emptyset$,*
- $S_n(\ell,\ r,\ ]\ell, r[\cap I,\ ]\ell, r[\cap -I)$ *whenever $\ell, r \notin -I \cup I$ and $]\ell, r[\setminus (-I \cup I) = \emptyset$.*

Proof. Just as we learned in Proposition 2.2.3, a ray is present in a quotient fan $\mathcal{F}^{\mathcal{B}}_{\equiv}$ if and only if all the shards that contain it in their interior are preserved by the congruence $\equiv^{\mathcal{B}}$. Using Proposition 2.2.3, we can describe the $\vec{\mathcal{A}}_{[\pm n]}$ shards which contain the ray $C(I)$ in their interior. The $\vec{\mathcal{B}}_n$ shards listed above are precisely those that correspond to these $\vec{\mathcal{A}}_{[\pm n]}$ shards through the projection $\varphi^{\mathcal{B}}$ on the centrally symmetric space $\mathcal{H}^{\mathcal{B}}_n$. □

We recall that an $\vec{\mathcal{A}}_{[\pm n]}$ shard is centrally symmetrizable if it corresponds to a $\vec{\mathcal{B}}_n$ shard as described in Definition 4.3.3. This property has implications on the rays in its interior and on their intersection with the centrally symmetric subspace $\mathcal{H}^{\mathcal{B}}_n \subset \mathbb{R}^{[\pm n]}$.

Observation 4.3.7 (Rays of Non-Symmetrizable Shards)**.** The interior of any $\vec{\mathcal{A}}_{[\pm n]}$ shard Σ that is not centrally symmetrizable does not intersect the centrally symmetric subspace $\mathcal{H}^{\mathcal{B}}_n$.

4.3.3 Quotientopes

We will now discuss the construction of quotientopes for lattice congruences on the weak order of $\mathfrak{S}^{\mathcal{B}}_n$ (equivalently, on the poset of regions $\mathrm{Pos}(\vec{\mathcal{B}}_n)$). The following statement follows from Corollary 4.3.4.

Corollary 4.3.8 ($\vec{\mathcal{B}}_n$ Quotientopes as Projections of $\vec{\mathcal{A}}_{[\pm n]}$ Quotientopes)**.** Let $\equiv$ be a lattice congruence on the poset of regions of $\vec{\mathcal{A}}_{[\pm n]}$. We set $\equiv^{\mathcal{B}}$ to be the lattice congruence on the poset of regions of $\vec{\mathcal{B}}_n$ that retains exactly the centrally symmetrizable $\vec{\mathcal{A}}_{[\pm n]}$ shards in $\mathbf{\Sigma}^{\checkmark}_{\equiv}$. Then the $\vec{\mathcal{B}}_n$ quotient fan $\mathcal{F}^{\mathcal{B}}_{\equiv}$ is the section of the $\vec{\mathcal{A}}_{[\pm n]}$ quotient fan $\mathcal{F}_{\equiv}$ by the centrally symmetric subspace $\mathcal{H}^{\mathcal{B}}_n$. Therefore, if $\mathsf{Quot}(\equiv)$ is a quotientope in $\mathbb{R}^{[\pm n]}$ for $\equiv$ (whose normal fan is thus equal to $\mathcal{F}_{\equiv}$), then the image of $\mathsf{Quot}(\equiv)$ by the projection $\varphi^{\mathcal{B}}$ is a quotientope in $\mathbb{R}^n$ for $\equiv^{\mathcal{B}}$.

If every quotient lattice of the weak order on $\mathfrak{S}^{\mathcal{B}}_n$ could be obtained in this way, then we could construct quotientopes for all lattice congruences $\equiv^{\mathcal{B}}$ in the above way. However, this is not the case as the forcing relation among $\vec{\mathcal{B}}_n$ shards is different from the forcing relation of their representative $\vec{\mathcal{A}}_{[\pm n]}$ shards as discussed in Observation 4.2.43. While every lattice congruence on $\mathrm{Pos}(\vec{\mathcal{A}}_{[\pm n]})$ corresponds to a lattice congruence on $\mathrm{Pos}(\vec{\mathcal{B}}_n)$, the converse is not true. In fact, only 12 of the 19 lattice congruences on $\mathrm{Pos}(\vec{\mathcal{B}}_2)$ can be constructed from centrally symmetrizing a congruence on $\mathrm{Pos}(\vec{\mathcal{A}}_{[\pm 2]})$, and only 1370 of 8368 do so for $n = 3$, as we computed using [SD19].

We will nevertheless construct quotientopes for all quotient fans of the $\vec{\mathcal{B}}_n$ arrangement fan. For the remainder of this chapter, we first construct shard polytopes for $\vec{\mathcal{B}}_n$ shards. With their help, we will be able to construct shardsumotopes for lattice congruences on the poset of regions $\mathrm{Pos}(\vec{\mathcal{B}}_n)$.

4.3.4 Shard Polytopes

We will use shard polytopes constructed for shards in the $\vec{\mathcal{A}}_{[\pm n]}$ arrangement and project them to the centrally symmetric subspace $\mathcal{H}^{\mathcal{B}}_n$. These polytopes will serve as shard polytopes for $\vec{\mathcal{B}}_n$ shards. Equivalently, they can be constructed directly from a $\vec{\mathcal{B}}_n$ shard by using shard matchings of its representative $\vec{\mathcal{A}}_{[\pm n]}$ shard.

Definition 4.3.9 ($\vec{\mathcal{B}}_n$ Shard Polytope)**.** Let S be a $\vec{\mathcal{B}}_n$ shard whose representative $\vec{\mathcal{A}}_{[\pm n]}$ shard is Σ. The **shard polytope** $\mathsf{SP}(S)$ is the convex hull of the characteristic vectors of all Σ-matchings, with the usual convention that $\mathbf{e}_{-i} = -\mathbf{e}_i$.

Observation 4.3.10. We remark that this implies that $\mathsf{SP}(S)$ is the image of the $\vec{\mathcal{A}}_{[\pm n]}$ shard polytope $\mathsf{SP}(\Sigma)$ under the projection $\varphi^{\mathcal{B}}$ onto the centrally symmetric subspace $\mathcal{H}^{\mathcal{B}}_n \subset \mathbb{R}^{[\pm n]}$ given in Definition 4.1.17, so we can write $\mathsf{SP}(S) = \varphi^{\mathcal{B}}(\mathsf{SP}(\Sigma))$.

See Figure 4.7 for an illustration of the shard polytopes of $\vec{\mathcal{B}}_2$ (top) and of $\vec{\mathcal{B}}_3$ (bottom).

Observation 4.3.11. Given a $\vec{\mathcal{B}}_n$ shard S represented by the $\vec{\mathcal{A}}_{[\pm n]}$ shard $\Sigma = \Sigma_{[\pm n]}(\ell, r, A, B)$, we first observe that the dimension of $\mathsf{SP}(S)$ is equal to $r - \ell$ if $\mathrm{family}(S) = 2$ and equal to r otherwise. To make some observations about the vertices of the shard polytope $\mathsf{SP}(S)$, we distinguish cases by the family that S belongs to.

- If $\mathrm{family}(S) = 1$, then the vertices of $\mathsf{SP}(S)$ are precisely the characteristic vectors of all those Σ-matchings that are centrally symmetric, as we will show in Lemma 4.3.17.
- If $\mathrm{family}(S) = 2$, then $\mathsf{SP}(S) = \mathsf{SP}(\Sigma)$, so the vertices of $\mathsf{SP}(S)$ are precisely the characteristic vectors of all Σ-matchings.
- If $\mathrm{family}(S) = 3$, then there is no bijection between the vertices of $\mathsf{SP}(S)$ and the Σ-matchings. In particular, there are Σ-matchings whose characteristic vectors are not vertices of $\mathsf{SP}(S)$ and there are vertices of $\mathsf{SP}(S)$ that are the characteristic vector of multiple Σ-matchings.

The following statement certifies that $\mathcal{B}_n$ shard polytopes have the crucial property that makes them suitable for our construction of quotientopes as shardsumotopes. It is the type $\mathcal{B}$ analogue of Proposition 3.3.3.

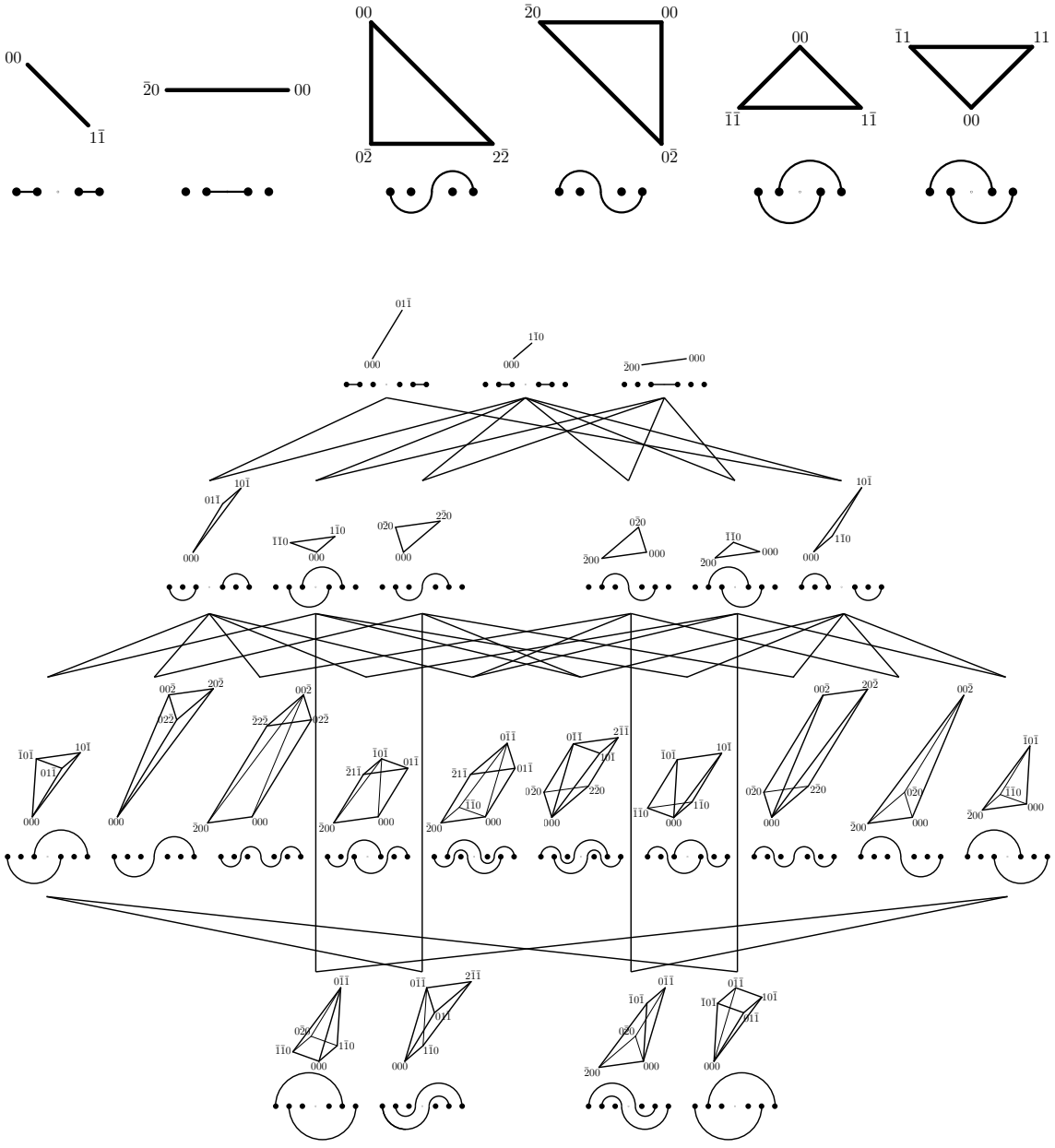

Figure 4.7: Shard polytopes for all six $\vec{\mathcal{B}}_2$ shards (top) and for all 23 $\vec{\mathcal{B}}_3$ shards (bottom). Each of them is labeled below by the arcs of their corresponding $\vec{\mathcal{A}}_{[\pm n]}$ shards. The numbers on the vertices indicate the characteristic vectors of the $\vec{\mathcal{A}}_{[\pm n]}$ shard matchings. In the diagram for $\vec{\mathcal{B}}_3$, the shard polytopes are arranged in the forcing order on $\vec{\mathcal{B}}_3$ shards. [Picture from [PPR20]]

Proposition 4.3.12 ($\vec{\mathcal{B}}_n$ Shard Fan Walls)**.** *Given a $\vec{\mathcal{B}}_n$ shard S, the union of the walls of the normal fan of the shard polytope $\mathsf{SP}(S)$ contains the shard S and is contained in the union of all shards S' that force S.*

The rest of this section is dedicated to the proof of Proposition 4.3.12. We first recall from Observation 4.3.10 that any $\vec{\mathcal{B}}_n$ shard polytope $\mathsf{SP}(S)$ is the image of the $\vec{\mathcal{A}}_{[\pm n]}$ shard polytope $\mathsf{SP}(\Sigma)$ under the linear projection $\varphi^{\mathcal{B}} : \mathbb{R}^{[\pm n]} \to \mathbb{R}^n$ (as defined in Observation 4.1.18), where Σ is the shard representing S. Similar to the arguments discussed in Observation 4.1.18, we observe that the normal fan of $\mathsf{SP}(S)$ is equal to the section of the normal fan of $\mathsf{SP}(\Sigma)$ with the centrally symmetric space $\mathcal{H}_n^{\mathcal{B}}$. In particular, the walls of the normal fan of $\mathsf{SP}(S)$ are exactly the intersection of the walls of the normal fan of $\mathsf{SP}(\Sigma)$ with $\mathcal{H}_n^{\mathcal{B}}$. This allows us to prove the first step towards Proposition 4.3.12.

Lemma 4.3.13 ($\vec{\mathcal{B}}_n$ Shards Are Contained in the Walls of Their Shard Fan)**.** *Any $\vec{\mathcal{B}}_n$ shard S is a subset of the union of the walls of the normal fan of $\mathsf{SP}(S)$.*

Proof. The $\vec{\mathcal{B}}_n$ shard S is equal to the intersection of its representative Σ with the centrally symmetric subspace $\mathcal{H}_n^{\mathcal{B}}$. We know from Proposition 3.3.3 that the union of the walls of the normal fan of $\mathsf{SP}(\Sigma)$ contains the shard Σ itself. This implies that $\Sigma \cap \mathcal{H}_n^{\mathcal{B}}$ is a subset of the union of walls of the normal fan of $\mathsf{SP}(S)$ as desired. □

Moreover, we can use this approach to make a step towards proving the opposite direction of Proposition 4.3.12.

Lemma 4.3.14 ($\vec{\mathcal{B}}_n$ Shards Fan Walls are Contained in a Union of Other Shards)**.** *The union of the walls of the normal fan of $\mathsf{SP}(S)$ is contained in the union of all $\vec{\mathcal{B}}_n$ shards S' whose representative Σ' forces the shard Σ representing S.*

Proof. The walls of the normal fan of $\mathsf{SP}(S)$ are exactly the intersections of the walls of the normal fan of $\mathsf{SP}(\Sigma)$ with the centrally symmetric subspace $\mathcal{H}_n^{\mathcal{B}}$. We know from Lemma 4.3.14 that the union of the walls of $\mathsf{SP}(\Sigma)$ is contained in the union of all shards Σ' that force Σ. This implies that the union of the walls of $\mathsf{SP}(S)$ is contained in the union of sets $\Sigma' \cap \mathcal{H}_n^{\mathcal{B}}$ for all shards Σ' forcing Σ and therefore in the union of those shards Σ'. □

As discussed earlier around Observation 4.2.43, the forcing of $\vec{\mathcal{A}}_{[\pm n]}$ representative shards does not guarantee the forcing of the respective associated $\vec{\mathcal{B}}_n$ shards. To prove Proposition 4.3.12, we therefore need to show for any $\vec{\mathcal{B}}_n$ shard S' that does not force S but has a representative Σ' that does force the representative Σ, that the centrally symmetric subspace $\mathcal{H}_n^{\mathcal{B}}$ does not intersect any wall of the normal fan $\mathsf{SP}(\Sigma)$ that is a subset of S'. We will prove this step by step depending on the family of the shard S.

Family 1 (Singular $\vec{\mathcal{B}}_n$ Arcs)

Definition 4.3.15 (Centrally Symmetric Matching)**.** Let Σ be an $\vec{\mathcal{A}}_{[\pm n]}$ shard. A Σ-matching M is called **centrally symmetric** if $M = -M$ holds.

We remark that centrally symmetric shards can have matchings that are not centrally symmetric (see for example the shard $\Sigma_{[\pm 2]}(-2, +2, \{+1\}, \{-1\})$ and the matching $M = \{1, 2\}$). Moreover, shards that are not centrally symmetric can have matchings that are centrally symmetric (see for example the shard $\Sigma_{[\pm 2]}(-2, +2, \{-1, +1\}, \emptyset)$ and the matching $M = \{-2, 2\}$). We take a closer look at characteristic vectors of centrally symmetric Σ-matchings.

Observation 4.3.16. Given a centrally symmetric $\vec{\mathcal{A}}_{[\pm n]}$ shard $\Sigma = \Sigma_{[\pm n]}(-r, r, A, B)$ and a centrally symmetric Σ-matching M, the k-th entry of its characteristic vector $\boldsymbol{\chi}(M) \in \mathbb{R}^n$ is either zero, or possibly $+2$ if $k \in A^+$, or possibly -2 if $k \in B^+ \cup \{r\}$.

We can now determine the vertices of the $\vec{\mathcal{B}}_n$-shard polytope $\mathsf{SP}(S)$.

Lemma 4.3.17 (Vertices of $\mathsf{SP}(S)$ for Family 1)**.** *Let S be a $\vec{\mathcal{B}}_n$ shard of the first family with representative $\vec{\mathcal{A}}_{[\pm n]}$-shard Σ. The vertices of the shard polytope $\mathsf{SP}(S)$ are exactly the characteristic vectors of those Σ-matchings that are centrally symmetric.*

Proof. We fix a Σ-matching $M = \{a_1 < b_1 < \cdots < a_k < b_k\}$. As the shard Σ is centrally symmetric, we know that the reflected set $-M := \{-b_k < -a_k < \cdots < -b_1 < -a_1\}$ is a Σ-matching as well. We observe that their characteristic vectors are identical in $\mathbb{R}^n$ because we have $\boldsymbol{\chi}(-M) = \sum_{i=1}^{k} (\mathbf{e}_{-b_i} - \mathbf{e}_{-a_i}) = \sum_{i=1}^{k} (\mathbf{e}_{a_i} - \mathbf{e}_{b_i}) = \boldsymbol{\chi}(M)$. We assume that M is not centrally symmetric, so that $M \neq -M$. As M and $-M$ cannot fall into any of the special cases of Lemma 3.2.13, so there are two Σ-matchings M_3 and M_4 distinct from M and $-M$ such that $2\boldsymbol{\chi}(M) = \boldsymbol{\chi}(M) + \boldsymbol{\chi}(-M) = \boldsymbol{\chi}(M_3) + \boldsymbol{\chi}(M_4)$. In particular, the vector $\boldsymbol{\chi}(M)$ is in the convex hull of $\boldsymbol{\chi}(M_3)$ and $\boldsymbol{\chi}(M_4)$, so it cannot be a vertex of $\mathsf{SP}(S)$. Therefore, every vertex of $\mathsf{SP}(S)$ has to be the characteristic vector of a centrally symmetric Σ-matching.

Conversely, we deduce from Observation 4.3.16 that any characteristic vector of a centrally symmetric Σ-matching is a vertex of the cube in $\mathbb{R}^n$ defined by the inequalities $0 \leq x_i \leq 2$ for all $i \in A^+$ and $-2 \leq x_j \leq 0$ for all $j \in B^+ \cup \{r\}$. Therefore, the shard polytope $\mathsf{SP}(S)$ is a subset of this cube and every characteristic vector of a centrally symmetric Σ-matching is an extremal point of the cube and thus a vertex of $\mathsf{SP}(S)$. □

We have another look at centrally symmetric matchings. We can partition them into two classes: Those that have a cardinality that is divisible by 4 (including the empty matching) and those that have a cardinality that is not divisible by 4.

Observation 4.3.18 (Partition of $\mathsf{SP}(S)$ Vertices)**.** Let $\Sigma = \Sigma_{[\pm n]}(\ell, r, A, B)$ be an $\vec{\mathcal{A}}_{[\pm n]}$ shard.

- A centrally symmetric Σ-matching M with $4 \mid |M|$ has an even number of negative and positive elements, and as they are strictly alternating between elements of $\{\ell\} \cup A$ and elements of $B \cup \{r\}$, both $M \cap [n]$ and $M \cap -[n]$ are Σ-matchings themselves. For its characteristic vector, we obtain $\langle \mathbf{1} \,|\, \boldsymbol{\chi}(M) \rangle = 0$.
- A centrally symmetric Σ-matching M with $4 \nmid |M|$ has an odd number of negative and positive elements. For its characteristic vector, we obtain $\langle \mathbf{1} \,|\, \boldsymbol{\chi}(M) \rangle = -2$.

Geometrically, as every vertex of $\mathsf{SP}(S)$ is equal to a characteristic vector of a centrally symmetric Σ-matching, the direction $\mathbf{1}$ defines two faces of $\mathsf{SP}(S)$ where we have either $\langle \mathbf{1} \,|\, \mathbf{x} \rangle = 0$ or $\langle \mathbf{1} \,|\, \mathbf{x} \rangle = -2$, and each vertex of $\mathsf{SP}(S)$ is contained in exactly one of these two faces.

We next have a look at the edge directions of $\mathsf{SP}(S)$.

Lemma 4.3.19 (Edge Directions of $\mathsf{SP}(S)$ for Family 1)**.** *Let S be a $\vec{\mathcal{B}}_n$ shard of the first family. The shard polytope $\mathsf{SP}(S)$ does not have any edge in a direction $\mathbf{e}_i + \mathbf{e}_j$ for any $1 \leq i < j \leq n$.*

Proof. Assume for a contradiction that $\mathsf{SP}(S)$ has two vertices $\boldsymbol{\chi}(M_1)$ and $\boldsymbol{\chi}(M_2)$ (where both M_1 and M_2 are centrally symmetric by Lemma 4.3.17) that form an edge in direction $\mathbf{e}_i + \mathbf{e}_j$. Then we have $\boldsymbol{\chi}(M_2) = \boldsymbol{\chi}(M_1) + \lambda(\mathbf{e}_i + \mathbf{e}_j)$ for some $\lambda \neq 0$. Without loss of generality, we may assume that $\lambda > 0$ (we can just exchange the roles of M_1 and M_2). We learned in the proof of Lemma 4.3.17 that the vertices of $\mathsf{SP}(S)$ have a k-th coordinate of 0 or 2 if $k \in A^+$ and a k-th coordinate of -2 or 0 if $k \in B^+ \cup \{r\}$. In any entry, two vertices of $\mathsf{SP}(S)$ can only differ either by 0 or by 2, so we need to have $\lambda = 2$. This gives us $\boldsymbol{\chi}(M_2) = \boldsymbol{\chi}(M_1) + 2\mathbf{e}_i + 2\mathbf{e}_j$, which

implies that $\langle \mathbf{1} \,|\, \boldsymbol{\chi}(M_2) \rangle = \langle \mathbf{1} \,|\, \boldsymbol{\chi}(M_1) \rangle + 4$. But we saw in Observation 4.3.18 that this scalar product is either 0 or -2 for all characteristic vectors of centrally symmetric Σ-matchings, which gives a contradiction. □

We can now prove the desired statement about first family shard polytopes without much effort.

Lemma 4.3.20 (Shard Fan Walls for Family 1)**.** *Let S be a $\vec{\mathcal{B}}_n$ shard of the first family. The union of the walls of the normal fan of the shard polytope $\mathsf{SP}(S)$ is contained in the union of the representatives Σ' for all $\vec{\mathcal{B}}_n$ shards S' that force S.*

Proof. Let Σ be the representative of S. As S is of the first family, it is only forced by those $\vec{\mathcal{B}}_n$ shards S' whose representative Σ' force Σ. With the help of Lemma 4.3.14, we only need to show that no wall of the normal fan of $\mathsf{SP}(S)$ is a part of a $\mathcal{B}_n$ hyperplane of the third family, or equivalently, that no edge of $\mathsf{SP}(S)$ is normal to a $\mathcal{B}_n$ hyperplane of the third family. This is certified by Lemma 4.3.19. □

Family 2 (Separated $\vec{\mathcal{B}}_n$ Arcs)

For $\vec{\mathcal{B}}_n$ shards of the second family, the desired result can be obtained in a straightforward way.

Lemma 4.3.21 (Shard Fan Walls for Family 2)**.** *Let S be a $\vec{\mathcal{B}}_n$ shard of the second family. The union of the walls of the normal fan of the shard polytope $\mathsf{SP}(S)$ is contained in the union of the representatives Σ' for all $\vec{\mathcal{B}}_n$ shards S' that force S.*

Proof. Let Σ be a $\vec{\mathcal{B}}_n$ shard of the second family with representative $\vec{\mathcal{A}}_{[\pm n]}$ shard Σ. We know from Observation 4.2.43 that the $\vec{\mathcal{B}}_n$ shards that force S are precisely those whose representative Σ' forces Σ. Therefore, the statement is an immediate consequence of Lemma 4.3.14. □

Family 3 (Overlapping $\vec{\mathcal{B}}_n$ Arcs)

The third family of $\vec{\mathcal{B}}_n$ shards is the one with the most complicated properties concerning both the notation we established and their relationship to the $\vec{\mathcal{A}}_{[\pm n]}$ arrangement. We will distinguish a number of cases for a $\vec{\mathcal{B}}_n$ shard depending on whether its dexter representative $\vec{\mathcal{A}}_{[\pm n]}$ shard is upper or lower. We will first make a few observations that help us in these case distinctions.

Observation 4.3.22. Let $S = S_n(\ell, r, A, B)$ be a $\vec{\mathcal{B}}_n$ shard of the third family in dexter notation (so that $0 < -\ell < r$). Let Σ be the representative of S and let α be the arc illustrating Σ and $-\alpha$ be the centrally symmetric image of α. We see immediately that α is above $-\alpha$ if and only if $0 \in A$. The vertical order of the arcs has some more implications:

- The arc α is above α' if and only if $-\ell \in A$ and $-i \in A$ for all $i \in B \cap]-\ell, \ell[$.
- The arc α is below α' if and only if $-\ell \in B$ and $-i \in B$ for all $i \in A \cap]-\ell, \ell[$.

Put differently, for any $\vec{\mathcal{B}}_n$ shard S, we are in one of the following cases:

- We have $0 \in A$ and$-\ell \in A$ and $-i \in A$ for all $i \in B \cap]-\ell, \ell[$.
- We have $0 \in B$ and $-\ell \in B$ and $-i \in B$ for all $i \in A \cap]-\ell, \ell[$.

The following result is a direct consequence of this observation.

Lemma 4.3.23 (Partial Central Symmetry Certified By Forcing)**.** *Let S be a $\vec{\mathcal{B}}_n$ shard of the third family with representative Σ. Let $S' = S_n(\ell', r', A', B')$ be another $\vec{\mathcal{B}}_n$ shard of the third family with representative Σ'. We set the position $m' := \min(|\ell'|, |r'|)$. If Σ' forces Σ and they are neither both upper nor both lower, then Σ is centrally symmetric on the interval $[-m, +m]$.*

We give another rather technical statement that we will use later to examine the $\vec{\mathcal{B}}_n$ shard fan for a shard of the third family.

Lemma 4.3.24 (Consequences of Non-Forcing Among Representative $\vec{\mathcal{A}}_{[\pm n]}$ Shards)**.** *Let S be a $\vec{\mathcal{B}}_n$ shard of the third family in dexter notation $S = S_n(\ell, r, A, B)$ with representative $\vec{\mathcal{A}}_{[\pm n]}$ shard Σ. Let $\Sigma' = \Sigma_{[\pm n]}(\ell', r', A', B')$ be another $\vec{\mathcal{A}}_{[\pm n]}$ shard that forces Σ. If Σ' does not force the centrally symmetric reflection of Σ, then*

- *either $r' > -\ell$,*
- *or $0 \in A$ and there is a $k \in]\ell', r'[$ such that $-k, k \in A$,*
- *or $0 \in B$ and there is a $k \in]\ell', r'[$ such that $-k, k \in B$.*

Proof. We denote the centrally symmetric reflection of Σ by $\Sigma^* := \Sigma_{[\pm n]}(-r, -\ell, -B, -A)$. As Σ' forces Σ, the sets A and A' (resp. B and B') agree on all positions in between ℓ' and r'. Moreover, we have either $[\ell', r'] \subseteq [-r, -\ell]$ or not.

- If $[\ell', r'] \not\subseteq [-r, -\ell]$, we remark that Σ is the dexter representative of S, so $-r < \ell < 0$. As Σ' forces Σ, we have $\ell \leq \ell'$. Together, these inequalities imply that $-r < \ell \leq \ell'$, so the case $[\ell', r'] \not\subseteq [-r, -\ell]$ can only occur if $r' > -\ell$.
- If $[\ell', r'] \subseteq [-r, -\ell]$, we have $-r \leq \ell \leq \ell' < 0 < r' \leq -\ell$. As Σ' does not force Σ^*, the set $-B$ does not agree with A' (and thus not with A) on the positions in between ℓ' and r' and the same argument holds for $-A$ and B. As they do not agree, there has to be some $k \in]\ell', r'[$ such that one of the following holds.
  - We have $k \in A \setminus (-B)$, so that $k \in A \cap (-A)$, and therefore $-k, k \in A$. Then Observation 4.3.22 implies that we are in the case where $0 \in A$.
  - We have $k \in B \setminus (-A)$, so that $k \in B \cap (-B)$, and therefore $-k, k \in B$. Then Observation 4.3.22 implies that we are in the case where $0 \in B$. □

The remainder of this section is dedicated to proving a statement on the walls of the normal fan of the shard polytope $\mathsf{SP}(S)$ analogous to those for the other families of shards.

Lemma 4.3.25 (Shard Fan Walls For Family 3)**.** *Let S be a $\vec{\mathcal{B}}_n$ shard of the third family. The union of the walls of the normal fan of the shard polytope $\mathsf{SP}(S)$ is contained in the union of the representatives Σ' for all $\vec{\mathcal{B}}_n$ shards S' that force S.*

Proof. For a $\vec{\mathcal{B}}_n$ shard S of the third family, the $\vec{\mathcal{B}}_n$ shards S' that force S are exactly those whose representative $\vec{\mathcal{A}}_{[\pm n]}$ shard Σ' forces Σ or its centrally symmetric image, except for those where S' is of the third family and Σ' does not force Σ (meaning that the upper $\vec{\mathcal{A}}_{[\pm n]}$ shard of S' does not force the upper $\vec{\mathcal{A}}_{[\pm n]}$ shard of S but the lower one and vice versa). We will therefore analyze the following situation:

- Let $S = S_n(\ell, r, A, B)$ be a $\vec{\mathcal{B}}_n$ shard of the third family in dexter notation.
- Let $\Sigma' = \Sigma_{[\pm n]}(\ell', r', A', B')$ be an $\vec{\mathcal{A}}_{[\pm n]}$ shard that forces Σ, such that
  - S' is a $\vec{\mathcal{B}}_n$ shard,
  - S' has Σ' as a dexter or sinister representative,
  - the upper representative of S' forces the lower representative of S,
  - and the upper representative of S' does not force the upper representative of S.
- Let $\mathbf{t} \in \Sigma' \cap \mathcal{H}_n^{\mathcal{B}} \subset \mathbb{R}^{[\pm n]}$ be a centrally symmetric $\mathbb{R}^{[\pm n]}$ vector in the shard Σ'. This holds exactly for those vectors $\mathbf{t} \in \mathbb{R}^{[\pm n]}$ with the properties

$$t_i = -t_{-i} \text{ for all } i \in [n] \tag{1}$$
$$t_{\ell'} = t_{r'} \tag{2}$$
$$t_i < t_{\ell'} = t_{r'} \text{ for all } i \in A \cap]\ell', r'[\tag{3}$$
$$t_j > t_{\ell'} = t_{r'} \text{ for all } j \in B \cap]\ell', r'[\tag{4}$$

We want to show that no edge of $\mathsf{SP}(\Sigma)$ has a normal cone that contains the vector $\mathbf{t}$. Such an edge would have to be in direction $\mathbf{e}_{\ell'} - \mathbf{e}_{r'}$.

We distinguish cases by the combinations of dexter/sinister and upper/lower representatives that force each other. We label the arcs of S by α and $-\alpha$ and the arcs of S' by α' and $-\alpha'$. We always assume that Σ' forces Σ while Σ' does not force the centrally symmetric image of Σ.

Case 1: Σ is lower dexter and Σ' is upper dexter

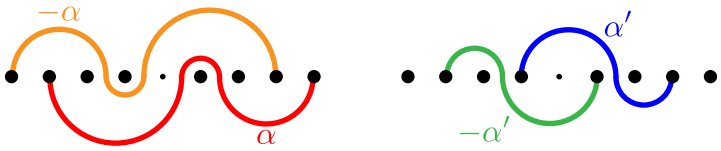

In this case, the order of the endpoints is $-r \leq -r' < \ell' < 0 < -\ell' < r' \leq r$ [Picture from [PPR20]]. As Σ' is upper, we have $-\ell' \in A'$ and therefore $-\ell' \in A$ by Observation 4.3.22. From (3), we have $t_{-\ell'} < t_{\ell'} = t_{r'}$ and by (1), we get $-t_{\ell'} < 0 < t_{\ell'}$.

As Σ is lower, we have $-\ell \in B$ and as $-\ell \in]\ell', r'[$, we know from (4) that $t_{-\ell} > t_{\ell'}$, which implies that $\ell \neq \ell'$. We deduce that $\ell' \in B$ as $\ell' \in]\ell, -\ell[$ and Σ is lower.

We now assume for a contradiction that $\mathbf{t}$ lies in the normal cone of an edge in direction $\mathbf{e}_{\ell'} - \mathbf{e}_{r'}$. As $\ell' \in B$, we know from Corollary 3.3.7 that there has to exist some $\ell \leq s < \ell'$ with $s \in \{\ell\} \cup A$ such that $\mathbf{t}$ lies in the normal cone of some Σ-matching containing the pair (s, ℓ'). By Corollary 3.3.5, this implies that

$$t_s \geq t_{\ell'} > 0. \tag{5}$$

We remark that $s \in [\ell, -\ell[$ and $s \in \{\ell\} \cup A$. We use Observation 4.3.22 to deduce that $-s \in B$. We distinguish two subcases depending on the order of s and $-r'$.

- If $s > -r'$, then $-s \in B \cap]\ell', r'[$, so (4) gives us $t_{-s} > t_{\ell'}$ while (1) gives us the equality $-t_s = t_{-s}$, allowing us to conclude that $-t_s > t_{\ell'} > 0$, which contradicts (5).
- If $s \leq -r'$, we have $r' \leq -s$ and $-s \leq -\ell$ by definition of s. This means that $r' \leq -\ell$, so we cannot be in the first case of Lemma 4.3.24. As Σ is lower, there is some $k \in]\ell', r'[$ such that $-k, k \in B$. By Lemma 4.3.23, Σ is centrally symmetric on the interval $[\ell', -\ell']$ as Σ' is dexter. Therefore, $k \in [-\ell', r'[$. Now $k < r'$ implies $s \leq r' < -k$, so $-k \in B \cap]s, \ell'[$. Now Corollary 3.3.5 implies that

  $$-t_k = t_{-k} \geq t_{\ell'} > 0. \tag{6}$$

  And from $k \in B \cap]\ell', r'[$ and (4), we deduce

  $$t_k \geq t_{\ell'} > 0. \tag{7}$$

  These two inequalities (6) and (7) contradict each other.

Case 2: Σ is lower dexter and Σ' is upper sinister

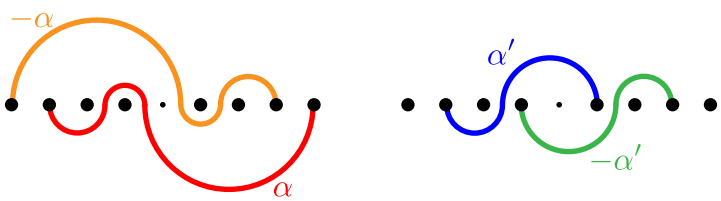

In this case, the order of the endpoints is $-r < \ell \leq \ell' < -r' < 0 < r' < -\ell' \leq -\ell < r$ [Picture from [PPR20]]. As Σ' is upper, we have $-r' \in A'$ and therefore $-r' \in A$ by Observation 4.3.22. From (3), we have $t_{-r'} < t_{\ell'} = t_{r'}$ and by (1), we get $-t_{r'} < 0 < t_{r'}$. As Σ' is sinister, we have $\ell' < -r' < -\ell'$. As Σ' forces Σ, we have $\ell \leq \ell'$. These imply

the inequalities $\ell < -r' < -\ell$. As Σ is lower, we then have $r' \in B$. As $r' < -\ell$, we learn from Lemma 4.3.24 that there is some $k \in]\ell', r'[$ such that $-k, k \in B$. Then Lemma 4.3.23 gives us $k \in]\ell', -r'[\subset]\ell', r'[$ and $-k \in]r', -\ell'[\subset]r', r]$. We distinguish two subcases depending on the order of t_{-k} and $t_{r'}$.

- If $t_{-k} \geq t_{r'}$, then (1) gives us
$$-t_k \geq t_{r'} > 0. \tag{8}$$
Moreover, as $k \in B \cap]\ell', r'[$, we learn from (4) that
$$t_k \geq t_{r'} > 0. \tag{9}$$
These two inequalities (8) and (9) contradict each other.
- Otherwise, we have $t_{-k} \geq t_{r'}$. We know from Corollary 3.3.7 that if $\mathbf{t}$ lies in the normal cone of an edge in direction $\mathbf{e}_{\ell'} - \mathbf{e}_{r'}$, where $r' \in B$, then $\mathbf{t}$ lies in the normal cone of some Σ-matching containing a pair (s, r') for some $s \leq \ell'$. With the help of Corollary 3.3.5, we deduce that for any $j \in]r', r[$ such that $j \in B \cup \{r\}$ and $t_j < t_{r'}$, there has to exist some $m \in]r', j[$ with $m \in A$ and $t_m \geq t_{r'}$. This holds in particular for $-k \in]r', r]$. Then there has to be some $m \in]r', -k[$ with $m \in A$ such that
$$t_m \geq t_{r'} > 0. \tag{10}$$
Moreover, as Σ is lower and $m \in]\ell, -\ell[$ with $m \in A$, we obtain $-m \in B$ and $-m \in]\ell', r'[$. With (4), we have
$$-t_m = t_{-m} \geq t_{r'} > 0. \tag{11}$$
These two inequalities (10) and (11) contradict each other.

Case 3: Σ is upper dexter and Σ' is lower dexter

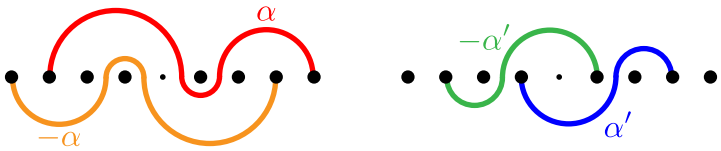

In this case, the order of the endpoints is $-r \leq -r' < \ell' < 0 < -\ell' < r' \leq r$ [Picture from [PPR20]]. As Σ' is lower, we have $-\ell' \in B$. Then (4) tells us that $t_{-\ell'} > t_{\ell'} = t_{r'}$ and by (1), we obtain $t_{\ell'} < 0 < -t_{\ell'}$. As Σ is upper, we have $-\ell \in A$ and therefore $\ell \neq \ell'$. This implies that $\ell' \in A$ because Σ is upper and $-\ell' \in]\ell, -\ell[$.

We now claim that there is some $u \in \{\ell\} \cup A$ with both $u \in [\ell, \ell'[$ and $u \in]-r', \ell'[$. We certify the existence of such an index u with the help of Lemma 4.3.24.

- Either $r' > -\ell$, then we set $u := \ell$. As Σ is upper, we have $-\ell \in A$ by Observation 4.3.22.
- or $r' \leq -\ell$ and there exists a $k \in]\ell', b'[$ with both $-k, k \in A$. In this case, we learn from Lemma 4.3.23 that $k \in]-\ell', r'[$ and we set $u := -k$.

For this position u, we have $-u \in A \cap]\ell', r'[$ and (3) gives us $t_{-u} \leq t_{\ell'} = t_{r'}$. Now (1) allows us to conclude that
$$-t_u \leq t_{\ell'} < 0. \tag{12}$$
We distinguish two subcases depending on the order of t_u and $t_{\ell'}$.

- If $t_u \leq t_{\ell'}$, we deduce from (12) that both $-t_u, t_u < 0$, which is impossible.
- Otherwise, $t_u > t_{\ell'}$. If $\mathbf{t}$ is in the normal cone of an edge in direction $\mathbf{e}_{\ell'} - \mathbf{e}_{r'}$ with $\ell' \in A$, then Corollary 3.3.7 states that $\mathbf{t}$ lies in the normal cone of a matching that contains a pair (ℓ', s) for some $s \geq r'$. Together with Corollary 3.3.5, we learn that for all $i \in [\ell, \ell'[$ with

both $i \in \{\ell\} \cup A$ and $t_i > t_{\ell'}$, there exists some $h \in]i, r'[$ with both $h \in B$ and

$$t_h \leq t_{\ell'} < 0. \tag{13}$$

On the other hand, Σ is upper and $h \in B \cap]\ell, -\ell[$, so Observation 4.3.22 gives us $-h \in A$. Furthermore, we have $-h \in]\ell', r'[$. Then (1) and (3) give us

$$-t_h = t_{-h} \leq t_{\ell'} < 0. \tag{14}$$

These two inequalities (13) and (14) contradict each other.

Case 4: Σ is upper dexter and Σ' is lower sinister

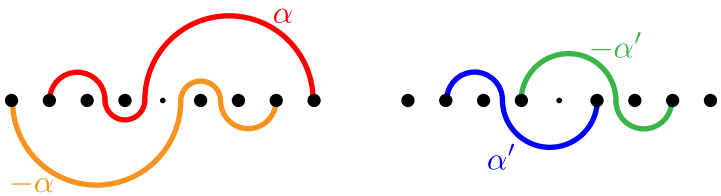

In this case, the order of the endpoints is $-r < \ell \leq \ell' < -r' < 0 < r' < -\ell' \leq -\ell < r$ [Picture from [PPR20]]. As Σ is lower, we have $-r' \in B$ by Observation 4.3.22. Then (4) gives us $t_{-r'} > t_{\ell'} = t_{r'}$ and (1) tells us that $t_{r'} < 0 < -t_{r'}$. As Σ is upper and $r' \in]\ell, -\ell[$, this also implies that $r' \in A$. As we have $r' < -\ell$, we learn from Lemma 4.3.24 that there exists some $k \in]\ell', r'[$ such that both $-k, k \in A$. This k must satisfy $k \in]\ell', -r'[$ by Lemma 4.3.23 and thus $k \in]\ell', r'[$. We know from (3) that

$$t_k \leq t_{r'} < 0. \tag{15}$$

If $\mathbf{t}$ lies in the normal cone of an edge in direction $\mathbf{e}_{\ell'} - \mathbf{e}_{r'}$ where $r' \in A$, then Corollary 3.3.7 tells us that $\mathbf{t}$ lies in the normal cone of a Σ-matching containing the pair (r', v) for some $v \in]r', r]$ with $v \in B \cup \{r\}$. Then Corollary 3.3.5 gives us

$$t_v \leq t_{r'} < 0. \tag{16}$$

We now distinguish two subcases by the order of v and $-\ell'$.

- If $v \geq -\ell'$, then $r' < -k < -\ell' \leq v$ certifies that $-k \in]r', v[$ and $-k \in A$. Together with (1) and Corollary 3.3.5, this gives us $-t_k = t_{-k} \leq t_{r'} < 0$. This contradicts (15).
- Otherwise, we have $v < -\ell'$. Since Σ is upper and $v \in]\ell, -\ell[$ with $v \in B$, we learn from Observation 4.3.22 that $-v \in A$. Moreover, we have $-v \in]\ell', -r[$. Then (4) certifies that $-t_v = t_{-k} \leq t_{r'} < 0$. This contradicts (16). □

This completes or work towards a proof of Proposition 4.3.12.

Proof of Proposition 4.3.12. We saw in Lemma 4.3.13 that the walls of $\mathsf{SP}(S)$ contain the shard S. We showed family for family in Lemma 4.3.20 and Lemma 4.3.21 and Lemma 4.3.25 that the union of the walls of $\mathsf{SP}(S)$ is always contained in the union of the representatives Σ' for all $\vec{\mathcal{B}}_n$ shards S' that force S. □

4.3.5 Shardsumotopes

We just learned that a $\vec{\mathcal{B}}_n$ shard polytope $\mathsf{SP}(S)$ as defined in Definition 4.3.9 has the crucial propery Proposition 4.3.12 that the union of the walls of its fans contains the shard S itself and

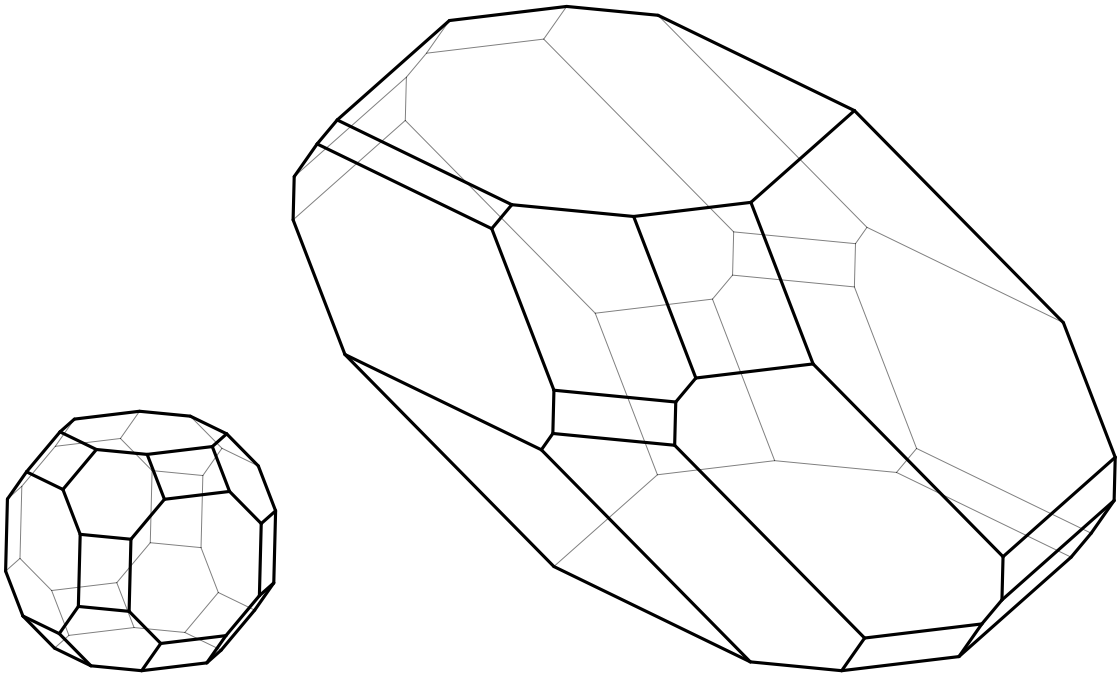

Figure 4.8: The $\mathcal{B}$ permutahedron $\mathsf{Perm}_3^{\mathrm{B}}$ as defined in Definition 4.1.16 (left) and the shardsumotope $\mathsf{SP}_+^{\mathcal{B}}(\mathbf{\Sigma}^{\mathcal{B}})$ as introduced in Example 4.3.28 (right). [Picture from [PPR20]]

does not contain any shard S' that is not forcing S. Of course, it would have been possible to build arbitrary Minkowski sums of $\vec{\mathcal{B}}_n$ shard polytopes and study their properties regardless of this result. But Proposition 4.3.12 now enables us to use $\vec{\mathcal{B}}_n$ shard polytopes to construct shardsumotopes that are quotientopes of lattice congruences on the weak order on $\mathfrak{S}_n^{\mathcal{B}}$ (or equivalently, on the poset of regions $\mathrm{Pos}(\vec{\mathcal{B}}_n)$.

Definition 4.3.26 ($\mathcal{B}$-Shardsumotope)**.** Given a lattice congruence $\equiv^{\mathcal{B}}$ of the weak order on $\mathfrak{S}_n^{\mathcal{B}}$ that retains the $\vec{\mathcal{B}}_n$ shards $\mathcal{S}^{\mathcal{B}}$, the **$\mathcal{B}$-shardsumotope** $\mathsf{SP}_+^{\mathcal{B}}(\equiv^{\mathcal{B}})$ is the Minkowski sum of the shard polytopes $\mathsf{SP}(S)$ for all $S \in \mathcal{S}^{\mathcal{B}}$, given by $\mathsf{SP}_+^{\mathcal{B}}(\equiv^{\mathcal{B}}) := \sum_{S \in \mathcal{S}^{\mathcal{B}}} \mathsf{SP}(S)$.

The following statement on $\mathcal{B}$-shardsumotopes is the type $\mathcal{B}$ analogue of Proposition 3.4.2 and a direct consequence of Proposition 4.3.12.

Corollary 4.3.27 ($\mathcal{B}$-Shardsumotopes are $\mathcal{B}$-Quotientopes)**.** For any lattice congruence $\equiv^{\mathcal{B}}$ on the poset of regions $\mathrm{Pos}(\vec{\mathcal{B}}_n)$, the quotient fan $\mathcal{F}_{\equiv}^{\mathcal{B}}$ is the normal fan of $\mathsf{SP}_+^{\mathcal{B}}(\equiv^{\mathcal{B}})$. In consequence, the $\mathcal{B}$-shardsumotope $\mathsf{SP}_+^{\mathcal{B}}(\equiv^{\mathcal{B}})$ is a quotientope for $\equiv^{\mathcal{B}}$.

Example 4.3.28. For the trivial lattice congruence on the weak order on $\mathfrak{S}_n^{\mathcal{B}}$ that retains all $\vec{\mathcal{B}}_n$ shards $\mathbf{\Sigma}^{\mathcal{B}}$, the normal fan of the shardsumotope $\mathsf{SP}_+^{\mathcal{B}}(\mathbf{\Sigma}^{\mathcal{B}})$ is the type $\mathcal{B}$ fan $\mathcal{F}_n^{\mathcal{B}}$. See Figure 4.8 (right) for an illustration in $\vec{\mathcal{B}}_3$.

Example 4.3.29. A well-studied example of lattice congruences of the weak order on $\mathfrak{S}_n^{\mathcal{B}}$ are **β-Cambrian congruences**. They were introduced and analyzed in the more general context of Coxeter groups in [Rea04] and [Rea06]. Given a β-Cambrian congruence $\equiv^{\mathcal{B}}$, the normal fan of the shardsumotope $\mathsf{SP}_+^{\mathcal{B}}(\equiv^{\mathcal{B}})$ is the quotient fan of this congruence. Their shardsumotopes are identical to the β-cyclohedra studied in [HL07]. This decomposition as a Minkowski sum of polytopes was already known from the context of brick polytopes (see [PS15]). See Figure 4.9 for some illustrations in $\vec{\mathcal{B}}_3$.

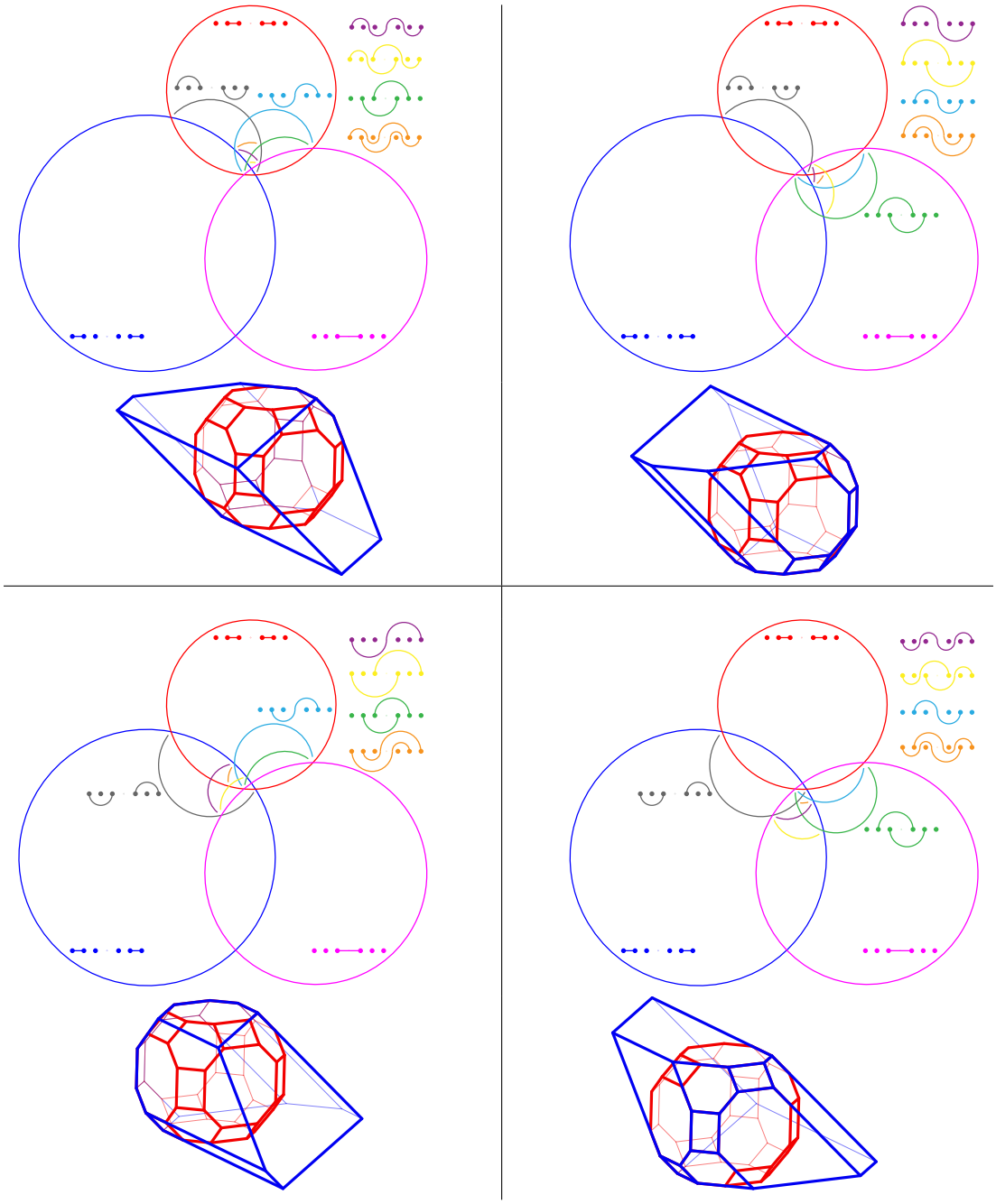

Figure 4.9: Several $\mathcal{B}$-shardsumotopes for β-Cambrian congruences. In each case, the upper diagram shows a steregraphic projection of the quotient fan with arc illustrations of all retained $\vec{\mathcal{B}}_n$ shards. The lower diagram shows the resulting shardsumotope in blue, which can equivalently obtained by removing inequalities from the facet description of the $\mathcal{B}$-permutahedron $\mathrm{Perm}_3^{\mathrm{B}}$ shown in red. [Picture from [PPR20]]

Bibliography

[ABD10] Federico Ardila, Carolina Benedetti, and Jeffrey Doker. Matroid polytopes and their volumes. *Discrete Comput. Geom.*, 43(4):841–854, 2010.

[AHBHY18] Nima Arkani-Hamed, Yuntao Bai, Song He, and Gongwang Yan. Scattering forms and the positive geometry of kinematics, color and the worldsheet. *J. High Energy Phys.*, (5):096, front matter+75, 2018.

[APR20] Doriann Albertin, Vincent Pilaud, and Julian Ritter. Removahedral congruences versus permutree congruences. Preprint, arXiv:2006.00264, 2020.

[BB05] Anders Björner and Francesco Brenti. *Combinatorics of Coxeter groups*, volume 231 of *Graduate Texts in Mathematics*. Springer, New York, 2005.

[BEZ90] Anders Björner, Paul H. Edelman, and Günter M. Ziegler. Hyperplane arrangements with a lattice of regions. *Discrete Comput. Geom.*, 5(3):263–288, 1990.

[CD06] Michael P. Carr and Satyan L. Devadoss. Coxeter complexes and graph-associahedra. *Topology Appl.*, 153(12):2155–2168, 2006.

[CFZ02] Frédéric Chapoton, Sergey Fomin, and Andrei Zelevinsky. Polytopal realizations of generalized associahedra. *Canad. Math. Bull.*, 45(4):537–566, 2002.

[Dev09] Satyan L. Devadoss. A realization of graph associahedra. *Discrete Math.*, 309(1):271–276, 2009.

[DLRS10] Jesús De Loera, Jörg Rambau, and Francisco Santos. *Triangulations: Structures for Algorithms and Applications*, volume 25. Springer Science & Business Media, 2010.

[Ede84] Paul H Edelman. A partial order on the regions of rn dissected by hyperplanes. *Transactions of the American Mathematical Society*, 283(2):617–631, 1984.

[HK10] Alan J Hoffman and Joseph B Kruskal. Integral boundary points of convex polyhedra. In *50 Years of integer programming 1958-2008*, pages 49–76. Springer, 2010.

[HL07] Christophe Hohlweg and Carsten Lange. Realizations of the associahedron and cyclohedron. *Discrete Comput. Geom.*, 37(4):517–543, 2007.

[HNT05] Florent Hivert, Jean-Christophe Novelli, and Jean-Yves Thibon. The algebra of binary search trees. *Theoret. Comput. Sci.*, 339(1):129–165, 2005.

[Hum90] James E. Humphreys. *Reflection groups and Coxeter groups*, volume 29 of *Cambridge Studies in Advanced Mathematics*. Cambridge University Press, Cambridge, 1990.

[KT97] Daniel Krob and Jean-Yves Thibon. Noncommutative symmetric functions. IV. Quantum linear groups and Hecke algebras at $q = 0$. *J. Algebraic Combin.*, 6(4):339–376, 1997.

[Lod04] Jean-Louis Loday. Realization of the Stasheff polytope. *Arch. Math. (Basel)*, 83(3):267–278, 2004.

[LP18] Carsten Lange and Vincent Pilaud. Associahedra via spines. *Combinatorica*, 38(2):443–486, 2018.

[LR98] Jean-Louis Loday and María O. Ronco. Hopf algebra of the planar binary trees. *Adv. Math.*, 139(2):293–309, 1998.

[McM73] Peter McMullen. Representations of polytopes and polyhedral sets. *Geometriae Dedicata*, 2:83–99, 1973.

[McM87] Peter McMullen. Indecomposable convex polytopes. *Israel J. Math.*, 58(3):321–323, 1987.

[MR95] Claudia Malvenuto and Christophe Reutenauer. Duality between quasi-symmetric functions and the Solomon descent algebra. *J. Algebra*, 177(3):967–982, 1995.

[Nov00] Jean-Christophe Novelli. On the hypoplactic monoid. *Discrete Math.*, 217(1-3):315–336, 2000. Formal power series and algebraic combinatorics (Vienna, 1997).

[Pil17] Vincent Pilaud. Which nestohedra are removahedra? *Rev. Colombiana Mat.*, 51(1):21–42, 2017.

[PK92] Aleksandr V. Pukhlikov and Askold G. Khovanskiĭ. Finitely additive measures of virtual polyhedra. *Algebra i Analiz*, 4(2):161–185, 1992.

[Pos09] Alexander Postnikov. Permutohedra, associahedra, and beyond. *Int. Math. Res. Not. IMRN*, (6):1026–1106, 2009.

[PP17] Vincent Pilaud and Viviane Pons. Permutrees. volume 61, pages 987–993. 2017. The European Conference on Combinatorics, Graph Theory and Applications (EUROCOMB'17).

[PPPP19] Arnau Padrol, Yann Palu, Vincent Pilaud, and Pierre-Guy Plamondon. Associahedra for finite type cluster algebras and minimal relations between g-vectors. Preprint, arXiv:1906.06861, 2019.

[PPR20] Arnau Padrol, Vincent Pilaud, and Julian Ritter. Shard polytopes. Preprint, arXiv:2007.01008, 2020.

[PRW08] Alexander Postnikov, Victor Reiner, and Lauren K. Williams. Faces of generalized permutohedra. *Doc. Math.*, 13:207–273, 2008.

[PS15] Vincent Pilaud and Christian Stump. Brick polytopes of spherical subword complexes and generalized associahedra. *Adv. Math.*, 276:1–61, 2015.

[PS19] Vincent Pilaud and Francisco Santos. Quotientopes. *Bull. Lond. Math. Soc.*, 51(3):406–420, 2019.

[Rea03] Nathan Reading. Lattice and order properties of the poset of regions in a hyperplane arrangement. *Algebra Universalis*, 50(2):179–205, 2003.

[Rea04] Nathan Reading. Lattice congruences of the weak order. *Order*, 21(4):315–344, 2004.

[Rea05] Nathan Reading. Lattice congruences, fans and Hopf algebras. *J. Combin. Theory Ser. A*, 110(2):237–273, 2005.

[Rea06] Nathan Reading. Cambrian lattices. *Adv. Math.*, 205(2):313–353, 2006.

[Rea15] Nathan Reading. Noncrossing arc diagrams and canonical join representations. *SIAM J. Discrete Math.*, 29(2):736–750, 2015.

[Rea16a] Nathan Reading. Finite Coxeter groups and the weak order. In *Lattice theory: special topics and applications. Vol. 2*, pages 489–561. Birkhäuser/Springer, Cham, 2016.

[Rea16b] Nathan Reading. Lattice theory of the poset of regions. In *Lattice Theory: Special Topics and Applications*, pages 399–487. Springer International Publishing Switzerland, 2016.

[RS09] Nathan Reading and David E. Speyer. Cambrian fans. *J. Eur. Math. Soc.*, 11(2):407–447, 2009.

[Sch13] Pieter Hendrik Schoute. *Analytical treatment of the polytopes regularly derived from the regular polytopes*, volume 11. J. Müller, 1913.

[SD19] The Sage Developers. *SageMath, the Sage Mathematics Software System (Version 8.9)*, 2019. https://www.sagemath.org.

[SS93] Steve Shnider and Shlomo Sternberg. *Quantum groups: From coalgebras to Drinfeld algebras*. Series in Mathematical Physics. International Press, Cambridge, MA, 1993.

[Sta63] Jim Stasheff. Homotopy associativity of H-spaces I, II. *Trans. Amer. Math. Soc.*, 108(2):293–312, 1963.

[Tam51] Dov Tamari. *Monoides préordonnés et chaînes de Malcev*. PhD thesis, Université Paris Sorbonne, 1951.

[You30] Alfred Young. On quantitative substitutional analysis. *Proceedings of the London Mathematical Society*, s2-31(1):273–288, 1930.

[Zie07] Günter M. Ziegler. *Lectures on Polytopes*, volume 152 of *Graduate Texts in Mathematics*. Springer-Verlag, New York, 7 edition, 2007.

ECOLE
DOCTORALE

Titre : Polytopes de tessons et quotientopes pour les congruences de treillis de l'ordre faible

Mots clés : ordre faible, congruence et quotient de treillis, éventail quotient et quotientope, arrangement d'hyperplans, cone de type, permutarbre

Résumé : Dans la combinatoire polyédrale, plusieurs polytopes bien connus sont reliés à des congruences de treillis de l'ordre faible. Deux exemples sont le permutaèdre et l'associaèdre. L'éventail normal du permutaèdre est l'éventail de tresses, donné par l'arrangement de tresses des hyperplans $x_i = x_j$ pour $1 \leq i < j \leq n$. L'éventail normal de l'associaèdre est l'éventail sylvestre. Parce qu'il est raffiné par l'éventail de tresses, l'associaèdre est un permutaèdre généralisé. De telles relations entre polytopes ne se limitent pas à l'éventail de tresses. Les cônes de tout arrangement réel d'hyperplans linéaires induisent un éventail qui est l'éventail normal d'un zonotope. De plus, le choix d'une région de l'éventail comme région de base induit un ordre partiel sur les régions, appelé le poset des régions, qui est un treillis dans certaines circonstances. Pour l'arrangement de tresses, ce poset est isomorphe à l'ordre faible sur le groupe symétrique. Pour l'arrangement de Coxeter de type B, il est isomorphe à l'ordre faible sur le groupe hyper-octaédrique.
N. Reading a montré qu'une congruence de treillis d'un treillis des régions induit un éventail quotient, où des cônes maximaux sont collés si leurs éléments de treillis correspondants sont équivalents sous la congruence de treillis. Par exemple, l'éventail normal de l'associaèdre est un éventail quotient induit par la congruence sylvestre. Un quotientope est un polytope dont l'éventail normal est un éventail quotient. Leur existence a été certifiée par une construction technique de V. Pilaud et F. Santos pour les éventails quotients basés sur l'ordre faible sur le groupe symétrique. L'objectif de cette thèse est d'étudier plus avant des constructions de quotientopes.
Notre première contribution concerne les constructions comme enlevoèdres qui sont des polytopes obtenus en enlevant des inégalités de la description de facettes du permutaèdre. Nous montrons que les permutarbrèdres sont les seuls quotientopes qui peuvent être obtenus comme enlèvoedres. Notre deuxième contribution est une construction simplifiée de quotientopes arbitraires comme sommes de Minkowski de polytopes élémentaires que nous appelons polytopes de tessons en raison de leur étroite relation aux tessons d'un arrangement d'hyperplans. Notre construction peut être adaptée pour construire des quotientopes pour tout congruence de treillis de l'ordre faible sur le groupe hyper-octaédrique.

Title : Shard Polytopes and Quotientopes for Lattice Congruences of the Weak Order

Keywords : weak order, lattice congruences and quotients, quotient fan and quotientope, hyperplane arrangement, type cone, permutree

Abstract : In polyhedral combinatorics, some well-known polytopes are related to lattice congruences of the weak order. Two examples are the permutahedron and the associahedron. The normal fan of the permutahedron is the braid fan, given by the braid arrangement of the hyperplanes $x_i = x_j$ for $1 \leq i < j \leq n$. The normal fan of the classical associahedron is the sylvester fan. Since it coarsens the braid fan, the associahedron is a generalized permutahedron. Such relationships between polytopes are not limited to the braid fan. The cones of any real central hyperplane arrangement induce a fan that is the normal fan of a zonotope. Moreover, choosing one of the regions of that fan as the base region induces a partial order on all the regions, called the poset of regions, which is a lattice under certain circumstances. For the braid arrangement, this poset is isomorphic to the weak order on the symmetric group. For the Coxeter type B arrangement, it is isomorphic to the weak order on the hyper-ocathedral group.
It was shown by N. Reading that applying a lattice congruence to a lattice of regions induces a quotient fan, where maximal cones are united if their corresponding lattice elements are equivalent under the lattice congruence. For example, the normal fan of the associahedron is a quotient fan induced by the sylvester congruence. A quotientope is a polytope whose normal fan is a quotient fan. Their existence was certified through a technical construction by V. Pilaud and F. Santos for those quotient fans based on the weak order on the symmetric group. The objective of this thesis is to study further constructions for quotientopes.
Our first contribution concerns constructions as removahedra which are polytopes obtained by removing inequalities from the facet description of the permutahedron. We show that the permutreehedra are the only quotientopes that can be obtained as removahedra. Our second contribution is a simplified construction of arbitrary quotientopes as Minkowski sums of elementary polytopes we call shard polytopes due to their close relation with the shards of a hyperplane arrangement. Our construction can be adapted to construct quotientopes for all lattice congruences of the weak order on the hyper-octahedral group.

Institut Polytechnique de Paris
91120 Palaiseau, France